UNITED STATES
DEPARTMENT OF THE INTERIOR
U.S.GEOLOGICAL SURVEY

GEOLOGICAL, GEOCHEMICAL AND GEOTECHNICAL OBSERVATIONS ON THE BERING SHELF, ALASKA

by

Matthew C. Larsen, C. Hans Nelson and Devin R. Thor

OPEN-FILE REPORT

80-979

This report is preliminary and has not been reviewed for conformity with U. S. Geological Survey editorial standards and stratigraphic nomenclature. Any use of trade names is for descriptive purposes only and does not imply endorsement by the USGS.

Table of Contents

Sedimentary processes and potential hazards on the sea floor of Northern Bering Sea
by: M.C. Larsen, C.H. Nelson, and D.R. Thor

Interplay of physical and biological sedimentary structures of the Bering epicontinental shelf
by: C. H. Nelson, R.W. Rowland, S.W. Stoker, B.R. Larsen

Ripples and sand waves in Norton Basin; bedform activity, and scour potential
by: C. H. Nelson, M.E. Field, D.A. Cacchione, D. E. Drake, and T. H. Nilsen

Graded storm sand layers offshore from the Yukon delta, Alaska
by: C. H. Nelson

Ice gouging on the subarctic Bering shelf
by: D. R. Thor and C. H. Nelson

Liquefaction potential of the Yukon prodelta, Bering Sea
by: E. C. Clukey, D.A. Cacchione, C.H. Nelson

Surface and subsurface faulting in Norton Sound and Chirikov Basin, Alaska
by: J. L. Johnson and M. L. Holmes

Hydrocarbon gases in near-surface sediment of northern Bering Sea (Norton Sound and Chirikov Basin)
by: K. A. Kvenvolden, G. D. Redden, D. R. Thor, and C. H. Nelson

Introduction to papers from Holocene Marine Sedimentation in the North Sea Basin
by: C. H. Nelson

Late Pleistocene-Holocene transgressive sedimentation in deltaic and non-deltaic areas of the Bering epicontinental shelf
by: C. H. Nelson

Microfaunal analysis of late Quaternary deposits of the northern Bering Sea
by: K. McDougall

Sedimentary structures on a delta-influenced shallow shelf, Norton Sound, Alaska
by: J. D. Howard, C. H. Nelson

Linear sand bodies in the Bering Sea epicontinental shelf
by: C.H. Nelson, W. R. Dupré, M.E. Field, and J. D. Howard

Depositional and erosional features of the inner shelf, northeastern Bering Sea
by: R. Hunter, D. R. Thor, and M. L. Swisher

Velocity and bottom-stress measurements in the bottom boundary layer, outer Norton Sound, Alaska
by: D. A. Cacchione, D. E. Drake, P. Wiberg.

Geotechnical characteristics of bottom sediments in the northern Bering Sea
by: H. W. Olsen, E. C. Clukey, and C. H. Nelson

Distribution of gas-charged sediment in Norton Basin, northern Bering Sea
by: M. L. Holmes and D. R. Thor

Appendix

GEOLOGICAL, GEOCHEMICAL, AND GEOTECHNICAL OBSERVATIONS ON THE BERING SHELF, ALASKA

M.C. Larsen, C.H. Nelson, and D.R. Thor

Multidisciplinary studies of Bering Sea shelf, Alaska, have been conducted by the U. S. Geological Survey in recent years. Our goal, as participants in this work, has been to assess the geochemical and geotechnical characteristics in northern Bering Sea and Norton Sound and the potential hazards to petroleum development due to various ongoing geologic processes. The studies have enabled us to examine a number of topical problems that are discussed in the 15 papers included in this report.

Many of the papers in this report will be published in The Eastern Bering Sea Shelf: Its Oceanography and Resources (edited by D.W. Hood) or Holocene Marine Sedimentation in the North Sea Basin (edited by S.D. Nio). This open-file report, however, was published because of the constant demand expressed by private companies and state and federal agencies for current information concerning our studies in the northern Bering Sea.

Acknowledgement

This study was supported jointly by the U.S. Geological Survey and by the Bureau of Land Management through interagency agreement with the National Oceanic and Atmospheric Administration, under which a multi-year program responding to needs of petroleum development of the Alaskan continental shelf is managed by the Outer Continental Shelf Environmental Assessment Program Office.

Sedimentary Processes and Potential Geologic Hazards on the Sea Floor of Northern Bering Sea

Matthew C. Larsen, C. Hans Nelson, and Devin R. Thor

U.S. Geological Survey, 345 Middlefield Road

Menlo Park, California 94025

ABSTRACT

A dynamic environment of strong bottom currents, storm waves, and gas-charged sediment on the shallow sea floor of northern Bering Sea creates several potential geologic hazards for resource exploration. Thermogenic gas seeps, sea-floor gas cratering, sediment liquefaction, ice gouging, scour-depression formation, coastal and offshore storm surge and associated deposition of storm-sand, and movement of large-scale bedforms all are active sedimentary processes in this epicontinental shelf region.

Interaction between the processes of liquefaction and the formation of shallow gas pockets and craters, scour depressions, storm-sand deposits, and slumps results in sediment instability. Liquefaction of the upper 1-3 m of sediment may be caused by cyclic storm-wave loading of the Holocene coarse-grained silt and very fine-grained sand covering Norton Sound. The widespread occurrence of gas-charged sediment with small surficial craters (3-8 m in diameter and less than 1 m deep) in central Norton Sound indicates that the sea-floor sediment is periodically disrupted by escape of biogenic gas from the underlying peaty mud. During major storms, liquefaction may not only help trigger crater formation but also magnify erosional and depositional processes that create large-scale scour areas and prograde storm sand sheets in the Yukon prodelta area.

Erosional and depositional processes are most intense in the shallower parts of northern Bering Sea and along the coastline during storm surge flooding. Ice gouges are numerous and ubiquitous in the area of the Yukon prodelta, where the sediment is gouged to depths of 1 m. Though much less common than in the prodelta, ice gouges are present throughout the rest of northern Bering Sea where water depths are less than 20 m and at times where water is as much as 30 m deep. In the Yukon prodelta area and in central Norton Sound, where currents are constricted by shoal areas and flow is made turbulent by local topographic irregularities (such as ice gouges), storm-induced currents have scoured large (10- to 150-m diamter), shallow (less than 1 m deep) depressions. The many storm-sand layers in Yukon prodelta mud show that storm surge and waves have generated bottom-transport currents that deposit layers of sand as thick as 20 cm as far as 100 km from land. Storm surge runoff may reinforce the strong geostrophic currents near Bering Strait, causing intermittent movement of even the largest sand waves (10-200 m wavelength, to 2 m height).

INTRODUCTION

Studies of potential geologic hazards on Norton Basin sea floor in northern Bering Sea have been conducted by the U.S. Geological Survey (USGS) in evaluating oil and gas lease tracts preparatory to Outer Continental Shelf (OCS) leasing. The data base for this evaluation included 9000 km of high-resolution geophysical tracklines (Nelson et al., 1978a; Thor and Nelson, 1978; Larsen et al., 1979) 1000 grab samples, 400 box cores and 60 vibracores; in addition, hundreds of camera, hydrographic, and current meter stations have been occupied during the past decade by USGS, National Oceanic and Atmospheric Administration (NOAA), and University of Washington oceanographic vessels (Figs. 1 and 2).

The northern Bering Sea is a broad, shallow epicontinental shelf region covering approximately 200,000 km^2 of subarctic sea floor between northern Alaska and the U.S.S.R. The shelf can be divided into four general morphologic areas: (1) the western part, an area of undulating, hummocky relief formed by glacial gravel and transgressive-marine sand substrate (Nelson and Hopkins, 1972); (2) the southeastern part, a relatively flat featureless plain with fine-grained transgressive-marine sand substrate (McManus, et al., 1977); (3) the northeastern part, a complex system of sand ridges and shoals with fine- to medium-grained transgressive sand substrate (Nelson, et al., 1978b); and (4) the eastern part, a broad, flat marine reentrant (Norton Sound) covered by Holocene silt and very fine sand (Nelson and Creager, 1977). A detailed discussion of bathymetry and geomorphology of northern Bering Sea is given by Hopkins and others (1976) (Fig. 3).

The northern Bering Sea is affected by a number of dynamic factors: winter sea ice, sea level setup, storm waves and strong currents (geostrophic, tidal, and storm). The sea is covered by pack ice for about half the year,

from November through May. A narrow zone of shorefast ice (sea ice attached to the shore) develops around the margin of the sea during winter months. Around the front of the Yukon River Delta, shorefast ice extends to 40 km offshore (Thor et al., 1978). During the open-water season, the sea is subject to occasional strong northerly winds, in the fall strong south-southwesterly winds cause high waves and storm surges along the entire west Alaskan coast (Fathauer, 1975). Throughout the year, there is a continual northward flow of water is present with currents intensifying on the east side of strait areas (Coachman et al., 1976). Although diurnal tidal ranges are small (less than 0.5 m), strong tidal currents are found in shoreline areas and within central Norton Sound (Fleming and Heggarty, 1966; Cacchione and Drake, 1979a).

This paper reviews basic sedimentary processes of this epicontinental shelf region and discusses certain potential geologic hazards related to these processes: thermogenic gas seepage, biogenic gas saturation of sediment and cratering, sediment liquefaction, ice gouging, current scouring, storm sand deposition, and mobile bedform movement (Fig. 4). These geologic hazards may pose problems for the future development of offshore resources in Norton Basin.

SEDIMENTARY PROCESSES

YUKON DELTA PROCESSES

The Yukon River drains an area a little less than 900,000 km^2, providing a water discharge of approximately 6000 m^3 per second and a sediment load of 70-90 million metric tons per year (Dupré and Thompson, 1979; Cacchione and Drake, 1979a). The sediment load, almost 90 % of all sediment entering the Bering Sea, is composed mainly of very fine sand and coarse silt with very little clay.

The Yukon delta plain, like many deltas described, is fringed by prograding tidal flats and distributary mouth bars. The delta front and prodelta are offset from the prograding shoreline by a broad platform (referred to as a subice platform) 30 km at its widest reach. This platform appears to be related to the presence of shorefast ice that fringes the delta for half the year. The term delta front describes the relatively steep margin of the offshore delta environment characterized by rapid deposition of sediment in water 2 to 10 m deep. The prodelta, an area of extremely gentle slopes, marks the distal edge of the deltaic sediments extending as far as 100 km offshore.

Processes on the Yukon Delta and offshore operate under seasonal regimens (Dupré and Thompson, 1979). The ice-dominated regimen begins with freeze-up in late October or November. Shorefast ice extends 10 to 40 km offshore where it is terminated by a series of pressure ridges and shear zones formed by the interaction of shorefast ice with the highly mobile seasonal pack ice.

River breakup, typically in May, marks the beginning of the river dominated regimen. Once the shorefast ice melts or drifts offshore, sedimentation is dominated by normal deltaic processes under the influence of the high discharge of the Yukon River.

Increasingly frequent southwest winds and waves associated with major storms during late summer mark the beginning of the storm-dominated regimen. High wave energy and decreasing sediment discharge from the Yukon cause considerable coastal erosion and reworking of deltaic deposits.

COASTAL STORM SURGE

In November 1974, a severe storm moved from southwest to northeast across the Bering Sea. Peak winds were 111 km per hour from the south, and nearshore waves were reported to be 3 to 4 m in height (Fathauer, 1975). Coastal flooding extended from Kotzebue Sound (north of Bering Strait) to just north

of the Aleutian Islands (Fathauer, 1975). The maximum sea level setup, measured by the elevation of debris lines along the coast of Norton Sound, ranged from 3 to 5 m above mean sea level (Sallenger et al., 1978). During this storm, extensive inland flooding occurred and erosion of 2 to 5 m high coastal bluffs took place near Nome. Irregular landward erosion, as much as 18 m, occurred west of Nome, where bluffs are 3 to 5 m high. East of Nome, where bluffs are 1.5 to 2 m high, landward erosion was as much as 45 m. Water level in the Norton Sound area reached its peak on 12 November, when as much as 2 m of water was standing in the village of Unalakleet and the static high-water line at Nome was 4 m above mean low low-water.

STORM CURRENTS

The transport of sediment in Norton Sound and Norton Basin can be described in terms of distinct quiescent and storm regimes (Cacchione and Drake, 1979a). The quiescent regime is characterized by generally low levels of sediment transport caused mainly by tidal currents. Fine silt and clay move as "wash load," and bedload transport is negligible except in shallow areas where surface waves become dominant. Current speeds in this regime are no greater than 30 cm/sec.

Although calm-weather conditions prevail for about 90% of the year in the northern Bering Sea, less than 50% of the sediment transport takes place under these conditions (Cacchione and Drake, 1979a). Norton Sound is commonly exposed to strong southerly and southwesterly winds generated by low-pressure weather systems in September, October and November. A two-day storm in September 1977 transported sediment equal to the transport that would occur during four months of quiescent conditions. Current speeds were as much as 70 cm/sec during this storm.

Graded storm-sand layers, to 20 cm thick (Nelson, 1977), occur in sea-floor strata of the northern Bering Sea, widespread evidence of major storm-surge events. The effects of storm surge are intensified by two factors: 1) extremely shallow water depth (less than 20 m), and 2) strong bottom return currents that may move large amounts of sediment northward to the Chukchi Sea. The thickness of Holocene sediment in Norton Sound, relative to Holocene sediment input from the Yukon River indicates that significant amounts of sediment have been resuspended and transported out of Norton Sound (Nelson and Creager, 1977). About 10% of the Yukon River input into Norton Sound may be carried as suspended sediment through the Bering Strait into the Chukchi Sea under nonstorm conditions (Cacchione and Drake, 1979a). As much as 40% of Holocene sediment discharged from the Yukon River appears to be missing from Norton Sound. This difference of 30% may be material that has been resuspended and transported during storms (Cacchione and Drake 1979a).

Storm currents not only resuspend and transport massive amounts of suspended sediment, but also appear to move large amounts of sand in bedload transport for considerable distances offshore. Graded storm-sand layers are extensive throughout southern Norton Sound; their thickening toward the Yukon subdelta, the apparent source region, suggests massive movement of bedload sediment away from the delta toward the adjacent offshore region during storms (Nelson, 1977).

WAVE EFFECTS

Waves and wave-induced currents are the dominant sedimentological agents on the inner shelf of northwestern Norton Sound and in the approaches to Bering Strait (Hunter and Thor, 1979). Sedimentary features common to both areas include sand and gravel patches and ribbons, wave ripples, sand waves, and ice gouges (Hunter and Thor, 1979).

Wave ripples with spacings to 2 m are common in both the Port Clarence and Nome areas in zones where sediment is well sorted and grain size ranges from coarse sand to pebbly gravel. Ripples in the Port Clarence area trend northwest-southeast and can be explained as the result of storm waves from the southwest Bering Sea. Trends of ripples in the Nome area indicate dominant wave activity from south to southwest.

Ribbons of sand and gravel are well developed near the entrance to Port Clarence. These bedforms may be produced by wave action or by wave-induced net water motion in the direction of wave propagation.

A rich assemblage of depositional and erosional features, both wave-formed and current-formed, occupy the floor in shallow water close to the southern shore of Seward Peninsula. Wave-formed features are more common; some of the current-formed features imply considerable sediment transport by strong bottom tidal currents.

Only the broad patterns of wave and current movement in southwestern Norton Sound are known. The major wave trains originate in the southern Bering Sea: waves move northward and refract clockwise around protruding Yukon shoals. Smaller waves with shorter periods are generated by northeasterly winds and move southwestward.

LIQUEFACTION

The Yukon River sediment that covers most of the bottom of Norton Sound (McManus et al., 1977) is primarily silt with considerable amounts of very fine sand in some areas and a generally minor content of clay-size material. The sediment thickness is generally less than 3 m, except near the Yukon Delta, where accumulations are as thick as 10 m (Olsen et al., 1979). The material is generally dense; there are zones of relatively loose sediment (material of low density) in gas-charged areas. In the delta areas sampled by

6-m vibracores, relatively loose zones of sediment were observed above and between dense layers.

Fresh-water peaty mud beneath Yukon marine silt is somewhat over-consolidated and contains substantial amounts of organic carbon and gas. The presence of gas indicates that the pore pressures in the peaty muds may be high. If it is, the strength of the material could be low despite its highly consolidated state.

The dominantly coarse-silt to fine-sand-size texture of the material, occurrence of loose sediment zones, and theoretical calculations utilizing GEOPROBE cyclic wave loading data (Olsen et al., 1979; Clukey et al., 1980) indicate that Yukon prodelta sediment in southwestern Norton Sound is susceptible to liquefaction. Potential liquefaction of the prodelta deposits is attributable to cyclic loading resulting from exposure of the Yukon prodelta to large storm waves from the southwest. Water depths are sufficiently shallow that much of the wave generated surface energy is imparted to the bottom sediment, possibly resulting in liquefaction of the upper 1-2 m of sediment during extreme storm surge events (Clukey et al., 1980). This liquefaction potential of prodelta sediment influences storm-sand transport, formation of sediment depressions, and gas cratering.

ICE SCOUR

Ice on the Bering shelf scours and gouges surficial sediment of the sea floor (Fig. 5). The annual ice cover in this subarctic setting is generally thin (less than 2 m); thick ice capable of gouging forms where pack ice collides with and piles up against stationary shorefast ice developing numerous pressure ridges (Thor and Nelson, this volume). A wide well-developed shear zone forms in southwest Norton Sound as ice moving southward from the northeast Bering Sea and westward along southern Norton Sound converges in the shallow water of the Yukon prodelta. Consequently, numerous

zones of pressure ridges are formed. This region at 10- to 20-m water depth has the maximum ice-gouge density. Gouges are found in water to 30 m deep, and furrows are as much as 1 m deep. Ice-gouging affects the sea floor under shorefast areas only minimally, or not at all (Thor and Nelson, 1980).

CURRENT SCOUR DEPRESSIONS

Zones of large flat-floored depressions in Norton Sound occur mainly in two areas: west of the Yukon prodelta and 50 km southeast of Nome, on the flank of a broad shallow trough (Fig. 6) (Larsen et al., 1979). These features range from individual more or less elliptical depressions 10 to 30 m in diameter to large areas with irregular margins, 80 to 150 m in diameter. The depressions are 60 to 80 cm deep (Larsen et al., 1980).

Bottom current speeds in depression areas are 20 to 30 cm per second under nonstorm conditions and were measured at 70 cm per second during a typical autumn storm (Cacchione and Drake, 1979a). Both zones of depressions are on flanks of gently sloping shoals, where strong tidal or geostrophic currents shear against the slopes. Small-scale ripple bedforms are associated with depression areas and mean grain size ranges from 4 phi to 4.5 phi (0.063 mm to 0.044 mm). Depressions in the Yukon delta area are associated with extensive ice gouging. The gouge furrows commonly expand into large shallow depressions (Larsen et al., 1979 and Thor and Nelson, this volume).

Experiments in flumes containing fine sand and silt have shown that currents flowing over an obstruction will scour material immediately downcurrent from the obstruction (Young and Southard, 1978). The large scour depressions observed in Norton Sound may be a characteristic erosional bedform developed during storms when strong currents and high wave energy are focused on silt-covered slopes where local topographic disruptions set off flow separation and downcurrent scour.

SANDWAVE DYNAMICS

Strong geostrophic currents prevail throughout much of the northern Bering Sea, particularly where westward land projections interject into the northward flow, as in the eastern Bering Strait area (Flemming and Heggarty, 1966; Coachman et al., 1976). In such regions large bedforms develop and migrate, forming an unstable sea floor (Nelson et al., 1978b). These large bedforms include large-scale sand waves 1 to 2 m high with wavelengths to 200 m, and small-scale sand waves 0.5-1 m high with wavelengths of 10 m. They occupy the crests and some flanks of a series of linear sand ridges 2 to 5 km wide and as much as 20 km long between Port Clarence and King Island.

Sand wave movement and bedload transport take place during calm weather (Nelson et al., 1978b), but maximum change apparently occurs when severe southwesterly storms generate sea level set-up in the eastern Bering Sea that enhances northerly currents. In contrast, strong north winds from the Arctic reduce the strength of the northerly currents and thereby arrest bedform migration.

SEDIMENT GAS CHARGING

The distribution of acoustic anomalies suggests that almost 7000 km^2 of sea floor in Norton Sound and Chirikov Basin is underlain by sediment containing gas sufficient (biogenic and/or thermogenic) to affect sound transmission through these zones (Holmes, 1979a). Core-penetration rates (Nelson et al., 1978c and Kvenvolden et al., 1979a) and sediment samples from 2- to 6-m vibracores confirm gas saturation of near-surface sediment at several locations characterized by acoustic anomalies. The isotopic compositions of methane at four of the sites range from -69 to -80°/oo ($\delta^{13}C_{PDB}$) (Kvenvolden et al., 1978, 1979b). This range of values clearly indicates that the methane is formed by microbial processes, possibly

operating on near-surface Pleistocene peat deposits that underlie Holocene deposits throughout the northern Bering Sea.

At one site in Norton Sound, near-surface sediment is apparently charged with CO_2 actively seeping from the sea floor accompanied by less than one percent hydrocarbon gases (Kvenvolden et al., 1979a). Methane in this gas mixture has an isotopic composition of -36°/oo, a value suggesting that it is derived mainly from thermal processes, probably operating at depth in Norton Basin (Kvenvolden et al., 1979a). Geophysical evidence indicates that the hydrocarbon gases migrate into the near-surface sediments along a fault zone (Nelson et al., 1978c). Subbottom reflector terminations on continuous seismic profiles near the fault zone outline a large zone of anomalous acoustic responses about 9 km in diameter and at a 100-m depth caused by a thick subsurface accumulation of gas. Gas geochemistry and extensive voids due to gas expansion in vibracores suggest a high degree of gas saturation at the seep site (Kvenvolden et al., 1979b).

BIOGENIC GAS CRATERING

Small circular pits on the sea floor are found over a 20,000-km^2 area of central and eastern Norton Sound (Fig. 7). The craters in the northern Bering Sea are young features, as shown by their presence within modern ice-gouge grooves and by the fact that relict buried craters have not been observed in seismic profiles (Nelson et al., 1979b). These craters range from 1 to 10 m in diameter, averaging 2 m, and are probably less than 0.5 m deep. They are associated with numerous acoustic anomalies observed on seismic profiles and with subsurface Pleistocene peaty mud that commonly is saturated with biogenic methane (Holmes 1979b; Kvenvolden, 1979c; Nelson et al., 1979). The extensive reflector-termination anomalies and peat with a high gas content in east-central Norton Sound suggest that gas-charged sediment may be the cause of crater formation.

Two basic mechanisms for gas venting can be proposed. The first is that continuous local degassing may maintain craters as active gas vents on the sea floor. The second and more likely mechanism is that gas is intermittently vented, particularly during severe storms when near-surface sediment may liquefy.

The occurrence of surface craters in overlying marine sediment and the presence of high quantities of methane trapped beneath cohesive marine mud in Norton Sound suggest that gas venting may be episodic in this lithologic setting. Absence of craters in the noncohesive near-surface fine to medium sand and gravel of Chirikov Basin indicates that gas probably diffuses gradually through this more porous sediment that overlies the peaty mud there. Further evidence for intermittent venting of gas is the broad, shallow shape of the craters, unlike the deep, conical, actively bubbling vents of the thermogenic seep. Lack of methane in bottom water also suggests that the craters are not continually active vents.

POTENTIAL GEOLOGIC HAZARDS

THERMOGENIC GAS CAP

The extent of active gas seepage into the water column and gas saturation in near-surface sediment above a thick sediment section with acoustic anomalies suggests a possible hazard for future drilling activity in the thermogenic gas seep area south of Nome. Artificial structures penetrating the large gas accumulation at 100 m or intersecting associated faults that cut the gas-charged sediment may provide direct avenues for uncontrolled gas migration to the sea floor.

SHALLOW GAS POCKETS

Gas-charged sediment creates potentially unstable surficial-sediment conditions in Norton Sound. Approximately 7,000 km^2 of Norton Sound is

underlain by acoustic anomalies with potential shallow gas pockets everywhere except under the Yukon prodelta (Holmes, 1979a; Nelson et al., 1979a). Pipelines built across areas of these potential gas pockets may be damaged by stress induced from the unequal bearing strength of gas-charged and normal sediment, particulary if the near-surface sediment is undergoing liquefaction caused by cyclic loading of storm waves. The gas saturation and lateral and subsurface extent of any shallow gas pockets will have to be detailed in any site investigations for platforms or pipelines.

GAS CRATERS

Gas craters cover a large area of north-central Norton Sound. During nonstorm conditions, near-surface gas in this area may be trapped by a 1- to 2-m thick layer of impermeable Holocene mud. We postulate that the gas escapes during periodic storms forming craters at the surface. The storm processes initiate rapid changes in pore-water pressures because of sea-level setup, seiches, erosional unloading of covering mud, and possible sediment liquefaction from cyclic wave loading (Clukey et al., 1980). Gas venting and sediment craters or depressions, which seem to form during peak storm periods, may be a potential hazard to offshore facilities because of rapid lateral changes in bearing strengths and sediment collapse that forms the craters. Sediment collapse may also expose pipelines to ice gouging hazards. During nonstorm conditions, the upper several meters of sediment at many locations has reduced shear strength because of the near-surface gas saturation and presence of peat layers. Siting of artificial structures will require extensive local testing of the substrate to determine the extent and activity of gas cratering at a given site.

LIQUEFACTION

The assessment and prediction of sea-floor stability is affected by the potential of a sedimentary deposit to liquefy under cyclic loading and behave as a viscous fluid. The liquefaction potential of Norton Sound sediment is great in central Norton Sound and in the vicinity of the western Yukon prodelta (Clukey et al., 1980; Olsen et al., 1979). Possible causes of liquefaction include upward migration of gas from thermogenic and biogenic sources, earthquakes, and ocean waves. Bottom features that may be caused in part by liquefaction include scour depressions and abundant sediment cratering where Yukon sediment is thin.

Loss of substrate support by sediment liquefaction is a problem that must be faced in the construction of pipelines, drilling platforms, and other types of structures resting on the sea floor. Full assessment of this problem requires extensive studies of in situ pore pressure, gas saturation, and wave cyclic loading during storms.

ICE SCOUR

The maximum intensity of ice-gouging occurs in central Norton Sound at 10- to 15-m depths in an area surrounding the Yukon Delta. The remaining area of Norton Sound, where depths are less than 10 m or more than 20 m, has a low density of gouging, or none at all. Special studies of nearshore areas off Nome and Port Clarence were made when they became potential centers for commercial development and activity. Offshore Nome, the focal point for logistics in the northern Bering Sea because it is an area of ice divergence, only a few gouges were found in water more than 8 m deep (Thor and Nelson, this volume). Several gouges were found at the northern end of Port Clarence spit and inside the tidal inlet, but again none occurred in water less than 8 m deep.

Ice gouging presents some design problems and potential hazards to installations in or on the sea floor. Pipelines and cables should be buried at a depth that allows for maximum ice gouging of 1 m, plus a safety factor for combined effects with current scour around the western Yukon prodelta front or gas cratering in central Norton Sound.

CURRENT SCOUR DEPRESSIONS

The highest density of scour depressions in Norton Sound is in two areas: (1) west and northwest of the Yukon delta and (2) southeast of Nome (Fig. 6). In areas of high density, artificial structures that disrupt current flow may cause extensive erosion of Yukon-derived silt or very fine-grained sand and create potentially hazardous undercutting of the structures. Even buried structures such as pipelines may be subject to scour because strong currents can greatly broaden and deepen naturally occurring ice gouges, thus exposing the structures. The severity of scour depressions is greatest where they occur with ice-gouging in the Yukon delta areas. Replicate surveys have shown that scour depressions recur annually. Full assessment of this geologic hazard requires long-term current monitoring in specific localities of scour to predict current intensity and periodicity, especially during severe storms, when measured current speeds have increased more than 100% under moderate storm conditions (Cacchione and Drake, 1979b).

MOBILE BEDFORMS

Large migrating bedforms form an unstable sea floor in the area west of Port Clarence. Actual rates of bedform movement are not known, but development and decay of sand waves up to 2 m in height has been observed during a one-year period. Pipelines could be subject to damaging stress if free spans developed where the structure crossed such areas of migrating 2-m high sand waves.

Studies made to this time indicate that potential for the most extreme scour exists in regions of sand ribbons and gravel plus shell pavement within the strait. Sea floor relief changes most rapidly in the Port Clarence sand-wave area, where the scour in sand-wave troughs may reach depths of 2 m. Replicate surveys have shown that such scour may occur each year in some areas of the Port Clarence sand wave field. Long-term monitoring of currents and bedform movement is particularly important in determining actual rates of change in this area, the only large natural harbor on the Alaskan coast north of the Aleutians.

COASTAL AND OFFSHORE STORM SURGE HAZARDS

The northern Bering Sea has a known history of major storm surges accompanied by widespread changes in sea-floor sedimentation (Cacchione and Drake, 1979a; Fathauer, 1975; Nelson, 1977); these changes complicate maintenance of sea-floor installations and mass transport of pollutants. The November 1974 storm is the most intense measured in historic time; storms of 1913 and 1946 caused considerable damage (Fathauer, 1975). Severe storms, such as the November 1974 storm, have caused extensive flooding along the Norton Sound coast between Nome and Unalakleet and on the St. Lawrence Island coast (Sallenger et al., 1978). At Nome, storm surge and waves overtopped a sea wall, causing damage reported at nearly 15 million dollars (Fathauer, 1975). Storm surge periodicity and intensity will have to be carefully studied in planning where and whether pipelines should come ashore in this area.

Rapid sedimentation of thick storm sand layers (15-20 cm) is a problem in the Yukon delta area. Pipelines, offshore facilities, and other structures impeding the erosion, transport, and redeposition of sediment in southern Norton Sound will require careful design. Accurate monitoring of the storm

surge process will require long-term deployment of an array of current meters and tide gauges in the northern Bering Sea.

ACKNOWLEDGMENTS

We thank Keith Kvenvolden for information concerning gas in Norton Sound sediment, David Cacchione and David Drake for data on current and sediment movement, William Dupré for information on deltaic processes, Abby Sallenger and Ralph Hunter for data concerning inner shelf processes, and Harold Olsen and Edward Clukey for data on geotechnical properties. We are grateful for the assistance of Phyllis Swenson, Marybeth Gerin, and Joan Esterle in drafting and preparation of figures and for the assistance of Helen Ogle in preparing the manuscript. David Drake and David Hopkins made helpful review comments.

The cruises were supported jointly by the U.S. Geological Survey and the Bureau of Land Management through interagency agreement with the National Oceanic and Atmospheric Administration under which a multiyear program responding to needs of petroleum development of the Alaska continental shelf is managed by the Outer Continental Shelf Environmental Assessment Program Office.

REFERENCES

Cacchione, D.A., and Drake, D.E., 1979a, Sediment transport in Norton Sound, Alaska: U.S. Geological Survey Open-File Report 79-1555.

Cacchione, D.A., and Drake, D.E., 1979b, Bottom shear stress generated by waves and currents in the northern Bering Sea, in: Abstracts volume, International Association of Sedimentologists, International meeting on Holocene marine sedimentation in the North Sea Basin, Paper no. 71.

Clukey, E.C., Cacchione, D.A., and Olsen, H.W., 1980, Liquefaction potential of the Yukon prodelta: Proceedings of the Offshore Technology Conference, Houston, Texas, 1980, Paper no. 3773, in press.

Coachman, L.K., Aagaard, K., and Tripp, R.B., 1976, Bering Strait: The Regional Physical Oceanography, Seattle, Washington University Press, 186 p.

Dupré, W.R., and Thompson, R., 1979, The Yukon delta: A model for deltaic sedimentation in an ice-dominated environment: Proceedings Offshore Technology Conference, Paper no. 3434, p. 657-661.

Fathauer, T.F., 1975, The great Bering Sea storms of 9-19 November, 1974: Weatherwise Magazine, American Meteorological Society, v. 28, p. 76-83.

Flemming, R.H., and Heggarty, D., 1966, Oceanography of the southeastern Chukchi Sea, in: Wilimovsky, N.J., and Wolf, J.M., eds., Environment of Cape Thompson Region, Alaska: U.S. Atomic Energy Commission, p. 679-694.

Holmes, M.L., 1979a, Distribution of gas-charged sediment in Norton Basin, northern Bering Sea, in: Abstracts volume, International Association of Sedimentologists, International meeting on Holocene marine sedimentation in the North Sea Basin, Paper no. 78.

Holmes, M.L., 1979b, Distribution of gas-charged sediment in Norton Sound and Chirikov Basin: in Environmental Assessment of the Alaskan Continental Shelf, Annual Report of Principal Investigators for the year ending March 1979, Environmental Research Laboratory, Boulder, Colorado, NOAA, U.S. Dept. of Commerce (in press).

Hopkins, D.M., Nelson, C.H., Perry, R.B., and Alpha, T.R., 1976, Physiographic subdivisions of the Chirikov Basin, northern Bering Sea: U.S. Geological Survey Professional Paper 759-B, 7 p.

Hunter, R., and Thor, D.R., 1979, Depositional and erosional features of the northeastern Bering Sea inner shelf, in: Abstracts volume, International Association of Sedimentologists, International meeting on Holocene marine sedimentation in the North Sea Basin, Paper no. 80.

Kvenvolden, K.A., Rapp, J.B., and Nelson, Hans, 1978, Low molecular weight hydrocarbons in sediments from Norton Sound (abs.): American Association Petroleum Geologists Bulletin., v. 62, p. 534.

_____, Weliky, K., and Nelson, Hans, 1979a, Submarine seep of carbon dioxide in Norton Sound, Alaska: Science, v. 205, p. 1264-1266.

_____, Redden, G.D., Nelson, C.H., 1979b, Gases in near-surface sediment of the northern Bering Sea, in: Abstracts volume, International Association of Sedimentologists, International meeting on Holocene marine sedimentation in the North Sea Basin, Paper no. 82.

_____, Nelson, Hans, Thor, D.R., Larsen, M.C., Redden, G.D., Rapp, J.B., and Des Marais, D.J., 1979c, Biogenic and thermogenic gas in gas-charged sediment of Norton Sound, Alaska: Proceedings Offshore Technical Conference, Paper No. 3412.

Larsen, M.C., Nelson, Hans, and Thor, D.R., 1979, Continuous seismic reflection data, S9-78-BS cruise, northern Bering Sea: U.S. Geological Survey Open File Report 79-1673, 7 p.

_____, _____, _____, 1979, Geologic implications and potential hazards of scour depressions on Bering shelf, Alaska: Environmental Geology, v. 3, p. 39-47.

McManus, D.A., Kolla, V., Hopkins, D.M., and Nelson, C.H., 1977, Distribution of bottom sediments on the continental shelf, northern Bering Sea: U.S. Geological Survey Professional Paper 759-C, 31 p.

_____, 1977, Storm surge effects, in: Environmental assessment of the Alaskan continental shelf, Annual Report of the Principal Investigators for the year ending March 1977, Environmental Research Laboratory, Boulder, Colorado, NOAA, U.S. Department of Commerce, v. 18, p. 111-119.

_____, and Hopkins, D.M., 1972, Sedimentary processes and distribution of particulate gold in the northern Beriang Sea: U.S. Geological Survey Professional Paper 689, 27 p.

_____, and Creager, J.S., 1977, Displacement of Yukon-derived sediment from Bering Sea to Chukchi Sea during the Holocene: Geology, v. 5, p. 141-146.

_____, Field, M.E., Cacchione, D.A., and Drake, D.E., 1978b, Activity of mobile bedforms on northeastern Bering shelf, in: Environmental Assessment of the Alaskan Continental Shelf, Annual Report of Principal Investigators for the year ending March 1978, Environmental Research Laboratory, Boulder, Colorado, NOAA, U.S. Dept. of Commerce, v.12 p. 291-307.

_____, Holmes, M.L., Thor, D.R., and Johnson, J.L., 1978a, Continuous Seismic reflection data, S5-76-BBS cruise, northern Bering Sea: U.S. Geological Survey Open File Report 78-609, 6 p.

_____, Kvenvolden, K.A., and Clukey, E.C., 1978c, Thermogenic gas in sediment of Norton Sound, Alaska, Proceedings of Offshore Technical Conference, 1978, Paper No. 3354, p. 1612-1633.

_____, Thor, D.R., Sandstrom, M.W., and Kvenvolden, K.A., (1980), Modern biogenic gas-generated craters (sea-floor "pockmarks") on the Bering shelf, Alaska. Geological Society of America Bulletin (in press).

Olsen, H.W., Clukey, E.C., and Nelson, C.H., 1979, Geotechnical characteristics of bottom sediments in the northern Bering Sea, in: Abstracts volume, International Association of Sedimentologists, International meeting on Holocene marine sedimentation in the North Sea Basin, Paper no. 91.

Sallenger, A.H., Dingler, J.R., and Hunter, R., 1978, Coastal processes and morphology of the Bering Sea coast of Alaska, in: Environmental Assessment of the Alaskan Continental Shelf, Annual Report of Principal Investigators for the year ending March 1978, Environmental Research Laboratory, Boulder, Colorado, NOAA, U.S. Dept. of Commerce, v. 12, p. 451-470.

Thor, D.R., and Nelson, Hans, 1978, Continuous seismic reflection data. S5-77-BS cruise, northern Bering Sea: U.S. Geological Survey Open File Report 78-608, 8 p.

_____, _____, and Williams, R.O., 1978, Environmental geologic studies in northern Bering Sea, in: Blean, K.M., ed., U.S. Geological Survey in Alaska, Accomplishments during 1977: U.S. Geological Survey Circular 772-B, p. B94-B95.

_____, _____, 1979, A summary of interacting surficial geologic processes and potential geologic hazards in the Norton Basin, northern Bering Sea: Proceedings Offshore Technical Conference, Paper No. 3400, p. 377-381.

_____, _____, (1980), Ice gouging on the subarctic Bering Shelf, in: Hood, D.W., ed., The Eastern Bering Sea Shelf: Its Oceanography and Resources.

Young, R.N., and Southard, J.B., 1978, Erosion of fine-grained marine sediments: Sea-floor and laboratory experiments: Geological Society of America Bulletin, v. 89, p. 663-672.

Figure Captions

Figure 1. Sampling station locations for U.S. Geological Survey research in northern Bering Sea between 1967 and 1978.

Figure 1a. Cross-hatched area of Figure 1, showing closely spaced sampling grid offshore Nome.

Figure 2. Geophysical trackline surveys for U.S. Geological Survey research in northern Bering Sea 1967-1978.

Figure 3. Generalized bathymetry of northern Bering Sea in 10-m contour intervals.

Figure 4. Potentially hazardous areas of northern Bering Sea (from Thor and Nelson, 1979).

Figure 5. Distribution and density of ice gouging, direction of movement pack ice, and limits of shorefast ice in northern Bering Sea (from Thor and Nelson, 1979).

Figure 6. Location of scour depressions, extensive scour and ripple zones, and strong bottom currents in Norton SOund, showing area of storm sand deposition (modified from Larsen et al., 1980).

Figure 7. Distribution and density of craters on sea floor of Norton Sound, showing isopachs of Holocene mud derived from the Yukon River and deposited since Holocene postglacial sea-level rise (from Thor and Nelson, 1979).

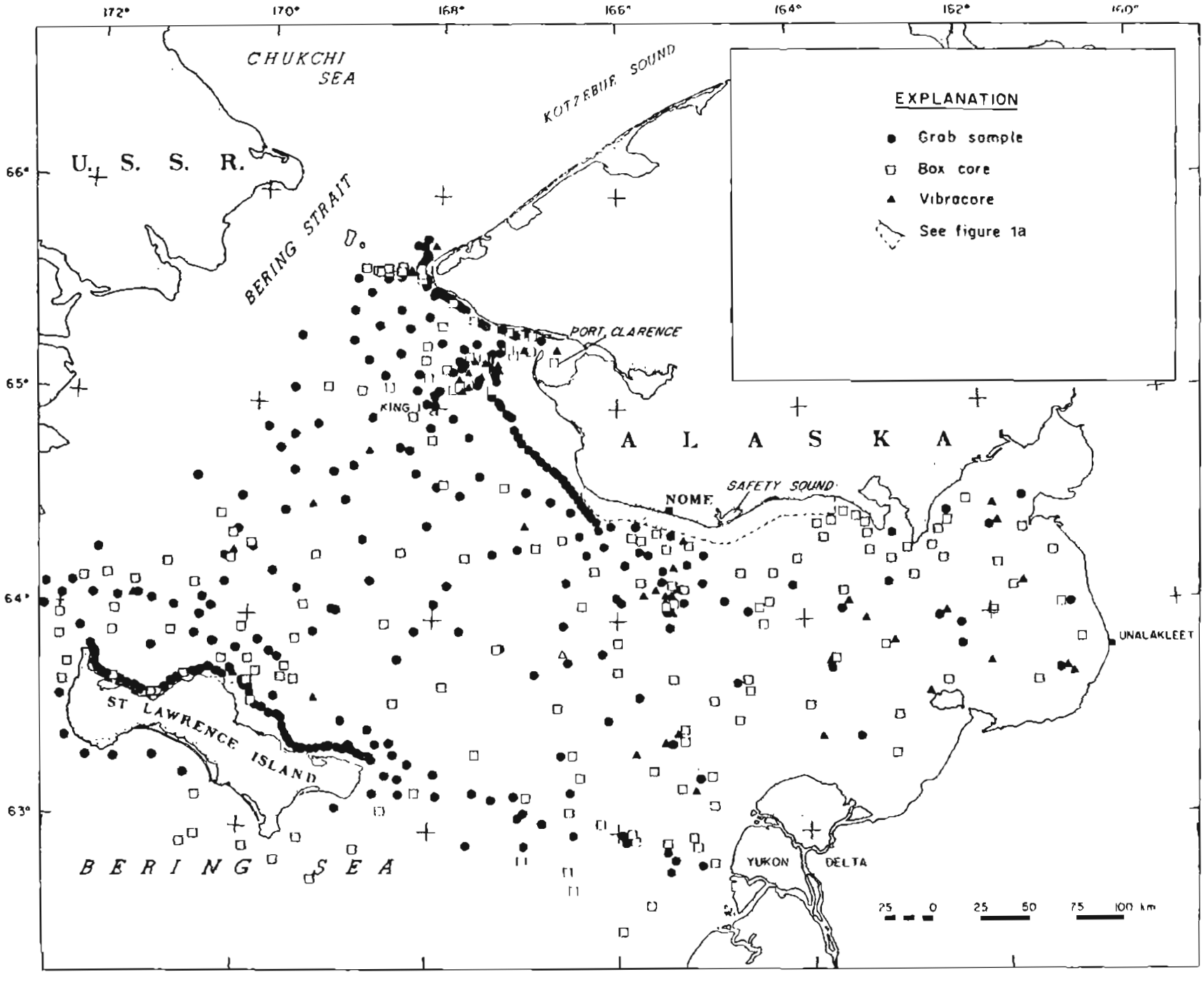
172°
170°
168°
166°
164°
162°
160°
66°
65°
64°
63°
CHUKCHI SEA
KOTZEBUE SOUND
U. S. S. R.
BERING STRAIT
PORT CLARENCE
KING
A L A S K A
NOME
SAFETY SOUND
UNALAKLEET
ST LAWRENCE ISLAND
BERING SEA
YUKON DELTA
EXPLANATION
Grab sample
Box core
Vibracore
See figure 1a
25 0 25 50 75 100 km

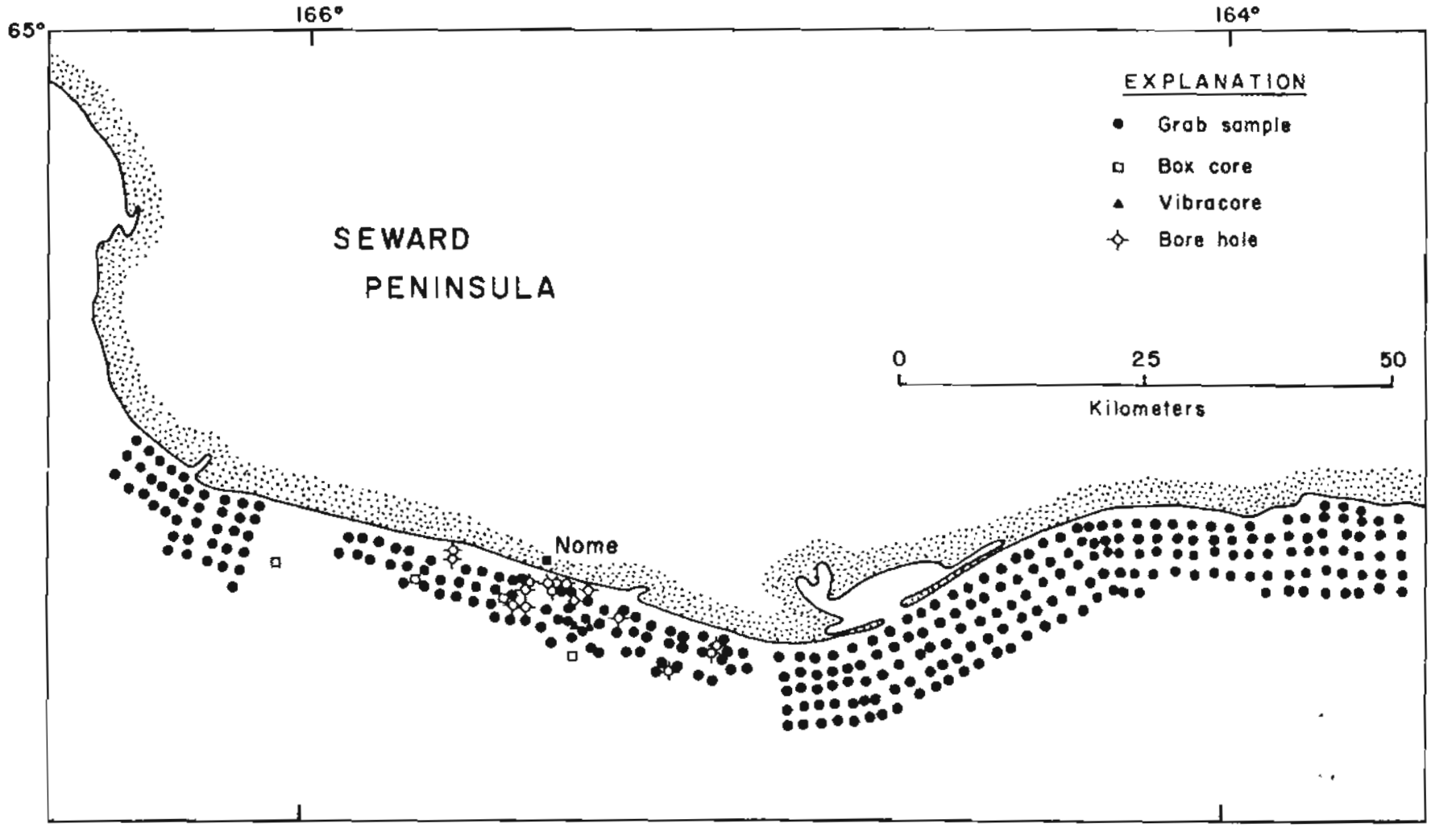
65°
166°
164°
EXPLANATION
Grab sample
Box core
Vibracore
Bore hole
SEWARD
PENINSULA
0
25
50
Kilometers
Nome

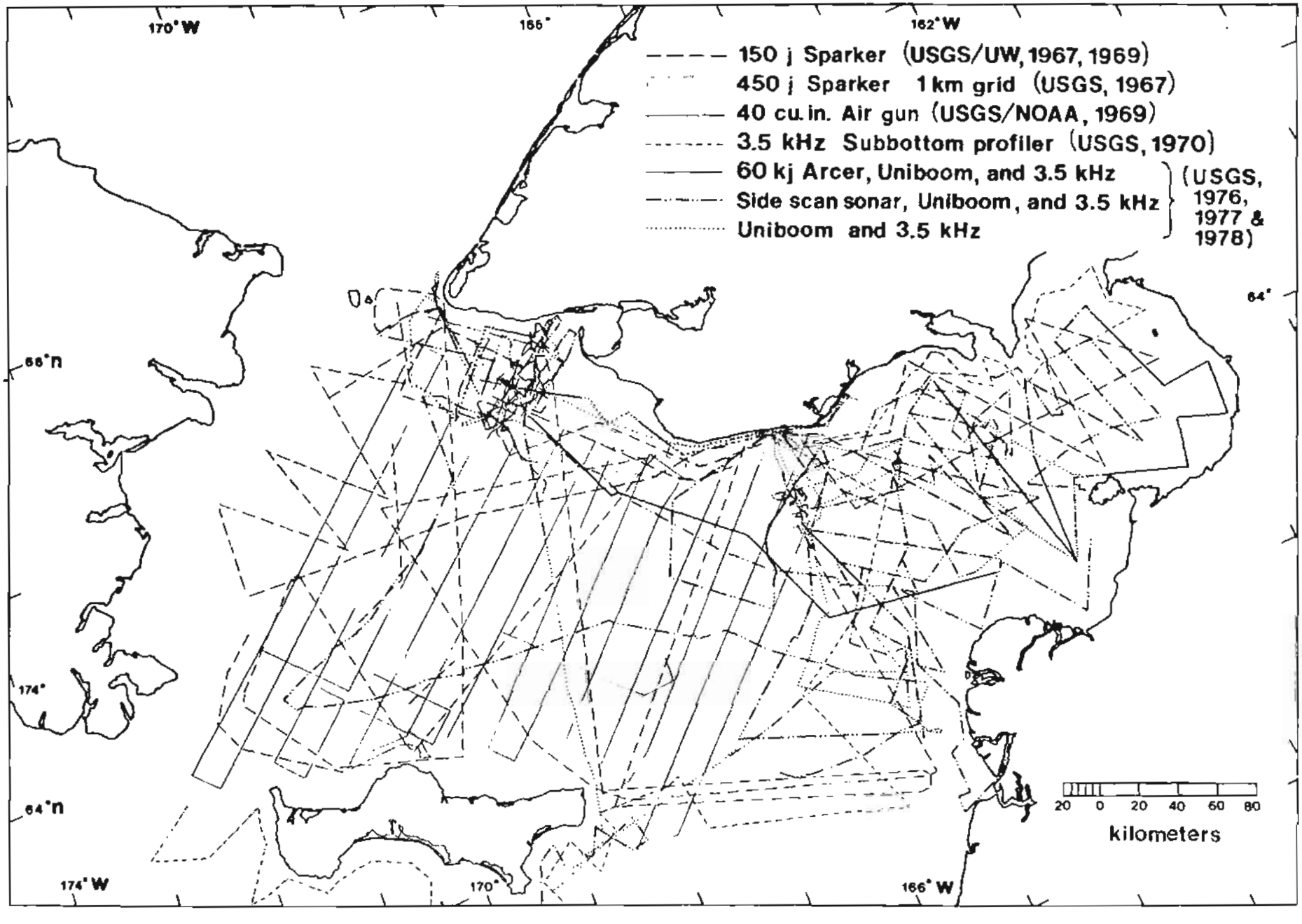
170°W
166°
162°W
150 j Sparker (USGS/UW, 1967, 1969)
450 j Sparker 1 km grid (USGS, 1967)
40 cu. in. Air gun (USGS/NOAA, 1969)
3.5 kHz Subbottom profiler (USGS, 1970)
60 kj Arcer, Uniboom, and 3.5 kHz
Side scan sonar, Uniboom, and 3.5 kHz
Uniboom and 3.5 kHz
(USGS, 1976, 1977 & 1978)
66°n
64°
174°
64°n
174°W
170°
166°W
20 0 20 40 60 80
kilometers

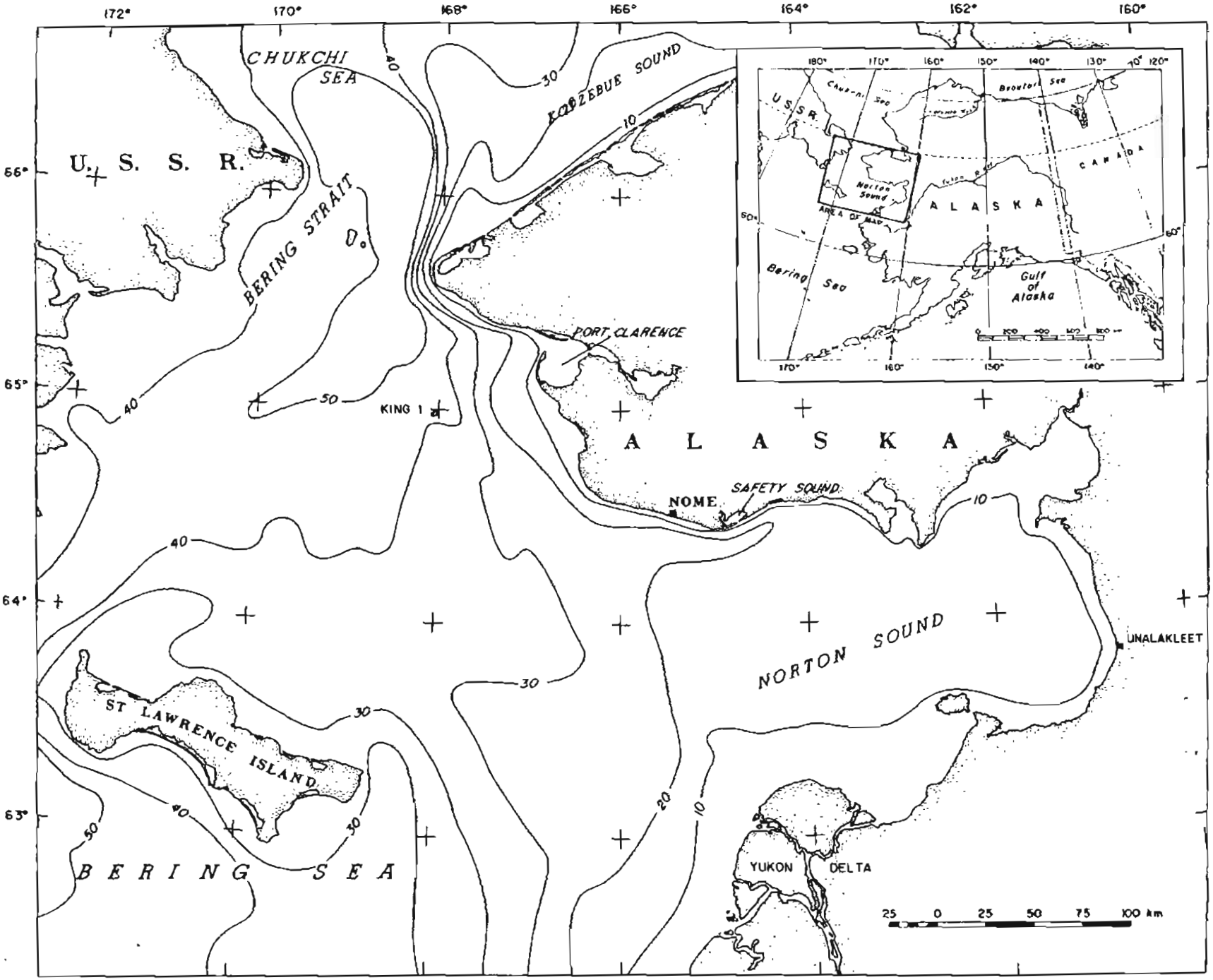
172°
170°
168°
166°
164°
162°
160°
66°
65°
64°
63°
CHUKCHI SEA
KOTZEBUE SOUND
U. S. S. R.
BERING STRAIT
PORT CLARENCE
KING I.
A L A S K A
NOME
SAFETY SOUND
ST LAWRENCE ISLAND
NORTON SOUND
UNALAKLEET
YUKON DELTA
B E R I N G S E A
40
30
10
50
20
25 0 25 50 75 100 km
Norton Sound
AREA OF MAP
Bering Sea
Gulf of Alaska
CANADA

Interplay of Physical and Biological Sedimentary Structures of the Bering Epicontinental Shelf

by

Hans Nelson
U.S. Geological Survey
Menlo Park, California 94025

Robert W. Rowland
U.S. Geological Survey
Reston, Virginia 22092

Sam W. Stoker
University of Alaska
Fairbanks, Alaska

Bradley R. Larsen
U.S. Geological Survey
Menlo Park, California 9405

ABSTRACT

Distinctive Holocene transgressive sand and post-transgressive mud with attendant physical and biological structures occur on the shallow (<60 m, shelf of the northern Bering Sea. Thin gravel lag layers, formed during the Holcene shoreline transgression, veneer exposed glacial moraines. Epifauna dominate these relict gravel areas and cause little disruption of physical structures. Some relict submerged beach ridges contain faint rippling that probably is caused by modern current reworking. Well-sorted medium sand on exposed shoal crests is reworked by the sand dollar and tellinid clam communities. Buried thin layers of transgressive beach sand and gravel retain rare original medium-scale cross-lamination and flat lamination that have been intensively bioturbated. A thin layer of an offshore fine-grained sand facies that was deposited by the Holocene transgression remains unburied by modern mud in central Chirikov Basin. Primarily because of ampeliscid amphipod bioturbation, this facies has no physical structures.

Post-transgressive silty mud from the Yukon River blankets the shallow (<20 m) areas of Norton Sound. In places the silty mud contains thin beds of shells and pebbles, and thin sand interbeds and lenses that exhibit ripples and small-scale flat and cross-lamination. These coarse-grained interbeds are interpreted to be storm layers formed by modern storm waves and storm surge currents. Physical sedimentary structures are well preserved only near the delta fringe; there, the frequency of physical reworking is highest, the potential for preservation by a high rate of deposition is greatest, and the inhibition of bioturbation by low salinity is most severe. At greater distances from shore, infaunal deposit-feeding bivalves, polychaete worms, and small amphipods cause progressively greater disruption of bedforms in prodelta mud. Almost all modern physical structures have been destroyed at water depths greater than 25 m. As a result the following sequence of storm deposits is characteristic of profiles extending away from the delta: thick (>5 cm) storm sand layers, thin storm sand layers, isolated and bioturbated sand lenses, faint bioturbated shell and pebble beds.

INTRODUCTION

Purpose

The northern Bering Sea region from St. Lawrence Island to Bering Strait Fig. 1) has continually strong bottom currents, an extremely rich benthic fauna, nd a wide variety of sediment substrates. These factors, coupled with shallow picontinental shelf depths that are affected by wave and tidal current activity, roduce a wide variety of physical and biological sedimentary structures. Our urpose is to map the distribution of these structures and to correlate the dis- ribution patterns with the controlling physical and biological factors. Such nalyses provide a model of factors controlling development of physical and bio- ogical structures on continental shelves in general and assist in specific aleoenvironmental reconstruction of ancient epicontinental shelf deposits.

Oceanographic Setting

Three water masses have been defined on the northern Bering shelf: Alaskan oastal Water, Bering Shelf Water, and Anadyr Water (Fig. 2, Coachman et al., 976). Alaskan Coastal Water, generated primarily from the Yukon and Kuskokwim ivers and other runoff (Fig. 2; Saur et al., 1954), has pronounced seasonal alinity changes. This is particularly true in southern Norton Sound, where reat changes in discharge from the Yukon River occur from summer to winter. efore June, salinities are close to 30 0/00 throughout southern Norton Sound. uring the summer and early fall salinities below 20 0/00 are common (Fig. 2; oodman et al., 1941; Sharma et al., 1974).

Typically, current speeds in the offshore part (>30 km from shore) of the laskan Coastal Water are 10 cm/s near the bottom and 20 cm/s near the surface, nd currents trend northward except for the counterclockwise gyre into Norton ound (Fig. 3). Nearshore surface and bottom water travels generally northward arallel to the Alaskan coast at typical speeds of 30-40 cm/s (Coachman and

Aagard, 1966; Fleming and Heggarty, 1966; Husby, 1969; 1971; McManus and Smyth, 1970; Coachman et al., 1976).

The maximum current speeds are found where the Alaskan coast protrudes westward and constricts water flow. At the smallest constriction, Bering Strait, bottom speeds reach 180 cm/s in water depths of 55 m (Fleming and Heggarty, 1966; Fig.). Currents in the other two water masses are generally slower, reaching a maximum of 50 cm/s in eastern Anadyr Strait and minimums of 5-15 cm/s in central Chirikov Basin (Fleming and Heggarty, 1966; Husby, 1971; McManus and others, 1977).

Changes in atmospheric pressure and wind velocity during storms can cause the current speed to fluctuate by as much as 100 percent over periods of a day or more (Coachman and Tripp, 1970) and can produce storm surges causing sea level set up of 4 m along the southern coast of Seward Peninsula (Fathauer, 1975).

Calculations based on linear wave theory suggest that the waves hindcasted for normal wind conditions can affect the bottom to water depths of 20 m (McManus et al., 1977). Wave reworking of bottom sediments may extend considerably deeper during intense storms. For example, the storm of November, 1974 generated waves 6-7 m high and may have produced water motion capable of affecting the bottom at depths exceeding any found in the northern Bering Sea (A. Sallenger, oral commun., 1977).

Geologic Setting

The entire northern Bering Sea floor is less than 60 m deep and generally flat, but it has distinctive topographic features in several locations (Fig. 1; Hopkins et al., 1976). The eastern margins of both Bering and Anadyr Straits exhibit relatively steep scarps. Southeast of Bering Strait and in central Shpanberg Strait, a series of linear ridges and depressions are found. Large linear shoals also occur off the northwestern and northeastern flanks of St. Lawrence Island. The shallowest area in northern Bering Sea is off the modern Yukon subdelta in southern Norton Sound.

The northern Bering epicontinental shelf is a mosaic of modern and relict surface sediments. The relict sediments formed in shallow water, at the strand, or in subaerial environments at times when sea level was lower than at present (Fig. 4). During these times continental glaciers pushed debris toward the center of Chirikov Basin, and valley glaciers deposited sediment several kilometers beyond the present shoreline of Seward Peninsula (Nelson and Hopkins, 1972). Shoreline regressions and transgressions, most recently during the rise of sea level since 18,000 BP, reworked the glacial moraines, leaving a lag gravel on the sea floor north and west of St. Lawrence Island and along the southern side of Seward Peninsula. Transgression of the shoreline across the Bering shelf blanketed the remainder of the Chirikov Basin with a relatively coarse-grained basal layer ranging from medium-grained sand to gravel with an overlying thin layer of fine-sand. Except in central Chirikov Basin, the transgressive deposits are only a few tens of centimeters thick and overlie Pleistocene glacial debris, alluvium, and freshwater mud and peat dated at 10,500 BP or older (Nelson and Hopkins, 1972; Nelson and Creager, 1977).

Holocene sandy silt, mainly originating from the Yukon River (called Yukon mud hereafter in the paper), has been deposited in Norton Sound. This sediment forms deposits tens of centimeters thick in parts of central Norton Sound and deposits several meters thick off the present subdelta and around the margins of Norton Sound (Nelson and Creager, 1977). Currents apparently have inhibited deposition of Holocene Yukon sand and silt over the older relict transgressive sand and gravel found in Chirikov Basin (McManus et al., 1974).

Biological Setting

The continental shelf of the northern Bering Sea is an area of rich macrobenthic standing stock (Neyman, 1961, Filatova and Barsanova, 1964; Kuznetzov, 1964; Rowland, 1972; Stoker, 1973), though it has a relatively low diversity in terms of major species (Stoker, 1973). While major faunal communities are as yet

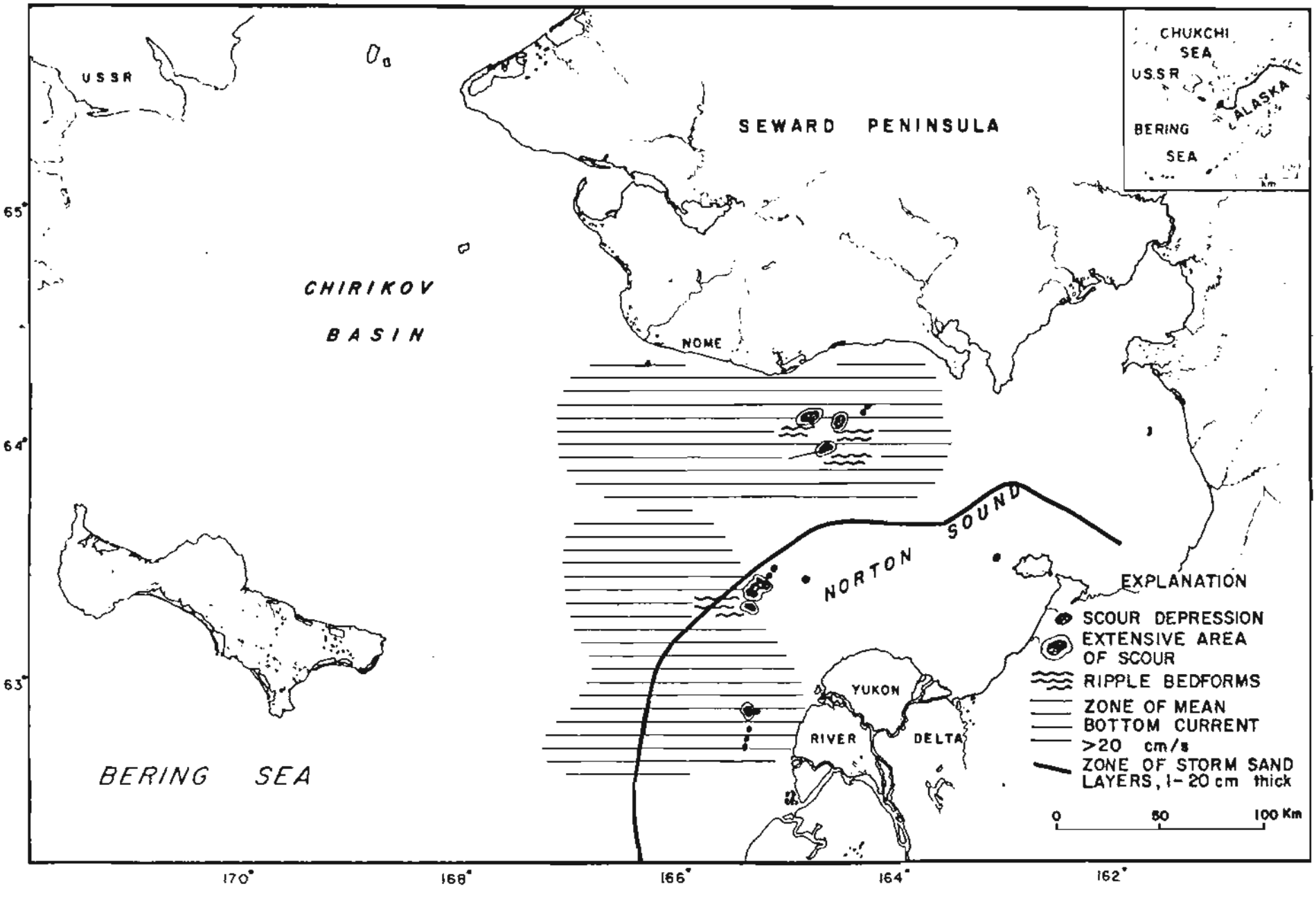
USSR
SEWARD PENINSULA
CHUKCHI SEA
U.S.S.R.
ALASKA
BERING SEA
CHIRIKOV BASIN
NOME
NORTON SOUND
YUKON RIVER DELTA
BERING SEA
65°
64°
63°
170°
168°
166°
164°
162°
EXPLANATION
SCOUR DEPRESSION
EXTENSIVE AREA OF SCOUR
RIPPLE BEDFORMS
ZONE OF MEAN BOTTOM CURRENT >20 cm/s
ZONE OF STORM SAND LAYERS, 1-20 cm thick
0
50
100 Km

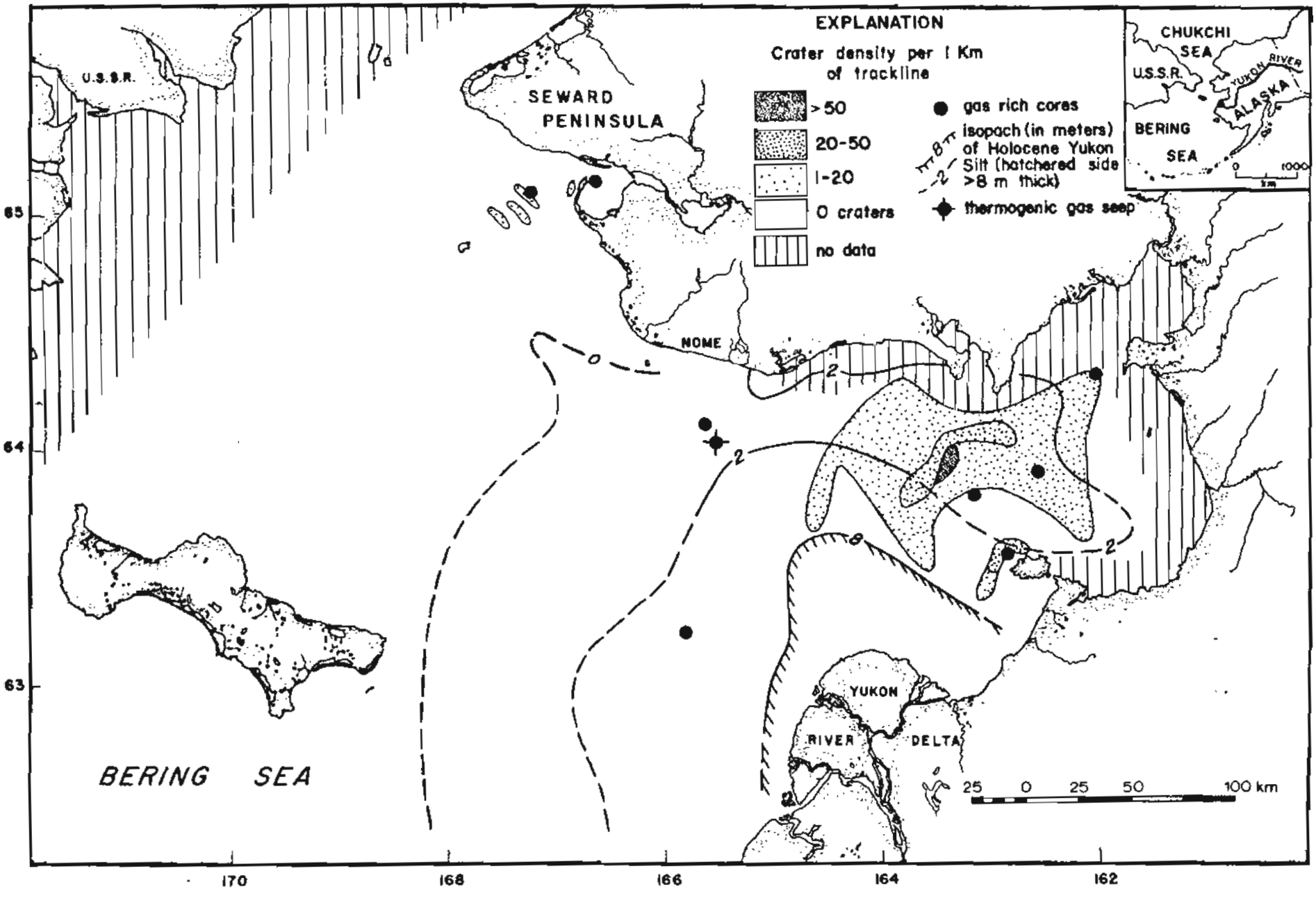
EXPLANATION
Crater density per 1 Km of trackline
>50
20-50
1-20
0 craters
no data
gas rich cores
isopach (in meters) of Holocene Yukon Silt (hatchered side >8 m thick)
thermogenic gas seep
U.S.S.R.
SEWARD PENINSULA
NOME
YUKON RIVER DELTA
BERING SEA
CHUKCHI SEA
U.S.S.R.
YUKON RIVER
ALASKA
BERING SEA
25 0 25 50 100 km
65
64
63
170
168
166
164
162

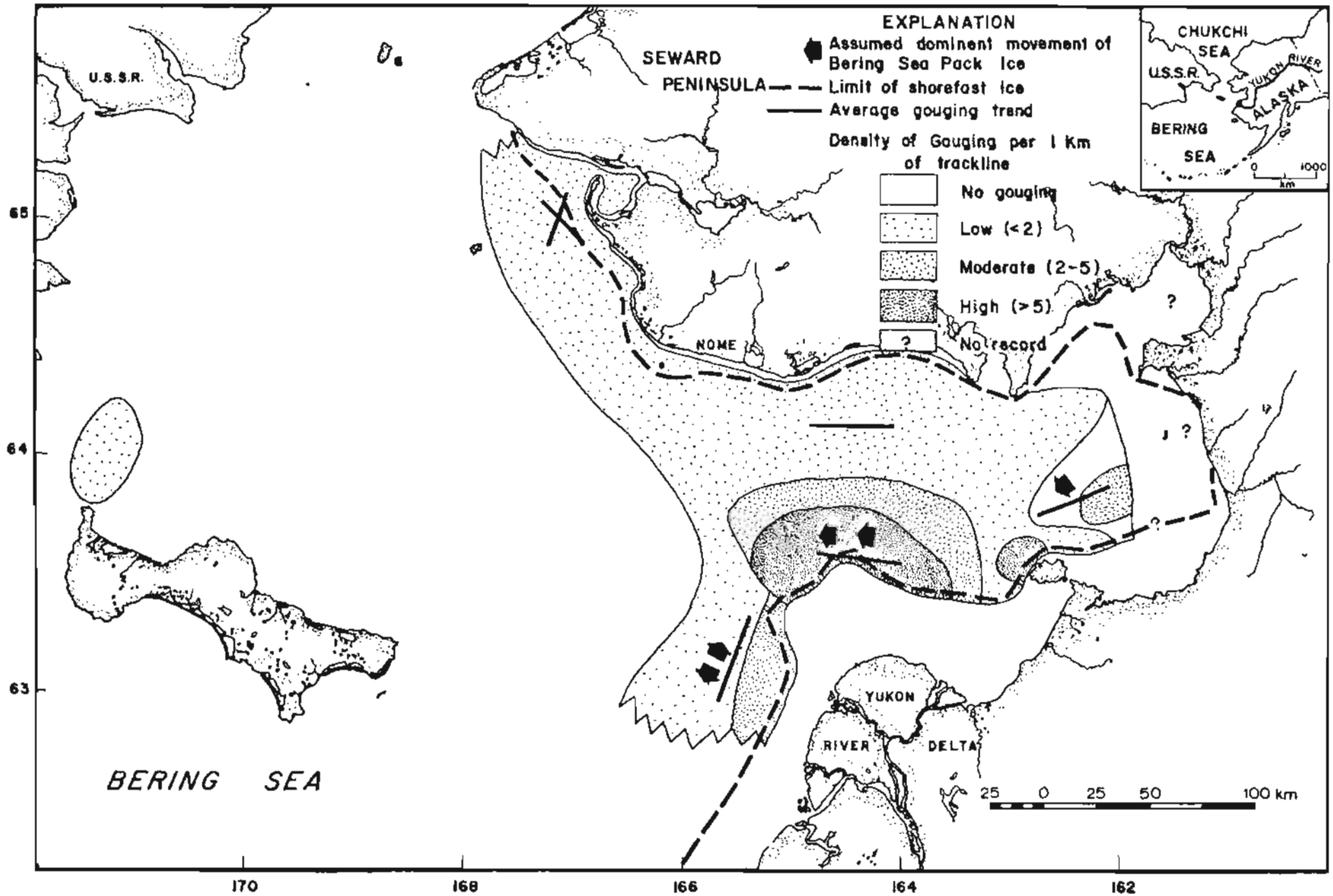
EXPLANATION
Assumed dominent movement of Bering Sea Pack Ice
Limit of shorefast ice
Average gouging trend
Density of Gouging per 1 Km of trackline
No gouging
Low (<2)
Moderate (2-5)
High (>5)
No record
SEWARD PENINSULA
U.S.S.R.
NOME
YUKON RIVER DELTA
BERING SEA
CHUKCHI SEA
U.S.S.R.
YUKON RIVER
ALASKA
BERING SEA
0 1000 km
25 0 25 50 100 km
65
64
63
170
168
166
164
162

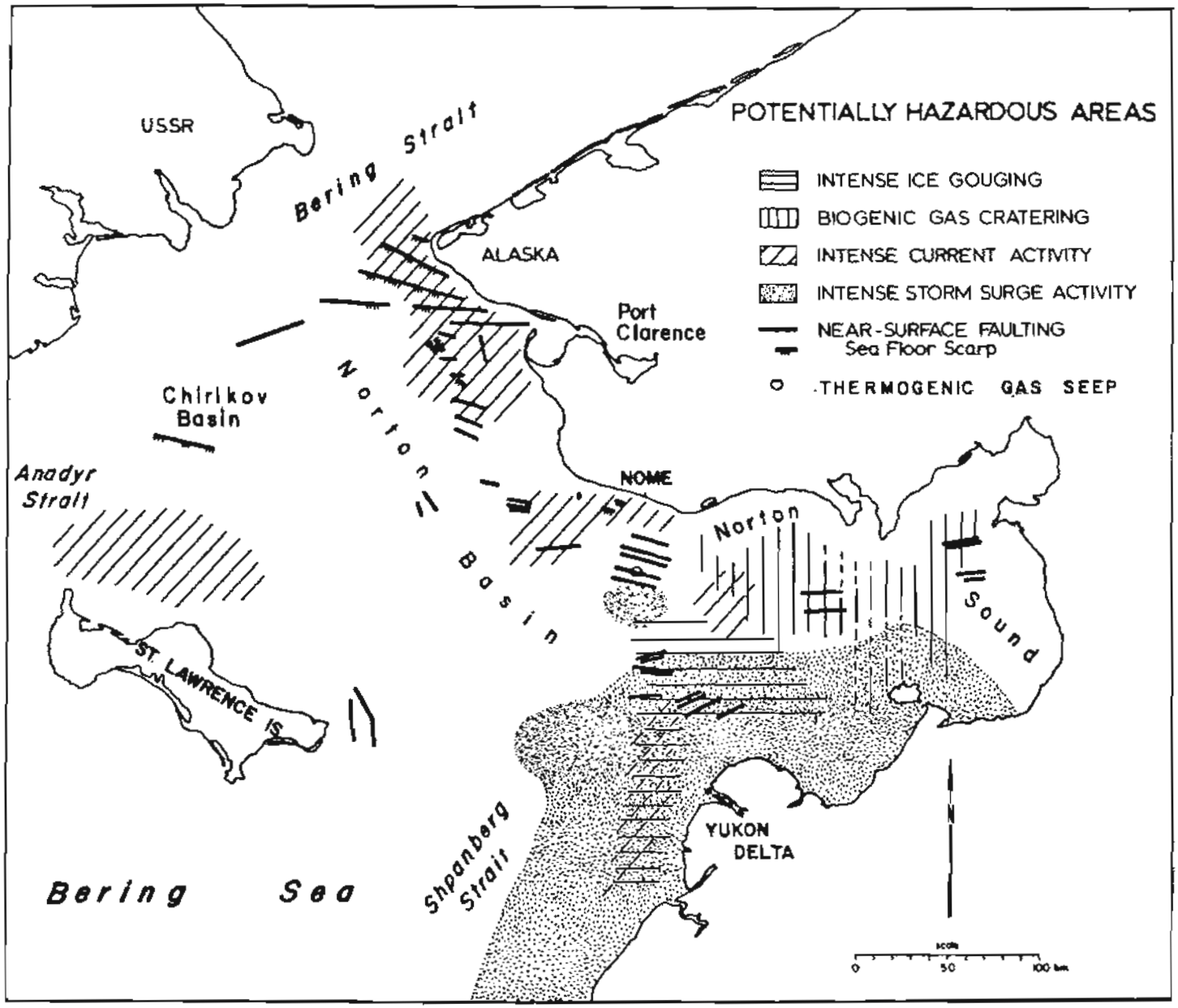
POTENTIALLY HAZARDOUS AREAS
INTENSE ICE GOUGING
BIOGENIC GAS CRATERING
INTENSE CURRENT ACTIVITY
INTENSE STORM SURGE ACTIVITY
NEAR-SURFACE FAULTING
Sea Floor Scarp
THERMOGENIC GAS SEEP
USSR
Bering Strait
ALASKA
Port Clarence
Chirikov Basin
Anadyr Strait
Norton Basin
NOME
Norton Sound
ST. LAWRENCE IS.
Shpanberg Strait
YUKON DELTA
Bering Sea
N
0
50
100 km

incompletely defined, affinities of species for sediment types have been defined for shelled forms (Rowland, 1973) and work is in progress to delineate overall association patterns (Stoker, unpub.). The primary benthic ecosystem is based mainly on a detrital food web (Kuznetzov, 1964), though other feeding types exist such as the sessile seston feeders of the Bering Strait.

A major problem in describing either trophic structure or distribution of the Bering Sea benthos is the extreme patchiness of the populations (Stoker, 1973). The reasons for such patchiness are incompletely understood but result from a combination of variable habitats and biological interactions (Stoker, 1973, and unpub.).

The major forms in the benthic macrofauna are bivalve mollusks, ophiuroid and echinoid echinoderms, ampeliscid amphipods, and polychaete worms; other forms, such as tunicates, holothurians, sipunculids, and gastropods, may be locally dominant (Neyman, 1961, Rowland, 1973; Stoker, 1973 and unpub.). Inferences on the bioturbating capabilities and substrate preference of some taxa can be drawn from general accounts of functional morphology (Stanley, 1970), distributional studies in other areas (Ockelmann, 1958) and recent Alaskan studies (Table 1).

Methods of Study

One hundred twenty box cores were obtained from the northern Bering Sea shelf at water depths greater than 10 m (Fig. 5). The cores were sectioned to 1 cm slabs, photographed, and x-rayed; the texture, stratigraphy, and structures were then described (Fig. 5). Identification of fauna was based primarily on specimens from the greater-than-2-mm sediment fraction of 25 kg Van Veen grab samples (Nelson and Hopkins, 1972; Rowland, 1973; Stoker, 1973). Photos of live fauna observed in box cores at the time of collection also were available. These data were compiled to estimate distribution and abundance of types of structures nd benthic fauna from the region.

PHYSICAL SEDIMENTARY STRUCTURES

External Form

Pebble Lag Layers consist predominantly of clasts from 4 to 64 mm in diameter (Fig. 6A and B) with little matrix, although large boulders have been reported by divers in lag areas off Nome (G. E. Greene, oral commun., 1967). Generally, th pebble lags occur at the sediment-water interface in layers 5 to 15 cm thick (Fig. 6A). However, a well-sorted "pea gravel" interpreted to be on an ancient beach strandline at -30 m in Anadyr Strait is more than 32 cm thick (Fig. 5B). These surficial pebble lags generally overlie glacial till but locally cover bedrock outcrops in topographically elevated regions (Nelson and Hopkins, 1972) (Figs. 1, 4, 5, 7).

Shell Lag Layers in the subsurface, several centimeters thick, and composed entirely of shell debris, were encountered in transgressive sands at several locations off north-central St. Lawrence Island (Fig. 6). They also were found in well-sorted, medium-grained sands on shoal crests of Shpanberg Strait and southeast Bering Strait (Fig. 6D). Clam shells predominate in layers off St. Lawrence Island, while sand dollar fragments make up layers of the shoal crests. In the region southeast of Bering Strait, basal coarse-grained, pebbly sands commonly have a high content of shell fragments, but not enough to be classed as shell layers.

Lag Layers of Mixed Pebbles and Shells are widespread in the upper subsurface, particularly in the mud of the shallow northern and eastern parts of Norton Sound (Figs. 5, 6G). However, a few such layers occur in subsurface basal coarse sand and gravel at water depths of 40 m or greater in the strait areas (Figs. 4, 5, 6H, and 7). In both cases, shell and pebble concentrations range from distinct layers a few centimeters thick, composed entirely of pebbles and shells (Fig. 6G), to diffuse zones 5-10 cm thick containing a matrix of sand and silt (Fig. 6H).

Solitary Rafted Pebbles are ubiquitous in all water depths, bathymetric settings, and sediment types (Figs. 4, 7). They are most common in sediment surrounding gravel deposits (Fig. 4), although solitary cobbles up to 20 cm in diameter were encountered in Yukon mud far from gravel sources (Fig. 6J).

Storm Sand Layers are most common in silty muds of the shallow parts of southern Norton Sound (Figs. 4, 5, 6E, F, G), but a few thin (<1 cm) coarse- and medium-grained sand storm layers are found in fine sand on deeper scarps (>40 m) southeast of Bering Strait (Figs. 4, 5, 6I, and 7). The sand layers in Norton typically are 1-2 cm thick except close to shore where they are thicker (Figs. 6E-G). In the shallowest sampling sites near the main distributaries of the present Yukon subdelta, surface sand layers from 4 to 12 cm thick have been detected in areas where mud was sampled in previous years.

In addition to the changes in distribution areally at the surface, the abundance of sand layers varies with depth in the subsurface. For example, off Stuart Island approximately 20 sand layers occur in the uppermost 12 cm of the core, and none are found in the 12 cm of the core beneath (Fig. 6F). In a long (132 cm) core of Yukon sediment from southeastern Norton Sound, four sand layers were found from 0 to 15 cm, two from 15 to 60 cm, and two from 60 to 132 cm.

Internal Structures

Flat Lamination is the most common and widely distributed internal structure in all sediment types, water depths, and topographic settings (Figs. 5, 7). It is observed most often in sand layers of Norton Sound, where the lamination is about 1 mm thick and is defined by minor variations in grain size (Fig. 6F and G). Lamination is least common in gravels, where layers are about 1 cm thick (Fig. 6B). The best examples of flat lamination are found in pre-Holocene deposits of limnetic mud (Fig. 8A). Although the whiteness of some laminae suggests volcanic ash or diatom varves, no glass shards or microfossils were found under the microscope.

Cross Lamination like flat lamination, is widely distributed and is best developed in the sand layers of Norton Sound. Characteristically the sets of cross-laminae are of small scale and are inclined at low angles (Figs. 4, 6F and G). Crossbedding in gravel is rare, but when observed is larger in scale and higher in dip angle than finer-grained sediment (Figs. 6B and 8A).

Ripples are very common at the tops of sand layers of Norton Sound and in sand at the margin of Chirikov Basin (Figs. 5 and 7). The ripples are generally asymmetric and small scale (6-8 cm wavelength, 5-1.5 cm wave height) and are interpreted to be current ripples and combined flow ripples commonly found in sand or silt (Harms and others, 1975) Figs. 6F and G). Where sand layers are thick, ripple forms appear to be nearly continuous (Figs. 6F and G), unless bioturbated, in which case the ripples are disrupted, producing sand lenses (Fig. 6E).

Miscellaneous Structures

Natural load and slump structures are observed in laminated Pleistocene lake deposits in a large depression off St. Lawrence Island (Fig. 8F). Other load-like features are present near the tops of some box cores, but they are suspected to be coring artifacts (Fig. 6F). Extremely disturbed sediment in a box core from the shallow area near the Yukon subdelta is the only apparent example of structures related to ice gouging (Fig. 8E). A paradox is that new studies show ice gouging to be ubiquitous at depths less than 20 m over the northern Bering Sea floor (Thor et al., 1978), but it rarely produces noticeable effects in box cores (Fig. 9). Large-scale bedforms such as sand waves have a wide distribution where topography and bathymetry constrict bottom currents (Figs. 1, 3 and 9) (Jordan, 1962; Grim and McManus, 1970). Characterization of these large bedforms and ice gouge effects must await detailed investigation with sidescan sonar.

BIOTURBATION

General

Once the primary physical structures associated with erosion and deposition have developed, secondary processes such as slumping, loading, and bioturbation begin. In this generally flat epicontinental shelf region, biogenic structures usually predominate over other secondary structures in the upper 30 cm of the sediment.

The size of the area and the patchiness of the benthos (Stoker, 1973) make it impossible to map benthic faunal distribution in detail or to correlate all types of structures with the organisms. Where single or very limited types of bioturbation characterize certain broad areas of sea floor, complete biologic structures can be traced to specific species. In other areas some species, for example, sand dollars are restricted to certain habitats (Table 1, Figs. 6I, 8C, 9 and 10) and can be documented to disturb shallow sands (Fig. 13A), but no distinct structures can be identified. Commonly only parts of burrows are observed in box cores, and the burrow may not be assignable to a single species (Figs. 13 and 14); this is particularly true for the numerous species of burrowing clams. Fortunately, distribution for each major group of bioturbating organisms (surface, shallow, intermediate, and deep can be outlined by analysis of screened megafauna from grab samples (Rowland, 1973; Stoker, 1973) (Figs. 10, 11).

Surface Disturbers

Several species of small organisms disturb the sediment surface over large areas of the Bering Sea floor (Fig. 10, 12). Brittle stars are one of the dominant organisms in eastern Bering Sea (Neyman, 1961), but they are most common in muddy areas closer to land and least common in central Chirikov Basin (in Fig. 10 note the absence of brittle stars at the predominant sandy 30-40 m depth of offshore Chirikov Basin). Distinctive surface tracks of brittle stars can be identified on the top surface of box cores, but burrows (Hertweck, 1972) are not

evident even where massive populations cover the bottom (Fig. 12).

The carnivorous gastropods occasionally leave surface trails also but may burrow to shallow depths after prey; they are widespread, being rare only in the shallow region around the Yukon subdelta (see Tachyrhynchus Fig. 10). Crabs and sea urchins typically are found on gravel substrates and both may excavate slight depressions, however, they are fewer in number than the other surface disturbers (Fig. 10). Crabs are common also in sandy areas except for central Chirikov Basin.

In response to the benthic food resources, large populations of walrus, bearded seal, and gray whale inhabit the northern Bering Sea on at least a seasonal basis and are likely to be responsible for considerable reworking of the shallow sediments over much of the northern Bering shelf. Gray whales are known to disturb bottom sediment to a depth of several centimeters to feed mainly on amphipods (Tomilin, 1957). The distribution of the large amphipod populations (Fig. 11) and the pathways of whale migration (Nasu, 1974) suggest that gray whales may cause surface disturbance of the Chirikov Basin area. Walrus and bearded seals also may disturb the sediment surface as they feed upon large bivalves and other infauna (Fay and Stoker, unpub. data).

Shallow Burrowers

The most widespread shallow burrowers (0-5 cm depth) are small, bright-colored amphipods possibly of the genus Protomedeia, Melita, or Hippomedon (Fig. 11). These taxa are most abundant off southeastern St. Lawrence Island and in the western and northern areas of Norton Sound, where they inhabit patches of Yukon-derived sediment. One or more of these species probably is the builder of U-shaped burrows about 5 mm in diameter (Fig. 11C, and D). Completely preserved burrows are distinctive, but fragments are not separable from burrows made by polychaete worms such as Nephthys (Fig. 13D). In general, we believe most incomplete burrows were constructed by the more abundant amphipods (Figs. 10 and 11).

Several species of shallow burrowing gastropods (Table 1) with no posi-

tively identified burrowing structures are present throughout northern Bering Sea except off the Yukon delta (Figs. 10 and 13). Tubes of the polychaete Pectenaria also are widespread (Fig. 10) (Stoker, 1973), and these organisms are known to develop shallow burrows (Hertweck, 1972), but no identification can be made in Bering Sea sediment . Numerous bivalves, such as Yoldia, Macoma, Nuculana, Tellina, and Nucula (Rowland, 1973; Stoker, 1973) are undoubtedly responsible for widespread shallow disturbance (Figs. 20 and 1A), but they also have produced no distinctive burrows.

Intermediate Burrowers

Intense bioturbation from the sediment surface to 10 cm depth can be defined in central Chirikov Basin and southwest and southeast of St. Lawrence Island. In these areas, abundant populations of large tube-building ampeliscid amphipods live in fine-grained sand (Figs. 20, 22B, 14A and B; Table 1). In most other areas, except central and southern Norton Sound, 1-mm-diameter burrows of small polychaete worms are common to abundant. These structures are particularly common in the silty mud on the northern and eastern margins of Norton Sound (Figs. 11, 6G, 14C and D). Bivalves such as Serripes and Clinodardium are particularly abundant throughout northern Bering sea region, however, the preponderance of amphipod aburrowing in Chirikov Basin and polychaete burrowing in Norton Sound appears to obliterate most other physical and biological structures at intermediate depths.

Deep Burrowers

Bivalves such as Mya and Spisula are the most common deep burrowing (0 to >10 cm depth) organisms. Their widespread distribution suggests that many deep burrows are caused by pelecypod bioturbation (Figs. 20, 11 and 15; Table 1). Only rarely (Fig. 8A) is it possible to correlate the burrow type with clam species, since normally only portions of the burrows are evident.

Several species of polychaete worms, holothurians, and sipunculids also burrow deeply into the sediments. Though deep-burrowing worm species occur

throughout the area, they are most common in silty and very fine-grained sand in deeper water (Figs. 10, 11 and 15A and B).

DISCUSSION

Factors Controlling Distribution of Physical Sedimentary Structures

Relict Structures in Relict Sediments

The physical sedimentary structures of northern Bering Sea are either relict from Quaternary conditions or developed by modern wave and bottom currents. In places, the Holocene shoreline transgression reworked Pleistocene moraines and bedrock outcrops exposed on the sea floor. The fine-grained debris was winnowed out leaving behind surface lag gravel deposits (Fig. 6A) (Nelson and Hopkins, 1972). These deposits remain on the surface of current-winnowed topographic elevations where deposition of Holocene muds has bee prevented. In the eastern parts of Anadyr and Bering Straits as well as along nearshore southwestern Seward Peninsula and St. Lawrence Island, the mineralogy and large grain size of gravel lags plus old radiocarbon dates (15-40,000 BP; Nelson, unpub. data) of underlying sediment both indicate deposition under older, high-energy conditions not present today (Nelson and Hopkins, 1972; McManus and others, 1974). The coarser grain size and different mineralogy of the Chirikov Basin sand blanket compared to the silty-sized sediment of the main modern Yukon sediment source suggest that Chirikov Basin sand also is relict.

Relict physical structures in relict sediments are best preserved in the subsurface sediment of strait areas with the deepest water, where present-day wave effects are minimal, coarse gravel armors the bottom surface, and strong currents prevent burial by modern deposits. Here box cores have penetrated into older transgressive sediments, and even into Pleistocene freshwater deposits with relict lamination (Fig. 8D). Coarse-grained relict sediment overlying Pleistocene tills contains flat lamination and associated high-angle, medium-scale cross bedding that evidently originated during the Holocene shoreline transgression (Figs. 6B, A, 4, 7). Subsurface shell and pebble horizons in such relict sedi-

ments are now in sufficiently deep water and buried deeply enough to ensure isolation from modern day storm wave and bottom current effects. These structures apparently formed as storm lags during lower sea level stands (Figs. 6C, 6H).

Modern Structures in Relict Sediments

The relict fine-grained sand of central Chirikov Basin is interpreted to have been deposited as a nearshore belt of sand that migrated along with the Holocene shoreline as it transgressed across the epicontinental shelf. The modern Yukon silt has not prograded over the transgressive sand, and it has, therefore, been exposed to intense bioturbation for thousands of years. Additionally, the Chirikov Basin sand has been covered by 35-55 m of water since the sea reached its present level several thousand years ago, and the development of physical sedimentary structures by waves thus has been limited. Bottom currents in this central area generally are sluggish (Fig. 3; McManus et al., 1977) and in most places probably are insufficient to develop structures. Even though waves or bottom currents occasionally possess sufficient energy to create structures in this noncohesive sediment, the binding effect of the dense network of ampeliscid amphipod tubes should inhibit formation of such structures (Fig. 14B; Rhoads, 1970). Consequently, the sand is completely devoid of sedimentary structures except on a few shoal crests where the sediments are reworked by strong bottom currents (Figs. 6I, 8C).

Recent evidence from sidescan sonar, underwater television, and vibracores verifies physical formation of sedimentary structures in certain shoal areas of relict sediment in Chirikov Basin. In the shallower upper parts of sand ridges with sand waves (Figs. 1, 4 and 9), the surface and near-surface coarse sand and shell storm lags (Fig. 6D) along with faint ripple structures (Figs. 6I and 8CK) appear to be near-surface modifications of relict sand by modern storm waves and bottom currents. On underwater television, storm waves have been observed to winnow shell pavement and to superimpose small-scale oscillation ripples over the larger sand-wave structures (Figs. 9A and B). Sidescan sonar records show large-

scale asymmetric sand waves covering ridge tops and trending northward in phase with the present strong northward bottom currents in northeastern Chirikov Basin (Fig. 3) (Fig. 9C, Nelson et al., 1977; Nelson, 1977); a thousand-year-old radiocarbon date (Teledyne Isotopes I-9773) on wood from 30 cm depth in a sand wave field documents that modification of sediments by sand wave formation has taken place recently during the present stand of high sea level.

Either wave or current effects could be responsible for individual faint ripple structures observed in specific box cores from sand ridges. However, the dominance and type of asymmetric sand wave and ripple fields in all sidescan records and bottom photographs from the region indicate that the majority of modern ripple structures in Chirikov Basin must derive from bottom current activity (Fig. 9).

Modern Structures in Modern Sediments

Numerous radiocarbon dates substantiate that the blanket of mud with interbedded sand in Norton Sound has a Holocene origin and contains contemporary sedimentary structures (Nelson et al., 1975; Nelson and Creager, 1977). Development and preservation of these physical structures varies widely both spatially and stratigraphically over the contemporary surface in Norton Sound. Historical change from complete bioturbation to complete preservation of physical structures within the past several thousand years can be demonstrated in several locations (Figs. 6F, G). In those locations closest to the Yukon delta, such dramatic alteration in preservation of physical structures may be attributable to salinity and circulation changes caused by a shift in location of a major Yukon distributary (Fig. 6F; Nelson and Creager, 1977).

The storm sand layers that are interbedded with mud surrounding the Yukon delta contain the best developed physical sedimentary structures because of several interacting factors. The prodelta area is subject to the most intense and frequent wave reworking of any northern Bering Sea area owing to its extreme shallowness. In addition, the Norton Sound shape acts to focus storm surge set-

up of water level (Fathauer, 1975) and this in turn results in development of strong bottom currents as storm-surge water runoff moves northward from the region (Fleming and Heggarty, 1965 ; Nelson and Creager, 1977). Such "runoff" currents may be the final mechanism to rework and form physical structures in sand layers of the prodelta area.

Formation of the thickest sand layers and their rapid burial due to the high sedimentation rates in the prodelta area both inhibit bioturbation and enhance preservation of the physical structures. Even more important, the low salinity and more extensive ice formation in the prodelta area (Figs. 2 and 11) appear to restrict faunal populations and consequent bioturbation of the physical structures. The complete bioturbation of physical structures at similar water depths but normal salinity on the northern side of Norton Sound appears to confirm this hypothesis.

Much of the cross-lamination and lenticularity in modern sand layers of Norton Sound appears to result from rippling by unidirectional bottom currents. The ripples are usually asymmetric, and the ripple form, where it can be observed in box cores, bottom photographs, underwater TV, and sidescan sonar, is sinuous and irregular, not straight-crested like oscillation ripples (Nelson, 1977), (Figs. 8 and 9). Furthermore, the basal surfaces on sand layers are regular, the internal structure conforms to ripple form, and bundlewise buildup or offshoots passing from adjoining troughs and crests are absent. Each of these points suggest formation primarily by unidirectional bottom currents (Reineck and Singh, 1973).

Waves still are important in forming bottom structures, and formation of oscillation ripples over asymmetric ripples and sand waves has been observed in Chirikov Basin at water depths similar to those of Norton Sound (Nelson et al., 1977) (Fig. 9). Hindcasting of wave data indicates that wave reworking can affect most of the Norton Sound sea floor (McManus et al., 1977). However, in the >10 m water depths with very fine sand that this study covers, Clifton's

(1976) conceptual model predicts that wave-related currents should not produce asymmetric rippling. Apparently, the dominant storm effect on sand layers is reworking by bottom currents, which are intensified by storm-induced sea level changes (Fathauer, 1975). Later modification by less intense wave effects may cause some oscillation ripples to be superimposed over the dominant unidirectional features, but in general they appear to be subordinate.

Eastward and northward from the present delta, storm sand layers become fewer and fewer, and only diffuse storm layers rich in shells and pebbles are observed. Near the delta, where biota appear to be restricted and no rocky headlands are present, few shells or pebbles are encountered in storm layers. With increasing distance from the delta into higher salinity water, more and more shells are encountered and bioturbation increases. In addition, the intensity of storm-wave reworking decreases and sand layers become thinner, while headlands along the coast away from the delta provide a pebble source. Figs. 6C–G, 6J, 13B–D exemplify such a proximal (delta) to distal (central Norton Sound) or shallow to deep sequence of storm layers. The change from sand layers to coarse lags of pebbles and shells offshore also suggests that processes change from dominantly transport and deposition of sand sheets to mainly erosion of mud leaving pebble and shell lags offshore.

The Yukon muds of Norton Sound, both massive and those interbedded with storm sand layers, remain nearly devoid of physical structures, except for occasional laminations (Fig. 13B,E). Because the mud deposition represents slow, continual deposition under non-storm conditions, bioturbation apparently can almost always keep pace with formation of physical structures, and thus physical structures are not generally preserved in muds.

Present-Day Pebble Rafting and Ice Gouging

Isolated pebbles are widespread in sediment of the Bering Sea region and may have been transported by several processes. Pebbles are most common in areas surrounding seafloor gravel(Fig. 4). This distribution pattern may result from

ice grounding in gravel areas. The ice may pluck pebbles from the gravel source and drop them nearby after the iceberg works free and begins melting. Other mechanisms such as transport of walrus gastroliths (stomach stones) (S.W. Stoker and F.H. Fay unpub. data) and sea grass rafting (Stoker, 1973) may also carry isolated pebbles offshore.

Recent studies indicate that gouging into the sea floor by icebergs occurs everywhere at depths shallower than 20 m (Thor et al., 1977) (Fig. 9), except in strait areas, where ice jams may cause gouging at much greater water depths (G. Bloom, oral commun, 1970). The gouging is most intense (reaching depths of up to 1 m in the sediment) in the prodelta area surrounding the modern Yukon subdelta; this is the same region where physical sedimentary structures are best preserved (Fig.5). The question remains, why does this intense gouging have such little effect on physical structures? Perhaps sediment rates are rapid enough near the modern subdelta to keep ahead of the rate of ice gouging.

Factors Controlling Bioturbation

Biological Factors

A few ubiquitous species show little environmental control and account for a significant amount of the bioturbation anywhere in the northern Bering Sea area. Examples of these species have been described in the previous bioturbation section such as the ophiuroid and gastropod (Tachyrhynchus erosus) surface disturbers, the clams (i.e. Yoldia myalis) and small amphipod shallow burrowers, the clams (i.e. Serripes groenlandicas) and small polychaete (thread worm) intermediate burrowers and the clams (i.e. Mya truncata) and large polychaete (i.e. Ampharete) deep burrowers (Table 1, Figs. 10, 11, and 12).

Except for the cosmopolitan species just mentioned, distribution of most species is controlled by environmental factors such as hydrographic conditions, morphologic setting, and substrate type. Consequently, bioturbation of most species has definite patterns of areal distribution (Figs. 10 and 11). All species appear to be restricted by the seasonally low salinity off the modern

Yukon subdelta (Figs. 2, 5 and 11; Lisitsyn, 1966). Regions of strong currents and resulting coarse-grained sediment support epifaunal communities such as the suspension-feeder assemblages found in straits, or the sand dollar (Echinarachnus parma) and bivalve community (Tellina lutea alternidentata, Spisula polynyma) found in sandy areas on crests of shoals (Fig. 10).

Because of the small depth range (0 - 50 m) on northern Bering shelf, water depth has little direct influence on abundance or type of bioturbating organisms. Instead, benthic communities typically show pronounced association with substrate. For example, the large ampeliscid amphipods are the dominant organisms disturbing the transgressive fine-grained sand in Chirikov Basin (Figs. 10 and 11; Table 2). They are not evident in Yukon silt of Norton Sound, where the smaller amphipods, brittle stars, and deposit-feeding worms and clams are predominant (Figs. 10 and 11, Table 1, Rowland, 1972, 1973). Gravel lags are habitats for an abundant epifauna of rocky substrate type consisting of bryozoans, barnacles and brachiopods. However, the thickness and coarseness of the lag layers and the sessile living habits of fauna on them seem to prevent significant bioturbation. Many other substrate associations of bioturbating organisms, particularly bivalves, have been outlined in other Bering Sea studies (Table 1; Rowland, 1972, 1973; Stoker, 1973 and unpub.).

Interplay of Biological and Physical Factors

Intensity of bioturbation is controlled by rates of several processes such as the frequency of formation of physical structures, rate of reworking by organisms, and sedimentation rate (Fig. 16). Changes in these rates through geologic time cause variations in the intensity of bioturbation at a site. The following physical factors cause a relative increase in the rate of formation of physical sedimentary structures and decrease in intensity of biogenic reworking: shallow water with intense wave reworking, swift bottom currents, rapid rates of deposition, and low-salinity water. These physical variables plus other environmental characteristics like those mentioned in the previous section control spe-

cies dispersal and cause patchiness of faunal distribution. As a result, the rate of biogenic reworking varies from one location to the next and with time at a given location.

In the shallow prodelta region off the Yukon River subdelta, bioturbation typically does not keep pace with the formation and rapid burial of physical structures (Fig. 5). An area just east of the prodelta near Stuart Island also shows no bioturbation in deposits of the last 5,000 years (Figs. 5 and 6J; Nelson and Creager, 1977). This is true even though the area has low sedimentation rates and is at a greater water depth, where the formation of wave-formed structures is expected to be slower. The well-developed physical structures probably result from the shoreline constriction of coastal currents. The extremely good preservation of physical structures here and in the prodelta area may result both from continued formation by bottom currents or waves and from the inhibition of biogenic activity by the great seasonal changes in salinity. Complete bioturbation of sediment older than 5,000 years near Stuart Island strongly suggests that Yukon delta distributaries shifted into the region after 5,000 BP (Nelson and Creager, 1977) and that salinity is the predominant factor controlling bioturbation in this area.

Another stratigraphic sequence for the last 2,000 years in eastern Norton Sound (Figs. 5 and 6G) shows complete bioturbation in the lower third of the sediment, nearly complete preservation in the middle, and complete bioturbation in the upper third. Either faunal populations diminished during the time of deposition of the middle sequence, or frequent storms prevented bioturbation from keeping pace with deposition.

GEOLOGIC SIGNIFICANCE

Geologic Effects of Bioturbation

In addition to disturbing physical structures and creating trace fossils, bioturbation may severely disrupt fossil assemblages and organic debris used in dating deposits. The disruption is especially severe in regions of thin trans-

gressive sequences such as the epicontinental shelf of the northern Bering Sea. In several cores (Figs. 8A and 8D), present-day burrows extend at least 30 cm into Pleistocene freshwater deposits that are tens of thousands of years old. As a result, in part because of this upward mixing of older materials, radiocarbon dates of 1,740 to 5,085 BP are found for bulk organic carbon in the top 1 - 2 cm of modern surface sediment on the northern Bering shelf (Teledyne Isotopes I-8134, 8135, 8226, Fig. 6F). Downward homogenization of Holocene sediment by bioturbation helps to explain radiocarbon dates of only a few thousand years for older buried transgressive deposits (Figs. 6I, 8D; Teledyne Isotopes I-7482, 7483).

Radiocarbon dates on calcium carbonate of shells again suggest significant biologic mixing of modern shells downward into buried transgressive gravel and sand (Fig.-6B, C, H, and I). Dates on fossil, surface-dwelling mollusk species are just several hundred years old, even though only those shells buried in older sediment far below their normal living habitat were dated (M. Rubin, USGS Radiocargon Lab. W-2462, 2464, 2466, 2467, 2681-2685). In Chirikov basin, where the transgressive sequences are thin and dates on shells do not appear to be reliable, mixed modern and transgressive foraminiferal assemblages are found throughout the entire transgressive sequences (Figs. 8A and 8D) (R. Echols, written commun., 1974). Only where sedimentation rates are high, producing rapid, deep burial such as near the modern Yukon subdelta, do radiocarbon dates on shells and organic carbon agree with stratigraphy (M. Rubin, USGS, Radiocarbon Lab W-26180; Teledyne Isotopes I-7316, 8134), and can unmixed transgressive sequences of microfossils be detected.

Rhoads (1973) points out another aspect of bioturbation that may have particular geologic significance for the northeastern part of the Bering shelf. The predominance of deposit feeders can reduce the bulk density of fine-grained sediment and greatly enhance the potential for erosion. The dominance of deposit feeders in Norton Sound (Figs. 10 and 14; Rowland, 1972) may be a contributing

factor to the resuspension of considerable fine-grained sediment there. The resuspension of sediment by storm waves and its removal by storm-generated and continuous currents may have displaced about half of the Holocene sediment of Yukon source from Norton Sound to the Chukchi Sea (Nelson and Creager, 1977).

Comparison of Bering Shelf and Similar Sedimentary Environments

Prodelta and Inner Shelf Facies

Prodelta mud facies develop in the shallow regions surrounding the Yukon River mouth where the low-salinity river plume is the dominant water mass (Figs. 2 and 5). The proximal deposits are characterized by thin mud interbedded with thick storm sand layers that contain well-developed sedimentary structures resulting from waves and currents generated by storm surge (Table 2, C_1). Offshore from the most proximal prodelta facies, layers become thinner, more highly rippled, well structured with cross lamination, and increasingly bioturbated. The most distal prodelta deposits are dominated by higly bioturbated muds with sand lenses containing bioturbated remnants of physical structures. Further seaward, shell and pebble-rich storm lag layers occur (see Figs. 6E, 6F, 6G, 13B and 14C for a specific sequence; Figs. 5 and 16 show general patterns of distribution). Bioturbation in the muddier facies is dominated by tube-building detritus feeders and burrowing deposit feeders (Table 1, G-C; Fig. 10 and 11; Table 2, C_1).

The physical and biological structures in similar ancient stratigraphic sequences reflect this same proximal to distal energy gradation. For example proximal to distal sequences of physical structures and storm sand layers like those in Norton Sound are described for Jurassic deposits by Anderton (1976). In the Upper Cretaceous Blackhawk formation in Utah, a regressive sequence begins with completely bioturbated offshore muds (Howard, 1972). Sand beds appear up-section and thicken upward with increasingly well-preserved physical structures, indicating greater wave energy. The faunas also change up-section from deposit to suspension feeders as the depositional environments shallowed.

Variations in wave climate and topographic setting can greatly extend or reduce proximal-to-distal offshore gradation of physical structures generated by waves. For example, in the Gulf of Gaeta in the low-energy wave climate of the Mediterranean, well-developed physical structures are limited to less than 6 m of water depth (Reineck and Singh, 1973) below which bioturbation predominates. In the higher energy environments of the northern Bering Sea and off Southern California, well-preserved recent physical structures exist to 15-20 m water depth (Figs. 5 and 7) (Karl, 1975). In the very high energy environment off Oregon, well-preserved physical structures occur in sediments in over 50 m of water (Kulm and others, 1975). Well-preserved physical structures also may exist anomalously far offshore on topographic elevations.

Sediment type and rate of influx also may influence the maximum offshore extent and water depth at which physical structures are preserved. In muddy areas, such as near deltas, fine-grained sand layers and their structures are readily identifiable in modern or ancient sequences (Fig. 6E-G) Moore and Scruton, 1957; Masters, 1967; Howard, 1972). Commonly, in the most distal locations of deposition, isolated pods or lenses of rippled and laminated sediment are the last recognizable vestige of a storm sand layer (Figs. 6J and 13B) (Reineck, 1970; Winston and Anderson, 1970). Such thin sand lenses are usually destroyed by bioturbation closer to shore or at shallower depths than are similar storm lag layers composed of shell and pebble lags (Figs. 5 and 7). For example, faint shell and pebble horizons of coarse-grained storm lags are identifiable to water depths of 30 m in modern sediments of Norton Sound even after very extensive bioturbation; the last vestiges of fine-grained sand layers occur in 25 m of water (Fig. 7). In most delta areas, the formation of such shell and pebble layers is inhibited by the paucity of rocky headland pebble sources and by the influx of fine-grained sediment and low salinity water, which appears to discourage large bivalve mollusk populations, the source of most shell material.

The distribution pattern of the prodelta facies may be controlled as much by water circulation and freshwater plume dispersal as by the shallow, nearshore location and shape of the prodelta topography (Figs. 2, 3 and 5). This is because variations in salinity and oxygen and nutrient content of sea water can influence benthic productivity and thus affect formation and preservation of physical structures. The best preservation of physical structures coincides with the location of the low-salinity plumes (Figs. 3 and 5; Nelson et al., 1975) surrounding the Mississippi and Yukon deltas; a progressive reduction in bioturbation also has been correlated with with decreasing salinity up estuaries (Winston and Anderson, 1970; Moore and Scruton, 1957). The importance of salinity compared to other factors, like rapid sedimentation, is suggested by thin (12 cm) late Holocene sequences that have remained unbioturbated for at least 5,000 years off the Yukon (Fig. 6F).

In some geographic settings physical structures may be preserved in unexpected epicontinental shelf areas where the benthic fauna is depauperate because of low oxygen content in bottom water (Seibold et al., 1971). Excellent preservation of physical structures found in the Mesaverde Formation of northwestern Colorado (Masters, 1967) suggests that these ancient deposits similar to those off the Yukon were formed under shallow, low-salinity water near a delta, or where environmental factors inhibited bioturbation.

Transgressive and Current-Winnowed Facies

The transgressive fine-grained sands in northern Bering Sea are characterized by a homogeneous texture, the general absence of physical structures, and intense bioturbation by tube-building detritus feeders (Table $2B_1$). This sediment facies may typify thin transgressive sands on epicontinental shelves with low wave energy, but where burial by offshore mud is prevented by strong bottom currents or isolation from sediment sources. In contrast, in areas where there is a very high energy wave regime, such as presently off Oregon, some physical structures are found in the offshore relict transgressive sand facies (Kulm and others, 1975).

The basal transgressive gravel and pebbly coarse to medium-grained sand of the Bering shelf in many places overlie Pleistocene moraines either as surface relict deposits or as subsurface strata beneath transgressive fine sand. These coarse-grained transgressive sediments take several forms that may be distinguishable in the stratigraphic record. The deposits with rounded pebbles, water-worn and thick-shelled mollusks, and medium-scale cross and flat lamination appear to be typical sediments associated with shoreline stillstands (Table 2, A_2; Clifton et al., 1971; Reineck and Singh, 1973). The angular pebble lags that develop over glacial till and bedrock apparently form during very rapid shoreline transgressions. Criteria for such deposits are angular gravels, little or no fine-grained matrix, and the remains of a rocky intertidal fauna (Table 2, A_1). Sessile benthic fauna consists largely of epifaunal forms (Craig and Jones, 1966). As a result, the thin pebble lags show little disruption from bioturbating organisms and may remain well preserved in the stratigraphic record For example, thin, structureless, transgressive sands overlying well-preserved glacial deposits have been noted in the Paleozoic transgressive sequence of the Algerian Sahara region (Beuf et al., 1971).

The well-sorted current-winnowed medium sand on the shoal crests of the northern Bering shelf is another sediment facies that may be recognizable in ancient shelf deposits (Table 2). Remnants of ripples and flat lamination are common; shell lag horizons and clay stringers, possibly representing major fluctuations in currents, are locally present. An important key to such deposits in ancient sequences would be dominance of sand dollars and filter feeding bivalves or similar ancient organisms (Table B_2).

Shelf Model

The physical and biological structures observed on the Bering shelf agree with other similar studies; these data permit conceptualization of a model of ty-

pical shelf sedimentary structures and factors controlling their distribution on an open shelf with clastic deposition dominated by muds and no organic reefs (Fig. 16). The inshore margin of the model presented here phases into the well-defined shoreline sequences of physical structures caused by breaking waves that have been depicted in the conceptual models outlined by Clifton et al. (1971). The model presented here does not consider the series of large-scale bedforms caused by extremely strong bottom currents in constricted bathymetric regions with high tidal or dynamic current flux. Such sequences have been described by Belderson et al. (1971) in the English Channel shelf and appear to be present in the Bering Strait area (Figs. 1, 4, and 16).

In the model we present, physical sedimentary structures caused by waves will dominate the open shelf sediment just offshore from beach-related features. The best developed physical sedimentary structures caused by strong bottom currents associated with periodic tides (Mofjeld, 1976), storm tides and shoreline constrictions of dynamic currents will generally occur just offshore from the wave-related structures. Seaward from strong wave- and tide-formed sedimentary structures, there occurs a spatial series of physical structures resulting from waning wave and bottom-current processes associated with storms. This complete sequence of storm sand to pebble- and shell-rich layers has been well documented in Norton Sound (Fig. 16).

As physical energy from waves and currents diminishes offshore, the frequency of physical sedimentary structures lessens and the physical structures are bioturbated and replaced by trace fossils to a progressively greater degree. The sequence of biological structures indirectly follows gradients of wave and current energy because these gradients regulate substrate types, which are the main control on biological assemblages (Craig and Jones, 1966; Rowland, 1973; Stoker, 1973). Typically, suspension-feeding organisms will be more prominent nearshore in coarse-grained substrates associated with high physical energy. In this environment, filtering apparatus is less likely to be clogged by fine-grained

debris (Rhoads and Young, 1970), and the circulation of suspended debris is vigorous. Suspension-feeding organisms will tend to disturb sediment less because they only need to anchor onto or into the bottom surface and do not need to burrow through the sediment to acquire food. In contrast, discrete burrows and complete bioturbation characterize offshore muds (Howard and Frey, 1973) because deposit feeders and detritus feeders require the higher content of organic debris found in fine-grained sediments of lower energy settings.

The conceptual model (Fig. 16) portrays an open graded shelf that gradually changes in depth, wave energy, sediment character, and current energy offshore. Evidence from the northern Bering epicontinental shelf and elsewhere indicates that many variables, including topographic setting, hydrographic characteristics, biologic productivity, and type and location of sediment sources can modify this idealized sequence. Several examples have already been cited to show that variation of wave climate can greatly extend or reduce offshore extent of physical structures generated by waves.

Topographic projections outward from the adjacent shorelines such as deltas or upward from the surrounding sea floor, such as offshore sand ridges (Nelson and others, 1975) are important variables controlling the development of current-formed physical structures. Where water circulation is constricted and strengthened by major shoreline projections as in the Bering Strait or English Channel (Belderson et al., 1970), bedforms and internal physical structures will be well developed no matter what the water depth or distance from shore. Offshore areas of sea-floor topographic relief such as sand ridges that constrict and focus bottom currents are also sites of well-developed physical structures without regard to their distance from shore (Fig. 6L).

Variation in the amount and type of sediment is another influence on the development and preservation of physical structures. Where rates of deposition are high and interbedded muds are common, as off the Yukon and Mississippi deltas (Moore and Scruton, 1957), preservation of physical structures is enhanced and

may extend to unusually great depths or distances from shore considering the wave-energy setting. The final shell and pebble remnants of an offshore storm layer may extend far offshore beyond the distance usually expected because of unusual sources of pebbles and mechanisms like ice or organic rafting to disperse them over the shelf.

All the factors of increased wave energy, current velocity and deposition rates, in addition to decreased benthic productivity will extend areas dominated by physical sedimentary structures farther seaward than bioturbation would otherwise allow (Fig. 16). These variations in basic physical, chemical, and biological factors are predictable at least partially and must be considered when sedimentary structures are utilized for paleoenvironmental reconstructions.

ACKNOWLEDGMENTS

Discussions with Asbury H. Sallenger, Jr. and H. Edward Clifton aided interpretations of physical structures, and George Mueller similarly helped with identifications of benthic fauna. Microfaunal analysis by Ronald Echols and Page Valentine plus radiocarbon dating by Meyer Rubin assisted stratigraphic interpretation. Excellent x-ray radiography was provided by David Pierce. Compilation of data and preparation of figures was ably completed by Dennis Kerr and Lee Bailey. For assistance with sample collection we thank scientists and crews of the following research ships: OSS "Oceanographer" (NOAA), OSS "Surveyor" OSS "Rainier" (NOAA), and R/V "Thompson" (University of Washington). Beneficial review comments were provided by Ralph E. Hunter and Asbury H. Sallenger, Jr.

REFERENCES CITED

Anderton, Roger, 1976, Tidal-shelf sedimentation: An example from the Scottish Dalradian: Sedimentology v. 23, p. 429-458.

Belderson, R.H., N. H. Kenyon, and A.H. Stride, 1971, Holocene sediments of the continental shelf west of the British Isles: in Delany, F.M. (ed.) ICSU/SCOR Working Party 31 Symposium, Cambridge 1970: The geology of the East Atlantic continental margin, v. 2: Europe. Rep. No. 70/14, Inst. Geol. Sci., p. 57-170.

Beuf, S., B. Biju-Duval, P. Rognon, O. Gariel, and A. Bennacef, 1971, Les gres du paleozoique inferieur au Sahara-Sedimentation et discontinuites evolution structurale d'un craton: Pub. de l'Inst. Francais du Petrole, Paris, Collection Sci. et Technique du Petrole No. 18, Part 1, ch. 4, p. 81-99, and Part 1, ch. 3, p. 222-257.

Chamberlain, J.L., and F. Stearns, 1963, A geographic study of the clams, Spisula polynyms: New York, American Geol. Soc., Serial Atlas of the Marine Environment, No. 3, 12p.

Clifton, H.E., 1976, Wave-formed sedimentary structures - conceptual model: Soc. Econ. Paleontologists and Mineralogists Spec. Pub.No.24, p. 126-148.

Clifton, H.E., R.E. Hunter, and R.L. Phillips, 1971, Depositional structures and processes in the non-barred high-energy nearshore; Jour. Sed. Petrology, v. 41, p. 651-670.

Coachman, L.K., and Knut Aagaard, 1966, On the water exchange through Bering Strait: Limnology and Oceanography, v. 11, p. 44-59.

Coachman, L.K., Knut Aagaard, and R.B. Tripp, 1976 Bering Strait: The regional physical oceanography: Univ. Washington Press, Seattle, 186 p.

Coachman, L.K., and R. B. Tripp, 1970, Currents north of Bering Strait in winter: Limnology and Oceanography, v. 15, no. 4, p. 625-632.

Coan, E.V., 1971, Northwest American Tellinidae: Veliger, v. 14, supplement, 63 p.

Craig, C.Y. and N.S. Jones, 1966, Marine benthos, substrate and paleoecology: Paleontology, v. 9, p. 30-38

Dörjes,J., S. Gadow, H.E. Reineck, and I.B. Singh, 1970, Sedimentologie and makrobenthos der Nordergrunde and der Außenjade (Nordsee): Senckenbergiana Maritima, v. 2, p. 31-59.

Fathauer, T.F., 1975, The great Bering Sea storms of 9-12 November 1974: Weatherwise Magazine, Am. Meteorol. Soc., v. 18, p. 76-83.

Filatova, Z.A., and N.G. Barsanova, 1964, Communities of benthic fauna in the western Bering Sea: Trudy Inst. Okean., LXIX, p. 6-97.

Fleming, R.H., and D. Heggarty, 1966, Oceanography of the southeastern Chukchi Sea, in Willimovsky, N.J., and J. M. Wolfe, (eds.), Environment of Cape Thompson Region, Alaska: U.S. Atomic Energy Comm., p. 697-754.

Frey, R.W., and J.D. Howard, 1972, Radiographic study of sedimentary structures made by beach and offshore animals in aquaria, in Hertweck, G. (ed.), Georgia coastal region, Sapelo Island, U.S.A.: Sedimentology and Biology: Senckenbergiana Maritima, v. 4, p. 169-182.

Goodman, J.R., J.H. Lincoln, T.G. Thompson, and F. A. Aewusler, 1942, Physical and chemical investigations: Bering Sea, Bering Strati, Chukchi Sea during the summers of 1937 and 1938: Univ. Washington Pubs. Oceanography, v. 3, no. 4, p. 105-169, and Appendix, p. 1-117.

Grim, M.W., and D.A. McManus, 1970, A shallow seismic-profiling survey of the northern Bering Sea : Marine Geology, v. 8, p. 293-320.

Hanor, J.S., and N.F. Marshall, 1971, Mixing of sediments by organisms, in Perkins, B.F., (ed.) Trace fossils - A field guide to selected localities in Pennsylvania, Permian, Cretaceous, and Tertiary rocks of Texas and related papers: Soc. of Econ. Paleontologists and Mineeralogists Field Trip, April 1-3, 1971, School of Geoscience, Louisiana State Univ. Misc. Pub. 17-1, Baton Rouge, La., p. 127-135.

Harms, J.C., J.B. Southard, D.R. Spearing, and R.G. Walker, 1975, Depositional environments as interpreted from primary sedimentary structures and stratification sequences: Soc. Econ. Paleontologists and Mineralogists Short Course No. 1, Dallas, 161 p.

Hertweck, G., 1972, Distribution and environmental significance of Lebensspuren and in-situ skeletal remains, in Hertweck, G., (ed.), Georgia coastal region, Sapelo Island, U.S.A.: Sedimentology and biology: Senckenbergiana Maritima, v. 4, p. 125-167.

Hopkins, D.M., Hans Nelson, R.B. Perry, and T.R. Alpha, 1976, Physiographic subdivisions of the Chirikov Basin, northern Bering Sea: U.S. Geol. Survey Prof. Paper, 1973, p. 31-37.

Howard, J.D., 1969, Radiographic examination of vatiations in barrier island facies; Sapelo Island, Georgia: Trans. Gulf Coast Assoc. Geol. Socs., v. 19, p. 217-232.

Howard, J.D., 1972, Trace fossils as criteria for recognizing shorelines in stratigraphic record, in Rigby, J.K., and W.K. Hambblin (eds.), Recognition of ancient sedimentary environments: Soc. Econ. Paleontologists and Mineralogists, Spec. Pub. No. 16, p. 215-225.

Howard, J.D., and R.W. Frey, 1973, Characteristic physical and biogenic sedimentary structures in Georgia estuaries: Am. Assoc. Petroleum Geologists Bull., v. 57, no. 7, p. 1169-1183.

Howard, J.D., and H.E. Reineck, 1972, Physical and biogenic sedimentary structures of the nearshore shelf, in Hertweck, G. (ed.), Georgia coastal region, Sapelo Island, U.S.A.: Sedimentology and Biology: Senckenberigiana Maritima v. 4, p. 81-123.

Husby, D.M., 1969, Report of oceanographic cruise U.S.C.G.C. NORTHWIND, U.S. Coast Guard Oceanog. Rept. No. 24, 75 p.

Husby, D.M., and G.L. Hufford, 1971, Oceanographic investigations in the northern Bering Sea and Bering Strait, 8-21 June, 1969: U.S. Coast Guard Oceanog. Rept. no. 42, 55 p.

Jordan, G.F., 1962, Large submarine sand waves: Science, v. 136, no. 3519, p. 839-848.

Karl, H.A., 1975, Distribution and significance of sedimentary structures and bedforms on the continental shelf, southern California: Geol. Soc. America Ab. with Progs., v. 7, no. 3, p. 331.

Knebel, H.J., and J.S. Creager, Sedimentary environments of the east central Bering Sea continental shelf: Marine Geology, v. 15, p. 25-47.

Kulm, L.D., R.C. Roush, J.C. Harlett, R.H. Neudeck, D.M. Chambers, and E.J. Runge, 1975, Oregon continental shelf sedimentation: Interrelationships of facies distribution and sedimentary processes: Jour Geology, v. 83, no. 2, p. 145-175.

Kusnetsov, A.A., 1964, Distributon of benthic fauna in western Bering Sea by trophic zone and some general problems of trophic zonation: Trudy Inst. Okean., v. LXIX, p. 98-117, (transl. by Office of Naval Intelligence).

Lisitsyn, A.P., 1966, Recent sedimentation in the Berng Sea: Akad. Nauk, U.S.S.R., Moscow, (English transl., 1969, Israel Prog. Scientific Translations), Natl. Sci. Found. - U.S. Commerce Dept., Clearinghouse for Scientific and Technical Information, Springfield, Virginia, 614 p.

Masters, C.E., 1967, Use of sedimentary structures in determination of depositional environments, Mesaverde Formation, Williams Fork Mountains, Colorado: Bull. Am. Assoc. Petroleum Geologists,;v. 51, no. 10, p. 2033 2043.

McManus, D.A., K. Venkataratham, D.M. Hopkins, and Hans Nelson, 1974, Yukon River sediment on the northernmost Bering Sea shelf: Jour. Sed. Petrology, v. 44, no. 4, p. 1052-1060.

McManus, D.A., and C.S. Smyth, 1970, Turbid bottom water on the continental shelf of northern Bering Sea: Jour. Sed. Petrology, v. 40, p. 869-877.

McManus, D.A., K. Venkataratham, D.M. Hopkins, and Hans Nelson, 1977, Distribution of bottom sediments on the continental shelf, northern Bering Sea: U.S. Geol. Survey Prof. Paper 759-C, 30 p.

Mofjeld, H.O., 1976, Tidal currents, in Stanley, D.J., and D.J. Swift (eds.), Marine sediment transport and environmental management: John Wiley and Sons, N.Y., p. 53-64.

Moore, D.G., and P.C. Scruton, 1957, Minor internal structures of some recent unconsolidated sediments: Am. Assoc. Petroleum Geologists Bull., v. 41, p. 2723-2751.

Nasu, K., 1974, Movement of whales in relation to hydrographic conditions in the northern part of the North Pacific Ocean and the Bering Sea, in Hood, D.W. (ed.), Oceanography of the Bering Sea: Occas. Pub. No. 2, Inst. Marine Sci., Univ. Alaska, Fairbanks, p. 345-362.

Nelson, Hans, D.A. Cacchione, M.E. Field, D.E. Drake, and T.H. Nilsen, 1977, Complex ridge and trough topography on a shallow current-dominated shelf, Northwest Alaska: Am. Assoc. Petroleum Geologists Bull., v. 6, p. 817.

Nelson, C.H., and J.S. Creager, 1977, Displacement of Yukon-derived sediment from Bering Sea to Chukchi Sea during the Holocene: Geology, v. 5, p. 141-146.

Nelson, Hans, and D.M. Hopkins, 1972, Sedimentary processes and distributon of particulate gold in the northern Bering Sea: U.S. Geol. Survey Prof. Paper 689, 27 p.

Nelson, Hans, B.R. Larsen, and R.W. Rowland, 1975, ERTS imagery and dispersal of the Yukon and Kuskokwim River plumes, in Carlson, P.R., T.J. Conomos, R.J. Janda, and D.H. Peterson (eds.), Principal sources and dispersal patterns of suspended particulate matter in nearshore surface waters of the northeast Pacific Ocean: ERTS Final Rept; Natl. Tech. Info. Service U.S. Dept. of Commerce, Rept. # E-75-10266, p. 26-40.

Nelson, Hans, 1978, Large-scale bedforms and potential scour areas in northern Bering Sea, in Environmental Assessment of the Alaskan Continental Shelf: annual reports of principal investigators, year ending March, 1977; U.S. Dept. Commerce, Natl. Oceanic Atmos. Admin., Envir. Research Laboratories, Boulder, Colo., p. 120-129.

Neyman, A.A., 1961, Nekotorye Zakonomernosti Kolichestvennogo Raspredeleniya Bentosay Beringovom More (Certain regularities in the quantitative distribution of the benthos in the Bering Sea): Okeanologiya, v. 1, p. 294-304.

Neyman, A.A., 1969, Kolichesvennoye Raspredeleniye bentosa vostochnoy chasti Beringova Morya: Aool. Ahar., v. 39, no. 9, p. 1281-1291, (transl. by Slessers, M., 1968, Quantitative distribution of benthos in Bering Sea: U.S. Naval Oceanographic Office, Wash. D.C., Trans. 402).

Ockelmann, W.K., 1958, Marine Lamellibranchiata (part of) Zoology of East Greenland: Neddelelser om Gronland v. 1222, p. 250.

Petrov, O.M., 1966, Stratigraphy and fauna of the marine mollusks in the Quaternary deposits of the Chukotsk Peninsula: Akad. Nauk SSSR, Geol. Inst., Trudy Moscow, v. 155, 290 p.

Quayle, D.B., 1970, Intertidal mollusks of British Columbia: British Columbia Prov. Mus., Victoria, Canada, Handbook 17, 104 p.

Reineck, H., 1970, Shichtungsarten and gefuge; in Reineck, H. (ed.),Das Watt: Verlag von Waldemer Kramer, Frankfurt-am-Main, p. 36-47.

Reineck, H.E., and I.B. Singh, 1973, Depositional sedimentary environments: Springer-Verlag, New York, 439 p.

Rhoads, D.C., 1970, Mass properties, stability, and ecology of marine muds related to burrowing activity, in Crimes, T.P. and J.C. Harper (eds.), Trace fossils - Proceedings of an international conference at Liverpool University, January 6, 7, and 8, 1970: Geol. Jour. Special Issue No. 3, p. 391-406.

Rhoads, D.C., and D.K. Young, 1970, The influence of deposit-feeding organisms on sediment stability and community trophic structure: Jour. Marine Research, v. 28, no. 2, p. 150-178.

Rowland, R.W., 1972, Ecology of the benthic fauna of the northern Bering Sea: Geol. Soc. of America Abs with Progs., v. 4, no. 7, p. 646.

Rowland, R.W., 1973, The benthic fauna of the northern Bering Sea: Ph.D. thesis, Univ. of Calif., Davis, 234 p.

Saur, J.F.T., J.P. Tully, and E.C. LaFond, 1954, Oceanographic cruise to the Bering and Chukchi Seas, summer 1949, Part IV: Physical oceanographic studies: U.S. Navy Electronics Lab. Rept. No. 416, v. 1, p. 31.

Schafer, Wilhelm, 1972, Ecology and Paleoecology of Marine Environment, University of Chicago Press, 568 p.

Seibold, E.S., N. Exon, M. Hartmann, F.C. Kogler, H. Krumm, G.F. Lutze, R.A.Newton and F. Werner, 1971, Geology of Kiel Bay: in Muller, G. (ed.), Sedimentology of parts of central Europe: VIII International Sedimentological Congress, 1971, International Assoc. of Sedimentology Guide Book: Verlag von Waldemer Kramer, Frankfurt-am-Main, p. 209-236.

Sharma, G.D., F.F. Wright, J.J. Burns, and D.C. Burbank, 1974, Sea-surface circulation, sediment transport, and marine mammal distributon, Alaska continental shelf: (prepared for) Natl., Aeronautics and Space Admin., Goddard Space Flight Center, Greenbelt, Maryland, ERTS Final Rept., Natl. Tech. Info. Service, E 74-107011, 77 p.

Stanley, S.M., 1970, Relation of shell form to life habits in the Bivalvia: Mollusca, Geol. Soc. America Mem. 125, p. 296.

Stoker, S.W., 1973, Winter studies of under-ice benthos on the continental shelf of the northeastern Bering Sea: M.S. thesis, Univ. of Alaska, College, Alaska, 60 p.

Swift, D.J., D.J. Stanley, J.R. Curry, 1971, Relict sediments on continental shelves: A reconsideration: Jour. Geology, v. 79, p. 322-346.

Thor, D.R., Hans Nelson, and J.E. Evans, 1978, Preliminary assessment of ice gouging in Norton Sound, Alaska, in Environmental Assessment of the Alaskan Continental Shelf, Annual Reports of principal investigators, U.S. Dept. Commerce, Natl. Oceanic Atmos. Admin., Envir. Research Laboratories, Boulder, Colo., p. 93 to 110.

Tomilin, A.G., 1957, Mammals of the USSR and adjacent countries, in Heptner, V.G., (ed.), Cetacea v. IX: Israel Prog. Sci. Transl., 1967, 717 p.

U.S. Coast and Geodetic Survey, 1964, United States Coast Pilot, v. 9, Pacific and Arctic Coasts, Alaska: Cape Spencer to Beaufort Sea, 7th Ed.: U.S. Govt. Printing Office, Washington, D.C., 330 p.

Winston, J.E. and F.E. Anderson, 1970, Bioturbation of sediments in a northern temperate estuary: Marine Geology, v. 10, p. 39-49.

TABLE 1 - LIST OF MOST COMMON BIOTURBATING ORGANISMS, AND, WHERE KNOWN, THEIR SUBSTRATE ASSOCIATIONS AND TYPE OF SEDIMENT DISTURBANCE IS GIVEN. WITHIN EACH GROUP THE SPECIES ARE LISTED IN ORDER OF ABUDANCE AND WHERE KNOWN, THE PERCENT OF OCCURRENCE AT SAMPLING STATIONS IS GIVEN IN PARENTHESES IN FRONT OF THE SPECIES.

Depth group	Organism	Substrate and Distribution	Living Habits	Data Source
SURFACE DISTURBERS	Brachyuran crabs *Chionoecetes opilio* *Chionoecetes bairdi* *Hyas coarctatus* *Telmessus cheiragonus*	 Ubiquitous do do	Create shallow surface depressions Same as above	Stoker, unpub Fig. 10
	Anamuran crabs *Pagarus* *Paralithodes* Crangonid shrimp *Crangon*	 Ubiquitous Seasonal and uncertain Ubiquitous		
	Ophiuroid echinoderms *Ophiura sarsi* *Ophiura maculata* *Stegaphiura nodosa* *Gorgonecephalus caryi*	 Muddy silt, nearshore Silty sand	Create extensive surface tracks	Fig.12; Heymen, 1960 Fig. 10 Stoker. unpub
	Echioid echinoderms (6%)*Strongylocentrotus drobachiensis*	 Gravel and pebble lags	Create shallow surface depressions	Fig. 10
SHALLOW BIOTURBATERS	Gastropod mollusks (19%)*Tachyrhynchus erosus* (15%)*Natica* (9%)*Neptunea* (7%)*Polinices* (2%)*Buccinum*	Ubiquitous, most common nearshore Ubiquitous do do	Surface trails and shallow burrows when preying Predatory, drilling bivalves Scavenger creating trails plus shallow burrows Predatory, drilling bivalves Scavenger	Fig. 10 Rowland, 1973 Schafer, 1972
	Bivalve molluska (36%)*Yoldia myalis*	Most common in muddy sediment , but widespread in all environments.	Deposit feeders?	Fig. 10, 11 Rowland, 1973 Stanley, 1970

›th ›up	Organism	Substrate and Distribution	Living Habits	Data Source
	(16%) Yoldia hyperborea or amygdalea	Mud or muddy sand	Deposit feeder?	Figs. 11, 14 Stanley, 197 Rowland, 197
	(15%) Nucula tenuis	do "	do	Figs. 11, Stanley, 197 Rowland, 197
	Nuculana radiata	do "	do	
	Clinocardium ciliatum	Sandy silt substrates	Suspension feeders	Petrov, 1966
	Tellina alternidentata	Current-winnowed clean sand		Figs. 13, 14
	Amphipoda			
	(27%) Protomedeia sp.	Mud and fine sand	Detritus feeders, one or more of these species create U-shaped and vertical burrows with widened circular area	
	(27%) Melita sp.	do		
	(27%) Hippomedon sp.	do		
	(27%) Haploops laevis	do		
	(27%) Pontoporeia femorata	do		
	Polychaeta			
	(8%) Nepthys	Ubiquitous	Errant polychaete Burrows parallel to bottom surface	Fig. 13 Fig. 10
	Haploscoloplos elongata			
	Sternaspis scutata			
	Pectinaria hyperborea	Fine, silty sand nearshore		
	Brada sp.			
	Echinoidea			
	(11%) Echinarachnius parma	Sorted-medium sand on shoals	Shallow horizontal burrows	Fig. 10 Lisitsyn, 19

Depth group	Organism	Substrate and Distribution	Living Habits	Data Source
INTERMEDIATE BIOTURBATERS	Bivalve mollusks			
	(58%) *Serripes groenlandicus*	Ubiquitous	Filter feeder	Fig. 10
	(45%) *Macoma calcarea*	Ubiquitous, sandy silt and sand	Detritus and filter feeder	Coan, 1971
	Venericardia crebricostata	Sandy silt	do	
	Liocyma fluctuosa	Sand and sandy silt	do	
	Echiroidea			
	Echiurus echiurus	Fine to coarse sand	Deposit feeder	
	Amphipoda			
	(28%) *Ampelisca* sp.	Silty sand	Detritus feeder that builds narrow, V-shaped, mucus-lined tube	Figs. 11, 14
	Byblis gaimardi			
	Polychaeta	Ubiquitous		
	Myriochele heeri	Fine sand		Figs. 10, 11
	Onuphis sp.			
	Spiophanes bombyx			
DEEP BIOTURBATERS	Holothuroidea			
	(1%) *Cucumaria calcigera*		Detritus feeder	Fig. 10
	Tunicata			
	(3%) *Polonia corrugata*	Sand to gravel	Filter feeder	Fig. 10
	Bivalve mollusks			
	(26%) *Nya truncata*	Ubiquitous, hard sand or mud	do	Figs. 10, 11 Quayle, 1970
	(1%) *Nya priapus*		do	
	(7%) *Spisula polynyma alaskana*	Sand	Deep burrowers and filter feeders	Chamberlain and Stearns, 1963

oth oup	Organism	Substrate and Distribution	Living Habits	Data Source
	(1%)Sipunculida Golfingia margaritaceum			
DEEP BIOTURBATERS	Polychaeta		All deposit feeders	
	(9%)Lumbrinereis	Ubiquitous	Errant Polychaeta(?)	Fig. 10
	(4%)Amphareta		Tube building	Fig. 10
	Maldane sarsi Praxillella praetermissa Axiothella catenate	Mud and silt	do	

TABLE 2 -CHARACTERISTIC PHYSICAL AND BIOLOGICAL STRUCTURES OF NORTHERN BERING SEA SEDIMENT FACIES

Sediment Facies	Physical Setting	Physical Structures	Biological Structures	Characteristic Biologic Community	Sedimentary Environment	Figures
Yukon Silt Prodelta F_2	Best developed <15 m water depth Low salinity water	Abundant to common-sand lags, sand lenses, small-scale flat and cross lamination, asymetric ripples Rare-ice push features	Rare - 1 mm worm burrows, U-shaped amphipods, deep worm and clam burrows, brittle star tracks	Mainly infauna abundant deposit and common detritus feeders	Suspension deposition with common sediment input and reworking by low-energy traction currents from storm waves and associated bottom currents. Bio-turbation, restricted low salinity.	6 F-G 8B,8E 12A
Yukon silt offshore C_1	<30 m and normal salinity water	Common to abundant sand lenses Rare to common shell and pebble lags with internal structures	Common to abundant 1-mm worm burrows, U-shaped amphipod tubes, deep worm and clam burrows, brittle star tracks	Same as prodelta	Like prodelta, but storm reworking less and bio-turbation not inhibited.	6C,12B 13B and C 13E 14C and D 15F and G
Sorted medium sand B_2	Shoal crests and other current-reworked areas	Common - faint ripples Rare - coarse sand and shell lags (sometimes of sand-dollar fragments) clay stringers, flat lamination	Abundant bivalve and sand dollar reworking - Rare to common 1 and 5 mm worm burrows	Mainly infauna, abundant suspension feeders especially sand dollars, tellinid clams, rare to common detritus and deposit feeders	Relict transgressive sand reworked by strong bottom currents	6I, 8C 13A and D
Chirikov fine sand B_1	Open shaft areas without Holocene hard cover	Absent, except rare storm shell and pebble lags	Rare-surface disturbance and deep burrows Common-small amphipods and 1-mm worm burrows - Common to abundant lg. amphipod burrows.	Mainly infauna with abundant detritus and common deposit feeders.	Relict transgressive sand deposited near-shore by wave suspension and traction processes, now below wave base.	6C and D 6H 14A and B 15A and D 15E
Gravelly medium sands to gravel A_2	Overlie bedrock outcrops or glacial till	Rare-medium-scale, cross-lamination and flat lamination; pebbles well rounded, gravels sorted	Predominant bivalve bioturbation with occasional worm and amphipod burrows	Mainly infauna with abundant suspension feeders and rare detritus and deposit feeders	Relict shoreline sedi-sediment winnowed lag (Swift and others, 1971), now preserved by burial or strong bottom currents	6B 8A 15C
Coarse pebble lags	Overlie bedrock outcrops or glacial till	Internal structures absent, but gravel lag layer is a distinct structure which overlies glacial till. Angular to rounded gravel without matrix	Bioturbation structures not evident, barnacle and bryozoan encrustations, brachipods present	Mainly epifauna anemones, bryazoas, sea urchins, barnacles, crabs, brachipods	Same as A, except not buried and usually present on scarps or elevated topography	6A

FIGURE CAPTIONS

Fig. 1 -Setting, physiography, and location of large-scale bedforms presently known in northern Bering Sea. Bathymetry modified from Hopkins et al. (1976). Large-scale bedforms from Jordan, 1962; Grim and McManus, 1970; L. Toimil, 1975, oral commun., and Nelson, unpublished data.

Fig. 2 -Water masses in northern Bering Sea (modified from Coachman et al., 1976). The Alaskan Coastal water (14 - 31.5 0/00, .8°C) occupies the eastern portion of the study area, the Bering Shelf Water (sometimes called Modified Shelf Water) (31.5-33 0/00, 0-4°C) covers the central area, and the Anadyr Water (33 0/00, 1-3°C) occurs in the western portion of the study area. Data on seasonal salinity changes from Goodman, et al., (1942), G.D. Sharma (1975, written commun.) and Nelson et al., (1975). Data on shorefast ice margin from Thor et al., (1977).

Fig. 3 -Offshore water circulation (from Goodman et al., 1942), and maximum bottom current velocities from available measurements in northern Bering Sea (from Fleming and Heggarty, 1966; Husby, 1971; McManus and Smyth, 1970; Nelson and Hopkins, 1972).

Fig. 4 -Surface sediment distributon in northern Bering Sea (modified from Nelson and Hopkins, 1972; Knebel and Creager, 1973; McManus et al., 1974, 1977).

Fig. 5 -Box core locations and descriptions of physical sedimentary structures observed in the upper 40 cm of sediment in northern Bering Sea. Structures in relict transgressive deposits and figure numbers of text photos are keyed to location.

Fig. 6 -Lag and storm layers in northern Bering Sea sediments: locations of box core photos shown in Fig. 5. Individual centimeter scale is shown in lower right corner of each photograph or radiograph.

Fig. 6A -Transgressive lag gravel over glacial till shown in box core slab face. Note Hemithyris psittacea (brachiopod) and bryozoan skeletons on surface. 41 m water depth.

Fig. 6B -Epoxy cast of box core containing thick, well-sorted transgressive lag gravel from -30 m shoreline stillstand (Nelson and Hopkins, 1972). Note faint cross-bedding in center of cast, 30 m water depth.

Fig. 6C -Box core slab face exhibiting shell lag at base of transgressive fine-grained sand. The shell layer was composed of equal amounts of Mya tella arctica and Macoma calcarea and probably formed as a storm lag during lower sea level. The layer was found in an isolated small basin at 43 m water depth.

Fig. 6D -Bioturbated coarse sand and shell layer composed entirely of Echinarachnius parma (sand dollars) in current-winnowed fine sand over a shoal crest, 35 m water depth.

Fig. 6E -Box core slab face showing thick light-colored storm sand layers in Yukon silt 30 km from the modern Yukon subdelta. Note that the thick upper sand most recently formed is not bioturbated, whereas only cross-laminated sand lenses remain in the lower bioturbated bed. 11 m water depth.

Fig. 6F -Radiograph of well-defined thin storm sand layers in late Holocene Yukon silt 75 km offshore from the present subdelta. Thoroughly bioturbated older Yukon silt underlies well-structured beds in younger Yukon silt (after Nelson and Creager, 1977). Note rippled and wavy bedded sand beds (light-colored) with small-scale cross and flat lamination. 16 m water depth.

Fig. 6G -Radiograph showing shell and pebble lags in the upper and lower parts of the core and numerous thin sand layers in between. Both probably developed by storm reworking of Yukon silt located 110 km from the present Yukon subdelta. Note that upper shell lag is only slightly disrupted, whereas basal layers are highly bioturbated. The middle unbioturbated section has sand beds (light-colored) that exhibit discontinuous parallel bedding in the upper two layers and nonparallel and lenticular bedding in the lower three layers. Wood at the core base had an age of 2,120 years BP (Teledyne Isotopes sample No. I-7320). Note the 1-mm-diameter burrows in the upper part of the core that probably are caused by polychaete worms (see Howard, 1969, Figs. 8, 13 and Hertweck, 1972, Figs. 3, 5). 14 m water depth.

Fig. 6H -Radiograph showing bioturbated shell and pebble lag layers (lower half of core) in transgressive coarse to medium sand. Lag apparently developed during the Holocene transgression. Overlying fine-grained transgressive sand in the upper half of the core is highly bioturbated by amphipods and clams. 47 m water depth.

Fig. 6I -Box core slab face of medium-grained sand from a shoal crest containing coarse sand lag layers and clay laminae probably formed by current reworking. 31 m water depth.

Fig. 6J -Yukon silt containing a large rafted pebble. Note thin sand lenses near the surface. 18 m water depth.

Fig. 7 Frequency of various physical sedimentary structures in different depth, substrate, and topographic settings.

Fig. 8 -Internal physical sedimentary structures.

Fig. 8A -Radiograph showing the following sequence: transgressive fine-grained sand overlying transgressive pebbly medium-grained sand with flat lamination and medium-scale cross-lamination, which overlies pre-transgressive limnetic clays with freshwater ostracodes (P. Valintin, written commun., 1971). Note deep burrowing probably by Mya sp., after marine transgression (see Fig. 29 of Mya arenaria burrows shown in Reineck, 1970). 36 m water depth.

Fig. 8B -Plan section of a ripple set impression at a parting surface near the bottom of a box core, together with an epoxy slab cross section (adjacent upper right) showing the same dark-colored lower sand layer and another surface sand layer. Note that apparent ripple crests (dotted line) are

irregular and asymmetric with tongue-like projections (cf. with Harms et al., 1975, Fig. 3-7 and Reineck and Singh, 1973, Fig. 30). Ripple index (length/height) is 5-8 basal and 10-12 for surface sand layers. 12 m water depth.

Fig. 8C -Radiograph of remnant asymmetric ripples that have been altered by bioturbation of medium-grained shoal crest sand. 21.9 m water depth.

Fig. 8D -Core slab face showing loading, slump or ice-disrupted structures (near the core bottom) in laminated late Pleistocene mud deposited before the Holocene transgression. Mud contains freshwater ostracodes (see reference for 8a). These have an age of 14,920 BP (Teledyne Isotopes No. I-7318) based on organic carbon from a whole sediment sample. 51 m water depth.

Fig. 8E -Radiograph showing highly contorted sand lags possibly caused by ice push or scour of the sea floor. Note shallow u-shaped burrows caused by small amphipods and large, deep burrow (on the right) probably made by a clam. 12 m water depth.

Fig. 9 -Sonographs and underwater TV and camera photographs of sea-floor surface features.

Fig. 9A -Sand dollar pavement covering current-winnowed shoal crest at 36 m.

Fig. 9B -Oscillation ripples on sand ridge crest at 9 m during severe storm.

Fig. 9C -Asymmetric ripples on similar shoal crest, as 9B, with strong unidirectional currents during non-storm conditions in 17 m water depth.

Fig. 9D -Sonograph showing large-scale sand waves over crests of sand ridges at 30 m water depth.

Fig. 9E -Sonograph showing intense ice scour that covers most of sea floor in 10-20 m of water (14 m water depth). There is no side-scan data in less than 10 m of water.

Fig. 10 -Frequency of various surface, shallow (0-5 cm), intermediate (0-10 cm) and deep (0->10 cm) bioturbating species versus water depth, substrate, and topographic setting.

Fig. 11 -Distribution of the most common shallow (0- 5 cm) (A), intermediate (0-10 cm)(B) and deep (0->10 cm) (C) biological structures that could be identified. Note that small amphipod tubes in A, ampeliscid tubes in B, and unidentified deep burrows in C are present everywhere in at least rare quantities.

Fig. 12 -Surface-disturbing organisms and sea-floor traces in northern Bering Sea. Fig. 12A-Photo of box core surface showing surface trails of brittle star Ophiura sarsi on Yukon silt. 14 m water depth.

Fig. 12B-Serripes groenlandicus that has severly disturbed the box core surface of Yukon silt. 18 m water depth.

Fig. 13 -Shallow burrowing (0-5 cm) organisms and their structures in Northern Bering Sea.

Fig. 13A-Ampharete sp. burrows shown in radiograph of core 207. Sediment type is claycy silt. 42 m water depth.

Fig. 13B-Field photograph of Amphicrete sp. tubes and worms from box core 207 surface just after collection.

Fig. 13C-Photograph of box core vertical and horizontal surface showing cemented tubes and subsurface mucus-lined burrows of sabellid-terribellid worms that occur in large numbers within muddy gravels. Note also the live shallow burrowing Yoldia sp. in the upper center of photograph. 27 m water depth.

Fig. 13D-Photograph of box core vertical slab face showing burrow of tunicate Pelonia corrugata in fine-grained transgressive sand. Note characteristic corrugations of burrow. 44 m water depth.

Fig. 13E-Field box core photograph showing Holothurian Cucumaria calcigera burrowing vertically downward through very fine sand. 37 m water depth.

Fig. 13F-Photo of box core vertical slab surface showing burrowing of polychaete worm (probably Lumbrinereis) in fine-grained sand. 19.6 m water depth.

Fig. 13G-Box core photo of horizontal burrow of Macoma brota from specimen living at the time of core collection. Sediment is Yukon silt and burrow is at a depth of 7 cm from the sediment water interface. 19 m water depth.

Fig. 14 -Intermediate burrowing (0-10 cm) organisms and their structures.

Fig. 14A-Radi-graph of large amphipod (Ampelisca macrocephala) tube structures occurring in great abundance in fine transgressive sand of central Chirikov Basin. Box core 237 from 27 m water depth.

Fig. 14B-Field photograph of surface of box core 237 taken immediately after collection. Silt-like, mucus-lined burrows shown are typical of large amphipod species Ampelisca macrocephala.

Fig. 15 -Deep burrowing structures and organisms.

Fig. 15A-Sand dollar (Echinarachnius parma) burrowing in medium sands of a shoal crest; photo of box core surface was taken in the field immediately after collection; it shows organisms in living position. 31 m water depth.

Fig. 15B-Radiograph of box core 103 from Yukon mud showing numerous u-shaped and straight 5-mm burrows assumed to result from burrowing of small amphiped species (see 11C). Note that nearly all storm sand layers structures are destroyed in the upper core but some sand lamination and rippling remain in the lower core. 19 m water depth.

Fig. 15C-Field photograph of surface of box core 103 taken immediately after collection; surface holes of small amphipods are apparent and appear to be responsible for u-shaped burrows observed in 11B.

Fig. 15D-Core photograph showing horizontal shallow burrowing pattern of polychaete Nepthys in Yukon silt. (T. Roonan, oral commun., 1976). 20 m water depth.

Fig. 15E-Field photograph of living Yoldia sp. on surface and intermediate burrowing Serripes groenlandicus within fine-grained sand. 20 m water depth.

Fig. 15F-Radiograph showing shallow burrowing tachyrhynchus crosus in Yukon silt. 14 m water depth.

Fig. 16 -Conceptual model showing importance of physical structures versus biological structures in shelf sediments. Thickness of wedge depicts relative intensity of process from high energy to low energy shelf environments. Current and wave fields could be various sizes depending on current or wave domination of a particular shelf. All areas of physical structures would shift seaward with higher energy (see arr or toward shore with lower energy. Unidirectional current features on shelves will be more common seaward of nearshore wave structures but the frequency of structures will relate to current intensity rather than distance seaward (for example, see Fig. 7)

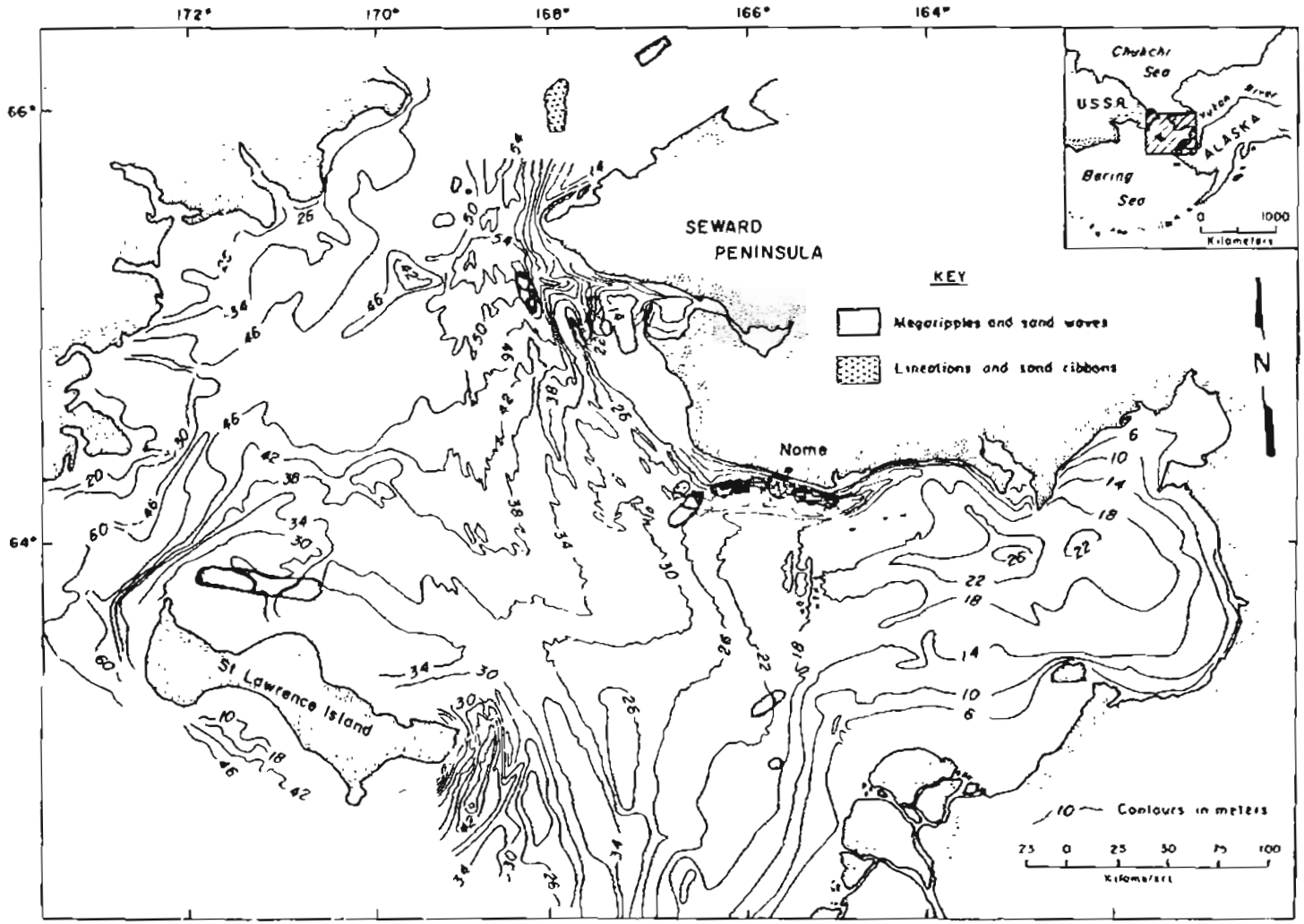
172°
170°
168°
166°
164°
66°
64°
SEWARD
PENINSULA
Nome
St Lawrence Island
KEY
Megaripples and sand waves
Lineations and sand ribbons
N
Chukchi
Sea
USSR
ALASKA
Bering
Sea
0
1000
Kilometers
10 — Contours in meters
25 0 25 50 75 100
Kilometers

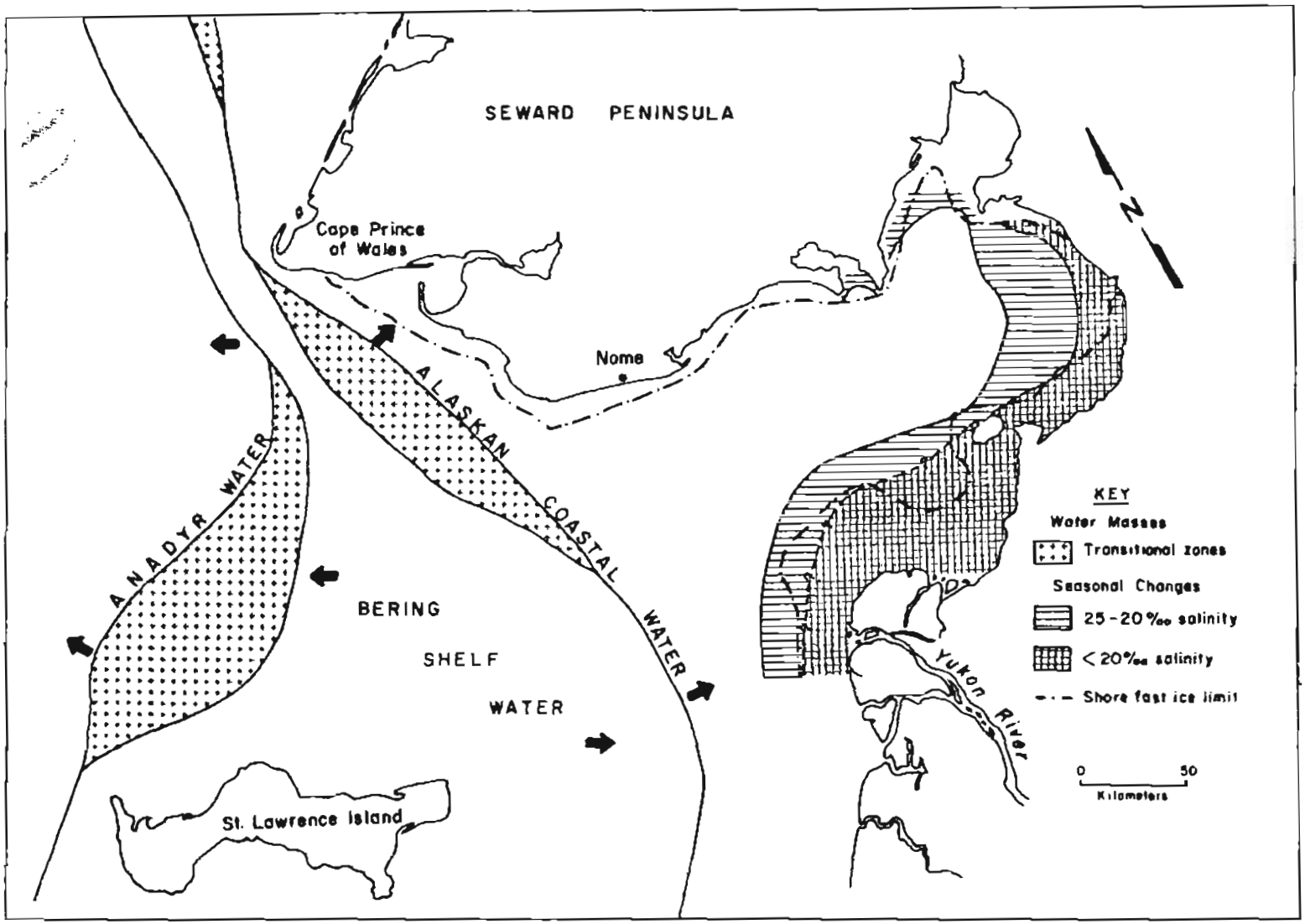
SEWARD PENINSULA
Cape Prince of Wales
Nome
ALASKAN COASTAL WATER
ANADYR WATER
BERING SHELF WATER
St. Lawrence Island
Yukon River
N
KEY
Water Masses
Transitional zones
Seasonal Changes
25-20‰ salinity
<20‰ salinity
Shore fast ice limit
0
50
Kilometers

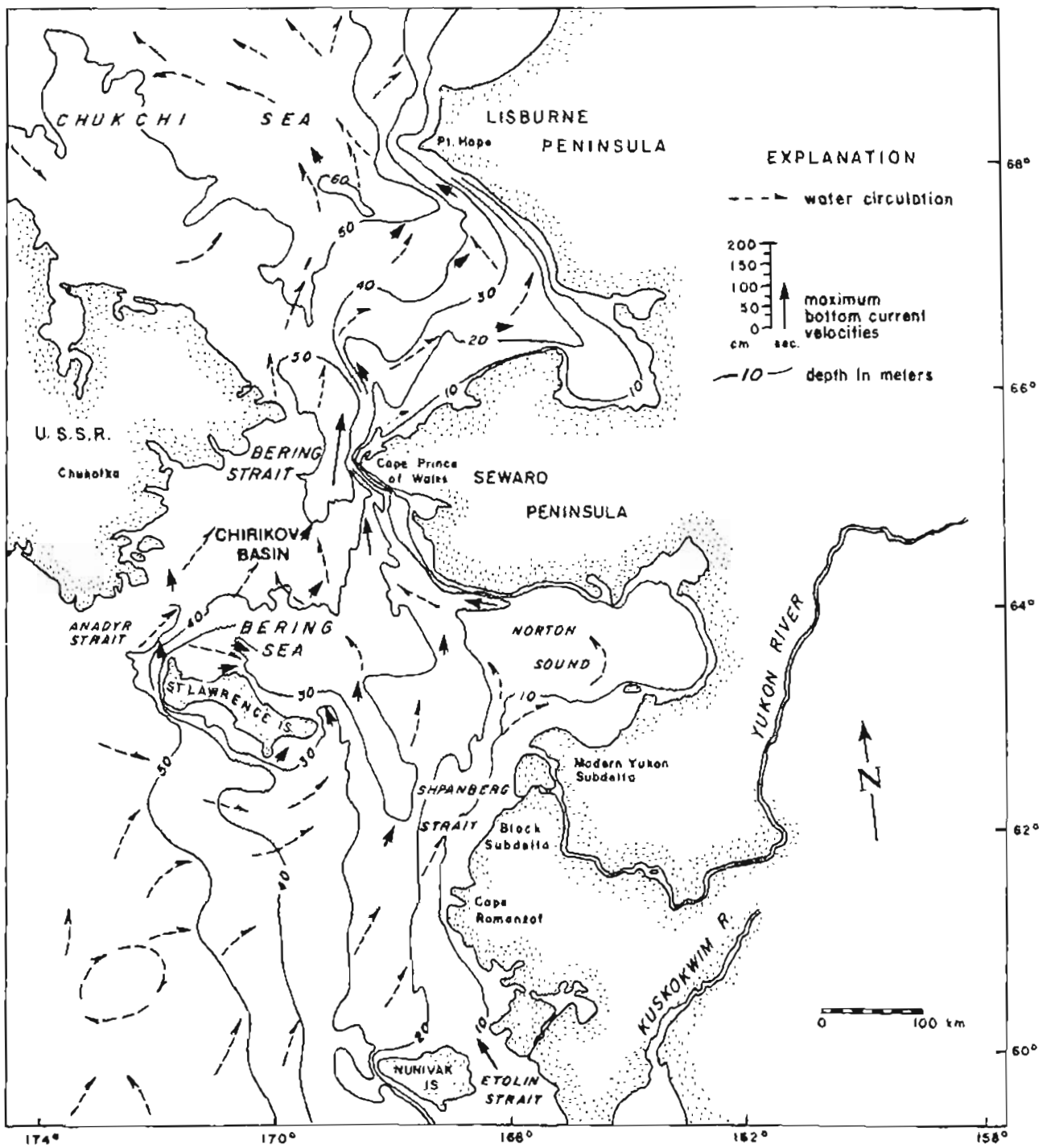
CHUKCHI SEA
LISBURNE PENINSULA
Pt. Hope
EXPLANATION
water circulation
200
150
100
50
0
cm sec.
maximum bottom current velocities
10
depth in meters
U.S.S.R.
Chukotka
BERING STRAIT
Cape Prince of Wales
SEWARD PENINSULA
CHIRIKOV BASIN
ANADYR STRAIT
BERING SEA
NORTON SOUND
YUKON RIVER
ST LAWRENCE IS
SHPANBERG STRAIT
Modern Yukon Subdelta
Block Subdelta
Cape Romanzof
KUSKOKWIM R.
NUNIVAK IS
ETOLIN STRAIT
N
0 100 km
68°
66°
64°
62°
60°
174°
170°
168°
162°
158°

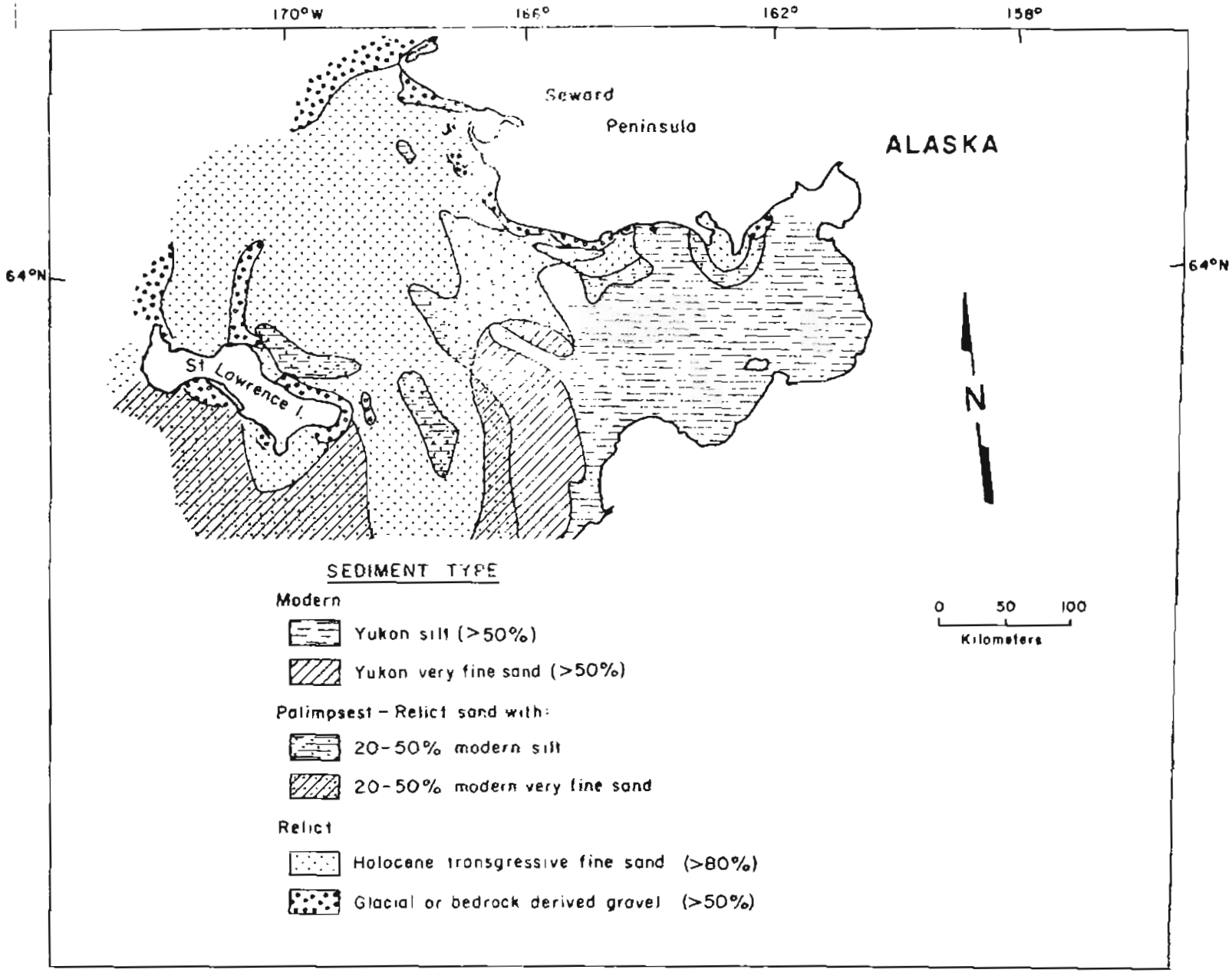
170°W
166°
162°
158°
64°N
64°N
Seward
Peninsula
ALASKA
St Lawrence I.
N
SEDIMENT TYPE
Modern
Yukon silt (>50%)
Yukon very fine sand (>50%)
Palimpsest – Relict sand with:
20-50% modern silt
20-50% modern very fine sand
Relict
Holocene transgressive fine sand (>80%)
Glacial or bedrock derived gravel (>50%)
0 50 100
Kilometers

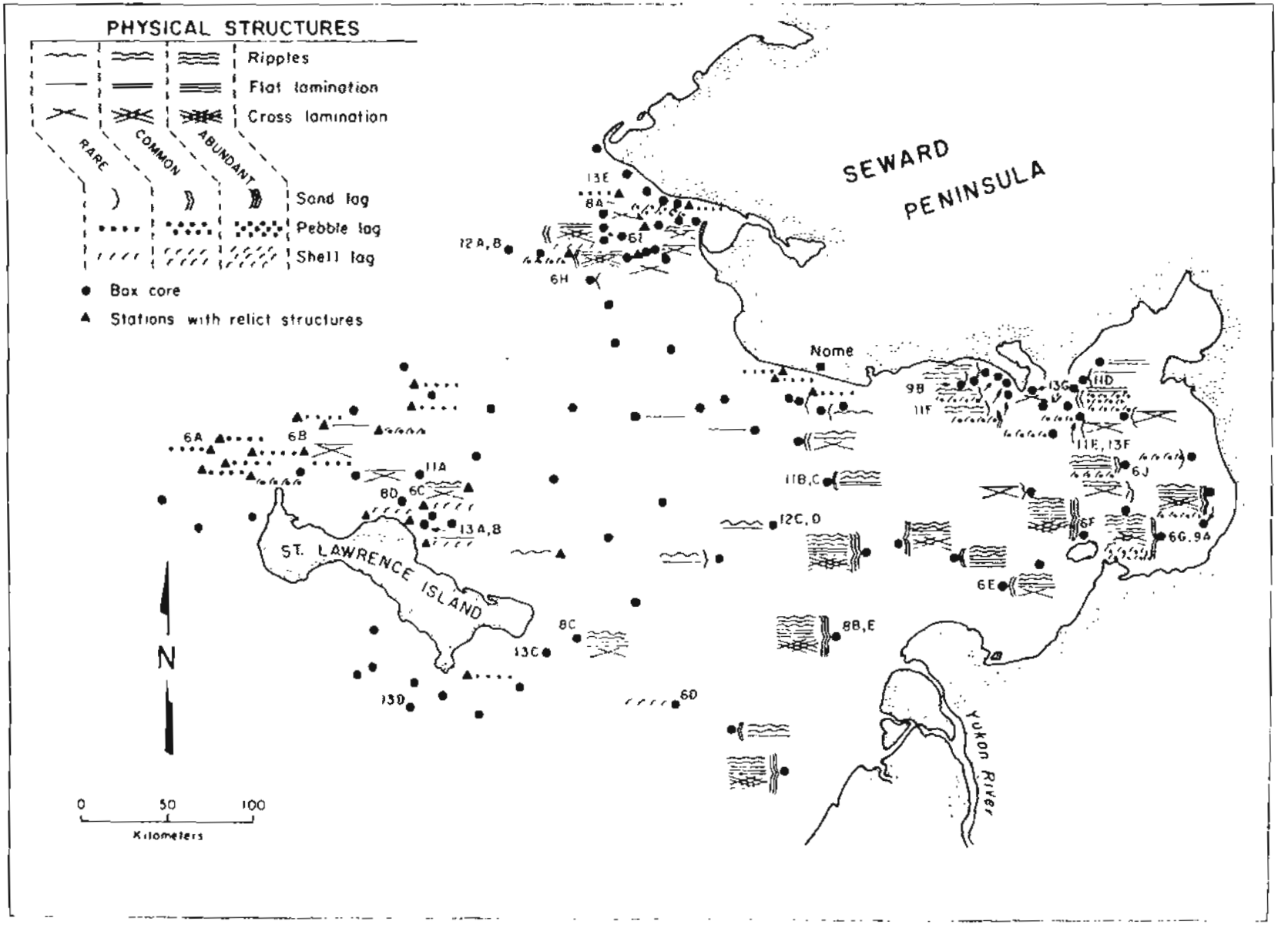
PHYSICAL STRUCTURES
Ripples
Flat lamination
Cross lamination
RARE
COMMON
ABUNDANT
Sand lag
Pebble lag
Shell lag
Box core
Stations with relict structures
SEWARD PENINSULA
Nome
ST. LAWRENCE ISLAND
Yukon River
N
0
50
100
Kilometers

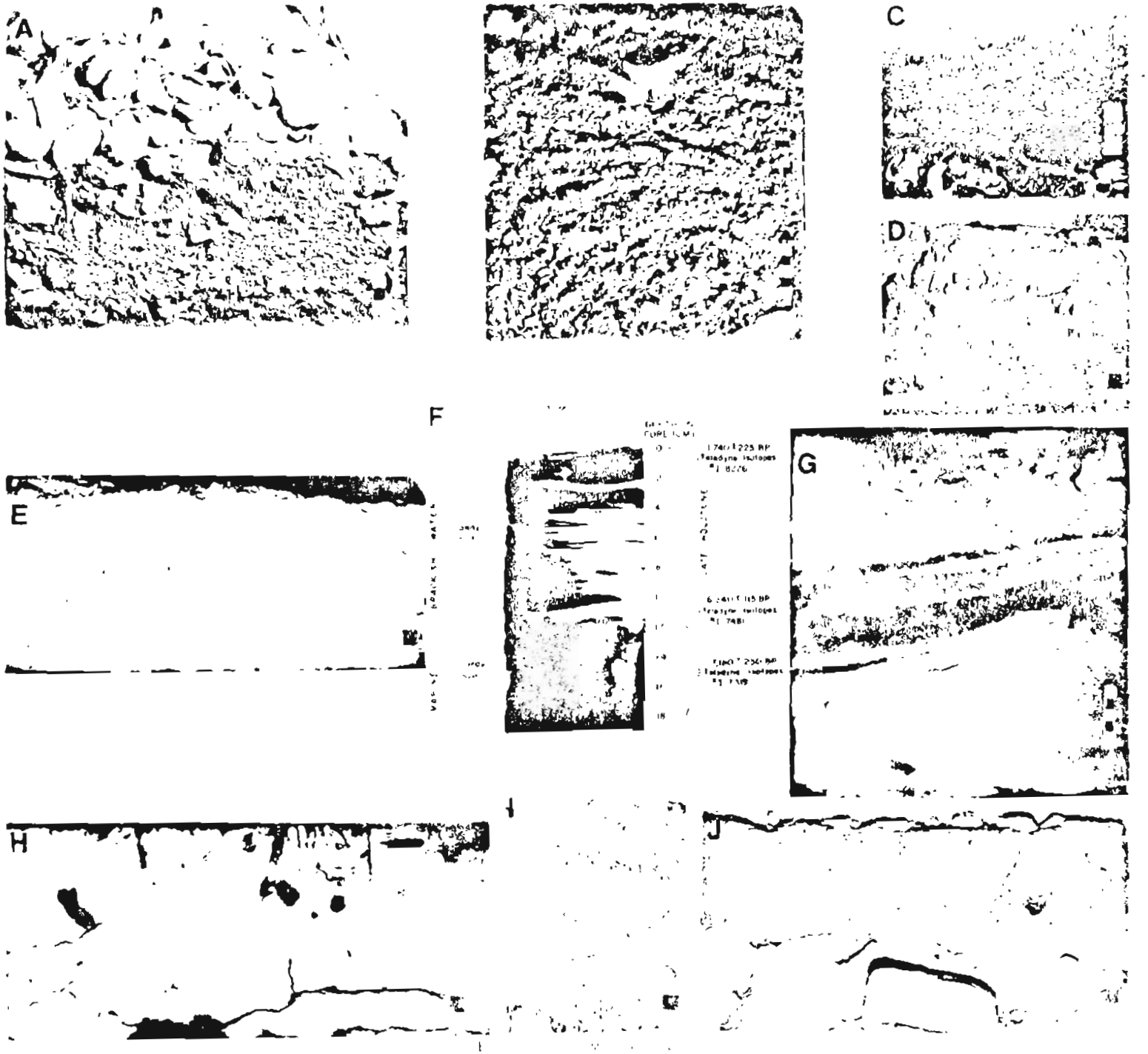
A
C
D
F
E
G
H
J

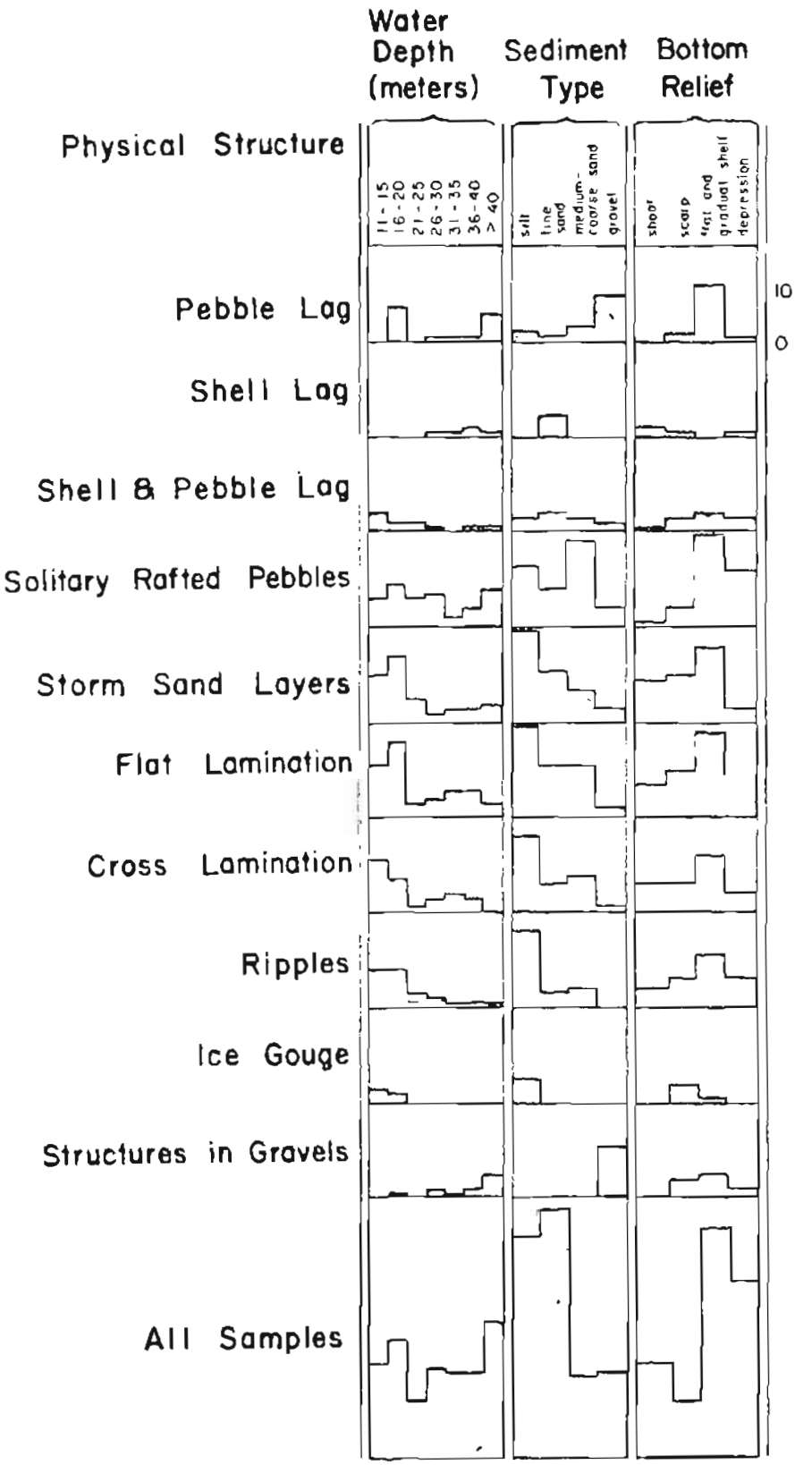
Water Depth (meters)
Sediment Type
Bottom Relief
Physical Structure
11 - 15
16 - 20
21 - 25
26 - 30
31 - 35
36 - 40
> 40
silt
fine sand
medium - coarse sand
gravel
shoal
scarp
flat and gradual shelf depression
Pebble Lag
Shell Lag
Shell & Pebble Lag
Solitary Rafted Pebbles
Storm Sand Layers
Flat Lamination
Cross Lamination
Ripples
Ice Gouge
Structures in Gravels
All Samples
10
0

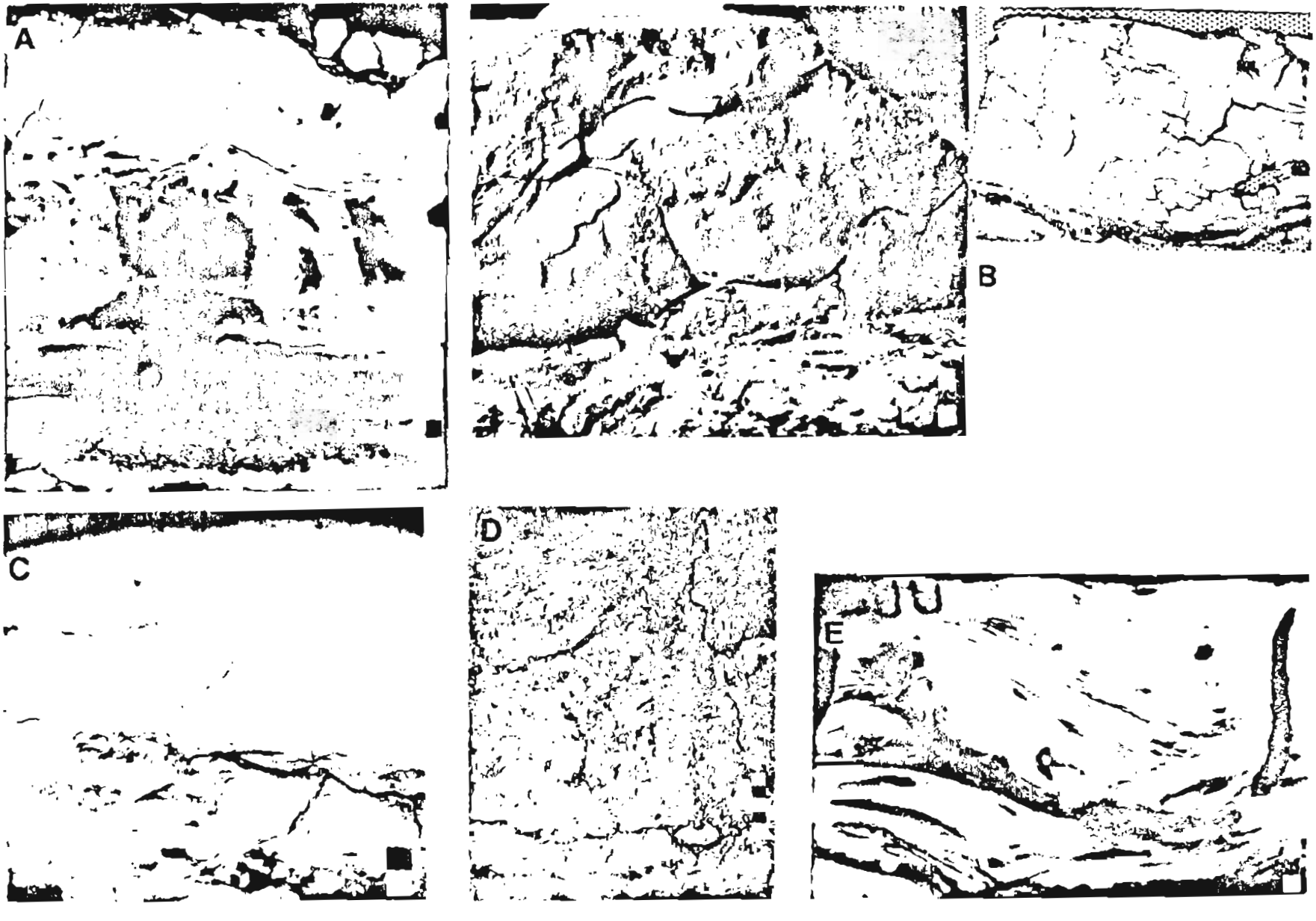
A
B
C
D
E

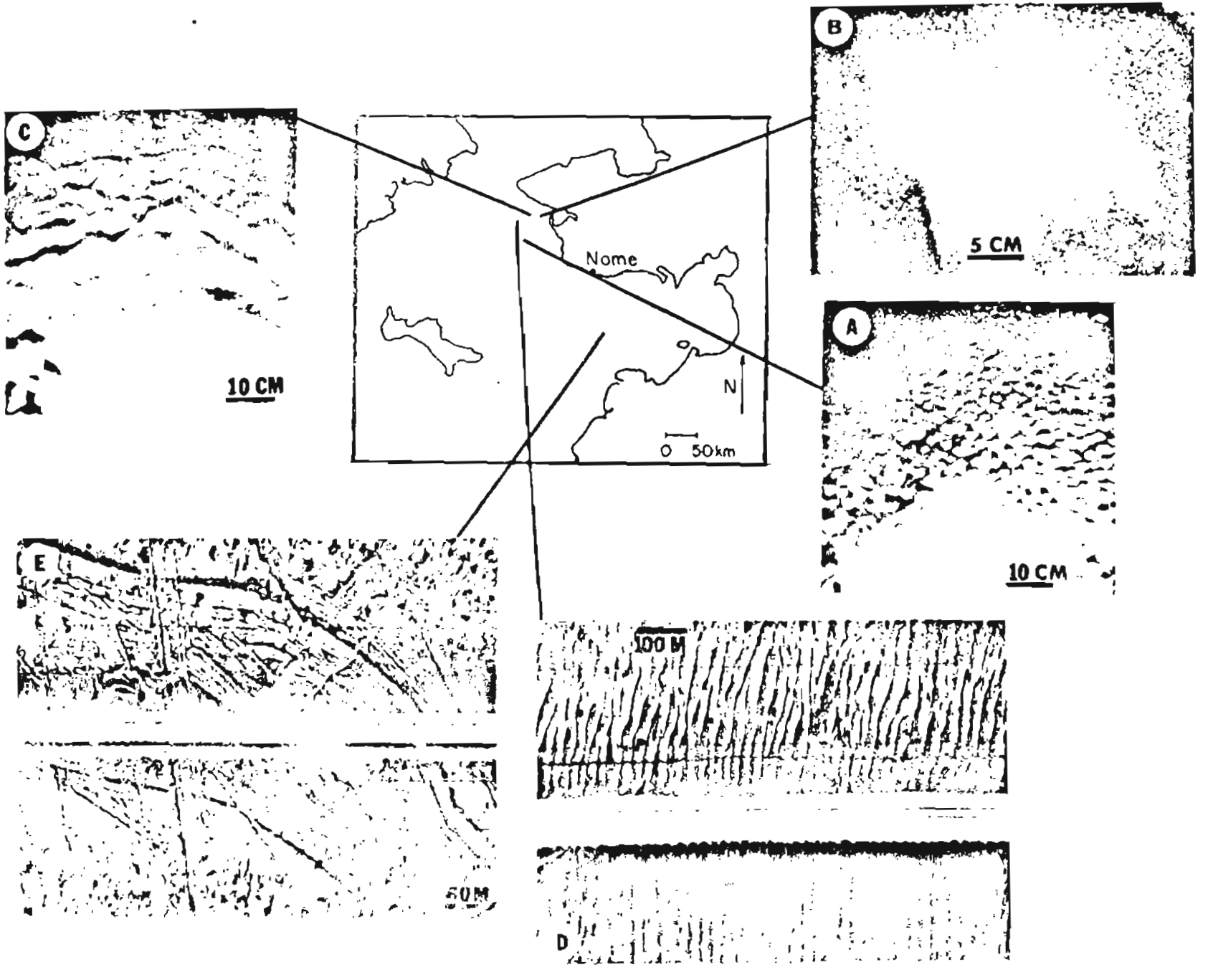
B
5 CM
C
10 CM
Nome
N
0 50km
A
10 CM
E
100 M
50M
D

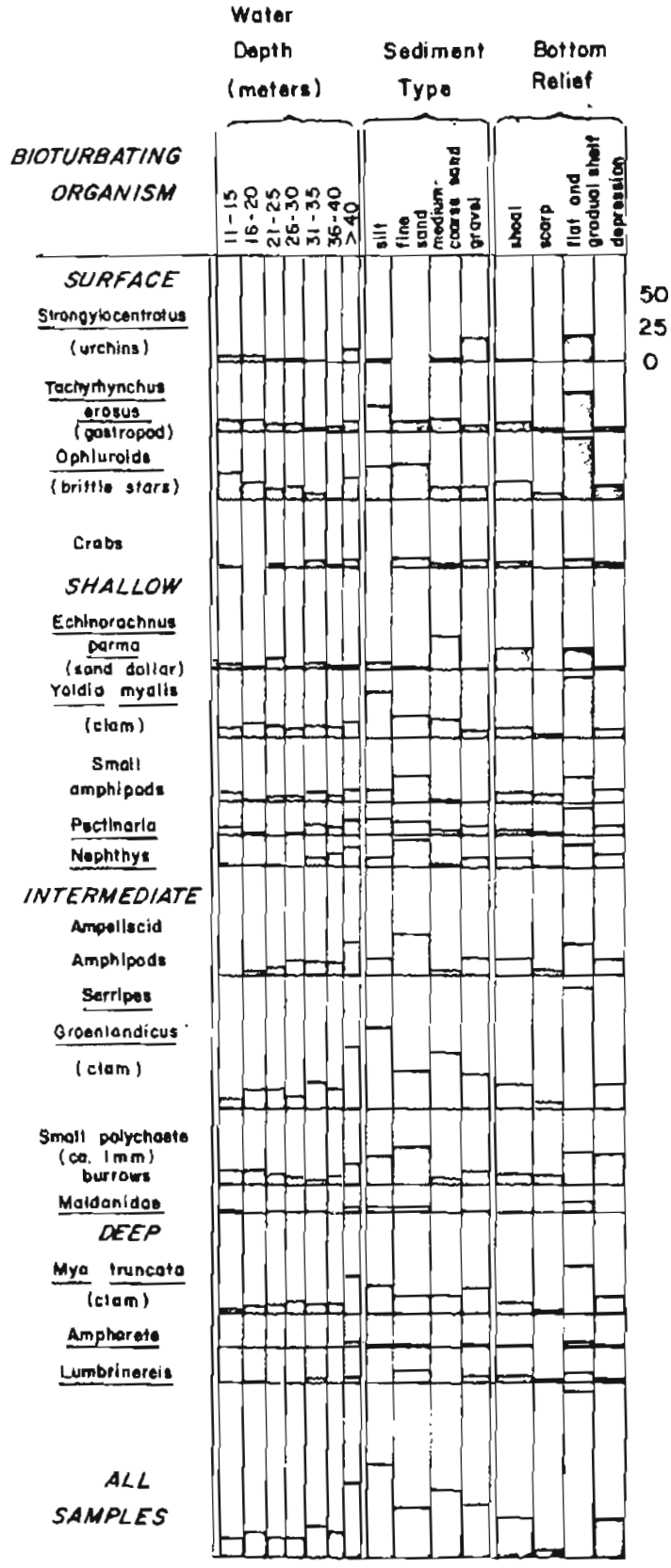
Water Depth (meters)
Sediment Type
Bottom Relief
BIOTURBATING ORGANISM
11 - 15
16 - 20
21 - 25
26 - 30
31 - 35
36 - 40
>40
silt
fine sand
medium - coarse sand
gravel
shoal
scarp
flat and gradual shelf
depression
SURFACE
Strongylocentrotus (urchins)
Tachyrhynchus erosus (gastropod)
Ophiuroids (brittle stars)
Crabs
SHALLOW
Echinarachnus parma (sand dollar)
Yoldia myalis (clam)
Small amphipods
Pectinaria
Nephthys
INTERMEDIATE
Ampeliscid Amphipods
Serripes Groenlandicus (clam)
Small polychaete (ca. 1mm) burrows
Maldanidae
DEEP
Mya truncata (clam)
Amphorete
Lumbrinereis
ALL SAMPLES
50
25
0

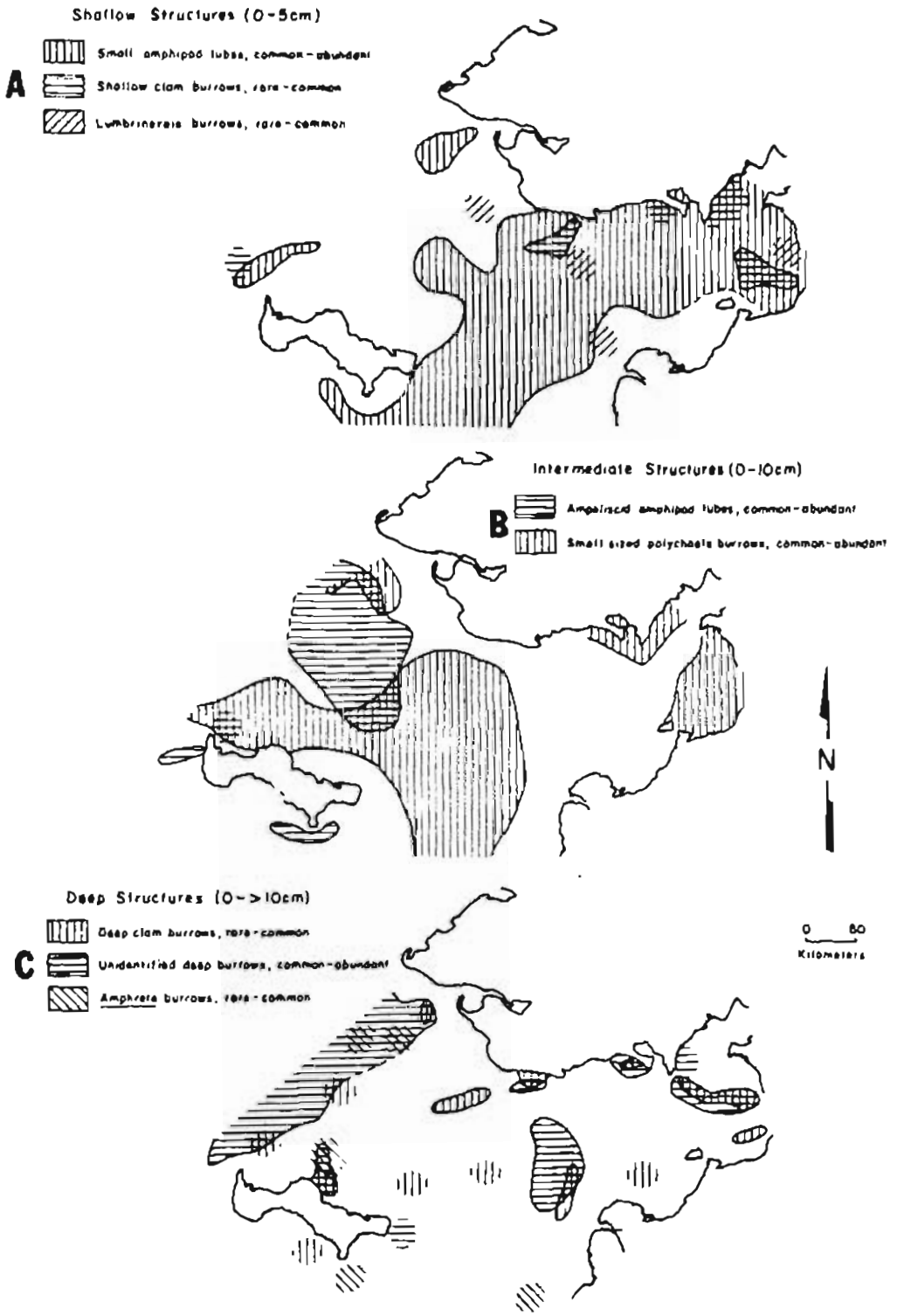
Shallow Structures (0-5cm)
A
Small amphipod tubes, common-abundant
Shallow clam burrows, rare-common
Lumbrineris burrows, rare-common
Intermediate Structures (0-10cm)
B
Ampelisca amphipod tubes, common-abundant
Small sized polychaete burrows, common-abundant
N
Deep Structures (0->10cm)
C
Deep clam burrows, rare-common
Unidentified deep burrows, common-abundant
Amphiura burrows, rare-common
0 80
Kilometers

SURFACE DISTURBERS.

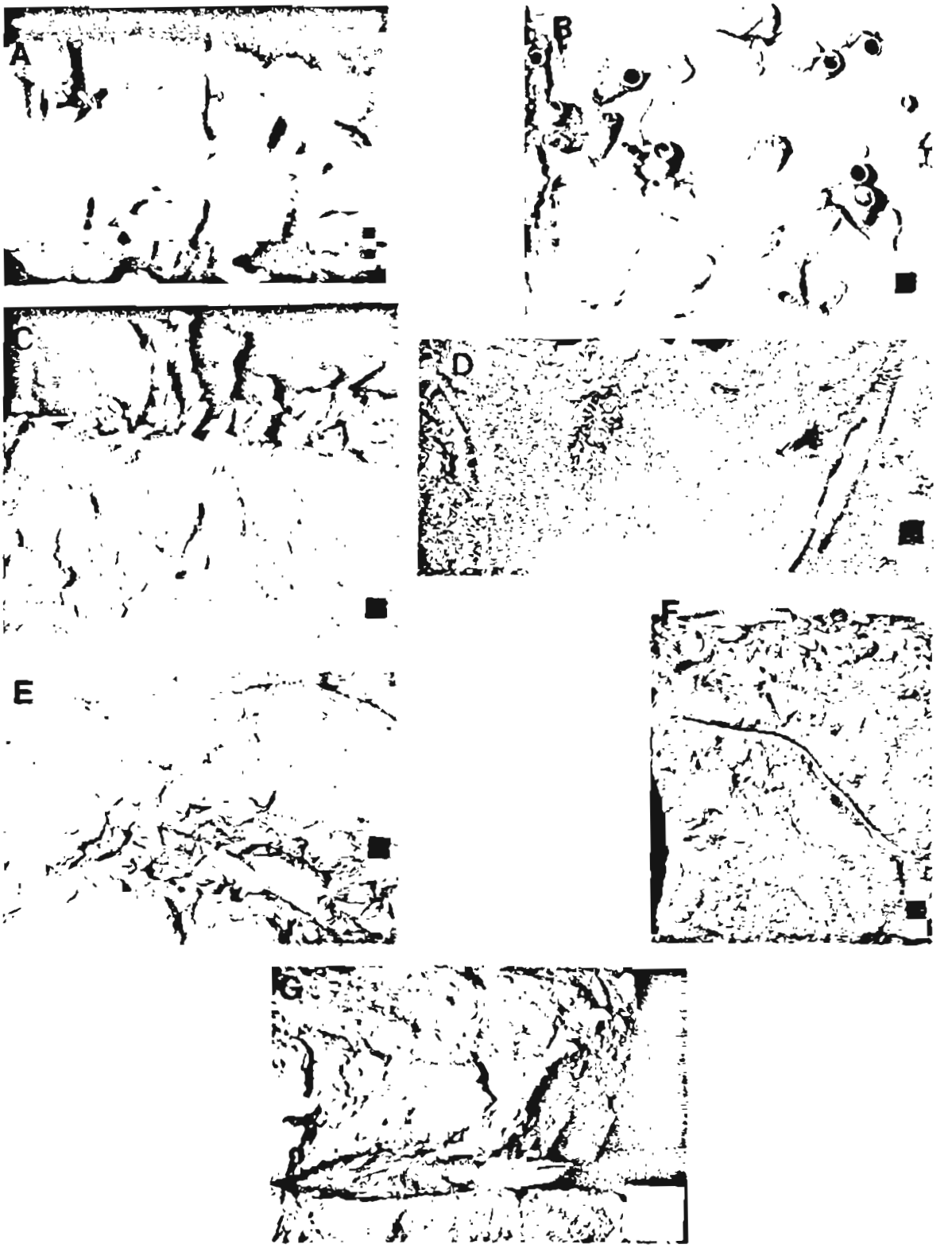

SHALLOW BURROWERS (0–5 CM DEPTH).

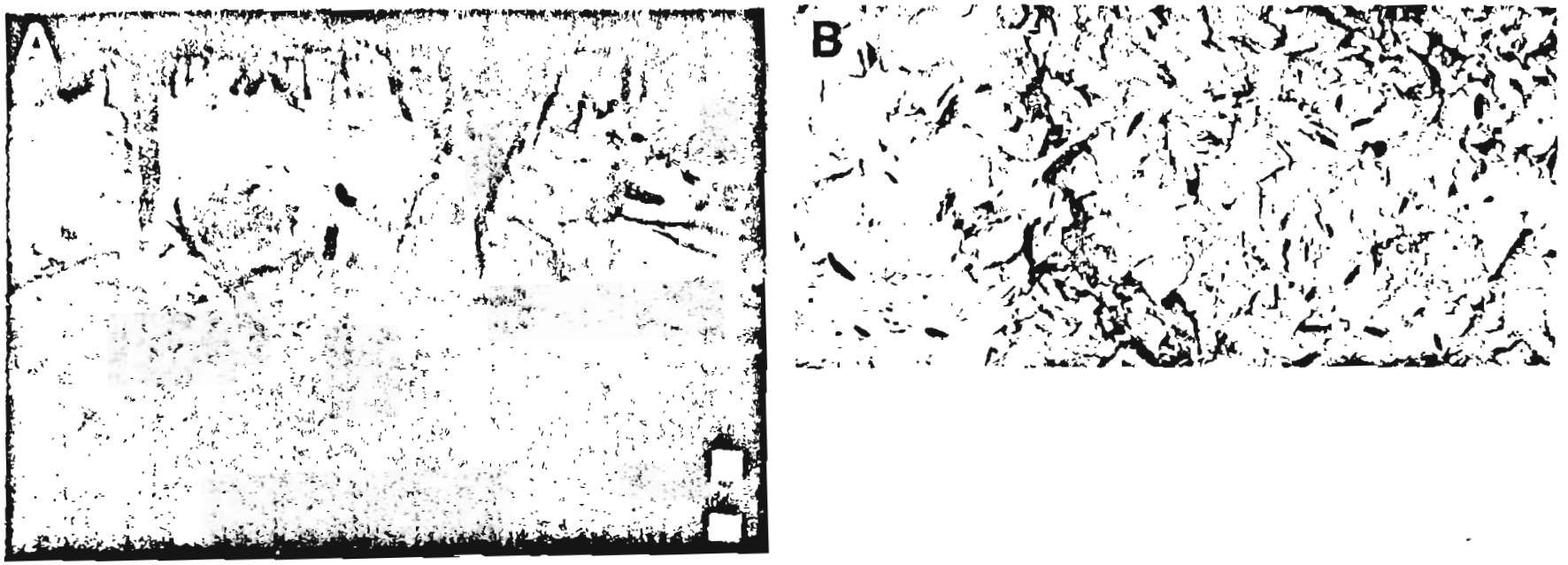

INTERMEDIATE BURROWERS (0-10 CM DEPTH)

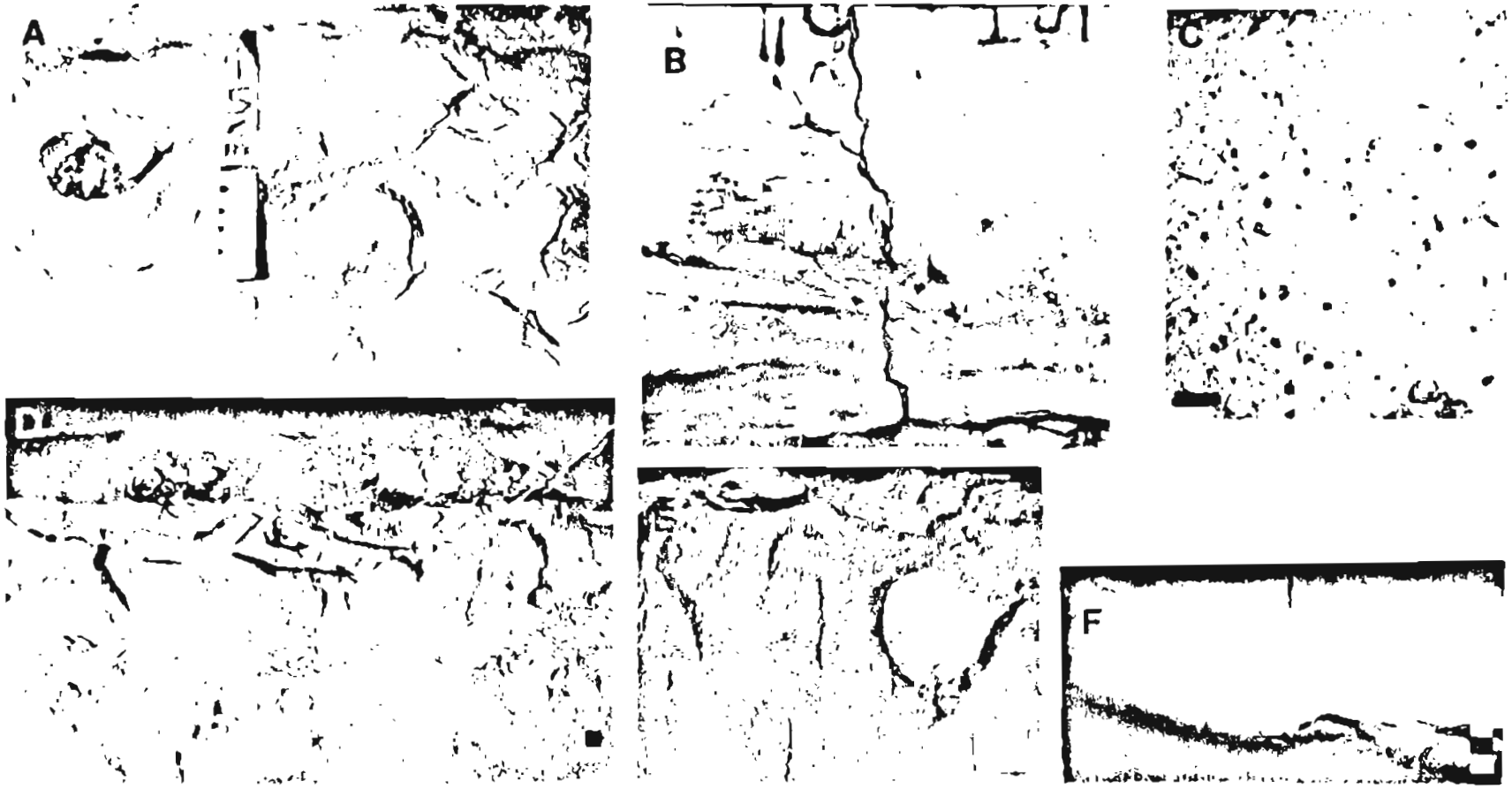

DEEP BURROWERS (0->10 CM DEPTH).

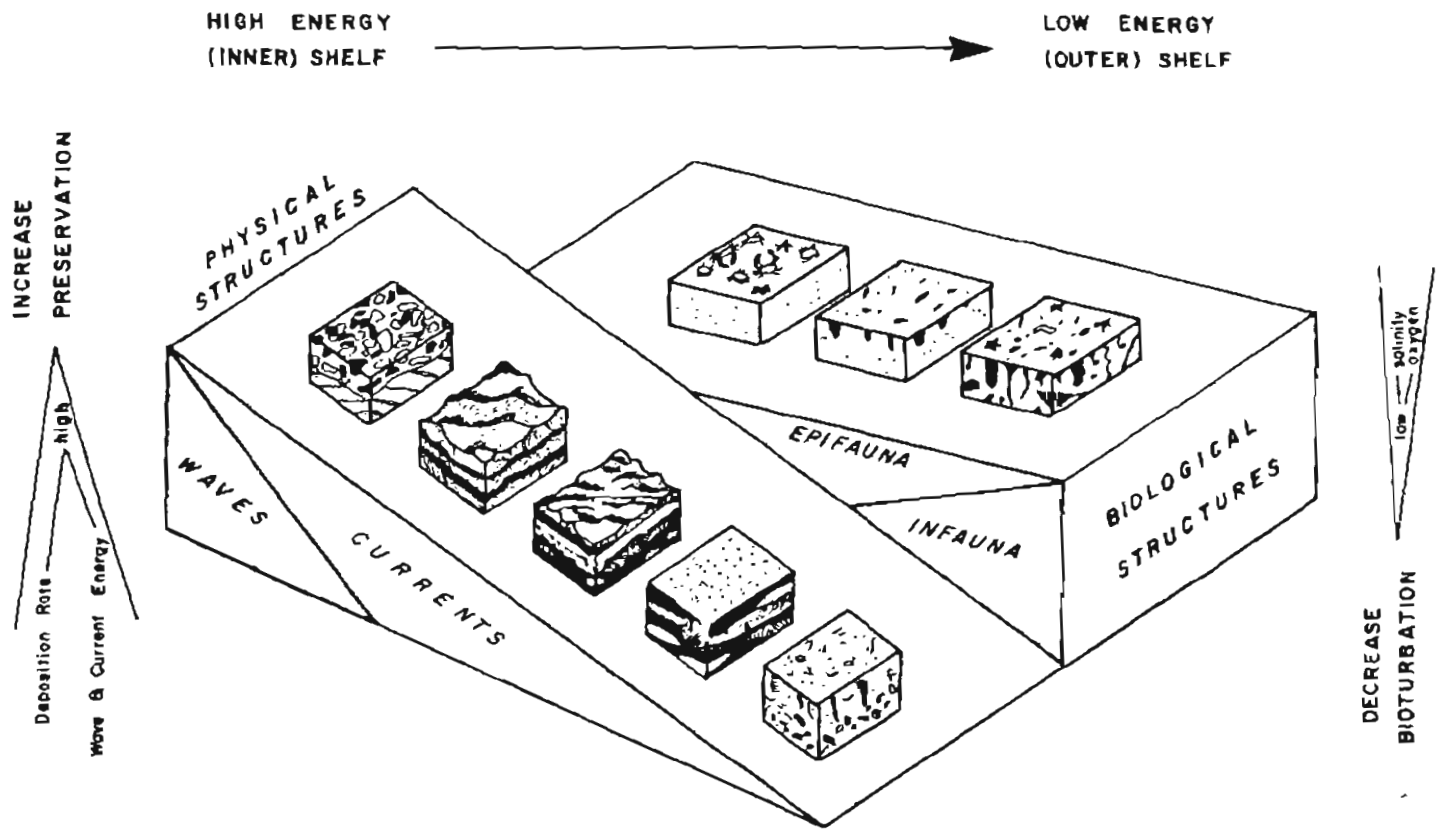
HIGH ENERGY
(INNER) SHELF
LOW ENERGY
(OUTER) SHELF
INCREASE
PRESERVATION
Deposition Rate
high
Wave & Current Energy
PHYSICAL
STRUCTURES
WAVES
CURRENTS
EPIFAUNA
INFAUNA
BIOLOGICAL
STRUCTURES
low
salinity
oxygen
DECREASE
BIOTURBATION

Ripples and Sand Waves in Norton Basin; Bed-form Activity, and Scour Potential

C. Hans Nelson, Michael E. Field, David A. Cacchione, David E. Drake, and Tor H. Nilsen

INTRODUCTION

Strong currents are present throughout much of the northern Bering Sea, particularly where westward land projections interject into the prevailing northward flow, such as in the eastern Bering Strait area (see fig 1, Nelson, Holocene transgression article this volume) (Fleming and Heggarty, 1966). In such regions large bedforms develop and migrate to form an unstable sea floor that can be a potential hazard to platform foundations and pipelines. Such potentially hazardous areas must be identified, their history assessed, and magnitude of future problems predicted. This paper outlines regions of mobile bedforms (fig. 1) and presently known aspects of their activity.

Identification and Distribution of Bedform and Scour Features

Large bedforms and scour features have been recognized and mapped with side-scan sonar profiles and basic internal structure sometimes has been determined by high-resoltuion profiles (fig. 2). Detailed surficial observations have been made with underwater television and bottom photos, and subsurface stratigraphic history has been determined by analyses of vibracores and box cores (figs. 3 and 4).

In general, only small-scale bedforms and large-scale scour features are found in Norton Sound (fig. 1) (Larsen et al., 1979). In contrast, Chirikov Basin is characterized by coarser grain size than Norton Sound (see fig. 6, Nelson, Holocene trangression article this volume) (Nelson and Hopkins, 1972; McManus et al., 1974 and 1977), and numerous fields of mobile bedforms (fig. 1). In the vicinity of Sledge Island, most of the sea floor has been stripped bare of sediment (Nelson and Hopkins, 1972), suggesting intense current scour (fig. 1). Just east and west of the scoured region and extending across the nearshore area of the Nome coastal plain, extensive sand wave and ripple fields are found (fig. 1) (Hunter and Thor, this volume).

From Pt. Spencer spit west to King Island a series of sand ridges and swales exist (fig. 2). The crest of each shoal is covered with sand waves of varying types and sizes (fig. 5). To the north of the ridge and swale area toward Bering Strait, extensive sand-ribbon fields are found with occasional sand dune areas (fig. 1); however, the area is not completely surveyed. The sand ribbon fields indicate a sediment-starved region and possibly one prone to current scour, since the current speeds intensify toward Bering Strait (see fig. 1, Nelson Holocene transgression article this volume). Further north within Bering Strait itself, gravel and shell pavements are noted (Nelson and Hopkins, 1972) in addition to sporadic occurrences of extremely large sand waves (Grim and McManus, 1970).

Off the eastern and western ends of St. Lawrence Island, major sand ridge and swale topography is known (Hopkins et al., 1976), and ripple fields are common to the northwest off St. Lawrence Island (fig. 1).

Character and Origin of Mobile Bedform Features

In the ridge and swale area between King Island and the mainland, swale areas appear to undergo erosion periodically. Generally, a thin veneer of fine, modern mud at the surface overlies Pleistocene peaty muds (fig. 6). Fine mud, signifying sluggish currents, is typically deposited rapidly in depressions (fig. 7). The lack of thick deposits, and very old radiocarbon dates close to the surface, however, suggest that muds have periodically been swept away so that there has been no net mud accumulation for thousands of years. In fact, a radiocarbon date on peat 20 cm below the surface of the swale between Tin City and York Shoal is >30,000 BP, indicating that significant quantities of younger sediment have been stripped away, possibly by currents (fig. 6).

In contrast to swales, sand ridges are definitely constructive as is shown in the sparker seismic profiles (figs. 8 and 9). The morphology of the more landward shoals mirrors the shape of the modern Pt. Spencer spit and these shoals may be ancient analogues (fig. 3). Indeed, depths of shoal crests coincide with proposed still-stand depths of ancient submerged strandlines noted elsewhere in northern Bering Sea (Nelson and Hopkins, 1972). Sand ridges behind large obstructions to the northward current flow, such as King Island and Cape Prince of Wales (see area north of station 88 in fig. 3), may be lee-side accumulations of sediment unrelated to past paralic environments.

Although formation of the basic ridge structures (15-30 km long, see cross-hatched areas in fig. 3) may relate to past transgressive history, these structures also have a modern history of modification by development of sand waves and ripple fields. Sand waves are 1 to 2 m high and have crest spacings of either 10 to 20 m or 150 to 200 m (figs. 9 and 10E). Superimposed on the sand waves are smaller-scale current-asymmetric (figs. 10B and C) and wave oscillation (fig. 10A) ripples with heights of approximately 4 to 10 cm and wavelengths of approximately 20 to 100+ cm. Except for the oscillation ripples, bedforms of all sizes are asymmetric to the north and their asymmetry coincides with the prevailing northward flowing currents (see fig. 1, Nelson, Holocene trangression article this volume) (Coachman et al., 1976).

Growth and movement of the sand wave fields on shoal crests is definitely intermittent, just like the apparent erosional history of the swales. Ice gouges observed to cut sand wave fields on inner shoals in the summer of 1976 proved that no major change in the sand-wave fields had occurred since the previous winter, or possibly for many years before, depending on how recently the gouge occurred. During the fall 1976 field season, only low speed oscillatory bottom currents up to 15 cm/sec (fig. 11) were measured. Underwater television observation showed only the development of oscillation ripples (fig. 10A) and sonographs showed only decayed, inactive sand waves (figs. 10D and E). Thus, sand waves were not active then or apparently for some time before. A piece of wood found at 30 cm depth in a sand wave, however, had an age of 1155 BP (Teledyne Isotopes #I-9773). This date proved that bedforms with heights of at least this order of magnitude (30 cm) had been actively migrating since sea level reached its present height, and that sand waves are not, therefore, relict features from some past time of lowered sea level.

Data collected in the field season of 1977 indicates that there had been significant bed-form activity since the 1976 survey. In some areas with replicate side-scan lines, large-scale sand waves reformed from decayed fields and developed subsets of superimposed smaller-scale sand waves offset at an angle (fig. 10E); however, sand waves on some other ridges remained unmodified from 1976 to 1977 (fig. 10D). Underwater television videotapes show that small-scale ripple fields were undergoing active modification at the time of observation in 1977. Instead of the oscillation ripples observed during the storm conditions in 1976, there were actively migrating asymmetric straight-crested ripples in the troughs (fig. 10C) and linguoid ripples on the upcurrent face of sand waves (fig. 10B). Northward-flowing bottom currents measured with the shipboard profiling current meter ranged from 20-40 cm/sec, with a near-bottom average current speed of 24 cm/sec (fig. 12).

Observations of a series of ice gouges also confirm that there has been recent, active migration of sand waves near Port Clarence (fig. 13). Ice gouges range from fresh to highly modified by sand wave migration (fig. 12F); thus, extensive movement within some sand-wave fields has occurred recently. Lack of modification of gouges (fig. 13) and continued presence of decayed bedforms in some locations indicates that current activity in the Port Clarence area varies both in time and space. Only long-term current measurements from from several locations will resolve this complex current regime and allow predictability of mobile-bedform activity.

Conclusions and Needs for Further Study

Surveys in September 1976, during a period of subsiding storm waves from the north, showed only oscillatory movement of sand on ripple crests. A maximum speed of the north-flowing coastal current of about 15 cm/sec was measured near the bottom and no net-bedload movement was observed. Fresh-looking ice gouges cutting inshore ripples indicated that bedload movement had been negligible in this zone since ice break-up in the spring. The second survey, in July 1977, was made during very calm weather, yet significant bedload movement was observed on ridge crests at water depths of 10 to 30 m. Northward flowing bottom currents measured up to 40 cm/sec. Linguoid ripples and straight-crested ripples were observed moving on the stoss slopes and troughs of sand waves, respectively. Ice gouges in varying states of preservation indicated active bedload transport on deeper ridge crests.

Sand-wave movement and thus bedload transport apparently occurs during calm weather, and maximum sediment transport apparently occurs when major southwesterly storms generate sea level set-up in the eastern Bering Sea that enhances northerly currents (Cacchione and Drake, 1979; Schumaker and Trip, 1979). Strong north winds from the Arctic, however, reduce the strength of the continuous northerly currents and thereby reduce the amount of bedload transport.

Studies to date indicate that the greatest potential for scour around obstructions exists in regions of sand ribbons and gravel-plus-shell pavements which occur within straits areas (fig. 1). The Port Clarence sand wave area has the most rapidly changing relief and the scour in sand wave crests may reach depths of up to 2 m (fig. 9). Data from replicate lines in 1976 and 1977 show that such scour may occur in some areas of the Port Clarence sand wave field each year (fig. 10).

ACKNOWLEDGMENTS

Devin Thor, Mathew Larsen, Terry Hallinan, William Richmond, Jeff Patry and James Evans compiled data and prepared figures. We thank the officers, crew, and shipboard scientific staff for their concerted effort in the detailed study of sand wave areas.

The cruises were supported jointly by the U.S. Geological Survey and by the Bureau of Land Management through interagency agreement with the National Oceanic and Atmospheric Administration, under which a multiyear program responding to needs of petroleum development of the Alaska continental shelf is managed by the Outer Continental Shelf Environmental Assessment Program (OCSEAP) Office.

REFERENCES CITED

Cacchione, D.A., and Drake, D.E., 1979) Sediment transport in Norton Sound, Alaska: Regional patterns and GEOPROBE system measurements: U.S. Geological Survey Open-File Report 79-1555.

Coachman, L.K., Aagaard, Knut, and Tripp, R.B., 1976, Bering Strait: The regional physical oceanography; Univ. of Washington Press, 186 p.

Fleming, R.H., and Heggarty, D., 1966, Oceanography of the southeastern Chukchi Sea, in Wilimovsky, N.J., Wolfe, J.M., (eds.), Environment of Cape Thompson Region, Alaska: U.S. Atomic Energy Commission, p. 697-754.

Grim, M.S., and McManus, D.A., 1970, A shallow seismic profiling survey of the northern Bering Sea: Marine Geology, v. 8, p. 293-320.

Hopkins, D.M., Nelson, Hans, Perry, R.B., and Alpha, Tau Rho, 1976 Physiographic subdivisions of the Chirikov Basin, northern Bering Sea; U.S. Geol. Survey Prof. Paper 759-B, p. B1-B7.

Larsen, M.C., Nelson, C.H., and Thor, D.R., 1979, Geologic implications and potential hazards of scour depressions on Bering shelf, Alaska: Environmental Geology, v. 3, p. 39-47.

McManus, D.A., Venktaratham, K., Hopkins, D.M., and Nelson, C.H., 1974, Yukon River sediment on the northernmost Bering Sea shelf: Jour. Sed. Pet., v. 44, no. 4, p. 1052-1060.

McManus, D.A., Venkataratham, Kolla, Hopkins, D.M., and Nelson, Hans, 1977, Distribution of bottom sediments on the continental shelf, northern Bering Sea: U.S. Geol. Survey, Prof. Paper 759-C, p. C1-C31.

Nelson, C.H., and Hopkins, D.M., 1972, Sedimentary processes and distribution of particulate gold in the northern Bering Sea: U. S. Geol. Survey Prof. Paper 689, 27 p.

Nelson, C. H., and Creager, J.S., 1977, Displacement of Yukon-derived sediment from Bering Sea to Chukchi Sea during Holocene time: Geology, v. 5, pp. 141-146.

Schumacher, J.D., and Tripp, R.B., 1979, Response of northeast Bering Sea shelf waters to storms: EOS, 60, 856.

Figure 1. Index map of Northern Bering Sea showing major areas of mobile bedforms.

Figure 2. Detailed high-resolution seismic profile and side-scan tracklines collected in 1976 and 1977 in northeastern Chirikov Basin. Miniranger precision navigation was used to replicate tracklines. Bathymetric contours are in meters: hachured areas outline major sand ridges that exhibit sand-wave fields.

Figure 3. Detailed transects of underwater television and bottom camera stations taken in northeastern Chirikov Basin. Bathymetric contours are in meters: hachured areas outline major sand ridges that exhibit sand-wave fields.

Figure 4. Location of detailed sampling stations in area of sand ridges west of Port Clarence, Alaska.

Figure 5. Location of active bedforms in northeastern Chirikov Basin. Bathymetric contours are in meters; hachured areas outline major sand ridges that exhibit sand-wave fields.

Figure 6. Stratigraphy of nearsurface sediment observed in box and vibracores from sampling transects across sand ridges near Port Clarence. Location of transects is shown in figure 2.

Figure 7. Grain-size distribution in sand ridge area west of Port Clarence.

Figure 8. Line drawings of high-resolution seismic profiles across major sand ridges shown in figure 2. Note that the "sand ridges" are constructional features overlying parallel or folded, older sediment. Names of ridges are given in figure 3.

Figure 9. 3.5 kHz seismic profiles with associated sonographs taken over sand ridges covered by large and small-scale, active sand waves. Records are from the York Shoal area shown in figure 3.

Figure 10. Bedforms and ice gouges observed on sand ridges west of Port Clarence. A-Videotape photo of oscillation ripples taken on the crest of Lost River Shoal in September, 1976 (ripple height approximately 4 cm and wave length about 20 cm; water depth 12 m). B-Bottom camera photo of asymmetric linguoid ripples on the stoss face of a sand wave on York Shoal taken in July, 1977 (ripple height approximately 2-3 cm and wave length about 10 cm; water depth 20 m). C-Bottom camera photo taken at same location as B showing asymmetric straight-crested ripples of the same scale, but located in a trough between sand waves of 0.5 m wave height, approximately. D-Sonographs of unchanged sand waves on the crest of Tin City Shoal. E-Sonographs of sand waves on York Shoal that changed from decayed bedforms in 1976 to two active sets of bedforms in 1977 (large-scale waves 2 m high and 150-200 m wave length; small-scale waves 0.5 m high and 10-20 m wave length). F-Series of sonographs showing different stages of ice gouge modification by actively migrating sand-wave fields.

Figure 11. Summary of profiling currert meter data collected at stations in the sand-wave fields west of Port Clarence in September, 1976. Hachured areas depict major sand ridges with sand-wave fields; contour interval is 4 m.

Figure 12. Summary of profiling current meter data collected at stations in the sand-wave fields west of Port Clarence and in Bering Strait during July, 1977. Hachured areas depict major sand ridges with sand wave fields; contour interval is 4 m.

Figure 13. Modification of ice gouges by actively migrating sand waves that is observed in sonographs taken in the area west of Point Spencer, Alaska. Hachured areas depict sand ridge crests with sand waves; contour interval is 4 m.

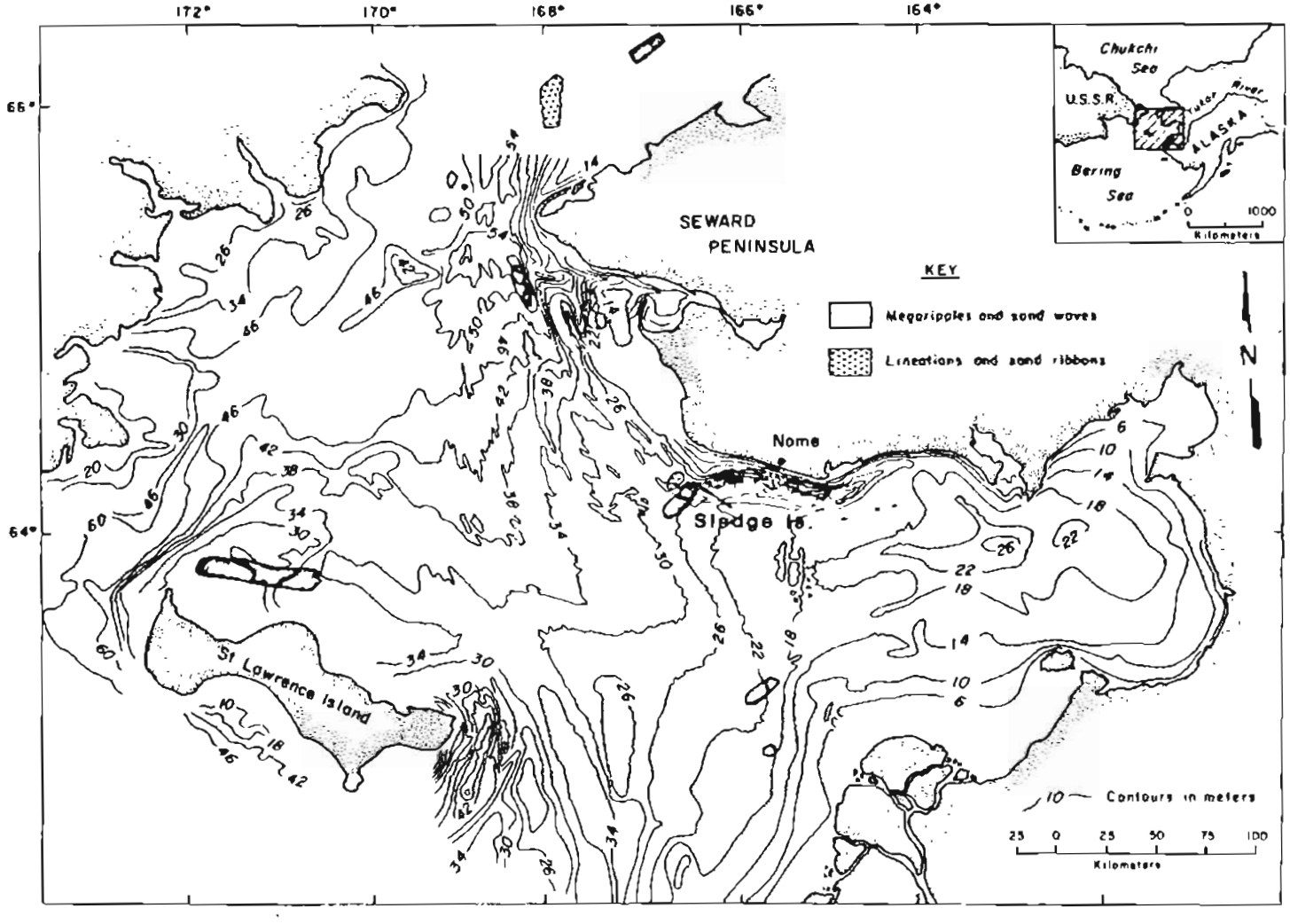
172°
170°
168°
166°
164°
66°
64°
SEWARD
PENINSULA
Nome
Sledge Is.
St Lawrence Island
KEY
Megaripples and sand waves
Lineations and sand ribbons
N
Chukchi
Sea
U.S.S.R.
Yukon River
ALASKA
Bering
Sea
0 1000
Kilometers
10 — Contours in meters
25 0 25 50 75 100
Kilometers

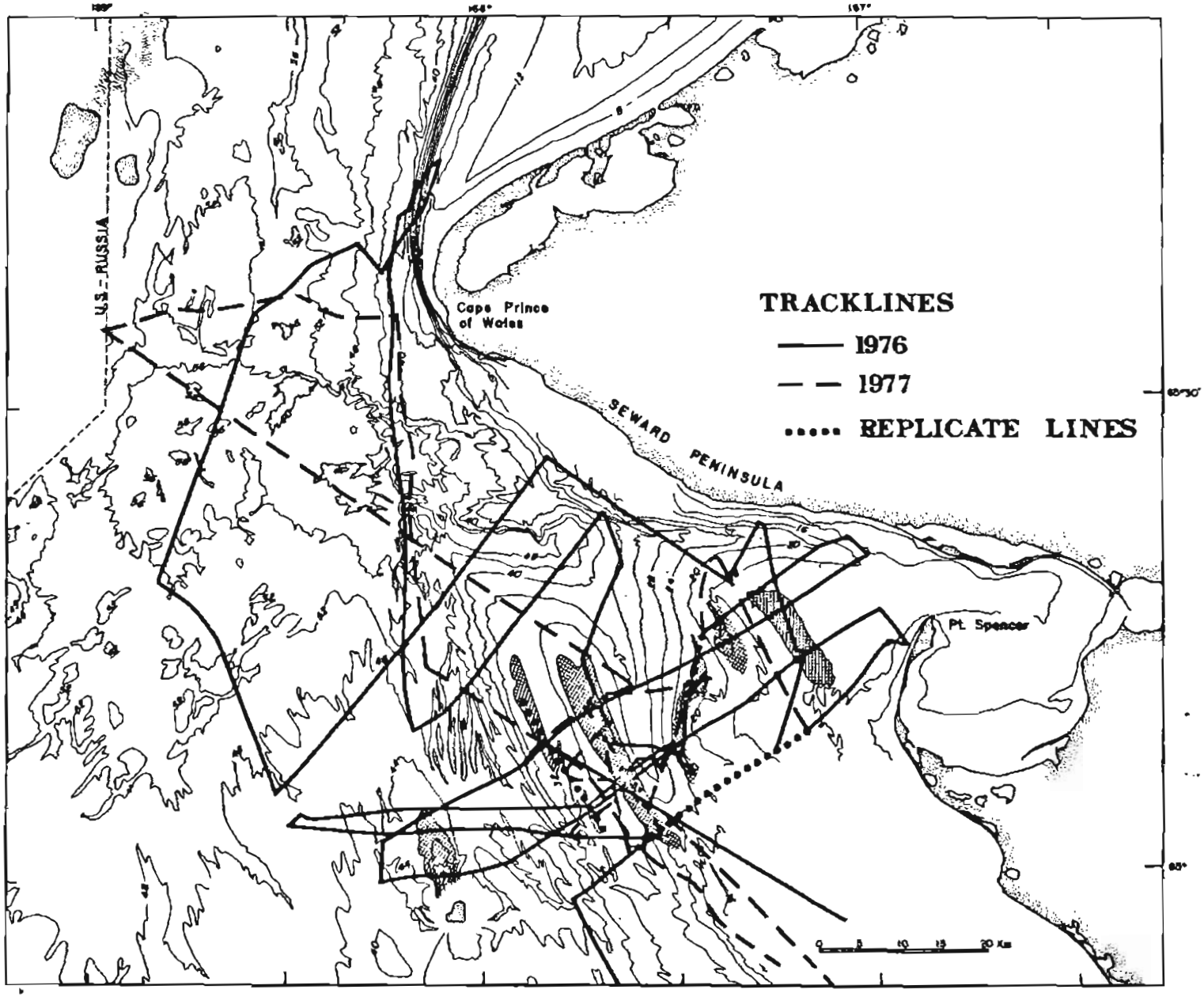
U.S. - RUSSIA
Cape Prince of Wales
SEWARD PENINSULA
Pt. Spencer
TRACKLINES
1976
1977
REPLICATE LINES
0 5 10 15 20 Km

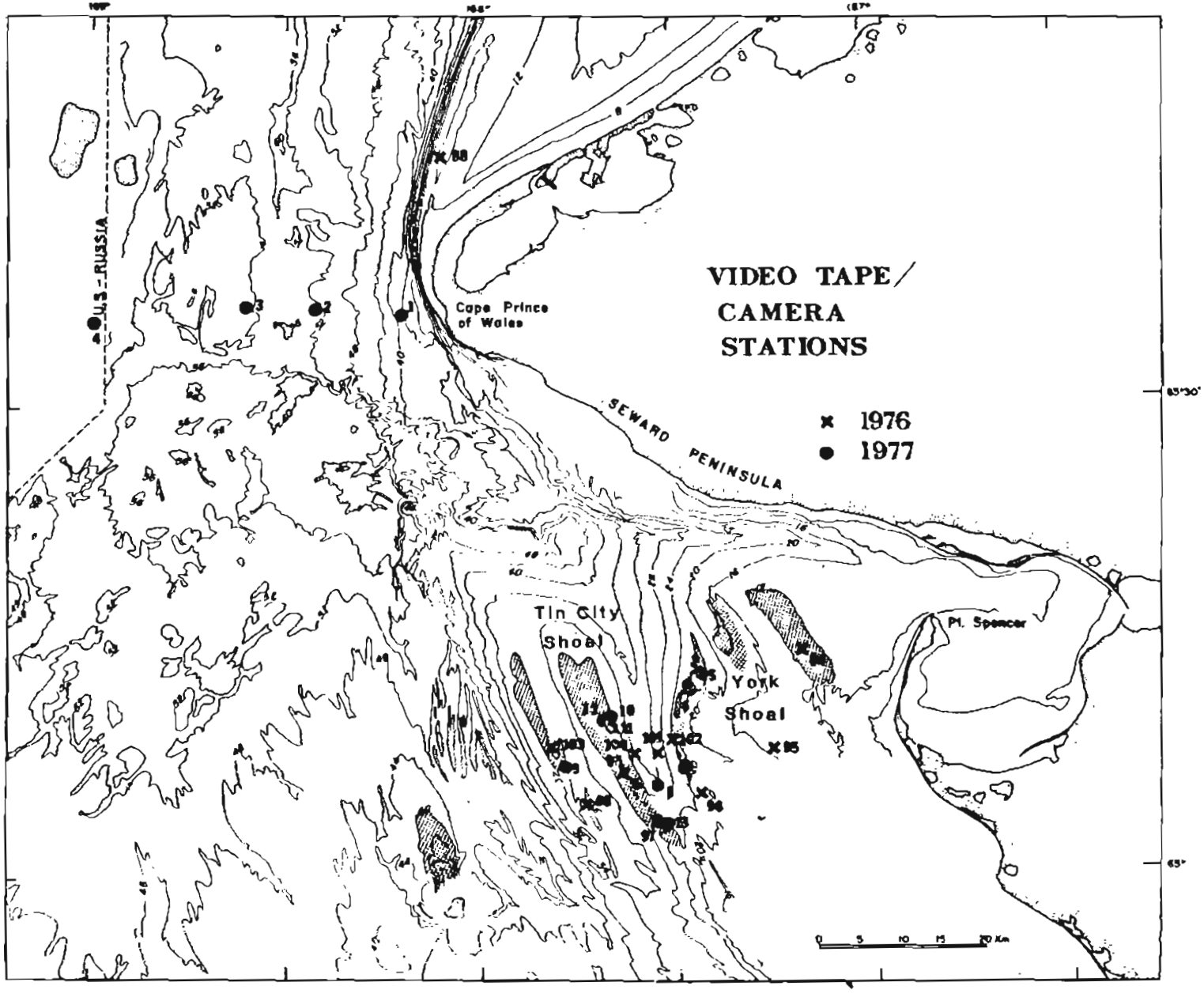
VIDEO TAPE/
CAMERA
STATIONS
× 1976
● 1977
U.S.-RUSSIA
Cape Prince
of Wales
SEWARD PENINSULA
Tin City
(Shoal)
York
Shoal
Pt. Spencer
65°30'
65°
0 5 10 15 20 Km

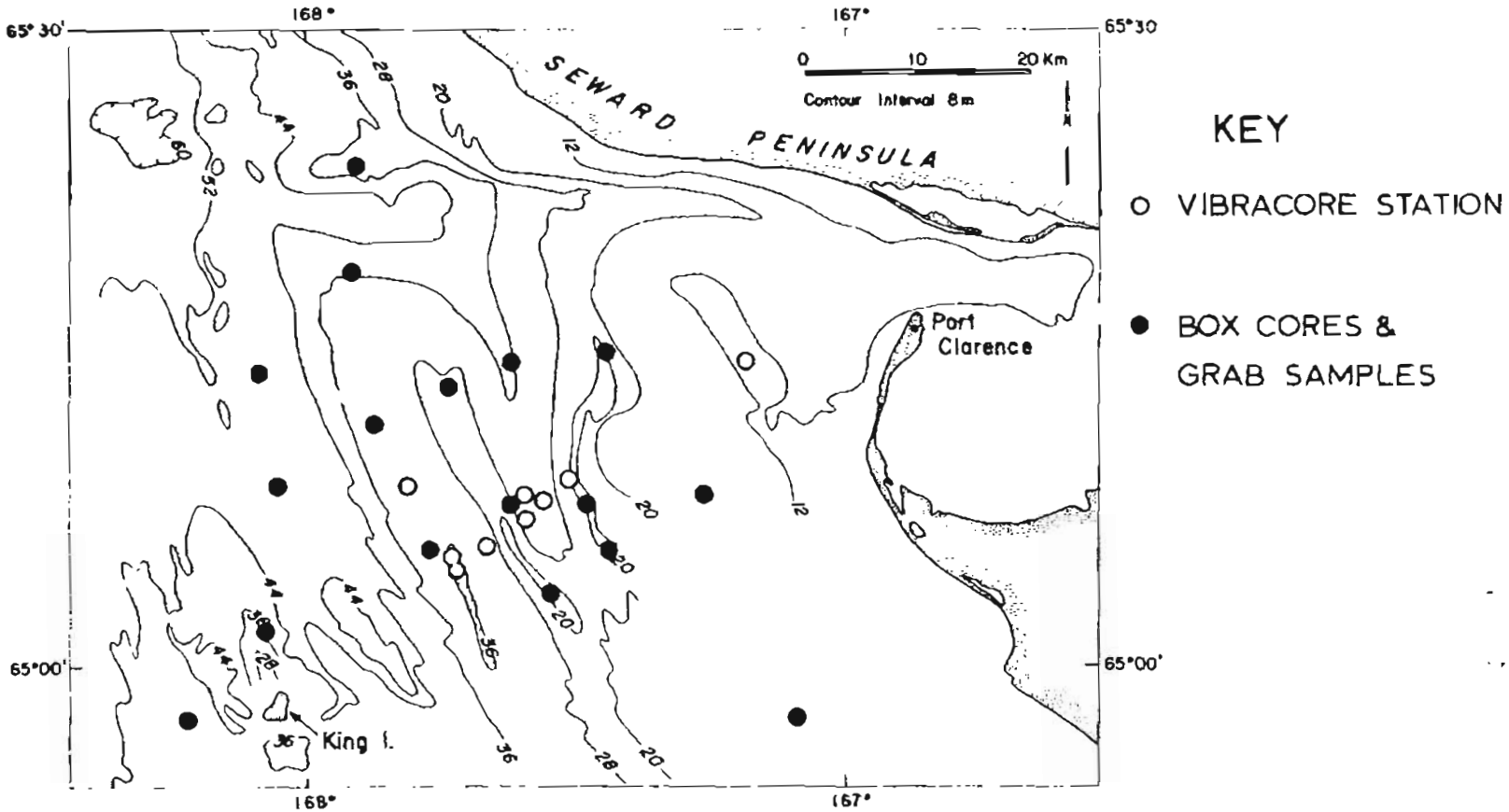
168°
167°
65°30'
65°00'
SEWARD PENINSULA
0 10 20 Km
Contour Interval 8m
Port Clarence
King I.
KEY
VIBRACORE STATION
BOX CORES & GRAB SAMPLES

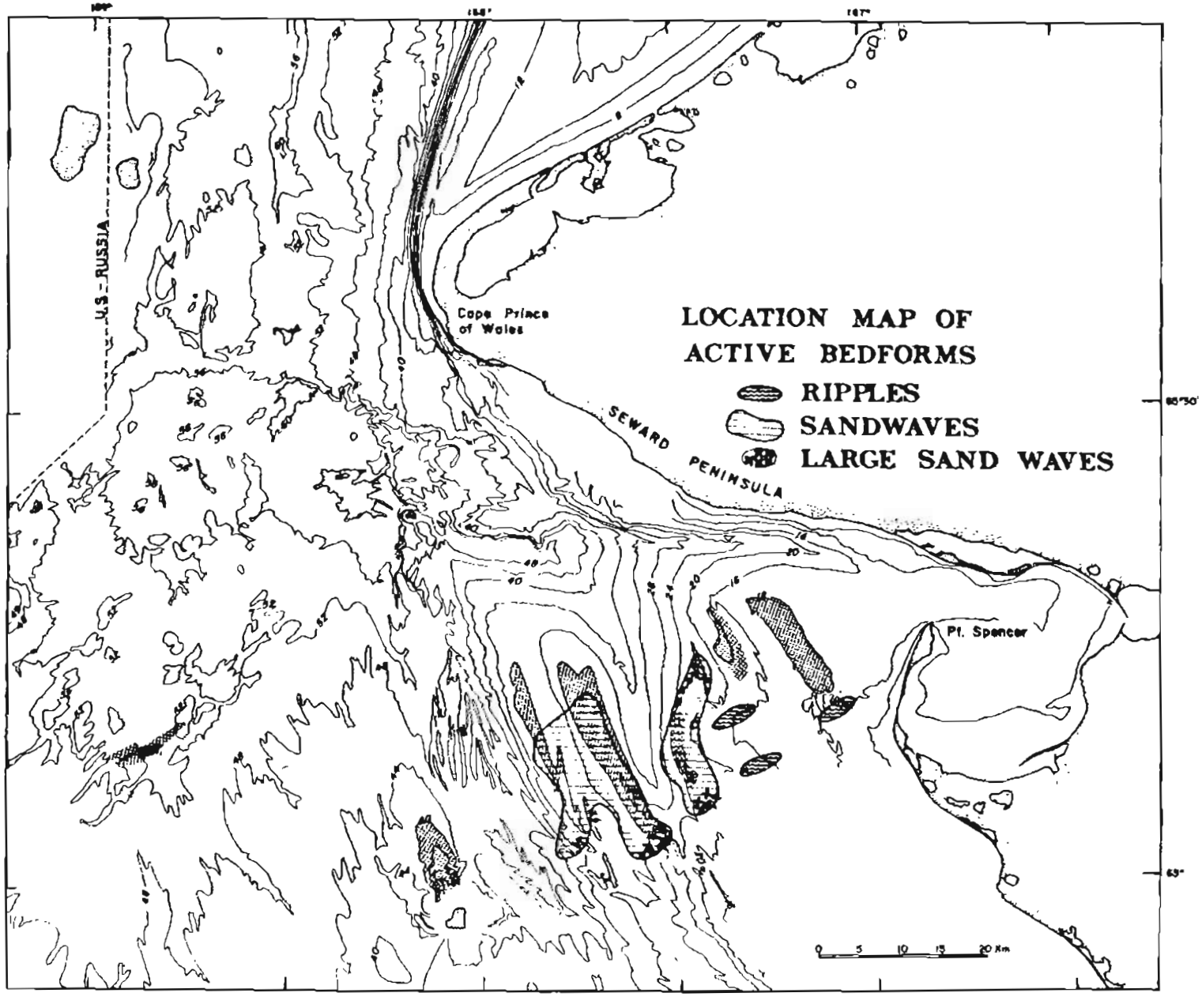
LOCATION MAP OF
ACTIVE BEDFORMS
RIPPLES
SANDWAVES
LARGE SAND WAVES
U.S. - RUSSIA
Cape Prince of Wales
SEWARD PENINSULA
Pt. Spencer
65°30'
65°
0 5 10 15 20 Km

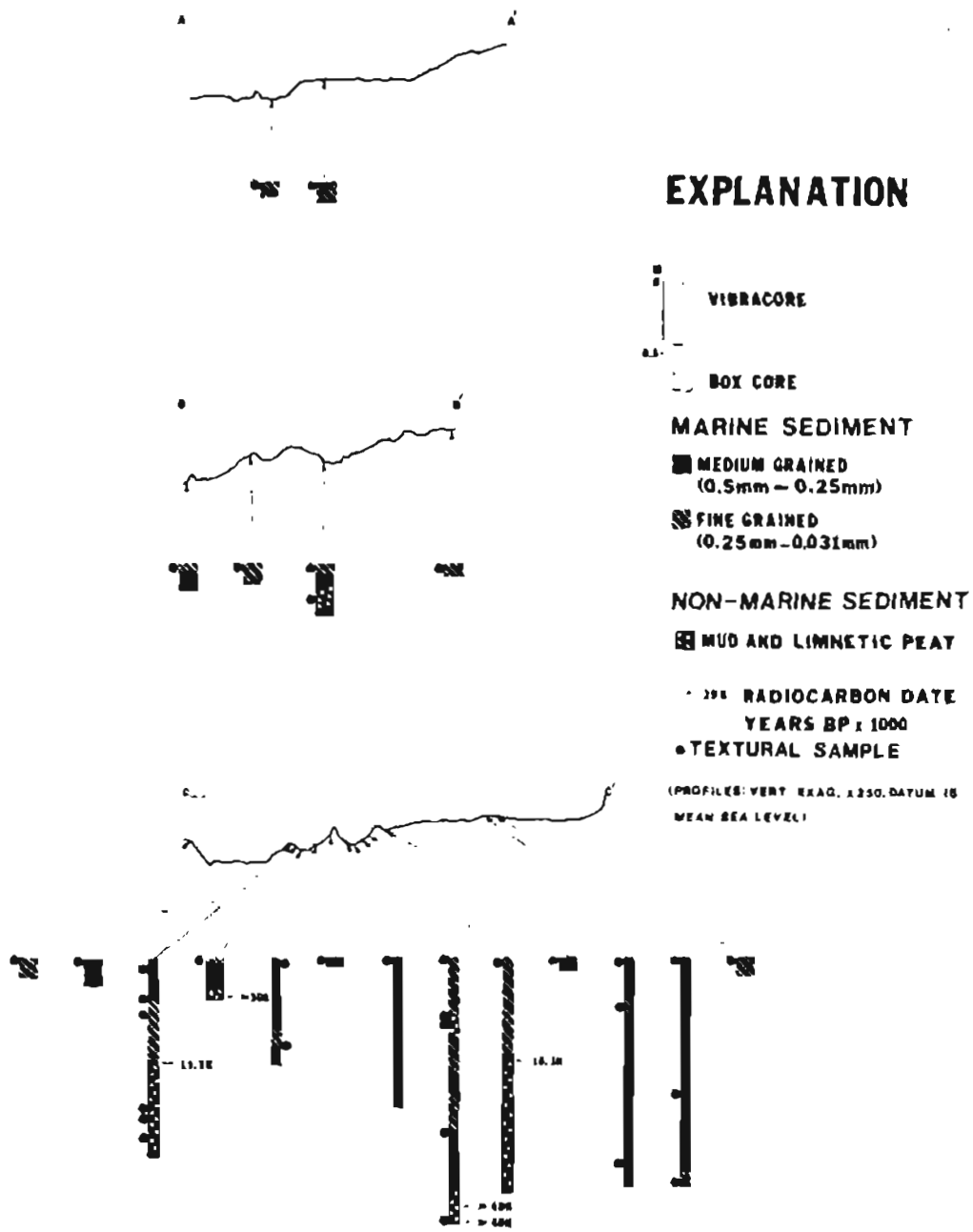
A
A'
B
B'
C
C'
EXPLANATION
VIBRACORE
BOX CORE
MARINE SEDIMENT
MEDIUM GRAINED
(0.5mm – 0.25mm)
FINE GRAINED
(0.25mm–0.031mm)
NON-MARINE SEDIMENT
MUD AND LIMNETIC PEAT
RADIOCARBON DATE
YEARS BP x 1000
TEXTURAL SAMPLE
(PROFILES: VERT. EXAG. x 250. DATUM IS
MEAN SEA LEVEL)

SEDIMENT DISTRIBUTION

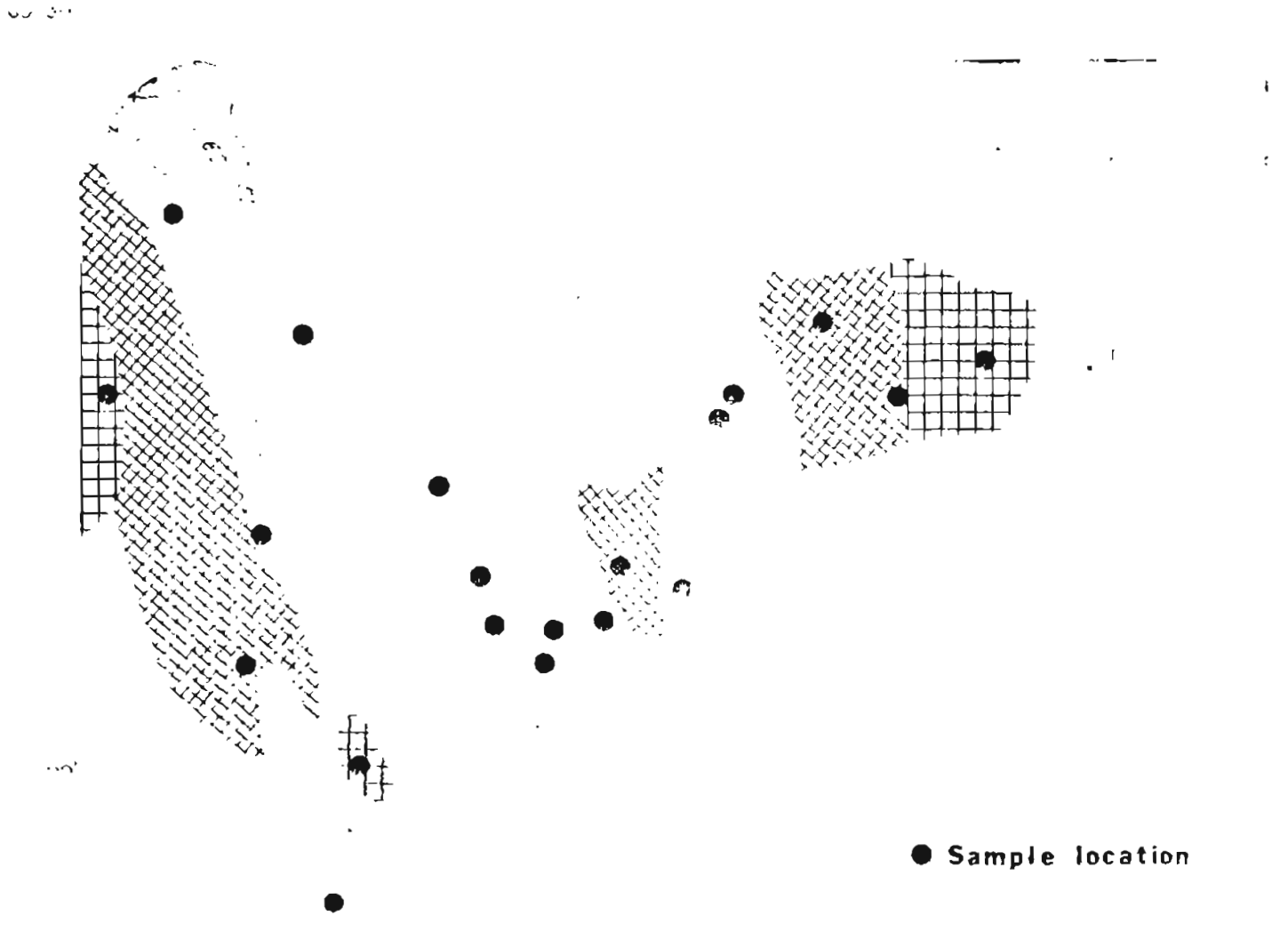

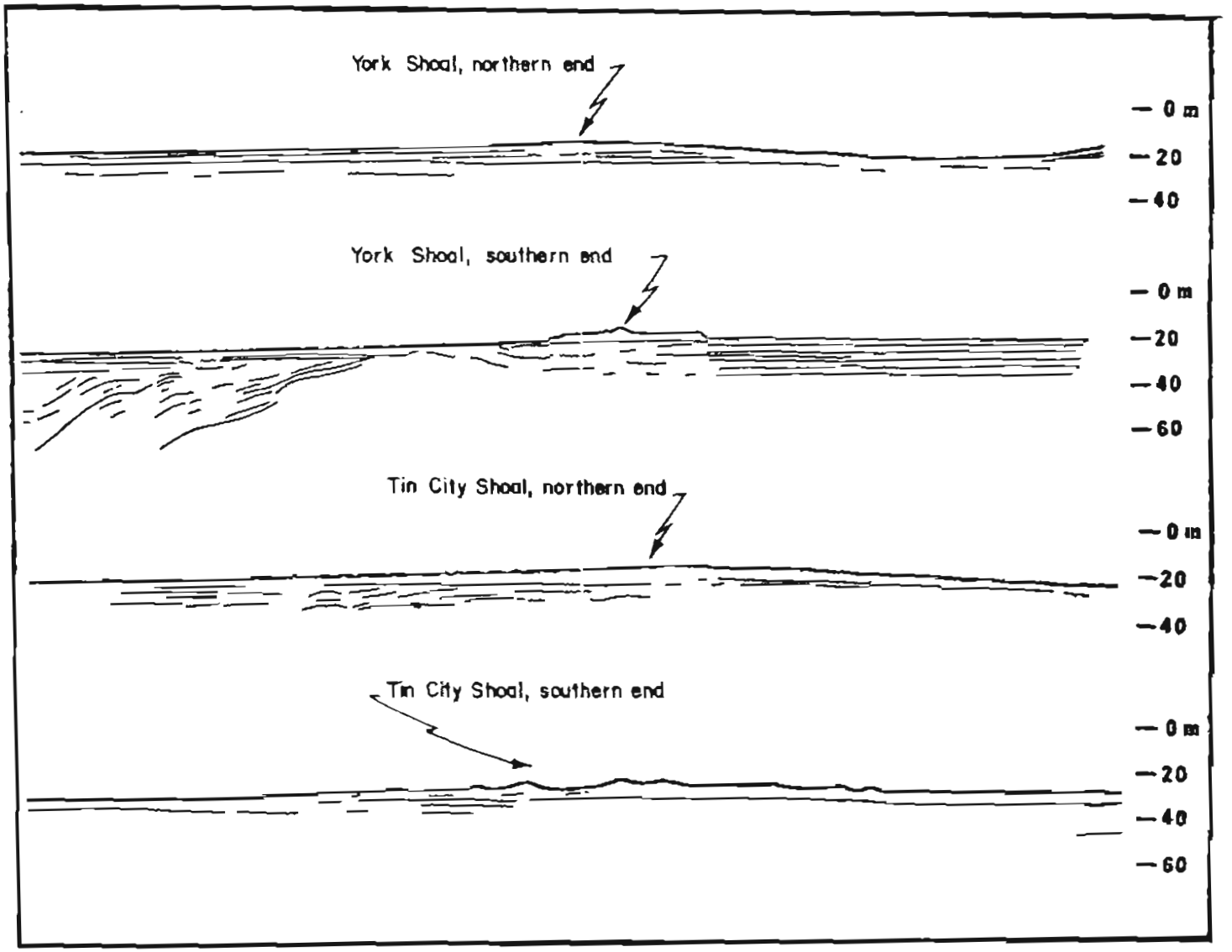
York Shoal, northern end
— 0 m
— 20
— 40
York Shoal, southern end
— 0 m
— 20
— 40
— 60
Tin City Shoal, northern end
— 0 m
— 20
— 40
Tin City Shoal, southern end
— 0 m
— 20
— 40
— 60

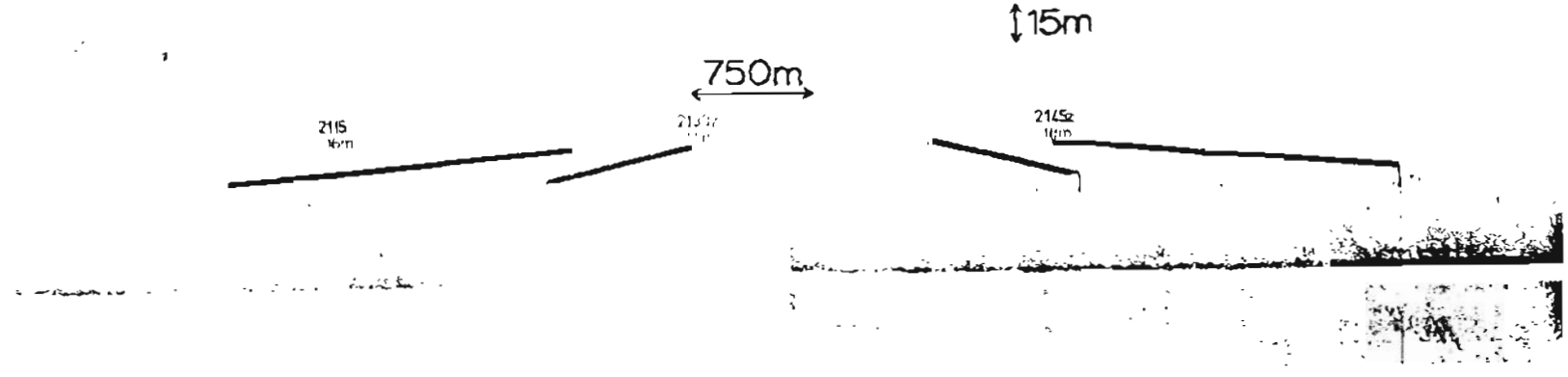
15m
750m

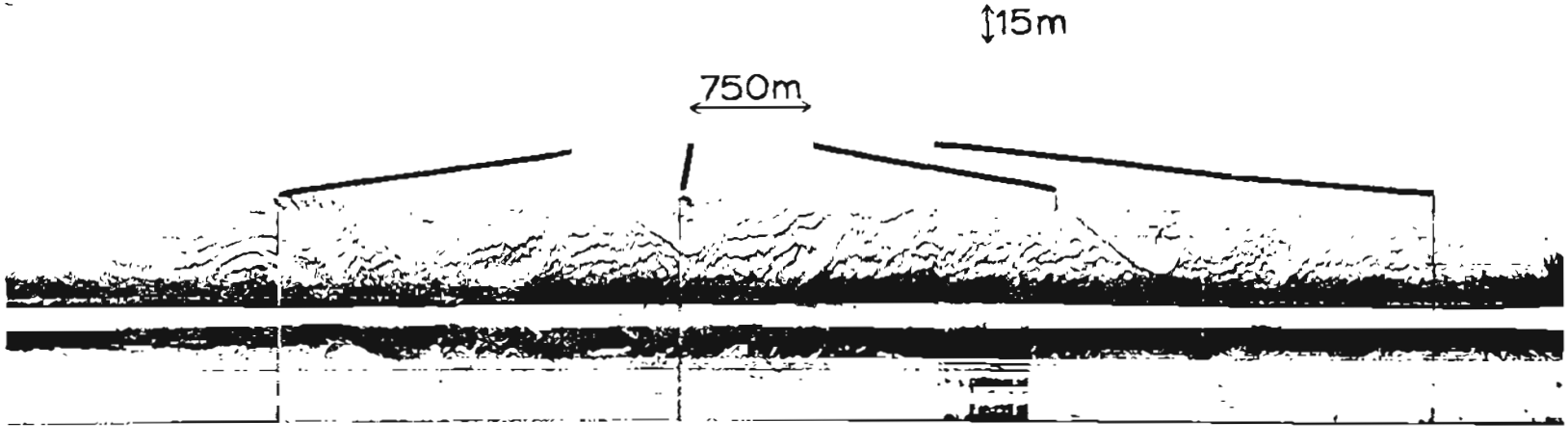
15m
750m

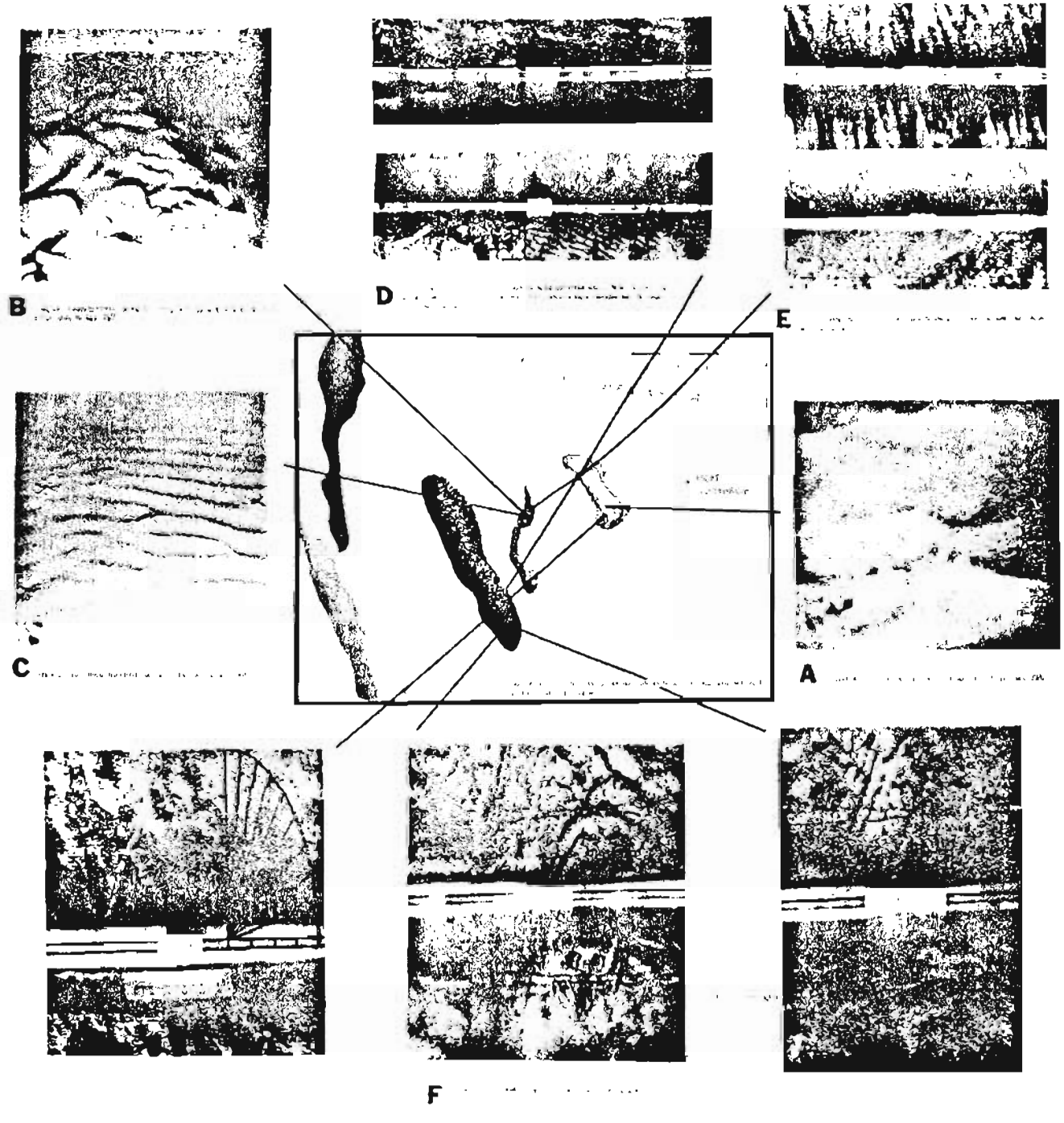
B
D
E
C
A
F

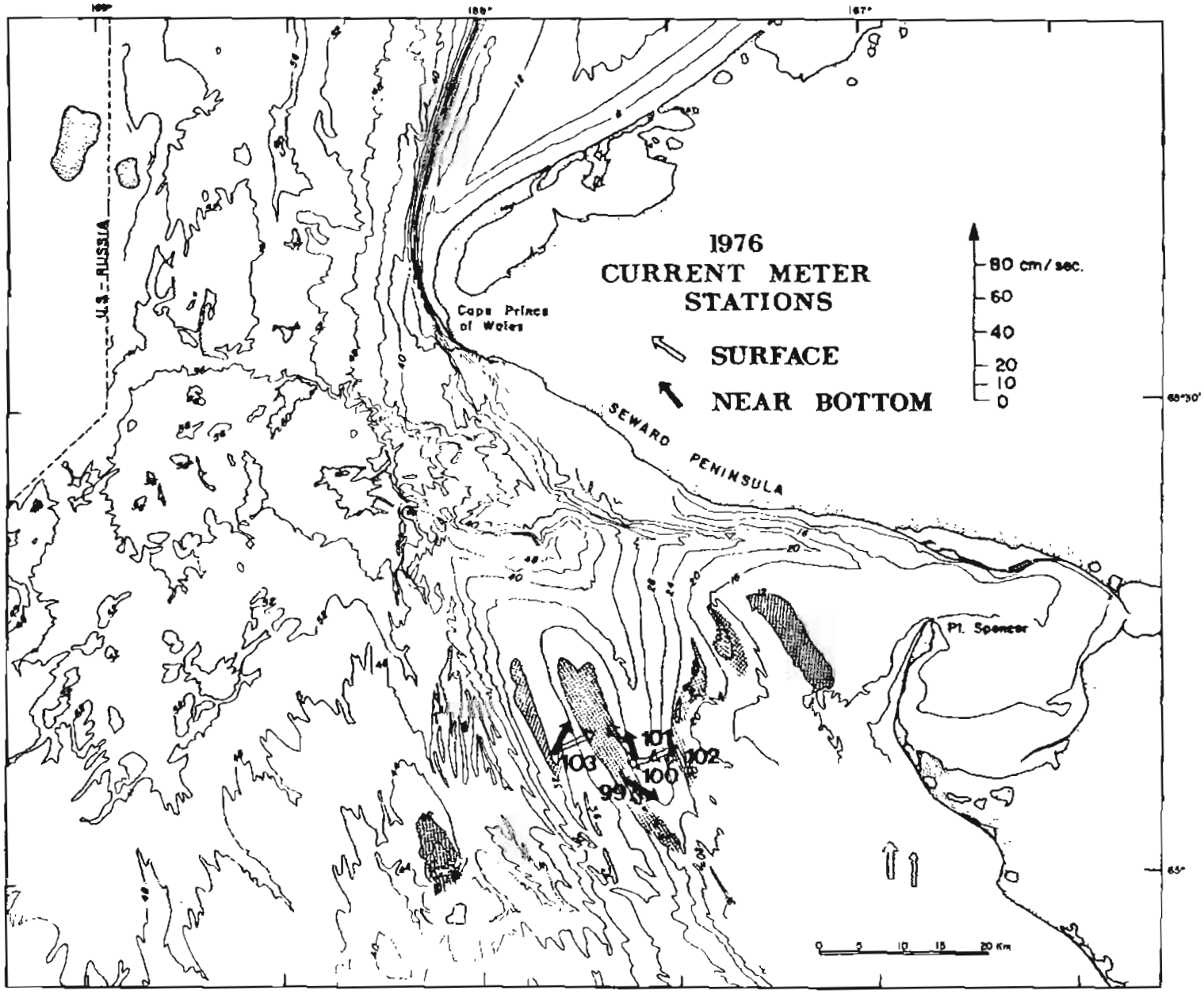
1976
CURRENT METER
STATIONS
SURFACE
NEAR BOTTOM
80 cm/sec.
60
40
20
10
0
U.S. - RUSSIA
Cape Prince of Wales
SEWARD PENINSULA
Pt. Spencer
103
101
100
102
99
0 5 10 15 20 Km

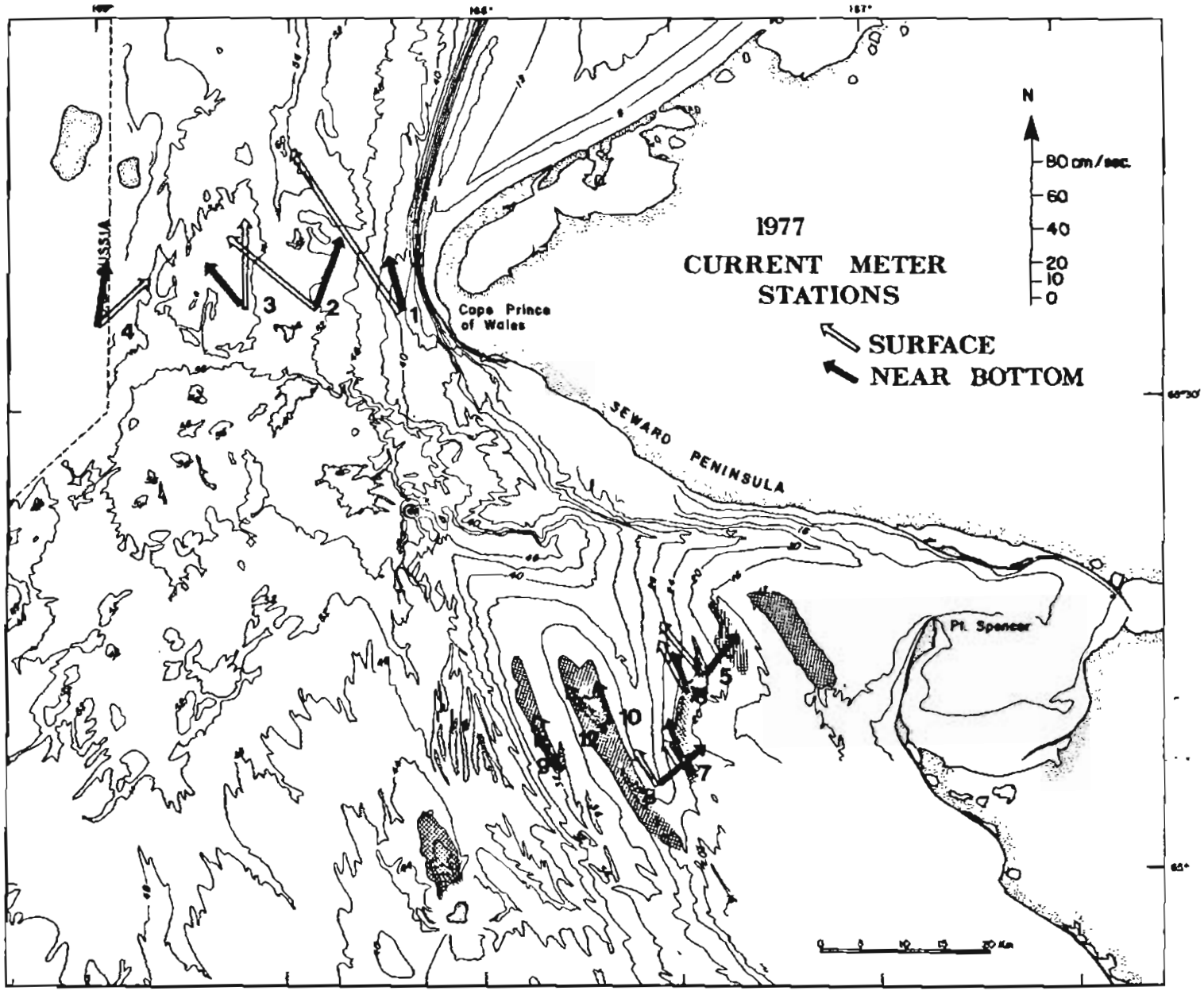
1977
CURRENT METER
STATIONS
SURFACE
NEAR BOTTOM
N
80 cm/sec.
60
40
20
10
0
Cape Prince
of Wales
SEWARD PENINSULA
Pt. Spencer
RUSSIA
1
2
3
4
5
6
7
8
9
10

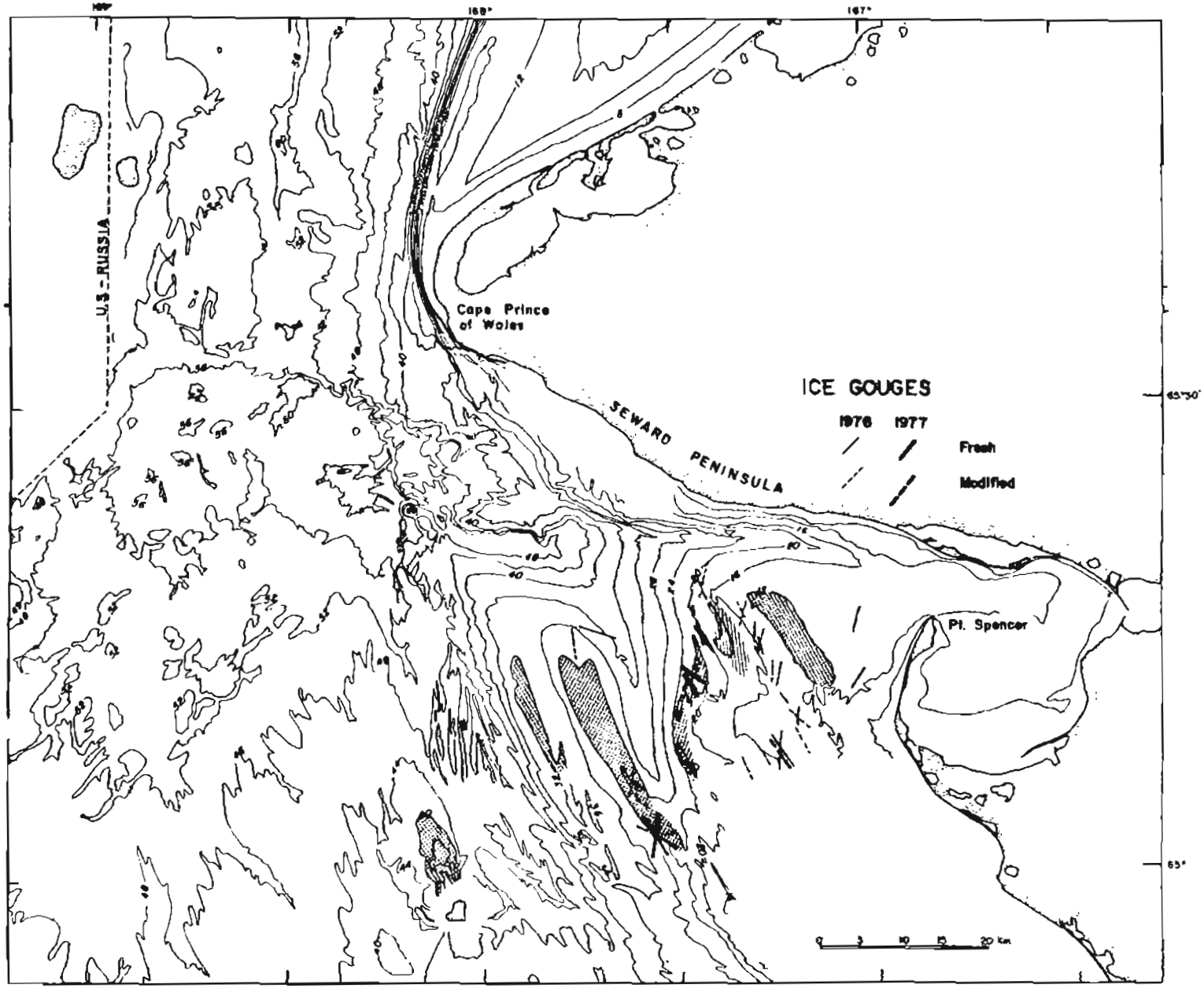
U.S. - RUSSIA
Cape Prince of Wales
SEWARD PENINSULA
ICE GOUGES
1976
1977
Fresh
Modified
Pt. Spencer
65°30'
65°
0 5 10 15 20 km

Graded Storm Sand Layers Offshore from the Yukon Delta, Alaska

C. Hans Nelson

Introduction

The northern Bering Sea has a history of severe storm surges. The most recent, and perhaps the worst in historical times, occurred in November, 1974 (Fathauer, 1975). Evidence of storm surge events is exhibited in sea-floor stratigraphy as well as shoreline flooding and indicates that significant widespread changes in sea-floor sedimentation take place (Nelson and Creager, 1977). These changes have implications for installations on the sea floor and for mass transport of pollutants.

This paper describes the interbedded sand layers found in southern Norton Sound off the modern Yukon Delta that are deposited by the storm surge events. Such deposits are evident in both modern and ancient deposits of epicontinental shelves (Hays, 1967; Howard and Reineck, in press; Anderton, 1976). These graded sand layers in very shallow water mimic many of the features of thin-bedded turbidite sands, although the shallow water deposits are thought to have a very different mechanism of deposition related to storm surge processes.

Two factors in the oceanographic setting of northern Bering Sea magnify the effects of storm surge. The sea floor is very shallow (less than 20 m deep over wide areas) particularly in Norton Sound. Consequently there is intensive wave reworking which causes extensive sea-floor erosion, mass movement, displacement, and offshore progradation of significant amounts of sediment during storm surges. The second factor is a system of strong dynamic bottom currents that can move large amounts of sediment northward to Chukchi Sea during normal weather. Much more sediment is moved when the current is reinforced by relaxing of the sea surface set-up caused by storm surge

(Fig. 1) (Flemming and Heggarty, 1966; Coachman et al., 1976; Cacchione and Drake, 1979; Schumacher and Tripp, 1979).

Another important influence on the sedimentation in southern Norton Sound is the effect of seasonal processes on the Yukon River delta. During the winter months from November to May the Yukon River averages 40,000 cfs when the ice-covered river is fed mainly by base flow (Dupré, 1976). Within less than a week of river breakup, peak discharges may reach 1,000,000 cfs or more and then decline throughout the summer.

Characteristics of Graded Sand Storm layers

Over 10,000 km^2 of southern Norton Sound display graded sand layers interbedded with silty mud. This paper focuses on the prominent interbedded very fine sand and coarse silt layers that show definite vertical size gradation of grain size and sedimentary structures. In addition to the vertical gradation within individual beds, there are lateral gradations in grain size, thickness of layers, and sedimentary structures for the complete system of beds from onshore to offshore. Vertical grading and areal gradations are found in a common surface sand layer throughout southern Norton Sound. Graded sand layers in the subsurface at each location are like the surface layer (Fig. 2) (Larsen et al. 1980). Patterns of grain size and layer thickness also vary areally from west to east across the front of the Yukon delta.

Onshore to offshore, the graded sand beds become finer grained and thinner, contain a smaller percentage of graded sand layers, and show less complete sequences of vertical sedimentary structures (Figs. 3 and 4). Inshore the graded sand layers make up 50-100 percent of the total sedimentary section (Fig. 3); they range from 10-20 cm thick and the basal part of the layer is made up of fine-grained sand (Fig. 5). Approximately 60-75 km from

the Yukon Delta shoreline, the graded sands are generally 1-2 cm thick, less than 35 percent of the total section, and the base of the layers is composed of very fine sand or coarse silt (Figs. 2-5).

The graded layers typically contain a vertical sequence of sedimentary structures (S_b-S_e, see Fig. 5). The base of a layer may or may not contain flat-laminated medium to fine sand (S_b). In the center section of a sand layer, cross lamination and convolute lamination are dominant (S_c). In the upper part of the layer, in the very fine sand or coarse silt, flat lamination again predominates and often laminated beds of epiclastic plant fragments become very prominent (S_d). The upper flat-laminated sequence of the individual sand beds grades into normal, continuous mud deposition (S_e)in most instances, although this mud cap may be lacking.

Going from nearshore to offshore, there is a less complete sequence of vertical structures in graded sand layers (Figs. 3 and 5). In the nearshore graded layers lower (S_b) flat lamination is often present whereas in distal layers, flat lamination at the base is not encountered (Figs 3 and 5). In addition, in the most distal layers, occasionally both the lower flat lamination and cross lamination are missing leaving only flat laminated sands. Trough cross lamination characterizes the nearshore graded sand beds whereas ripple lamination or starved ripple drift prevails in the distal graded sand beds (Fig. 5).

A surface sand layer is present in many of the cores and could potentially be a correlative layer from the 1974 storm surge (Fathauer, 1975) (Fig. 2). Such a continuous layer was not encountered at the surface and sand content was 30% less over wide regions of Norton Sound in field seasons prior to 1974 (Fig. 6) (Nelson et al., in press). Oxidized grain coatings also were noted in surface sands, giving the thicker sands a yellowish color rather than

the usual olive drab hue. Such coatings suggest a subareal source and that progradation of sand layers offshore may correlate with extensive shoreline erosion. Such shoreline erosion extended up to several hundred meters inland in the 1974 storm (Sallenger et al., 1978). Offshore movement of extensive sand masses from delta source areas from the 1974 storms is also indicated by the grading of thicker to thinner layers offshore (Fig. 2). It is not possible to confirm the dating of this upper sand layer, but it does exhibit a consistent pattern of trends in thickness, grain size and vertical sequence of sedimentary structures that is the same as the average of these characteristics throughout the entire core sequences. Thus, the surface layer appears to be a verification of the areal patterns of gradation in these vertical sequences of graded sand beds.

In addition, extensive change in surface texture of the sediment since 1974 can be shown in certain areas of the sea floor (Fig. 6). Change is most prominent nearshore off the modern Yukon subdelta where storm sand layers are thicker than they are far offshore. Coarser texture is found in most inshore areas where pre and post 1974 data is available. A 30-50 percent increase in sand content is noted in these regions. In the furthest offshore region of the central sound, no change is apparent, as would be expected in ths distal region where storm sands are poorly developed at best and are subject to more intense bioturbation (Nelson et al., in press).

Characteristics of graded sand beds also vary from the western side of the delta to the eastern nearshore area of the delta. In the western delta the individual sand layers are approximately 18 cm thick whereas in the eastern area most sand layers are 8-9 cm thick with occasional layers of up to 20 cm in thickness (Fig. 5). Similarly, in the distal areas off the western delta, sand layers average 5-10 cm thick whereas off the eastern area sand layers average 1-2 cm thick (Fig. 2).

Thickness of graded sand layers varies areally, depending on local morphology vertically in different stratigraphic horizons. Some cores change from thicker to thinner layers from base to top (Fig. 5) and others change from thinner to thicker layers from base to top. The cores taken in channels consist almost entirely of sand and may or may not contain thick graded sands, whereas cores taken on the flanks of the channels and on the delta front platform have well-developed graded beds; these become thinner at greater distances from the channels.

Depositional Processes of the Graded Sand Layers

The vertical and areal trends of graded sand layers permits speculation concerning the method of deposition. The well-developed vertical sequence of sedimentary structures and vertical gradation of grain size in the individual beds suggests that a rapidly waning current deposits these beds. It is apparent that this rapidly waning current is stronger inshore and gradually relaxes offshore, as shown by the pronounced change to thinner beds, fewer beds, and finer-grained beds offshore. In addition, it is apparent that sources vary and that pathways of the rapidly waning current are influenced by the sub-ice channel system (Dupré, 1979). It seems that the western delta, where 90 percent of the sediment is introduced, has a much more vigorous transport of the prograded sand beds from onshore to offshore. In contrast, the eastern delta is a region with much less effective sand transport from onshore to offshore.

Two possible mechanisms may be suggested for deposition of prograding graded sand beds in southern Norton Sound. One possible cause, particularly associated with inshore sub-ice channel locations, may be the sudden high river discharge at the time of spring breakup. The graded sand sheets may be deposited annually during the high discharge. The lack of evidence of an even

cyclic event in the stratigraphy and the extent of deposition over 100 km from shore, suggest that such a deposit is unlikely from a freshwater flood plume entering salt water.

The second and favored hypothsis is that the prograding sand beds are deposited by storm surge runoff currents that develop from the relaxation of sea level set-up after passage of the strong south to southwesterly winds that usually accompany the major low-pressure storms in this region (Fathauer, 1975) (Fig. 7). In small storms, sea surface set up of a meter and current speed increases of over 100% have been measured in central Norton Sound (Cacchione and Drake, 1979; Schumacher and Tripp, 1979). Measurement of offshore set-up nearly equal to shoreline set-up and known occurrences of up to 5 m of shoreline set-up (Sallenger et al., 1978) indicate storm surge runoff currents several orders of magnitude greater than normal current speeds are possible.

The progradation of sand from onshore to offshore is potentially enhanced by cyclic wave loading on the delta front that can interact with the favorable grain size that is present. The possibility of cyclic wave loading and liquefaction potential appears to be verified by theoretical calculations based on wave pressures measured at the GEOPROBE site (Cacchione and Drake, 1979; Clukey et al., 1980). Consequently, a synergistic effect of sea level set-up, wave cyclic loading and liquefaction, and strong bottom return flow onshore toward offshore, is reinforced by the relaxing of the sea surface set-up. The pathway of the bottom return flow is apparently affected by the onshore channel systems whereas offshore, beyond the 30 km reach of the channel, sheet flow apparently gives a uniform distribution of thin sands (Fig. 7).

Another possible gradational process may be due to the greater effect of

waves inshore. There, trough cross lamination predominates, whereas offshore current ripple lamination and starved ripple drift are apparent as the sand progradation process may be dominated mainly be bottom current flow with lesser influence of waves and a waning source of sand in the distal regions.

Isopach thicknesses of Holocene sediment in Norton Sound (Nelson and Creager, 1977) and comparison of these thicknesses with total sedment input from the Yukon River during the Holocene, indicate that significant amounts of sediment have been removed from the sea floor by sediment resuspension (Nelson and Creager, 1977). Detailed stratigraphy and lithology suggest the same conclusion. The section of Yukon Holocene muds is exceptionally thin in many places adjacent to the delta source region and this indicates sediment removal. Numerous lag layers of pebbles and shells and thin sands are apparent in the distal areas of Yukon muds of central and northern Norton Sound (Fig. 5). These form when storm waves resuspend the bottom mud but leave behind coarse ice-rafted pebbles, shell fragments, and coarse fraction in the bottom muds.

Additional new evidence of resuspension appears in the form of a thick storm sand layer now observed on the surface of southern Norton Sound; a layer of this thickness is not apparent in the past thousands of years of stratigraphy. This suggests that originally thick sand layers of major storms are eroded away due to resuspension by smaller storm events subsequent to the major event, so that the stratigraphic record may preserve storm sand layers that are thinner than those originally deposited. A generally thicker surface sand, compared to the other sand layers in each individual core, verifies the model of sediment resuspension.

Resuspension of bottom sediment by waves is also suggested by side-scan sonar and underwater television videotapes which show large scour depressions and formation of oscillation ripples by storm waves (Larsen et al., 1979).

Ice gouges covered by sediment in regions of intense ice scouring again suggest significant sediment resuspension and movement in southern Norton Sound (Thor and Nelson, 1980).

Potential Hazards and Storm-surge Deposition and Erosion

All evidence indicates that unusually large amounts of sediment are resuspended and then transported from Bering Sea to Chukchi Sea (Nelson and Creager, 1977) consequently any structure impeding this movement requires careful design. Data on suspended sediment verifies that about 10 percent of the Yukon River input to Norton Sound may be carried as part of the normal suspended sediment load that is bypassing through the Bering Strait. Because as much as 40 percent of the late Holocene discharge of the Yukon River appears to be missing from Norton Sound (Nelson and Creager, 1977), then, up to 20 million metric tons of sediment per year, on the average, may be suspended and carried to Chukchi Sea by the strong northward flowing currents. The several hundred percent increase of suspended sediment transport, observed during a small storm in 1977, by Cacchione and Drake (1979), suggests that most of the 40 percent displacement of the suspended sediment occurs during storm events.

In summary, there are extremely large amounts of suspended sediment moving rapidly in the coastal waters along Alaska, often in intermittent large concentrations generated by storms and the early summer seasonal runoff. The fall storm season consequently could cause extremely wide dispersal of any oil spill material residing on the sea floor. Recent data by Drake (in press) suggest sediment resuspension may also be vigorous, even during the season of ice cover, because of greater constriction of currents in the delta region where the most rapid deposition occurs. Thus, any pollutants residing on the sea floor face extremely wide dispersal from northern Bering Sea to distances as far as a thousand kilometers to the north into the Arctic Ocean.

Storm surges generally dominate the mass movements of suspended sediment and also can be seen to move large amounts of rapidly prograding sand in bedload transport for distances of up to 60 km offshore. This intensive transport and deposition could affect offshore facilities, especially pipelines. Storm sand layers deposited by such events could be impeded in their transport by any structures that protrude on the sea floor. These protruding structures could act as a dam, holding back the sediment transport and of course, would be put under severe stress if the sediment piled up rapidly against any feature such as a pipeline on the sea floor.

Conclusions and Suggestions for Future Work

A complex and vigorous set of sedimentary processes are apparent in the shallow Yukon Delta front platform and prodelta regions. A major depositional sequence of graded sands may prograde offshore in storm surges. These graded sand beds with a vertical sequence of structures that mimic those of turbidites (Bouma, 1962) provide an example of shallow water deposition from rapidly waning storm surge currents that is very much like that of turbidity currents.

Storm surges and their concommitant wave and current activity have important effects on this basin that must be considered in planning for offshore development. Extensive erosion of the sea floor, resuspension of sediment, and transport of materials and any attached pollutants is one aspect. The second potential effect is movement of extensive sand sheets from shoreline and nearshore sources to offshore areas. Rapid deposition of 15 cm or more of sand can smother biota immediately and alter texture of the substrate over extensive areas for a number of years. Thus, a sea-floor baseline measured at one time, alters markedly in post-storm conditions. Future studies should monitor conditions with an instrument such as the

GEOPROBE which can help to determine the severity of sea-floor erosion in different locations during a storm. A number of deep vibracores are needed to determine recurrence intervals of such events and charateristics before and after such a catastrophic episode.

Acknowledgments

Discussion with Hans Reineck, Ed Clifton, Bill Dupré, Jim Howard and Ed Clukey has enhanced my conceptual development of storm sand layer sedimentation. Collection of inshore cores and preparation of excellent peel structures by James Howard, Devin Thor, and Rick Brokaw was a key to complete assessment of this storm sand system. Brad Larsen, Devin Thor, Jeff Patry, Carol Hirozawa, Joan Esterle, and Carol Madison have assisted in preparation of figures and compilation of data.

References Cited

Anderton R., 1976, Tidal shelf sedimentation: an example from the Scottish Dalradian: Sedimentology, v. 23, no. 4, p. 429-458.

Cacchione , D.A., and Drake, D.E., 1979, Sediment transport in Norton Sound, Alaska, Regional Patterns and GEOPROBE SSystem measurements: U.S. Geological Survey Open-File Report 79-1555, 88 p.

Clukey, E., Cacchione, D.A., Nelson, C.H., 1980, Liquefaction potential of the Yukon prodelta, Bering Sea: Offshore Technology Conference, Houston, Proceedings, v. 1, paper 3773, p. 315-325.

Coachman, L.K., Aagaard, Knut, and Tripp, R.B., in press, Bering Strait: The regional physical oceanography: University of Washington Press.

Dupré, W.R., 1976, Yukon delta coastal processes study: Environmental Assessment of the Alaskan Continental Shelf, Annual Report of Principal Investigators for year ending March, 1977, Environmental Research Laboratory, Boulder, Colo., NOAA, U.S. Dept. of Commerce, v. 13, p. 5-40.

Dupré, W.R., 1980, Deltaic sedimentation on the epicontinental shelf of the northern Bering Sea: in Nio, S.C., Schattenhelm, R.T., and Van Weering, T.C.E. eds., Holocene Marine Sedimentation in the North Sea Basin, Special Publication No., Intl. Assoc. Sedimentologists, Blackwell Scientific Publications, London, (in press).

Fathauer, T.F., 1975, The Great Bering Sea Storms of 9-12 November 1974: Weatherwise Magazine, Am. Meteorological Society, v. 28, pp. 56-84.

Fleming, R.H., and Heggarty, D., 1966, Oceanography of the southeastern Chukchi Sea, in Wilimovsky, N.J., Wolfe, J.M., eds., Environment of Cape Thompson Reigon, Alaska: U.S. Atomic Energy Commission, p. 697-754.

Howard, J.D., and Reinick, H., 1980, Sedimentary structures of a "high energy" beach-to-offshore sequence; Ventura-Port Hueneme area, California, U.S.A., University of Georgia Marine Institute, contribution no. 371. (in press).

Hayes, M.O., 1967, Hurricanes as geological agents: case studies of Hurricane Carla, 1961 and Cindy, 1963: Report Inves. No. 61, Bur. Econ. Geol., University of Texas, Austin, Texas, 54 p.

Larsen, B.R., Nelson, C.H., Larsen, M.C., Thor, D.R., Olsen, H.W., Clukey, E.C., Howard, J.D., Esterle, J.S., and Kilty, L.A., 1980, Physical properties of Norton Basin sediment. U.S. Geological Survey Open-File Report (in press).

Larsen, M.C., Nelson, C. Hans, and Thor, D.R., 1979, Geologic implications and potential hazards of scour depressions on Bering shelf, Alaska: Environmental Geology, v. 3, p. 39-47.

McManus, D.A., Venkatarathnam, K., Hopkins, D.M., and Nelson, C.H., 1974, Yukon River sediment on the northernmost Bering Sea shelf: Jour. Sedimentary Petrology, v. 44, no. 4, p. 1052-1060.

Nelson, C. Hans, and Creager, J.S., 1977, Displacement of Yukon-derived sediment from Berng Sea to Chukchi Sea during Holocene time: Geology, v. 5, p. 141-146.

Nelson, C.H., Rowland, R.W., Stoker, S.W., and Larsen, B.R., 1980, Interplay of physical and biological sedimentary structures: in: Hood, D.W., ed., The Eastern Bering Shelf: its Oceanography and Resources, (in press).

Olsen, H.W., CLukey, E.C., and Nelson, C.H., 1980, Geotechnical characteristics of bottom sediment in the northern Bering Sea: in Nio, S.C., Schattenhelm, R.T., and Van Weering, T.C.E. eds., Holocene Marine Sedimentation in the North Sea Basin, Special Publication No., Intl. Assoc. Sedimentologists, Blackwell Scientific Publications, London, (in press).

Sallenger, A.H., Dingler, J.R., and Hunter, R., 1978, Coastal processes and morphology of the Bering Sea coast of Alaska, in: Environmental Assessment of the Alaskan Continental Shelf, Annual Report of Principal Investigators for the year ending March 1978, Environmental Research Laboratory, Boulder, Colorado, NOAA, U.S. Dept. of Commerce, v. 12, p. 451-470.

Schumacher, J.D., and Tripp, R.B., 1979, Response of northeast Bering Sea shelf waters to storms: EOS, v. 60, p. 856.

Thor, D.R., and Nelson, H., 1980, Sea ice as a geologic agent on the subarctic Bering shelf, in: Hood, D.W., ed., The Eastern Bering Sea Shelf: Its Oceanography and Resources, (in press).

Figures

Figure 1. Bottom water currents and bathymetry of the northern Bering Sea.

Figure 2. Thickness and distribution of a surface sand layer in samples taken after the 1974 storm surge.

Figure 3. Distribution of vertical sequences of sedimentary structures in storm sand layers in southern Norton Sound and thickness of graded sand beds expressed as a prercent of total core length.

Figure 4. Mean Grain size change in graded sand layers with distance from the Yukon Delta shoreline.

Figure 5. Sedimentary structures of storm sand layers
A. Homogeneous trough cross-bedded sand from the thalweg of the sub-ice channel extending off the southwest distributary of the Yukn River, 3 km from shoreline.
B. Inshore (5 km from shoreline) graded sand layer from interchannel area of sub-ice channel off the southwest distributary showing lower flat lamination S_b, cross lamination S_c, upper flat lamination and S_e mud cap.
C. Offshore graded sand showing S_{c-e} and $S_{d,e}$ sequences from a 2 m vibracore, 22 km from shoreline off the northeastern part of the delta.
D. Radiograph of distal graded sands and pebble and shell lags from a box core 115 km from Yukon Delta shoreline.

Figure 6. Model depicting sedimentary processes of a storm surge runoff current that may deposit graded storm sand layers off the Yukon Delta in Norton Sound.

Figure 7. Change in surface texture, pre- and post-1974 storm surge in Norton Sound.

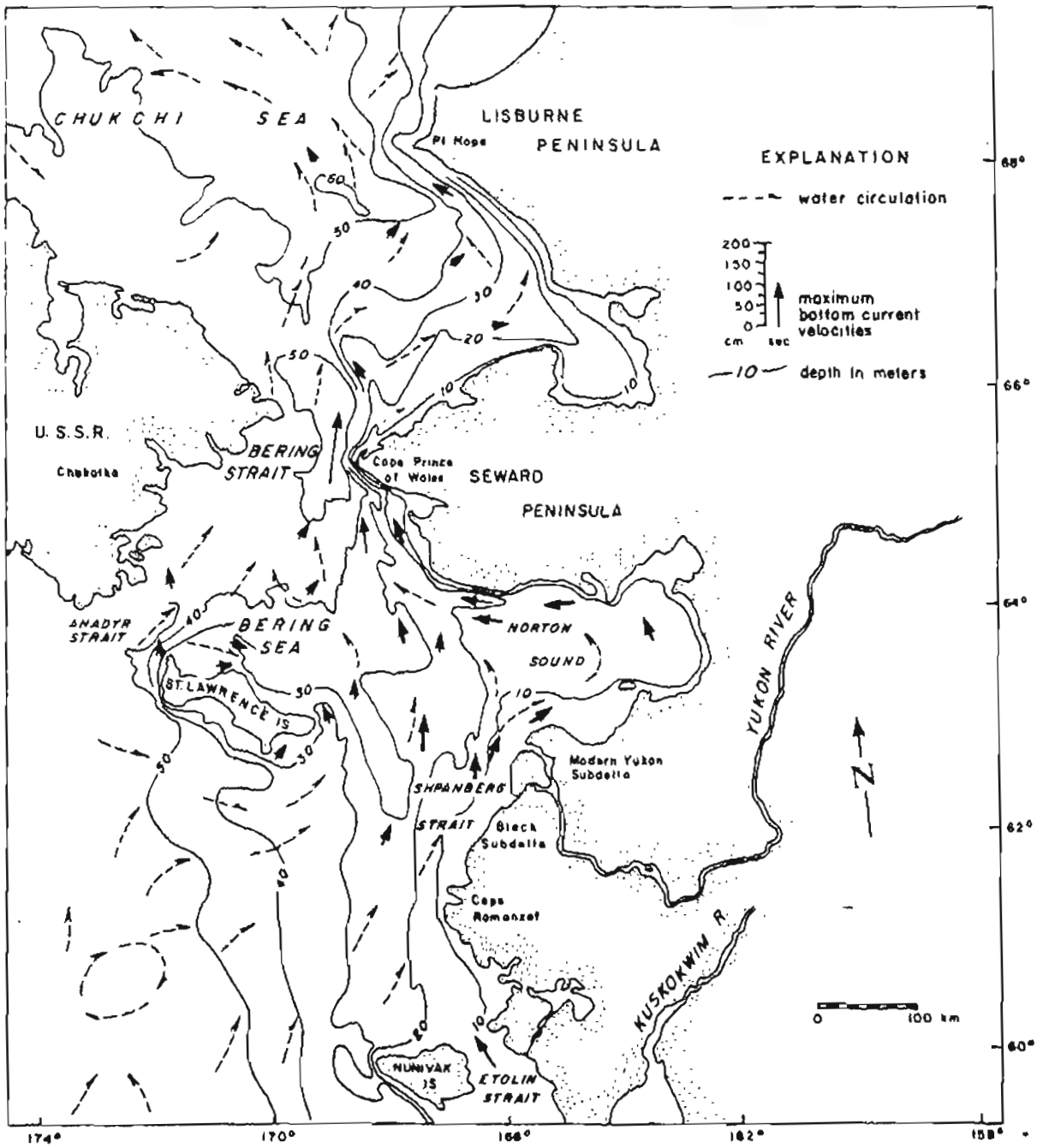
CHUKCHI SEA
LISBURNE PENINSULA
Pt Hope
EXPLANATION
water circulation
200
150
100
50
0
cm sec
maximum bottom current velocities
10
depth in meters
U. S. S. R.
Chukotka
BERING STRAIT
Cape Prince of Wales
SEWARD PENINSULA
ANADYR STRAIT
BERING SEA
NORTON SOUND
YUKON RIVER
ST. LAWRENCE IS.
SHPANBERG STRAIT
Modern Yukon Subdelta
Block Subdelta
Cape Romanzof
KUSKOKWIM R.
NUNIVAK IS.
ETOLIN STRAIT
N
0
100 km
66°
64°
62°
60°
174°
170°
166°
162°
158°

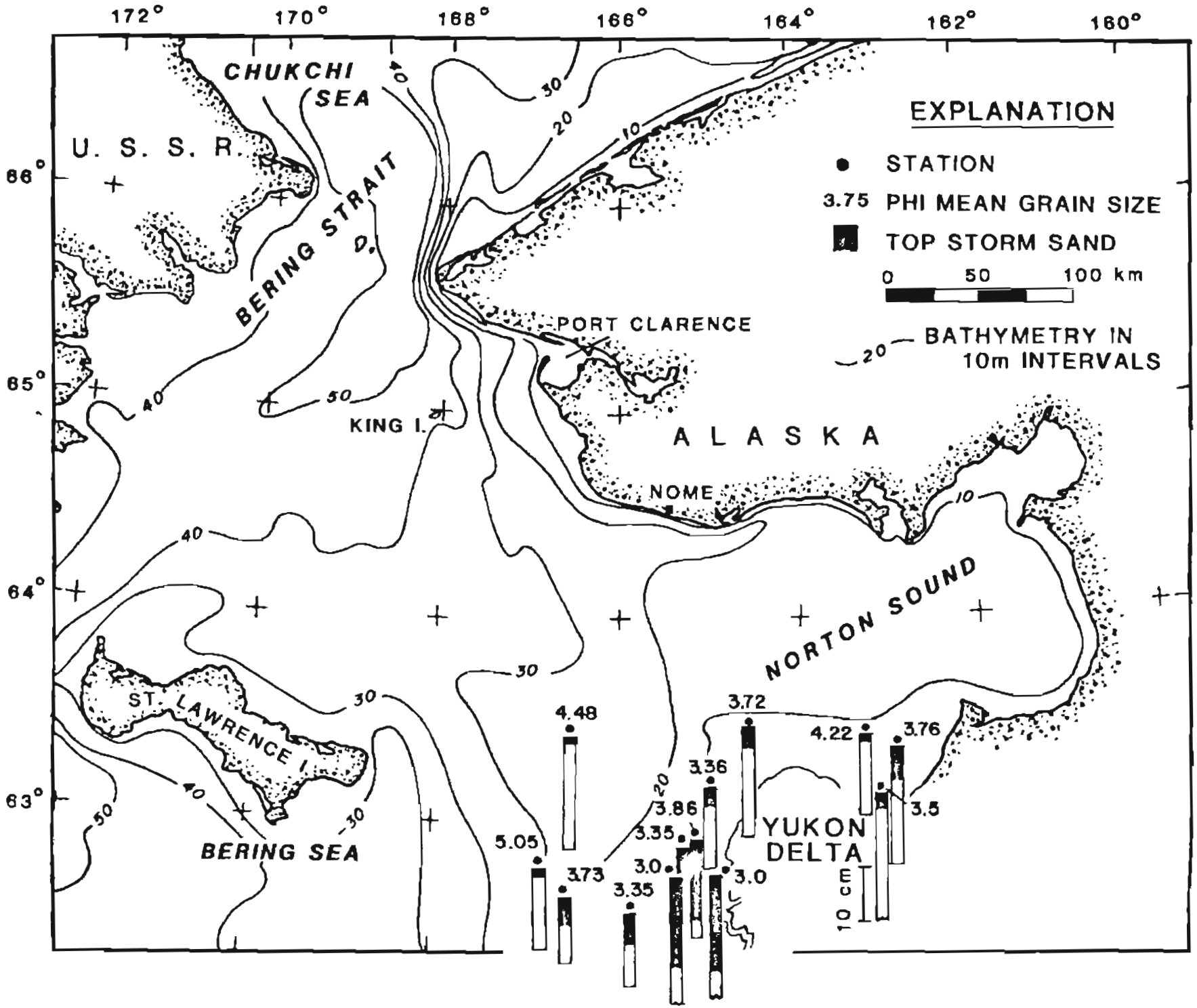
172°
170°
168°
166°
164°
162°
160°
66°
65°
64°
63°
CHUKCHI SEA
U. S. S. R.
BERING STRAIT
PORT CLARENCE
KING I.
ALASKA
NOME
NORTON SOUND
ST. LAWRENCE I.
BERING SEA
YUKON DELTA
EXPLANATION
STATION
3.75 PHI MEAN GRAIN SIZE
TOP STORM SAND
0 50 100 km
BATHYMETRY IN 10m INTERVALS
10 cm
4.48
5.05
3.73
3.35
3.0
3.86
3.35
3.36
3.0
3.72
4.22
3.76
3.5

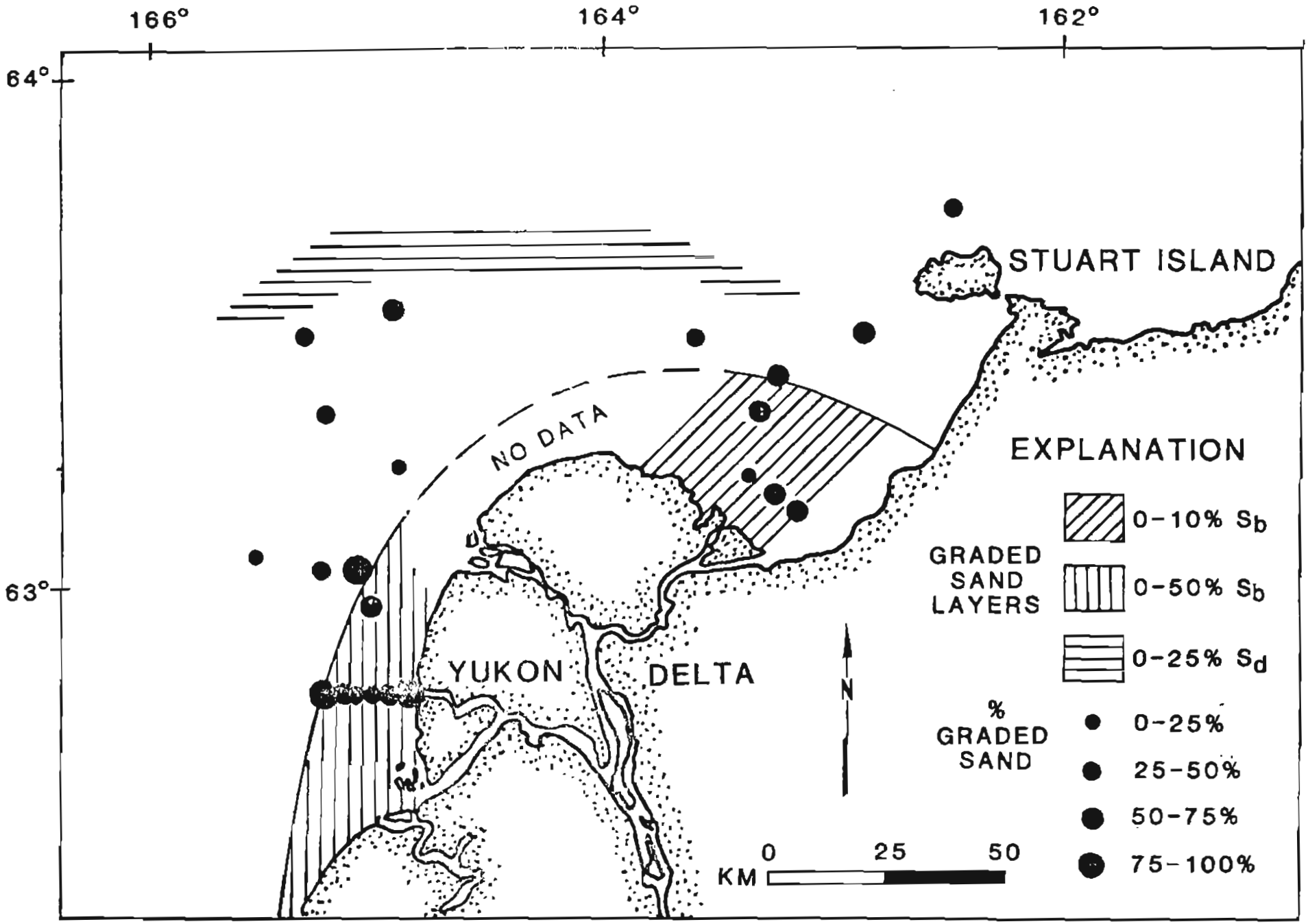
166°
164°
162°
64°
63°
STUART ISLAND
NO DATA
YUKON
DELTA
EXPLANATION
GRADED SAND LAYERS
0-10% Sb
0-50% Sb
0-25% Sd
% GRADED SAND
0-25%
25-50%
50-75%
75-100%
N
0
25
50
KM

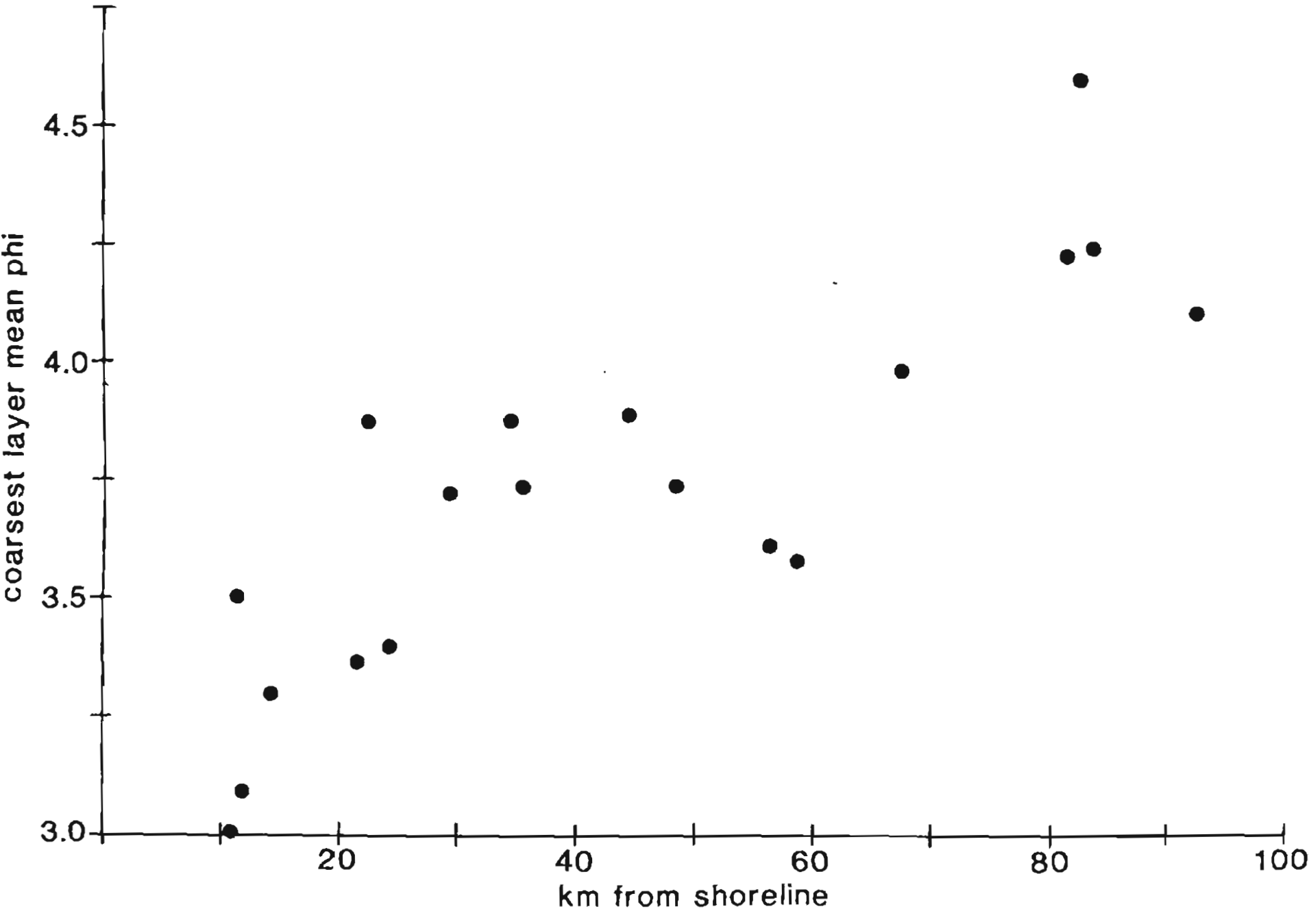
coarsest layer mean phi
4.5
4.0
3.5
3.0
20
40
60
80
100
km from shoreline

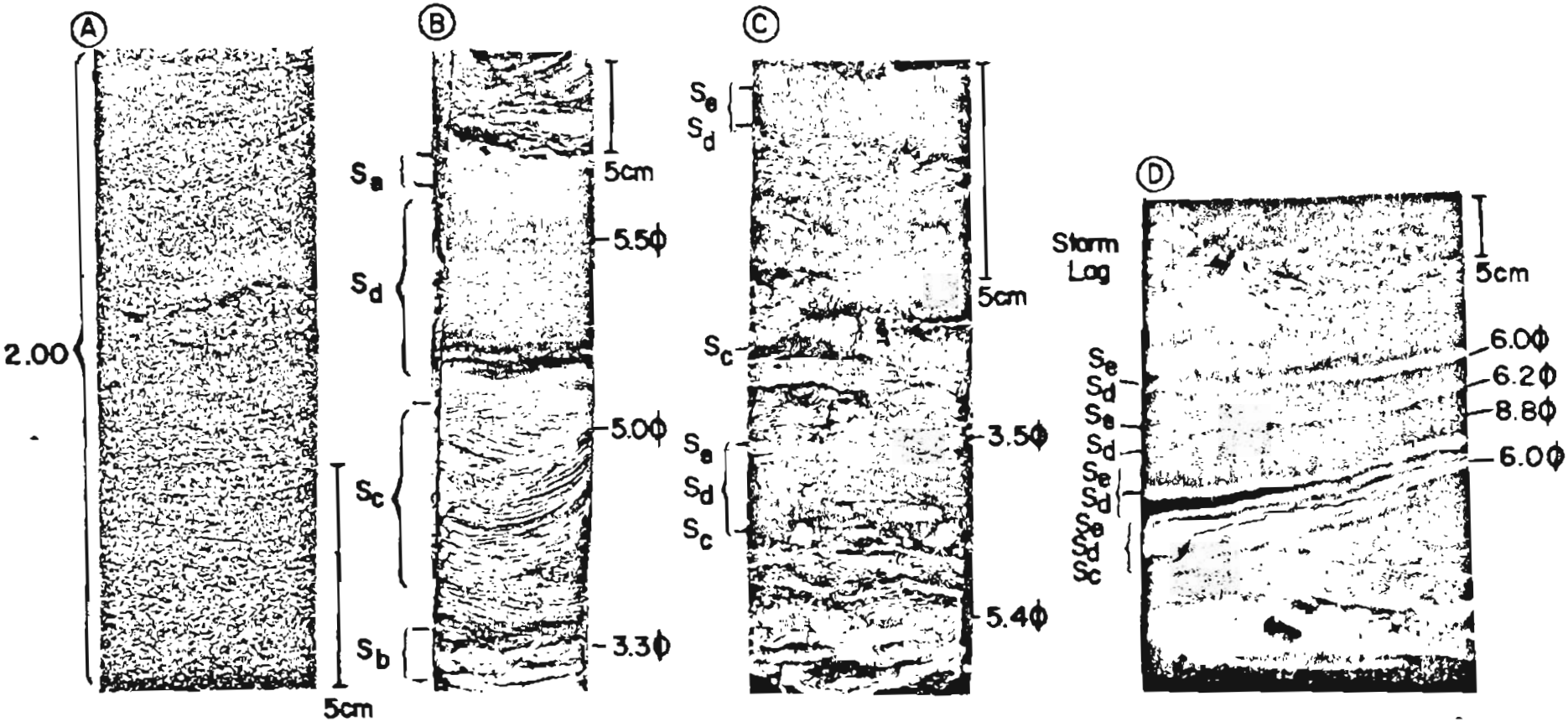
A
B
C
D
2.00
5cm
S_a
S_d
S_c
S_b
5.5ϕ
5.0ϕ
3.3ϕ
S_e
S_d
S_c
3.5ϕ
5.4ϕ
Storm Lag
6.0ϕ
6.2ϕ
8.8ϕ
6.0ϕ

STORM SURGE PROCESSES

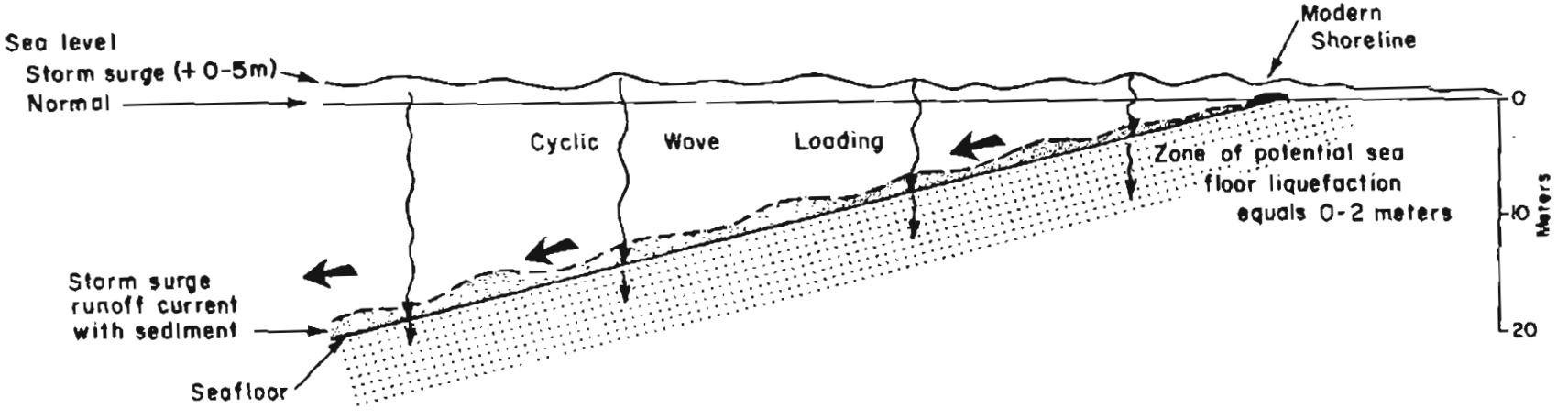

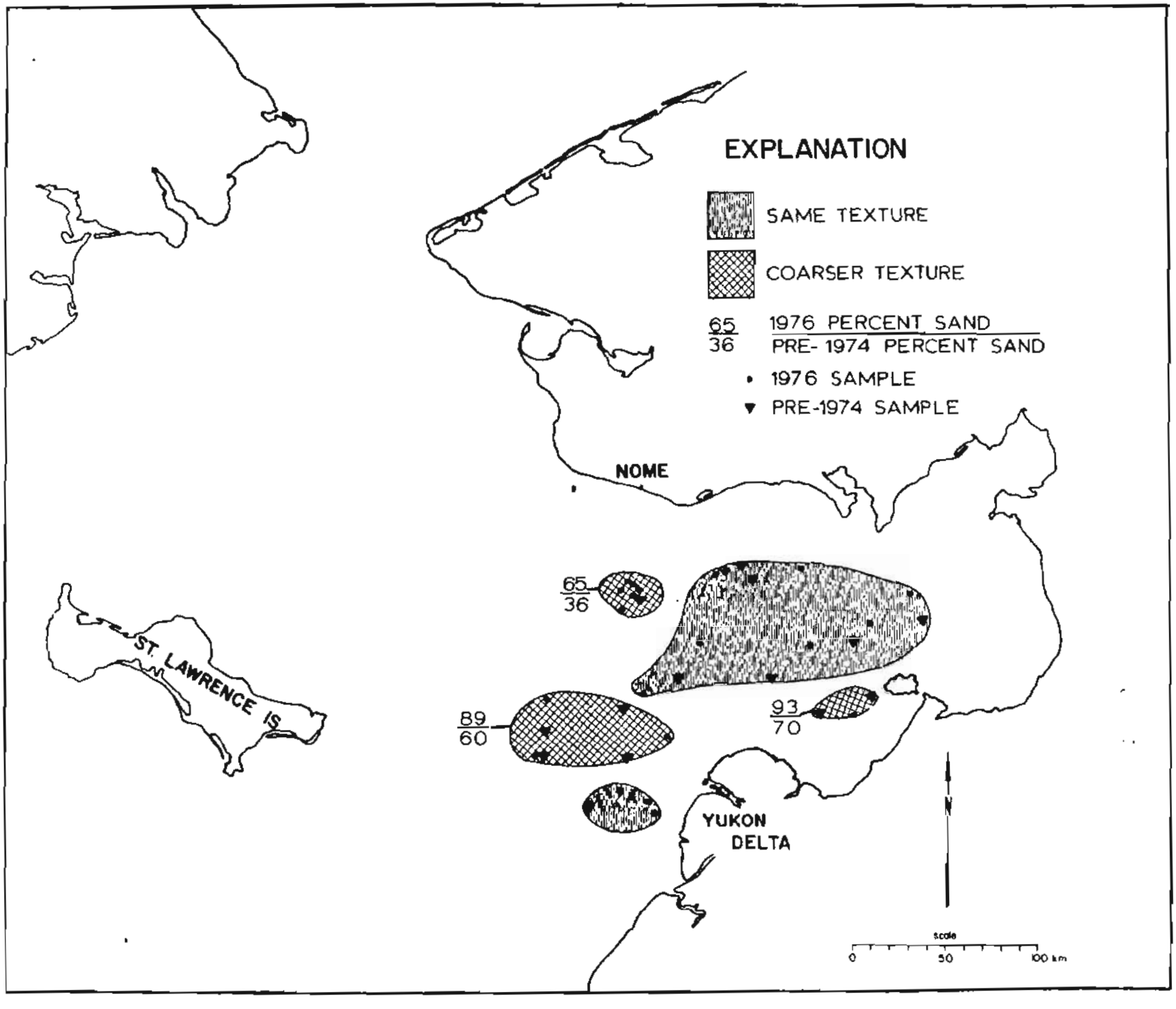
EXPLANATION
SAME TEXTURE
COARSER TEXTURE
65/36 1976 PERCENT SAND / PRE-1974 PERCENT SAND
1976 SAMPLE
PRE-1974 SAMPLE
NOME
ST. LAWRENCE IS.
65/36
89/60
93/70
YUKON DELTA
N
scale
0
50
100 km

ICE GOUGING ON THE SUBARCTIC BERING SHELF

Devin R. Thor and C. Hans Nelson

U. S. Geological Survey, Menlo Park, California 94025

ABSTRACT

Ice impacting the sea floor gouges surficial sediment of the shallow, Bering epicontinental shelf, Alaska. Two types of ice gouge have been recognized: the single gouge, a single gouge furrow, and multiple gouges or raking, a wide zone of numerous, subparallel gouge furrows. Single gouges, the most common type, are cut by single-keeled pieces of thick ice, whereas multiple gouges are formed by multikeeled, thick, pressure-ridge ice. Gouges occur in water depths of 30 m or less, but are most dense in water 10 to 20 m deep. Although some gouge incisions are as deep as 1 m, most gouges are 0.5 m or less. Ice gouges trend parallel to pack ice movement, which in turn generally moves parallel to isobaths and coastline configuration. Mean gouge trend in Norton Sound is west-east, in northeastern Bering Sea north-south.

The annual ice cover in this subarctic setting is thin (less than 2 m). Ice thick enough to gouge the substrate forms in compression and in shear zones; there moving pack ice collides with and piles up against other pack ice or stationary shorefast ice to develop numerous pressure ridges. Southward-moving pack ice in northeastern Bering Sea and westward-moving pack ice in Norton Sound converge with, and shear past, a 10-30-km wide shorefast ice zone that covers the shallow water offshore of the Yukon Delta. The intensity of ice deformation in this zone causes the highest gouge density in the study area. In contrast, northeastern Norton Sound is an area of ice divergence and only minimal ice gouging. The rest of Norton Sound and northeastern Bering Sea is either in ice-divergence areas or water depths are too great for ice to touch bottom, thus ice gouge density in these places is low. Gouging is extremely rare inshore of the shear zone, because shorefast ice is relatively static and protects inshore areas from the dynamics of the shear or compression zone and consequent ice gouging.

INTRODUCTION

Development of natural resources in northern latitudes has led to increased research on the effects of ice on shelf sediment in arctic regions such as the Beaufort Sea (Reed and Sater, 1974; Reimnitz and others, 1973; Reimnitz and others, 1977; Barnes and others, 1978). Until recently, however, research on ice gouging had not been done in subarctic regions such as the Bering Sea. A variety of gouge features are found in many areas of northeastern Bering Sea, even though ice conditions there are not as severe as in high-latitude arctic regions. Ice gouging into the sea floor is a potential hazard to future resource development and sea-floor installations such as pipelines and wellheads.

This paper discusses general ice conditions and ice movement in northeastern Bering Sea, the effect of ice as an erosional and depositional agent that influences the geomorphology and depositional history of the shallow subarctic Bering Sea shelf, and ice gouging as a potential hazard to resource development in and around Norton Basin. Terminology used is adopted from Barnes and others (1978), particularly in the use of the word "gouge"to describe the feature and the process of ice interacting with the sea floor.

Geographic Setting

The floor of northeastern Bering Sea is a broad, shallow epicontinental shelf (Figs. 1 and 2). Water depths in Chirikov Basin range from 20 m on the eastern side to 50 m in the central part. The shelf is generally flat and featureless except for a prominent series of ridges and swales that subparallel the coastline off Port Clarence. A large, elongate marine re-entrant forms Norton Sound, bounded on the north by Seward Peninsula, on the east by the Alaskan mainland, and on the south by the Yukon Delta. Except in

a broad trough in the northern part of the sound, where depths are as great as 27 m, water depths in Norton Sound range from 10 to 20 m. The offshore part of the Yukon Delta is a zone of extensive shoals covering about 8000 km^2 (Fig. 2). Water depths 10 to 30 km offshore do not exceed 3 m, at which point there is a gentle break in slope and the depth increases to 10 m as far as 50 to 70 km from shore. The substrate of the Yukon prodelta, derived from the Yukon River, consists of coarse silt to very fine sand, whereas sediment in Chirikov Basin consists mostly of glacial gravel and transgressive fine sand (Nelson and Hopkins, 1972; McManus and others, 1977).

Ice Conditions and Movement

Ice overlies northern Bering Sea annually from November through June (Muench and Ahlnas, 1976; Shapiro and Burns, 1975). Depending on the severity of the winter, multiyear ice may migrate into Bering Sea from southern Chukchi Sea. Keel depth of 90% of the pack ice (any free-floating ice regardless of origin) is less than 1 m, although depths to 20 m have been reported (Arctic Research Laboratory, 1973).

Ice in open sea pans in Norton Sound is 0.7 to 1.2 m thick (Brower, and others, 1977), but can get as thick as 2 m (Carole Pease, 1979, pers. comm.). Shorefast ice (ice anchored to the land) extends seaward to about the 10 m isobath and is best developed in the southern part of Norton Sound, around the Yukon Delta (Ralph Hunter, written comm., 1976; Dupré, 1977, Stringer and others, 1977) (Fig. 2).

Analysis of Landsat photographs (Dupré and Ray, Sec. II, this volume; Stringer and others, 1977; Muench and Ahlnas, 1976; Shapiro and Burns, 1975) has contributed to a preliminary understanding of ice dynamics in the Bering Sea. Pack ice in the northern Bering Sea originates from (1) *in situ* northeastern Bering Sea ice and (2) advected Chukchi Sea ice. Chukchi Sea ice can move through the Bering Strait and into the northern Bering Sea during episodes of rapid deformation and subsequent rapid southerly movement of pack ice caused by episodes of strong northerly winds (Shapiro and Burns, 1975).

Ice movement in the northeastern Bering Sea is controlled by the interplay of: (1) prevailing winter northeasterly geostrophic wind (Muench and Ahlnas, 1976), (2) erratic onshore wind (NOAA, 1974), (3) northward-flowing water current on the eastern side of the Bering Sea (Coachman and others, 1976) (Fig. 2), and (4) a counterclockwise current gyre in Norton Sound (Nelson and Creager, 1977) (Fig. 2). Late winter and early spring winds tend to push ice generally southward in northeastern Bering Sea, whereas waning late spring winds allow pack ice to be increasingly influenced by the northward-flowing water currents (Fig. 2).

In Norton Sound the dominant direction of ice movement is southwestward out of the sound. This drift creates a zone of divergence in the northeastern part of the sound and a zone of convergence in the southwestern or Yukon prodelta area of the sound (Dupré and Ray, Sec. II, this volume; Stringer and others, 1977) (Fig. 2). Periodic changes in wind and water current tend to move ice in and out of the sound, thereby making it possible for Bering Sea ice, or even advected Chukchi Sea ice, to work its way into the sound.

Zones of convergence can be zones of pressure-ridge or shear-ridge formation characterized by colliding, piling up, and deforming of the edges of

fast ice and of pack ice (Reimnitz and Barnes, 1974). The best-developed pressure ridges in northeastern Bering Sea form around the Yukon Delta, where Bering Sea pack ice on the western prodelta and Norton Sound pack ice on the northern prodelta collides with the Yukon Delta fast ice (Dupré and Ray, Sec. II, this volume; Stringer and others, 1977).

Methods

Data for this study were gathered by the U.S. Geological Survey during September 1976, July 1977, and September 1978 aboard R/V SEA SOUNDER and during June and July 1978 aboard R/V KARLUK. Approximately 5,100 km of side-scan sonar trackline was obtained (Fig. 1). Normally, seismic units with energy sources of 200 kHz, 12 kHz, 7 kHz, 3.5 kHz, and 2 kHz were run simultaneously with side scan for additional bottom and subbottom information. The 6-m keel depth of the R/V SEA SOUNDER limited ship operations to water deeper than 8 m, whereas the shallow draft of the R/V KARLUK (1 m) allowed surveying in nearshore areas and in the shallow waters off the Yukon Delta. Geophysical and navigational operations are described in Thor (1978).

An EG and G side-scan sonar system*, consisting of a dual-channel graphic recorder and a towed transducer fish, was used to survey the sea floor. Side-scan sonar, an alternative method to conventional vertical echo sounding, employs a 105 kHz acoustic beam whose axis is slightly below horizontal. This acoustic beam can resolve topographic irregularities and objects on the sea

*Any use of trade names and trademarks in this publication is for descriptive purposes only and does not constitute endorsement by the U.S. Geological Survey.

floor with as little as 10 cm of relief. Reflected echoes are graphically recorded in a form that approaches a plan view map. Discussions on theoretical and practical aspects of side-scan operation and interpretation can be found in Belderson and others (1972) and Flemming (1976). Normally the side-scan was operated at 100-m sweep (the scan range on either side of the ship); although at times, the 50-m sweep was used to help resolve details of the gouging. In addition, a 200 kHz high-resolution fathometer was operated to measure the incision depth of ice gouges (Fig. 3). Vertical relief of gouges on the fathometer record or on the horizon line of sonographs is generally masked by the recording of sea swell or ship's motion on the chart paper.

Gouge data were collected from the sonographs by counting the number, measuring the trend, and noting the time of occurrence of all gouges seen on the records. Distortion of sea floor features on the sonograph occurs parallel to the line of travel because of the difference in ship's speed and the recorder's paper-advance speed. To obtain absolute compass trend of gouges, a distortion ellipse protractor, which corrects for the apparent angle produced by ship paper speed, was used to measure gouge angle with respect to ship's track. This information was then normalized at 10-km intervals. Normalization entailed two procedures: (1) correction of the number of observed gouges and (2) averaging of observed gouge trends. The number of observed gouges per 10-km interval was multiplied by 1/sin (where angle equals the angle between ship's course and gouge trend) to correct for the fact that ship's course usually was not normal to the gouge trend. Any angle other than 90^0 between ship's course and gouge trend will give a false picture of gouge density (Barnes and others, 1978). Averaging observed gouge trends

involved graphing the measured trends for the 10-km intervals and noting the average dominant and subordinate trend or trends. Each average trend per 10-km interval was then plotted on the base map to define areas of similar gouge trend.

GEOMETRY AND TYPE OF ICE GOUGING

Two basic types of ice gouge have been recognized on the sea floor of northeastern Bering Sea: (1) single gouges and (2) multiple gouges or raking. A single gouge, the dominant type of ice-produced mark on the Bering Sea floor, is a groove produced by a single ice keel plowing through the surficial sediment (Figs. 3-A, 3-B, 4-A, 4-B, and 4-C) (Reimnitz and others, 1973; Reimnitz and Barnes, 1974). Single gouges are ubiquitous throughout Norton Sound; although the highest density occurs around the prodelta of the Yukon River (Fig. 5).

Single gouge widths range from 5 to 60 m; a width of 15 to 25 m is most common. Gouge patterns range from straight, through sinuous, to sharp-angled turns (Fig. 4). Incision depths of gouges, as measured on the sea-floor profile of sonographs (Fig. 4-E) and on the 200 kHz fathometer record (Fig. 3-B), can be as deep as 1 m. Most gouges range in depth from 0.25 to 0.5 m or less. These figures may be conservative because of the geometric relation between the narrow width of the gouge and the spread of the acoustic cone of the fathometer transducer (Reimnitz and others, 1977). The original incision depth is impossible to determine unless the gouge is seen as the keel plows the bottom, because the gouge has subsequently been infilled.

Multiple gouges or raking (Figs. 4-F and 4-G) are produced when multi-keeled floes (such as pressure ridges) plow or rake the bottom sediment, creating numerous parallel furrows (Reimnitz and others, 1973; Reimnitz and

Barnes, 1974). Unlike single gouges, raking is not ubiquitous, but in the Yukon prodelta area the raking process is locally more prevalent than single gouging. Zones of raking are 50-100 m to several kilometers wide. The deepest incisions caused by raking observed on the records are about 1 m; but raking, like single gouges, usually produces incisions less than 0.25-0.5 m deep.

TREND AND DISTRIBUTION OF GOUGES

Analysis of the trend and distribution of gouges allows recognition of five areas of gouging with similar trends (areas I - V), and two large areas almost devoid of gouges (VI and shorefast ice zone) (Fig. 5). Absolute direction of ice movement cannot be predicted because criteria needed to make certain distinctions, such as gouge terminations, were not seen on the sonographs.

In areas I and II (Fig. 5), the dominant trend of gouges is distinctly subparallel to isobaths and the coastline. There is more data scatter in areas III, IV, and V, but gouges again are generaly parallel to isobaths and the coastline. The greatest data scatter is seen in area V, but this may reflect the irregular bathymetry of ridge and swale topography off Port Clarence. Except for a couple of gouges off the northwestern end of St. Lawrence Island, area VI is devoid of ice gouges.

Density of ice gouges is as much as 25 times higher around the Yukon Delta area, where the water is 10 to 20m deep, than in other areas of northeastern Bering Sea (Table I and Fig. 5, areas I and II). Not coincidentally, the Yukon prodelta is the largest expanse of shallow water in the study region. Here density of ice gouges can be as high as 75 gouges/km^2. Density of ice gouging is 60 times higher in water 10 to 20 m deep than in water 5 to 10 m deep or in water 20 to 39 m deep (Table II). Gouging has not been seen in water shallower than 5 m or deeper than 30 m.

Table I

Gouge Density by Area

Area	km^2	Trackline km	Total number of gouges	Average density (gouges/km^2*)
I	5,500	530	1,684	3.18
II	8,000	1,005	5,080	5.05
III	9,500	1,100	917	0.83
IV	15,500	400	993	2.48
V	7,900	1,120	216	0.19
VI	50,400	766	4	0.03

*Assuming 1 km trackline of side-scan sonar is representative of 1 km^2.

Table II

Gouge Density by Water Depth Interval

Depth interval(m)	km^2	Trackline km	Total number of gouges	Gouges/km^2*
0-10	16,500	480	147	0.31
10-20	24,600	2100	8,593	4.09
20-30	32,700	1300	143	0.11
30-40	26,000	750	0	0
40-50	12,600	450	0	0
>50	5,400	170	0	0

*Same as Table 1.

GEOLOGICAL SIGNIFICANCE

Trend and Density of Gouges

The interplay of geomorphology, water depth, oceanic conditions, and location of compression or of shear zones (Fig. 2) determines the pattern of ice gouging in northern Bering Sea (Figs. 5 and 6). The orientation of ice gouges is dependent on the direction of ice drift under the influence of wind and water current. The dominant trend of ice gouges, therefore, in Norton Sound is east-west and in the Bering Sea north-south (Figs. 5 and 6).

Land promontories, such as the Yukon Delta, tend to block ice movement and to cause the formation of compression and shear zones. Formation of ice ridges around the Yukon Delta by the collision and shearing of moving pack ice with stationary shorefast ice accounts for the high density of ice gouges in areas I and II (Fig. 5). Areas within the zone of shorefast ice, such as the large area around the Yukon Delta (Fig. 5), are devoid of gouges. This is because only the edge of the shorefast ice is deformed by the pack ice, and subsequent deformation occurs continually seaward through a process of migration of the compression/shear zone through time (Dupré, 1978). Areas III and IV are characterized by low density of ice gouges (Fig. 5). Gouging in areas III and IV is the product of ridges formed in an ice-divergence zone by intercollisions of pack ice. Density of ice gouges in area V is low because this area is not in a convergence zone and at most places water depth exceeds normal ice-keel depths. Area VI does not seem to have any ice gouging because water depths (Fig. 2) exceed normal ice-keel depths (Fig. 5).

Age of Ice Gouges

Although no specific studies were made to determine the age and longevity of gouges, the gouges seem to be modern ephemeral phenomena that recur annually. West of Port Clarence and in the nearshore area of Nome, ice gouges cut through ripple- and sand-wave fields that are in dynamic equilibrium with present wave or current motion (Nelson and others, 1978; Hunter and Thor, 1979) (Figs. 4-A and B). Here old gouges, highly modified by ripples or sand waves and new gouges suggests that gouges are being formed each winter.

A number of geologic processes act to rapidly destroy gouges once they have formed. Initial smoothing of ice gouges can be enhanced by: (1) the saturated, silty substrate that tends to seek a minimum relief equilibrium

with sides of the gouge flowing or slumping toward the center of the gouge, and (2) the constant oscillatory pounding of wave motion on the sea floor that causes shear failure in the soft sediment (Henkel, 1970), causing gouge sides to collapse toward the center. The 'dish-shape' profiles of most gouges (Figs. 4-E and G) indicate that these are normal factors in the process of gouge destruction.

Repeated surveys of ice gouges in water less than 20 m deep in the Beaufort Sea have shown that gouges are frequently smoothed over completely in one season (Barnes and Reimnitz, 1979). In the Bering Sea, the ice-free season is 3 to 4 months longer than in the Beaufort Sea, allowing more time for considerably stronger open-water wave and current regimes of the Bering Sea to destroy gouges. In Norton Sound, storm waves and currents caused by advance and retreat of storm-surge water, in addition to normal tidal and geostrophic currents, resuspend and transport large quantities of surficial sediment (Cacchione and Drake, 1978; Nelson and Creager, 1977). Destruction of gouges is augmented by biological reworking of surficial sediment, an active process in Norton Sound (Nelson and others, in press). In summary, gouges will tend to be either eroded or buried because they are not in equilibrium with the dynamic physical processes on the sea floor. This reinforces the hypothesis that gouges in Bering Sea are present-day phenomena involving development of some new gouges each ice season.

Ice/Sediment Interaction

Ice acts as both an erosional and a depositional agent. Ice gouges, mixes, and deforms the substrate, and promotes current scour. Ice partially controls the geomorphology of the Yukon Delta (Dupré and Thompson, 1979).

Sediment mixing and deformation of the substrate are important processes in densely gouged areas such as the Yukon prodelta where pressure-ridge raking can gouge 1 m into the sediment. One event of pressure ridge raking can affect several square kilometers of sea floor.* Such an event can mix or disrupt several million cubic meters of sediment. A zone of deformed sediment in box core No. 48 (11-18 cm interval, Fig. 3-C) possibly represents an ice-gouge event.

Sharpness of gouge morphology is highly dependent on the type of substrate being gouged. The sediment of the Yukon prodelta is a moderately cohesive sandy silt that will hold a shape better than the coarser-grained sediment of central Norton Sound or offshore from Port Clarence (Clukey and others, 1978; Nelson and Hopkins, 1972; McManus and others, 1977). The gouge shown in figure 5-A and some gouges shown in figure 4 are examples of forms with sharp relief in a competent substrate. Gouges shown in figure 4-A are smoother in form because they cut into a cohesionless sand substrate in the Port Clarence area.

Prominent broad (50-150 m wide), shallow (0.6-0.8 m deep) depressions on the western Yukon prodelta are associated with areas of intense ice gouging and strong bottom currents (Larsen and others, 1979). Topographic disruption by ice gouges in these areas apparently causes flow separation in the strong

*Area of gouging times depth of gouging. Ex. 2000 m (length of gouged zone) x 1000 m (width of gouged zone) x 0.5 m (depth of gouge) = 1,000,000 m^3.

currents, thereby initiating scour depression for extensive distances downstream. Consequently, large regions of scour may continue to expand away from intensely gouged areas (Fig. 4-H).

The extensive depositional sand shoals of the Yukon Delta front coincide with the seaward extent of shorefast ice, stamukhi (grounded pressure ridges) and zones of dense ice gouging (Figs. 2 and 6). Reimnitz and Barnes (1974) have noted this relation in the Colville Delta area of the Beaufort Sea. They postulate that pressure ridges and stamukhi act as sediment traps or dams, channelize winter currents, or bulldoze sediment to form shoals. Thus, a cycle is formed in the sense that shoal areas determine the extent of shorefast ice and the location of a shear zone and pressure ridges, which in turn cause shoals to develop. Dupré (1979) hypothesizes that the geomorphology of onshore and offshore parts of the Yukon Delta are similarly controlled by ice.

RESOURCE DEVELOPMENT: POTENTIAL HAZARDS

To summarize, gouges are ubiquitous throughout northeastern Bering Sea in water depths of 5 to 30 m. Ice-gouge density varies from rare to sparse in northeastern Bering sea and northern Norton Sound; maximum density is around the Yukon Delta (Fig. 6). Depth of ice gouges is fairly uniform throughout northeastern Bering Sea and seems to be independent of gouge density. Although maximum observed ice-gouge depth is about 1 m and maximum observed current scour about 1 m, the combination of these forces could affect the bottom to depths of several meters, thus presenting some design problems and potential hazards to installations in or on the sea floor. Pipelines and

cables should be buried below the combined effective depth of ice gouging and current scour, plus a safety factor.

Special studies of nearshore areas off Nome and Port Clarence were conducted because both are potential centers for commercial development and activity. Nome, already a well established small city, is the focal point for barge traffic in the northern Bering Sea. Port Clarence, the only natural harbor in the northern Bering Sea has high potential for development as a site for future shipping activity.

Offshore Nome, being an area of ice divergence, is not heavily gouged. Although several gouges were found offshore, none were in water shallower than 8 m. Several of these gouges are probably not related to ice. They are very narrow (less than 1 m) compared to typical ice gouges (more than 5 m wide) and are possibly produced by anchor, anchor chain, or cable drag from the tugs and barges that frequent the port of Nome.

Several gouges were found near Port Clarence at the northern end of the Port Clarence spit and on the northern side of Port Clarence inside the tidal inlet. But, none occurred in water less than 8 m deep.

ACKNOWLEDGMENTS

We thank William Dupré, University of Houston, for data concerning pack ice movement and shorefast ice limits; Ralph Hunter, U. S. Geological Survey, for data on shorefast ice limits; and David Drake U. S. Geological Survey, for data on ice thickness. Jim Evans and Ron Williams compiled data on gouges from sonographs. Valuable discussions on ice processes and interpretation of sonographs were held with Peter Barnes, Erk Reimnitz, and Larry Toimil, U.S. Geological Survey. Marybeth Gerin helped with figure layout and drafting. Erk Reimnitz and Harry Cook, U.S. Geologcial Survey, made helpful comments on

the manuscript. The officers, crew, and technical staff of the R/V SEA SOUNDER made data collection a successful and enjoyable endeavor.

The cruises were supported jointly by the U.S. Geological Survey and by the Bureau of Land Management through interagency agreement with the National Oceanic and Atmospheric Administration, under which a multi-year program responding to the needs of petroleum development of the Alaska continental shelf is managed by the Outer Continental Shelf Environmental Assessment Program (OCSEAP) Office.

REFERENCES CITED

Arctic Research Laboratory

1973 Ice Character in Bering and Chukchi Seas Naval Oceanic Systems Center, Dept. of Navy, San Diego, CA.

Barnes, P.W., David McDowell, and Erk Reimnitz

1978 Ice gouging characteristics: Their changing patterns from 1975-1977, Beaufort Sea, Alaska: U. S. Geological Survey Open File Report 78-730, 42 pp.

Barnes, P.W., and Erk Reimnitz

1979 Ice gouge obliteration and sediment redistribution event; 1977-1978, Beaufort Sea, Alaska, U.S. Geological Survey Open File Report 79-848, 22 pp.

Belderson, R.H., N.H. Kenyon, A.H. Stride, and A.R. Stubbs

1972 Sonographs of the sea floor: Elsevier Pub. Co., New York, 185 pp.

Brower, W.A., and others

1977 Climatic atlas of the outer continental shelf waters - coastal region of Alaska: v. 2 - Bering Sea, Arctic Environmental Information and Data Center, Anchorage, Alaska.

Cacchione, D.A., and Drake, D.E.

1978 Sediment transport in Norton Sound, Northern Bering Sea, in Environmental Assessment of the Alaskan Continental Shelf, Annual Report of Principal Investigators for the year ending March 1978, Environmental Research Laboratory, Boulder, Colorado, NOAA, U.S. Department of Commerce, 12: 308-450.

Clukey, E.C., Hans Nelson, and J.E. Newby,

1978 Geotechnical properties of northern Bering Sea sediment: U.S. Geological Survey Open File Report 78-408, 48 pp.

Coachman, L.K., K. Aagaard, and R.B. Tripp

1976 Bering Strait: The regional physical oceanography: Washington University Press, Seattle, 186 pp.

Dupré, W.R.

1977 Yukon Delta coastal processes study: Environmental Assessment of the Alaskan Continental Shelf, Annual Report of Principal Investigators for the year ending March 1977, Environmental Research Laboratory, Boulder, Colorado, NOAA, U.S. Department of Commerce, 14: 508-553.

Dupré, W.R.

1978 Yukon Delta coastal processes study: Environmental Assessment of the Alaskan Continental Shelf, Annual Report of Principal Investigators for the year ending March 1978, Environmental Research Laboratory, Boulder, Colorado, NOAA, U.S. Department of Commerce, 11: 384-446.

Dupré, W.R., and R. Thompson

1979 The Yukon Delta: A model for deltaic sedimentation in an ice dominated environment: Proceedings Offshore Technology Conference, v. 1, paper no. 3434: 657-664.

FATHAUER, T.F.

1975 The great Bering Sea storms of 9-19 November, 1974: Weatherwise Magazine, American Meterological Society, 28: 76-83.

Flemming, B.W.

1976 Side-scan sonar: A practical guide, in Side Scan Sonar, A comprehensive presentation: E.G. and G. environmental Equipment Division, Waltham, MA, A-1 - A-45.

Fleming, R.H., and Heggarty, D.,

1966 Oceanography of the southeastern Chukchi Sea, in: Willimovsky M.H., and J.M. Wolfe, eds., Environment of Cape Thompson region Alaska: Washington, D.C., U.S. Atomic Energy Commission 697-754.

Goodman, J.R., Lincoln, J.H., Thompson, T.G., and Zeusler, F.A.

1941 Physical and chemical investigations: Bering Sea, Bering Strait, Chukchi Sea during the summers of 1937 and 1938: Washington University publications in Oceanography, v. 3, no. 4 105-169 and appendix 1-117.

HENKEL, D.J.,

1970 The role of waves in causing submarine landslides: Geotechnique, v. 10, 75-80.

Hunter, R. E., and Thor, D.R.

1979 Depositional and erosional features of the northeastern Bering Sea inner shelf (abs.): Amsterdam, International Association of Sedimentologists, Program and Abstracts, Eleventh International Congress in Sedimentology, (in press).

Husby, D.M.

1969 Report of oceanographic cruise U.S.C.G.C. NORTHWIND, northern Bering Sea-Bering Strait-Chukchi Sea, July 1969: U.S. Coast Guard Oceanographic Report, no. 24, 75 pp.

Busby, D.M.

1971 Oceanographic investigations in the northern Bering Sea and Bering Strait, June-July 1969: U.S. Coast Guard Oceanographic Report no. 49, 50 pp.

LARSEN, M.C., HANS NELSON, and D.R. THOR

1979 Geologic implications and potential hazards of scour depressions on Bering shelf, Alaska: Environmental Geology, v. 3, 39-47.

McManus, D.A., V. Kolla, D.M. Hopkins, and C.H. Nelson,

1977 Distribution of bottom sediments on the continental shelf, northern Bering Sea: U.S. Geological Survey Professional Paper 759-C, C1-C31.

McMANUS, D.A., and C.S., SMYTH

1970 Turbid bottom water on the continental shelf of northern Bering Sea: Journal of Sedimentary Petrology, v. 40, 869-877.

MUENCH, R.D., and K. AHLNAS

1976 Ice movement and distribution in the Bering Sea from March to June 1974: Journal of Geophysical Research, v. 81, no. 24, 4467-4476.

National Oceanic and Atmospheric Administration

1974 Local climatological data - annual summary with comparative data for Nome, Unalakeet, Shismaref and Wales, Alaska.

NELSON, HANS, and J. CREAGER

1977 Displacement of Yukon-derived sediment from Bering Sea to Chukchi Sea during Holocene time: Geology, v. 5, 141-146.

Nelson, Hans, M E. Field, D.A. Cacchione, and D.E. Drake

1978 Areas of active large-scale sand wave and ripple fields with scour potential on the Norton Basin sea floor, in: Environmental Assessment of the Alaskan Continental Shelf, Annual Report of Principal Investigators for the year ending March 1978, Environmental Research Laboratory, Boulder, Colorado. NOAA, U.S. Department of Commerce, v. 12, 291-307.

Nelson, Hans, and D.M. Hopkins

1972 Sedimentary processes and distribution of particulate gold in the northern Bering Sea: U.S. Geological Survey Professional Paper 689, 27 pp.

Nelson, Hans, R.W Rowland, Sam Stoker. and B.R. Larsen

1980 Interplay of physical and biological sedimentary structures of the Bering Sea epicontinental shelf, in Hood. D. (ed.), Bering Sea Shelf: Oceanography and Resources: NOAA, (in press).

Pratt, R., and F. Walton,

1974 Bathymetric map of the Bering shelf: Boulder, Colorado, Geological Society of America, scale 1:1,440,000.

Reed, J.C., and J.E. Sater, (eds.)

1974 The coast and shelf of the Beaufort Sea: Arlington, Virginia Arctic Institute of North America, 750 pp.

Reimnitz, Erk, and P.W. Barnes

1974 Sea ice as a geologic agent on the Beaufort Sea shelf of Alaska in Reed, J.C., and J.E. Sater (eds.), The coast and shelf of the Beaufort Sea: Arlington, Virginia, Arctic Institute of North America, 301-351.

Reimnitz, Erk, P.W. Barnes, and T.R. Alpha

1973 Bottom features and processes related to drifting ice: U.S. Geological Survey Miscellaneous Field Studies Map MF-532.

REIMNITZ, ERK, P.W. BARNES, L.J. TOIMIL, and JOHN MELCHIOR

1977 Ice gouge recurrence and rates of sediment reworking, Beaufort Sea, Alaska: Geology, v. 5, 405-408.

Sackinger, W.M., and J.C. Rogers

1974 Dynamics of break-up in shorefast ice in Reed, J.C., and J.E. Sater (eds.), The coast and shelf of the Beaufort Sea: Arlington Virginia, Arctic Institute North America, 367-376.

Shapiro, L.H., and J.J. Burns

1975 Satellite observations of sea ice movement in the Bering Strait region: Climate of the Arctic, Report, University of Alaska, Fairbanks, 379-386.

Stringer, W.J., S.A. Barrett, Nita Blavin, and Diane Thomson

1977 Morphology of Beaufort, Chukchi, and Bering Seas nearshore ice conditions by means of satellite and aerial remote sensing: Environmental Assessment of the Alaskan Continental Shelf, Annual Report of Principal Investigators for the year ending March 1977, Environmental Research Laboratory, Boulder, Colorado, NOAA, U.S. Department of Commerce, v. 15, 42-150.

Thor, D.R., and Hans Nelson

1978 Continuous seismic reflection profile records, SEA 5-77-BS Cruise northern Bering Sea: U.S. Geological Survey Open File Report 78-608, 8 pp., 2 pls.

List of Figures

Figure 1. Index map and chart of high-resolution geophysical and side-scan sonar tracklines covered by the R/V SEA SOUNDER and R/V KARLUK in northeastern Bering Sea during 1976, 1977, and 1978.

Figure 2. Northeastern Bering Sea and southern Chukchi Sea, showing water circulation and bathymetry. Compliation sources include Goodman and others (1942), Fleming and Heggarty (1966), Husby (1969, 1971), McManus and Smyth (1970), Nelson and Hopkins (1972), Pratt and Walton (1974), and Coachman and others (1976). Drift directions of pack ice in northern Bering Sea adapted from Muench and Ahlnas (1976) and Duprè (1978).

Figure 3. A - solitary gouge on a sonograph. B - 200 kHz fathometer profile and diagrammatic representation of gouge shown in A. Features of gouge include a) incision depth as measured from gouge bottom to a horizontal line projected across sediment surface, b) height of sediment mounded on the gouge edge, c) width of incision, d) width of disruption zone caused by the gouging process. C - box core slab showing subsurface (11-18 cm interval) disruption possibly caused by a past gouge event.

Figure 4. Sonographs showing ice gouges of the northeastern Bering Sea. A and B - solitary gouges in sand-wave and ripple fields. C, D, and E - solitary gouges. Example E shows depth of incision on the sonograph horizon line. F and G - examples of pressure ridge raking. Example G shows depth of incision on the sonograph horizon line. H - example of depressions associated with ice gouging.

Figure 5. Rose diagrams representing trend and density of gouges. Division into areas I - V based on zones of similar trending gouges. Zone of shorefast ice based on evaluation of Landsat imagery (Duprè, 1977, 1978; Ralph Hunter, pers. comm., 1977).

Figure 6. Summary of ice gouging: density, shorefast ice limits, and ice movements in northeastern Bering Sea.

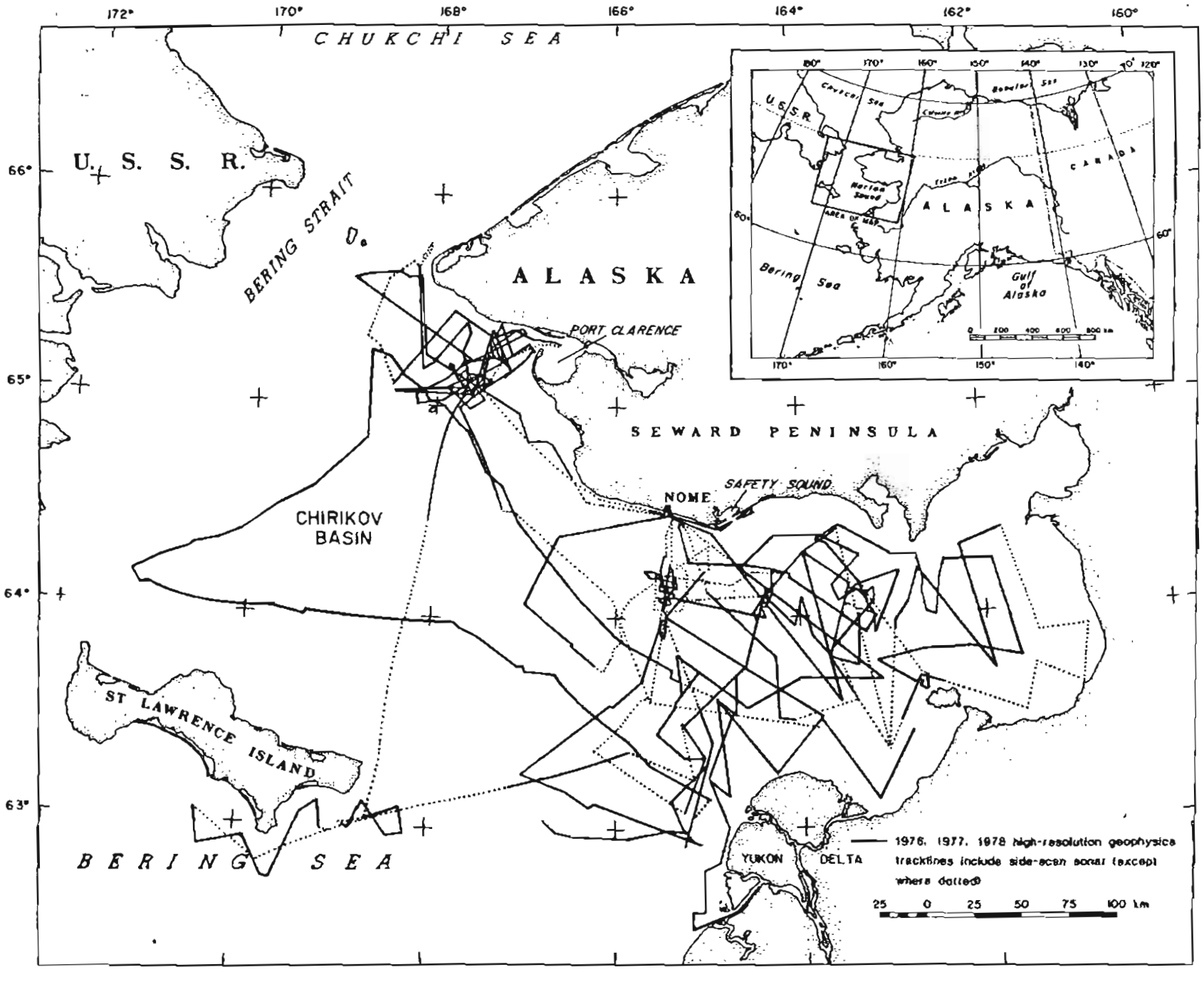
172°
170°
168°
166°
164°
162°
160°
66°
65°
64°
63°
CHUKCHI SEA
U. S. S. R.
BERING STRAIT
ALASKA
PORT CLARENCE
SEWARD PENINSULA
NOME
SAFETY SOUND
CHIRIKOV BASIN
ST LAWRENCE ISLAND
BERING SEA
YUKON DELTA
1976, 1977, 1978 high-resolution geophysics tracklines include side-scan sonar (except where dotted)
25 0 25 50 75 100 km
U.S.S.R.
CANADA
ALASKA
Bering Sea
Gulf of Alaska
170°
160°
150°
140°

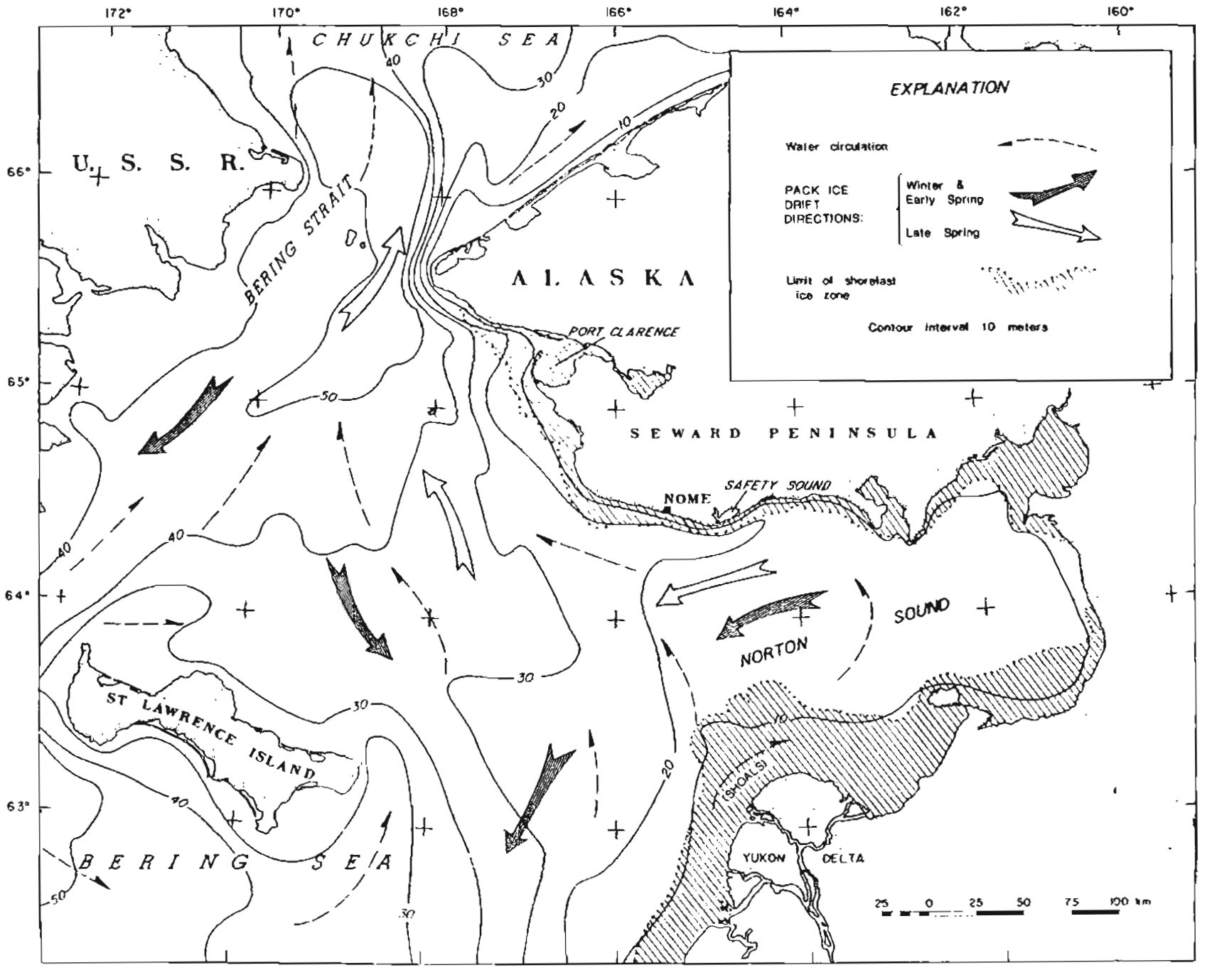
172°
170°
168°
166°
164°
162°
160°
66°
65°
64°
63°
CHUKCHI SEA
U. S. S. R.
BERING STRAIT
ALASKA
PORT CLARENCE
SEWARD PENINSULA
NOME
SAFETY SOUND
NORTON SOUND
ST LAWRENCE ISLAND
BERING SEA
SHOALS
YUKON DELTA
40
30
20
10
50
EXPLANATION
Water circulation
PACK ICE DRIFT DIRECTIONS:
Winter & Early Spring
Late Spring
Limit of shorefast ice zone
Contour interval 10 meters
25 0 25 50 75 100 km

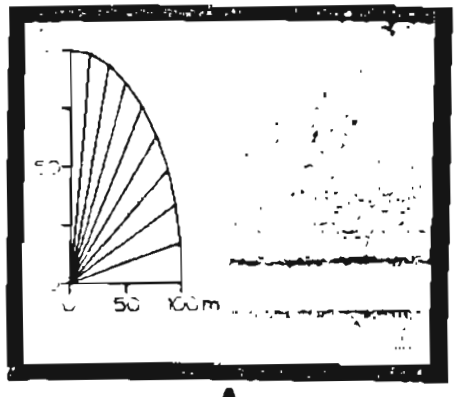

A

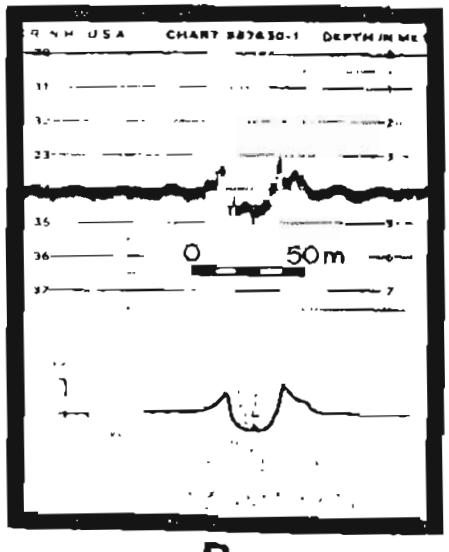

B

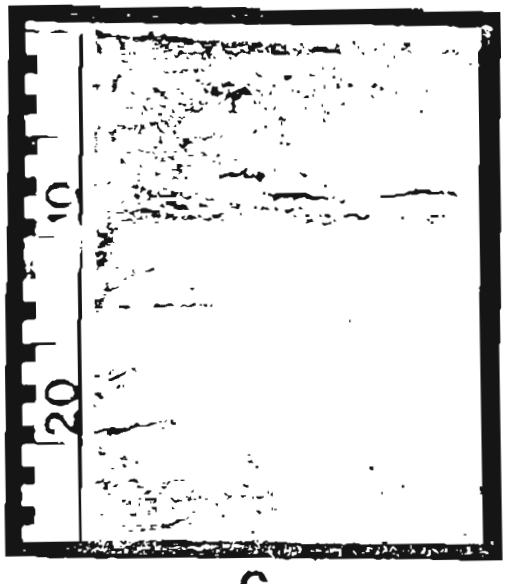

C

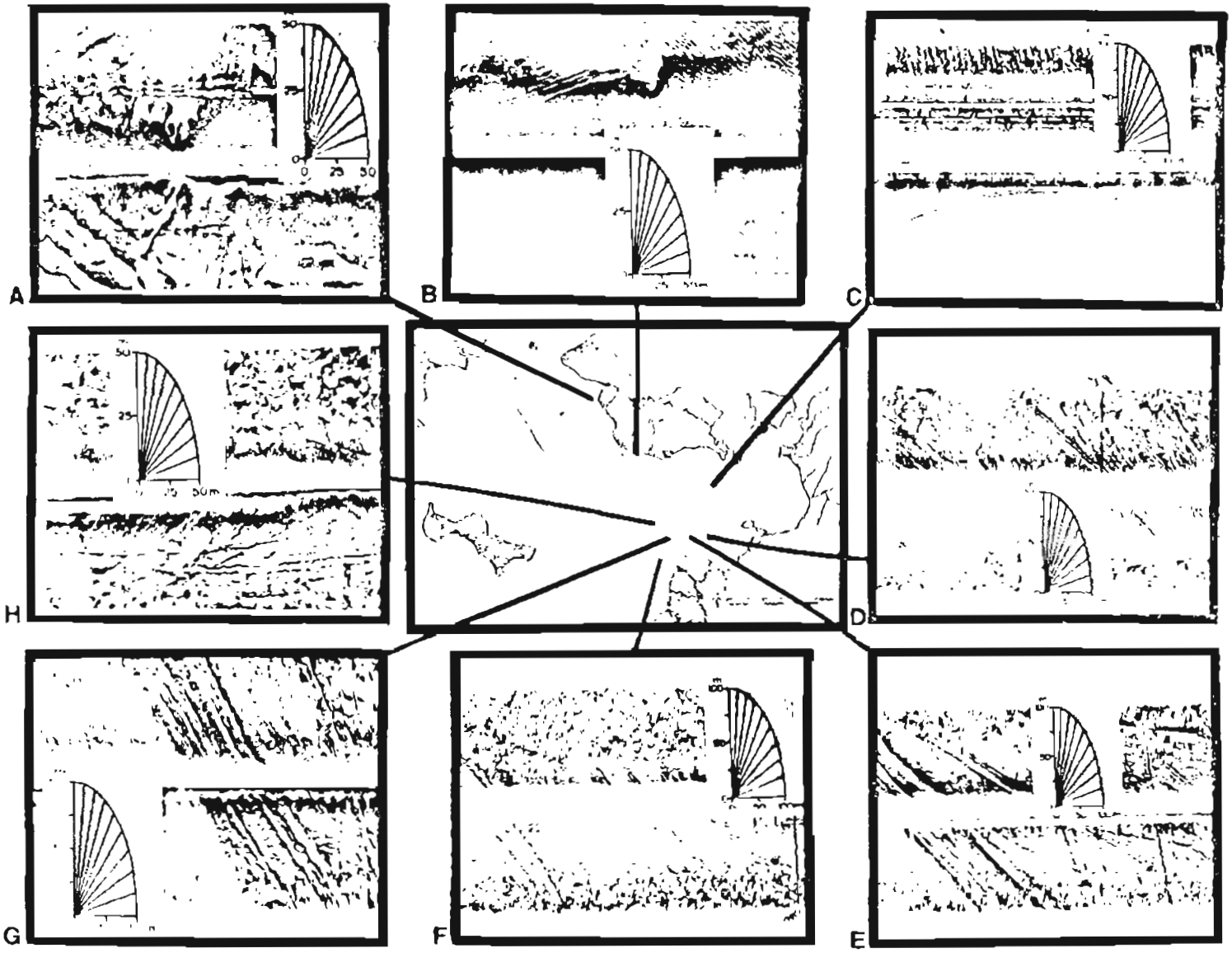
A
B
C
H
D
G
F
E

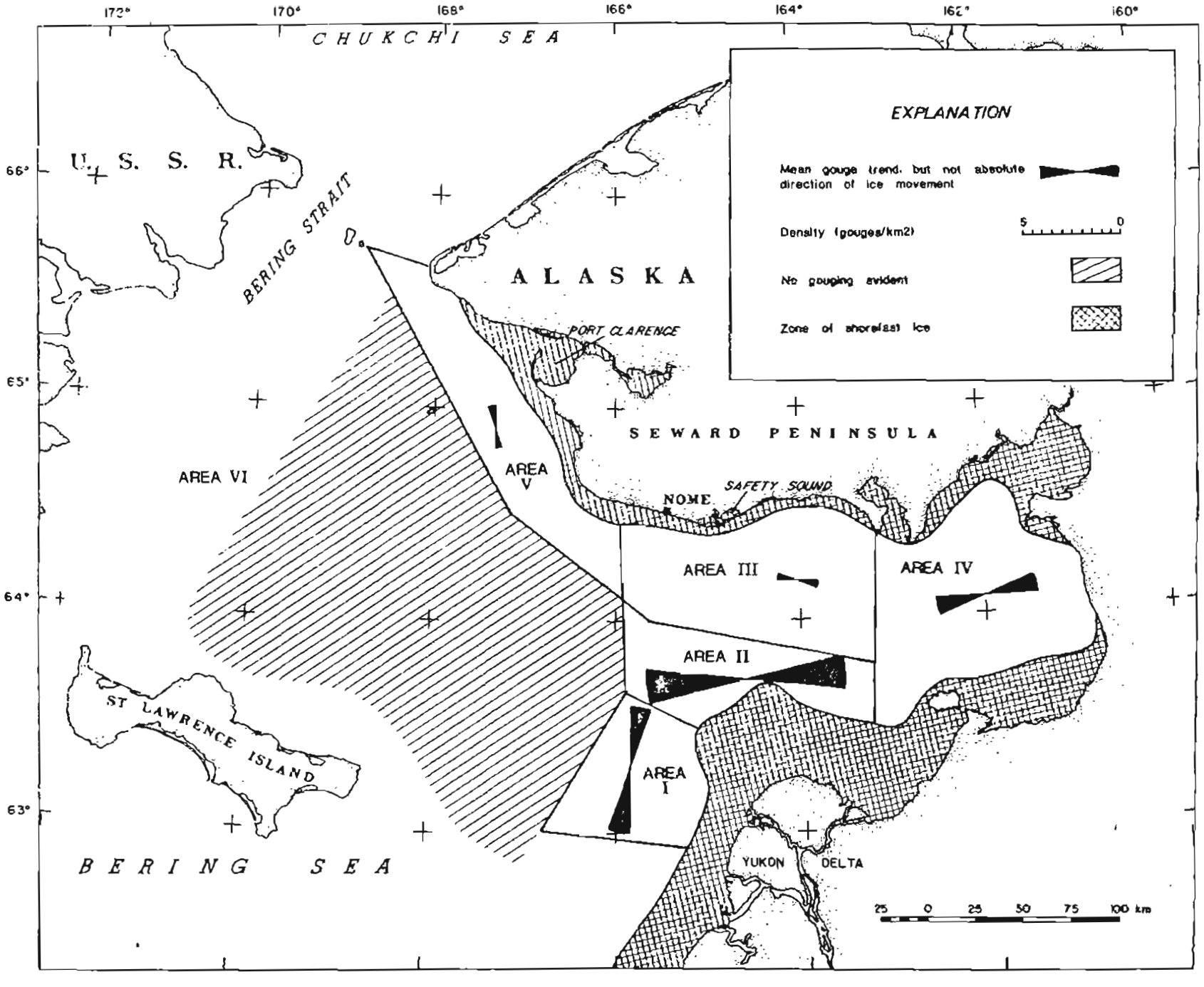
172°
170°
168°
166°
164°
162°
160°
66°
65°
64°
63°
CHUKCHI SEA
U. S. S. R.
BERING STRAIT
ALASKA
PORT CLARENCE
SEWARD PENINSULA
NOME
SAFETY SOUND
AREA VI
AREA V
AREA III
AREA IV
AREA II
AREA I
ST LAWRENCE ISLAND
BERING SEA
YUKON DELTA
EXPLANATION
Mean gouge trend, but not absolute direction of ice movement
Density (gouges/km2)
5
0
No gouging evident
Zone of shorefast ice
25 0 25 50 75 100 km

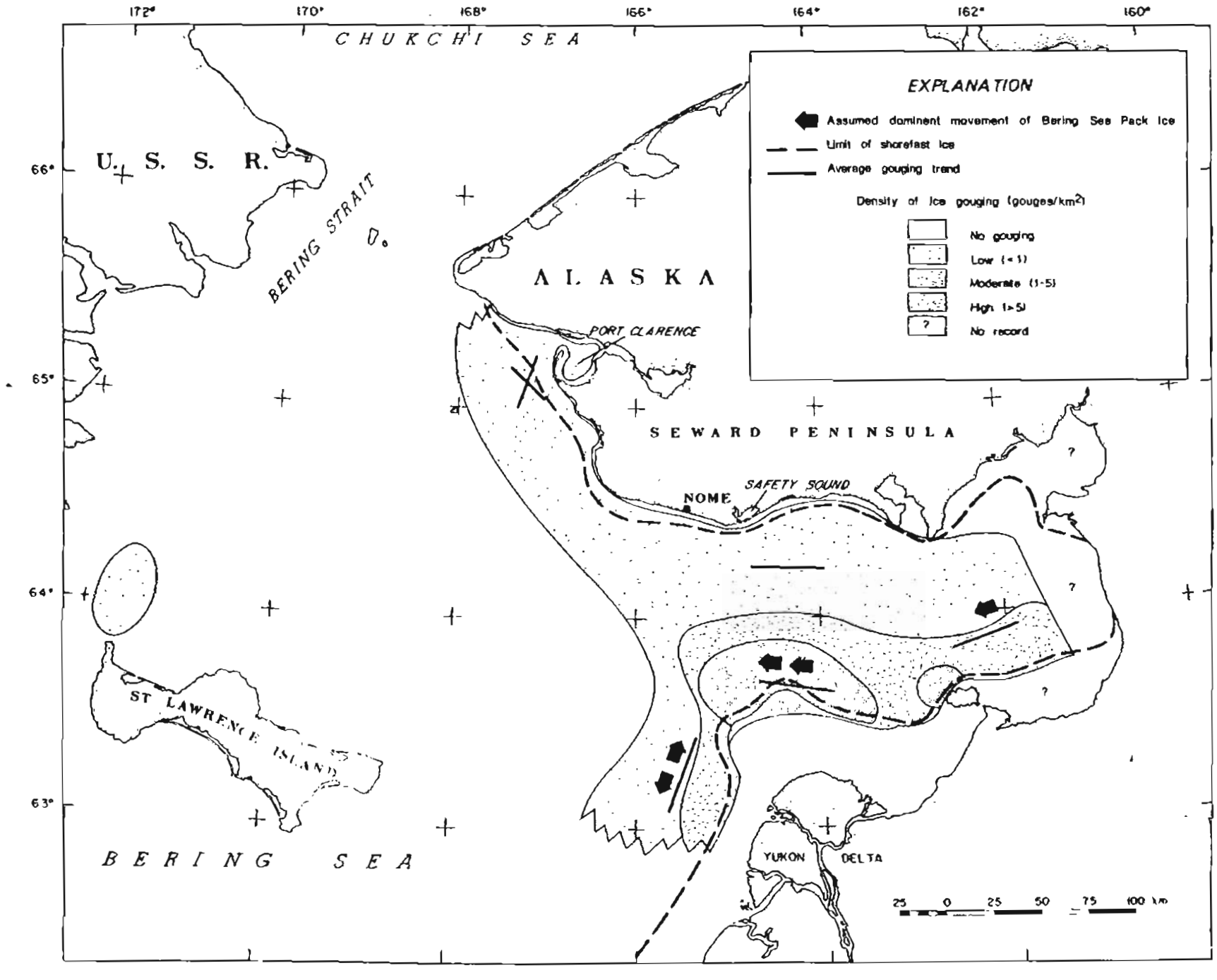
172°
170°
168°
166°
164°
162°
160°
66°
65°
64°
63°
CHUKCHI SEA
U. S. S. R.
BERING STRAIT
ALASKA
PORT CLARENCE
SEWARD PENINSULA
SAFETY SOUND
NOME
ST LAWRENCE ISLAND
YUKON DELTA
BERING SEA
EXPLANATION
Assumed dominant movement of Bering Sea Pack Ice
Limit of shorefast ice
Average gouging trend
Density of ice gouging (gouges/km²)
No gouging
Low (< 1)
Moderate (1-5)
High (>5)
No record
25 0 25 50 75 100 km

UNITED STATES DEPARTMENT OF THE INTERIOR
GEOLOGICAL SURVEY

Liquefaction Potential of the Yukon Prodelta, Bering Sea

by

Edward Clukey, David A. Cacchione, and C. Hans Nelson

This report is preliminary
and has not been edited or
reviewed for conformity with
Geological Survey Standards
and nomenclature.

ABSTRACT

The Yukon prodelta is exposed to large storm waves propagating northward from the southern Bering Sea. Shallow water depths of the prodelta enhance the transfer of energy from the surface waves to the bottom. As the bottom deposits are cyclically loaded by large storm waves, potential decrease in their resistance to shear could ultimately cause liquefaction. A preliminary assessment of the engineering properties of Yukon sandy silt suggests that the prodelta deposits may be susceptible to wave-induced liquefaction during severe storm events. In addition, erosion and resuspension of sediment in the prodelta may be intensified because of the liquefaction process.

INTRODUCTION

The stability of granular sea-floor deposits can be upset by liquefaction of the deposits under cyclic loading and their behavior as a viscous fluid. This liquefaction or fluidization of bottom sediment may pose severe problems to the integrity of offshore installations. The bearing capacity of the sea floor beneath offshore structures (Lee and Focht, 1975; Rahman et al., 1977) may be seriously impaired if the upper few meters of deposits liquefy and mass flows result. Erosion and sediment scouring caused by current-induced bottom shear stresses are other processes significantly related to liquefaction vulnerability. The net effect may be the erosion of foundation-bearing sediment beneath platforms sited on the bottom. The extent of the damage potential would depend on the areal distribution of the liquefiable material and recognition of the liquefaction potential in design considerations.

The liquefaction of sea-floor sediment results from repeated loading during either earthquakes or high-intensity storm waves, when pore-water pressures reduce the shearing resistance of the material. In this report we

consider the potential of Yukon prodelta deposits (Fig. 1) to liquefy under large-amplitude surface water waves. Although Norton Basin does possess several active faults that could pose a moderate seismic risk, the liquefaction potential under wave loading is considered particularly destabilizing on the basis of sediment-type (borderline sand-silt) in the prodelta (Fig. 2) and exposure of the prodelta to large storm waves. Typical late-fall storms in Bering Sea generate large-amplitude low-frequency waves that propagate into Norton Sound from the southern Bering Sea. Water depths (Fig. 1) throughout Norton Sound are also sufficiently shallow (<20 m), that most wave-generated surface energy is imparted to the bottom deposits. Under these conditions, bottom deposits may liquefy during storms. To investigate this possibility, we have made a preliminary assessment of the liquefaction potential of Yukon prodelta deposits.

This study was in part based on samples from, and bottom-pressure measurements in, the Yukon prodelta (Fig. 1). At present, however, no direct cyclic strength data have been gathered on undisturbed samples from the area, and thus our conclusions should be considered tentative. This assessment of the liquefaction potential was supplemented by results obtained by other investigators on similar sediment. The dissipation of pore-water pressures for a typical and an extreme storm event was modeled by an isoparametric one-dimensional finite-element method (FEM) of analysis. Although our results are not site specific, they do represent the general sea-floor conditions throughout the prodelta area and provide insights for more detailed studies aimed at defining the degree of liquefaction susceptibility on a regional basis, using techniques recently devised for onshore deposits (Youd and Perkins, 1978).

DATA COLLECTION

Data for this investigation were collected aboard the research vessel Sea Sounder during 1976, 1977, and 1978. Bottom pressure measured at 2.2 m above the sea floor and current measurements taken at 1 m above the sea floor were recorded with a multi-instrumented bottom tripod, GEOPROBE (Cacchione and Drake, 1979), used to investigate sediment transport on continental shelves. The GEOPROBE (Fig. 3) collected 80 days of bottom data during July-September 1977 at a water depth of 19 m approximately 50 km south of Nome, Alaska (Fig. 1). During that time, data were collected on one moderate storm that generated 3-m surface waves with approximately 10- to 12-s periods (Fig. 4).

Core samples were taken with a variety of coring devices including shallow grab samplers as well as 2- and 5-m vibracoring samplers (Fig. 1). Only rarely did core stratigraphy appear to be disturbed by coring.

The cores were subsampled at sea immediately after collection, typically at the core surface and at 0.5-m intervals thereafter, and above and below distinct stratigraphic changes. Grain-size distributions were determined from subsamples using wet-sieve splits made at 2 mm (Sieve 18) and at 0.0625 mm (sieve 230), and the mud fraction was run in a hydrophotometer measuring silt and clay grain sizes less than 0.0625 mm (Clukey and others, 1978).

Bulk densities were determined on a few whole-core sections before opening. Generally, the in-situ density was estimated by taking small plugs of known volume. The densities of samples could also be determined from their water content (assuming 100-percent pore-water saturation). Appropriate corrections were made in all cases for the salinity of the pore water. Minimum and maximum densities were calculated on the basis of mean grain size and sorting characteristics of the deposits, and from results obtained by other investigators on approximately similar types of deposits.

GEOLOGIC AND OCEANOGRAPHIC SETTING

The Yukon prodelta is in the southwest part of Norton Sound in the northern Bering Sea (Fig. 1). During the Pleistocene, tundra-derived peat deposits formed when the entire northern Bering shelf, including Norton Sound, was emergent because of lowered sea levels (Nelson, in press). These peaty deposits generally overlie Pleistocene glacial and alluvial deposits that are underlain by pre-Quaternary bedrock. About 12,000 years B.P. Sphanberg Strait (Fig. 1) was flooded during sea-level transgression, and transgressive fine sand and silt began to be deposited there. By 9500 B.P. Norton Sound had been indundated by water, and modern Holocene sandy-silty mud began prograding over the Pleistocene freshwater peaty mud (Nelson and Creager, 1977). The modern Yukon subdelta moved north to its present position about 5000 years B.P. or later.

The Yukon River presently carries 60 to 100 million tons of sediment into the Bering Sea each year (Lisitsyn, 1966). Currents transport much of the Yukon-derived sediment into the Chukchi Sea (Drake and others, 1980). Sediment remaining in Norton Sound is deposited onto a deltaic wedge that thickens from 2- to 10-m depth toward the modern Yukon subdelta (Fig. 2) (Nelson and Creager, 1977). The southwest margin of the prodelta consists of well-sorted silty sand grading northward to moderately sorted silty sand and eastward to poorly sorted sandy silt and silt (Dupre and Thompson, 1978). The Holocene sandy and silty mud of the Yukon River (Fig. 2) covers central and northern Norton Sound with surficial deposits as thick as 2 m. Chirikov basin, west of Norton Sound is entirely bypassed, and no modern very fine sand and silt are deposited there (Nelson, in press).

Investigation of large-scale current patterns in the northern Bering and Chukchi Seas were summarized by Coachman and others (1976). The regional

circulation is relatively simple: Bering shelf water flows northward into the Arctic basin throughout most of the year. This flow is principally driven by sea-level differences across the Bering Strait and is modified by surface-wind stresses generated by large-scale atmospheric-pressure systems. Surface-wind stresses associated with the predominant northerly winds decrease the magnitude of this nrthward flow and occasionally reverse the surface-current direction. When the flow is northward, topographic constriction approaching the Bering Strait effectively enhances the current speed north of about latitude 64°30′ N. Bottom deposits in the approaches to the Bering Strait are predominantly made up of sand that has been molded into a variety of bedforms characteristic of progressively stronger bottom currents.

Energetic atmospheric storms normally transit the northern Berng Sea with increasing frequency, commencing in September. Typically, these early storms have low-pressure centers that pass north of Nome, Alaska. These storm tracks are favorable for the formation of large surface waves by sustained strong southwesterly winds blowing across a relatively unimpeded fetch that terminates along the outer northern margin of Norton Sound (Fig. 1). Such conditions have historically caused intense storm surges and extensive wave erosion of the Nome coastline (Sallenger and Dingler, 1978).

Monthly averages of sea state and winds compiled by the Arctic Environmental Information and Data Center (1977) indicate that over the last 35 years, in the northwestern Bering Sea (the area contained within latitude 60°N and the coastline to longitude 175° W). the maximum observed wave heights have been 7 m in September and 8 m in October. The statistical recurrence interval for extreme waves of 24-m height in the deeper southernmost part of the study area is only 5 yr; the maximum significant wave height for this same recurrence period is 13.5 m (Arctic Environment Information and Data Center,

1977, p. 438). At Nome, Alaska, the recurrence period for sustained windspeeds of 50 knots is 5 yr. We note that during the period November 11-13, 1974, a storm surge estimated to be a once-in-30-yr occurrenee severely damaged the Nome area; during this storm an estimated water rise of 7.6 m caused extensive flooding over the entire north margin of Norton Sound (Sallenger and Dingler, 1978). Normal tidal range for that period was 1.2 m.

These data indicate the extreme importance of wind-driven and wave events in the study area. Estimates of bottom erosion and sediment transport must include measurement and evaluation of not only normal fair-weather turbulent shear stresses but also excessive stresses induced by high waves.

LIQUEFACTION OF A SEDIMENTARY DEPOSIT

Temporary or permanent loss in the strength of ocean deposits generally occurs in loose fine-grained sand to coarse silty sediment (Lee and Fitton, 1969). In extreme cases, this loss in strength can cause liquefaction of the deposits. Liquefaction is controlled by the buildup of excess pore-water pressures, that is, above hydrostatic, as the deposits are subjected to cyclically induced shear stresses. As the material responds to these shear stresses, the particles tend to compact. If the permeability of the deposits is insufficient to allow for instantaneous reorientation of the particles, excess pore-water pressures develop. As these pressures increase with successive cycles, the deposits weaken and become less resistant to the imposed load. The shear resistance is then associated with a critical level of repeated loading (Sangrey and others, 1978). As pore-water pressures dissipate over time, the particles tend to move closer together, and the deposits become more stable. If the rate of pore-water-pressure dissipation is sufficiently rapid relative to the rate of pore-water-pressure generation,

the deposits will remain stable under the prevailing load. If, however, the applied load is sufficient to overcome dissipation effects, the deposits will tend to fail and may ultimately liquefy.

The permeability of the deposits controls the rate of pore-pressure dissipation. Thus, the more permeable the deposits, the greater will be the critical level of repeated loading required to induce liquefaction. In an earthquake-related situation, in which the frequency of loading is relatively high, pore-water-dissipation effects are generally negligible. The loading frequencies for storm waves, however, can be an order of magnitude less than those associated with earthquake frequencies, so dissipation of pore-water pressures over time must be considered.

Deposits that are sufficiently dense before loading do not generate long-term positive excess pore-water pressures. The soil particles in these deposits after finite displacements tend to dilate when sheared and thereby generate a negative pore-water pressure that temporarily increases the strength of the deposit. The relative density D_r, numerically expresses the relation of the onsite density to the maximum and minimum densities of the deposits; that is,

$$D_r = \frac{\gamma_{max}(\gamma - \gamma_{min})}{(\gamma_{max} - \gamma_{min})} \qquad (1)$$

where: γ = the in-situ dry unit weight

($\gamma = \rho g$, where ρ = density and

g = acceleration due to gravity)

γ_{max} = the maximum dry unit weight of sediment

and γ_{min} = the minimum dry unit weight of sediment

This relative density commonly is used as an index for the density state of granular material. Deposits with greater relative densities tend to be less

susceptible to liquefaction and therefore require higher critical levels of repeated loading in order to liquefy. The liquefaction potential then depends on the integrated effects of:

(1) the density state of the deposits,

(2) the level of loading imposed by storm waves,

and

(3) pore-water-dissipation effects.

A fourth parameter, the relation between the effective confining stress and the density state of the deposits, is also important in evaluating the liquefaction potential. Unfortunately, more detailed laboratory data are necessary before its importance can be assessed. In the absence of these data, in the present study we consider the deposits to be normally consolidated, and so the density state, level of loading, and dissipation effects will govern the response.

LIQUEFACTION ASSESSMENT

To evaluate the liquefaction potential from wave loading, we can effectively apply techniques used in earthquake engineering with some minor modifications (Nataraja and Singh, 1979). Once the level of imposed stresses has initially been determined, the number of cycles required to liquefy the sediment calculated under undrained conditions, at a given relative density, can be calculated (Seed and Rahman, 1978). The effects of drainage on bed response can then be modeled by an FEM analysis (Seed and Rahman, 1978). This model includes the dissipation of pore-water pressure after the passage of each wave. The total pore-pressure buildup as a function of the overburden pressure is then continually monitored throughout the duration of the storm or until 100-percent pore-water-pressure response is achieved. Although 100-percent pore-water-pressure response is not necessarily sufficient for

liquefaction, it does represent a condition whereby at least a temporary loss in strength occurs as a result of excess pore-water pressures.

WAVE-INDUCED STRESSES

Several techniques are presently available to determine both the pore-water-pressure response and the cyclically imposed shear and normal stresses in the deposits (Fig. 5). Moshagen and Tørum (1975) used the heat-conduction equation, together with the assumptions that the pore-water is incompressible and that the porous bed is undeformable, to predict the transitory wave-induced pore-water-pressure response; these responses are infiltration pore-water pressures, not those associated with shear stresses. This approach, however, does not predict the induced stresses in the deposits. Other investigators (Prevost and others, 1975), concerned with bed deformation and the resulting stresses, assumed the bed to be elastic and not to interact with the pore-water; the conclusions reached from this approach are those derived from classical solid mechanics. More recently, Yamamoto (1978) and Madsen (1978) have used a three-dimensional consolidation model for the bed to predict the wave-induced pore-water-pressure and effective-stress changes in the bed during a single wave cycle. The results of their work indicate that the bed response is strongly affected by the permeability and stiffness of the sediment as well as by the thickness of the bed.

None of these solutions, however, considers the response of the bed under repeated loading. Pore-water pressures would increase under application of cyclic shear stresses. This increase in pore-water pressure varies as a function of the number of applied loads, that is, waves, and reduces the normal effective stresses acting on the bed. This increase in pore-water pressure also depends on the drainage characteristics, frequency of loading, and duration of loading. Seed and Rahman (1977) considered the cyclic-loading

effects of storm-generated waves and proposed an FEM solution to model the pore-water-pressure dissipation effects throughout a storm. In their solution the wave-induced stresses were calculated by considering the total stress state in the bed and applying an appropriate stress function. Their solution is similar to that proposed by Prevost and others (1975). Where the deposits are idealized as a semi-infinite half-space, the expression for the horizontal (1977), is identical to that of Yamamoto (1978) and Madsen (1978); that is,

$$\tau_h = 2\pi\Delta p \left(\frac{z}{L}\right) \exp\left(\frac{2}{L} z\right), \qquad (2)$$

where: p = the bottom wave-induced pressure,

L = the wavelength,

and z = the depth in the sediment.

The geometry is illustrated in Figure 5. If we subtract the pore-water pressures determined by Moshagen and Tørum (1975) from the total stresses, the effective principal stresses are also identical to those determined by Yamamoto (1978) and Madsen (1978).

The horizontal shear stress can then be normalized with respect to the overburden stress σ'_{v_o}, that is,

$$\sigma'_{v_o} = \gamma_b \, z \qquad (3)$$

where: γ_b = the buoyant unit weight of the sediment.

The resulting expression then gives the maximum shear-stress ratio at a depth depth z:

$$\frac{\tau_h}{\sigma'_{v_o}} = 2 \frac{\overline{\lambda p}}{\gamma_b^1} \exp -\{\frac{2\theta}{1} z\}. \qquad (4)$$

Once the maximum shear-stress ratio has been determined, the number of cycles required to cause liquefaction under undrained conditions (for a given relative density) can be calculated from an experimental curve similar to that shown in Figure 6. Although data from actual tests performed on Yukon prodelta sediment may differ from these results, the curve in Figure 6 can be used to make a preliminary estimate of the response characteristics of sandy marine deposits under cyclic loading. The shear-stress ratios (τ_c / σ'_{v_o}), with depth for 3- and 6-m surface waves are shown in Figure 7. The 3-m wave was selected to represent the maximum storm conditions recorded by the GEOPROBE, whereas the 6-m wave would have a 1-percent occurence frequency for the months of September and October (Arctic Environmental Information and Data Center, 1977).

DENSITY STATE

The relative density of the sediment must be determined to correlate the number of cycles required to cause liquefaction at the imposed-stress level (Fig. 6). Higher relative densities would transpose the curve in Figure 6 upward, whereas lower relative densities would transpose it downward. Typical maximum and minimum density values can be estimated from the grain sizes and sorting characteristics of the deposits. The grain-size analyses of several grab samples are summarized in Table 1. The average-uniformity coefficient c_u for this sand (2.2) indicates a well-sorted material. On the basis of data presented by Johnston (1973) for a similar sand, the respective minimum and maximum densities for Yukon prodelta material were estimated at between 1280-

1320 kg/m^3 and 1600-1630 kg/m^3. These values were increased slightly to take into account the average percent fines in the samples tested (Townsend, 1973). The final minimum and maximum densities were then estimated to be 1370 and 1760 kg/m^3, respectively. These values were somewhat corroborated in tests by other investigators (Lee and Focht, 1975) on marine sediment from the North Sea with similar grain-size characteristics (d_{50} = 0.11 mm, c_u = 2.0). Their results show minimum and maximum densities of 1340 and 1740 kg/m^3, respectively, in good agreement with the values in this study.

Thus, relative density of typical Yukon prodelta sediment can be calculated on the basis of estimated minimum and maximum densities, and the in-situ densities determined from water-content or bulk-density estimates (Table 2). Although the relative densities obtained using the above methods rely on limited data and are initial estimates, they do suggest that the relative density of deposits throughout the study area varies considerably and is not restricted to a unique value or range of values. Thus, pockets or lenses of loose material could conceivably exist throughout the prodelta that would be susceptible to pore-water-pressure generation and possible liquefaction. Despite the variations in the data, a relative density of 54 percent is considered an approximate upper estimate for the sediment within the prodelta. Several of the higher relative densites listed in Table 2 are attributable to dense layers of different material within the stratigraphic section, or to compaction due to vibracoring action.

LIQUEFACTION SUSCEPTIBILITY

We can assess the liquefaction susceptibility for undrained conditions by correlating the number of cycles necessary to cause liquefaction with the shear-stress ratio ($^{\tau}h/\sigma'_{v_o}$), as shown in Figure 6. The 3-m storm-wave height would appear to require an extremely large number of cycles to cause

liquefaction, and the deposits would be even less susceptible if drainage were allowed to occur throughout the storm. Failure, as defined by Egan and Sangrey (1978), could possibly occur, however, if an effective-stress approach similar to Yamamoto's (1978) and Madsen's (1978) were used and the entire stress state were considered in the analysis. On the basis of our analysis, the likelihood of liquefaction from storm waves of 3-m height appears extremely small.

For the 6-m storm wave height, however, full pore-water-pressure response could occur in the upper several meters of sediment within a relatively small number of cycles under undrained conditions in the bed. If drainage were allowed, a greater number of cycles would be necessary to liquefy the deposits; an FEM analysis can then be used to investigate the effects of drainage during the storm. The 6-m storm- wave height was investigated with this technique for a storm duration of one hour. Because the dissipation effects depend on the permeability and compressibility of the deposits, two different permeability-compressibility combinations were used in the analysis. The buildup of pore pressure for each time increment was governed by the equation

$$r_u = \frac{2}{\pi} \text{ arc } \sin(x^{1/2\theta} z) \qquad (5)$$

where: r_u = the ratio of excess pore-water pressure to initial vertical effective stress,

x = the ratio of the applied cycle (n) to the number of cycles (n_1) required to cause liquefaction,

and θ = an empirical shape constant for the pore-water-pressure curve (1.2 in this analysis).

The results of the analysis indicate (Fig. 8) that even with pore-water-pressure dissipation taken into consideration, the deposits will liquefy to a depth of 3 to 3.5 m. The permeability of the material significantly - influences the time required for liquefaction to occur. For a coefficient of permeability of of 5 x 10^{-5}m/s, which would correspond to a medium- to coarse-grained sand like that encountered in Chirikov Basin, the sediment would not liquefy. The coefficients of permeability, derived from laboratory consolidation test results (1.5 x 10^{-6} - 1.5 x 10^{-7}ms), that represent a range of values typical for Yukon prodelta sandy silt show that liquefaction is possible. In this case pore-wateer pressure dissipation effects do not preclude full pore-water pressure response and possible liquefaction.

GEOLOGICAL IMPLICATIONS; HAZARD POTENTIAL

The present analysis suggests that modern Yukon prodelta sediment could at least temporarily liquefy to significant depths during severe storms. The widespread distribution of thick storm-sand layers within 50 km of the modern prodelta shoreline (Nelson, 1977) suggests that liquefaction and mass movement processes may be important mechanisms in the movement of major sheets of sand offshore. These sand layers range from 1 cm thick in central Norton Sound to over 20 cm thick within 30 km of the delta (Nelson, 1977). The more massive sand layers close to the delta may in part result from mass movement of liquefied material under major storm-wave and surge conditions. Bottom-friction velocities from tidally dominant bottom currents are insufficient to transport massive quantities of material. Drake and others (1980) suggest (from GEOPROBE data) that the very fine sand consituting about 50 percent of the sediment on the outer part of the Yukon prodelta is mostly transported during a few late summer and fall storms each year. The mean transport velocities for the September 1977 storm that generated 3-m-high waves, as

recorded by the GEOPROBE, were well in excess of those required to initiate transport of sediment (Cacchione and Drake, 1980). The effects of this transport mechanism during more severe storm events would be magnified if the bed were partially softened by liquefaction and the zone of material influenced by the mean transport velocity were several meters thick. Integration of the liquefaction susceptibility with the critical mean transport velocity in future sediment-transport models could provide useful insights into the rate and amount of sediment transport in this area.

Severe erosional effects can be observed in the delta area in the form of large scour depressions (Larsen and others, 1979). These depressions, which range as large as 250 m in diameter and 1 m in depth, are triggered by local topographic disruptions in prodelta areas where strong currents shear against steeper offshore topography. The potential for liquefaction in this area may greatly enhance the formation of these scour depressions. Weakening of the deposits by increased pore-water pressures, along with mixing of the deposits with water by storm-wave action, could lead to erosion and transport of sediment from scour depressions.

Liquefaction to a depth of 2.5 to 3 m and consequent movement of massive storm-sand sheets could cause severe hazards to sea-floor structures; this is particularly true if the protective sedimentary cover were removed from buried pipelines, or the sea floor around foundations were undermined. The undermining of a foundation can be partly predicted by more extensive and detailed site investigation, whereas pipeline construction must rely on a more regional data base and interpretation. Techniques similar to those presented herein would be useful in the selection of possible pipeline routes leading to onshore terminal facilities.

Preliminary strength tests on several samples from the study area (Olsen and others, 1979) suggest that some of the Yukon prodelta sediment may be significantly overconsolidated. This overconsolidation is due to the removal of past higher stresses from the deposits or the effects of a constant wave stress over a prolonged period. The overconsolidation leads to increased shear resistance in the deposits. For deposits with the same relative density, those that are overconsolidated would be less prone to liquefy (Seed, 1977) than those that are normally consolidated. Additional tests are required, however, for a more comprehensive assessment of such overconsolidation effects on the liquefaction potential.

SUMMARY

The vulnerability of Yukon prodelta sandy silt to wave-induced liquefaction has been evaluated using engineering analysis and data on storm-wave and sediment characteristics. The combination of sediment type, exposure to large storm systems, shallow water depths, and at least some fairly loose layers of material suggests that the prodelta may be susceptible to the generation of excess pore-water pressures and to consequent loss in strength and ultimate liquefaction. Geologic evidence of potential liquefaction effects includes the presence of prograded storm sand sheets and fairly broad scour depressions throughout the prodelta area.

We adapted methods currently practiced in earthquake engineering to our analysis, which considers two simplified storm systems. The principal difference between the earthquake- and storm-wave-based analyses is a longer duration for the storm event and consequently greater dissipation of pore-water pressures. A 3-m surface wave height was found to be insufficient to liquefy the deposits, even when the effects of pore-water-pressure dissipation were neglected. However, a storm event with 6-m wave heights theoretically

would generate 100-percent pore-water-pressure response and liquefaction in the sediment to a depth of approximately 3.5 m in one hour. Recent preliminary strength tests, however, indicate significant overconsolidation of the same Yukon deposits that may decrease the liquefaction danger, although the significant reduction in strength within the upper several meters of sediment may remain as a hazard to construction in the study area. Liquefaction, coupled with the shallow gas-charged deposits that are widespread in this area, (Nelson and others, 1979), may further complicate foundation engineering. Additional testing, however, is clearly needed before any final assessment of the extent of hazard potential can be properly made.

ACKNOWLEDGMENTS

The authors thank David Drake for his assistance with the GEOPROBE analysis and Devin Thor for his compilation of the Yukon sediment isopach map. This study was supported in part by the U.S. Geological Survey and the Bureau of Land Management through interagency agreement with the National Oceanic and Atmospheric Administration, under which a multiyear program responding to the needs of petroleum development of the Alaskan Continental Shelf is managed by the Outer Continental Shelf Environmental Assessment Program (OCSEAP) office.

REFERENCES

Arctic Environmental Information and Data Center, 1977: Climatic Atlas of the outer continental shelf waters and coastal regions of Alaska, v. 2, Bering Sea, Anchorage, University of Alaska, 443 p.

Beckman, W.J., 1970, Engineering considerations in the design of ocean outfall: Journal WPCF, v. 42, no. 10, p. 1805-1831.

Brown, R.J., 1971, How deep should an offshore line be buried for protection: Oil and Gas Journal, v. 69, p. 151-155.

Cacchione, D.A., and Drake, D.E., 1979, A new instrument to investigate sediment dynamics on continental shelves: Marine Geology, v. 30, p. 299-312.

Cacchione, D.A., and Drake, D.E., 1980, Storm-generated sediment transport on the Bering continental shelf, Alaska: Journal of Geophysical Research, in press.

Clukey, E.C., Nelson, H.C., and Newby, J.E., Geotechnical properties of northern Bering Sea Sediment: U.S. Geological Survey Open-File Report 78-408, 29 p.

Coachman, L.K., Aagaard, K., and Tripp, R.B., 1976, Regional Physical Oceanography: Seattle, University of Washington Press, 186 p.

Drake, D.E., Cacchione, D.A., Muench, R.D., and Nelson, C.H., 1980, Sediment transport in Norton Sound: Marine Geology, in press.

Dupré, W.R., and Thompson, R., 1979, A model for deltaic sedimentation in an ice dominated environment, Offshore Technology Conference, Houston, Texas: Proceedings, Paper 3434.

Egan, J.A., and Sangrey, D.A., 1978, Critical state model for cyclic load pore pressure: Proceedings of ASCE Geotechnical Engineering Division Specialty Conference, Pasadena, California, Earthquake Engineering and Soil Dynamics, p. 410-424.

Holmes, M.L., and Thor, D.R., 1980, Distribution of gas-charged sediment in Norton Basin, northern Bering Sea, in Nio, S.D., Van den Berg, J.H., and Siegenthaler, C., eds.: International Association of Sedimentologists, International meeting on Holocene marine sedimentation in the North Sea Basin, in press.

Johnson, J.L., and Holmes, M.L., 1978, Surface and subsurface faulting in Norton Sound and Chirikov Basin, Alaska, in Environmental Assessment of the Alaskan continental shelf, Annual Report of Principal Investigators, Environmental Research Laboratory, Boulder, Colorado, v. 12, p. 203-227.

Johnston, M.M., 1973, Laboratory studies of maximum-minimum densities of cohesionless soils, in The evolution of relative density and its role in geotechnical projects involving cohesionless soils, Selig and Ladd, eds.: ASTM STP 523, p.133-140.

Kvenvolden, K.A., Nelson, C.H., Thor, D.R., Larsen, M.C., Redden, G.D., Rapp, J.V., and Des Marias, D.J., 1979, Biogenic and thermogenic gas in gas-charged sediment of Norton Sound, Alaska: Offshore Technology Conference, Houston, Texas: Proceedings, Paper 3412, p. 479-483.

Larsen, M.C., Nelson, C.H., and Thor, D.R., 1979, Geologic implications and potential hazards of scour depressions on Bering shelf, Alaska: Environmental Geology, v. 3, p. 39-47.

Lee, K.L., and Fiton, J.A., 1969, Factors affecting the cyclic loading strength of soil: ASTM STP 450, p. 77-95.

Lee, K.L., and Focht, J.A., 1975, Liquefaction potential of Edofisk Tank in North Sea, Journal of the Geotechnical Engineering Division, ASCE, v. 100, no. GT1, p. 1-18.

Lisitsyn, A.P., 1966, Recent sedimentation in the Bering Sea, Moscow, Akad., Nauk, SSSR; English Trans., 1969, Israel Program of Scientific Translation (Springfield, Virginia, U.S. Dept. of Commerce Federal Science Technical Information), 614 p.

Madsen, O.S., 1978, Wave induced pore pressures and effective stresses in a porous bed: Geotechnique, v. 28, no. 4, p. 377-393.

Moshagen, H., and Trum, A., 1975, Wave induced pressures in permeable seabeds, Journal of Waterways, Harbors and Coastal Engineering, ASCE, v. 101, no. WW1, p. 49-58.

Nataraja, M.S., and Singh, H., 1979, A simpllified procedure for ocean-wave-induced liquefaction potential: Proceedings of Civil Engineering in the Oceans, Special Conference IV by ASCE Technical Council on Ocean Engineering, v. 2, p. 949-963.

Nelson, C.H.,1977, Storm surge effects, in: Environmental assessment of the Alaskan continental shelf: Annual Report of Principal Investigators, U.S. Department of Commerce, Environmental Research Laboratory, Boulder, Colorado, v.18, p. 120-129.

Nelson, C.H., 1980, Holocene transgression in deltaic and non-deltaic areas of the Bering epicontinental shelf, in Proceedings of the International Meeting on Holocene Marine Sedimentation in the North Sea Basin, International Association of Sedimentologists, Nio, S.D., Schuttenheln, R.T., and Weering, T.C.E., eds., 30 p., in press.

Nelson, C.H., and Creager, J.S., 1977, Displacement of Yukon sediment from Bering Sea to Chukchi Sea during Holocene time, Geology: v. 5, p. 141-146.

Nelson, C.H., Thor, D.R., Sandstrom, M.W., and Kvenvolden, K.A., 1979, Modern biogenic gas-generated craters (sea-floor "pockmarks") on the Bering shelf, Alaska: Geological Society of America Bulletin v. 90, p. 1144-1152.

Olsen, H.E., Clukey, E.C., and Nelson, C.H., 1979, Geotechnical characteristics of bottom sediments in the northern Bering Sea, in Proceedings of the International Meeting on Holocene Marine Sedimentation in the North Sea Basin, International Association of Sedimentologists, Nio, S.D., Schuttenheln, R.T., and Weering, T.C.E., eds., p. 91-92.

Prevost, J.H., Eide, O., and Andersen, K., 1975, Wave induced pressures in permeable seabeds: Journal of Waterways, Harbors and Coastal Engineering, ASCE, v. 101, no. WW4, p. 464-465.

Sallenger, A.H., Jr., and Dingler, J.E., 1978, Coastal processes and morphlogy of the Bering Sea coast of Alaska, Final Report of Research Unit 431 in Outer continental shelf environmental assessment Program, Juneau, Alaska, National Oceanographic and Atmospheric Administration, U.S. Department of Commerce, 66 p.

Sangrey, D.A., Castro, G., Poulos, S.J., and France, J.W., 1978, Cyclic loading of sands, silts, and clays: ProceeCalifornia, of ASCE Geotechnical Engineering Division Conference, Pasadena, Earthquake Engineering and Soil Dynamics, p. 836-851.

Seed, H.B., 1979, Soil liquefaction and cyclic motility evaluation for level ground during earthquakes: Journal of Geotechnical Engineering Division, ASCE, v. 105, no. GT2, p. 201-255.

Seed, H.B., and Rahman, M.S., 1978, Analysis for wave-induced pore pressure relation to ocean floor stability of cohesionless soils: Marine Geotechnology, v. 3, no. 2, p. 123-150.

Townsend, F.C., 1973, Comparisons of vibrated density and standard compaction tests on sands with varying amounts of fines, in The evaluation of relative density and its role in geotechnical projects involving cohesionless soils, Selig and Ladd, eds., ASTM STP 523, p. 348-363.

Yamamoto, T., 1978, Sea bed instability from waves, Offshore Technology Conference, Houston, Texas: Proceedings, Paper 3263, p. 1819-1824.

Youd, T.L., and Perkins, D.M., 1978, Mapping liquefaction induced ground failure potential: Journal of the Geotechnical Division, ASCE, v. 104, no. GT4, p. 433-446.

TABLE 1

Table 1.--Results of grain-size analyses of sediment samples from the Yukon prodelta

Box core	Core Depth (cm)	Sand (%)	Silt (%)	Clay (%)	D_{60} (mm)	D_{10} (mm)	$C_u = D_{60}/D_{10}$[1]
164	4	96.9	2.6	0.4	0.187	0.101	1.83
166	11	92.6	6.3	1.1	0.135	0.072	1.86
162	12	86.0	12.3	1.7	0.108	0.042	2.58
168	11	90.6	7.9	1.5	0.109	0.062	1.76
157	4	77.2	22.1	0.7	0.101	0.035	2.89

[1]Average = 2.18

Table 2.--Density data on samples from Norton Sound

Sample Designation	Depth (cm)	Water content (%) corrected	Dry unit weight γ(lbs/ft)	Dry density (Kg/m	Relative density D_x l
Box 147	2-6	30.9	96	1.54	51
Sutar 149	Surface	106.1	45	0.72	*
Box 154	4-5	43.0	72	1.15	*
	13-14	56.1	70	1.12	*
	10-18	46.6	77	1.23	*
	26-29	45.0	80	1.28	*
Box 156	33-35	81.7	55	0.88	*
Box 161	2-12	51.8	73	1.17	*
Vibracore					
17	6-8	37.6	87	1.39	9
	23-25	37.8	85	1.36	*
	40-42	31.6	94	1.51	42
	54-56	34.5	90	1.44	26
	72-74	32.3	93	1.49	39
	90-92	31.7	94	1.51	43
	123-125	73.3	59	0.95	*
	134-136	26.5	102	1.63	*
Box 17	0-2	35.9	89	1.43	18
	8-10	49.1	75	1.20	*
	13-15	39.5	84	1.35	*
	18-20	38.0	86	1.38	*
	24-26	29.1	99	1.59	58
	19-21	42.7	81	1.30	*
Vibracore					
16	10-12	30.6	96	1.54	49
	29-31	33.3	92	1.47	33
	39-41	26.9	101	1.62	69
	49-51	29.2	98	1.57	57
	64-66	28.3	99	1.59	62
	74-76	27.2	100	1.60	68
	84-86	26.6	101	1.62	71
	109-111	22.0	109	1.75	98
	119-121	19.3	114	1.83	100
	129-131	28.7	98	1.57	59
	139-141	24.0	106	1.70	87
Box 27A	0-3	44.7	77	1.23	-
	5-7	37.6	84	1.35	-
	15-17	35.4	87	1.39	22
	18-20	41.1	82	1.31	-

Figures

Figure 1. Station locations for core samples taken during 1976, 1977, and 1978 field seasons; site of GEOPROBE deployment during July-September 1977. The Yukon prodelta extends out to 90 km into North basin; isopach contours in Figure 2.

Figure 2. Surficial sediment distribution in Norton Sound (modified after Nelson, 1980) and isopach thickness of Holocene-Yukon derived sediment (modified after Thor, in prep.).

Figure 3. GEOPROBE tripod during launch into Norton Sound, July 1977. Horizontal distance between attachment points of footpads is 3.2 m; overall height is about 3.5 m. Flotation package in upper part of photograph rests on plastic (PVC) buckets containing recovery line. Current sensors are visible within center of tripod. Undersea strobe attached to leg at right; pressure cases contain electronic systems and sensor packages (see Cacchione and Drake, 1979).

Figure 4. Current-meter and pressure data taken with GEOPROBE during storm on Sept. 14, 1977, in Norton Sound, Alaska. Data were taken every second for 60 s. Current speeds (computed from north-south and east-west components) at 0.2, 0.5, 0.7, and 1 m above sea floor are designated by CM1, CM2, CM3, and CM4, respectively. Pressure (PRS) is measured at 2 m above sea floor and expressed in equivalent meters of water. Averages have not been removed from data.

Figure 5. Simplified wave profile used in liquefaction-potential analysis. Bottom-pressure wave data were obtained from linearized wave theory. Bottom pressures induce horizontal shear stresses that cause a pore-water-pressure response and reduced strength.

Figure 6. Normalized cyclic horizontal shear-stress ratio (τ_h / σ'_{v_o}) vs number of cycles required for initial liquefaction (undrained conditions) for deposits with a relative density of 54 percent (Seed, 1977).

Figure 7. Wave-induced shear stress ratio (τ_h / σ'_{v_o}) vs depth (Z) for 3- and 6-m-surface wave heights during storm events.

Figure 8. Results of preliminary analysis of wave-induced liquefaction potential of Holocene Yukon sandy silt near Yukon prodelta: H, wave height; T, wave period; D_r, relative density; K, coefficient of permeability; u/σ'_v ratio of wave-induced excess pore-water pressure to initial effective overburden stress.

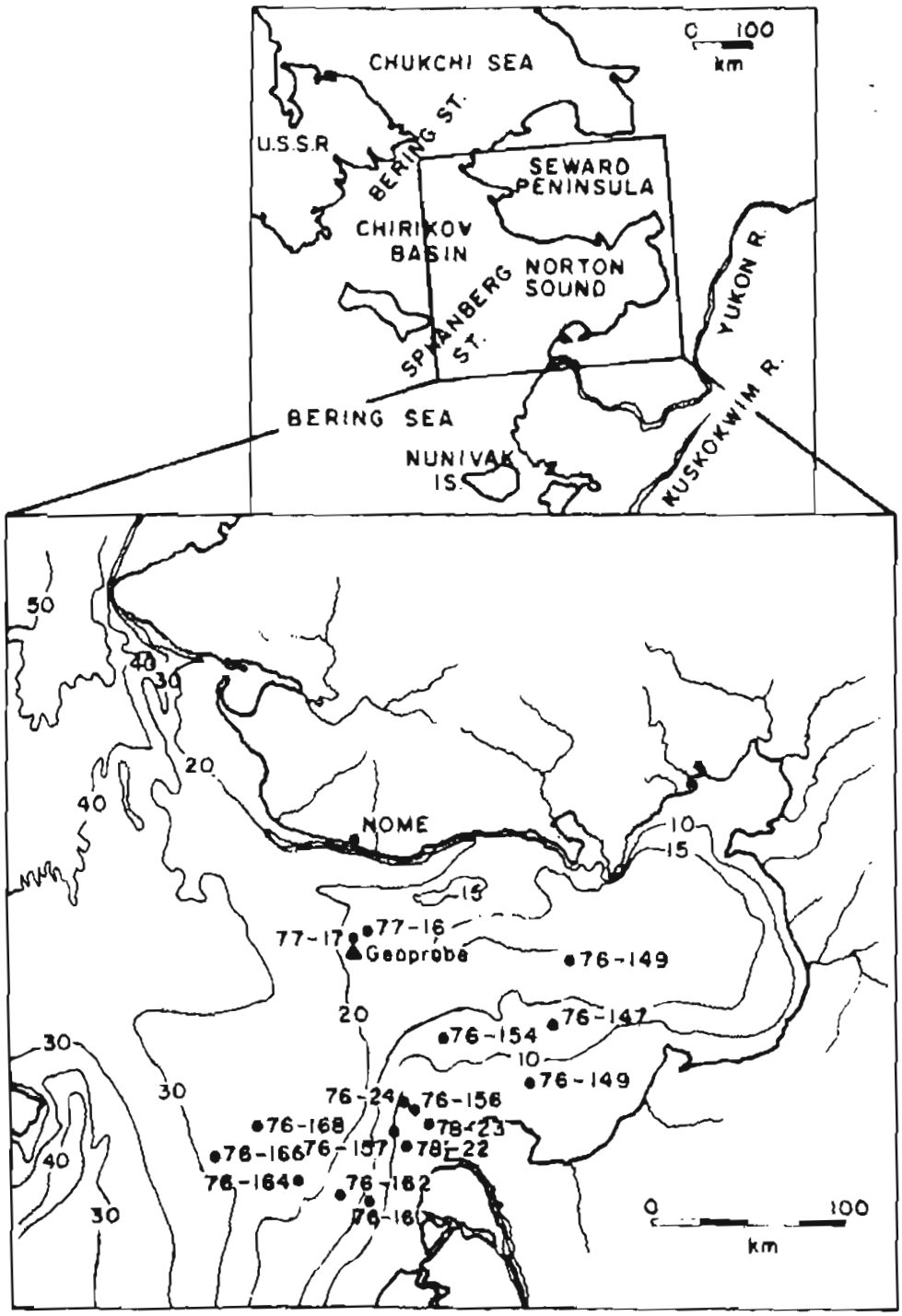
0 100
km
CHUKCHI SEA
U.S.S.R
BERING ST.
SEWARD PENINSULA
CHIRIKOV BASIN
NORTON SOUND
SPAANBERG ST.
YUKON R.
KUSKOKWIM R.
BERING SEA
NUNIVAK IS.
50
40
30
20
40
NOME
10
15
15
77-17
77-16
Geoprobe
76-149
20
76-154
76-147
30
10
30
76-149
76-24
76-156
76-168
76-23
76-166
76-157
76-22
40
76-164
76-162
76-161
30
0 100
km

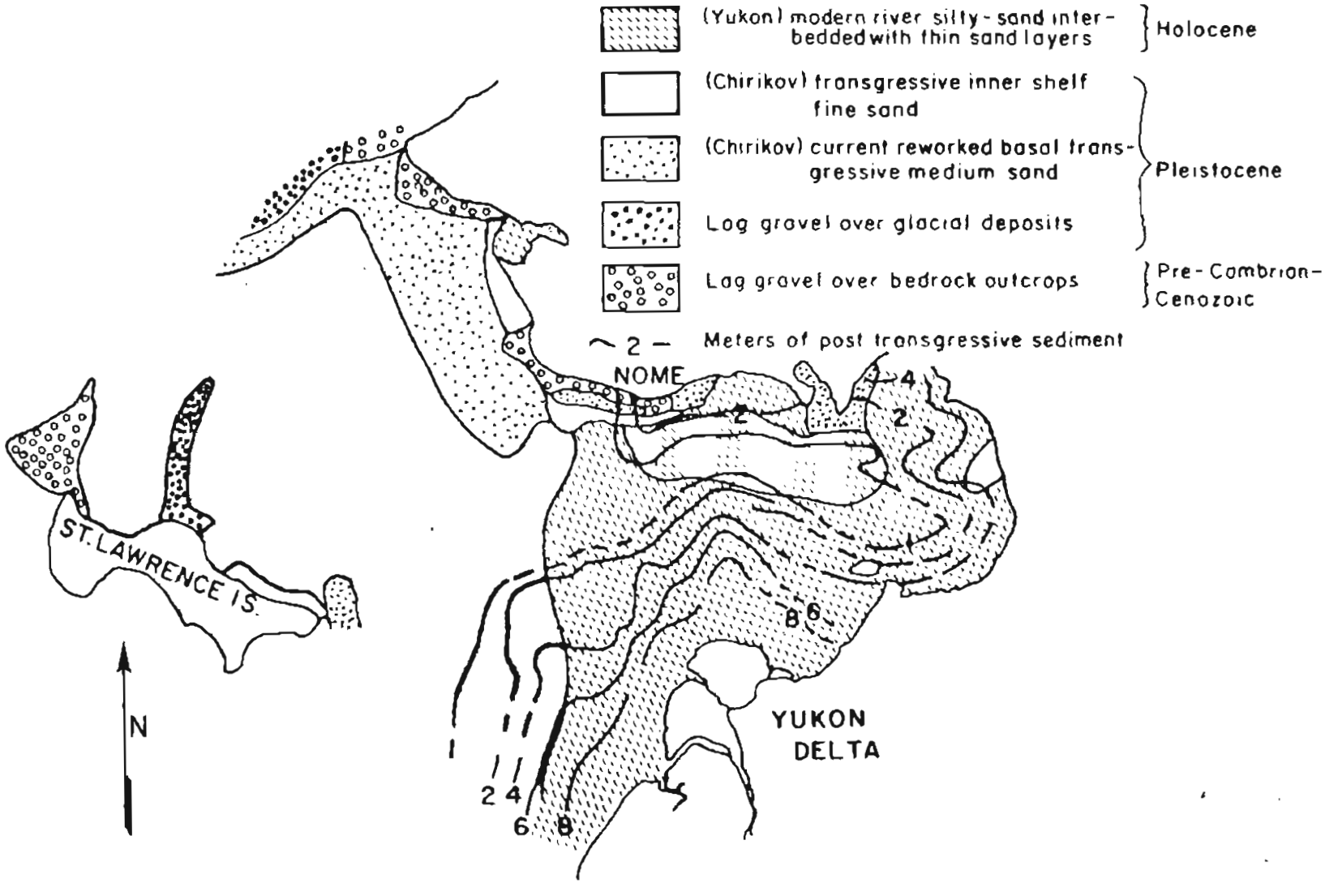
(Yukon) modern river silty-sand interbedded with thin sand layers
Holocene
(Chirikov) transgressive inner shelf fine sand
(Chirikov) current reworked basal transgressive medium sand
Pleistocene
Lag gravel over glacial deposits
Lag gravel over bedrock outcrops
Pre-Cambrian-Cenozoic
~2~ Meters of post transgressive sediment
NOME
ST. LAWRENCE IS.
N
YUKON DELTA
1
2
4
6
8

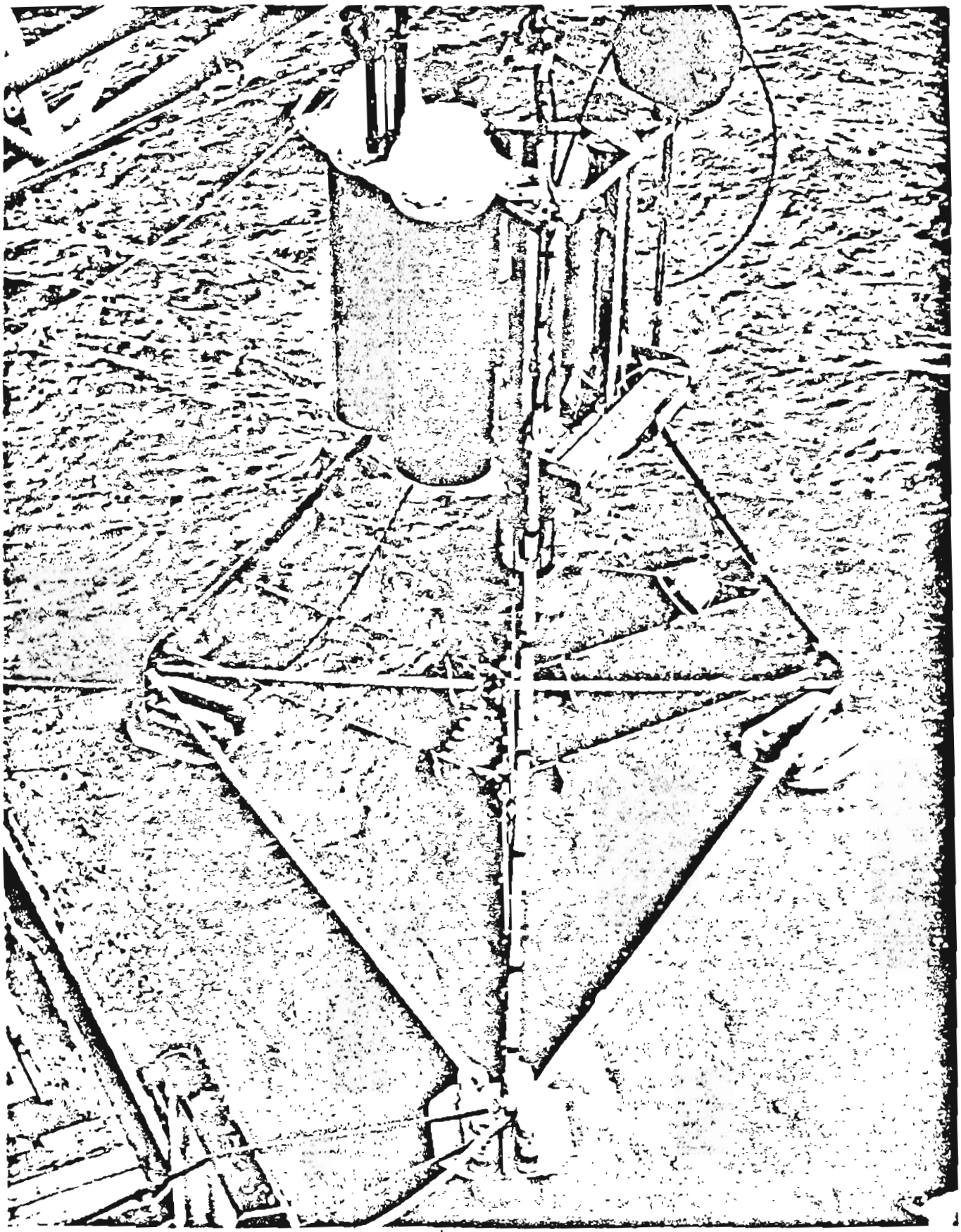

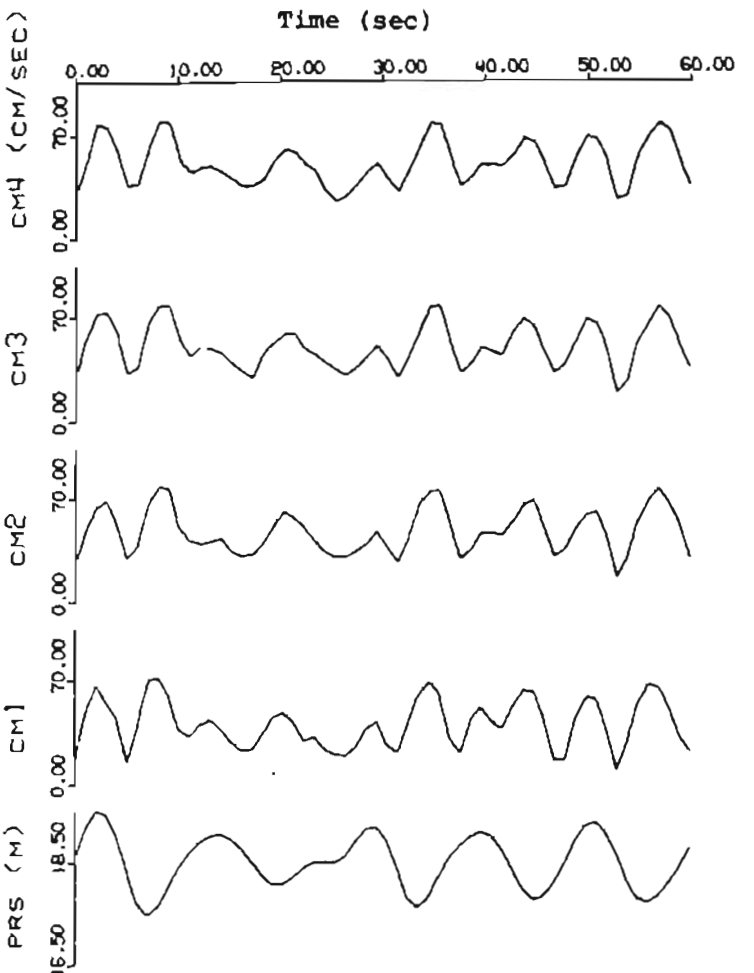
Time (sec)
0.00
10.00
20.00
30.00
40.00
50.00
60.00
CM4 (CM/SEC)
70.00
0.00
CM3
70.00
0.00
CM2
70.00
0.00
CM1
70.00
0.00
PRS (M)
18.50
16.50

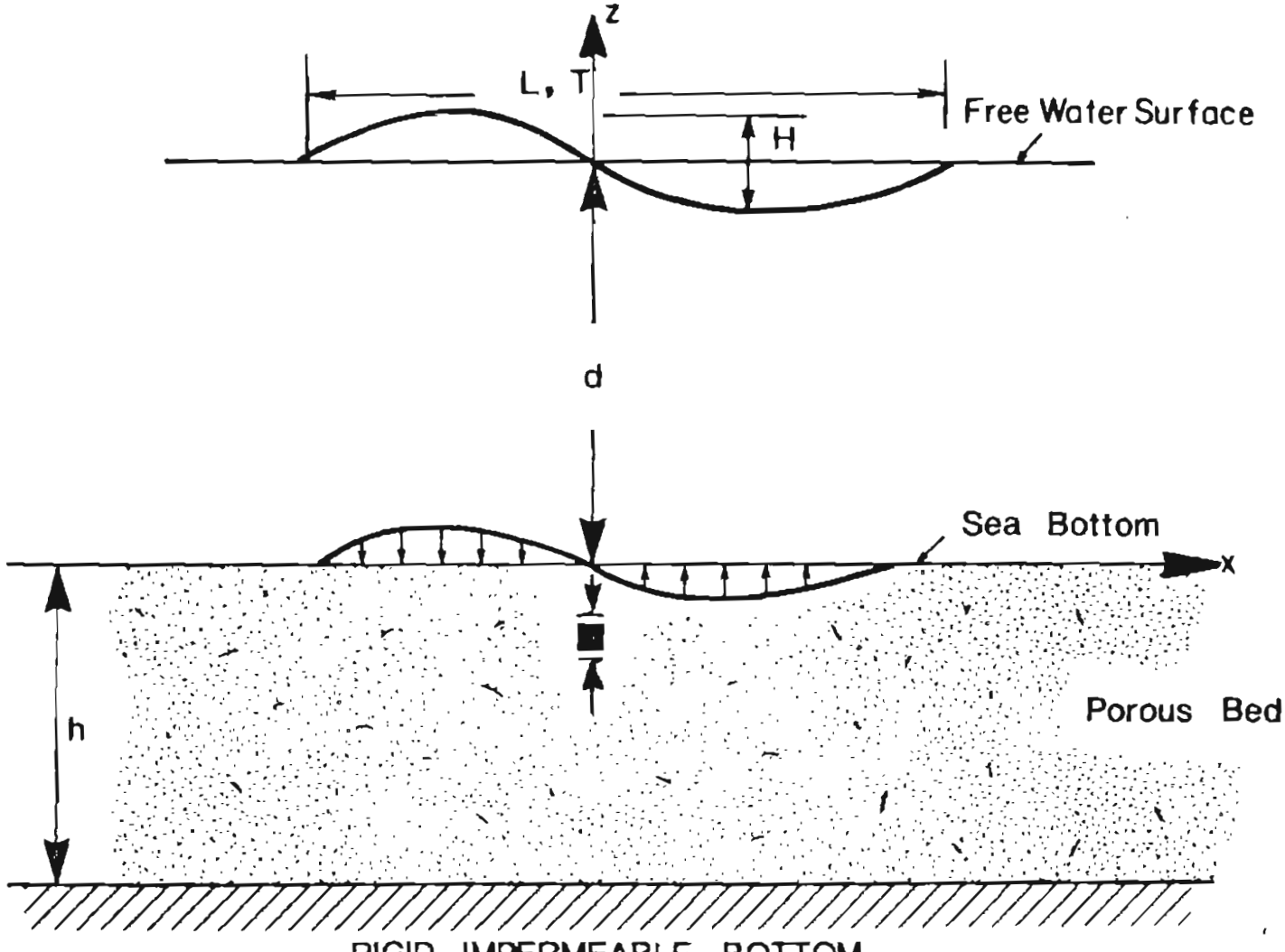
z
L, T
H
Free Water Surface
d
Sea Bottom
x
h
Porous Bed
RIGID IMPERMEABLE BOTTOM

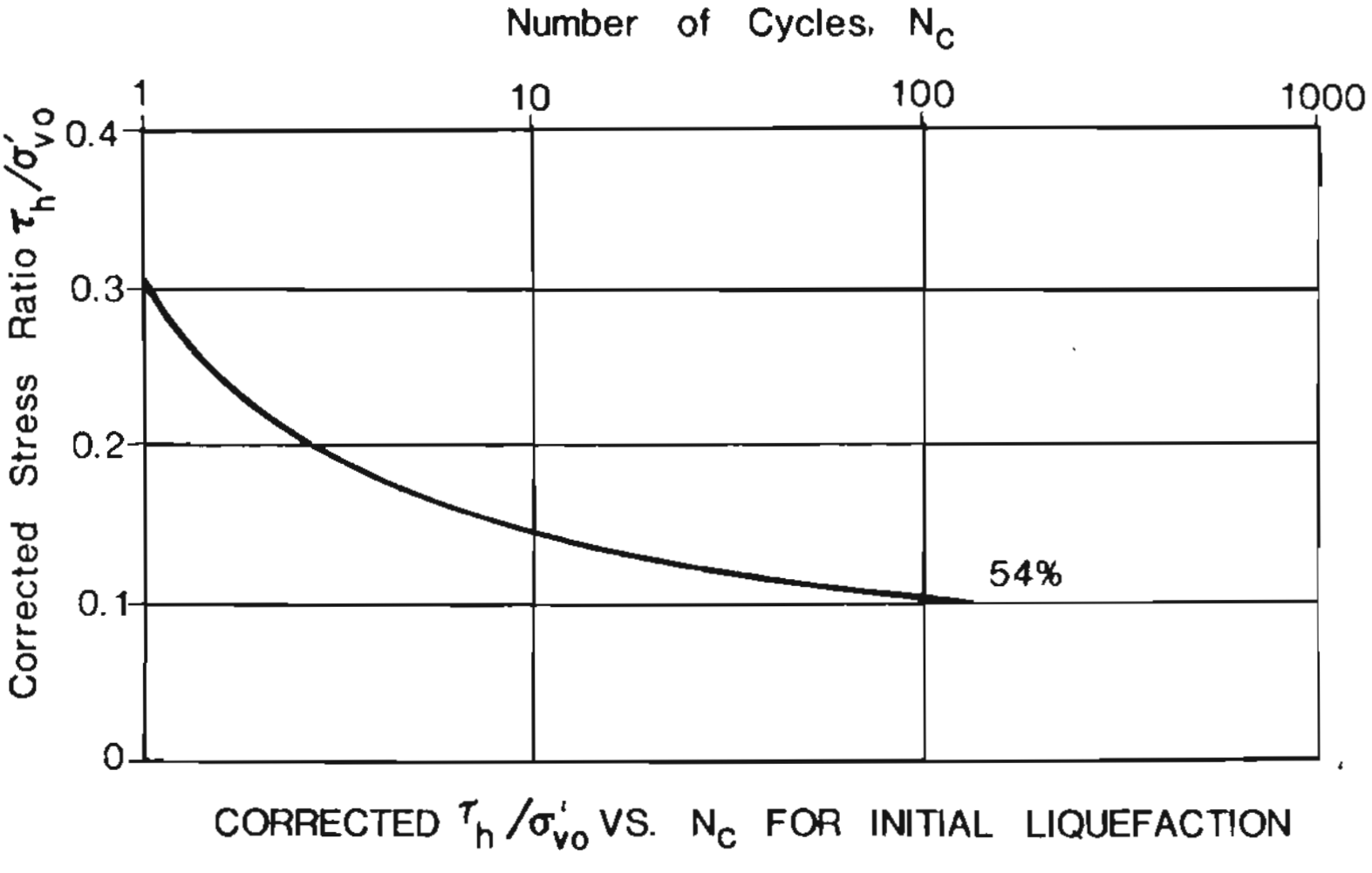

CORRECTED τ_h/σ'_{vo} VS. N_c FOR INITIAL LIQUEFACTION

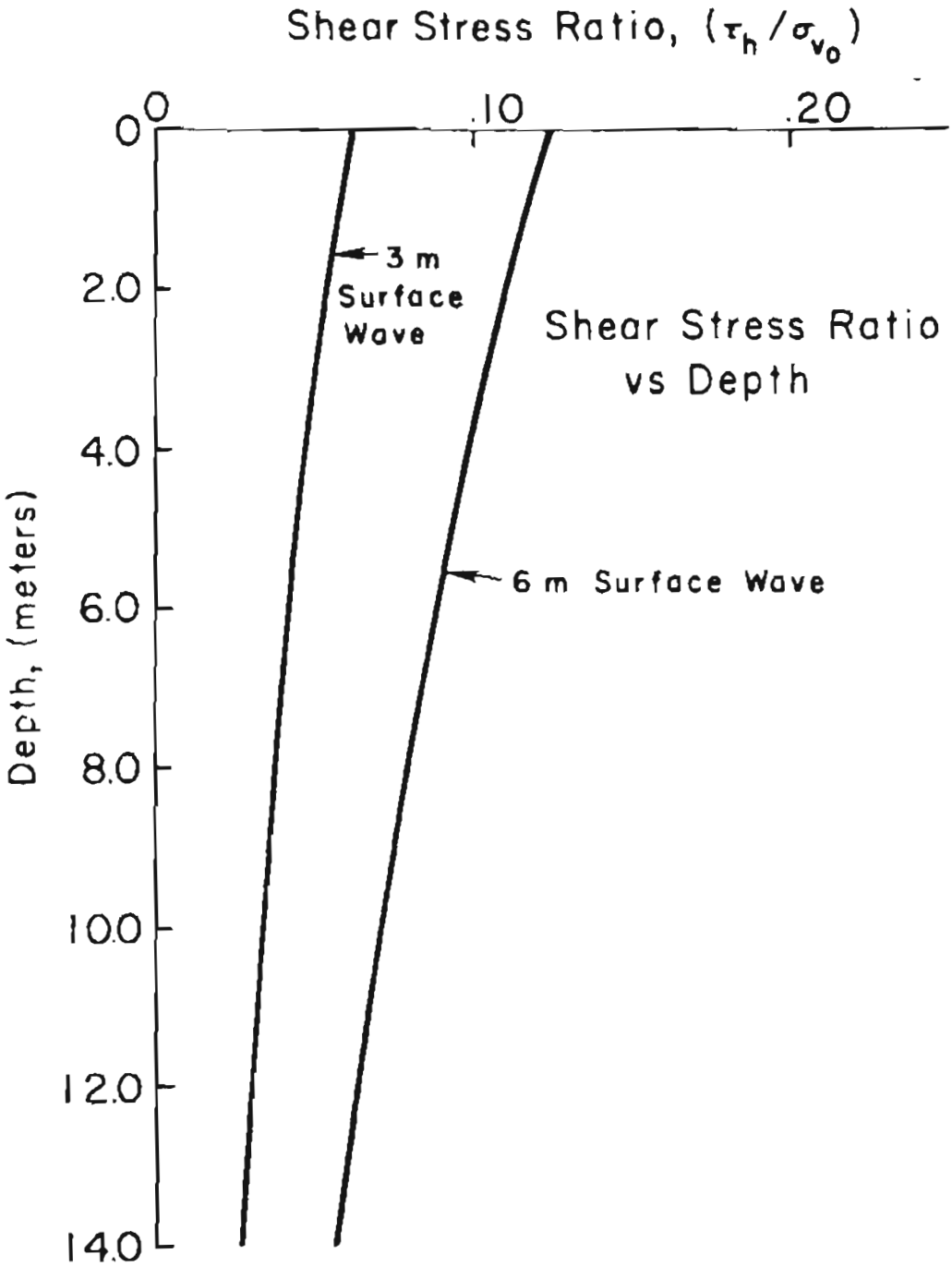
Shear Stress Ratio, (τ_h / σ_{v_0})
0
.10
.20
0
2.0
4.0
6.0
8.0
10.0
12.0
14.0
Depth, (meters)
3 m Surface Wave
6 m Surface Wave
Shear Stress Ratio vs Depth

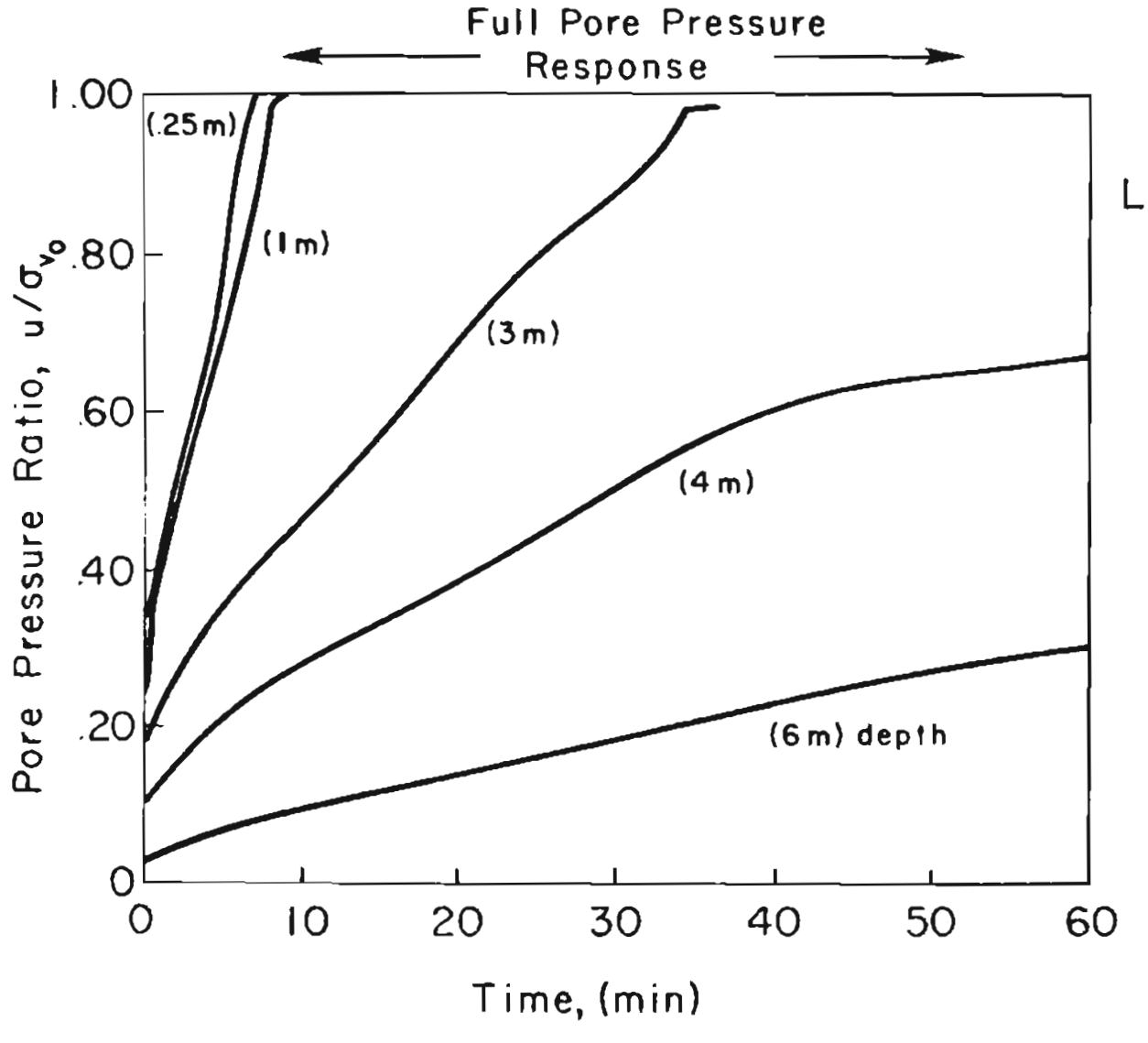

Wave
Liquefaction Analysis

Norton Sound

H = 6m, T = 10 s

D_r = 54%

k = 1.50×10^{-6} m/sec

SURFACE AND SUBSURFACE FAULTING IN NORTON SOUND AND CHIRIKOV BASIN, ALASKA

By

Janice L. Johnson and Mark L. Holmes

SUMMARY

Seismic reflection data were obtained in July 1977 by the U. S. Geological Survey aboard R/V SEA SOUNDER along 2800 km of track in Norton Sound and northeastern Chirikov basin. These data and records from several previous surveys were analyzed in order to determine the location, extent, and possible age and activity potential of offshore faulting. Acoustic reflection records were obtained using sparkers (160 and 0.8 kilojoule), Uniboom (1200 joule), and 3.5 kHz subbottom profiler. Sidescan sonar measurements were made along some of the tracklines whenever the large sparker was not deployed.

Maps showing the distribution of surface, near-surface, and deeper subbottom faults show that faulting occurs most commonly within 50 km of the margins of Norton basin, the deep sedimentary trough which underlies Norton Sound and Chirikov basin. A smaller number of faults were detected in the central regions of the basin.

Surface fault scarps were seen in several places in northern Chirikov basin. These sea-floor offsets ranged in height from 5 to 15 m along several west-trending faults which may be associated with some of the major transcurrent faults in Alaska. The existence of these scarps

indicates possible disturbance of sedimentary deposits over the fault, although the scarps may have been maintained by non-deposition. Evidence from both onshore and offshore field studies indicate that movement along these faults may have occurred between 12,000-120,000 years ago.

Many northwest-trending faults were mapped around the margins and in the central regions of Norton basin; they appear to show increasing displacement with depth and a thickening of the strata as they dip basinward away from the fault. These characteristics indicate a more or less continual movement along the faults as Norton basin was subsiding. The lack of recorded earthquakes in Norton basin during historical time implies that either activity along the offshore faults has ceased, or that movement is taking place at a slow but steady rate, preventing a buildup of strain and consequent earthquake-producing ruptures.

The west-trending faults in northern Chirikov basin appear to offset, and therefore postdate, the northwest trending faults which parallel the Norton basin axis. These two intersecting trends may have resulted from a change in the direction of regional compression during late Tertiary or early Quaternary time.

Considerable sea-floor relief hampered identification of surface scarps associated with offshore faults near St. Lawrence Island; and horizontal (transcurrent) motions along these faults may have taken place during Quaternary time in conjunction with movements on the Kaltag Fault which displaced Pleistocene deposits in western Alaska.

CONTENTS

	Page
INTRODUCTION	3
METHODS	5
Navigation	5
Acoustic Survey Techniques	6
Sparker	6
Uniboom	7
Bathymetry/Subbottom Profiler	8
Sidescan Sonar	8
GEOLOGIC SETTING	9
Tectonic Framework	9
Regional Geology	10
Norton Basin	10
Acoustic Basement	12
RESULTS AND DISCUSSION	12
Observed Faults and Structures	12
Fault Activity and Hazard Potential	15
CONCLUSIONS	18
REFERENCES	20

INTRODUCTION

Geological and geophysical studies were carried out by U. S. Geological Survey personnel aboard R/V SEA SOUNDER in Norton Sound and Chirikov basin during July 1977 (Fig. B1). Acoustic survey systems used included 160 and 0.8 kilojoule sparkers, a 1200 joule (four transducer) Uniboom, a 3.5 kHz bathymetric/subbottom profiling system, and sidescan sonar. This section of the annual report deals primarily with an interpretation of the extent and hazard potential of the surface and subsurface faults shown on the sparker and Uniboom records. Discussions of the 3.5 kHz and sidescan sonar data will be found in other sections.

The geophysical data obtained on this recent USGS cruise has been supplemented in places by seismic reflection information which was collected on previous expeditions by the USGS, NOAA, and the University of Washington (Fig. B1). In 1967 a joint USGS/University of Washington cruise obtained 4200 km of 150 joule sparker data (Grim and McManus, 1970), and 3200 km of 120 kilojoule sparker records (Scholl and Hopkins, 1969). High-resolution seismic reflection surveys were conducted in 1967 in the nearshore region south of Nome between Sledge Island and Cape Nome (Tagg and Greene, 1973). Walton et al. (1969) shot 3840 km of single channel 40 in^3 air gun records during a joint USGS/NOAA (then ESSA) survey in 1969, and that same year an additional 800 km of 150 joule sparker records were collected in Chirikov basin on a joint USGS/University of Washington cruise. Johnson and Holmes (1977) reported on preliminary results of a study of recent faulting in the northern Bering Sea, based primarily on examination of approximately 3000 km of seismic reflection data collected aboard R/V SEA SOUNDER in September and October 1976. Holmes

et al. (1978) obtained an additional 675 km of single channel air gun reflection data and 13 refraction profiles in Norton Sound during a survey conducted by the USGS aboard R/V LEE in October 1977.

All seismic records, sidescan records, and navigational data from the 1976 and 1977 R/V SEA SOUNDER cruises are on microfilm. Copies can be obtained from the National Geophysical and Solar-Terrestrial Data Center, EDS/NOAA, Boulder, Colorado 80302, or from the Alaska Technical Data Unit, USGS, 345 Middlefield Road, Menlo Park, California 94025.

METHODS

This section discusses the instrumentation and procedures used in collecting navigation and acoustic survey data on the R/V SEA SOUNDER cruise in July 1977.

Navigation

Navigational information was obtained by two independent systems. A Magnavox satellite navigator with integrated Teledyne Loran C received inputs from the ship's speed log and gyro. This system computed dead reckoning positions every two seconds and the data were stored on magnetic tape and a teleprinter. Performance of the system was degraded somewhat by proximity to the Loran C master station at Port Clarence and the high elevation of many of the satellites during transit.

A Motorola mini-Ranger system was used to obtain fixes every seven and one-half minutes which were recorded on paper tape in digital form. This system measures the range to two or more shore-based transponders which were maintained by survey personnel on land. On a few occasions the included angle between the transponders was too small to permit obtaining reliable fix information.

Fixes were plotted at least every fifteen minutes on the navigational charts with appropriate notations made at the time of major course and speed changes. Radar and line-of-sight bearings were sometimes used to augment the other navigational information, and navigational accuracy probably averaged ± 150 m.

Acoustic Survey Techniques

Figure B1 shows the tracklines for the 1977 R/V SEA SOUNDER cruise, as well as those of previous expeditions on which seismic reflection data were collected. The figure also notes which acoustic systems were used during the various cruises. The bathymetry-subbottom profiler and sidescan sonar systems used aboard R/V SEA SOUNDER will be briefly discussed, although interpretation of these data will be, as previously mentioned, found in other sections of the report.

Seismic profiling operations aboard R/V SEA SOUNDER were carried out at speeds ranging from 4-6 knots. It was found that speeds greater or less than this range resulted in generation of "ship noise" by the propulsion machinery which produced a significant amount of interference on the records.

Sparker. A Teledyne SSP (Seismic Section Profiler) was used to obtain 325 km of single channel seismic reflection records in Norton Sound and northeastern Chirikov basin. Power output was normally 160 kilojoules, but was reduced to 120 kilojoules at times because of equipment casualties. The signals were received by a Teledyne 100-element Hydrostreamer and processed through a Teledyne seismic amplifier before being printed off a modified Raytheon PFR (Precision Fathometer Recorder). Frequency pass band was normally set at 20-98 Hz, and sweep and fire rate was 4 seconds. The records were annotated at 30 minute intervals with date, time (GMT), line number, water depth, and appropriate instrument settings. Changes in course, speed, or instrumentation were noted when they occurred.

Maximum penetration achieved by the sparker was approximately 2.1 km. The quality of the records was affected adversely by the shallow water and the generally flat nature of the bottom and subbottom reflectors. The shallow depth caused the water bottom multiple to appear at small distances below the initial sea-floor reflection, thus partially obscuring signals from deeper reflectors. The flat subbottom layering produced intra-formational or "peg-leg" multiples which also obscured or interfered with the primary reflections. In only a few places was an acoustic basement detected; more commonly the reflection amplitudes slowly decreased as the signal was attenuated in the sedimentary section.

Uniboom. Approximately 2800 km of high-resolution records were obtained using a hull-mounted EG & G Uniboom system consisting of four transducer plates. Total power level for this array was 1200 joules. An EG & G model 265 hydrophone streamer (10-element) was used as a receiver. Records were printed on an EPC 4100 recorder after passing through a Krohn-Hite filter. Sweep and fire rate was normally 1/4 second, although a 1/2 second sweep was used on occasion. The filter pass band was typically set from 400-4000 Hz. Time marks were made at 5 minute intervals and record annotations similar to those for the sparker were made at 15 minute intervals.

The quality of the Uniboom records was most affected by sea state, surficial bottom sediment type, and machinery generated ship noise. The hydrophone streamer was towed alongside the ship and only 20-30 cm below the surface. Consistently choppy seas were responsible for a significant amount of noise on the record which sometimes totally obscured subbottom

reflectors. Maximum penetration achieved was approximately 100 m, but was typically less than 75 m. Whenever coarse-grained and hard sediments were encountered penetration was severely reduced, and in some instances, such as near the Yukon Delta, the records are very poor.

Bathymetry/Subbottom Profiler. These data were collected along 2800 km of track using a Raytheon 3.5 kHz CESP II system. A hull-mounted transducer array consisting of 12 TR-109A units was used to send and receive the signals. Pulse generation and correlation functions were done by a CESP II (Correlator Echo Sounder Processor) and a PTR-105B (Precision Transmitter Receiver) was used as a tone burst amplifier during pulse transmission. Sweep and fire rates were normally 1/2 second. Time marks were made every 5 minutes and the records were annotated and depth measurements taken at 15-minute intervals.

Clarity of the records and amount of penetration varied considerably over the survey area. This system seemed less sensitive to ship-generated noise than the Uniboom, but the 3.5 kHz records were more adversely affected by hard bottom sediment. The long (50 msec) pulse generated during transmission also created an internal "ringing" in the transducer array which masked not only the weak subbottom reflections but sometimes the bottom echo as well in shallow water. Penetration ranged from 0-20 m.

Sidescan Sonar. An EG & G sidescan sonar system was used to record 1000 km of good to high quality data. Scales (sweeps) of 50 m and 100 m were used, and the "fish" altitude above the sea-floor was maintained at approximately 10 percent of the scale being used. The sidescan system was used in shallow water areas of known or suspected sand waves and ice-gouge features, and at such times the sparker system was shut down and its associated arc cables and hydrostreamer were brought aboard to prevent their fouling the sidescan cable.

GEOLOGIC SETTING

Tectonic Framework

The structural features and evolution of the Bering Sea continental shelf have been discussed by Scholl and Hopkins, 1969; Scholl et al., 1968; Pratt et al., 1972; Churkin, 1972; Lathram, 1973; Nelson et al., 1974; and Marlow et al., 1976. Figure B2 shows the major Cenozoic structures of western Alaska and eastern Siberia.

The general tectonic framework is characterized by large scale oroclinal bending forming two distinct flexures in central Alaska and eastern Siberia concave toward the Pacific Ocean. The Bering and Chukchi continental shelves are part of the broad intervening structural arc which is concave toward the Arctic Ocean.

This large scale oroclinal folding appears to have been completed before Oligocene time (Nelson et al., 1974), but continued activity along the major Alaskan transcurrent faults has displaced upper Tertiary and Quaternary sediment in several places on land and beneath the shelf areas (Patton and Hoare, 1968; Scholl et al., 1970; Grim and McManus, 1970). Total horizontal (right-lateral) movement along some of these large transcurrent faults has been approximately 130 km since the beginning of the Tertiary (Grantz, 1966; Patton and Hoare, 1968).

Regional Geology

Norton Basin. The geology of Norton basin has been discussed by Moore, 1964; Scholl and Hopkins, 1969; Grim and McManus, 1970; Tagg and Greene, 1973; Nelson et al., 1974; and Holmes et al., 1978. A submarine seepage of natural gas 40 km south of Nome has been described by Cline and Holmes (1977). Seismic reflection data suggest that the basin area is about 130,000 km^2; maximum basin depth has recently been estimated to be approximately 5.5 km (Anon., 1976). The basin probably contains as much as 180,000 km^3 of sediment.

The basin fill consists of three major stratified units (Homes et al., 1978), which are in turn covered by a thin mantle of Quaternary sediment (Grim and McManus, 1970; Tagg and Greene, 1973; Nelson and Creager, 1977). The lowermost unit in the basin, with a velocity of 4.9 km/sec (Holmes et al., 1978), may consist of Cretaceous nonmarine sandstones similar to those mapped onshore in the Koyukuk geosyncline (Patton and Hoare, 1968; Cobb, 1974). A velocity discontinuity at the top of this unit indicates that this interface may be an erosional unconformity.

Two other units of the basin fill can also be distinguished on the basis of compressional velocities (Holmes et al., 1978). A strong reflector on the reflection records corresponds to an apparent unconformity separating those units; the unconformity lies at a depth of about 1.2 km near the basin axis and approaches to within a few tens of meters of the sea floor near the basin margins. The compressional velocities above this unconformity are low, ranging from 1.6 to 2.1 km/sec; this section is probably composed of recent marine and glaciomarine sediment and loosely cemented sandstones and shales. The higher velocities (2.3-3.7 km/sec) below the

unconformity are more characteristic of compact or indurated sandstones and shales (Grant and West, 1965; Gardner et al., 1974). The unconformity was probably formed during the late Miocene marine transgression which inundated the northern Bering Sea continental shelf (Nelson et al., 1974). Strata of the unit below the unconformity form a broad synclinorium whose principal axis trends generally northwest; the beds of the upper unit are more nearly flat-lying.

Although younger Quaternary deposits everywhere cover the older Cenozoic and Mesozoic basin fill, some onshore outcrops and drill-hole data give clues as to the nature of the two upper units. Nonmarine coal-bearing strata of late Oligocene age are exposed on northwestern St. Lawrence Island (Patton and Csejtey, 1970), and several offshore holes drilled by the U.S. Bureau of Mines near Nome encountered marine sands and clayey silts of early Pliocene age at a subbottom depth of approximately 18 m (Scholl and Hopkins, 1969; Nelson et al., 1974). Late Miocene or early Pliocene marine limestone was recovered from a dredge haul 30 km south of St. Lawrence Island, just outside the basin.

These facts and the regional stratigraphic patterns indicate that the basin fill probably consists of late Cretaceous and lower to middle Tertiary sedimentary rock in the lower two units and upper Tertiary and Plio-Pleistocene sedimentary rocks and sediment in the upper unit. All direct evidence suggests that the lower units are nonmarine, but the size of the basin is such that unseen transitions to marine facies could occur within this sequence.

Acoustic Basement. The high compressional velocity contrast across the acoustic basement is indicative of a marked lithologic change at this interface (Holmes et al., 1978). Velocities of 5.5 to 6.5 km/sec are characteristic of igneous and metamorphic rocks (Grant and West, 1965), indicating that Norton basin is probably floored by a basement surface formed on strata which are analogous to the diverse older rocks which occur on land around the basin margins. Sedimentary, metamorphic, and igneous rocks of Precambrian through Mesozoic age are exposed on the Chukotka Peninsula (Nalivkin, 1960); and Seward Peninsula is formed primarily of Paleozoic sedimentary and metamorphic units with some Mesozoic and Cenozoic intrusive and extrusive rocks. Mesozoic sedimentary rocks (some slightly metamorphosed) and Cenozoic volcanics have been mapped onshore in the Yukon-Koyukuk basin east and southeast of Norton Sound (Miller et al., 1959; Patton and Hoare, 1968). At the southern margin of Norton basin, St. Lawrence Island is constructed mainly of Paleozoic, Mesozoic, and Cenozoic intrusive and extrusive rocks with some Cenozoic sedimentary deposits (Miller et al., 1959; Scholl and Hopkins, 1969; Patton and Csejtey, 1970). The acoustic basement probably represents an erosional surface which has been steepened by tectonic subsidence during development of Norton basin.

RESULTS AND DISCUSSION

Observed Faults and Structures

Locations of faults observed on seismic reflection profiles from Norton Sound and Chirikov basin are shown in Fig. B3. The majority of faults, especially those extending close to the sea floor, occur within 50 km of the basin margins. Most faults in Chirikov basin and western

Norton Sound trend northwest in alignment with the major axis of Norton basin. Synclinal and anticlinal axes mapped by Greene and Perry (unpub.), and shown in Johnson and Holmes (1977, Fig. B3), reflect this same trend. In eastern Norton Sound, the structural grain is nearly east-west.

Seismic records from the basin margins generally show sediments of the upper two units of basin fill, the Main Layered Sequence of Scholl and Hopkins (1969), resting with onlap unconformity against the eroded surface of the acoustic basement. The single channel seismic reflection systems were unable to resolve acoustic basement in the deeper basin areas where sediment thickness exceeded 2 km. Numerous faults offset the acoustic basement, often displacing overlying sediments. Many normal and antithetic faults displace the basin fill and extend to within 100 meters of the sediment surface. A few of these have topographic expression as fault scarps.

Faulting appears to be most complex, and the fault density is highest, in the area west of Port Clarence (Fig. B3). Several west-trending faults appear to intersect, and can be seen to offset, the dominant pattern of northwest-trending faults. These west-trending faults must therefore be younger than the others, and may be indicative of a change in the direction of regional compression during Quaternary time.

One of the major faults comprising this major east-west trend is the Bering Strait Fault (BSF) of Hopkins (unpub.). It forms the northern boundary of the Bering Strait Depression (BSD) named by Greene and Perry

(unpub.) and appears to extend for over 90 km west from Port Clarence (Fig. B3). A south-facing scarp 5 meters high marks the fault near the Bering Strait Depression. The scarp decreases in height eastward; no trace of the fault has been found beneath Port Clarence. This fault appears to have been active as recently as 12,000 years ago (Hopkins, unpub.).

The Port Clarence Rift (PCR) (Hopkins, unpub.) is a narrow fault-bounded depression extending eastward from the Bering Strait Depression; the fault along the northern margin of the depression is probably equivalent to the Cape York Fault of Greene and Perry (unpub.). This northern fault has a scarp 9 meters high near the Bering Strait Depression, which decreases to the east. No trace of this fault has been observed beneath Port Clarence, but displacement of bedrock beneath Grantley Harbor has been suggested as evidence for extension of the Port Clarence Rift further to the east. The Rocks beneath Grantley Harbor have experienced 16 km of left-lateral movement (Hopkins, unpub.). Several other west-trending faults with scarps up to 15 m high have been observed in the area west of Port Clarence (Fig. B3).

The rough seafloor topography north of St. Lawrence Island made identification of fault scarps difficult, but a few have been tentatively mapped (Fig. B3). A large west-trending fault has been inferred by Hopkins (unpub.) to parallel the northern coast of St. Lawrence Island and bend northward before reaching the western end of the island (Fig. B3). Existence of the St. Lawrence Fault Zone (SLF) is based on swarms of volcanic vents which trend N80°W through the axis of the Kookooligit

Mountains, and on the extension of these volcanic rocks into offshore regions. Hopkins has suggested that movement along this fault has been left-lateral. Possibly it is related to movement along the Kaltag Fault (KF), a large transcurrent fault in western Alaska that has been known to displace Pleistocene sediments onshore.

Many deep-seated and near-surface normal faults occur in the central part of Norton basin, although no surface expressions of these have been identified. An increase in displacement with depth, and apparent thickening of beds on the downthrown side of these faults, indicates that they are probably growth faults along which movement has taken place more or less continuously during the major episodes of basin subsidence.

Several subbottom faults occur along the southern and eastern margins of Norton Sound (Fig. B3). Short line segments indicate faults have been observed on one crossing, and therefore, their exact orientation is unknown. However, several faults appear to parallel the trend of the Kaltag Fault; others may represent splays of the Kaltag Fault. No surface scarps were associated with the near-surface faults along the eastern margin of Norton Sound.

Fault Activity and Hazard Potential

Surface fault scarps in northern Chirikov basin are associated with the Bering Strait Fault, the Port Clarence Rift, and other nearby faults (Fig. B3). The Bering Strait Fault and Port Clarence Rift may represent extensions or splays of the large transcurrent faults which have been mapped in western Alaska and Seward Peninsula (Fig. B2). The scarps may have been caused by recent vertical movement on these faults, and therefore would indicate a definite hazard to man-made structures placed over

or near these fault zones. There is also the possibility, that the faults have been inactive for some time, and the scarps have been maintained by nondeposition or lack of erosion. Currents west of Port Clarence flow almost normal to the trend of these scarps, and carry almost one third of the Yukon River sediment load into the Chukchi Sea (Nelson and Creager, 1977). The persistence of the surface expression of the faults in spite of apparently vigorous erosional agents would argue for the fault scarps to be recently formed features.

The Bering Strait Fault must have formed between 12,000 and 120,000 years ago; evidence exists that a lake was formed during the Wisconsin glaciation when development of the fault scarp dammed a northward-flowing river west of present day Port Clarence. Marine terraces on Seward Peninsula may have been uplifted during the Illinoian glaciation as a result of movement along the fault 130,000 years ago. Although no specific age can be given to movements along these faults in northern Chirikov basin, the area should definitely be considered as potentially hazardous to placement of structures on the bottom in the vicinity of the fault scarps.

Only a few surface scarps have been noted in association with faults along the northern side of the St. Lawrence Island or in southern and eastern Norton Sound; the rough sea-floor topography in this area makes identification of fault scarps difficult. Movement may have occurred along these faults during Tertiary and Quaternary time in conjunction with known displacement in western Alaska along the large transcurrent Kaltag Fault. Further study is necessary to determine if this represents a hazard to resource development.

Earthquake records show an almost complete lack of epicenters beneath Norton basin. This lack of seismicity can be interpreted to indicate either inactivity or, conversely, that strain release is being accomplished by small but frequent adjustments along the faults. The growth nature of most of the northwest trending faults which parallel the Norton basin axis support the latter interpretation, although the rate of basin subsidence may have decreased since the end of Pleistocene time when rising sea-level opened Bering Strait and resulted in a significant change in deposition patterns in the northern Bering Sea.

CONCLUSIONS

Based on the foregoing discussion, the following conclusions may be made regarding the faulting observed in Norton Sound and Chirikov basin:

1. Faults are most numerous in a belt approximately 50 km wide around the margins of Norton basin. Near surface faults are more numerous in central Norton basin than previously reported, but are still less prevalent than around the periphery of the basin. Most of the faults trend generally northwest, with the basinward sides down-dropped; antithetic faults are also common, resulting in series of narrow horsts and grabens along the basin margins. These faults and the many associated anticlinal and synclinal folds involving the basin fill and acoustic basement are the result of tectonic activity which occurred during subsidence and filling of the 5.5-km deep Norton basin. Initial subsidence of the basin probably began during late Cretaceous time, and has continued to the present with two apparent major interruptions during early and late Tertiary time.

2. Surface scarps up to 15 m high are associated with some of the long west-trending faults in northern Chirikov basin. These scarps can indicate either recent activity or persistence due to lack of erosion or burial by sedimentation since the last movement. Scarps occur on the Bering Strait Fault and on the northern side of the Port Clarence Rift, and movement along these faults possibly occurred as recently as 12,000 years ago in conjunction with uplift of marine terraces on Seward Peninsula.

3. The west-trending faults in northern Chirikov basin intersect and appear to offset the northwest-trending faults and structures south of Bering Strait. This relationship implies that the west-trending features postdate the main Norton basin structures; the different trends could also be indicative of a shift in regional compressive axes.

4. None of the faults can definitely be classed as historically active, however the area of northern Chirikov basin west of Port Clarence should be considered potentially hazardous to any bottom mounted structures. The fault scarps in this region are still well defined in spite of the swift currents and bottom sediment transport which occur normal to the trend of the fault zones. Basin subsidence is probably still taking place, and the lack of recorded earthquakes beneath Norton basin may indicate that strain release is being accomplished by small but frequent movement along some of these faults.

5. West-trending subbottom faults without surface fault scarps occur along the southern margin of Norton basin. These may represent splays or displacements related to the Kaltag Fault, one of the major transcurrent faults in western Alaska. Movement along onshore portions of the Kaltag Fault have displaced Pleistocene deposits, but data regarding age of movements along the offshore portion are inconclusive.

REFERENCES

Anonymous, 1976, Prospective basins included in Alaska OCS sale plans: The Oil and Gas Journal, v. 74, p. 126-130.

Churkin, M., Jr., 1972, Western boundary of the North American continental plate in Asia: Geol. Soc. America Bull., v. 83, p. 1027-1036.

Cline, J. D., and M. L. Holmes, 1977, Submarine seepage of natural gas in Norton Sound, Alaska: Science, v. 198, p. 1149-1153.

Cobb, E. H., 1974, Synopsis of the mineral resources of Alaska: U.S. Geological Survey Bull. 1307, 53 p.

Gardner, G.H.F., L. W. Gardner, and A. R. Gregory, 1974, Formation velocity and density--the diagnostic basis for stratigraphic traps: Geophysics, v. 39, p. 770-780.

Grant, F. S., and G. F. West, 1965. Interpretation theory in applied geophysics: McGraw-Hill, New York, p. 8.

Grantz, A., 1966, Strike-slip faults in Alaska: U.S. Geol. Survey Open-File Report, 82 p.

Grim, M. S., and D. A. McManus, 1970, A shallow seismic-profiling survey of the northern Bering Sea: Marine Geology, v. 8, p. 293-320.

Holmes, M. L., J. D. Cline, and J. L. Johnson, 1978, Geological setting of the Norton basin gas seep: Proceedings, 1978 Offshore Technology Conference (in press).

Johnson, J. L., and M. L. Holmes, 1977, Preliminary report on surface and subsurface faulting in Norton Sound and northeastern Chirikov basin, in Environmental Assessment of the Alaskan Continental Shelf, v. XVIII, Hazards and Data Management, Annual Reports of Principal Investigators: U.S. Dept. of the Interior, Bureau of Land Management, p. 14-41.

Lathram, E. H., 1973, Tectonic framework of northern and central Alaska, in Pitcher, M. G., ed., Arctic Geology: Tulsa, Okla., American Assoc. Petroleum Geologists Mem. 19, p. 351-360.

Marlow, M. S., D. W. Scholl, A. K. Cooper, and E. C. Buffington, 1976, Structure and evolution of Bering Sea shelf south of St. Lawrence Island: American Assoc. of Petroleum Geologists Bull., v. 60, p. 161-183.

Miller, D. J., T. G. Payne, and G. Gryc, 1959, Geology of possible petroleum provinces in Alaska: U.S. Geol. Survey Bull. 1094, 131 p.

Moore, D. G., 1964, Acoustic reconnaissance of continental shelves: Eastern Bering and Chukchi Seas, in Miller, R. L., ed., Papers in Marine Geology, Shepard commemorative volume: New York, MacMillan Co., p. 319-362.

Nalivkin, D. V., 1960, The geology of the U.S.S.R.: New York, Pergamon Press, 170 p.

Nelson, C. H., D. M. Hopkins, and D. W. Scholl, 1974, Tectonic setting and Cenozoic sedimentary history of the Bering Sea, in Herman, Y., ed., Marine Geology and Oceanography of the Arctic Seas: New York, Springer-Verlag, p. 119-140.

Nelson, C. H., and J. S. Creager, 1977, Displacement of Yukon-derived sediment from Bering Sea to Chukchi Sea during Holocene time: Geology, v. 5, p. 141-146.

Patton, W. W., Jr., and J. M. Hoare, 1968, The Kaltag fault, west-central Alaska: U.S. Geol. Survey Prof. Paper 600-D, p. D147-D153.

Patton, W. W., Jr., and B. Csejtey, Jr., 1970, Preliminary geologic investigations of western St. Lawrence Island, Alaska: U.S. Geol. Survey Prof. Paper 684, 15 p.

Pratt, R. M., M. S. Rutstein, F. W. Walton, and J. A. Buschur, 1972, Extension of Alaskan structural trends beneath Bristol Bay, Bering shelf, Alaska: Jour. Geophys. Research, v. 77, p. 4994-4999.

Scholl, D. W., E. C. Buffington, and D. M. Hopkins, 1968, Geologic history of the continental margin of North America in Bering Sea: Marine Geology, v. 6, p. 297-330.

Scholl, D. W., and D. M. Hopkins, 1969, Newly discovered Cenozoic basins, Bering Sea shelf, Alaska: Amer. Assoc. Petroleum Geologists Bull., v. 53, p. 2067-2078.

Scholl, D. W., M. S. Marlow, J. S. Creager, M. L. Holmes, S. C. Wolf, and A. K. Cooper, 1970, A search for the seaward extension of the Kaltag fault beneath the Bering Sea: Geol. Soc. America, Abs. with Program, Cordilleran Sect., v. 2, p. 141-142.

Tagg, A. R., and H. G. Greene, 1973, High-resolution seismic survey of an offshore area near Nome, Alaska: U.S. Geol. Survey Prof. Paper 759-A, 23 p.

Walton, F. W., R. B. Perry, and H. G. Greene, 1969, Seismic reflection profiles, northern Bering Sea: ESSA Operational Data Report C+GS DR-B

Figure 1. Coverage of geophysical studies conducted in northeastern Bering Sea.

Figure 2. Regional tectonic map of northern Bering Sea area.

Figure 3. Faults in Chirikov Basin and Norton Sound.

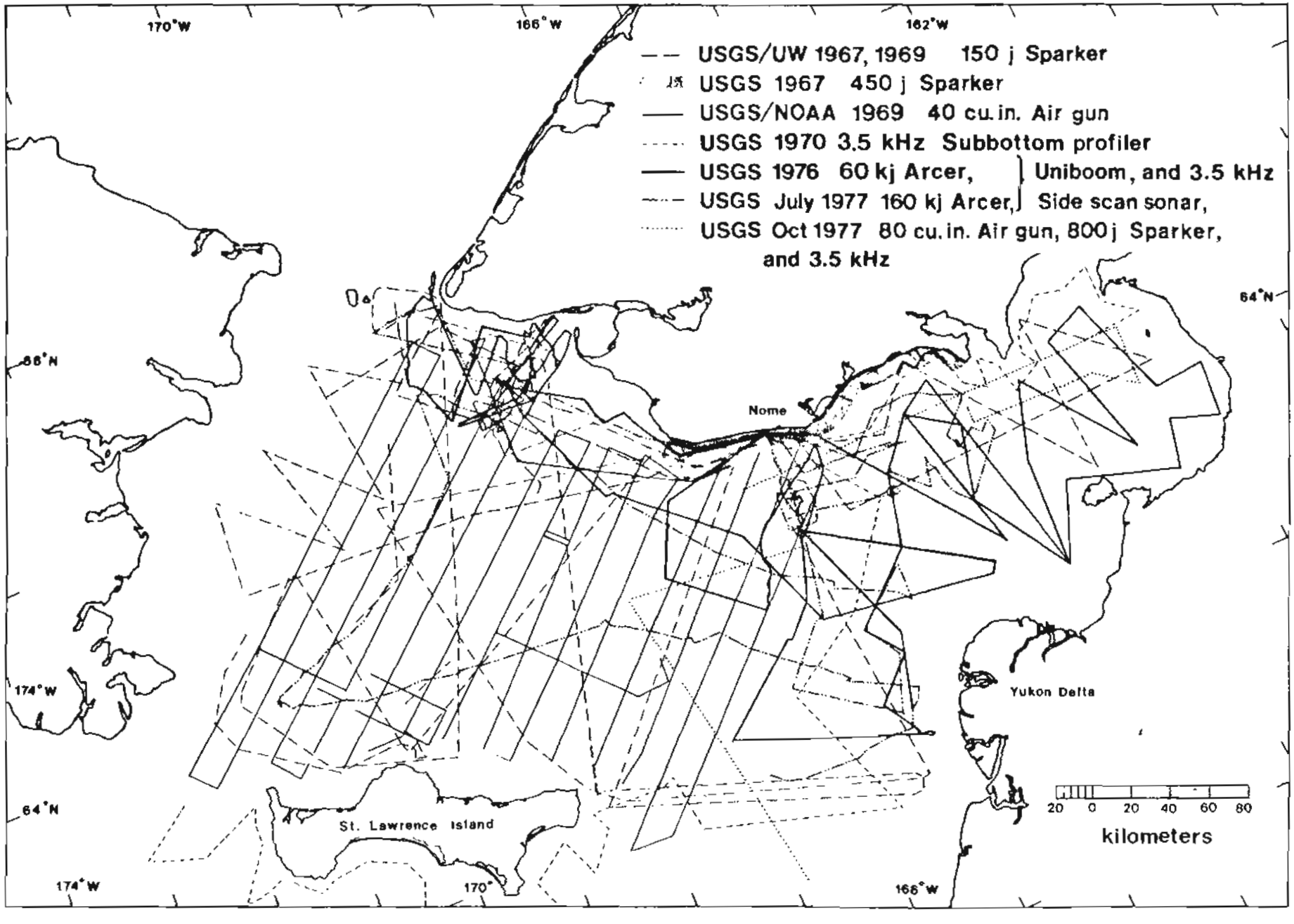
170°W
166°W
162°W
USGS/UW 1967, 1969 150 j Sparker
USGS 1967 450 j Sparker
USGS/NOAA 1969 40 cu.in. Air gun
USGS 1970 3.5 kHz Subbottom profiler
USGS 1976 60 kj Arcer, Uniboom, and 3.5 kHz
USGS July 1977 160 kj Arcer, Side scan sonar,
USGS Oct 1977 80 cu.in. Air gun, 800j Sparker,
and 3.5 kHz
64°N
66°N
Nome
174°W
Yukon Delta
64°N
St. Lawrence Island
174°W
170°
166°W
20 0 20 40 60 80
kilometers

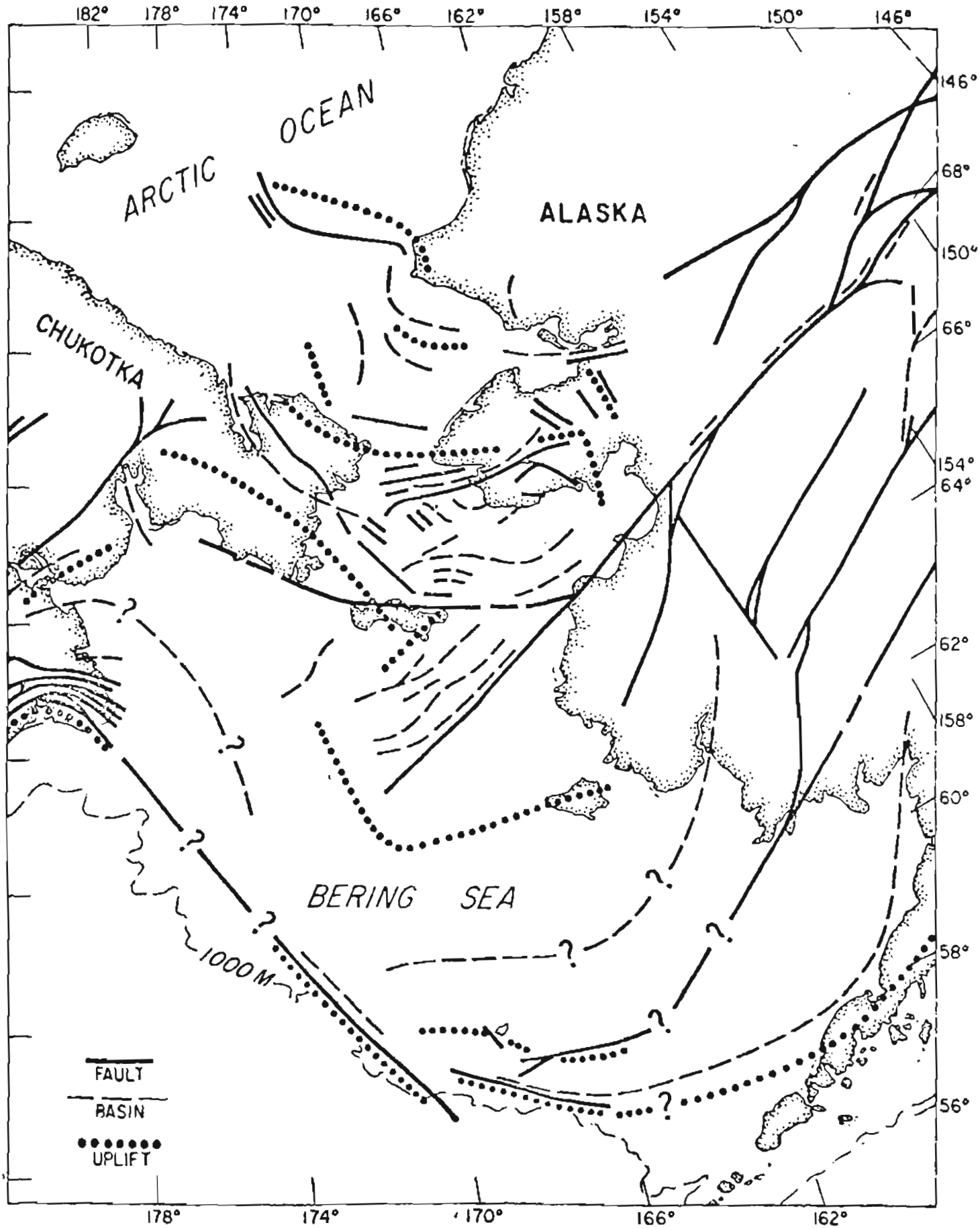
182°
178°
174°
170°
166°
162°
158°
154°
150°
146°
ARCTIC OCEAN
ALASKA
CHUKOTKA
BERING SEA
1000 M
FAULT
BASIN
UPLIFT
146°
68°
150°
66°
154°
64°
62°
158°
60°
58°
56°
178°
174°
170°
166°
162°

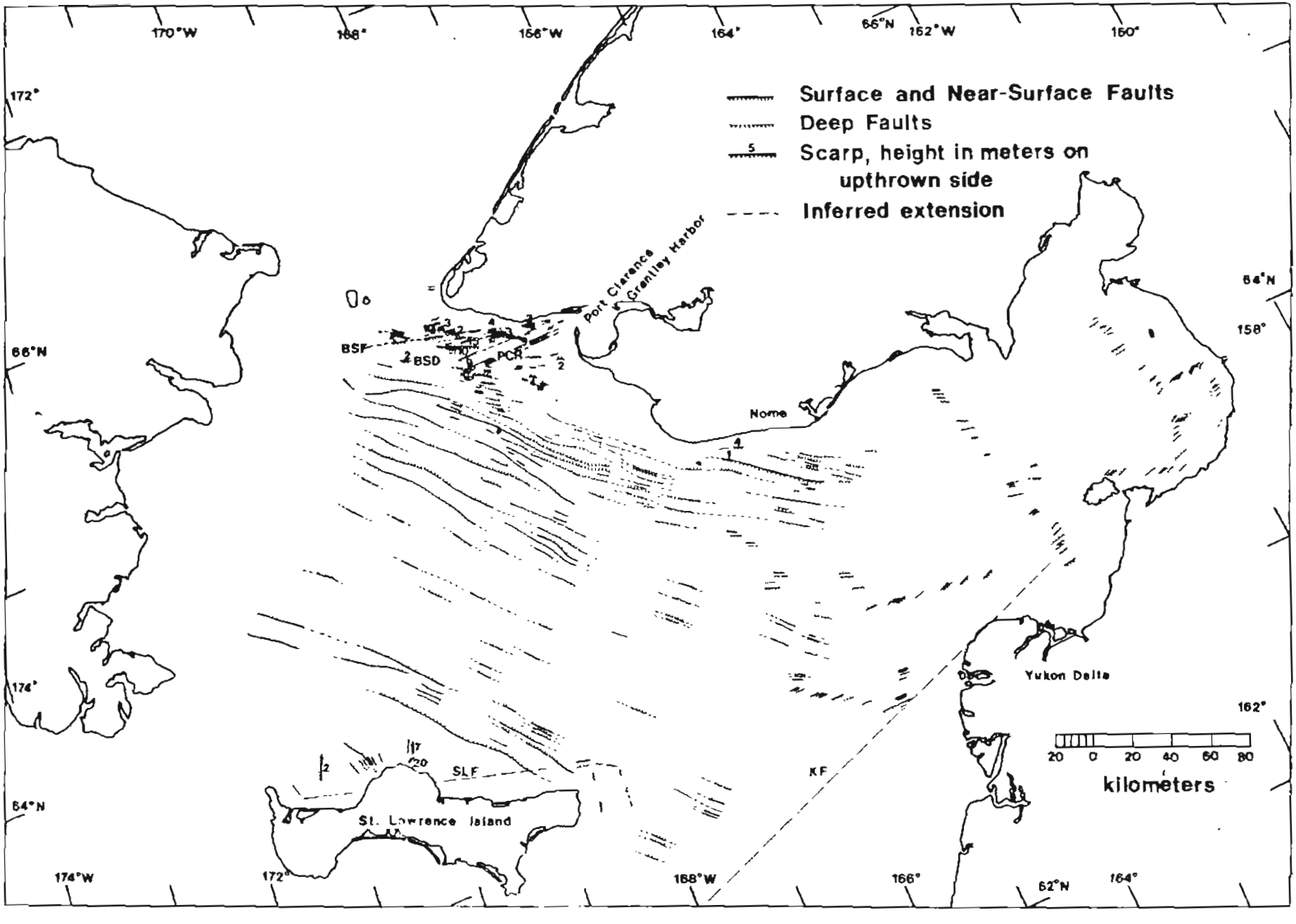
Surface and Near-Surface Faults
Deep Faults
5
Scarp, height in meters on upthrown side
Inferred extension
Port Clarence
Grantley Harbor
Nome
BSF
BSD
PCF
SLF
KF
St. Lawrence Island
Yukon Delta
20 0 20 40 60 80
kilometers
170°W
168°
166°W
164°
66°N
162°W
160°
172°
66°N
64°N
158°
174°
162°
64°N
174°W
172°
168°W
166°
62°N
164°

HYDROCARBON GASES IN NEAR-SURFACE SEDIMENT OF NORTHERN BERING SEA (NORTON SOUND AND CHIRIKOV BASIN)

Keith A. Kvenvolden, George D. Redden,

Devin R. Thor, and C. Hans Nelson

U.S. Geological Survey, Menlo Park, California 94025

Prepared for publication in book "Eastern Bering Sea Shelf: Oceanography and Resources"

ABSTRACT

Methane, ethane, ethene, propane, propene, n-butane, and isobutane are common in bottom sediment of the northern Bering Sea. At eight sites the content of methane rapidly increases downward within the first four meters of sediment. These concentration gradients, and absolute methane concentrations, indicate that the interstitial water of the near-surface sediment at these sites may be gas saturated. These gas-charged sediments may be unstable, creating potential geologic hazards and, in certain areas, causing the formation of seafloor craters.

The isotopic compositions of methane at four of the sites range from -69 to -80°/$_{oo}$ ($\delta^{13}C_{PDB}$). This range of values clearly indicates that the methane derives from microbial processes, possibly within the near-surface Pleistocene peat deposits that are common throughout the northern Bering Sea. At one site in Norton Sound, near-surface sediment is charged with CO_2, accompanied by minor concentrations of hydrocarbons, that is seeping from the seafloor. Methane in this gas mixture has an isotopic composition of -36°/$_{oo}$, a value that suggests derivation from thermal processes at depth in Norton Basin.

The presence of sediment charged with methane or CO_2 cannot in general be predicted from analyses of surface sediment, which usually contains hydrocarbon gases and CO_2 at low concentrations. Sampling beneath a sediment depth of about 0.5 m is generally required to detect high concentrations of gas. Acoustic anomalies detected on high-resolution seismic records indicate the presence of gas-charged sediment, but gas analyses of sediment samples from areas with these anomalies do not always confirm that high concentrations of gas are there. Conversely, high concentrations of methane are sometimes found at sites where no acoustic anomalies are obvious on high-resolution records.

INTRODUCTION

About twenty years ago Emery and Hoggan (1958) described the occurrence of hydrocarbon gases in near-surface marine sediment from Santa Barbara Basin, off southern California. These anoxic sediments contain methane, ethane, propane, butanes, pentanes, and hexanes, with methane being one to almost five orders of magnitude greater in concentration than any of the other hydrocarbons. Geochemical studies that followed have generally focused on methane and the processes that can account for its occurrence and distribution in a variety of aquatic sediments (Reeburgh, 1969; Whelan, 1974; Martens and Berner, 1974; Claypool and Kaplan, 1974; Oremland, 1975; Barnes and Goldberg, 1976; and Kosiur and Warford, 1979). Recently Bernard et al. (1978) described the distribution of methane, ethene, propane, and propene in sediment from shelf and slope sediment in the Gulf of Mexico, and Kvenvolden and Redden (1980) reported on the occurrence of these gases in sediment from the outer shelf, slope and basin of the Bering Sea. The present study examines inner shelf areas of the Bering Sea and considers the hydrocarbon gases methane (C_1), ethane (C_2), ethene ($C_{2:1}$), propane (C_3), propene ($C_{3:1}$), isobutane ($\underline{i}$-C_4), and $\underline{n}$-butane ($\underline{n}$-C_4) in sediment of the inner Bering Shelf in Norton Sound and the adjacent eastern Chirikov Basin (Fig. 1).

Norton Sound is an elongate, east-west trending bay in the western coast of Alaska bounded on the north by the Seward Peninsula, on the east by the Alaskan mainland, on the south by the Yukon Delta, and on the west by the Chirikov Basin. The floor of the sound is very flat, and water depths average about 20 m. To the west into the Chirikov Basin water depths increase to about 50 m, especially in the northern part of the basin at the Bering Strait.

When sea level lowered in late Pleistocene time, the floor of Norton Sound and

eastern Chirikov Basin became exposed (Nelson and Hopkins, 1972). During this time fluvial processes and tundra vegetation characterized the area (Hopkins, 1967), and peaty mud was deposited over much of the region. This mud contains 2 to 8 percent organic carbon. As sea level rose during latest Pleistocene time, marine sedimentation resumed. In Holocene time, fine-grained, sandy silt derived mainly from the Yukon River blanketed the area with a cover up to 10 m thick (McManus et al., 1977; Nelson and Creager, 1977). In contrast to the nonmarine sediment, the organic content of the overlying sediment ranges from 0.5 to 1.0 percent (Nelson, 1977).

METHODS

The analytical procedures for this work have been described previously (Nelson et al., 1978; Kvenvolden et al., 1979a). Vibracores and surface samples were taken during three summer field seasons in 1976, 1977 and 1978. Hydrocarbon gases and carbon dioxide were extracted from sediment recovered from the surface and from various intervals in cores. Sediment samples were extruded into 0.95-L double-friction-seal cans which had two septa-covered holes near the top. Helium-purged distilled water was added to each can until a 100-mL headspace remained. Each can was closed with a lid, and the headspace was purged with helium through the septa. The cans were shaken for ten minutes to release gases into the headspace. Exactly one milliliter of the headspace gas mixture was analyzed by gas chromatography using both flame ionization (for hydrocarbons) and thermal conductivity (for carbon dioxide) detectors. Calculations of gas concentrations were determined by peak height measurements on chromatograms. Partition coefficients were used to correct for the different solubilities of the hydrocarbon gases. Concentrations are reported in nL, μL, or mL per liter of wet sediment.

RESULTS

C_1 is the most abundant hydrocarbon gas found in the first five meters of

sediment in Norton Sound and the eastern Chirikov Basin. Figure 2 shows the geographic distribution of maximum concentrations of C_1. At eight sites this concentration exceeds 1 mL/L, and at five of these sites (8-4, 8-8, 8-15, 8-21 and 8-22) concentrations exceed 10 mL/L. At the other stations the maximum amount of C_1 measured was less than 100 µL/L with two exceptions at 7-33 and 8-6 where it was about 200 µL/L at each site. The amount of C_1 found depends to some extent on the depth of core, for concentrations of C_1 generally increase with depth. Thus, surface samples and short cores usually have lower amounts of C_1 than do samples taken from greater depths. The vertical distribution of C_1 at the eight sites mentioned above is shown in Figure 3. For these sites the concentration of C_1 increases by 4 or 5 orders of magnitude within the top four or five meters of sediment. Also shown is the distribution of methane at Sites 7-17 and 8-3. The data for these sites are combined because the sites are at essentially the same location sampled during two different field seasons. Here the C_1 concentrations, especially in deeper samples, are much lower than at the eight sites. The major gas at 7-17/8-3 is not C_1 but CO_2.

The second most abundant hydrocarbon gas in this area is C_2; C_3 concentrations are usually slightly lower and generally parallel C_2 concentration profiles with depth. The geographic distribution of $C_2 + C_3$ is shown in Figure 4. The maximum concentrations of these two hydrocarbons are usually less than 1 µL/L. At two sites, 8-4 and 8-17, maximum $C_2 + C_3$ concentrations are slightly higher (1.2 and 1.1 µL/L, respectively), but at Site 7-17/8-3, $C_2 + C_3$ maximum concentration is almost 8 µL/L. At the eight sites where C_1 show 4-5 orders of magnitude increase in concentrations with depth, $C_2 + C_3$ increases by about two orders, but the profiles of concentration are more variable (Fig. 5) than the C_1 concentration profile (Fig. 3). The concentrations of $C_2 + C_3$ in samples from 7-17/8-3 are much higher than in all other samples.

Both $C_{2:1}$ and $C_{3:1}$ are present in all samples analyzed. Concentrations are variable, but as a general rule $C_{2:1}$ exceeds C_2 in surface samples and with increasing depth the reverse is observed. At Site 7-17/8-3, C_2 is much more abundant than $C_{2:1}$, with the $C_2/C_{2:1}$ ratio reaching a maximum of 340 at 60 cm depth. A similar relation holds for $C_{3:1}$ and C_3. At the surface $C_{3:1}$ is usually more abundant than C_3, and the reverse is true for deeper samples. At 7-17/8-3, C_3 is always more abundant than $C_{3:1}$ being larger by a factor of 47 at 200 cm depth.

The concentrations of i-C_4 and n-C_4 are lower in concentration than the lighter hydrocarbon gases and in many cases reach the limit of detection of the method, about 2 nL/L. In general the concentrations of i-C_4 + n-C_4 are less than 100 nL/L, and the distribution with depth is variable. In samples from 7-17/8-3, concentrations of i-C_4 + n-C_4 reach a maximum of 14 µL/L at a depth of 200 cm.

Hydrocarbons from C_5 to C_7 are measured in a single backflush peak from chromatography and are designated C_{5+}. C_{5+} hydrocarbons commonly occur in low concentrations in surface samples from this area and in core samples from 7-17/8-3.

BIOGENIC METHANE

The occurrence in anoxic sediment of high concentrations of C_1 resulting from microbial decomposition of organic matter is well established (Emery and Hoggan, 1958; Barnes and Goldberg, 1976; Reeburgh and Heggie, 1977; and Kosiur and Warford, 1979). C_1 is both produced and consumed by microorganisms, and models for these processes have been devised (Claypool and Kaplan, 1974; Martens and Berner, 1974; Barnes and Goldberg, 1976; Kosiur and Warford, 1979). In less reducing sediments of open marine environments, C_1 is also present but at concentrations as much as five orders of magnitude less than those observed in

anoxic marine sediments (Bernard et al., 1978; Kvenvolden and Redden, 1980). Although there is much less C_1 in sediments of open marine environments, the processes that generate gas are probably similar to those in anoxic sediments, but much slower.

At eight sites in Norton Sound and the eastern Chirikov Basin abundances of C_1 increase by four or five orders of magnitude within the first five meters of sediment, reaching concentrations near or exceeding saturation of the interstitial water. These shallow sediments are likely anoxic, and the C_1 probably is being generated by the decomposition of peaty mud that contains 2 to 8 percent organic carbon, and is buried under marine sediment of lower carbon content (0.5 to 1.0 percent). This sediment cover is thickest near the front of the Yukon Delta and thins to the north (McManus et al., 1977; Nelson and Creager, 1977; Nelson, 1977). The depth of burial of the peaty mud may account for the groupings of the C_1 concentration profiles shown in Figure 3. Seven of the sites (6-121, 6-125, 6-131, 8-4, 8-8, 8-15, and 8-21) have profiles that group together. These seven sites are located in the eastern and northern parts of Norton Sound and in the Chirikov Basin near Port Clarence (Fig. 2). In these areas, peaty sediment is buried under about 2 meters of sandy silt. The seven profiles show maximum concentrations below about 1.5 meters. Therefore, if peaty mud is the source of the methane, the depth of its burial accounts for the depth at which high C_1 concentrations are found. In contrast, one C_1 concentration profile (8-22) reaches maximum values below 3 meters. This site was located northwest of the Yukon Delta in the southern part of Norton Sound where the sediment cover is thicker and the peaty mud is more deeply buried. Thus there is a correlation between the depth of buried organic matter and the depth at which C_1 concentrations reach high values. At Site 7-17/8-3, C_1 concentrations follow a different trend to be discussed below.

That the high concentrations of C_1 at eight sites result from microbiological

processes is supported by both chemical and isotopic data. Higher molecular weight hydrocarbons accompany C_1, and the ratio $C_1/(C_2 + C_3)$ can be used as a guide to interpret mode of formation. Likewise, the carbon isotopic composition of C_1 can be used to interpret process of formation (Bernard et al., 1976, 1977). Microbial degradation of organic matter produces hydrocarbon gases with $C_1/(C_2 + C_3)$ ratios greater than 1000, and with $\delta^{13}C_{1PDB}$ lighter than $-60°/_{oo}$. Table 1 shows these parameters for samples from the eight sites. Clearly, based on the criteria stated above, the C_1 at the eight sites was derived from microbiological processes, and the buried peaty mud, in which the organic carbon has as isotopic composition of $-28°/_{oo}$ (Kvenvolden et al., 1979 a,b) is the likely source.

Other sites may exist in Norton Sound and eastern Chirikov Basin where C_1 concentrations exceed 1 mL/L. Finding these locations will require sampling below about one meter of sediment (three meters or more off the Yukon Delta), because the occurrence of high amounts of C_1 at shallow depths is not manifest at the surface. The surface layer of sandy silt either seals the C_1 preventing its migration to the surface or the rate of consumption or diffusion of C_1 in the upper meter is very rapid, leading to low concentrations of C_1 at the surface. At two sites, 8-6 and 7-33 (Fig. 2), maximum concentrations of C_1 of 224 and 196 µL/L, respectively, may hint that much higher concentrations are present at greater depths. At Site 7-33, the deepest sample (Fig. 1) came from 70 cm. If this sample, containing 196 µL/L, were plotted on Figure 3 it would fall within the envelope of C_1 -concentration profiles of cores in which C_1 exceeds 1 mL/L at depth. The case for Site 8-6 is not so clear. The sample containing 224 µL/L comes from a depth of 220 cm (Fig. 1). If plotted on Figure 3, this value would fall below the envelope of C_1 -concentration profiles. At Site 8-6, peaty mud may be more deeply buried than at other sites in northern Norton Sound. Only deeper sampling can directly verify the presence of higher

Table 1.

$C_1/(C_2+C_3)$ ratios and $\delta^{13}C_1$ values for samples containing C_1 concentrations in excess of 1 mL/L

Site	Maximum $C_1/(C_2+C_3)$	$\delta^{13}C_1$* (°/₀₀)
8-4	24000	-80[1]
8-8	71000	nd
8-15	28000	nd
8-21	440000	nd
8-22	88000	nd
6-121	6500	-72[2]
6-125	28000	-69[2]
6-131	5400	-75[2]

*relative to the PDB standard

[1]Kvenvolden et al. (1979a,b)

[2]Nelson et al. (1979)

amounts of C_1. At other sites in Norton Sound and eastern Chirikov Basin, C_1 concentrations are below 100 µL/L and at many sites below 10 µL/L (Fig. 2).

POSSIBLE BIOLOGIC ORIGIN OF OTHER HYDROCARBONS

Besides C_1, other hydrocarbon gases are present in these sediments, but quantitatively, they have much less significance than C_1. The maximum concentrations of $C_2 + C_3$ are in the same range as the minimum concentrations of C_1. At sites where C_1 increases rapidly with depth (Fig. 3), $C_2 + C_3$ also generally increases (Fig. 5) but much more slowly than C_1. Concentrations of i-C_4 and n-C_4 are even lower than concentrations of $C_2 + C_3$, and the i-C_4 + n-C_4 concentrations are erratic with depth. As a generalization, however, the abundances of the higher hydrocarbons, C_2, C_3 and C_4, are greater in samples where concentrations of C_1 are larger. Therefore, the processes that produce C_1 may also be responsible in part for the generation of the higher hydrocarbons. Microbiological production and consumption provides a reasonable mechanism to account for C_1 at the eight sites where C_1 concentrations increase beyond 1 mL/L. Therefore, microbial processes may also explain the occurrence of the higher molecular weight hydrocarbons, although evidence for this process remains circumstantial. Laboratory experiments have demonstrated the microbial formation of C_2 and C_3 (Davis and Squires, 1954). Thus, there is support for the suggestion that the C_2 and the C_3 hydrocarbons at these sites can come from microbial processes, but there is no precedent in the literature on microbiology for the production of C_4 hydrocarbons.

The presence and distribution of $C_{2:1}$ is probably controlled by biological processes, but these processes likely differ from those which account for the very high C_1 concentrations. These unsaturated hydrocarbons have been formed by microbial action in the laboratory (Davis and Squires, 1954), and $C_{2:1}$ is produced in soils by bacteria (Primrose and Dilworth, 1976). In the sediment the process seems to take place uniformly, because there is no obvious concentration gradient with depth. In surface samples concentrations of $C_{2:1}$ and $C_{3:1}$ are

larger respectively than concentrations of C_2 and C_3. With depth, concentrations of C_2 and C_3 increase slightly so that below the surface ratios of $C_2/C_{2:1}$ and $C_3/C_{3:1}$ are usually equal to or greater than one.

THERMOGENIC HYDROCARBONS

The above discussion focused mainly on sites where C_1 concentration increases rapidly with depth, and consideration has been given to the heavier hydrocarbons associated with this C_1. At one site, 7-17/8-3, however, C_1 concentrations are not unusually high, less than 100 µL/L (Fig. 3), but concentrations of $C_2 + C_3$ (Fig. 5) and $i\text{-}C_4 + \underline{n}\text{-}C_4$ are unusually large relative to concentrations seen elsewhere in the sediments of this area, or for that matter, anywhere else in marine sediments off Alaska.

Site 7-17/8-3 has been studied in great detail since anomalous hydrocarbon concentrations were first discovered in the water column at the site (Cline and Holmes, 1977). Nelson et al. (1978) showed that the sediments here also contain anomalous hydrocarbon concentrations. Kvenvolden et al. (1979a, b) confirmed the hydrocarbon chemistry and discovered that the major gas component within the sediment and escaping into the water column is CO_2. The $C_1/(C_2+C_3)$ ratios in sediment at this site are less than 10 and the $\delta^{13}C_1$ is $-36°/_{oo}$. These numbers differ greatly from those discussed earlier where microbiological processes were inferred.

The hydrocarbons at Site 7-17/8-3 are likely derived from thermochemical processes, judging from the molecular distribution of C_1, C_2, and C_3 and the isotopic composition of C_1. In addition, anomalously high concentrations of $i\text{-}C_4$, $\underline{n}\text{-}C_4$ and C_{5+} (gasoline-range hydrocarbons) support the mechanism of thermochemical processes (Kvenvolden and Claypool, unpublished). Heat for this process must be available at depth in Norton Basin. The hydrocarbons resulting from the thermal decomposition of organic matter within the basin must migrate along with CO_2 up fault zones to the surface and escape as a seep. Although the hydrocarbon

chemistry indicates that the hydrocarbons at Site 7-17/8-3 likely migrate from depth, the concentration profiles (Figs. 3 and 5) indicate that special conditions of migration must exist. The fact that hydrocarbons are leaking into the water column suggests that surface sediments should contain large amounts of these hydrocarbons. On the contrary, surface samples at this site contain very low concentrations of hydrocarbons. In fact, surface samples (0-10 cm) at this site show no evidence of the high concentrations of hydrocarbons deeper in the sediment. The gradients of C_1 (Fig. 3), $C_2 + C_3$ (Fig. 5) and $i\text{-}C_4 + \underline{n}\text{-}C_4$ decrease rapidly toward the sediment surface. This rapid decrease and lack of significant quantities of hydrocarbons at the sediment surface can be explained by rapid diffusion of hydrocarbons into the water column from the first few centimeters of sediment or the presence of discrete gas vents that pipe the hydrocarbons through the sediment leaving few hydrocarbons remaining in the sediment. The second explanation is more reasonable, because active gas vents were seen by television in 1978 (Kvenvolden et al., 1979a). The concentration profiles (Figs. 3 and 5) at Site 7-17/8-3 reach a maximum value at about 1 to 2 meters depth and then decrease. This profile suggests that migration from greater depths does not involve diffusion of hydrocarbons within the underlying sediment but rather that the hydrocarbons are following distinct conduits such as faults. Near the surface the hydrocarbons are dispersed into the sediment where they eventually vent along with CO_2 into the water. That the hydrocarbons from this seep are present in the water column has been documented by Cline and Holmes (1977). The waters of Norton Sound and the eastern Chirikov Basin also contain a regional distribution of hydrocarbon gases (Cline et al., 1978) whose sources, in part, may be the underlying surface and near-surface sediment.

GEOPHYSICAL EVIDENCE

The presence of gas in near-surface sediments can cause acoustic anomalies

on high-resolution geophysical records where the gas is no longer in solution in the interstitial water but takes the form of bubbles. Schubel (1974), for example, demonstrated how high concentrations of gas affect acoustic properties of sediments. At the eight sites where C_1 concentrations exceeded 1 mL/L and may have reached and exceeded interstitial water solubility, bubble-phase C_1 may be present. Acoustic anomalies would be expected on high-resolution records from these sites if free gas is indeed present.

Geophysical transects, utilizing 800-J boomer, 3.5 kHz subbottom profiler and 120 kJ sparker systems, indicate that near-surface acoustic anomalies are widespread i Norton Sound. Figure 6 shows those sites, sampled for hydrocarbon gases, at which acoustic anomalies are seen on geophysical records. At three sites (6-125, 8-4, and 8-21), acoustic anomalies correspond to samples having high concentrations of C_1. The acoustic anomaly and associated C_1 at 8-4 were discussed in detail by Kvenvolden et al. (1979a,b). The characteristics of the acoustic anomaly at 8-21 suggest that the cause may be controlled more by the presence of glacial till deposits than by gas. At Sites 7-17/8-3, geophysical records show both near-surface and deeper acoustic anomalies. There the sediment is charged with CO_2 rather than C_1, and the CO_2 is escaping from the seafloor as a submarine seep, observed acoustically and by television (Kvenvolden et al., 1979a). At five sites (6-121, 6-131, 8-8, 8-15, and 8-22) on Figure 6, where high concentrations of C_1 were measured, no acoustic anomalies were detected. At sites 6-121 and 6-131 no geophysical records were obtained; therefore, it is uncertain whether or not acoustic anomalies are present at these sites. At Sites 8-8, 8-15, and 8-22, high-resolution geophysical records show no evidence of acoustic anomalies although the geochemical measurements indicate high concentrations of C_1 (Figs. 2 and 4). Apparently the gas concentrations at these sites were not in the proper range to produce anomalies on the records of the geophysical systems employed. On the other hand, acoustic anomalies were observed on

records at Sites 8-1, 8-9, and 8-10, but maximum C_1 abundances in cores at these sites were only 6, 4, and 15μL/L, respectively. Concentrations this low are not expected to produce acoustic anomalies. In addition, acoustic anomalies were found in geophysical records at Sites 6-168, 7-22, and 7-25, but sampling at these sites was not deep enough (Fig. 1) to test the presence of high C_1 or CO_2 concentrations at depth.

High concentrations of C_1 in near-surface sediment may cause instability and may lead to crater formation whenever the gas vents abruptly into the water column. Nelson et al. (1978) discussed some preliminary engineering information related to the stability of gas-charged sediment in Norton Sound, and Nelson et al. (1979) proposed that the craters found in central Norton Sound may result from the rapid escape of gas from gas-charged sediments.

SUMMARY

Hydrocarbon gases, methane, ethane, ethene, propane, propene, isobutane, and n-butane are common in surface and near-surface sediment of Norton Sound and eastern Chirikov Basin. From a quantitative standpoint methane is the most important hydrocarbon gas. At eight sites in this area methane abundances increase with depth in the sediment by four or five orders of magnitude, reaching concentrations near or exceeding saturation of the interstitial water. The highest value measured is about 55 mL/L. This methane is probably being generated by microbial decomposition of peat that is buried with mud under a cover of fine-grained, sandy silt derived from the Yukon Delta. Maximum ratios of methane to ethane plus propane at the eight sites are large, ranging from about 5×10^3 to 440×10^3. Carbon isotopic compositions range from -69 to -80°/₀₀ (relative to the PDB standard). These molecular and isotopic compositions strongly suggest that microbiological processes are involved in the production of at least methane. Higher molecular weight hydrocarbons are present in much lower concen-

trations than methane, but, as a general rule over the area, the trends in concentrations of the hydrocarbons, at least through propane, are roughly the same. Therefore, microbiological processes may also be responsible for the hydrocarbon gases heavier than methane.

At one site in Norton Sound the concentrations of all hydrocarbon gases are anomalous. For example, methane is anomalously low in concentration relative to the methane at the eight sites mentioned above. On the other hand, ethane, propane, and the butanes are all anomalously high in concentration. The ratios of methane to ethane plus propane are less than 10 and the isotopic compositon of methane is about $-36^{\circ}/_{\circ\circ}$. The magnitude of these parameters sharply contrasts with the values obtained elsewhere in the area and indicates that thermochemical rather than biochemical processes are at work. The maximum concentration of hydrocarbons from samples at this site is about 100 µL/L.
The major component is carbon dioxide. The carbon dioxide and hydrocarbons are actively seeping from the sediment into the water column.

A number of geological consequences result from the presence of gases in near-surface sediment of this area. Where gas concentrations approach and exceed their solubilities in the interstitial water, free gas in the form of bubbles occurs. This gas modifies the acoustic properties of the sediments, and near-surface acoustic anomalies are detected on high-resolution geophysical records. Acoustic anomalies were observed at three of the eight sites where methane is very abundant and also at the site where carbon dioxide was observed along with hydrocarbons. On the other hand, acoustic anomalies were also seen in geophysical records from three sites where maximum gas concentrations in core samples were too low to cause anomalies. At three other sites there was no geophysical evidence for acoustic anomalies although geochemical measurements indicated high methane concentrations in the sediment. The presence of high gas concentrations in near-surface sediments can lead to sediment instability and the

possibility of seafloor cratering. Finally, the thermochemical hydrocarbons, observed at one site, may have been produced deep within Norton Basin and be migrating to the surface. These hydrocarbons have petroleum-like characteristics and may be indicative of petroleum generation and accumulation at depth.

REFERENCES CITED

Barnes, R.O. and Goldberg, E.D. (1976) Methane production and consumption in anoxic marine sediments: Geology 4, 297-300.

Bernard, B.B., Brooks, J.M., and Sackett, W.M. (1976) Natural gas seepage in the Gulf of Mexico. Earth and Planet. Sci. Lett. 31, 48-54.

Bernard, B.B., Brooks, J.M., and Sackett, W.M. (1977) A geochemical model for characterization of hydrocarbon gas sources in marine sediments: Proc. 9th Offshore Tech. Conf., 1, 435-438.

Bernard, B.B., Brooks, J.M., and Sackett, W.M. (1978) Light hydrocarbons in recent Texas continental shelf and slope sediments. Jour. Geophys. Res., 83, 4053-4061.

Claypool, G.E. and Kaplan, I.R. (1974) The origin and distribution of methane in marine sediments. In Natural Gases in Marine Sediments, Kaplan, I.R., ed., Plenum, New York, 99-139.

Cline, J.D., Feely, R.A., and Young, A. (1978) Identification of natural and anthropogenic petroleum sources in the Alaskan shelf areas utilizing low molecular weight hydrocarbons: Environmental Assessment of the Alaskan Continental Shelf, Ann. Report, v. 8, NOAA, BLM, p. 73-198.

Cline, J.D. and Holmes, M.L. (1977) Submarine seepage of natural gas in Norton Sound, Alaska: Science, 198, 1149-1153.

David, J.B. and Squires, R.M. (1954) Detection of microbially produced gaseous hydrocarbons other than methane. Science, 119, 381-382.

Emery, K.O. and Hoggan, D. (1958) Gases in marine sediments. Am. Assoc. Petrol. Geol. Bull., 42, 2174-2188.

Hopkins, D.M. (1967) Quaternary marine transgression in Alaska. In The Bering Land Bridge, Hopkins, D.M., ed., Stanford University Press, Stanford, California, 47-90.

Kosiur, D.R., and Warford, A.L. (1979) Methane production and oxidation in Santa Barbara Basin Sediments: Estuarine and Coastal Marine Science, 8, 379-385.

Kvenvolden, K.A., Nelson, C.H., Thor, D.R., Larsen, M.C., Redden, G.D., Rapp, J.B., and DesMarais, D.J. (1979a) Biogenic and thermogenic gas in gas-charged sediment of Norton Sound, Alaska. Proc. 11th Offshore Tech. Conf. 1, 479-486.

Kvenvolden, K.A., Weliky, K., Nelson, C.H., and DesMarais, D.J. (1979b) Submarine seep of carbon dioxide in Norton Sound, Alaska: Science, 205, 1264-1266.

Kvenvolden, K.A. and Claypool, G.E. (1980) Migration of gasoline-range hydrocarbons by solution in carbon dioxide as observed in Norton Basin, Alaska: (unpublished).

Kvenvolden, K.A. and Redden, G.D. (1980) Hydrocarbon gas in sediment from the shelf, slope and basin of the Bering Sea: Geochim. Cosmochim. Acta, (submitted).

Martens, C.S. and Berner, R.A. (1974) Methane production in the interstitial waters of sulfate-depleted marine sediments. Science, 185, 1167-1169.

McManus, D.A., Venkatarathan, K., Hopkins, D.M., and Nelson, C.H. (1977) Distribution of bottom sediments on the continental shelf, northern Bering Sea: U.S. Geol. Survey Prof. Paper 759-C, 31 pp.

Nelson, C.H. (1977) Potential seafloor instability from gas-rich sediments and sediment depression craters. In Environmental Assessment of the Alaskan Continental Shelf, Ann. Rept. Prin. Inv. for 1977, NOAA, Env. Res. Lab, U.S. Dept. of Commerce, Boulder, Colo., 79-92.

Nelson, C.H. and Creager, J.S. (1977) Displacement of Yukon-derived sediment from Bering Sea to Chukchi Sea during Holocene time: Geology, 5, 141-146.

Nelson, C.H. and Hopkins, D.M. (1972) Sedimentary processes and distribution of particulate gold in northern Bering Sea: U.S. Geol. Survey Prof. Paper 689, 27 pp.

Nelson, C.H., Kvenvolden, K.A., and Clukey, E.C. (1978) Thermogenic gases in near-surface sediments of Norton Sound, Alaska. Proc. 10th Offshore Tech. Conf. 4, 2623-2633.

Nelson, C.H., Thor, D.R., Sandstrom, M.W., and Kvenvolden, K.A. (1979) Modern biogenic gas-generated craters (seafloor "pockmarks") on the Bering Shelf. Geol. Soc. Am. Bull. (accepted).

Oremland, R.S. (1975) Methane production in shallow-water, tropical marine sediments. Appl. Microbiol. 30, 602-608.

Primrose, S.B. and Dilworth, M.J. (1976) Ethylene production by bacteria: Jour. General Microbiology, 93, 177-181.

Reeburgh, W.S. (1969) Observations of gases in Chesapeake Bay sediments. Limnol. Oceanog. 14, 368-375.

Reeburgh, W.S. and Heggie, D.T. (1977) Microbial methane consumption reactions and their effect on methane distributions in freshwater and marine environments. Limnology and Oceanography 22, 1-9.

Schubel, J.R. (1974) Gas bubbles and the acoustically impenetratable, or turbid, character of some estuarine sediment. In Natural Gases in Marine Sediments, Kaplan, I.R., ed., Plenum Publ. Corp., New York, 275-298.

Whelan, T. (1974) Methane, carbon dioxide and dissolved sulfide from interstitial water of coastal marsh sediments: Estuarine and Coastal Marine Science 2, 407-415.

FIGURE CAPTIONS

Figure 1. Location of hydrocarbon gas sampling sites in Norton Sound and Chirikov Basin (dots). Sites are designated with the last digit of the year when the site was occupied followed by the station number. In parentheses is the interval in centimeters from which samples were taken. After the colon is the number of samples analyzed for hydrocarbon gases in that interval.

Figure 2. Distribution of maximum concentrations of C_1 in µL/L and mL/L of wet sediment at each site.

Figure 3. Graph of concentrations of C_1 in µL/L and mL/L of wet sediment vs. depth (cm) for sediment samples from cores taken at nine sites in Norton Sound and eastern Chirikov Basin. Site 7-17 and 8-3 are the same location; results are combined into one curve.

Figure 4. Distribution of maximum concentrations of $C_2 + C_3$ in nL/L and µL/L of wet sediment at each site.

Figure 5. Graph of concentrations of $C_2 + C_3$ in nL/L and µL/L of wet sediment vs depth (cm) for sediment samples from cores taken at nine sites in Norton Sound and eastern Chirikov Basin.

Figure 6. Distribution of acoustic anomalies and sites with high concentrations of gas.

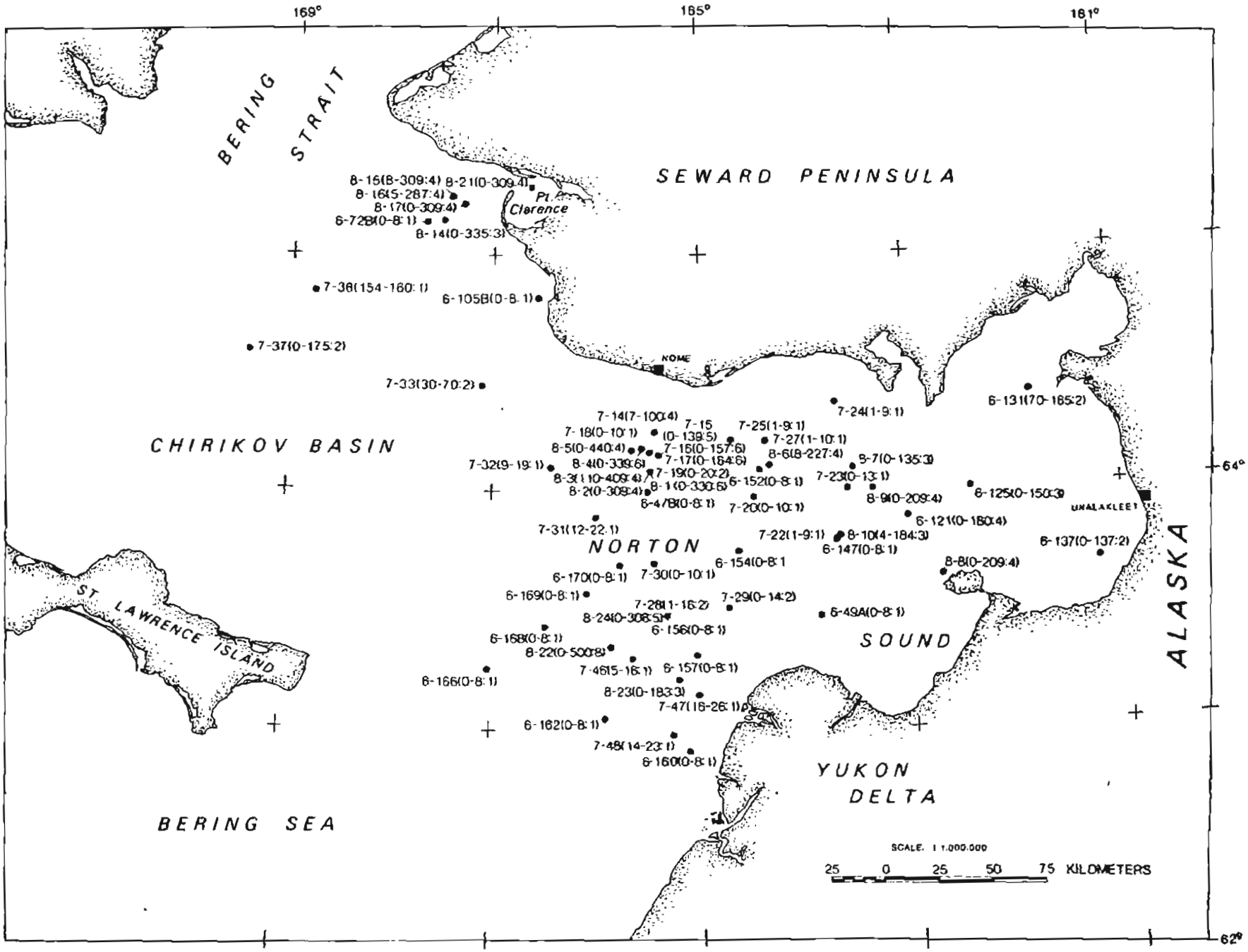
169°
165°
161°
64°
62°
BERING STRAIT
SEWARD PENINSULA
Pt. Clarence
NOME
CHIRIKOV BASIN
NORTON SOUND
ST LAWRENCE ISLAND
BERING SEA
YUKON DELTA
ALASKA
UNALAKLEET
8-16(8-309:4) 8-21(0-309:4)
8-16(5-287:4)
8-17(0-309:4)
6-128(0-8:1)
8-14(0-335:3)
7-36(154-160:1)
6-105B(0-8:1)
7-37(0-175:2)
7-33(30-70:2)
7-24(1-9:1)
6-131(70-185:2)
7-14(7-100:4)
7-15
7-25(1-9:1)
7-18(0-10:1)
(0-139:5)
7-27(1-10:1)
8-5(0-440:4)
7-16(0-157:6)
8-6(8-227:4)
7-32(9-19:1)
8-4(0-339:6)
7-17(0-184:6)
8-7(0-135:3)
8-3(110-409:4)
7-19(0-20:2)
7-23(0-13:1)
8-2(0-309:4)
8-1(0-330:6)
6-152(0-8:1)
8-9(0-209:4)
6-125(0-150:3)
8-4/8(0-8:1)
7-20(0-10:1)
6-121(0-180:4)
7-31(12-22:1)
7-22(1-9:1)
8-10(4-184:3)
6-137(0-137:2)
6-147(0-8:1)
6-154(0-8:1
8-8(0-209:4)
6-170(0-8:1)
7-30(0-10:1)
6-169(0-8:1)
7-28(1-16:2)
7-29(0-14:2)
8-24(0-308:5)
6-49A(0-8:1)
6-156(0-8:1)
6-168(0-8:1)
8-22(0-500:8)
7-46(5-16:1)
6-157(0-8:1)
6-166(0-8:1)
8-23(0-183:3)
7-47(16-26:1)
6-162(0-8:1)
7-48(14-23:1)
6-160(0-8:1)
SCALE 1:1,000,000
25 0 25 50 75 KILOMETERS

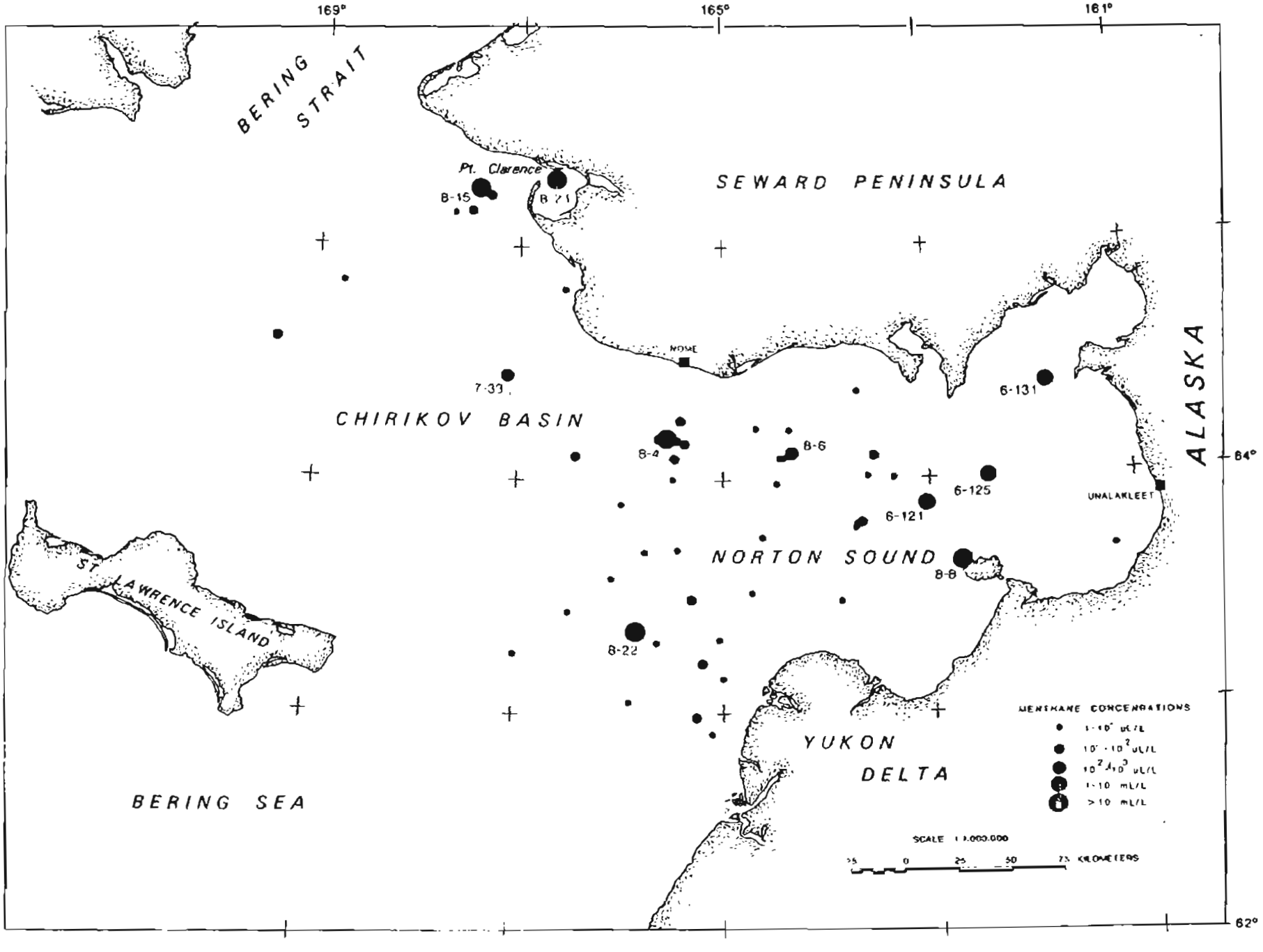
169°
165°
161°
BERING STRAIT
Pt. Clarence
B-15
B-21
SEWARD PENINSULA
NOME
7-33
CHIRIKOV BASIN
B-4
B-6
6-131
ALASKA
64°
6-125
6-121
UNALAKLEET
NORTON SOUND
B-8
ST LAWRENCE ISLAND
B-22
YUKON
DELTA
BERING SEA
METHANE CONCENTRATIONS
1-10 µL/L
10-10² µL/L
10²-10³ µL/L
1-10 mL/L
>10 mL/L
SCALE 1:3,000,000
25 0 25 50 75 KILOMETERS
62°

CONCENTRATIONS OF C_1

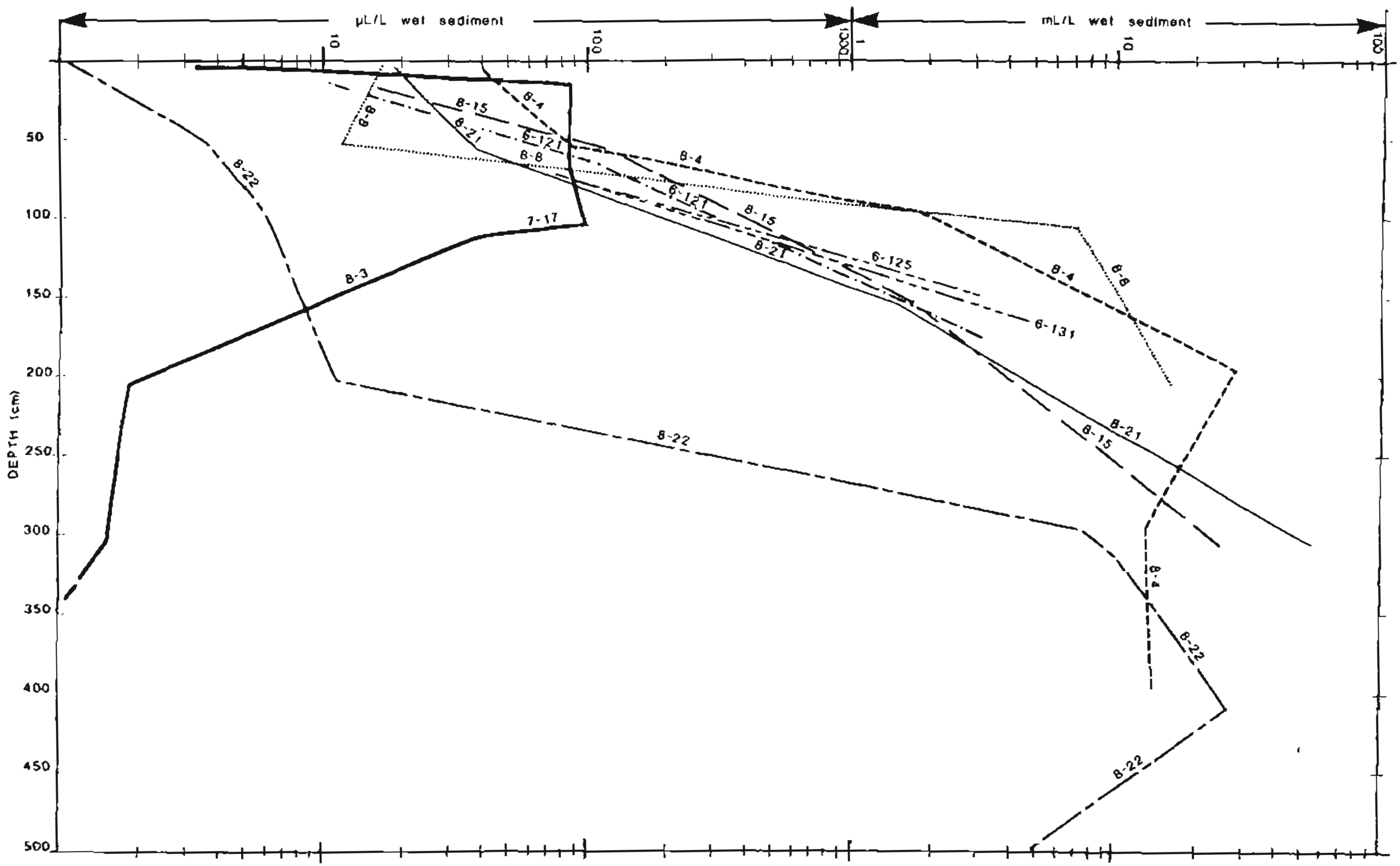

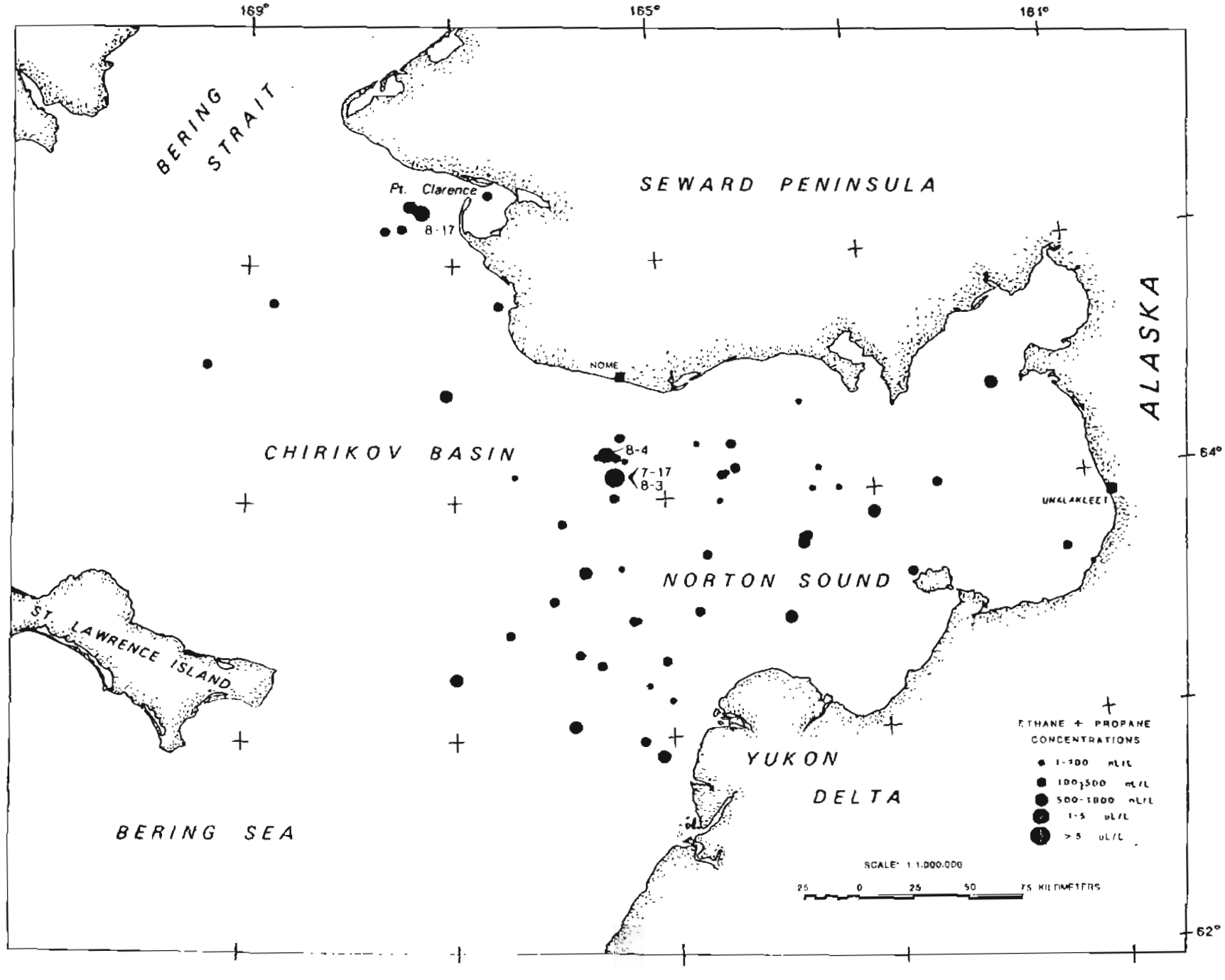
169°
165°
161°
64°
62°
BERING STRAIT
SEWARD PENINSULA
ALASKA
Pt. Clarence
8-17
NOME
CHIRIKOV BASIN
8-4
7-17
8-3
UNALAKLEET
NORTON SOUND
ST. LAWRENCE ISLAND
YUKON
DELTA
BERING SEA
ETHANE + PROPANE
CONCENTRATIONS
1-100 nL/L
100-500 nL/L
500-1000 nL/L
1-5 uL/L
>5 uL/L
SCALE: 1:1,000,000
25 0 25 50 75 KILOMETERS

CONCENTRATIONS OF $C_2 + C_3$

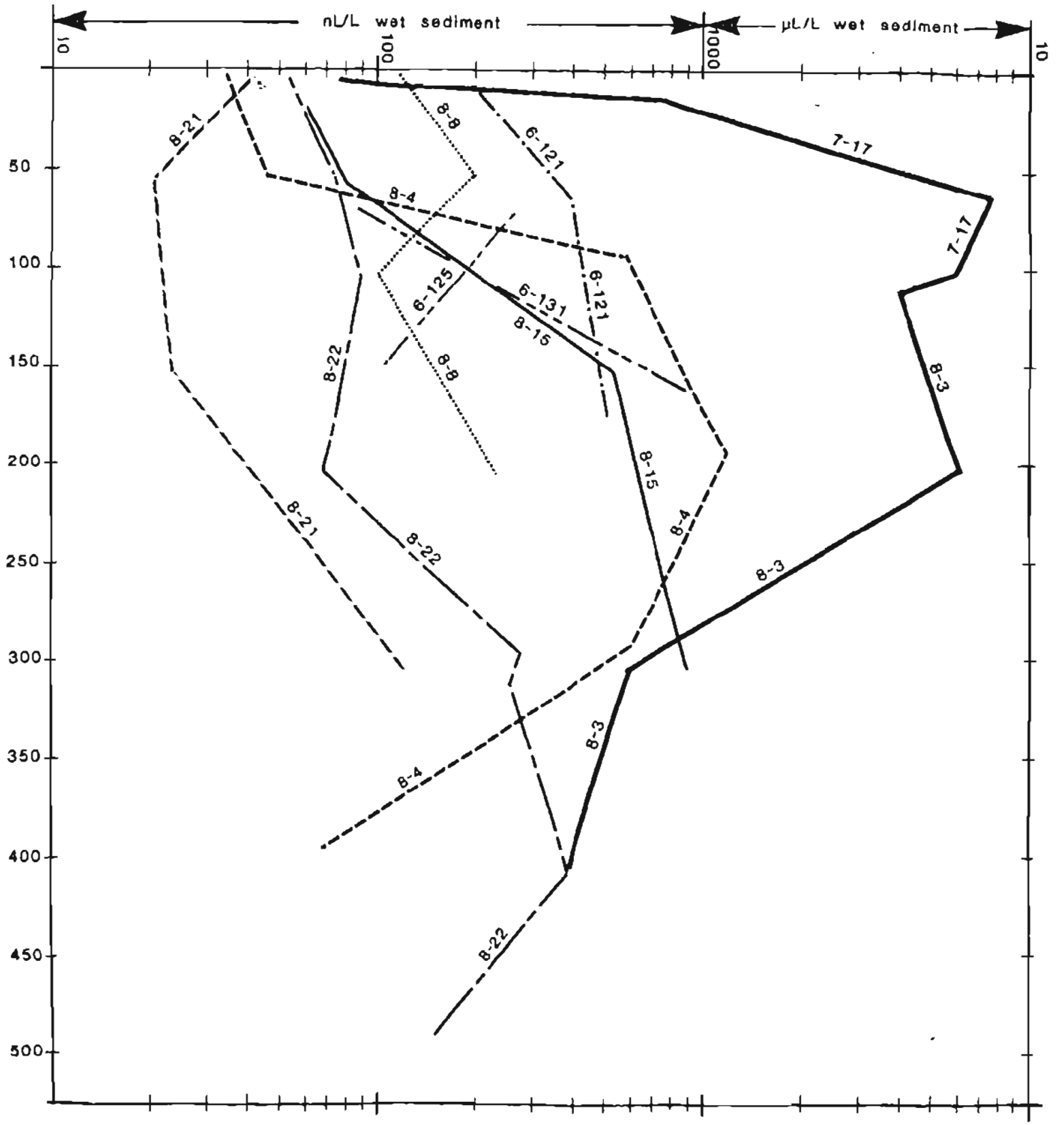

GPO 689-143/11

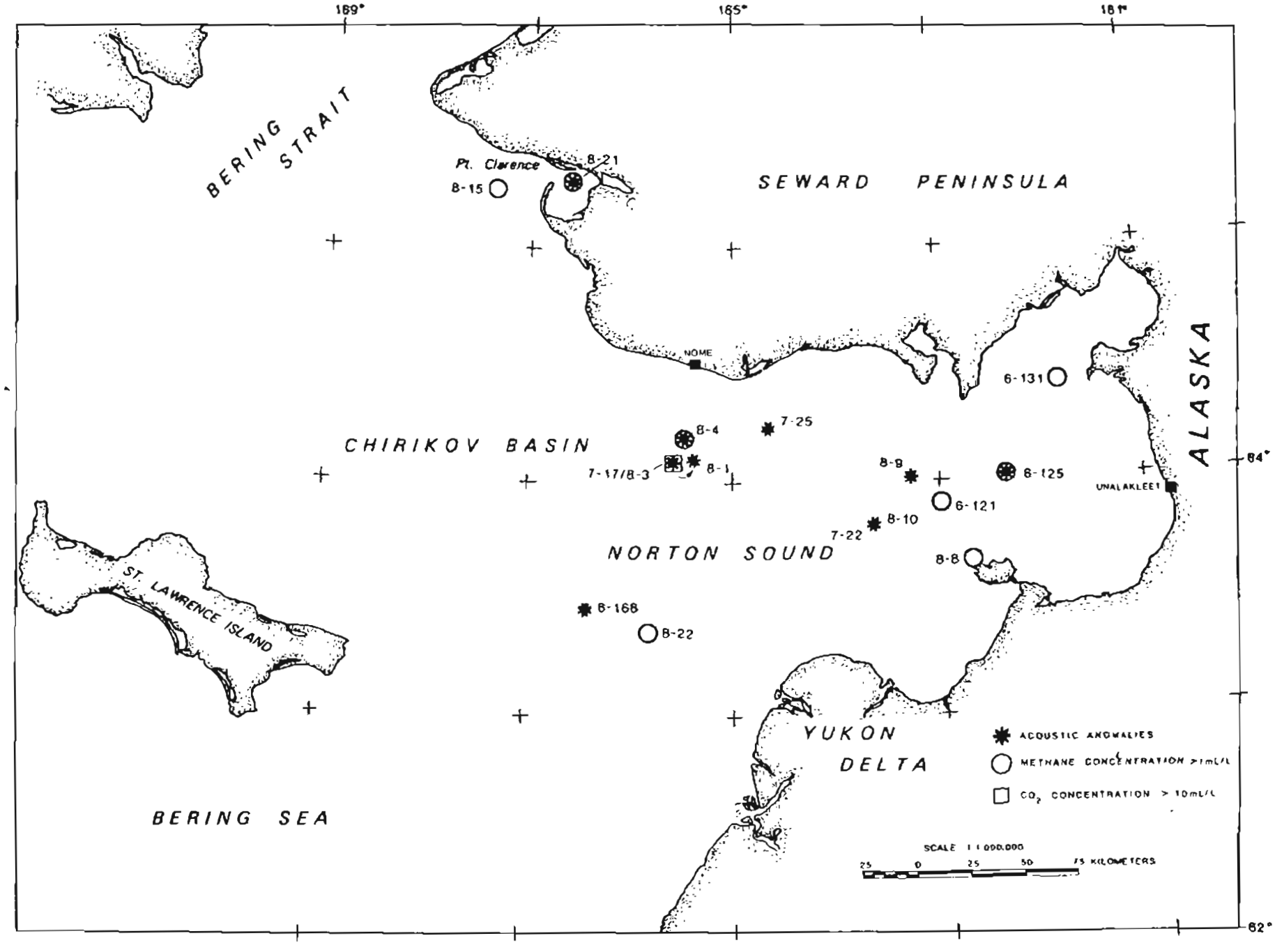
169°
165°
161°
64°
62°
BERING STRAIT
Pt. Clarence
8-21
8-15
SEWARD PENINSULA
NOME
6-131
ALASKA
8-4
7-25
CHIRIKOV BASIN
7-17/8-3
8-1
8-9
6-125
UNALAKLEET
6-121
8-10
7-22
NORTON SOUND
8-8
ST. LAWRENCE ISLAND
6-168
8-22
YUKON DELTA
BERING SEA
ACOUSTIC ANOMALIES
METHANE CONCENTRATION >1mL/L
CO_2 CONCENTRATION > 10mL/L
SCALE 1:1,000,000
25 0 25 50 75 KILOMETERS

Introduction to papers from: Holocene Marine Sedimentation in the North Sea Basin

The papers that follow cover a decade of interdisciplinary research on Holocene sedimentation in the northern Bering Sea. The U.S. Geological Survey environmental assessment studies in this region result in interfacing studies of a number of marine geologic, physical oceanographic, geochemical, and geotechnical specialists. This epicontinental shelf research focuses on a poorly known, but significantly large type of environment of northern North America. Although nearly half of the continental shelf area of the United States is made up of epicontinental shelves that surround Alaska, most studies of Holocene shelf sedimentation in north America have focused either on the narrow, tectonically active Pacific coast shelves or the Atlantic continental margin shelves. The general lack of information on modern epicontinental shelves is a severe handicap to understanding the extensive ancient rock record of these types of environments, for example, the Mesozoic of the interior of western North America.

We feel it is most useful for modern and ancient comparative studies to incorporate our papers into this volume containing the significant body of European work on the North Sea. The environment of the northern Bering Sea is similar in many ways to that of the North Sea. Both shelf areas are dominated by strong currents constricted by land masses. As a result, large sand ridges and sand-wave fields are common, and significant reworking, resuspension, and relocation of Holocene sediment masses is apparent on both shelves. Storm waves are common to all shelf areas, but large storm surges and strong storm-driven currents are more restricted, occurring mostly in broad shallow embayments such as those found in the North and Bering Seas. Wide variation in tidal range and sediment input in different parts of the basins is also

characteristic of both regions and results in similar Holocene sediment types and distribution patterns in the two areas.

The first paper on the late Pleistocene to Holocene sedimentation points out that two very different sequences of transgressive deposits can develop within the same shelf region. In Chirikov Basin, Pleistocene peaty mud is covered by typical, but extremely thin, basal and inner shelf transgressive sand units. The strong currents and circulation of water masses, however, prevent deposition of a modern mud blanket to complete a normal transgressive sequence. Instead, currents rework the surface sediment into a distribution that conforms to the strong geostrophic flow patterns rather than a wave-generated gradation from coarse-grained deposits in shoreline regions to finer-grained deposits in offshore regions.

The seafloor of Norton Sound is overlain by Pleistocene peaty mud but, in contrast to Chirikov Basin, it lacks transgressive sand layers. Here marine transgressive sequences consist of mud interbedded with thick storm sand layers which grade upsection to thinner storm sands and then to bioturbated mud facies. Progradation of the modern Yukon prodelta reverses this sequence in southern Norton Sound so that storm sand layers are found in the uppermost Holocene sediment. Patterns of late Pleistocene-Holocene sedimentation in both Chirikov Basin and Norton Sound are different from those in southern Bering shelf where a classic wave-generated seaward-fining is found in Holocene deposits. Thus, when interpretations are made of ancient epicontinental shelf sequences, deposits in current-dominated settings like the North Sea and the northern Bering Sea must be considereded because gradations in sediment texture and thickness may have little relation to shoreline location or depth-related variations in wave energy.

The second paper analyzing microfauna in shelf deposits of the northern

Bering Sea shows that biostratigraphical changes and paleoecological patterns may aid in reconstruction of epicontinental shelf environments. In Chirikov Basin there is a vertical change from freshwater to marine facies. In Norton Sound the same change is evident, but nearshore and offshore faunal assemblages can be distinguished in thicker transgressive deposits. In the late Holocene sediment, however, a reversal back to brackish water environments is encountered because of formation of the present active delta lobe in southern Norton Sound.

Sedimentary structures in Norton Sound described in the third paper also mirror the effects of the transgressive and progradational history. Nearshore physical structures occur at the base of the sequence and grade upsection to bioturbated mud; the uppermost sequence, however, changes to well-developed nearshore structures in southern Norton Sound where the delta progrades over the offshore sequences laid down in the earlier Holocene. Because of the delta progradation in southern Norton Sound, well-developed physical structures in surface sediment grade offshore to highly bioturbated deposits as might be expected in onshore to offshore sequences. The high degree of bioturbation nearshore in northern Norton Sound, however, it is unexpected near shorelines and reflects low sedimentation rates caused by resuspension and advection of most Holocene sediment from this region by the Alaska Coastal Water. Because of the large freshwater discharge from the Yukon River into southern Norton Sound, bioturbation there is similar to that found in local coastal embayments and estuaries elsewhere, even though Norton Sound is an open-shelf region. Again, this is an example to be kept in mind when interpreting ancient epicontinental shelf deposits.

The fourth paper, describing the Bering shelf sand body types and their processes of formation, provides new information to trace petroleum reservoirs

in ancient shelf systems. The sand bodies of the Bering shelf, although similar to one another in their linearity, size, and sediment types; can be separated into genetic types based on subtleties of grain size, sedimentary structure, morphology, and orientation. Recognition of leeside sand bodies formed of very fine sand may help to distinguish large sand bodies deposited far offshore and not parallel to shorelines, from the more common and generally coarser-grained, shore-parallel sand bodies of the inner shelf.

Several of the process-oriented papers that follow the first four papers describing sedimentary features show that development of different sand body types is a result of a wide variation in hydrographic setting and sediment input on the Bering shelf. In the modern inner shelf area, out to water depths of 10-15 m, the sea floor is typically affected by wave energy. Along southern Seward Peninsula, however, a complex pattern of bedforms related to wave and unidirectional currents is evident. Interplay of current-formed features with ice scour in this subarctic environment adds to the complexity of bedforms in this region. The result is a mosaic of oscillation and unidirectonal current ripples, ice-gouge features, and a complex pattern of varying sediment types.

The inner shelf off the Yukon delta complex of southern Norton Sound contrasts with that of the rocky headland and coastal plain coast of the Seward Peninsula. It is dominated by deltaic sedimentation and a seasonal set of fluvial, hydrographic, and ice processes. In winter, river discharge is almost totally lacking and extensive shorefast ice develops. The wide apron of shorefast ice results in much further extension of distributary channels offshore from the delta than is the case in temperate or tropical deltas. The sub-ice channels serve as sediment conduits during maximum discharge conditions in late spring and summer. Thus, extremely large

quantities of sediment enter the sound in a very short period of time and accumulate rapidly in southern Norton Sound. Major storms in the fall rework, resuspend, and remove large quantities of sediment from Norton Sound. Occasional extremely large storm-surge events cause progradation of major sand sheets from the delta shoreline out over southern Norton Sound.

Quantitative measurements of significant reworking and resuspension of bottom sediment during storms have been made in northern Norton Sound using GEOPROBE instrumentation. The longterm in situ measurements of currents and suspended sediment made with the GEOPROBE in the benthic boundary-layer provide new information that has broad implications for any epicontinental shelf region. The continuous monitoring of shear velocities proves that storm-related currents are the major process in the constricted shallow waters of epicontinental shelf regions like northern Bering Sea. Measurements also show the importance of continual advective suspended sediment transport over northern Bering shelf and sediment resuspension and transport during spring tidal conditions.

In contrast to the more classic wave and current processes outlined in several papers, new concepts of epicontinental shelf processes are suggested by the geotechnical, geochemical, and geophysical studies. Poorly consolidated mud of restricted quiet-water lagoons and sheltered, but open-shelf embayments, contrasts with other regions of highly overconsolidated sediment; there, fetch of the open sea permits strong cyclic loading on shallow bottom sediment by large open-shelf waves. Biogenic gas trapped beneath Holocene mud of Norton Sound can create poorly consolidated zones and regions of gas-charged sediment traced by acoustic anomalies in geophysical records. New studies also show that cyclic wave loading during major storm surge events may have the potential to liquefy the very fine sand of the Yukon

delta region. Thus, liquefaction may be a very important process in conjunction with strong, storm-generated currents to develop the prograding storm-sand sheets and extensive scour observed on epicontinental shelves like Bering Sea.

Our research on Bering shelf suggests that sedimentary processes on shallow epicontinental shelves include synergistic effects of wind, tidal, and barotrophic-driven currents and also poorly understood effects of instability due to sediment gas-charging and cyclic wave loading. Future interdisciplinary research on epicontinental shelves is required to define the relative importance of these factors in sediment transport.

We hope that this set of papers on the Bering epicontinental shelf will show some similarities and contrasts with the North Sea as well as provoke some new thoughts regarding Holocene sedimentation processes common to all epicontinental shelf settings. Large new studies are being instigated in other epicontinental shelves like the east China Sea and it appears that commonalities of Holocene transgressive sedimentation and modern sedimentary processes are present. Once this modern data base is provided from a wide variety of settings like the east China, Bering and North Seas, new refined interpretations can be applied to similar ancient environments.

Hans Nelson

Late Pleistocene-Holocene Transgressive Sedimentation in Deltaic and Non-Deltaic Areas of the Bering Epicontinental Shelf

by C. Hans Nelson

United States Geological Survey, Menlo Park, California 94025

ABSTRACT

The distribution of late Pleistocene (>10,000 years BP)[1] and Holocene (≤10,000 years BP) surface sediment on the northern Bering Sea floor is patchy and dependent upon locations of seafloor bedrock and pre-late Pleistocene glacial debris, late Holocene river sediment influx, and modern strong bottom currents. Seafloor vibracores and high-resolution profiles record two different sedimentary environments in the northern Bering shelf: late Pleistocene-Holocene shoreline transgression (≤16,000 years BP) in Chirikov Basin, and Holocene deposition from the Yukon River in Norton Sound.

Lag gravels remain exposed on the margins of Chirikov Basin where the transgression of the late Pleistocene-Holocene shoreline reworked pre-Quaternary bedrock and glacial moraines deposited during earlier low sea levels. The shoreline transgression over most of central Chirikov Basin left a cover of inner-shelf fine-sand facies that is underlain in places by a pebbly to medium sand basal transgressive facies, both of which overlie Pleistocene limnic peaty mud of emergent shelf deposition. Water circulation patterns have inhibited deposition of Holocene Yukon River silt over transgressive sand and lag gravels of Chirikov Basin.

About 9,500 BP, rapid marine transgression of Norton Sound began, to deposit a basal nearshore facies of thick storm-sand layers in marine silt overlain by an offshore bioturbated silt, both deposited over the Pleistocene freshwater peaty mud. Progradation of thick storm-sand layers and Holocene brackish-water silt deposits (up to 14 m) in southern Norton Sound is attributed to a shift of the present active Yukon delta lobe into its present position after about 2,500 BP.

Late Pleistocene and Holocene sedimentation on Bering shelf has implications for interpretation of ancient epicontinental shelf deposits. In Norton Sound, early Holocene transgressive sequences of coarser to fine muddy facies up-section are covered by regressive coarser facies in areas of deltaic progradation. In contrast, Chirikov Basin displays extremely thin transgressive deposits (<1 m) that are a complex mosaic of gravel, sand, and mud lenses unrelated to shoreline sources, just as sediment thickness is in parts of Norton Sound. Holocene sediments derived from the Yukon River bypass Chirikov Basin to accumulate hundreds of kilometers away in the Arctic Ocean in deposits averaging 10 m thick; however, thin accumulations (<2 m) occur in northern Norton Sound near the present Yukon Delta. In contrast to the complex transgressive sequences of the northern Bering shelf, the southern Bering shelf exhibits generally classic offshore gradation of coarse- to fine-grained Holocene deposits.

[1]For consistant stratigraphic nomenclature, deposits 10,000 years BP and younger are defined as Holocene in this paper (see Hopkins, 1975).

INTRODUCTION

The Bering epicontinental shelf is much like the North Sea shelf because of its strong currents (Cacchione and Drake, 1979) and numerous insular and peninsular constrictions. In addition, input of the Rhine and Elbe Rivers into the North Sea results in deltaic and non-deltaic areas of Holocene sedimentation (Nio et al., 1979) similar to those caused by discharge of the Yukon River on Bering shelf. On the northern Bering shelf during shoreline transgression of the late Pleistocene to Holocene, different transgressive sedimentary facies developed in the non-deltaic region of Chirikov Basin to the west and the deltaic area of Norton Sound to the east (Fig. 1). Definition of these two types of transgressive sedimentation in the Bering epicontinental shelf region provides important information to compare with similar deposits in other areas, like the North Sea, and to distinguish similar facies in ancient analogs.

The extremely thin transgressive sandy facies of the Chirikov Basin is described in this paper and compared to the thick, muddy sequence of Yukon-derived Holocene deposits in Norton Sound. In these different environments, the general lithology, sedimentary processes, and sedimentary history are outlined throughout the late Pleistocene and Holocene time. The present distribution of transgressive late Pleistocene and Holocene deposits is also explained in terms of modern oceanographic processes. Sediment distribution patterns and processes of northern Bering shelf are then compared to the overall patterns of epicontinental shelf sedimentation in the eastern Bering Sea. In the geologic significance section description of these highly variable sediment facies patterns on Bering shelf is used to provide new insights for the interpretation of similar ancient shelf deposits.

METHODS

The summary of late Pleistocene and Holocene history of sedimentation on the northern Bering shelf spans a decade of marine geologic research by the U.S. Geological Survey in this region. The findings in this paper are based on box cores and vibracoring up to 6 m into the seafloor and on more than 10,000 km of tracklines covered by high-resolution sparker, Uniboom, and 3.5-kHz continuous seismic profiling systems. Nearly 50 vibracores and 250 box cores have been described from lithologic analyses, X-ray radiography and epoxy peels. Samples also have been analyzed for texture, microfauna, and radiocarbon dates (see also McDougall, this volume).

OCEANOGRAPHIC SETTING

The northern Bering Sea is a very shallow epicontinental shelf area (<60 m deep) that can be divided into two provinces, Chirikov Basin and Norton Sound (Fig. 1). The shallow eastern half of the area, the Norton Sound embayment, is generally less than 20 m deep (Fig. 1). The very shallow prograding Yukon Delta wedge in southern Norton Sound is an important morphologic feature of Norton Sound that influences wave and storm-surge processes in this region. The western region, Chirikov Basin, is surrounded by projecting land masses on the northwest and northeast, and the large St. Lawrence island on the south that constrict and reinforce the strong geostrophic current flow (Fig. 1).

The Bering shelf, like that of the North Sea, is dominated by currents. Whereas all the North Sea shelf is strongly tidal, only the north part of Norton Sound is dominated by tidal currents; Chirikov Basin is influenced mainly by the strong northward geostrophic current (Fig. 1) (Cacchione and Drake, 1979). Currents are intensified along the eastern Bering Sea margin wherever land projects westward into them. Even more important is the

increase in geostrophic current speeds, which have been observed to double, during moderate storm events (Cacchione and Drake, 1979; Schumacher and Tripp, 1979). As in the North Sea, storm-surge set-up along the Alaskan coast results in storm-related currents that cause major sedimentation events (Nelson, 1977).

GEOLOGIC BACKGROUND

A number of past eustatic sea-level changes determine distribution of the present Holocene and late Pleistocene shelf deposits. The most important influence, the last late Pleistocene and Holocene transgression, began about 12,000 to 13,000 years ago in straits where the water was deepest (Hopkins, 1973). At first a narrow seaway developed from Anadyr Strait to Bering Strait (Hopkins, 1979) and then from Shpanberg Strait to Bering Strait (Nelson and Creager, 1977). The narrow seaways expanded southeastward to fill out the deeper western area of Chirikov Basin until about 10,000 years ago. During shoreline transgression in Chirikov Basin a number of stillstand features were created. For example, ancient shorelines remain as large submerged sand ridges between King Island and Port Clarence (Figs. 2 and 3, B-B′), (see Nelson et al., this vol.), and recognizable ancient strandlines occur in numerous other locations, particularly off Nome (Nelson and Hopkins, 1972; Hopkins, 1973).

The entire Norton Sound region remained emergent until about 10,000 years ago. Sea-level fluctuations determined elsewhere (Field et al., 1979) and radiocarbon dates in Norton Sound show that from 10,000 to 9,500 years B.P., the shoreline rapidly transgressed eastward over Norton Sound, and buried tundra peat deposits.

The transgressing shoreline planed over a number of previous alluvial, glacial, and bedrock exposures. Bedrock remains exposed on the seafloor in

regions near insular and peninsular granitic stocks and volcanic outcrops, such as near Cape Prince of Wales, King Island, and off northern St. Lawrence Island (Fig. 4) (Nelson and Hopkins, 1972). Another extensive area of sea-floor bedrock occurs north of a major fault scarp (Johnson and Holmes, 1978) along the subsurface channel west of Port Clarence (Fig. 4) to the Cape Prince of Wales shoreline, and is perhaps correlative with Precambrian to Paleozoic limestone of the adjacent shoreline area (Nelson and Hopkins, 1972).

Numerous subsurface alluvial channels covered by the transgressive deposits have been mapped in the Norton Sound region where the most detailed grid of seismic profiles is present (Fig. 4). In Chirikov Basin the limited grid of seismic profiles (Fig. 2) does not permit detailed mapping of the subsurface channels, but major subsurface channels are known to exist west of Port Clarence, extending toward Bering Strait, and in the sea valley extending south from King Island (Hopkins et al., 1976) (Fig. 4).

Early and middle Pleistocene continental glaciation extending off (U.S.S.R.-Chukotka) to central Bering Sea, and local valley glaciation offshore from Seward Peninsula have been determined both by seismic profiling and by sediment sampling (Grim and McManus, 1970; Nelson and Hopkins, 1972; Tagg and Greene, 1973; Hopkins, 1975 and 1979). The glacial moraines extend in the subsurface of the central Chirikov Basin and emerge toward land as gravel ridges (Figs. 4 and 5A). Complete sequences of moraines and outwash were documented in the nearshore areas off Nome from detailed profiling (Tagg and Greene, 1973) and drillholes as deep as 75 m below the seafloor (Nelson and Hopkins, 1972).

The other major geologic event that significantly influenced the distribution of late Pleistocene and Holocene deposits is the change in position of the active Yukon delta lobe on the Bering shelf. About 16,000

years ago, the Yukon River apparently crossed the present Bering shelf in the vicinity of Cape Romanzof and deposited a deltaic sequence south of St. Lawrence Island (Knebel and Creager, 1973a). As sea level rose in the the early Holocene, various active lobes developed far south of Norton Sound in the Black subdelta and Cape Romanzof regions (Fig. 1) (Nelson and Creager, 1977). The present active delta lobe first developed in southern Norton Sound after 2,500 years BP as shown by dating of onshore delta deposits (Dupré, this volume) and of offshore change from marine to brackish-water fauna (see core C in Fig. 3, A-A′) (McDougall, this volume). Since then the Yukon River has prograded significantly into Norton Sound and altered biological activity and attendent bioturbation patterns (Nelson et al., in press; Howard and Nelson, this volume).

LATE PLEISTOCENE TRANSGRESSIVE SEDIMENTATION IN CHIRIKOV BASIN

Transgressive Deposits

The late Pleistocene to Holocene shoreline transgression deposited a thin sequence of transgressive deposits on the margins of Chirikov Basin. On some margins, only a thin gravel lag is found over bedrock outcrops or glacial deposits (Fig. 3, B-B′, core D, and Figs. 4 and 5B). On other margins, the typical sequence is late Pleistocene freshwater peaty silt overlain by transgressive sand (Figs.3, B-B′ and Fig. 5B). The Pleistocene peaty silt occurs near the seafloor in troughs between sand ridges where strong bottom currents have either prevented deposition or have scoured through the transgressive sand into the peaty mud (Fig. 3, B-B′, King Is. shoal to Port Clarence). The presence of very old radiocarbon dates from peaty mud in some trough locations suggests that significant scour has taken place there.

A typical trough sequence is fine sand above medium-grained sand overlying the peaty freshwater silt (Fig. 3, B-B′). An example of a complete

eustatic cycle in northeastern Chirikov Basin is found in Core No. 247, taken between Tin City and York shoal (Figs. 3, B-B′ and Fig. 5B). At the very base, a thin layer of coarse-grained regressive sand containing a fauna typical of cold, brackish water (P. Valentine, U.S. Geological Survey Woods Hole, 1976, written commun.) is overlain by a 20-cm-thick sequence of freshwater mud (McDougall, this volume) cut into by sand-filled burrows of marine clams. Above this is medium sand showing good trough cross-lamination that in turn is overlain by flat-laminated to massive fine sand (Fig. 5B).

The different transgressive gravel and sand facies exhibit an areal pattern related to underlying older deposits. The thin gravel lags are found close to shore over bedrock and parallel to emergent seafloor moraines that project into central Chirikov Basin south from Cape Prince of Wales and north from St. Lawrence Island (Fig. 3, B-B′, Core D and Figs. 4 and 5A). Offshore from the bedrock gravel lag of Seward Peninsula, medium-grained sand fringes the northeastern edge of Chirikov Basin (Fig. 6). The surface of central and southern Chirikov Basin is covered by fine sand that overlies the medium sand or late Pleistocene freshwater muds (Figs. 3, B-B′, and 5B and C).

Transgressive History

The oldest deposits in Chirikov Basin are the gravel lags that occur over bedrock and pre-late Pleistocene glacial deposits (Fig. 6). These lags developed as the late Pleistocene-Holocene transgessive shoreline reworked bedrock or glacial deposits, removed fine-grained sediment and left a gravel lag deposit over their surface (Nelson and Hopkins, 1972). In places, the lags are much better rounded, contain higher percentages of quartz, and exhibit modes of medium- to coarse-grained sand, all of which indicate late Pleistocene-Holocene stillstands of the strand line at these particular depths of 10-12 m, 20-24 m, 30 m, and 38 m (Nelson et al., 1969; Nelson and Hopkins, 1972; Hopkins, 1973).

At locations where topographic elevations of bedrock and glacial moraines were not present, late Pleistocene tundra and freshwater silt with occasional alluvial deposits developed (Figs. 3 and 4). As the shoreline transgressed over the freshwater peaty mud of the once emergent seafloor, a basal coarse- to medium-grained sand, only a few centimeters thick, was deposited and remains uncovered in northern Chirikov Basin (Fig. 6). A fine-grained, inner shelf sand (Nelson et al., 1969) was laid down immediately off the shoreline as it transgressed; this generally overlies the basal coarser sand facies and forms a blanket deposit now covering most of the surface of central and southern Chirikov Basin (Fig. 6). The few vibracores from central Chirikov Basin suggest that this inner-shelf sand facies is no more than a few tens of centimeters thick (Fig. 3, B-B′, cores E and F). The mineralogy and texture of this sand contain no evidence of the modern Yukon River sediment source (McManus et al., 1974). Thus, the Yukon sediment entering this region during the Holocene has bypassed northward to deposit in southern Chukchi Sea (Nelson and Creager, 1977) and no Holocene sediment is found in Chirikov Basin, except for that temporarily ponded in the troughs between sand ridges (Fig. 3, B-B′).

HOLOCENE SEDIMENTATION IN NORTON SOUND

Holocene Deposits

As in much of Chirikov Basin, freshwater late Pleistocene silt and interbedded peat or peaty mud is the oldest stratigraphic unit observed in Norton Sound (Fig. 3, A-A′). Overlying the freshwater peaty mud is marine sandy silt with interbedded very fine sand layers in the southern Norton Sound region and deeper parts of the Holocene section in central Norton Sound. Above this sequence in central Norton Sound and throughout the northern area is bioturbated sandy silt derived from the Yukon River (McManus et al., 1977) (Howard and Nelson, this volume).

From onshore to offshore, the interbedded sand beds become finer grained, thinner, contain a smaller percentage of graded sand layers, and exhibit less complete sequences of vertical sedimentary structures (Nelson, 1977) (Fig. 5E and F). Nearshore, the graded sand layers make up 50-100% of the total sedimentary section; they range from 10 to 20 cm in thickness and have a mean grain size of about 0.250 mm in the coarsest part of the layer (Fig. 5E) (also see Fig. 4G of Nelson et al., this volume). At the outer extremity of the distribution of interbedded sand layers, usually 60 to 75 km from the Yukon Delta shoreline, the graded sands are generally 1-2 cm thick, make up less than 35 percent of the total section, and have mean grain sizes of 0.125 mm or less (Fig. 5F).

The surficial Holocene deposits in Norton Sound vary from fine-grained sand surrounding the delta and trough along northern Norton Sound to very fine sand and coarse silt in central and eastern Norton Sound (Fig. 6) (see Fig. 3 of Howard and Nelson, this volume). Not only is sediment coarser in the northern trough, but the mineralogy also shows a mixed derivation from Seward Peninsula and Yukon River sources (McManus et al., 1974). Bioturbated mud is present in the surface of most of Norton Sound (Fig. 5F), except surrounding the modern Yukon subdelta where fine to very fine sand layers may be present at the surface (Nelson, 1977) (Fig. 5E).

Holocene Transgressive and Deltaic History

In contrast to the thin transgressive sequence of sand deposited in Chirikov Basin, Norton Sound contains a thin to thick blanket of Holocene silt and interbedded sand layers derived from the Yukon River. Thick sections of Holocene sediment have been deposited in southern Norton Sound because of progradation of the Yukon delta; only 2 m or less of bioturbated mud has been deposited in the more distal areas of northern and eastern Norton Sound

(Fig. 4B). The bathymetric trough in northern Norton Sound is an exception that appears to be an area of nondeposition through the Holocene because of tidal current flushing in the trough (Figs. 1 and 6) (Cacchione and Drake, 1979). Coarser texture than Yukon deposits (Fig. 6) and mineralogic origin from Seward Peninsula (Fig. 6) (McManus et al., 1974) suggests that Holocene trangressive sand remains in the tidally scoured trough. Elsewhere, Yukon mud with marine fauna has been deposited directly over late Pleistocene freshwater silt, and basal transgressive sand is not found as it is in Chirikov Basin (Fig. 3, A-A′). Although late Pleistocene alluvial deposits are shown incising the freshwater silt in seismic profiles, these deposits have not been identified in cores. Thick nearshore sand layers at depth (Fig. 3, A-A′, core G), in central Norton Sound, however, suggest that the transgressive shoreline was close to this location early in Holocene Time. As the shoreline transgressed, deposition of the interbedded nearshore sand ceased, resulting in sedimentation of the upper sequence of offshore massive silt without interbedded sand (Fig. 3, A-A′, core G, and Fig. 7).

Just as transgression of the shoreline is evident in the lower Holocene stratigraphy of central Norton Sound, migration of the active Yukon delta lobe from the Cape Romanzof region (Knebel and Creager, 1973a; Dupré, this volume) into southern Norton Sound and progradation of brackish-water delta deposits is evident in the upper Holocene stratigraphy of the Sound. When the delta shifted to its present position after 2500 BP (Fig. 3, A-A′, core C) (Dupfe, this volume), influx of low-salinity water into southern Norton Sound caused a change in fauna (see McDougall, this volume) and fluctuation in the rate of bioturbation, so that well-bioturbated mud was locally overlain by unbioturbated sequences of sand and interbedded mud (Fig. 3, A-A′, core C, and Fig. 5D) (Nelson and Creager, 1977). Progradation of the active delta wedge with

with its unbioturbated sequences of thick sand layers interbedded in silt is shown in all upper Holocene sequences surrounding the delta (Fig. 3, A-A′, cores C, H, I, Figs. 5, D-F, and Fig. 7) (Howard and Nelson, this volume; Nelson et al., in press). The vertically and horizontally graded sand layers in the near-surface sediment off the Yukon Delta appear to be prograding sand sheets deposited by currents (Cacchione and Drake, 1979; Schumacher and Tripp, 1979) associated with large-scale storm surge that occurs in Norton Sound (Nelson, 1977; Nelson and Creager, 1977).

Resuspension and removal of large quantities of Yukon sediment from Norton Sound (Fig. 8) by storm-related currents is another significant factor throughout Holocene depositional history. When the estimated discharge of Yukon sediment for the Holocene is compared with the isopach thickness of Holocene sediment in Norton Sound (Fig. 4B), about half of the estimated sediment introduced into Norton Sound is missing, but is found in a 10-m-thick blanket of Holocene mud in the southern Chukchi Sea (Fig. 9) (Nelson and Creager, 1977). Effects of the extensive storm resuspension of sediment are shown by the old radiocarbon dates yielded by modern surface mud (Figs. 5D and 3, A-A′, core I) and the pebble and shell lags found within the bioturbated mud (Fig. 5F). The lag layers are produced by storm-wave and current reworking of sediment to concentrate the coarser fragments from the resuspended mud. New evidence for this resuspension process has recently been acquired in central Norton Sound by *in situ* sediment dynamic and current meter probes (GEOPROBE) that showed several hundred percent increase in suspended sediment transport during a moderate storm event (Cacchione and Drake, 1979).

GEOLOGIC SIGNIFICANCE OF BERING SHELF FACIES PATTERNS

Comparison of the Chirikov Basin and Norton Sound regions shows that strong currents have influenced late Pleistocene and Holocene deposition in

both regions. The strong currents and lack of sediment input into Chirikov Basin have resulted in a transgressive sand sequence that has no Holocene mud over it. Instead, on the northeastern margin of Chirikov Basin, non-deposition and/or scour have taken place so that in nearshore areas, where maximum geostrophic current shear occurs (Fig. 1), the basal coarse-sand facies remains exposed on the seafloor; farther inshore only bedrock outcrops with gravel lags are present (Fig. 6 and 8). Topographic elevations projecting upward into currents in this region (1) retain relict gravel lags over glacial or bedrock outcrops or (2) contain basal sands that are reworked into large-scale mobile bedforms (see Figs. 4C and H and Fig.5 of Nelson, et al., this vol.)

Offshore from the inshore bands of gravel and basal transgressive sand facies in northeast Chirikov Basin (Fig. 8), a parallel band of transgressive inner shelf sand occurs where the geostrophic current flow becomes considerably weaker to the west (Fig. 1). Although the surface sediment patterns of increasing coarseness inshore (Fig. 8) parallel those of increasingly stronger geostrophic current flow toward the northeast side of Chirikov Basin (Fig.1), the shore-parallel facies patterns in these areas could suggest equilibrium with offshore to inshore gradients of increasing wave energy. However, the sheltering and limitation of fetch by St. Lawrence Island, plus the occurrence of an inshore mud blanket parallel to the Port Clarence coastline (Fig. 8), eliminate wave energy as a possible cause of the shore-parallel transgressive facies.

The region west of the modern Yukon subdelta in Shpanberg Strait is another area of strong geostrophic current shear that has important implications for the facies distribution (Fig. 1). The southwest distributary discharges most of the Yukon River sediment load at this location, and parallel banding of sediment facies patterns develops. Here, fine-grained

deposits are found closer to shore near the sediment source and become progressively coarser toward the center of the strait (Fig. 8). McManus et al. (1974) suggested that the central part of the strait is underlain by an older transgressive sand deposited in the narrow early Holocene seaway that extended from a more southerly Yukon Delta source in central Bering Sea (Knebel and Creager, 1973a) to Bering Strait. Therefore, sediments become increasingly coarser grained offshore where current erosion prevents prograding of modern fine sand and silt deposits over the coarse-grained, older transgressive sand.

Comparison of the current-dominated deposition of northern Bering Sea with sedimentation in the central Bering shelf shows the following. Just south of St. Lawrence Island, inner shelf sand like that in Chirikov Basin is present (Fig. 9) (Knebel and Creager 1973a and b; Knebel et al., 1973). Progressively to the south, and toward the edge of the shelf, surface sediment becomes finer grained, and a prograding mud blanket beginning in the mid-central shelf area extends as an increasingly thick wedge to the edge of the continental shelf; an exception is an area where islands are surrounded by coarse-grained relict deposits (Fig. 9).

Studies of Sharma et al. (1972) and Gardner et al. (in press) show that from the Bristol Bay shoreline out toward the shelf edge of southern Bering Sea, deposits become increasingly fine grained. In contrast to the northern Bering shelf, where deposition has been completely dominated by strong bottom current regimes a classic wave-graded pattern of sediment size distribution has developed on the epicontinental shelf in southern Bering Sea (Fig. 9).

The extreme variance of Holocene sedimentation patterns within single epicontinental shelf depositional systems like those of the Bering and North Seas has important implications for studies of ancient analogs. Epicontinental shelf deposits may be classically wave graded from the

shoreline out in one part of a shelf and show similar gradations that are in equilibrium with offshore current regimes in nearby areas (Fig. 9). A major sediment source may reverse the normal onshore- to- offshore facies pattern and lithology of transgressive sequences in two adjacent regions of an epicontinental shelf like Chirikov Basin and Norton Sound (Fig. 8). Norton Sound and related southern Chukchi Sea deposits show that large quantities of sediment introduced into one part of Bering shelf are removed and displaced by currents from storms and related geostrophic circulation to create a major depocenter hundreds of kilometers from the source in another shelf area (Fig. 9) (Nelson and Creager, 1977). Thus, contrary to stratigraphic concepts, prograding prodelta deposits may be extremely thin on the shelf close to a major river source, yet thick hundreds of kilometers from the source; also they may grade from fine to coarse-grained proceeding offshore because of geostrophic current patterns. On the other hand, in normal transgressive sequences, onshore to offshore gradation to finer sediment may occur because geostrophic currents strengthen shoreward rather than as usually expected because of increasing wave energy shoreward (Fig. 8).

Analysis of Holocene sedimentation on Bering shelf has important implications for stratigraphic analysis in similar ancient sequences. Because of the local influence of deltaic sedimentation, currents and topography, areas of transgressive (Chirikov Basin) and regressive (Norton Sound) deposits may develop and coexist in the same area during rising sea levels. In a broad epicontinental shelf area like Chirikov Basin with no prograding delta, the rapid shoreline transgression and strong geostrophic currents result in thin late Pleistocene and Holocene transgressive basal and inner shelf sands without deposition of an overlying offshore mud sequence (Figs. 3 and 6). In inshore regions of strongest currents only thin basal transgressive lags may occur because finer grained offshore facies have been stripped off (Fig. 6).

In contrast to thin transgressive sand sequences of Chirikov Basin, in Norton Sound a thick sequence consisting of transgressive mud and interbedded nearshore storm sands, covered by offshore bioturbated mud is in turn overlain by a regressive sequence of thicker storm sands in mud deposited by the prograding delta in the late Holocene (Figs. 3 and 6).

ACKNOWLEDGMENTS

I thank Devin Thor and Kristin McDougall for contributing background information on seismic stratigraphy and biostratigraphy, respectively. Bob Muench kindly provided new bottom current information from NOAA long-term *in situ* current stations. I am also indebted to Meyer Rubin and Steven Robinson for the radiocarbon dates from the U.S. Geological Survey Radiocarbon Laboratories. Beneficial review comments were made by Monty Hampton and Les Magoon. Mathew Larsen assisted in compilation of data and figures and Tau Rho Alpha drew the three dimensional drawing of Figure 7.

The cruises were supported jointly by the U.S. Geological Survey and by the Bureau of Land Management through interagency agreement with the National Oceanic and Atmospheric Administration, under which a multiyear program responding to needs of petroleum development of the Alaska continental shelf is managed by the Outer Continental Shelf Environmental Assessment Program (OCSEAP) Office.

Any use of trade names or trademarks in this publication is for descriptive purposes only and does not constitute endorsement by the U.S. Geological Survey.

REFERENCES

Cacchione, D. A., & Drake, D. E. (1979) Sediment transport in Norton Sound, Alaska: Regional patterns and GEOPROBE system measurements. U.S. Geological Survey Open-file Report 79-1555.

Field, M. E., et al. (1979) Upper Quaternary peat deposits on the Atlantic inner shelf of the United States. Geological Society of America Bulletin, 90, 618-628.

Gardner, J. V., Dean, W. , & Vallier, T. (1980) Sedimentology and geochemistry of surface sediments, outer continental shelf, southern Bering Sea. Marine Geology, (in press).

Grim, M. S., & McManus, D. A. (1970) A Shallow-water seismic profiling survey of the northern Bering Sea. Marine Geology, 8, 293-320.

Hopkins, D. M. (1973) Sea level history in Beringia during the past 250,000 years. Quat. Res. 3, 520-540.

Hopkins, D. M. (1975) Time stratigraphic nomenclature for the Holocene Epoch. Geology, 3, 10.

Hopkins, D. M. (1979) Landscape and climate of Beringia during late Pleistocene and Holocene time. In: The first Americans: origins, affinities, and adaptations, Eds. W.S. Laughlin and A.B. Harper 1979. Gustav Fischer, New York, 15-41.

Hopkins, D. M., Nelson, C. H., Perry, R. B., & Alpha, Tau Rho (1976) Physiographic subdivisions of the Chirikov Basin, northern Bering Sea. United States Geological Survey Professional Paper 759-B.

Johnson, J. L, & Holmes, M. L. (1978), Surface and subsurface faulting in Norton Sound and Chirikov Bain, Alaska, Environmental Assessment of the Alaskan Continental Shelf, Annual Report of Principal Investigators, Environmental Research Lab., Boulder, Colo., NOAA, U.S. Dept. of Commerce 12, 203-227.

Knebel, H. J., & Creager, J. S. (1973a) Yukon River - evidence for extensive migration during the Holocene transgression. Science, 79 1230-1231.

Knebel, H. J., & Creager, J. S. (1973b) Sedimentary environments of the east-central Bering Sea epicontinental shelf. Marine Geology, 15, 25-47.

Knebel, H. J., Creager, J. S. & Echol, R. D. (1973) Holocene sedimentary framework, east-central Bering Sea continental shelf. Arctic Geology and Oceanography, (Ed. by V. Herman) Springer Verlag, 157-172.

McManus, D. A. et al. (1974) Yukon River sediment on the northernmost Bering Sea shelf. Journal of Sedimentary Petrology, 44, 1052-1060.

McManus, D. A. et al. (1977) Distribution of bottom sediments on the continental shelf, northern Bering Sea. U.S. Geological Survey Professional Paper 759-C.

Nelson, C. H.(1977) Storm surge effects. Environmental Assessment of the Alaskan Continental Shelf, Annual Report of the Principal Investigators for the year ending March, 1977, Environmental Research Laboratory, Boulder, Colo., NOAA, U.S. Dept. of Commerce, 18, 111-119.

Nelson, C. H., Hopkins, D. M., & Ness, G. (1969) Interpreting complex relict and modern sediment patterns on the Bering Shelf Geological Society of America Annual Meeting, Abstracts w/programs 7, 159.

Nelson, C. H., & Hopkins, D. M. (1972) Sedimentary processes and distribution of particulate gold in northern Bering Sea. U.S. Geological Survey Professional Paper 689.

Nelson, C. H., & Creager, J. S. (1977) Displacement of Yukon-derived sediment from Bering Sea to Chukchi Sea during the Holocene. Geology, 5, 141-146.

Nelson, C. H. et al., (1980) Interplay of physical and biological sedimentary structures of the Bering epicontionental shelf. The Eastern Bering Sea Shelf: Its Oceanography and Resources, (Ed. by D.W. Hood) (in press)

Nio, S. D., Schuttenhelm, R. T., & Van Weering, T. C. E., eds., (1979) Shelf Sedimentation. Theme 4 International Association of Sedimentologists, International Meeting on Holocene Marine Sedimentation in the Norton Sea Basin, Texel, The Netherlands (Abstracts) , 40-56.

Schumacher, J. D., & Tripp, R. B. (1979) Response of northeast Bering Sea shelf waters to storms. EOS, 60, 856.

Sharma, G. D., Naidu, A. S., & Hood, D. W. (1972) Bristol Bay: A model contemporary graded shelf. American Association of Petroleum Geologists Bulletin, 56, 2000-2012.

Tagg, A. R., & Greene, H. G. (1973) High-resolution seismic survey of a nearshore area, Nome Alaska. U.S. Geological Survey Professional Paper 759-A.

Figure Captions

Figure 1. Northeastern Bering Sea and southern Chukchi Sea, showing water circulation, maximum measured bottom-current velocities, and bathymetry. Modified from Nelson and Creager (1977) including new long-term *in situ* current measurements from Cacchione and Drake (1979) and R. Muench (written commun., NOAA-PMEL, Seattle, Wash., 1979).

Figure 2. Location of sampling stations and geophysical tracklines for U.S. Geological Survey research in northern Bering Sea between 1967 and 1978. Lines A-A′ and B-B′ show locations of cross-sections shown in Figure 3. Single letters A-F show station locations of core photographs in Figure 5.

Figure 3. Near-surface late Pleistocene and Holocene stratigraphy in Chirikov Basin (B-B′) and Norton Sound (A-A′) (see Fig. 2 for locations). Corrected dates with stars are calculated by the method shown in Figure 5D. In profile A-A′ the date of 1500 years BP in core C approximately dates freshwater influx of the modern Yukon delta lobe. In profile B-B′, the region of sand ridges in northeast Chirikov Basin extends from King Island shoal to Port Clarence.

Figure 4. A. Elements of pre-transgressive geologic history in northeastern Bering Sea showing locations of seafloor and near-surface bedrock outcrops, glacial moraines, and alluvial channels. Details of subsurface channels are incomplete, particularly in Chirikov Basin, because of insufficient geophysical trackline coverage. Information on glacial moraines is based on Nelson and Hopkins (1972) and on bedrock outcrops and subsurface channels is modified from Devin Thor (written communication, 1979).

B. Thickness of Holocene sediment based on seismic profiles (modified from Nelson and Creager, 1977) (Devin Thor, written communication, 1979).

Figure 5. Internal sedimentary features of late Pleistocene and Holocene deposits in northeastern Bering Shelf. Numbers to the left in B and C show percent of gravel and coarse to medium sand in transgressive and regressive sand layers. See Figure 2 for core locations.

A. Transgressive lag gravel over glacial till shown in a box core slab face. 41 m water depth.

B. Box core no. 247 radiograph showing cross-laminated transgressive fine-grained inner shelf sand overlying limnic clays with freshwater ostracodes (P. Valentine, written commun., U.S.G.S. Woods Hole, Mass., 1971). Note deep pelecypod burrowing into freshwater mud after the marine transgression. 36 m water depth.

C. Box core slab showing transgressive inner shelf fine sand overlying basal transgressive medium to fine sand. 48 m water depth.

D. Radiograph of cross-laminated and wavy bedded sand layers (light colored) in late Holocene Yukon silt (<5,000 years old) based on bulk sample radiocarbon dates (corrected for surface sample age) underlain by bioturbated older Yukon silt (>5,000 years old) (after Nelson and Creager, 1977). Located 75 km from the Yukon Delta in 16 m water depth.

E. Box core slab face showing a surface and a deeper bioturbated sand layer (light colored) in Yukon silt 30 km from the modern Yukon subdelta. 11 m water depth.

F. Radiograph showing shell and pebble storm lag layers near the surface and base of the core in addition to a series of thin sand layers (light colored) and parallel and lenticular bedding in the center of the core. Radiocarbon date at the core bottom is based on a piece of wood. Located 110 km from the Yukon Delta in 14 m water depth.

Figure 6. Preliminary map of the northeastern Bering shelf surficial geology.

Figure 7. Conceptual model showing importance of physical structures versus biological structures in epicontinental shelf deltaic sequences (after Nelson et al., in press). Thickness of wedge depicts relative intensity of process from lower salinity and higher energy to higher salinity and lower energy shelf environments offshore. Relative thickness of storm sand sequences from inshore to offshore also is shown (Nelson, 1977). Area of thick storm sands and physical structures shifts seaward with influx of a prograding delta lobe and low-salinity water.

Figure 8. Transgressive sediment facies patterns based on grain-size modes (from McManus et al., 1977).

Figure 9. Generalized late Pleistocene and Holocene deposits of the eastern Bering Shelf, Alaska. Compiled from Gardner et al., (in press); McManus et al., (1977); Nelson and Creager, (1977); Knebel and Creager, (1973b); Nelson and Hopkins, (1972); Sharma et al., (1970).

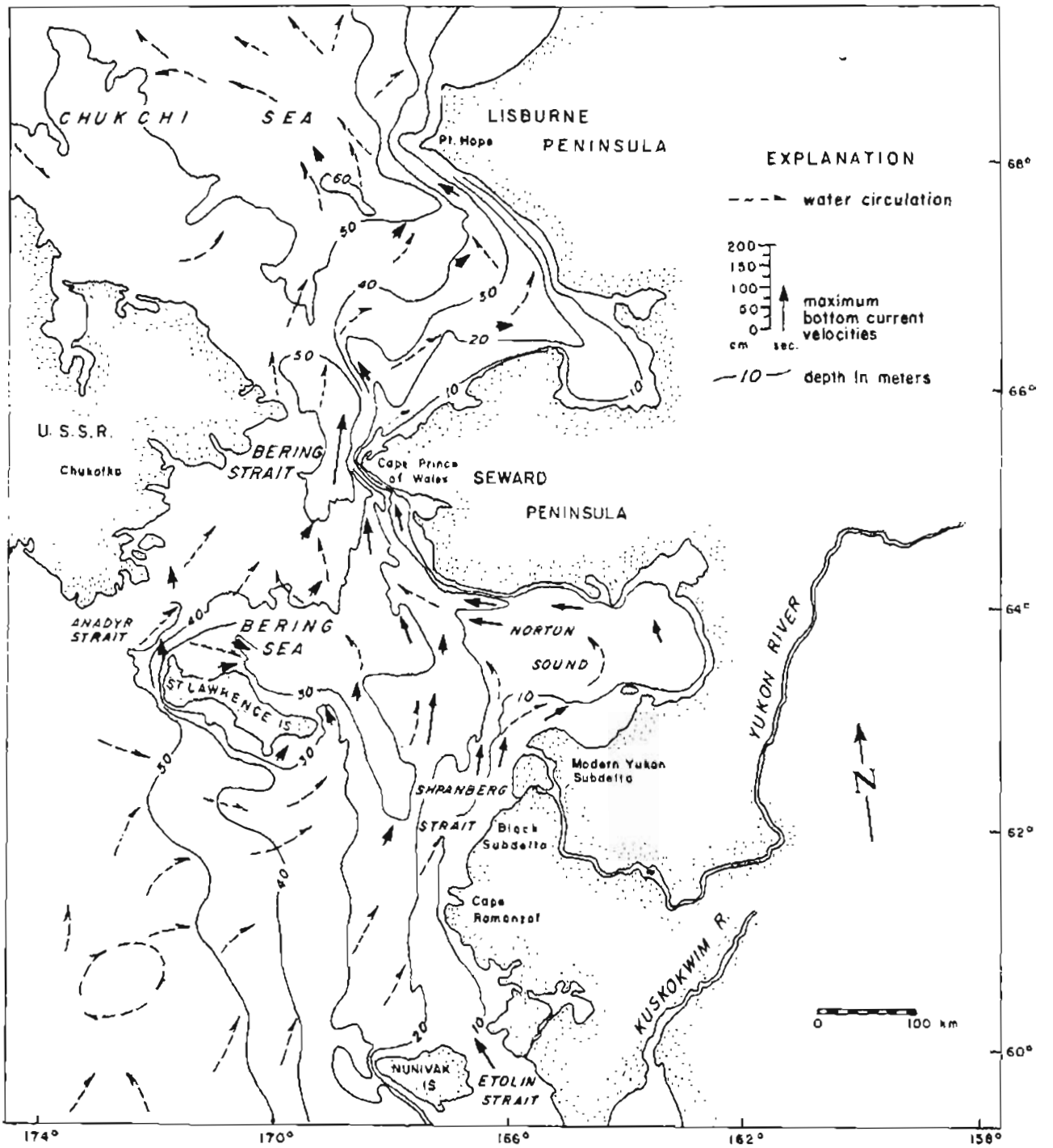
CHUKCHI SEA
LISBURNE PENINSULA
Pt. Hope
EXPLANATION
water circulation
200
150
100
50
0
cm sec.
maximum bottom current velocities
10
depth in meters
U.S.S.R.
Chukotka
BERING STRAIT
Cape Prince of Wales
SEWARD PENINSULA
ANADYR STRAIT
BERING SEA
NORTON SOUND
ST LAWRENCE IS
YUKON RIVER
Modern Yukon Subdelta
SHPANBERG STRAIT
Black Subdelta
Cape Romanzof
KUSKOKWIM R.
NUNIVAK IS
ETOLIN STRAIT
N
0 100 km
66°
64°
62°
60°
174°
170°
166°
162°
158°

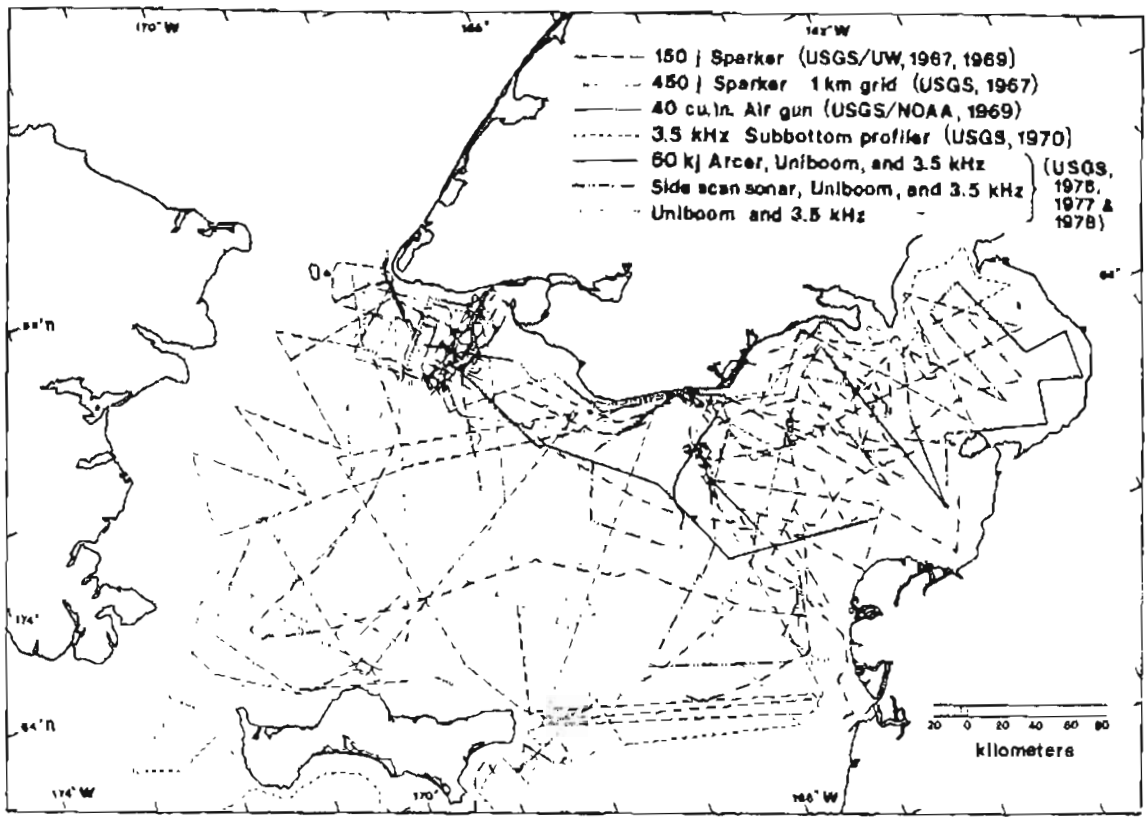
150 j Sparker (USGS/UW, 1967, 1969)
450 j Sparker 1 km grid (USGS, 1967)
40 cu.in. Air gun (USGS/NOAA, 1969)
3.5 kHz Subbottom profiler (USGS, 1970)
60 kj Arcer, Uniboom, and 3.5 kHz
Side scan sonar, Uniboom, and 3.5 kHz
Uniboom and 3.5 kHz
(USGS, 1976, 1977 & 1978)
kilometers

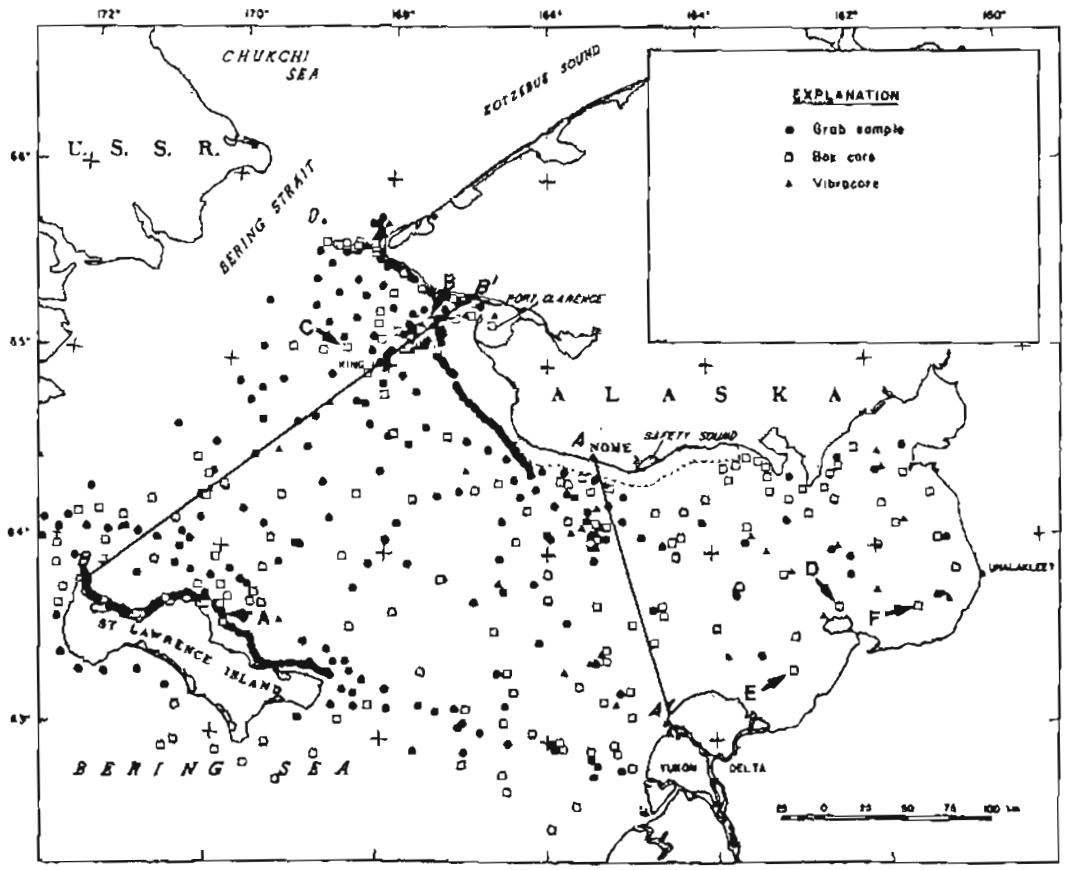
CHUKCHI SEA
KOTZEBUE SOUND
U. S. S. R.
BERING STRAIT
EXPLANATION
Grab sample
Box core
Vibrocore
FORT CLARENCE
A L A S K A
NOME
SAFETY SOUND
ST LAWRENCE ISLAND
BERING SEA
YUKON DELTA

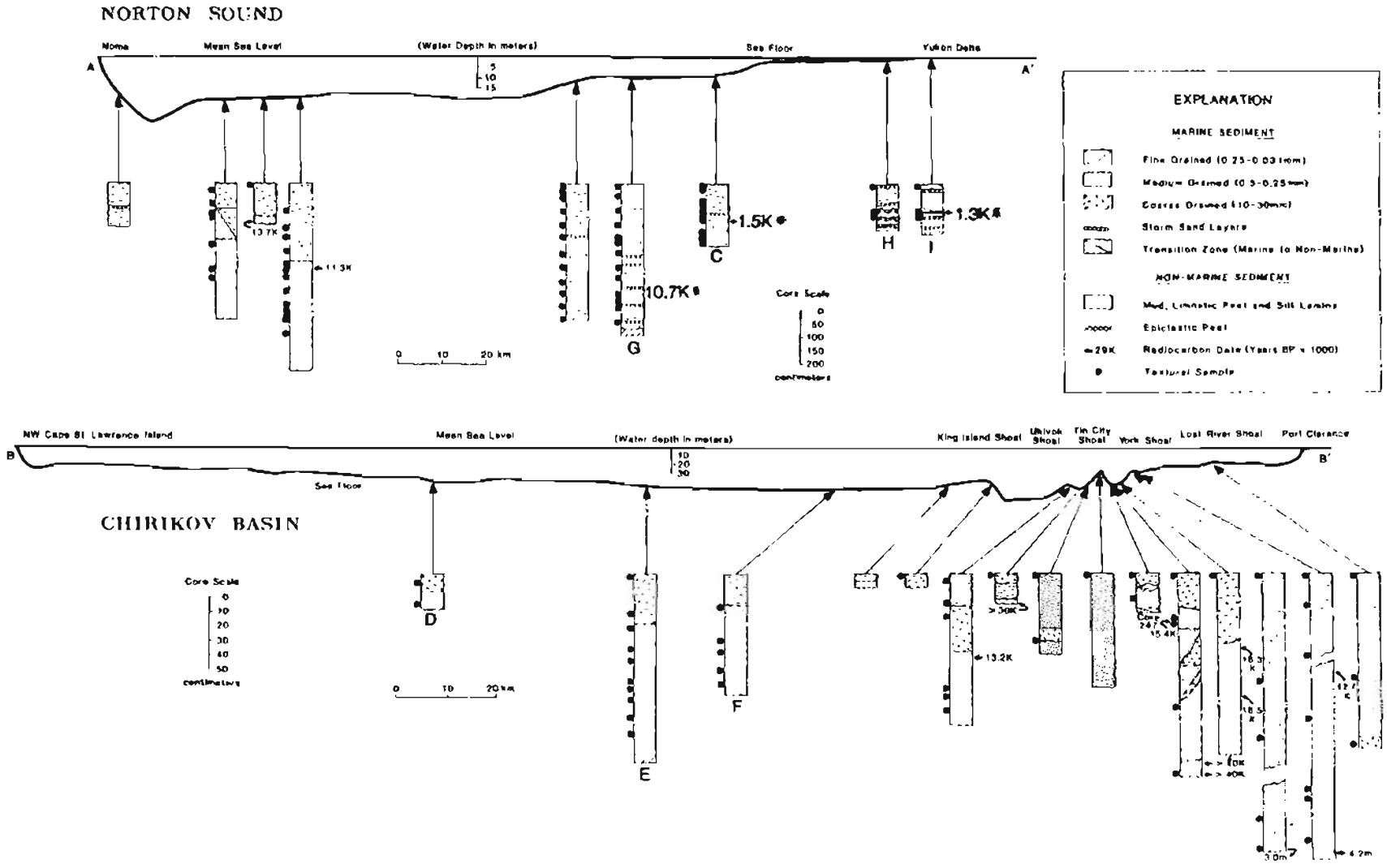
NORTON SOUND
Nome
Mean Sea Level
(Water Depth in meters)
Sea Floor
Yukon Delta
A
A'
5
10
15
13.7K
11.3K
10.7K
1.5K
1.3K
C
G
H
I
0 10 20 km
Core Scale
0
50
100
150
200
centimeters
EXPLANATION
MARINE SEDIMENT
Fine Grained (0.25-0.03 mm)
Medium Grained (0.5-0.25 mm)
Coarse Grained (1.0-.50 mm)
Storm Sand Layers
Transition Zone (Marine to Non-Marine)
NON-MARINE SEDIMENT
Mud, Limnetic Peat and Silt Lenses
Epiclastic Peat
Radiocarbon Date (Years BP x 1000)
Textural Sample
NW Cape St Lawrence Island
Mean Sea Level
(Water depth in meters)
King Island Shoal
Uhlvok Shoal
Tin City Shoal
York Shoal
Lost River Shoal
Port Clarence
B
B'
10
20
30
Sea Floor
CHIRIKOV BASIN
Core Scale
0
10
20
30
40
50
centimeters
0 10 20 km
D
E
F
> 30K
13.2K
15.4K
> 40K
3.0m
4.2m

A

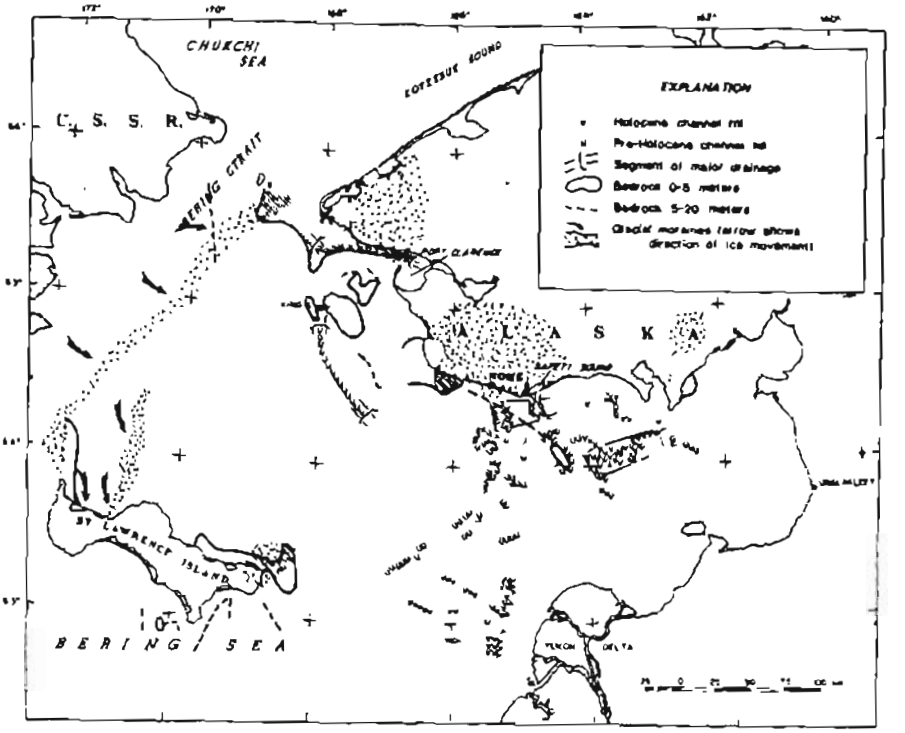

PRELIMINARY MAP OF SURFACE AND NEARSURFACE BEDROCK, GLACIAL MORAINES AND BURIED CHANNELS

B

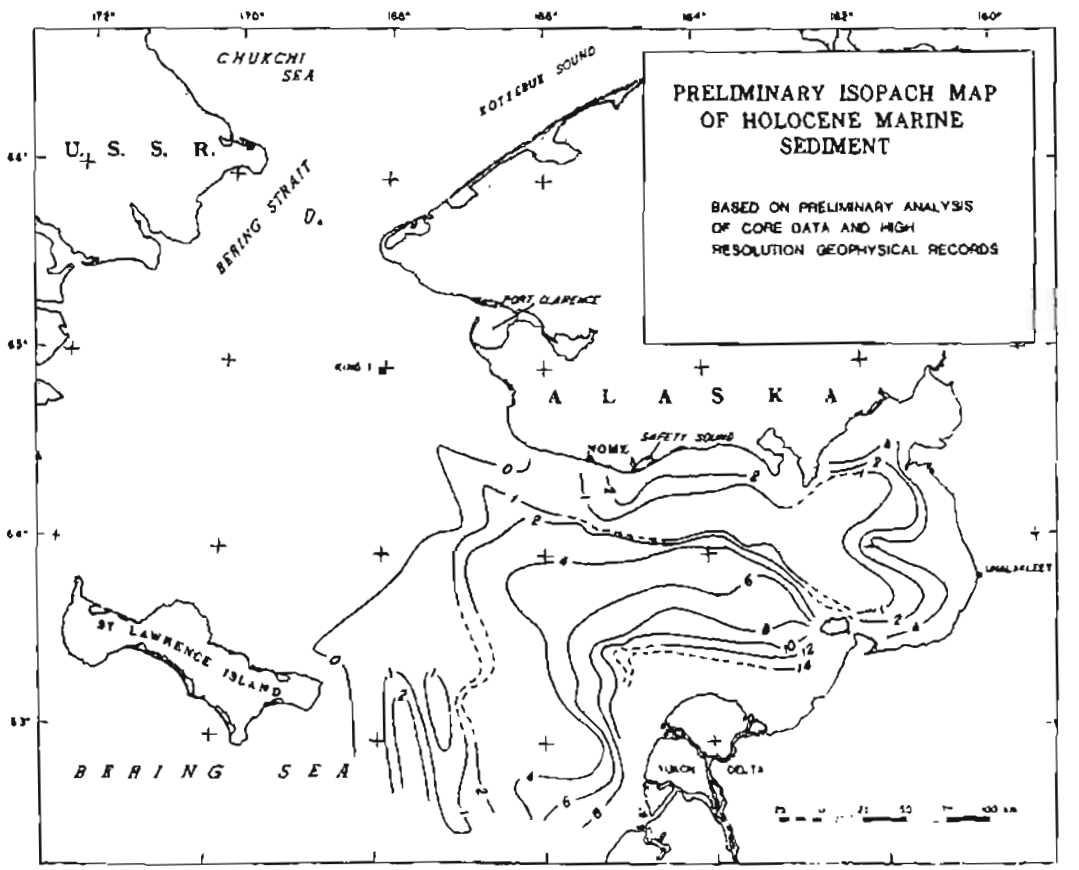

CHIRIKOV BASIN LATE PLEISTOCENE TRANSGRESSIVE DEPOSITS

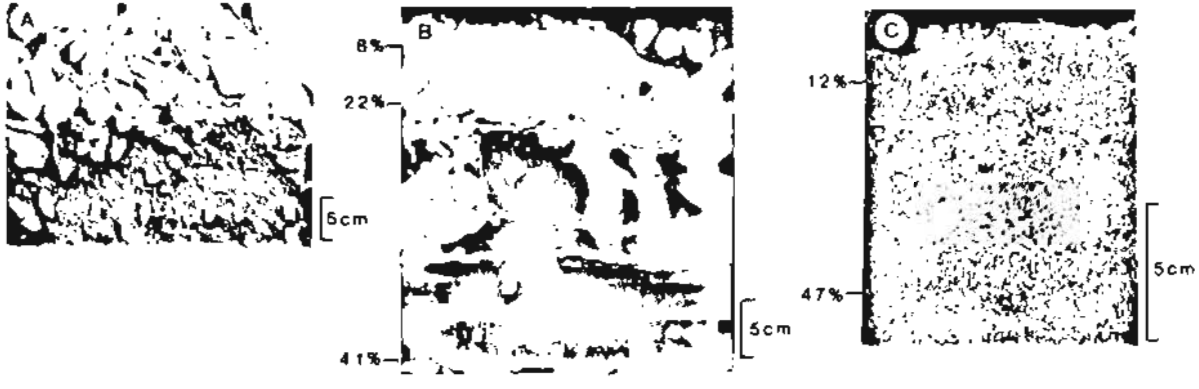

NORTON SOUND HOLOCENE DEPOSITS

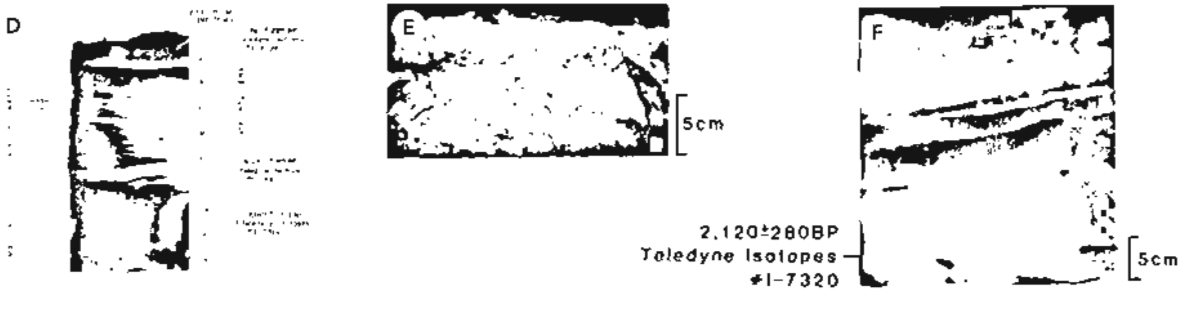

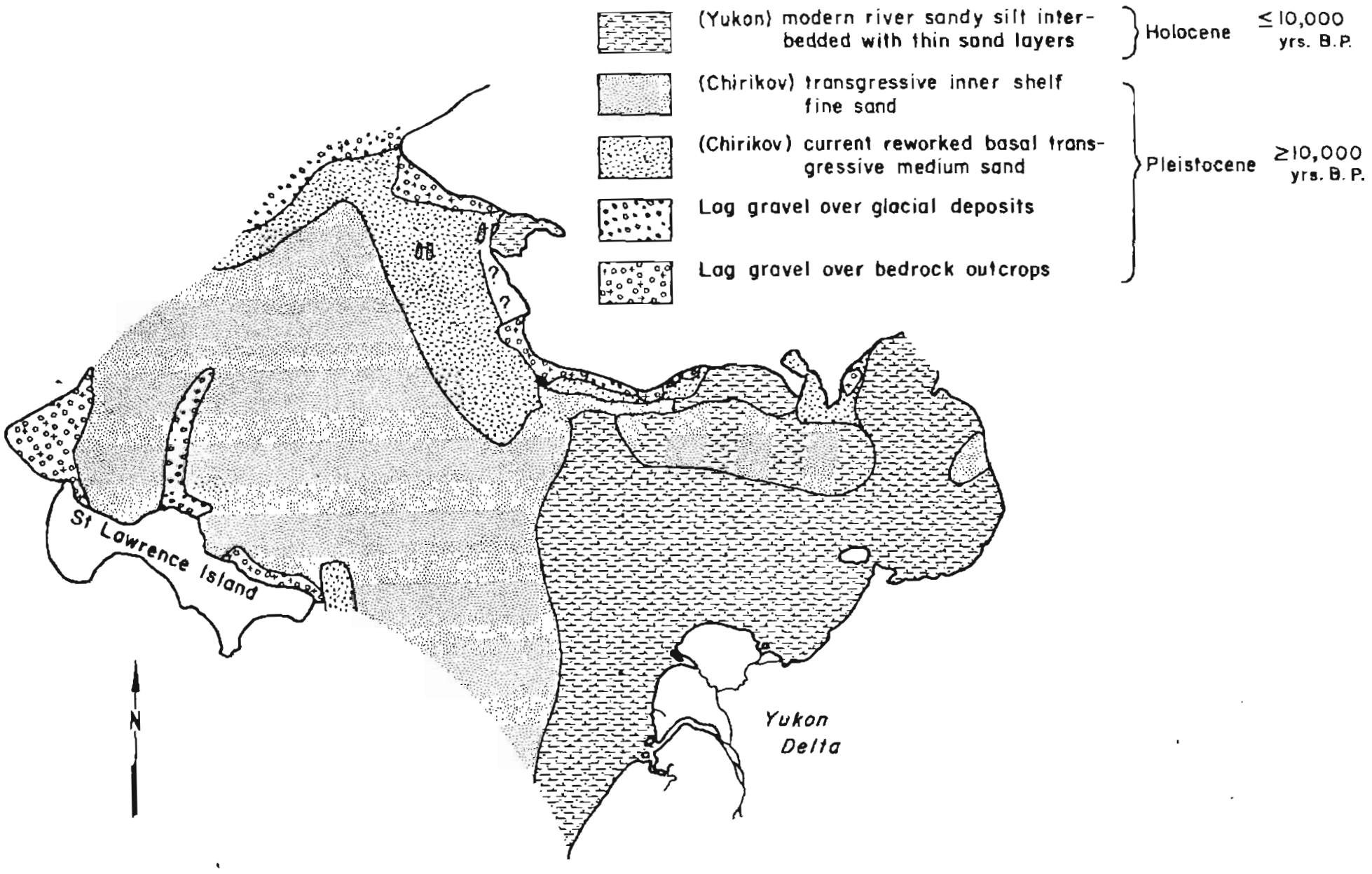
(Yukon) modern river sandy silt interbedded with thin sand layers
Holocene
≤ 10,000 yrs. B.P.
(Chirikov) transgressive inner shelf fine sand
(Chirikov) current reworked basal transgressive medium sand
Pleistocene
≥10,000 yrs. B.P.
Lag gravel over glacial deposits
Lag gravel over bedrock outcrops
St Lawrence Island
Yukon Delta
N

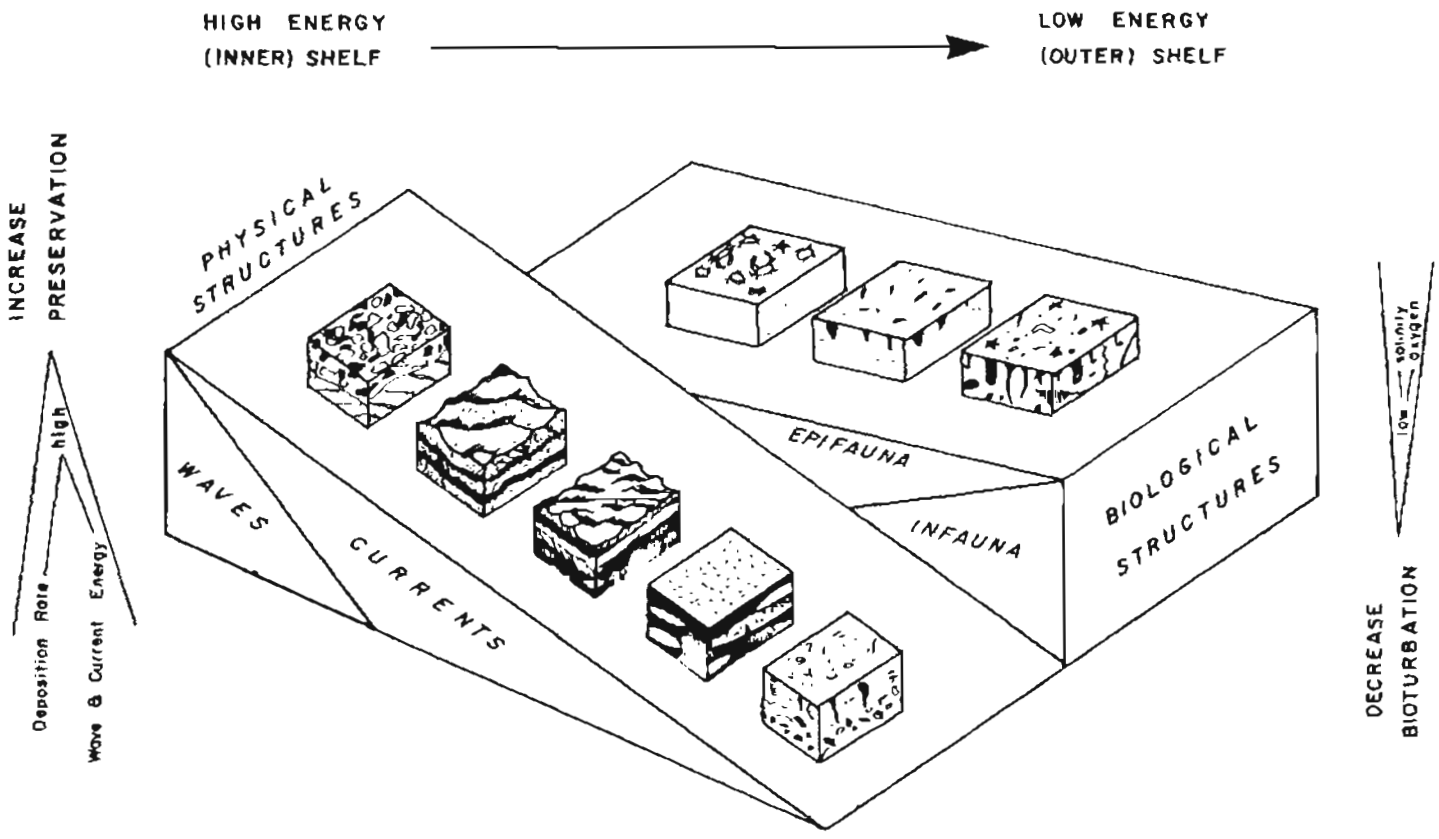
HIGH ENERGY
(INNER) SHELF
LOW ENERGY
(OUTER) SHELF
INCREASE
PRESERVATION
high
Deposition Rate
Wave & Current Energy
PHYSICAL
STRUCTURES
WAVES
CURRENTS
EPIFAUNA
INFAUNA
BIOLOGICAL
STRUCTURES
low
salinity
oxygen
DECREASE
BIOTURBATION

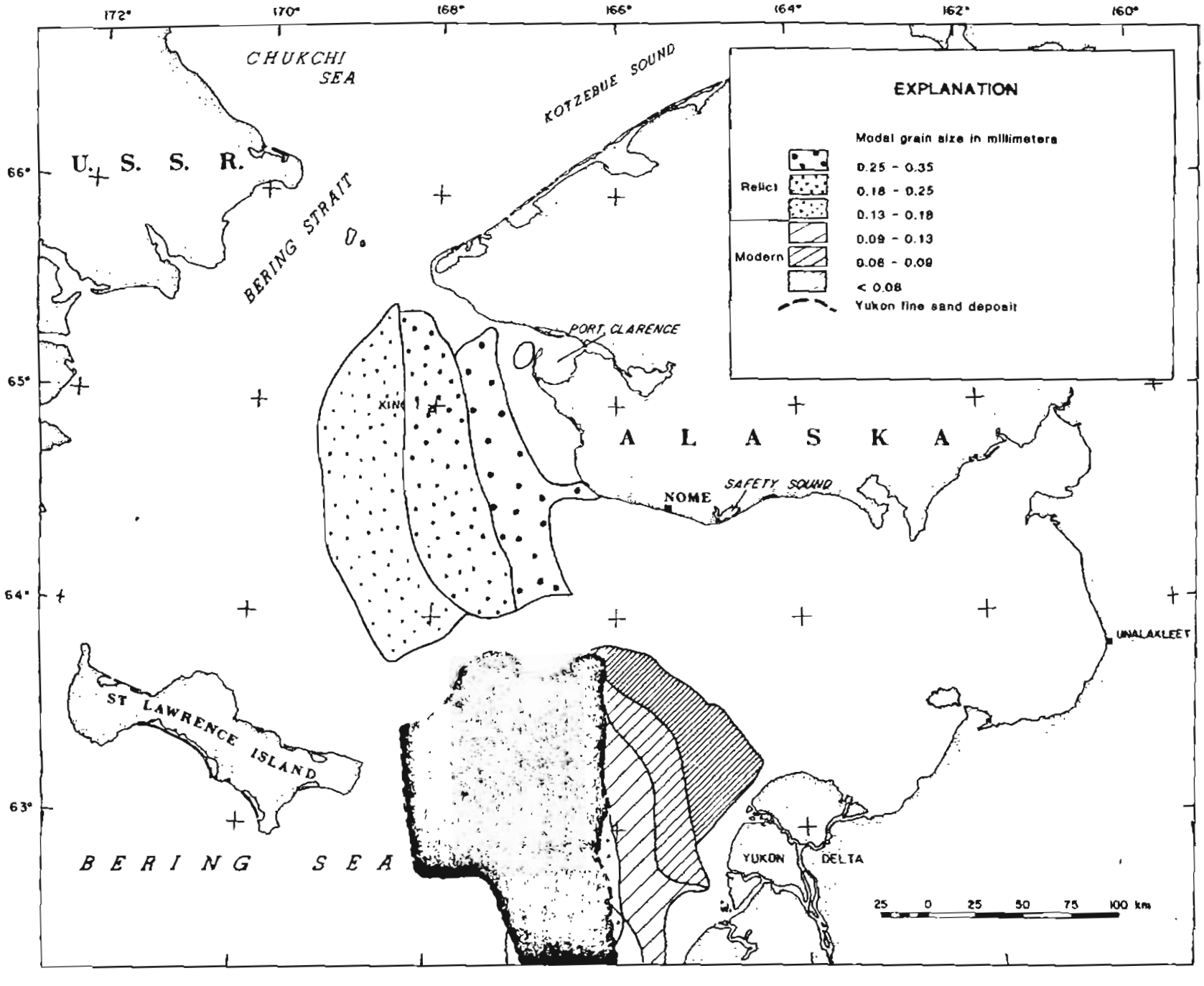

PRELIMINARY ISOPACH MAP OF HOLOCENE MARINE SEDIMENT

BASED ON PRELIMINARY ANALYSIS OF CORE DATA AND HIGH RESOLUTION GEOPHYSICAL RECORDS

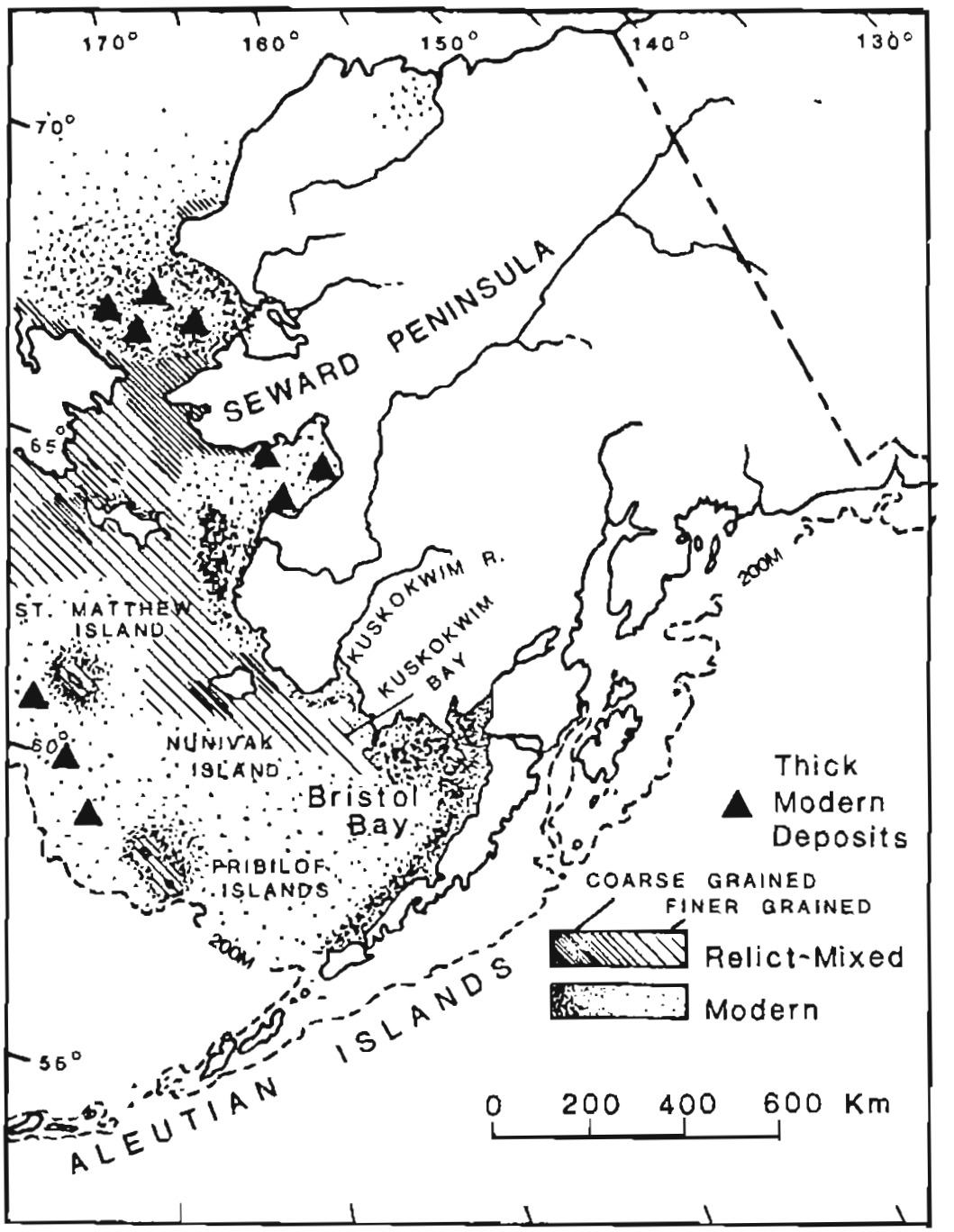
170°
160°
150°
140°
130°
70°
65°
60°
55°
SEWARD PENINSULA
ST. MATTHEW ISLAND
NUNIVAK ISLAND
KUSKOKWIM R.
KUSKOKWIM BAY
Bristol Bay
PRIBILOF ISLANDS
200M
ALEUTIAN ISLANDS
Thick Modern Deposits
COARSE GRAINED
FINER GRAINED
Relict-Mixed
Modern
0 200 400 600 Km

Microfaunal analysis of late Quaternary deposits of the northern Bering Sea

by

Kristin McDougall

U.S. Geological Survey, Menlo Park, Calif. 94025

Abstract

Holocene microfaunal associations and distribution patterns define three inner-shelf (<20 m) biofacies in Norton Sound, northern Bering Sea. The first biofacies is composed of typical bay faunas dominated by the species Eggerella advena, Buccella frigida, Ammotium cassis, and Reophax dentaliformis. The second biofacies contains bay to inner-shelf faunas indicative of deeper, more marine waters; such inner-shelf species as Reophax arctica, R. fusiformis, Spiroplectammina biformis, and Textularia torquata dominate. The third biofacies, common in deltaic areas with high sedimentation rates and freshwater input, is characterized by abundant Elphidium orbiculare and E. clavatum. The distribution of other microfaunal groups (diatoms, ostracods, tintinnids, and fragments of larger invertebrates and plants) corresponds to current and sedimentary patterns.

These Holocene facies relations are the basis for interpreting early Holocene and late Pleistocene environmental conditions in the northern Bering Sea area. Within older deposits the sequence of biofacies can be used to interpret the Holocene transgressive cycle in Norton Sound. Norton Sound cores provide evidence of two marine transgressions and varying river input.

Introduction

Shpanberg Strait, northern Bering Sea, was breached by marine waters about 11,800 B.P., when sea level rose to -30 m. This event separated Saint Lawrence Island from the Alaskan mainland and marked the beginning of the Holocene transgression in Norton basin (Hopkins, 1973). The rising sea level and warming climate brought about a sequence of physical and biologic changes that transformed the basin from a tundra-covered plain containing peat bogs to a shallow sea. This transformation is recorded in a thin veneer of Holocene sedimentary deposits in Norton Sound.

Holocene and older transgressive-regressive cycles in the Bering Sea have been studied by McManus and others (1969), Hopkins (1972, 1973), Nelson and Hopkins (1972), Knebel and Creager (1973), Herman (1974), McManus and others (1974, 1977), Coachman and others (1975), Hopkins and others (1976), Cacchione and others (1977), Nelson and Creager (1977), and Nelson (this volume). Few of these studies have considered the biologic changes and faunal distributions that reflect these cycles. In particular, data on foraminifers, which are sensitive ecologic indicators, have not been previously reported for the northern Bering Sea.

Holocene foraminiferal studies along the west coast of Alaska considered the ecologic relations of inner-shelf (<20 m) assemblages of the southern Bering Sea (Anderson, 1963) and the Chukchi Sea (Cooper, 1964). Fossil foraminiferal studies include those by R. J. Echols (in Knebel and others, 1974) south of Saint Lawrence Island and Beljaeva (1960; see also Kummer and Creager, 1971) in the Gulf of Anadyr. These works recognized inner-shelf assemblages, using criteria formulated during Holocene studies to interpret the paleoenvironment. Faunas from depths of less than 20 m were not identified. Because Norton Sound is mostly shallower than 20 m (McManus and others, 1977), foraminiferal assemblages and faunas representing the Holocene transgression could only be considered as representative of the inner neritic biofacies of earlier workers. Microfaunal analysis limited by this conceptual framework would provide little or no further information on the Holocene transgression. This investigation was conducted to determine what biofacies, if any, could be recognized in the shallow marine waters of Norton Sound, what physical parameters might be related to any of the biofacies found, and which of these biofacies relations might be useful in interpreting the paleoecology of the Holocene transgression.

Norton Sound is a shallow epicontinental shelf sea bounded on the southwest by the Yukon delta and on the north by Seward Peninsula, Alaska (fig. 1). Water depths are commonly less than 20 m (McManus and others, 1977). Warmer (6°-9°C avg summer temperature), less saline (≤31°/₀₀) Alaskan coastal water fills Norton Sound and, circulating in a counterclockwise direction, moves generally northward (Anderson, 1963; Coachman and others, 1975; McManus and others, 1977). Runoff from the Yukon River carries sand, silt, and low-salinity water into Norton Sound, where little of the sediment actually accumulates beyond the modern prodelta (Nelson and Creager, 1977). Strong storm surges frequently resuspend the sediment and periodically disrupt the substrate (Nelson, this volume).

From an analysis of 35 stained surface samples from Norton Sound, three foraminiferal biofacies can be recognized: bay, bay/inner-shelf, and delta. The bay biofacies is associated with slightly higher salinities, lower water temperatures, and fine sand. The bay/inner-shelf biofacies is associated with cool water temperatures, normal salinity, and greater depths. The delta biofacies is associated with shallow water depths, low salinity, warmer water temperatures, and sandy substrates (Howard and Nelson, this volume). Other microfaunal and microfloral groups (diatoms, ostracods, tintinnids, and fragments of larger invertebrates and plants) are also associated with specific environmental conditions in Norton Sound. Fossil assemblages interpreted as representing the Holocene transgression contain many of the species presently living in Norton Sound. These assemblages indicate a progressive change in Norton Sound from a tundra-covered plain to a shallow sea. Foraminiferal assemblages from earlier transgressive-regressive cycles are not included in this discussion.

Holocene microfaunas

During 1976 and 1977 surface (box cores) and subsurface (vibracores and piston cores) samples were taken from Norton Sound, northern Bering Sea (fig. 2). Of these samples 35 surface samples form the basis of the Holocene surface data; these samples were collected from the top 1 to 2 cm of the box cores and were stained with rose bengal solution onboard the research vessel Sea Sounder. Subsequent laboratory processing of both surface and subsurface samples included soaking samples in water and wet sieving through a 63-mesh (250 μ) screen. From the dried residues, 300 organic specimens (foraminifers, diatoms, ostracods, tintinnids, and fragments of larger invertebrates and plants) and, where possible, 300 foraminiferal specimens were counted and identified. These microfaunal data (total assemblages) were subjected to both visual and statistical (cluster and factor) analysis.

Benthic foraminiferal species constitute one of the major microfaunal groups in the Holocene surface samples. In all, 53 foraminiferal species were recorded; although diversity ranges from 1 to 17 species, most assemblages are dominated by 3 or 4 species. By cluster and factor analysis these assemblages were separated into three groups, identified here as the bay, bay/inner-shelf, and the delta biofacies (figs. 3-5).

The bay biofacies is characterized by Eggerella advena, Buccella frigida, Ammotium cassis, and Reophax dentaliformis. E. advena is the most abundant, and makes up 10 to 80 percent of the faunas. Stained specimens were difficult to recognize because most of the tests are yellow to brown and thus obscure the red stain. Living specimens were, however, noted in samples south of Nome, Alaska, and west of Port Clarence (an embayment northwest of Nome). Buccella frigida and Ammotium cassis, the next most abundant species, range in abundance from 1 to 35 percent. A. cassis is more abundant in areas where the bay assemblages make up less than 40 percent of the faunas and the sedimentary material is coarser; no living specimens were recognized. B. frigida, which is more evenly distributed, increases in abundance in the central parts of Norton Sound and in the bay/inner-shelf assemblages; living specimens are present in both the bay and bay/inner-shelf biofacies.

Faunas dominated by the bay biofacies are most abundant in the northeastern and central parts of Norton Sound as well as around Port Clarence. These faunas are absent in samples from off the Yukon delta and Cape Rodney, northwest of Nome (fig. 3). This distribution correlates with water depths between 10 and 30 m (Hopkins and others, 1976; McManus and others, 1977) salinites of 29 to 31.5°/$_{oo}$ (Coachman and others, 1975), and temperatures below 12°C (avg summer temperature). The substrate in these areas is a fine sand (<4.0 ø) derived from the Yukon River or Seward Peninsula (McManus and others, 1977).

The bay/inner-shelf biofacies is characterized by Spiroplectammina biformis, Textularia torquata, Reophax arctica, and R. fusiformis. R. arctica and R. fusiformis, the most common of the four diagnostic species, together average more than 20 percent of the bay/inner-shelf biofacies; Spiroplectammina biformis and Textularia torquata are less common and occur more sporadically. Inner-shelf species that occur infrequently in association with this biofacies are Cassidulina islandica, Buliminella elegantissima, and Nonionella auricula.

The bay/inner-shelf biofacies makes up about 20 percent of the species in the depression in Norton Sound, southeast of Nome, and higher percentages of the assemblages in the western part of Norton Sound (fig. 4). Species diagnostic of this biofacies frequently occur in association with the species characteristic of the bay biofacies, although little to no overlap with the delta biofacies is evident. Water depths are generally 20 m or greater, summer water temperatures are below 12°C, and salinities are 29°/$_{oo}$ or higher (Coachman and others, 1975). The substrate is composed of several sedimentary types in these areas and fine sand predominates (McManus and others, 1974).

The delta biofacies is characterized by Elphidium clavatum and E. orbiculare; these two species together constitute greater than 50 percent of the delta faunas. Four other species of Elphidium were identified in the Norton Sound assemblages: E. albiumbilicatum, E. bartletti, E. incertum, and E. frigidum. These other species do not occur frequently or abundantly but could be included as species characteristic of the delta biofacies. They occur most frequently in the outer fringes of the delta biofacies--areas where the delta and bay faunas are mixed. E. frigidum occurs principally in the bay/inner-shelf assemblages and thus cannot be used as diagnostic of the delta biofacies.

Specimens of Elphidium were the most commonly stained group; the rose bengal stain colored all chambers except the last (living) chamber. Because of this staining pattern, none of the specimens are believed to have been alive at the time of collection.

Faunas dominated by the delta biofacies are concentrated around the Yukon delta, the southeastern part of Norton Sound, and in an area immediately south of Nome, Alaska (fig. 5). This distribution correlates with the shallowest water depths (<10 m) to about 20 m, warmer water temperatures (to 12°C average summer temperature; Coachman and others, 1975), and lower salinities (≤29°/₀₀). The substrate is dominated by Yukon silt and fine (<4.0 ϕ) sand (McManus and others, 1974).

The interrelation of the three biofacies is evident in two transects of surface samples across Norton Sound. Most faunal assemblages contain species from all three biofacies. Species diagnostic of each biofacies are present in every assemblage except those directly affected by the Yukon River (samples Mf4763, Mf5461, Mf5462). The bay/inner-shelf biofacies exists principally in the deeper waters and only where the delta species make up less than 50 percent of the assemblage (figs. 6, 7).

The three biofacies recognized here refine the inner-shelf sublittoral biotopes recognized in the southern Bering Sea and the faunal assemblages recognized in the Chukchi Sea. The deltaic biotope of Anderson (1963) and the delta biofacies of this study are equivalent. Both the delta biofacies and biotope are dominated by species of Elphidium and controlled largely by salinity. No clearly deltaic assemblage was recognized in the Chukchi Sea. The bay and bay/inner-shelf biofacies of this study resemble the inner shelf biotope of Anderson (1963) of which they may be subdivisions. The transitional biotope of Anderson (1963) was not recognized in the Norton Sound surface samples but was recognized in the subsurface samples; this biotope contains abundant occurrences of Buccella frigida and Buliminella elegantissima and is therefore unlike the bay or bay/inner-shelf biofacies of this study. The group II and group III faunal assemblages in the Chukchi Sea (Cooper, 1964) resemble the bay and bay/inner-shelf biofacies in Norton Sound, although Cooper's groups are not so clearly defined or restricted.

Other faunal and floral groups recognized are plant fragments, larger invertebrate fragments, ostracods, diatoms, and tintinnids. Plant fragments were present in every sample and very high abundances were observed in samples from near the Yukon delta. Larger invertebrates include worm tubes, crustaceans, and mollusks, present throughout Norton Sound and generally the only living (stained) component of the assemblages. Ostracods were considered separately from the other invertebrates; this faunal group is concentrated in the eastern part of Norton Sound, where they make up as much as one-fourth of the faunas (fig. 8). Elsewhere in Norton Sound, ostracods were only minor components (<5%). Larger diatoms, which occur in the foraminiferal residues, are present throughout and increase in abundance from east to west as the water becomes deeper and more normal marine (fig. 8). Smear slides contained oceanic, neritic marine, benthic marine, and freshwater diatoms; no particular pattern has yet been recognized. Tintinnids (Tintinnopsis fimbriata) are minor members of all assemblages, except in a few samples from the extreme eastern part of Norton Sound (fig. 8), where the tintinnids make up as much as one-fifth of the organic remains. Abundant tintinnids are also found in the depression south of Nome, a distribution that probably reflects the current pattern and transport of fine-grained sediment. Echols and Fowler (1973) reported this same species in the Chukchi Sea and note that it may be used as an indicator of Yukon River sediment.

Holocene transgresion

Refinement of the shallow-water biofacies serves as a basis for interpreting environmental changes during the Holocene transgression. Five cores from different parts of Norton Sound were selected for study. In these cores the biologic changes, particularly in the benthic foraminiferal faunas, were examined and related to paleoenvironmental conditions to provide a clearer picture of the transition taking place during the transgression. Sample preparation was the same as for the surface samples discussed previously.

Core 78-22 (fig. 2) was northwest of the present Yukon delta (lat 63.21° N., long 165.50° W.) in an area now dominated by the bay biofacies. Subsurface samples were taken at about 50-cm intervals between -2 and -513 cm. Faunal analyses indicate a progression from an interval dominated by plant fragments, assumed to represent a nonmarine environment (-513 cm), to one dominated by the delta biofacies (-450 to -250 cm). The benthic foraminiferal assemblages in this fossiliferous interval also contained a few species of the bay biofacies and the transitional biotope of Anderson (1963). Samples between -250 and -50 cm were dominated by plant fragments. One specimen of Eggerella advena occurred at -200 cm, and several diatoms were present in the sample at -250 cm. The sample at -2 cm was, as expected, dominated by bay species and included rare delta species.

Core 76-145 (including 76-145B) was northeast of the present Yukon delta (lat 63.22° N., long 163.07° W.; fig. 2), in an area dominated by the delta biofacies. Subsurface samples were at -3, -9, -10, -15, -20, and -85 cm; the beginning of the Holocene transgression was not reached in this core. The lowest sample (-85 cm) contained an assemblage composed of 60 percent bay species and 40 percent delta species. Plants were the only organic remains in the samples at -20 and -15 cm. The higher samples (-10, -9, and -3 cm) were all dominated by deltaic species, which make up the modern Norton Sound faunas in this area (fig. 10).

Core 78-3 and core 77-17 were south of Nome, Alaska (lat 64,55° N., long 165.29° W., and lat 64.05° N., long 165.29° W., respectively; fig. 2), in an area dominated by the bay biofacies. Assemblages containing as much as 20 percent bay/inner-shelf biofacies were obtained just east of these sites, and assemblages dominated by the delta biofacies just west of the sites. Information from core 77-17 was used to supplement the unsampled part of core 78-3. Samples in core 78-3 were taken at approximately 50-cm intervals between -100 and -550 cm; core 77-17 was sampled at 50-cm intervals from -5 to -130 cm. The Holocene transgression begins above the plant-dominated assemblages at -30 cm in core 78-3 (C. H. Nelson, oral commun., 1980). The benthic foraminiferal assemblages between -5 and -300 cm in these cores are dominated by species indicative of the bay biofacies. Evidence of an initial delta fauna was not found in these cores. A minor number of bay/inner-shelf species appeared at -5 cm. Delta species also appear as minor components in the assemblages at -50 and -5 cm. No plant-fragment-dominant interval was evident in the upper part of the core (fig. 11).

Core 78-15 was west of Port Clarence (lat 65.14° N., long 167.25° W.; fig. 2), in an area now dominated by bay and bay/inner-shelf species. The Holocene transgression begins above the peat at -144 cm (C. H. Nelson, oral commun., 1980). The upper part of the core was sampled at -130, -80, -30, and -3 cm. Benthic foraminifers at -130 cm represent the delta biofacies. The delta assemblage is overlain by plant dominated intervals at -80 and -30 cm. The highest sample resembles the modern fauna in this area: 17 percent delta biofacies, 67 percent bay biofacies, and 15 percent bay/inner-shelf biofacies (fig. 12).

PALEOENVIRONMENTAL INTERPRETATION OF THE HOLOCENE TRANSGRESSION

Biofacies analysis of these five cores indicates changes in the biologic and physical conditions of Norton Sound. Two benthic assemblages are recognized in the cores examined. The lower benthic foraminiferal faunas indicate biofacies patterns that differ from the modern pattern; the upper benthic foraminiferal faunas resemble modern faunas and represent similar biofacies patterns. The two assemblages are separated by several plant-fragment-rich intervals in all cores but one.

When the Shpanberg Strait was breached, marine waters encroached from the south. The initial benthic foraminiferal faunas indicate very shallow water depths (<10 m) and low salinities; these initial faunas were observed only in the western cores (78-22, 78-15). The next fauna to appear is dominated by species of the bay biofacies. Environmental changes included increased water depths and increased salinities. The presence of bay/inner-shelf and transitional species in several lower samples suggests that transgressive water depths reached the present level or that salinities increased to 31°/₀₀.

In cores 78-22, 76-145, and 78-15, an interval barren of benthic foraminifers and dominated by plant fragments separates the lower from the upper assemblages and abruptly alters the benthic foraminiferal assemblages. This change in faunas may indicate the time at which the Yukon River began actively to influence the water quality and sedimentation in Norton Sound (Nelson, this volume). The upper benthic foraminiferal assemblages and biofacies patterns resemble modern assemblages and patterns. The modern foraminiferal assemblage is strongly influenced by the Yukon River.

Conclusions

Three biofacies can be recognized in the shallow waters of Norton Sound: bay, bay/inner-shelf, and delta. The faunal species and the distribution of the biofacies are influenced by such physical factors as salinity, water temperature, and sedimentation. These modern biofacies are useful in interpreting the paleoenvironmental conditions in Norton Sound since the Holocene transgression began. As sea level rose Norton Sound was first occupied by low-salinity waters that became progressively more marine and deeper. Then water quality or sediment regime changed possibly because of changes in the Yukon River discharge and formation of the modern lobe about 2,500 B.P. (Nelson, this volume). Above the level of this change, benthic foraminiferal assemblages have the same distribution and interrelations as the modern faunas.

Acknowledgments

C. H. Nelson directed the surface and subsurface sampling of Norton Sound. J. A. Barron examined the smear slides for floral groups. M. G. Murphy and Jonathan Schneider prepared the samples and figures.

References cited

Anderson, G. J., 1963, Distribution patterns of Recent foraminifera of the Bering Sea: Micropaleontology, v. 9, no. 3, p. 305-317.

Beljaeva, N. V., 1960, Distribution of Foraminifera in the western part of the Bering Sea: Akademiya Nauk SSSR Institut Okeanologii Trudy, v. 32, p. 158-170.

Cacchione, D. A., Drake, D. E., and Nelson, C. H., 1977, Sediment transport in Norton Sound, Alaska [abs.]: EOS (American Geophysical Union Transactions), v. 58, no. 6, p. 408.

Coachman, L. K., Aagaard, K., and Tripp, R. B., 1975, Bering Strait, the regional physical oceanography: Seattle, University of Washington Press, 172 p.

Cooper, S. C., 1964, Benthonic foraminifera of the Chukchi Sea: Cushman Foundation for Foraminiferal Research Contributions, v. 15, p. 79-104.

Echols, R. J., and Fowler, G. A., 1973, Agglutinated tintinnid loricae from some Recent and Late Pleistocene shelf sediments: Micropaleontology, v. 19, no. 4, p. 431-443.

Herman, Yvonne, 1974, Marine geology and oceanography of the Arctic seas: New York, Springer-Verlag, 397 p.

Hopkins, D. M., 1972, The paleogeography and climatic history of Beringia during late Cenozoic time: Inter-Nord 12, p. 121-150.

_____1973, Sea level history in Beringia during the past 250,000 years: Quaternary Research, v. 3, no. 4, p. 520-540.

Hopkins, D. M., Nelson, C. H., Perry, R. B., and Alpha, T. R., 1976, Physiographic subdivisions of the Chirikov Basin, northern Bering Sea: U.S. Geological Survey Professional Paper 759-B, p. B1-B7.

Knebel, H. J., and Creager, J. S., 1973, Sedimentary environments of the east-central Bering Sea continental shelf [Alaska]: Marine Geology, v. 15, no. 1, p. 25-47.

Knebel, H. J., Creager, J. S., and Echols, R. J., 1974, Holocene sedimentary framework, east-central Bering Sea continental shelf, in Herman, Yvonne, ed., Marine geology and oceanography of the Arctic seas: New York, Springer-Verlag, p. 157-172.

Kummer, J. T., and Creager, J. S., 1971, Marine geology and Cenozoic history of the Gulf of Anadyr: Marine Geology, v. 10, no. 4, p. 257-280.

McManus, D. A., Kelley, J. C., and Creager, J. S., 1969, Continental shelf sedimentation in an Arctic environment: Geological Society of America Bulletin, v. 80, no. 10, p. 1961-1983.

McManus, D. A., Kolla, Venkatarathnam, Hopkins, D. M., and Nelson, C. H., 1974, Yukon River sediment on the northernmost Bering Sea Shelf: Journal of Sedimentary Petrology, v. 44, no. 4, p. 1052-1060.

_____1977, Distribution of bottom sediments on the Continental Shelf, northern Bering Sea: U.S. Geological Survey Professional Paper 759-C, p. C1-C31.

Nelson, C. H., 1978, Faulting, sediment instability, erosion, and depositional hazards of the Norton Basin seafloor, in Annual report of the principal investigator for the year ending March 1978: Boulder, Colo., U.S. Department of Commerce, NOAA Environmental Research Laboratory, p. A1-617.

Nelson, C. H., Cacchione, D. A., Field, M. E., and others, 1977, Complex ridge and trough topography on shallow, current-dominated shelf, northwest Alaska [abs.]: American Association of Petroleum Geologists Bulletin, v. 61, no. 5, p. 817.

Nelson, C. H., and Creager, J. S., 1977, Displacement of Yukon-derived sediment from Bering Sea to Chukchi Sea during Holocene time: Geology, v. 5, no. 3, p. 141-146.

Nelson, C. H., and Hopkins, D. M., 1972, Sedimentary processes and distribution of particulate gold in northern Bering Sea: U.S. Geological Survey Professional Paper 689, 27 p.

Nelson, C. H., Hopkins, D. M., and Scholl, D. W., 1974, Tectonic setting and Cenozoic sedimentary history of the Bering Sea, in Herman, Yvonne, ed., Marine geology and oceanography of the Arctic seas: New York, Springer-Verlag, p. 119-140.

Plate 1

1. Psammosphaera fusca Schulze, sample Mf3928, 0-1 cm. Bar equals 100 um.
2. Protoschista findens (Parker), sample Mf3928, 0-1 cm. Bar equals 100 um.
3. Reophax arctica Brady, sample Mf3934, 0-1 cm. Bar equals 100 um.
4. Reophax curtus Cushman, sample Mf5036, 0-1 cm. Bar equals 100 um.
5. Reophax scotti Chaster, sample Mf3934, 0-1 cm. Bar equals 100 um.
6. Reophax subfusiformis Earland, sample Mf3934, 0-1 cm. Bar equals 300 um.
7. Milliammina fusca (Brady), sample Mf3934, 0-1 cm. Bar equals 300 um.
8. Ammotium cassis (Parker), sample Mf3934, 0-1 cm. Bar equals 300 um.
9. Trochammina nitida Brady, sample Mf5028, 0-1 cm. Bar equals 30 um.
10. Eggerella advena (Cushman), sample Mf3934, 0-1 cm. Bar equals 100 um.
11. Quinqueloculina sp., sample Mf5036, 0-1 cm. Bar equals 30 um.
12. Quinqueloculina subrotunda (Montagu), sample Mf3934, 0-1 cm. Bar equals 100 um.
13. Guttulina lactea (Walker and Jacob), sample Mf3928, 0-1 cm. Bar equals 30 um.
14. Guttulina austriaca d'Orbigny, sample Mf3934, 0-1 cm. Bar equals 100 um.
15. Discorbis baccata (Heron-Allen and Earland), sample Mf3928, 0-1 cm. Bar equals 30 um.
16. Neoconbrina sp., sample Mf3934, 0-1 cm. Bar equals 100 um.
17. Buccella frigida (Cushman), sample Mf3934, 0-1 cm. Bar equals 100 um.
18. Elphidium bartletti Cushman, sample Mf3934, 0-1 cm. Bar equals 100 um.
19. Elphidium clavatum Cushman, sample Mf5028, 0-1 cm. Bar equals 30 um.
20. Elphidium albiumbilicatum (Weiss), sample Mf3934, 0-1 cm. Bar equals 100 um.

Figure 1.--Index map of study area in northern Bering Sea and southern Chukchi Sea.

Figure 2.--Locations of surface samples (▲) and cores (0). East-west and north-south lines indicate cross sections in figures 6 and 7.

Figure 3.--Distribution of bay biofacies in Norton Sound. Percentage of indicative bay specimens in each sample is contoured to show distribution pattern.

Figure 4.--Distribution of bay/inner-shelf biofacies in Norton Sound. Percentage of indicative bay/inner-shelf specimens in each sample is contoured to show distribution pattern.

Figure 5.--Distribution of delta biofacies in Norton Sound. Percentage of indicative delta specimens in each sample is contoured to show distribution pattern.

Figure 6.--Foraminiferal composition and depth. West-to-east transect through Norton Sound shows that percentage of bay/inner-shelf species (vertical lines) in surface samples decreases as water depths decrease, whereas percentage of the bay (dots) and delta (horizontal lines) species increases. The unpatterned area represents those species not associated with any of the three recognized biofacies.

Figure 7.--Foraminiferal composition and depth. North-to-south transect through Norton Sound shows that bay/inner-shelf species (vertical lines) occur only in deeper northern part of Norton Sound and that percentage of delta species (horizontal lines) increases rapidly near the Yukon River. Only a small percentage of foraminiferal faunas is not associated with one of the recognized biofacies.

1
2
3
4
5
6
7
8
9
10
11
12
13
14
15
16
17
18
19
20

Figure 8.--Distribution of associated microfossil groups. Ostracods and tintinnids were common in eastern part of Norton Sound, whereas diatoms were common in samples from western part.

Figure 9.--Faunal composition of core 78-22. Foraminiferal assemblages in lower part of core are dominated by delta species (horizontal lines); bay species (dots) and species representing transitional biotope of Anderson (1963) are also present. Above interval of plant fragments, benthic foraminiferal species of bay biofacies predominate.

Figure 10.--Faunal composition of core 76-145 (including core 76-145B). Foraminiferal assemblages in lower part of core contain nearly equal proportions of delta (horizontal lines) and bay (dots) species. Above interval of plant fragments, delta species predominate.

Figure 11.--Faunal composition of cores 78-3 and 77-17. Benthic foraminiferal species characteristic of bay biofacies (dots) predominate throughout.

Figure 12.--Faunal composition of core 78-15. Benthic foraminiferal species characteristic of delta biofacies (horizontal lines) predominate in assemblages below plant-fragment-dominated interval, whereas bay (dots) predominate above.

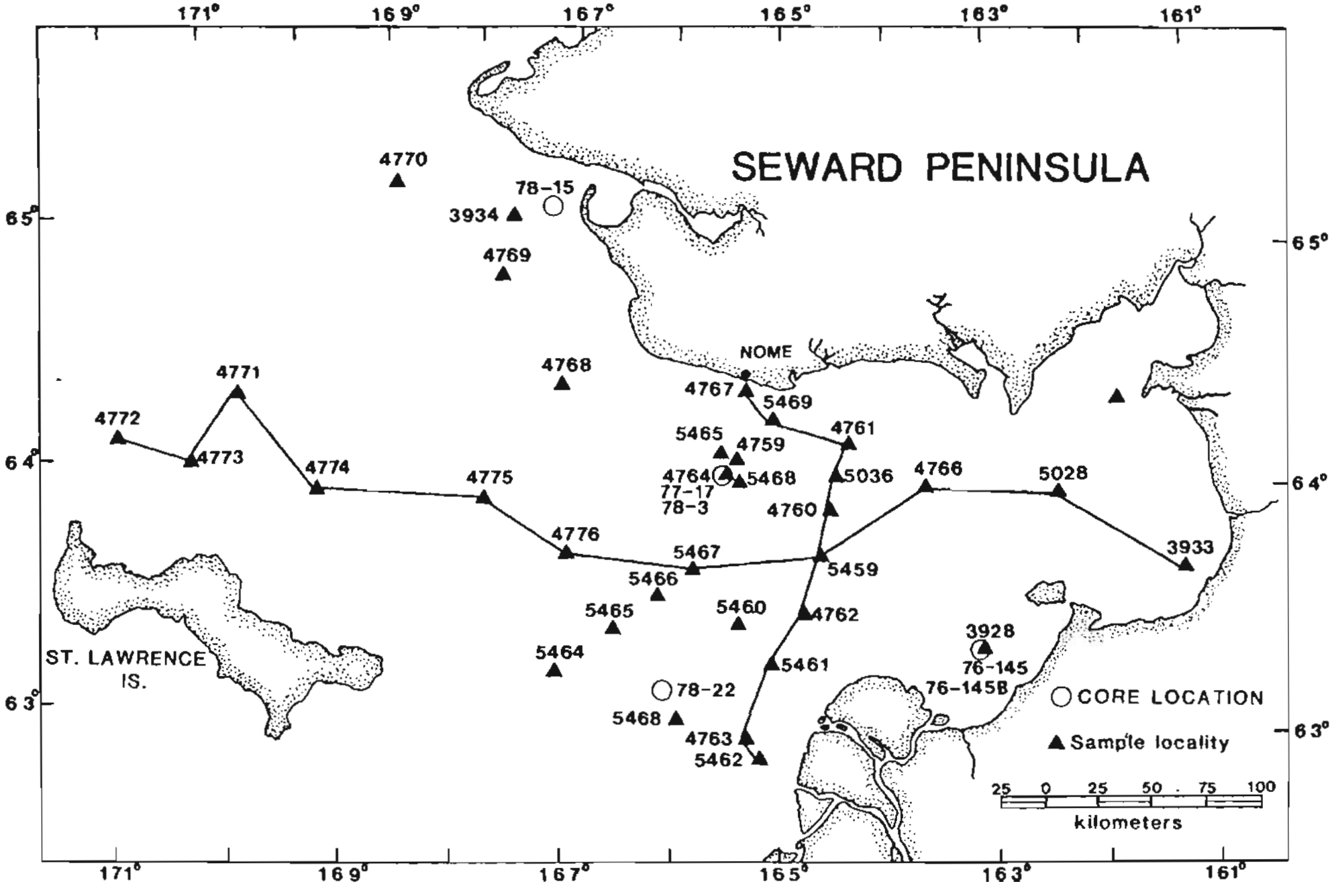
SEWARD PENINSULA
NOME
ST. LAWRENCE IS.
171°
169°
167°
165°
163°
161°
65°
64°
63°
4770
78-15
3934
4769
4768
4771
4772
4773
4774
4775
4776
4767
5469
4761
5465
4759
4764
77-17
78-3
5468
5036
4766
5028
4760
3933
5467
5459
5466
5465
5460
4762
3928
76-145
5464
5461
76-145B
78-22
5468
4763
5462
CORE LOCATION
Sample locality
25 0 25 50 75 100
kilometers

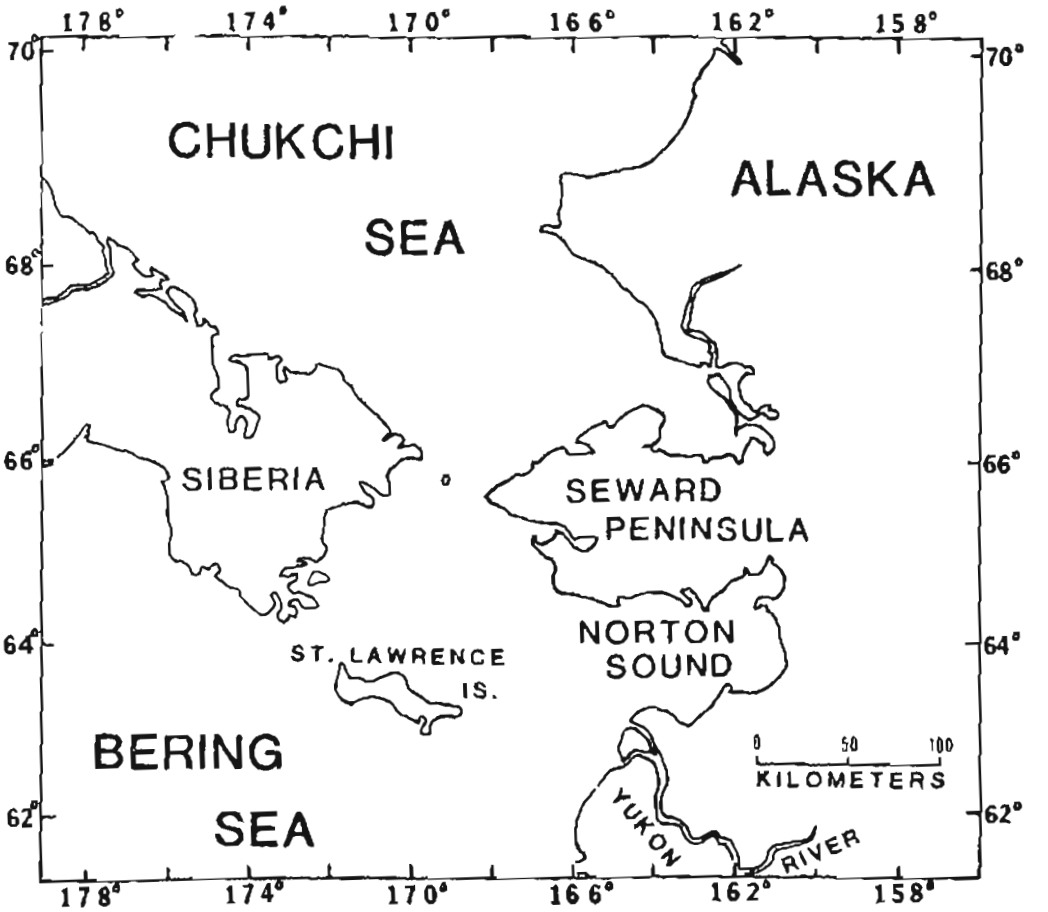
178°
174°
170°
166°
162°
158°
70°
68°
66°
64°
62°
CHUKCHI
SEA
ALASKA
SIBERIA
SEWARD
PENINSULA
NORTON
SOUND
ST. LAWRENCE
IS.
BERING
SEA
0 50 100
KILOMETERS
YUKON
RIVER

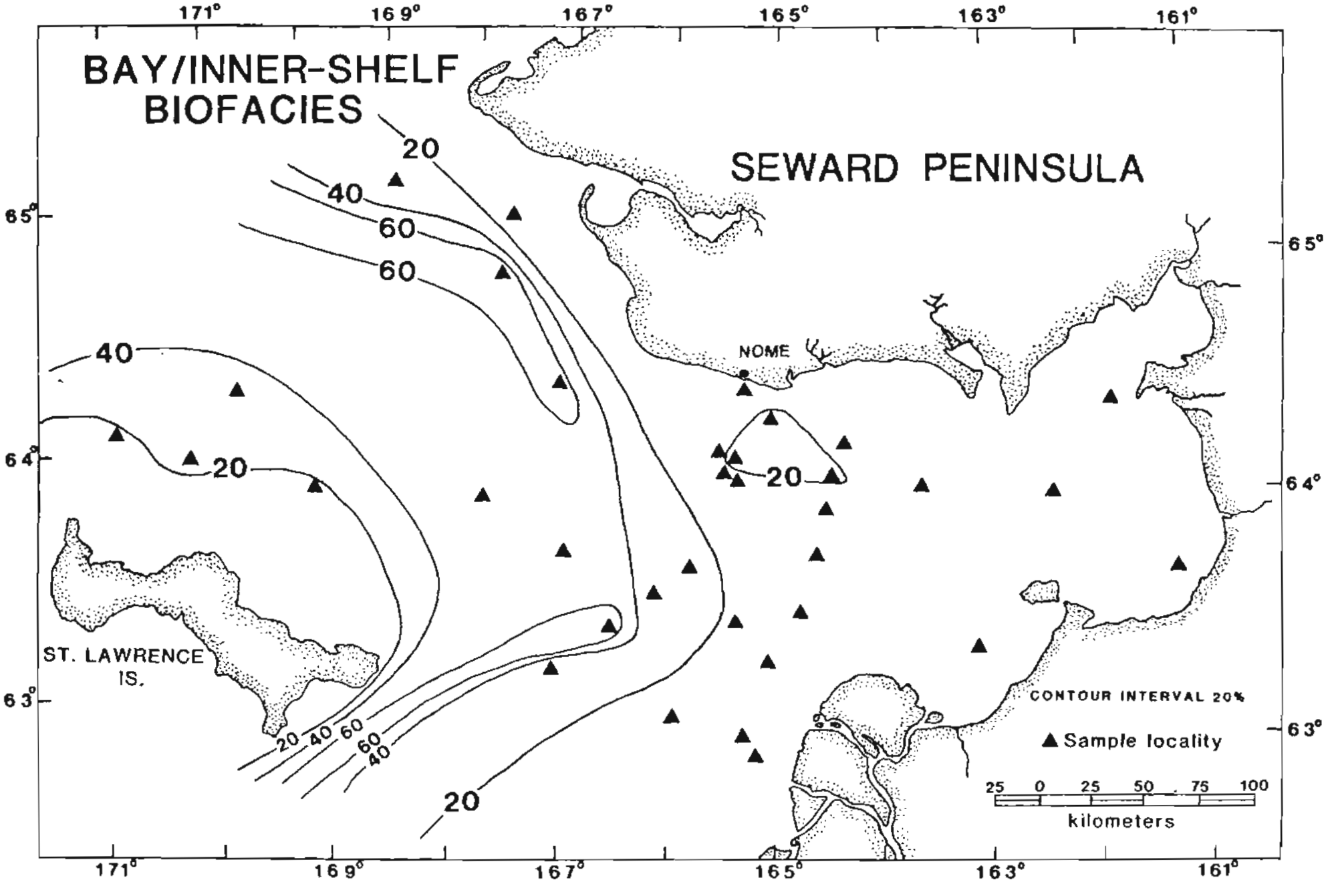
BAY/INNER-SHELF
BIOFACIES
SEWARD PENINSULA
NOME
ST. LAWRENCE
IS.
20
40
60
60
40
20
20
20
40
60
60
40
20
171°
169°
167°
165°
163°
161°
65°
64°
63°
CONTOUR INTERVAL 20%
Sample locality
25 0 25 50 75 100
kilometers

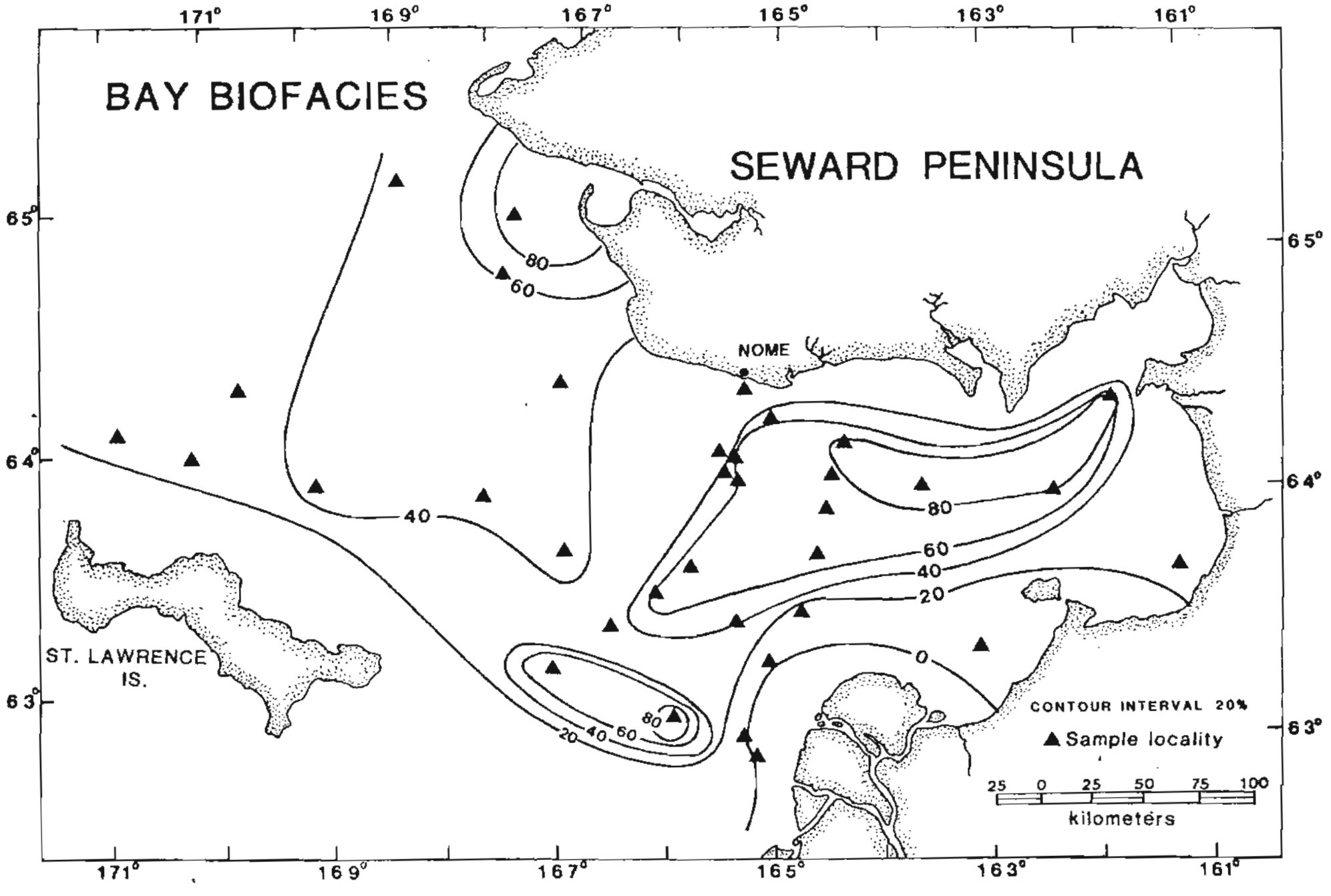
BAY BIOFACIES
SEWARD PENINSULA
NOME
ST. LAWRENCE IS.
171°
169°
167°
165°
163°
161°
65°
64°
63°
80
60
40
20
0
CONTOUR INTERVAL 20%
▲ Sample locality
25 0 25 50 75 100
kilometers

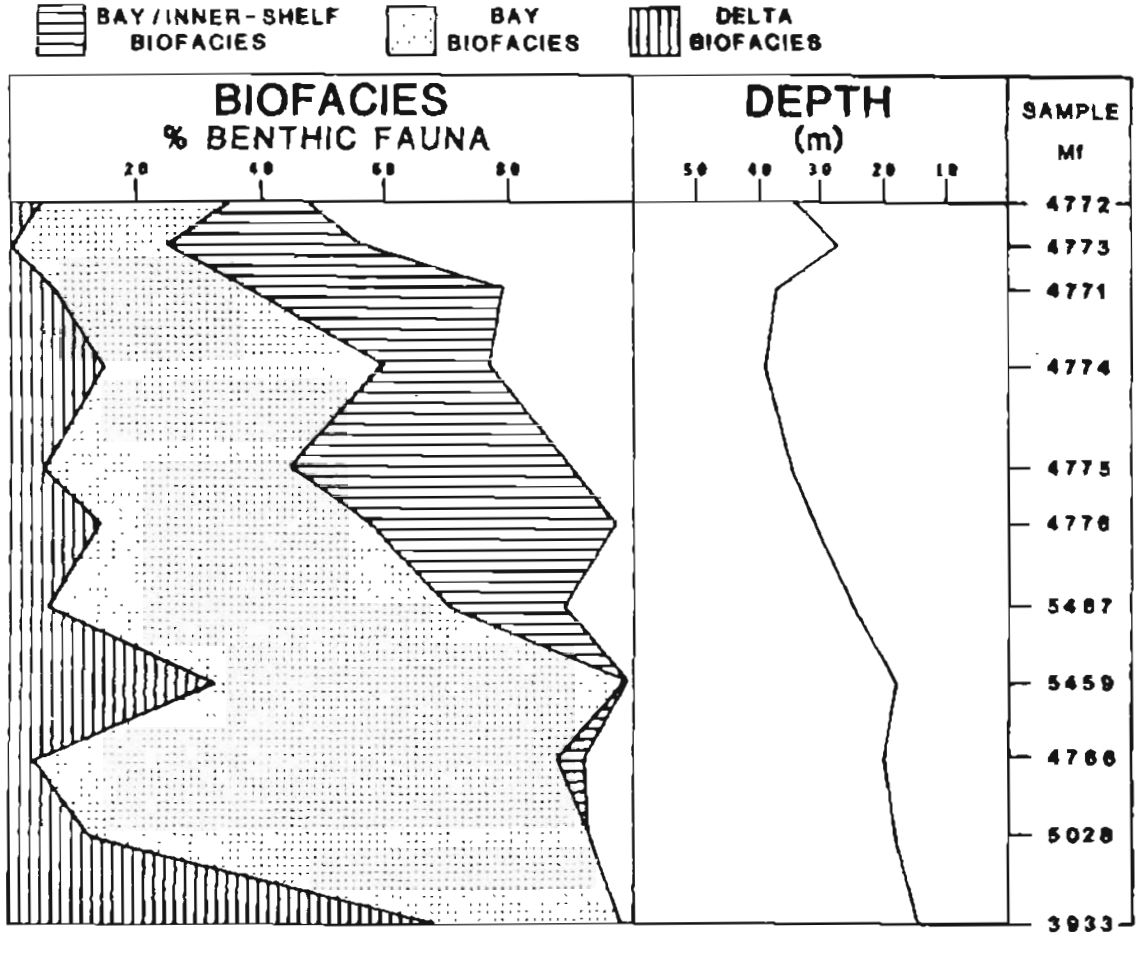
BAY / INNER-SHELF BIOFACIES
BAY BIOFACIES
DELTA BIOFACIES
BIOFACIES
% BENTHIC FAUNA
20
40
60
80
DEPTH
(m)
50
40
30
20
10
SAMPLE
Mf
4772
4773
4771
4774
4775
4776
5487
5459
4766
5028
3933

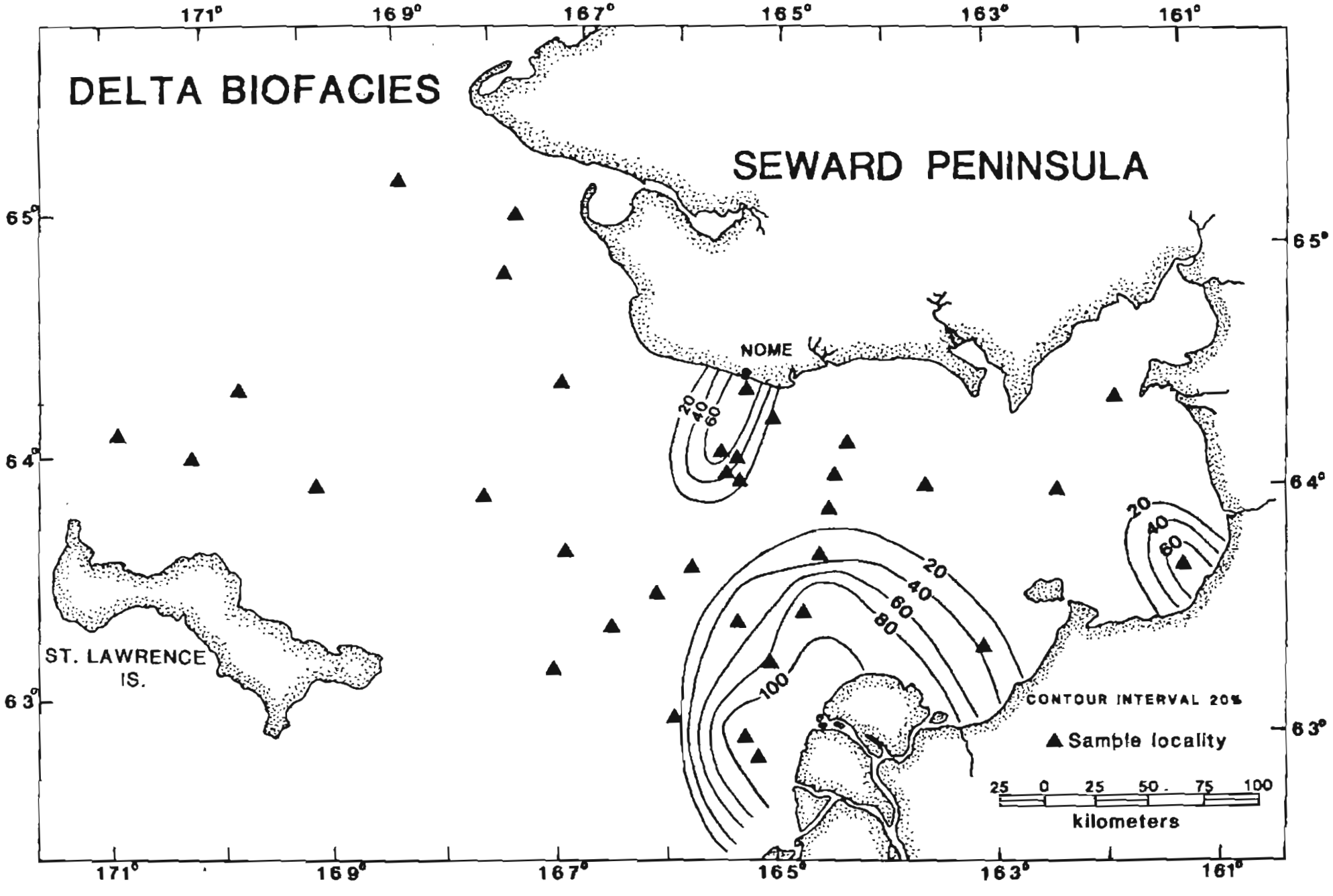
DELTA BIOFACIES
SEWARD PENINSULA
171°
169°
167°
165°
163°
161°
65°
64°
63°
NOME
20
40
60
80
100
ST. LAWRENCE
IS.
CONTOUR INTERVAL 20%
Sample locality
25 0 25 50 75 100
kilometers

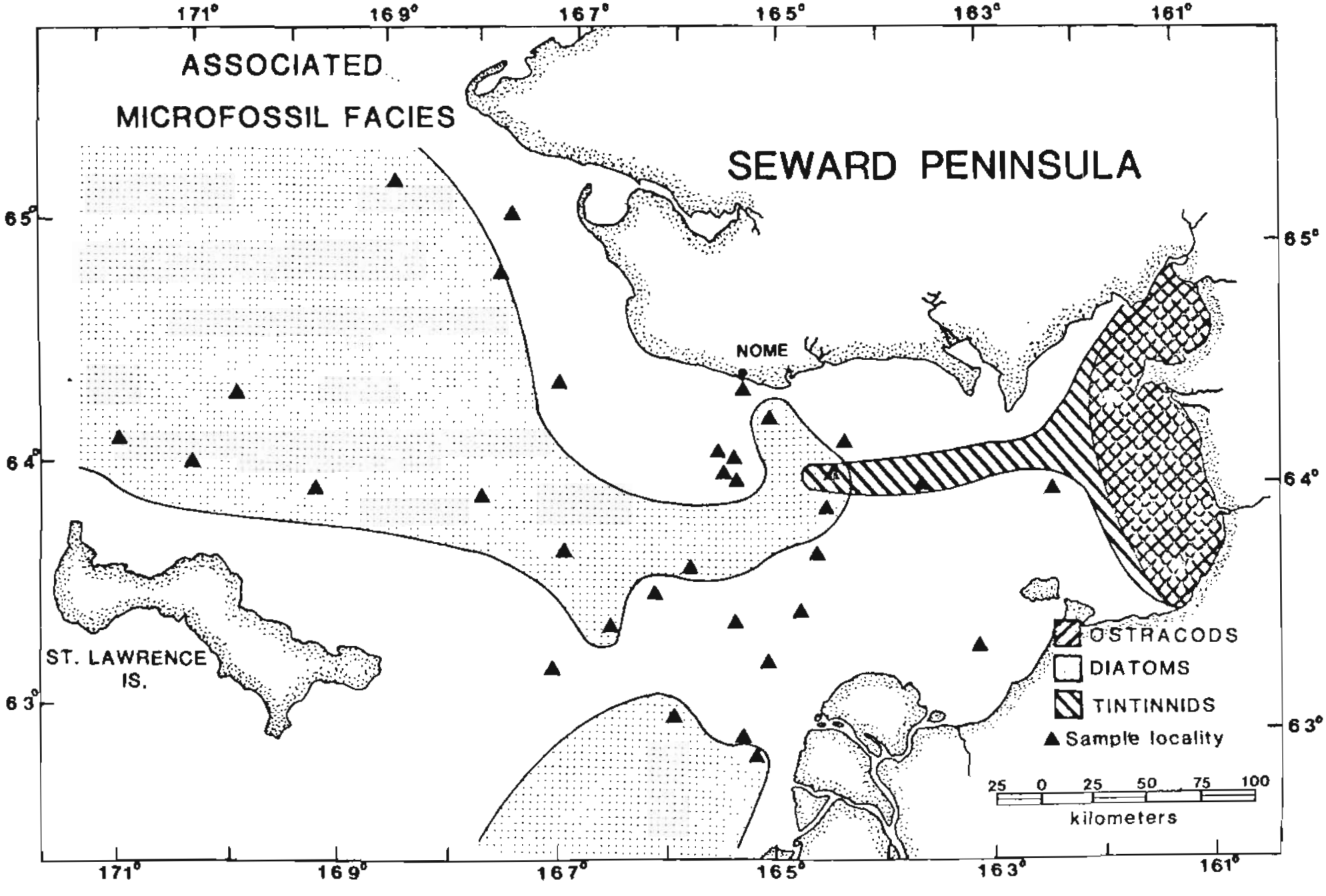
ASSOCIATED
MICROFOSSIL FACIES
SEWARD PENINSULA
NOME
ST. LAWRENCE
IS.
171°
169°
167°
165°
163°
161°
65°
64°
63°
OSTRACODS
DIATOMS
TINTINNIDS
Sample locality
25 0 25 50 75 100
kilometers

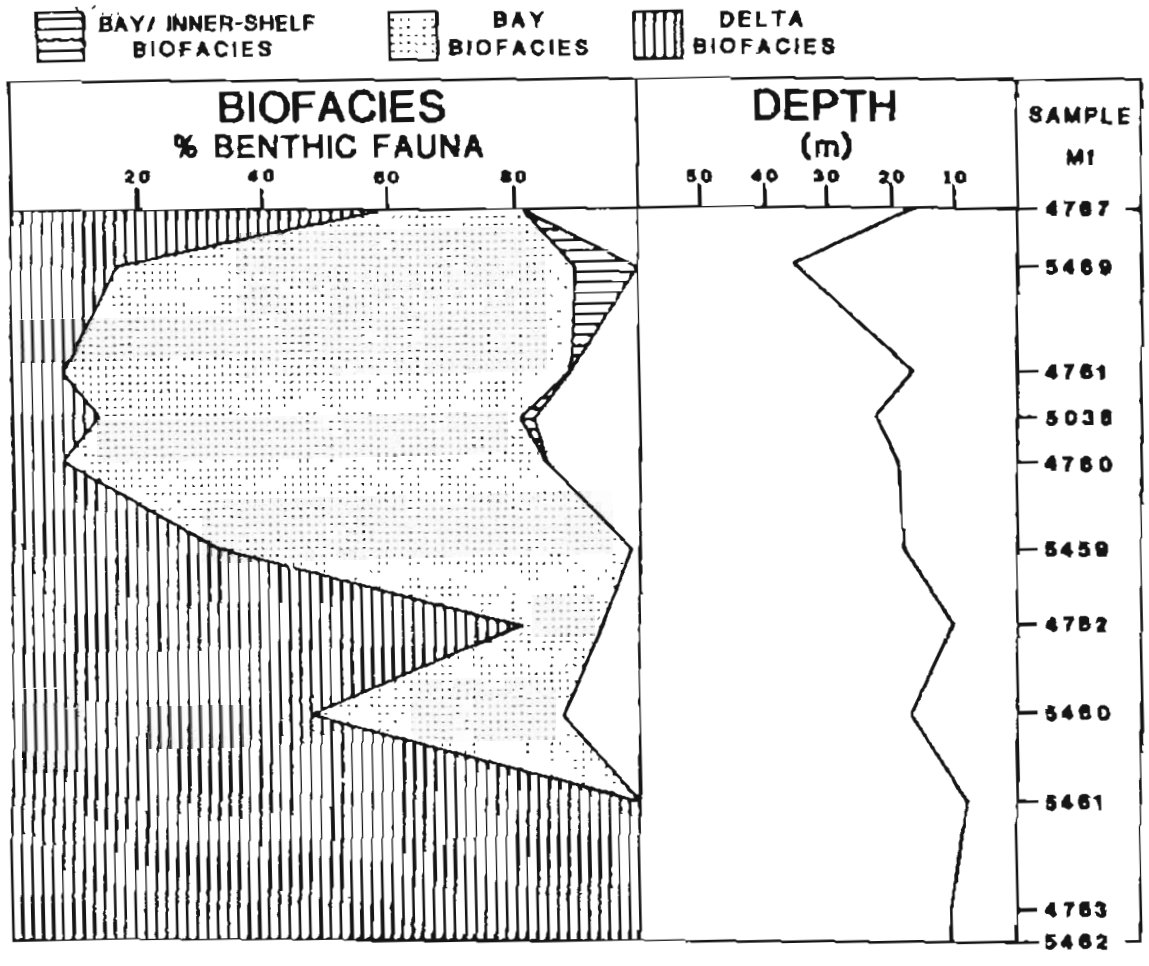
BAY/ INNER-SHELF BIOFACIES
BAY BIOFACIES
DELTA BIOFACIES
BIOFACIES
% BENTHIC FAUNA
20
40
60
80
DEPTH
(m)
50
40
30
20
10
SAMPLE
M1
4787
5469
4761
5038
4760
5459
4782
5460
5461
4763
5462

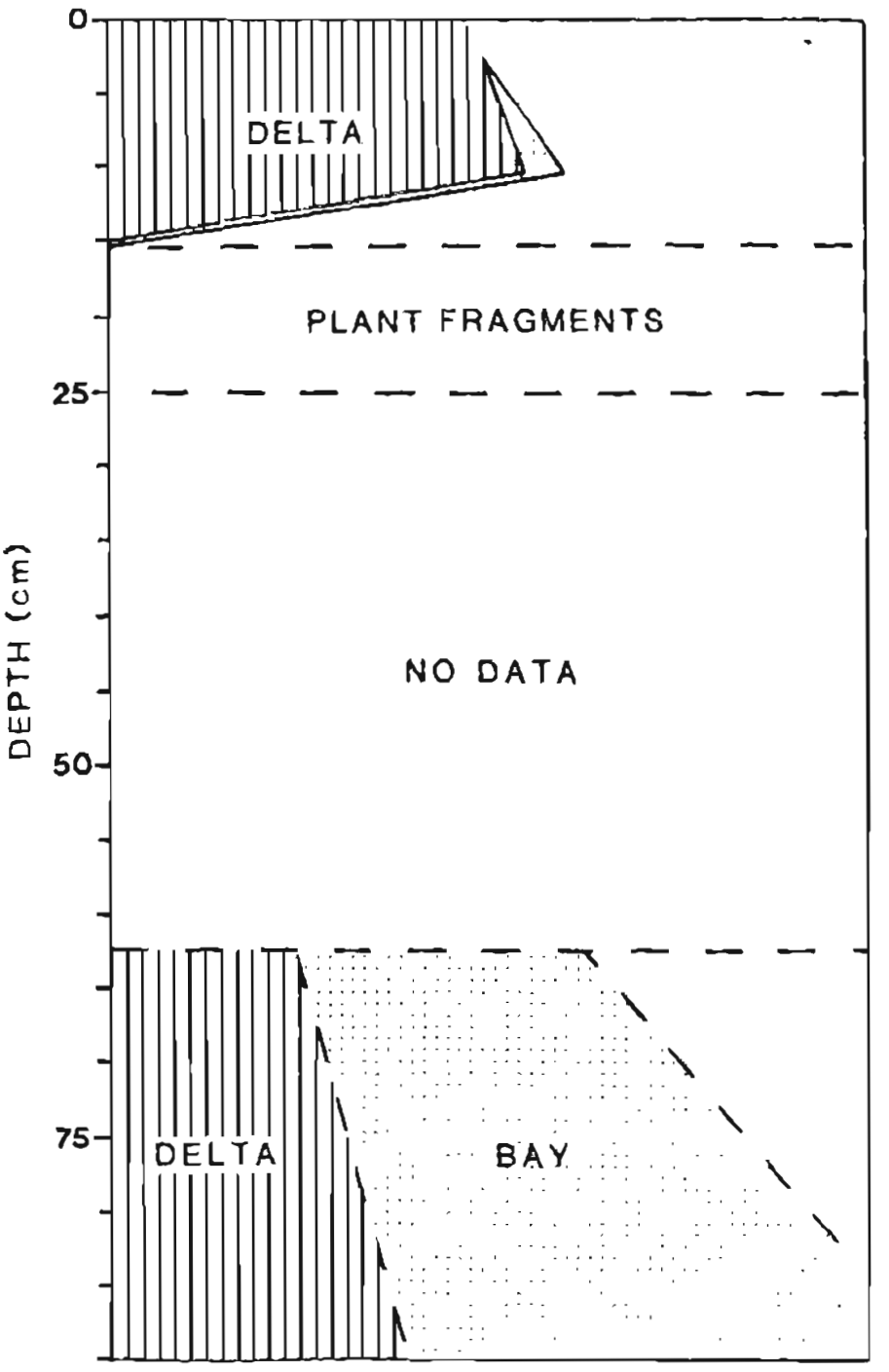
CORE 76-145
0
DELTA
PLANT FRAGMENTS
25
NO DATA
50
DEPTH (cm)
75
DELTA
BAY

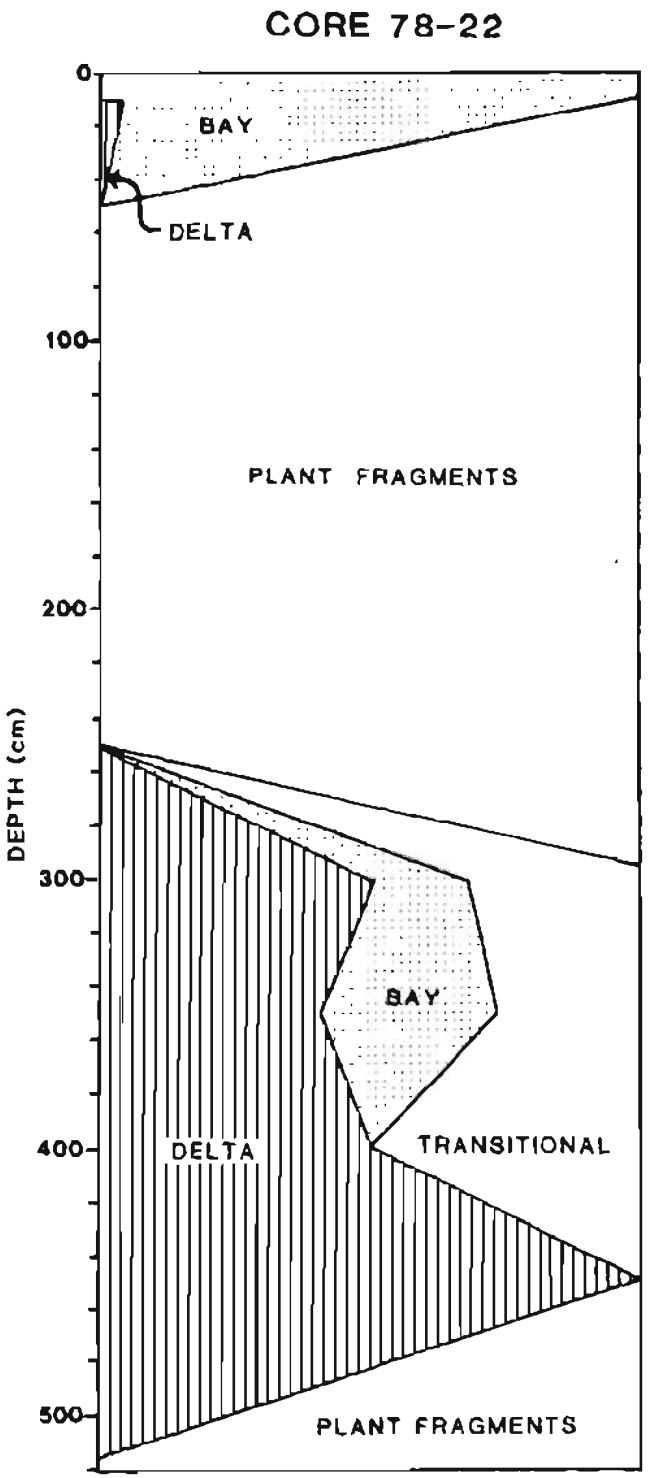
CORE 78-22
0
100
200
300
400
500
DEPTH (cm)
BAY
DELTA
PLANT FRAGMENTS
BAY
DELTA
TRANSITIONAL
PLANT FRAGMENTS

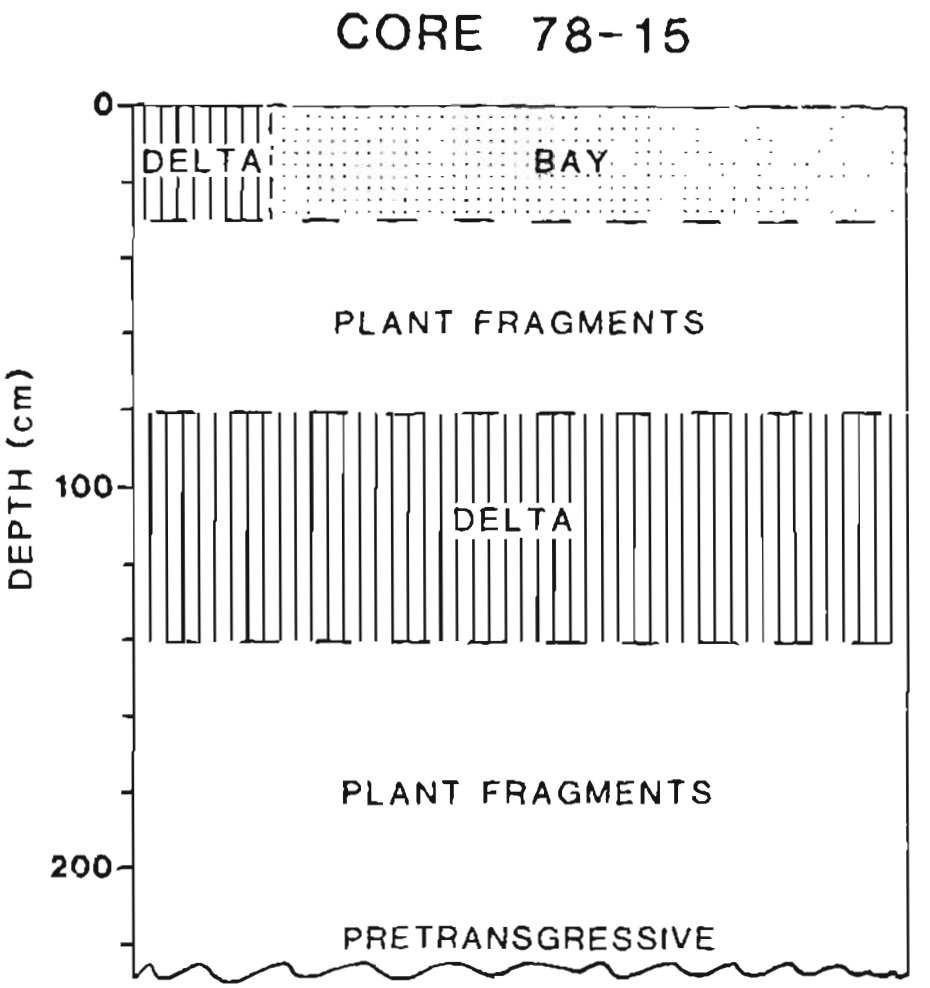
CORE 78-15
0
DELTA
BAY
PLANT FRAGMENTS
DEPTH (cm)
100
DELTA
PLANT FRAGMENTS
200
PRETRANSGRESSIVE

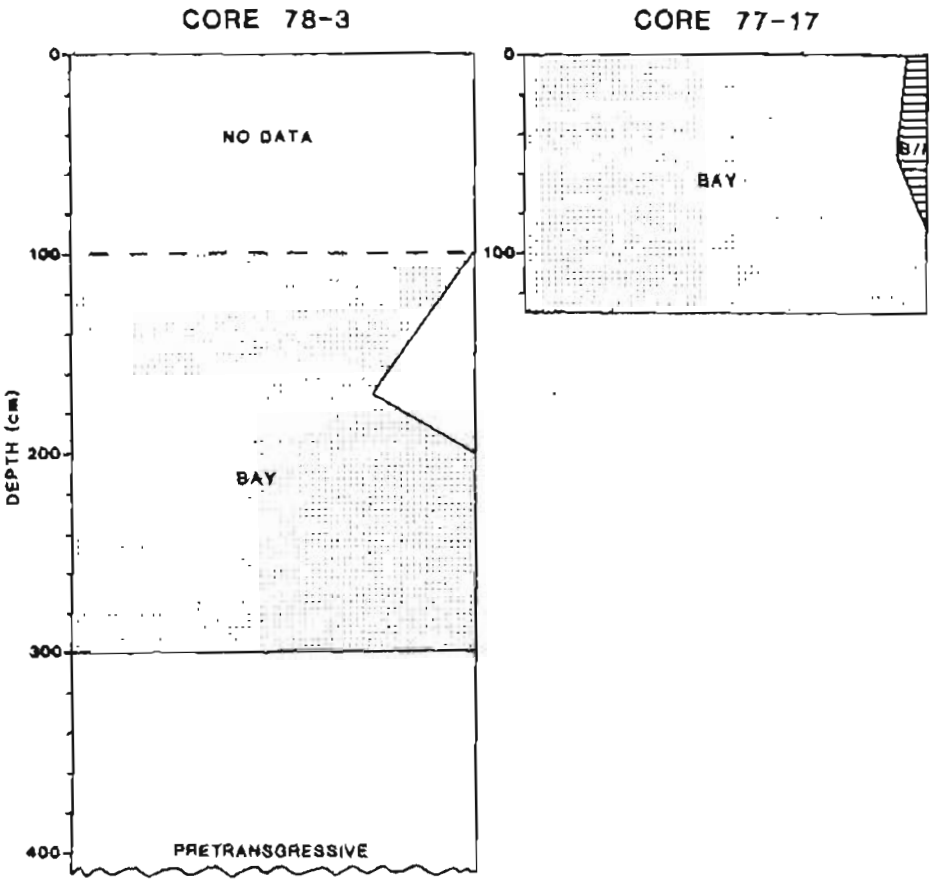
CORE 78-3
CORE 77-17
0
100
200
300
400
DEPTH (cm)
NO DATA
BAY
PRETRANSGRESSIVE
BAY

INTRODUCTION

Norton Sound is a large shallow reentrant of the Bering Sea with water depths of less than 25 m, mostly less than 20 m, over an area of 24,000 km^2 (Fig. 1). Sediment is primarily derived from the Yukon River, one of the largest sources in North America, and discharges via the active Yukon Delta lobe in southern Norton Sound (Dupre, this volume). Much of this sediment, however, has a short residence time in the Norton Basin; instead, it is transported northward into the Chukchi Sea by the Alaskan Coastal Water (Nelson and Creager, 1977) that flows north along the west side of the Yukon Delta and Norton Sound. Thus, although the Yukon Delta is presently prograding into Norton Sound, relatively little sediment is accumulating beyond the delta front because large quantities of sediment are resuspended by storm-surge events and carried off by strong geostrophic currents (Drake et al., 1980). This is an atypical delta-influenced system because the delta is building into a non-subsiding depositional basin across a sequence of relict sediments that were subaerially exposed during Pleistocene time (Nelson and Creager, 1977).

Sediment facies in the wedge of delta-front platform deposits and prodelta bioturbated muds are defined in this paper. Past changes in sea level and progradation of the delatic facies here result in an alternating stratigraphic sequence of nearshore and offshore facies.

Sediment cores in Norton Sound were collected using a Naval Electronics Lab (NEL) box corer modified from the origial Kastengrifer of Reineck (1963). The box core is capable of taking a large (20 x 30 x 64 cm) undisturbed core. However, maximum penetration of 64 cm was rarely achieved because of substrate resistance.

SEDIMENTARY STRUCTURES ON A DELTA-INFLUENCED SHALLOW SHELF, NORTON SOUND, ALASKA

James D. Howard, Skidaway Inst. of Oceanography, Savannah, Georgia

C. Hans Nelson, U.S. Geological Survey, Menlo Park, California 94025

ABSTRACT

Sedimentation in an epicontinental sea influenced by deltaic progradation is exemplified by the Norton Sound-Yukon Delta region. Norton Sound is a large embayment of more than 24,000 km^2 with water depths of less than 25 m. The Yukon Delta, on the south side, is a major North American source of sediment that enters the Sound. Progradational deposits on the seaward part of the delta are highly reworked by storm waves and currents, and serve as a model for a depositional sequence that encroaches on a shallow shelf. To describe the primary physical and biogenic sedimentary structures of the several facies in this embayment, we utilized X-ray radiographs, relief casts, and grain-size analyses of 83 box cores.

Primary physical sedimentary structures are best developed in and adjacent to the Yukon Delta and include parallel- and ripple-laminated sand and silt and crossbedded sand. Biogenic sedimentary structures are found throughout Norton Sound and, in the northern part, completely obliterate physical sedimentary structures. Bioturbation close to the northern shoreline suggests that rates of sedimentation there are low. Dominance of physical structures near the delta results from (1) increased wave and current energy in this very shallow water, (2) reduced biological activity in brackish water, and (3) increased rates of deposition. As a result, the Holocene progradational sequence in Norton Sound consists of basal beds with well-developed physical structures deposited during lower eustatic sea level, a thin middle interval of bioturbated mud and a thick upper section of structured beds deposited by the prograding delta.

Clean sand (less than 10% silt and clay) is limited mostly to the delta-front platform and the seafloor on the western side of Norton Sound (Fig. 3). As discussed by Duprè and Thompson (1979), clean sand on the Yukon Delta front is the result of wave reworking that removes the finer fraction. The presence of clean sand to the southwest of the delta and in the tongue in the southwest part of the study area (Fig. 3) reflects the current shear of the Alaska Coastal Water on the eastern side of Shpanberg Strait as the water moves toward the Bering Strait and into the Chukchi Sea. Currents in this area during storms reach 100 cm/s and are more than adequate to remove the silt and clay fractions (see Fig. 1 of Nelson, this volume).

Silty sand that dominates most of the western open area of Norton Sound is likewise a reflection of the influence of the Alaskan Coastal Water. The eastern margin of the silty sand in this area appears to mark the western edge of the principal path of the north-moving water mass containing Yukon sediment. Elsewhere in Norton Sound two patches of silty sand appear to be controlled by bathymetry.

Sandy silt makes up most of the central Norton Sound area. The distribution pattern for this sediment shows (1) the influence of sediment delivered from the Yukon River discharge, (2) the reduced current speed of the Alaskan Coastal Water, and, (3) the presence of a trough deeper than 20 m water depth oriented roughly east-west in the north-central part of the Basin.

Silt is the dominant sediment along the eastern margin of Norton Sound north of St. Michaels. The area is a protected corner of the Sound without a local sand source.

In spite of the distinct and recognizable depositional patterns that emerge from this mapping of textures from box-core samples, it is important to point out that the box cores rarely penetrated more than 30 cm. From our

INTRODUCTION

Norton Sound is a large shallow reentrant of the Bering Sea with water depths of less than 25 m, mostly less than 20 m, over an area of 24,000 km^2 (Fig. 1). Sediment is primarily derived from the Yukon River, one of the largest sources in North America, and discharges via the active Yukon Delta lobe in southern Norton Sound (Dupre, this volume). Much of this sediment, however, has a short residence time in the Norton Basin; instead, it is transported northward into the Chukchi Sea by the Alaskan Coastal Water (Nelson and Creager, 1977) that flows north along the west side of the Yukon Delta and Norton Sound. Thus, although the Yukon Delta is presently prograding into Norton Sound, relatively little sediment is accumulating beyond the delta front because large quantities of sediment are resuspended by storm-surge events and carried off by strong geostrophic currents (Drake et al., 1980). This is an atypical delta-influenced system because the delta is building into a non-subsiding depositional basin across a sequence of relict sediments that were subaerially exposed during Pleistocene time (Nelson and Creager, 1977).

Sediment facies in the wedge of delta-front platform deposits and prodelta bioturbated muds are defined in this paper. Past changes in sea level and progradation of the delatic facies here result in an alternating stratigraphic sequence of nearshore and offshore facies.

Sediment cores in Norton Sound were collected using a Naval Electronics Lab (NEL) box corer modified from the origial Kastengrifer of Reineck (1963). The box core is capable of taking a large (20 x 30 x 64 cm) undisturbed core. However, maximum penetration of 64 cm was rarely achieved because of substrate resistance.

interbedded sand and mud are also important bedding types. Most of the box cores were taken in water 10 m deep or more and lie in the prodelta facies of Dupré (this volume). Cores on the delta front (29, 47A, 49, 61, 157, and 160) are mostly characterized by ripple and parallel laminae that reflect wave reworking. Cores 49 and 61, which are well bioturbated, are obvious exceptions, but they occur at the margin of a now-abandoned delta distributary.

Biogenic Sedimentary Structures

Organisms have significantly affected the surface sediment of Norton Sound. Figures 2 and 4 depict the influence of biogenic activity in three ways. Figure 2 shows the degree of bioturbation in specific layers of the cores and the specific biogenic sedimentary structures recognized from examination of peels and X-ray radiographs; Figure 4 illustrates the basin-wide pattern of bioturbation. Because the cores were taken without an accompanying zoological study, the specific origin of many of the biological structures is unknown, but some have been identified in another study with associated biological research (Nelson et al., in press). In addition, the identity of some organisms can be inferred based on core studies from other areas and from studies of specific organisms in sediment-filled aquaria (Howard and Frey, 1975a,b).

Most obvious in the Norton Sound box cores is the widespread occurence of total bioturbation (Fig. 4). In the area shown as 90% bioturbated there is little evidence of primary physical sedimentary structures except for an occasional hint of remnant stratificaton. This degree of bioturbation is characteristic of areas that lie below wave base or that are receiving very little new sediment. In the case of Norton Sound, this intensity of bioturbation is probably due to very low rates of accumulation, in places

experience with box coring in a wide variety of environments, this indicates hard substrates and probably low rates of sedimentation. In fine-grained sediment, as most of these are, sediment deposited rapidly is relatively easily penetrated. Furthermore, recently acquired vibracores used in Norton Sound, which provide deeper penetration, show the presence of deep facies different from those that exist today. Radiocarbon dates substantiate that present-day sedimentation in Norton Sound is low except for the immediate vicinity of the delta (see Figs. 3 and 4B of Nelson, this volume).

Plant fragments and shells are accessory sediment components found in the Norton Sound box cores. Thin layers of plant material occur in four cores on the delta margin. All of this material is apparently derived from the delta, which contains abundant organic detritus in platform and channel sediment.

Shells and shell fragments are found in cores throughout the Sound. Most are single or broken valves of pelecypods, and some are whole gastropod shells. The shells appear to be mainly storm transported and reworked into a bioturbated matrix. A few articulated pelecypods and shells in growth positions are observed.

Physical Sedimentary Structures

Most of the Norton Sound box cores are 90% bioturated and the majority are entirely reworked by benthic organisms. It thus appears that rates of sediment accumulation are low in most of Norton Sound. Primary physical sedimentary structures are abundant only in the vicinity of the Yukon Delta where better sorted, cleaner sand occurs. Dominance of physical over biogenic sedimentary structures is apparently in response to shallower water where wave reworking, rapid deposition and low-salinity water inhibit biota development on the delta front. Wave-formed ripple laminae and parallel laminae are the predominant physical sedimentary structures, but crossbedded sand and

structures because polychaetes are somewhat limited in the variety of patterns they can create.

Amphipods created U-shaped burrows, branching burrows and the amphipod bioturbation in the Norton Sound cores. This conclusion is based on comparisons with cores from other areas where more detailed studies have been carried out (Howard and Frey, 1975a,b). Also, in several of the cores containing these structures we found living amphipods. Amphipod-created structures are present throughout Norton Sound, but are least abundant in the vicinity of the Yukon Delta and in the muddy coarser sediment in the northwest part of the basin. The U-shaped burrows attributed to amphipods are most abundant in the northeast part of the Sound, although some similar appearing structures were also found in cores from the central part of Norton Sound. As is true of polychaete burrows, various species of amphipods are capable of making similar structures.

A biogenic structure referred to as "streaked bioturbation" was a prominent feature in five cores in the western, open part of Norton Sound. Although not specifically identified, it is likely that this structure was formed by brittle stars (ophiuroids) because of its strong similarity to features known to be formed by this organism elsewhere (Howard and Frey, 1975b). Another very restricted form, referred to as "concentric-walled burrows," occurs in the vicinity of the Yukon Delta. This burrow is very similar to a structure found in a previous study (Howard and Frey, 1975b) which was referred to as unidentified worm burrow, possibly formed by the polychaete Nereis.

Three adjacent cores (20, 21 and 154) contain spreite structures or concentric vertical burrows (Fig. 2). Such structures, especially when vertically oriented, commonly indicate periods of relatively rapid

<2 cm/1000 years (Nelson and Creager, 1977). As pointed out by Drake et al. (1980), storms can easily rework the substrate of Norton Sound, and most of the shallow floor of the Sound is above storm wave base. Indeed, many of the box cores from water less than 20 m deep show some evidence of stratification. One exception is the nearshore area in the north-central part of the Sound east of Nome. Here a series of cores (25, 27, 33, 34, 35, 36, 37, 101, and 150) are entirely bioturbated. However, all are very short cores owing to the substrate resistance, a characteristic of bottoms that are not receiving new sediment and are commonly erosional.

In the gravelly area near Nome, the degree of bioturbation is speculative. Sediment there appears to be totally bioturbated because there is no hint of any primary physical sedimentary structures; this absence in part may relate to the glacial origin of the sediment (Nelson and Hopkins, 1972). On the other hand, there is no indication of any specific biogenic structures either, which may be due to the predominance of a relict rocky-intertidal-type fauna associated with coarse gravel lag deposits (Nelson et al., in press).

In spite of the highly bioturbated character of most of the Norton Sound sediment, we were able to recognize a number of specific biogenic sedimentary structures. Most were probably formed by polychaete worms and amphipods. The assumed polychaete burrows include large and small, simple, vertical to nearly vertical burrows and, in one core, a horizontal burrow referred to as a polychaete tunnel. These various structures occur throughout the Sound without any apparent relation to water depth or sediment type, except that they are scarce in the vicinity of the Yukon Delta. This lack of variation with depth and texture is not surprising, because in most shelf environments polychaetes are ubiquitous. Probably a variety of species have created these

wave energy that creates physical structures and it traps sediment only intermittently that is carried in by the Alaskan Coastal Water (Nelson and Creager, 1977; Drake et al., 1980).

Another noteworthy aspect of the Norton Sound cores is the abundance of distinct burrows. In offshore sediment it is common to see, as we do here, a higly bioturbated substrate. Generally, however, the resulting fabric has a homogeneity that precludes recognition of any specific structure. In most of the Norton Sound cores, in contrast, we were able to recognize some specific burrow types. The probable reason is a restricted number of species (Nelson et al., in press), and hence the effect of one burrow type cancelling out another is less likely.

The restricted fauna may be due to the harshness of this depositional environment because of large sediment loads and reduced salinity from the nearby discharge of the Yukon River. In addition, most of the species present appear to be suspension rather than substrate feeders and leave no subsurface traces. Whatever the cause, it is surprising that the burrow types and variety and the general biogenic record in Norton Sound, exclusive of the area immediately adjacent to the Yukon Delta, are similar to the biogenic records in Georgia estuarine sediment (Howard and Frey, 1975b). In both areas, polychaete burrows are the dominant preserved biogenic structures, brittle-star-type bioturbaton occurs, and truncated sand-filled burrows and spreite are found locally. This is not to imply that the stratigraphic record of Norton Sound would be confused with an estuarine depositional sequence. It probably would not, but there are many similarities: Norton Sound is a restricted depositional embayment with a large discharge from the Yukon River, low rates of deposition, and occasional storms that cause local scour and at times, rapid deposition.

sedimentation (Howard, 1978). Five cores (15, 16, 25, 122 and 152), from an area immediately northeast of the areas exhibiting spreite, all contain well-defined sand-filled burrows in an otherwise silty substrate. In all cases the burrows are truncated and lie several centimeters below the sediment-water interface. Such features suggest that there was (1) erosion that opened the burrow, followed by (2) transport of sand across the eroded surface that filled the open burrow, then, (3) resumption of normal slow sedimentation and attendant biogenic reworking.

DISCUSSION

An overview of the Norton Sound sediment shows some expected and some unexpected results. In general, an increase in bioturbation away from shore is observed as water depth increases and sediment becomes finer grained. Such a pattern is typical of normal nearshore to shelf sequences because fewer physical structures form as wave energy decreases in deeper water (Howard and Reineck, 1972). This is essentially the case in Norton Sound, where the central basin cores are all highly bioturbated and physical sedimentary structures dominate in the vicinity of the Yukon Delta. However, this is not the case in other parts of Norton Sound where highly bioturbated sediment occurs close to shore.

The reasons for the anomalous bioturbation patterns differ in various parts of Norton Sound. South and west of Nome, strong longshore tidal currents and generally coarse lag sediments occur and no new sediment is being deposited. Likewise, to the east of Nome, in the area of stations 33, 34, 35 and 36, poor penetration by the corer suggests that this is dominantly an erosional coastal zone. The eastern end of Norton Sound is characterized by highly bioturbated cores, and probably is an area of active sedimentation, because cores penetrate deeply. This area appears to be protected from large

ACKNOWLEDGMENTS

We appreciate numerous beneficial discussions with William Dupré on the physical environment of the delta, and with Robert Rowland and Sam Stoker on the biological environment. Richard Brokaw and Matthew Larsen assisted with compilation of data and they, Louise Jaffe, and other scientific staff and crew of the R.V. SEA SOUNDER provided field assistance. Ralph Hunter and Kenneth Bird provided beneficial review comments.

The cruises were supported jointly by the U.S. Geological Survey and by the Bureau of Land Management through interagency agreement with the National Oceanic and Atmospheric Administration, under which a multi-year program responding to the needs of petroleum development of the Alaska continental shelf is managed by the Outer Continental Shelf Environmental Assessment Program (OCSEAP) Office.

Preliminary examination of vibracores taken in 1978 indicates that sediment in central Norton Sound just a few tens of centimeters below the surface was caused by a significantly different set of depositional processes dominated by an energetic depositional system leaving abundant physical sedimentary structures (see Nelson, this volume).

CONCLUSIONS

What is the significance of the present-day sediment of Norton Sound? If we can assume continuation of present-day processes through an extended period of geologic time, the record of today's events would be that of a relatively thin unit of highly bioturbated sediment. It is reasonable to expect that the Yukon Delta will continue to prograde across the basin. Progradation of the delta would provide increasing protection and restriction to eastern Norton Sound, and sediment laterally equivalent to the delta-front facies would be highly bioturbated silt and sandy silt similar to that observed in the cores north and northeast of St. Michaels. The present-day Norton Sound floor would be preserved as a thin bioturbated unit separating two thick sequences dominated by physical sedimentary structures. The underlying unit would represent higher energy nearshore environments of lower sea levels in the early Holocene. The similar upper unit with well-developed physical structures would represent progradation of the active delta lobe across the offshore bioturbated mud.

Figure Captions

Figure 1. Location map of study area. Shaded portion is Norton Sound.

Figure 2. Physical and biogenic sedimentary structures and intensity of bioturbation in Norton Sound, Alaska.

Figure 3. Generalized sediment types of Norton Sound, Alaska.

Figure 4. Bioturbation in Norton Sound, Alaska.

REFERENCES

Drake, D.E., Cacchione, D.A., Muench, R. A. & Nelson, C.H. (1980) Sediment transport in Norton Sound, Alaska. Marine Geology, in press.

Howard, J.E. (1978) Sedimentology and trace fossils. In: Basan, P.B., Trace fossil concepts. Soc. Economic Paleontologists and Mineralogists Short Course no. 5, 13-45.

Howard, J.D., & Frey, R.W. (1975a) Estuaries of the Georgia coast, U.S.A.: sedimentology and biology, I. Introduction. Senckenbergiana Maritina 7, 1-31.

Howard, J.D., & Frey, R.W. (1975b) Estuaries of the Georgia coast, U.S.A.: sedimentology and biology. II. Regional animal-sediment characteristics of Georgia estuaries. Senckenbergiana Maritina 7, 33-103.

Howard, J.D. & Reineck, H.E. (1972) Georgia coastal region, U.S.A.: Sedimentology and biology. IV. Physical and biogenic sedimentary structures of the nearshore shelf. Senckenbergiana Maritina, 4, 8-123.

Nelson, C.H., & Creager, J.S.,(1977) Displacement of Yukon-derived sediment from Bering Sea to Chukchi Sea during the Holocene. Geology, 5, 141-146.

Nelson, C.H. & Hopkins, D.M. (1972) Sedimentary processes and distribution of particulate gold in the northern Bering Sea. U.S. Geological Survey Professional Paper 689, 27 p.

Nelson, C.H., Rowland, R.W., Stoker, S.W., & Larsen, B.R. (1980) Interplay of physical and biological sedimentary structures of the Bering epicontinental shelf. In: The eastern Bering Sea shelf: Its oceanography and resources (Ed. by Hood, D.W.) (in press).

Reineck, H.E. (1963) Der Kastengreiter: Natur and Museum 93, 102-108.

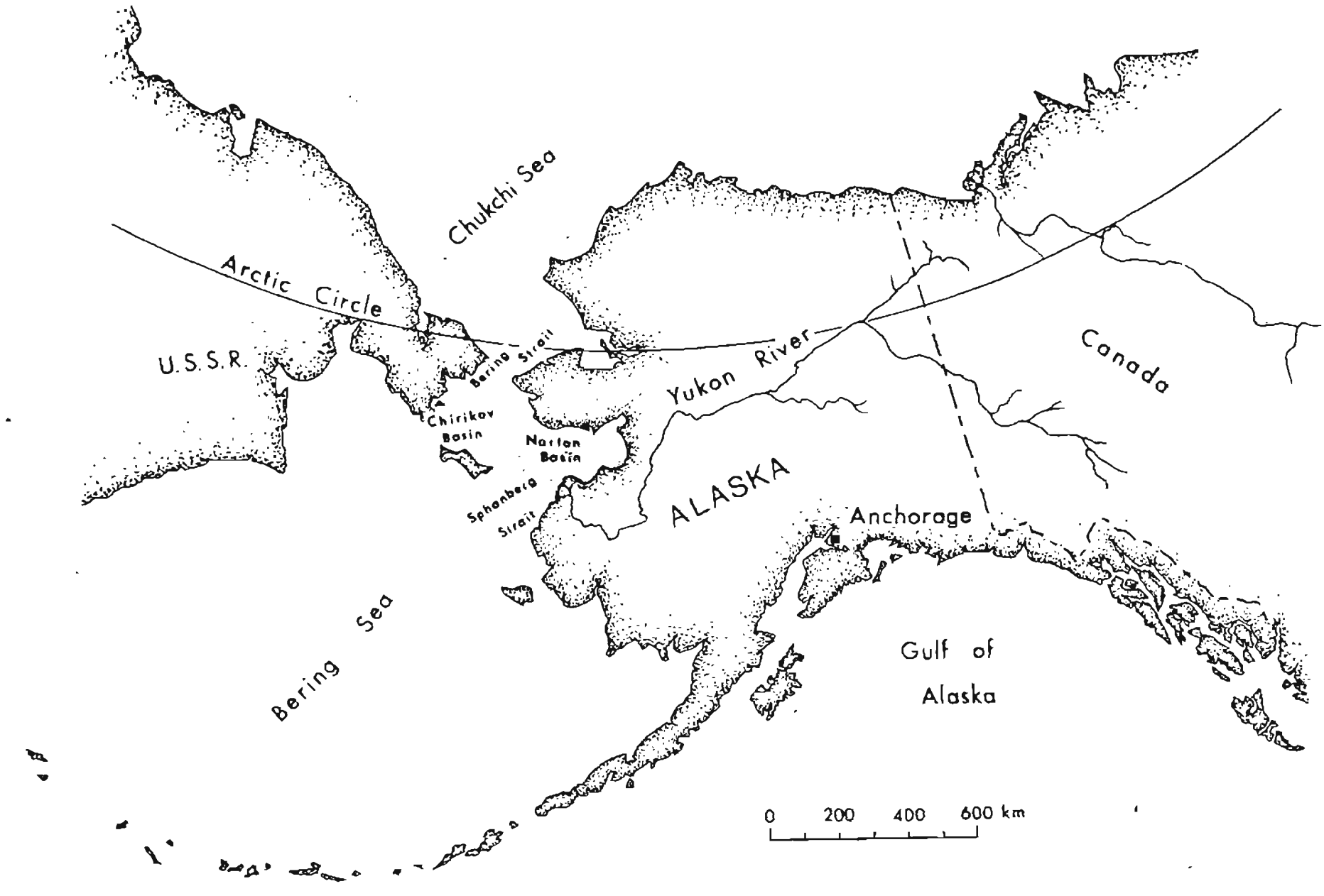
Chukchi Sea
Arctic Circle
U.S.S.R.
Bering Strait
Chirikov Basin
Norton Basin
Sphenberg Strait
Yukon River
Canada
ALASKA
Anchorage
Bering Sea
Gulf of Alaska
0 200 400 600 km

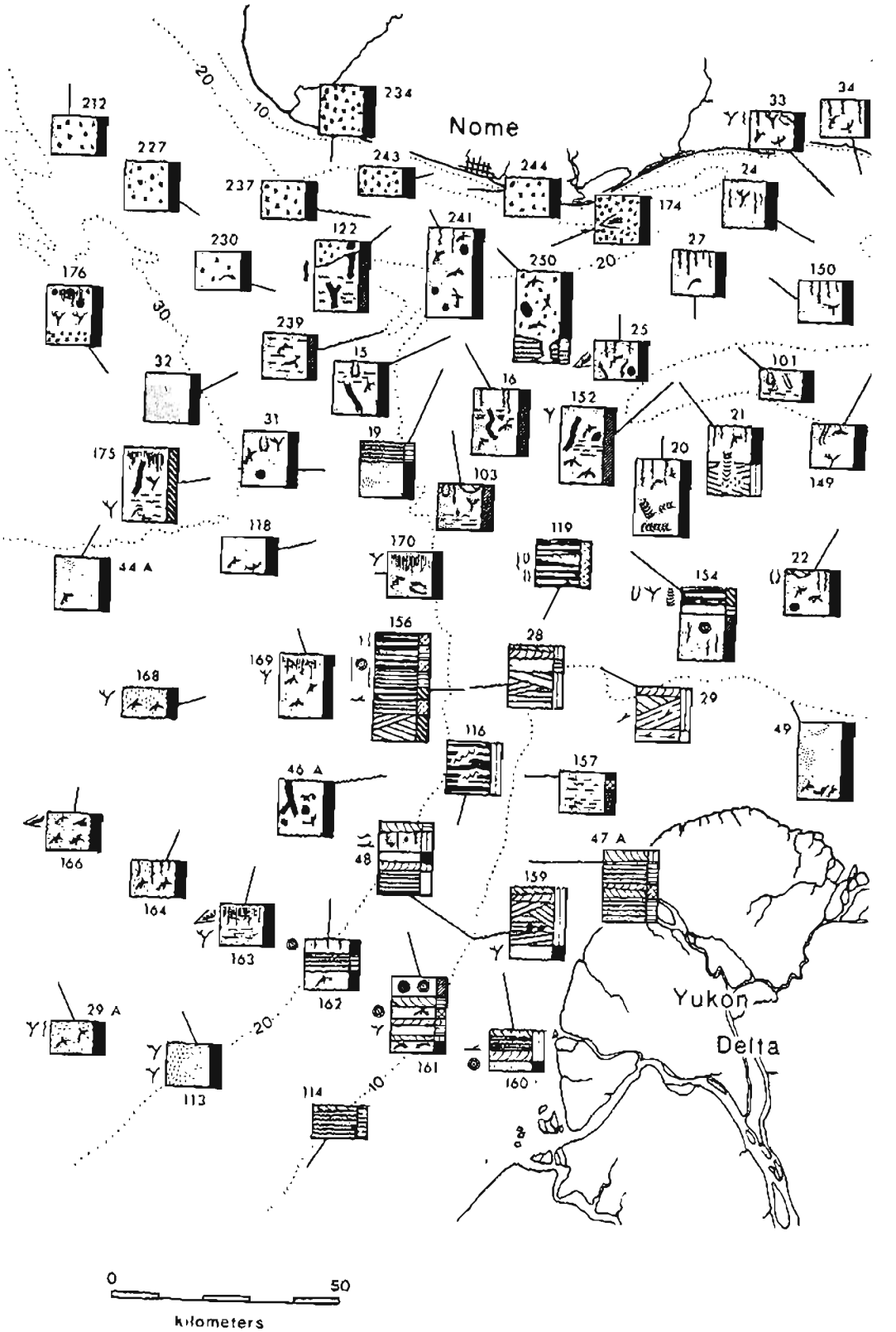
Nome
Yukon
Delta
0
50
kilometers

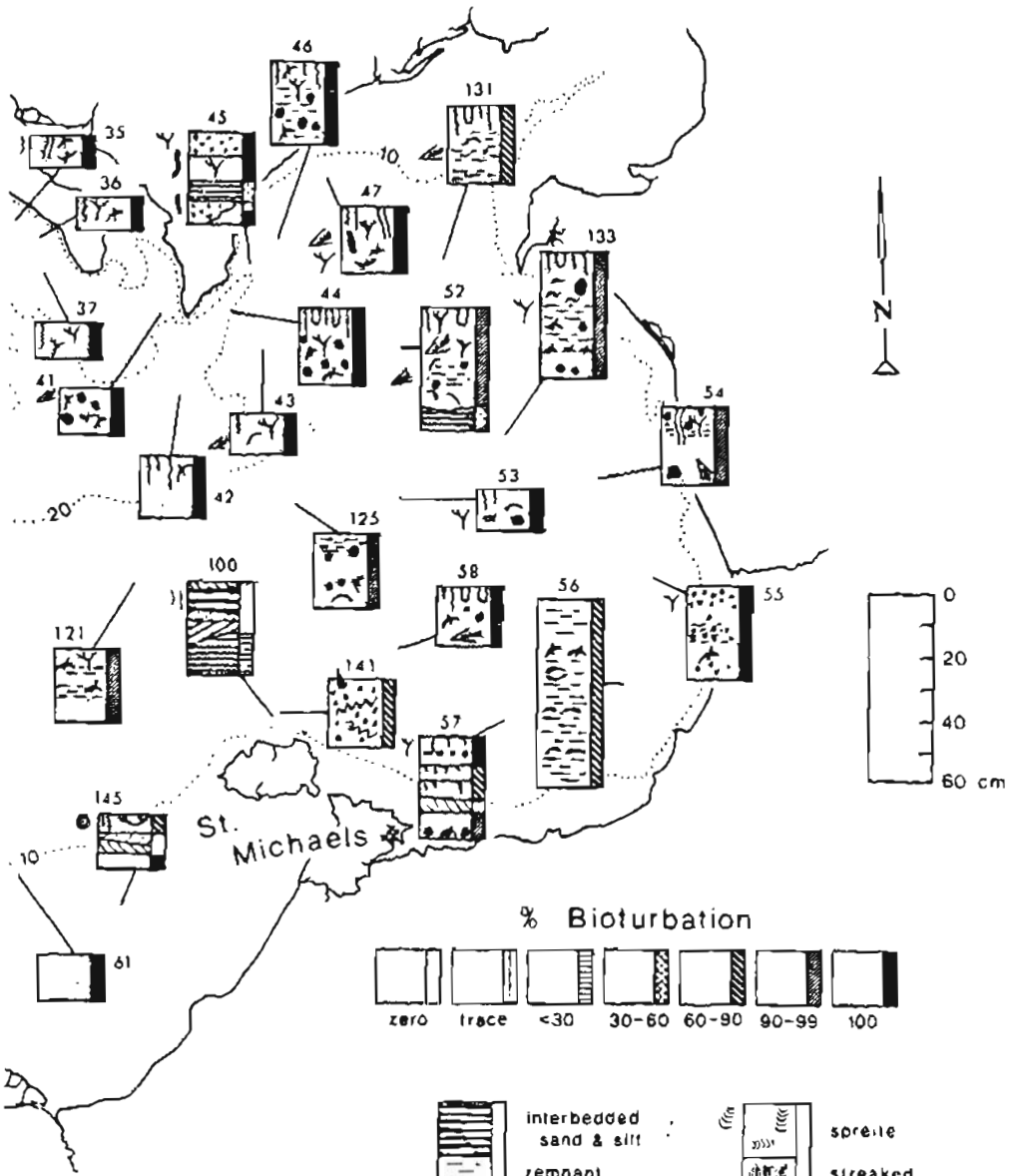

% Bioturbation

zero trace <30 30-60 60-90 90-99 100

gravel
sand
silty sand
sandy silt
silt
parallel laminae
ripple-laminated sand
crossbedded sand

interbedded sand & silt
remnant stratification
large polychaete burrows
simple polychaete burrows
branching burrows
polychaete tunnels
u-shaped burrows
concentric-walled burrows
gastropod
amphipod bioturbation

spreite
streaked bioturbation
Pectinaria sp
shell fragments
shell
shell in growth position
isolated, round pebbles
sand-filled burrows
plant fragments
physical disturbance

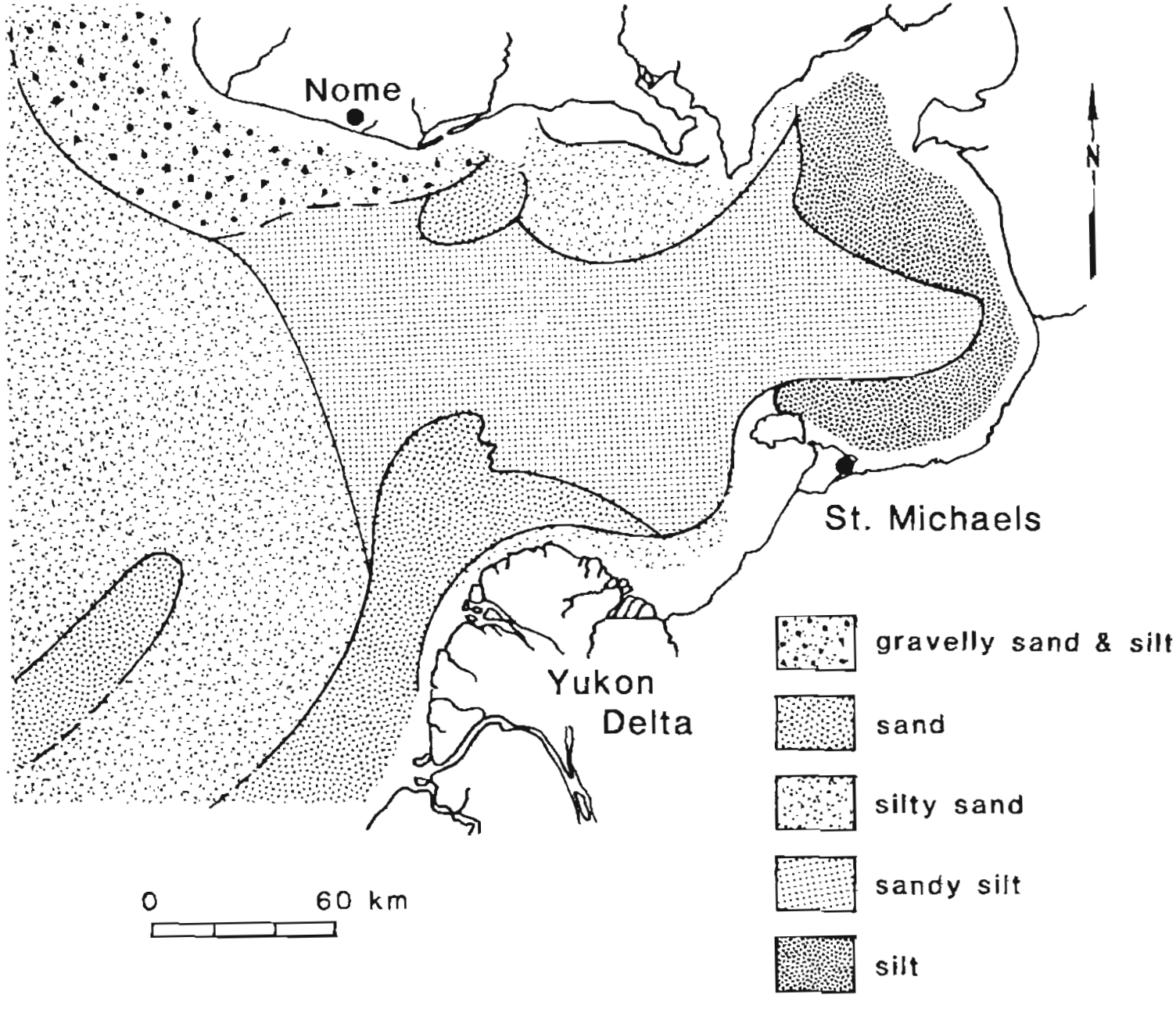
Nome
N
St. Michaels
Yukon
Delta
gravelly sand & silt
sand
silty sand
sandy silt
silt
0
60 km

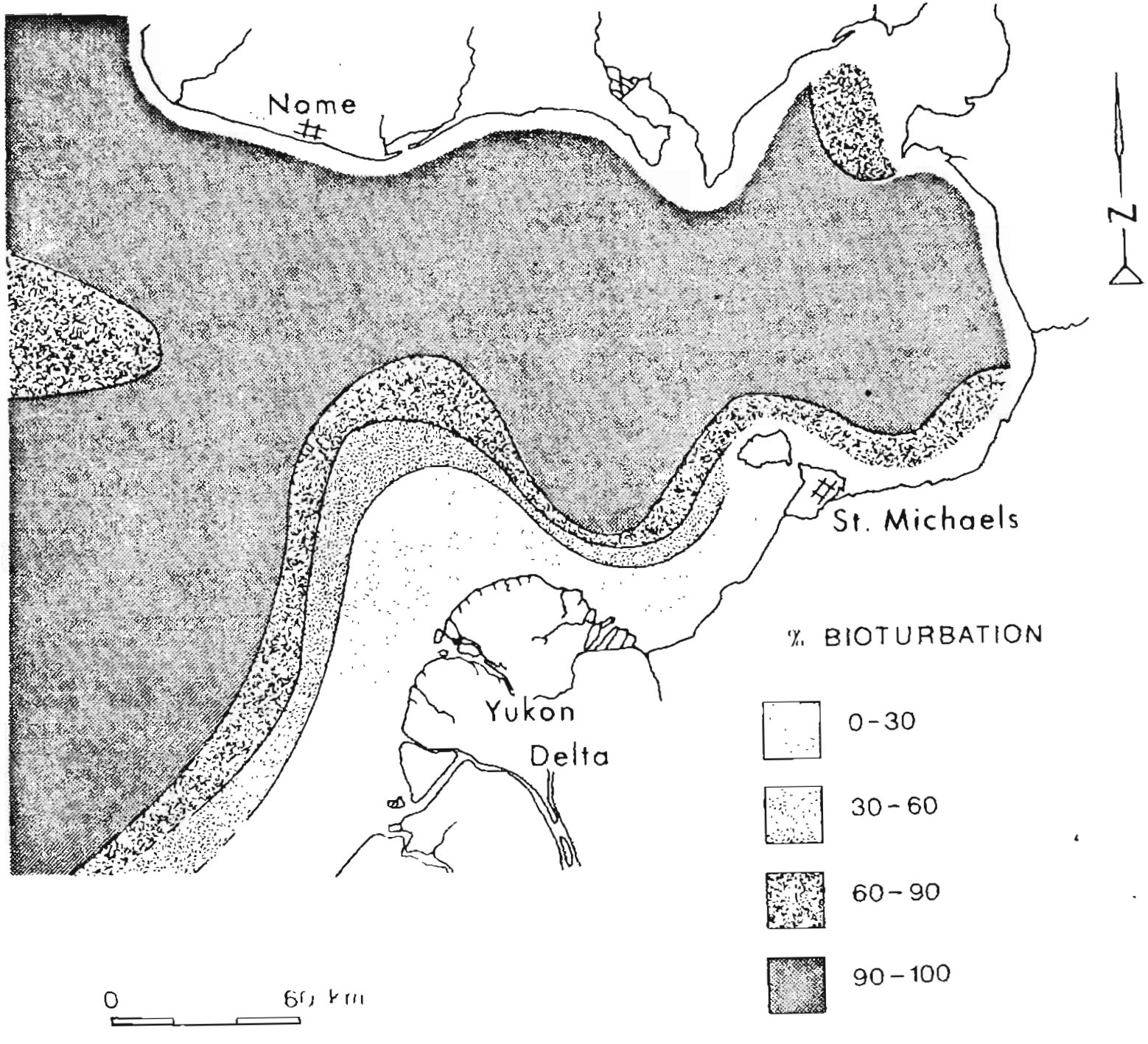
Nome
St. Michaels
Yukon
Delta
N
% BIOTURBATION
0-30
30-60
60-90
90-100
0
60 km

Linear Sand Bodies in the Bering Sea Epicontinental Shelf

by

C. Hans Nelson[1], William R. Dupré[2], Michael E. Field[1], and James D. Howard[3]

ABSTRACT

The epicontinental shelf of the Bering Sea is characterized by variations in river and glacial sediment supply, wave energy, tidal range (microtidal to mesotidal), and tidal, geostrophic, and storm-induced currents. These factors, combined with the effects of the Holocene rise in sea level, have resulted in the formation of a complex assemblage of linear sand bodies of similar morphology and lithology, but different origins. The sand bodies are large features <10 km long found from the present shoreline to tens of kilometers offshore in water depths up to 50 m. They include modern sand bodies formed by present-day processes; relict sand bodies formed during lower stands of sea level; and palimpsest sand bodies formed under past conditions but modified by modern day processes. Together they reflect the wide variety of offshore sand bodies that may be found in epicontinental settings like the modern North Sea or some ancient shelves.

The different types of sand bodies (linear tidal sand ridges, shore parallel shoals, delta front channels, leeside shoals, ancient shoreline shoals and morainal features) may be identified by variations from the norm: linear morphology, orientation parallel to the strand line, enclosure by shelf sand or mud, fine sand texture, and horizontal lamination. Linear tidal sand ridges (5-35 by 1-3 km) which form at the present time in the macrotidal, funnel-shaped Kuskokwim Bay, are oriented perpendicular to the shoreline, enclosed by tidal flat and shelf mud, and sometimes sigmoidal in shape. The modern shore parallel shoals (including barrier islands) (5-10 by .5-1 km) form in mesotidal environments, are the smallest of the shelf sand bodies, and typically are bounded by tidal flat mud inshore and shelf mud offshore. Delta front channels (20 -30 by 2-4 km) extend seaward from the modern river distributaries and form sand bodies perpendicular to the shoreline; they are enclosed by graded overbank sand beds and mud, and are characterized by large- to small-scale trough cross lamination. Leeside shoals, (25-100 by 5 to 25 km) which form now and in the past behind obstructions to unidirectional shelf currents, are the longest, possess the finest grain size, and exhibit the most consistent rhythmic flat lamination of any sand bodies encountered on the Bering shelf. Ancient shoreline shoals (15-30 by 3-7 km) are remnant shoreline features paralleling strand lines of lower sea levels; they contain cycles of ripple and trough cross lamination alternating with high angle foreset beds formed by modern sand waves that cover crests of these sand bodies. Relict sand and gravel bodies deposited in moraines are distinguished by their coarse grain size and irregular size and shape.

[1]U.S. Geological Survey, Menlo Park, Ca.
[2]University of Houston, Geology Department, TX
[3]Skidaway Institute of Oceanography, Savannah, GA.

INTRODUCTION

The epicontinental shelf of the eastern Bering Sea is characterized by large variations in fluvial input at different locations and in the energy of systems that distribute and deposit the load. Sediment is distributed not only by wave and tidal currents but also by strong geostrophic and storm-induced currents. The wide variety of processes, combined with the effects of the Holocene rise in sea level, has resulted in the deposition of sand bodies with similar linear morphology but different depositional settings, orientations, and origins that this paper describes. Examples include: linear tidal sand ridges, and shore-parallel shoals (including barrier islands) like those in the North Sea, as well as delta-front (sub-ice) channels, leeside shoals, ancient shoreline shoals, and morainal features that may be more specific to the Bering shelf.

The Bering epicontinental shelf contains a combination of (1) modern sand bodies formed by present-day processes, (2) relict sand bodies formed under past conditions, and (3) palimpsest sand bodies formed under past conditions but modified by modern-day processes. The variety of modern sand bodies on Bering shelf may be similar to that found on ancient shelves. The recognition of these differences is crucial to reconstruction of ancient epicontinental shelf facies and the task of hydrocarbon exploration.

Methods

The morphology, geometry, and lithology of the sand bodies on the Bering shelf have been studied over the past decade using a combination of high-resolution bathymetry, seismic profiling, side-scan sonar, vibracores of 2-6 m, box cores, and grab samples. Sediment samples have been analyzed for grain size and X-rayed to determine internal sedimentary structures. Grain-size distributions have been mapped vertically and horizontally using standard

grain-size techniques, although the degree of detail varies in different locations. In some areas of extremely shallow water of Kuskokwim Bay and off the Yukon Delta, shipboard surveys and sampling have not been possible. There, sediments have been sampled by helicopter and sand bodies have been mapped using satellite imagery.

Geologic and oceanographic settings

Tidal range and wave climate vary greatly in different locations of the eastern Bering shelf. Waves with 10-12-second periods and with heights of 10-20 m are possible in the southern shelf, but maximum wave heights are only 7 m on the northern Bering shelf (Arctic Environmental Information, 1977). Similarly, maximum spring tidal heights range from up to 5 m in the upper Kuskokwim Bay to less than 0.5 m in the northeastern Bering shelf. Where the Alaskan Coastal Water flows northward and is constricted by the eastern Seward Peninsula side of Bering Strait, bottom current speeds of over 200 cm/s occur (see Fig. 1 of Nelson, this volume). In the constrictions of Anadyr and Shpanberg Straits, maximum current speeds are 100-150 cm/s. In Norton Sound even small-scale storm tide events have been observed to increase current speeds of the northward geostrophic flow from less than 30 to 70 cm/s (Cacchione and Drake, 1979).

Quaternary glaciations and sea-level fluctuations on the northern Bering shelf have been crucial to the development of morainal and ancient shoreline sand bodies. Continental and valley glaciers near the eastern side of Anadyr Strait and off Nome, respectively, have left moraines that have been reworked by the Pleistocene-Holocene transgression of the past 20,000 years (see Fig. 4 in Nelson, this volume). Sea-level stillstands accompanying the late Pleistocene-Holocene transgression remain as coast-parallel offshore bars (Nelson and Hopkins, 1972; Tagg and Greene, 1973). The stillstands are most

apparent at depths of 10 to 12 m, 20 to 24 m, 30 m, and 38 m (see Nelson, this volume).

Both the Yukon and Kuskokwim Rivers contribute large amounts of sediment to the northeastern Bering Sea and this input is a significant factor in the development of presently forming sand bodies. The Yukon provides $60\text{-}90 \times 10^6$ t, or 90% of the modern fluvial sediment introduced into the entire Bering Sea; the second largest source is the Kuskowkim River which yields nearly 4×10^6 t of sediment annually (Drake et al., 1980).

TIDAL SAND RIDGES

Linear tidal sand ridges form in structurally subsiding macrotidal (>4 m) embayments (Hayes, 1975) such as Kuskokwim Bay (Fig. 1). Tidal sand ridges are best developed in the bay at the mouth and offshore from the Kuskokwim River but also occur in other nearby macrotidal embayments (e.g., Bristol Bay). The tidal sand ridges in Kuskokwim Bay typically are 0.5 to 4 km wide, 4 to 50 km long, and range in relief from 4 to 10 m near the mouth of the river to 32 m offshore (Fig. 2). Some of the Kuskokwim tidal sand ridges, like those in the North Sea, are asymmetric in cross section and slightly sigmoidal in plan view, a configuration that reflects opposing tidal currents (Caston, 1972).

The grain size on the emergent surface of the tidal ridges consists of fine, well-sorted sand (Fig.2). The tidal mud flats that flank the ridges consist of very poorly sorted silt (Fig. 3). Bedforms on ridge surfaces consist of sand waves of about 50 m wavelength that contain superimposed current ripples. The only internal structures observed in shallow trenches cut into the emergent ridges were horizontal parallel laminations. Apparently, like the predominance of parallel lamination observed on the ebb-dominated side of the tidal sand ridges of the Oosterscheld Estuary in the

Netherlands (Nio and others, 1979), preservation of internal structures of large-scale bedforms is limited in Kuskokwim Bay tidal ridges.

Orientation of the tidal sand ridges is roughly parallel to the rectilinear tidal currents (Fig. 2). The currents range from slightly over 50 cm/s in the outer part of the bay to nearly 150 cm/s knots at the mouth of the Kuskokwim River (U.S. Department of Commerce, NOAA, 1977). The landward increase in tidal current velocity is also paralleled by a landward increase in tidal range, the maximum of which is 5 m at the river's mouth. Current attenuation within the river channel results in an upstream decrease in tidal amplitude to slightly less than 1.5 m approximately 100 km inland and also causes an asymmetry in the tidal currents to flood-dominated in the lower part of the river, similar to that described in the Ord River, Australia by Coleman and Wright (1978).

Most sand ridges in Kuskokwim Bay appear to be formed by present-day tidal reworking of sand by the river. Some of the sand bodies farthest offshore may have formed during intervals of lowered sea level and thus may be palimpsest or relict features like the "moribund" sand ridges described by Kenyon and others (1979). The sand ridges in the nearshore regions of the bay are slightly offset to the east of the main trend, smaller in scale and size, and more closely spaced than are the ridges farther offshore (Fig. 2). The sand ridges that trend more northwesterly are more sigmoidal in shape, possibly because of the increased tidal amplification and flood-dominated tidal asymmetry toward the river's mouth. The longest and straightest ridges are found in the southeastern part of the region, where it is possible that ebb and flood currents are more equal (Fig. 2).

SHORE-PARALLEL SAND SHOALS AND ASSOCIATED BARRIER ISLANDS

The linear tidal ridges of the macrotidal upper Kuskokwim Bay region grade westward into mesotidal (2-4 m) areas where wide tidal flats, large tidal channels, and an outer fringe of submergent to emergent shoals occur (Fig. 3). The shoals nearest the mouth of the Kuskokwim River are approximately 30 km offshore and are emergent only during lowest spring tides. They grade westward into low-lying barrier islands approximately 10 km offshore. Similar barrier islands present in mesotidal areas along the western margin of the Yukon-Kuskokwim delta complex off Cape Romanzof were not studied.

The shore-parallel shoals (including barrier islands) in Kuskokwim Bay are 5 to 10 km long, 0.5 to 1 km wide, and may have as much as 15 m of relief above the adjacent seafloor. They, like the tidal shoals, are characterized by well-sorted fine sand (Fig. 2) and are enclosed by silty sand that grades inshore to the silty mud of the tidal flats (Figs. 2 and 3). The barrier islands rise approximately 2 m above sea level, but unlike those formed in drier temperate climates, they lack eolian dunes. When the easternmost shoals are emergent, however, sand waves are seen that sometimes intersect each other at right angles (Fig. 4-I). The sand waves, although planed to small amplitudes, are covered by sets of divergently oriented ripples formed by diversely oriented nearshore waves and tidal currents. The only observed internal sedimentary structures of these ephemeral ripples and sand waves are parallel laminations.

The shore-parallel sand bodies and barrier islands form in equilibrium with the mesotidal setting on the west. Emergent barrier islands grade eastward to submergent shoals where there is an increase in tidal range. Barrier islands decrease in length and tidal channels become more numerous.

Tidal flats increase in width to more than 10 km. Farther to the east the shore-parallel shoals grade into the shore-perpendicular linear tidal ridges in a macrotidal setting.

The barrier island, shore-parallel shoals and tidal sand ridges forming in equilibrium with tidal and wave energy today in Kuskokwim Bay are similar to those in the Rhine River estuary of the North Sea (Hayes, 1975; Nummendal, 1979). The size and setting of the Kuskokwim system make it essentially a replica of the Rhine River-North Sea system if Kuskokwim Bay were inverted from north to south. Sand bodies in both systems are representative of epicontinental shelf macrotidal, funnel-shaped estuary systems with a significant sediment input (Coleman and Wright, 1978).

DELTA FRONT (OR SUB-ICE) CHANNELS

The Yukon River mouth, in contrast to the funnel-shaped estuary of the nearby Kuskokwim River, has a constructional, lobate delta (Fig. 1). The delta shoreline is an area of relatively low wave energy and tides (typically 1 m or less) (Arctic Environmental Information, 1977). Deltaic sedimentation also is strongly affected by the presence of shorefast ice that fringes the delta for almost seven months of the year (Duprè, this volume). The shorefast ice forms over the sub-ice platform that is typically 2-3 m deep and extends as far as 30 km offshore. The platform is crossed by a series of subaqueous channels that extend offshore from major distributaries of the delta (see Fig. 5 in Duprè, this volume). These channels are typically 5 to 10 m deep, and 0.5 to 1 km wide; lateral migration of the channels produces sand bodies approximately 10 m thick and 1 to 4 km wide that extend up to 25 km beyond the shoreline.

The grain size of the channel fill varies widely from well-sorted medium to fine sand in thalwegs of the inshore active channel (Fig. 4-F) to graded

sand beds interbedded with silty mud that flank and may in part fill abandoned channels (Fig. 4-G). Individual graded units up to 30 cm thick vary from well-sorted fine sand at the base to poorly sorted silt at the top. Off the eastern delta, where current channel fill is low, fine sand occurs and the sand beds in the upper sequence of channel fill are only a few centimeters thick.

Large-scale megaripples on the floor of active subaqueous channels appear to be represented by large-scale, moderately dipping crossbedding (Fig. 4-F). Subaqueous point-bar sequences presently form in meandering sub-ice channels and consist of trough cross-laminated sand fining upward into interbedded silt and peat. A complete vertical sequence of sedimentary structures in ascending order is flat-laminated, trough cross-laminated and flat-laminated sand (Fig. 4-G). Farther offshore the basal flat-laminated beds may be replaced by mainly trough cross-laminated or ripple-laminated units with thin, flat-laminated upper parts.

The presence of the sub-ice platform and associated subaqueous channels appears to be restricted to the ice-dominated deltas (see Fig. 5 in Duprè, this vol.) that are common in arctic and sub-arctic shelves today. The effect of the shorefast ice is to extend the well-sorted distributary sand far beyond the shoreline, resulting in elongate sand bodies enclosed in thinner sand and mud overbank deposits.

LEESIDE SHOALS

Leeside shoals are large accumulations of sand deposited in the current lee behind land barriers that interrupt continuous, strong geostrophic current flows in the northern Bering Sea (see Fig. 1 in Nelson, this volume). These shoals are most typically found on the east sides of straits where land projects westward into the strongest current flow. Examples are north of Cape

Romanzof, the Yukon delta, and northwest of Cape Prince of Wales (Fig. 1). Leeside shoals also form in the north lee of King and St. Lawrence Islands which obstruct the strong northerly water circulation (Fig. 1).

Leeside shoals vary in size and shape from long and narrow behind King Island (20 by 5 km) and Cape Prince of Wales (100 by 14 km) (Fig. 1) to broad and diffuse sand bodies (45 by 25 km) north of the modern Yukon delta. Their relief ranges from 10 to 20 m, and their orientation generally parallels the current flow direction rather than the shape of the coastline, from which they are typically detached.

The grain size of the leeside shoal in all settings is very fine sand (Fig. 1), and consequently, asymmetric current ripples are the typical surface bedform. Sedimentary structures of the shoal north of Cape Prince of Wales, where geostrophic current shear is maximum and most continuous, are very even parallel flat laminations and intermittent ripple laminations (Fig. 4-D). The leeside shoal north of the Yukon delta (Fig. 1) exhibits well-developed alternating layers of crossbedded and horizontally laminated sand (see Fig. 2 in Howard and Nelson, this volume). Large-scale tabular foresets also develop as the sand body apparently grows offshore from the edge of the the Yukon delta-front platform (Fig. 4-E).

Because deposition results from flow separation on the lee side of obstructions (Middleton and Southard, 1977), the sediment source for leeside shoals is entrainment of sediment that has been stripped from adjacent coastlines, river mouth discharge, or upcurrent shelf sand. One sand source of the Cape Prince of Wales leeside shoal is believed to be very fine sand eroded from the southern Seward Peninsula beaches between Cape Prince of Wales and Port Clarence. These beaches lack very fine sand (<5% at 8 stations) whereas the leeside shoal and beach on the north side of Cape Prince of Wales

are composed of dominantly very fine sand (>97% at 6 stations). The very fine sand fraction normally eroded from beaches and deposited in offshore bars during storm events apparently is entrained and carried northward through the Bering Strait by the geostrophic current. Because of flow separation on the lee side north of Cape Prince of Wales, the entrained very fine sand is deposited on the beaches and leeside shoal.

The leeside shoal north of the modern Yukon delta contains very fine sand derived from the southwest distributary that is the main discharge point of the Yukon River (Dupré, this volume). This distributary is located in the maximum current-shear region of eastern Shpanberg Strait (see Fig. 1 of Nelson, this volume), where strong geostrophic currents are located. These currents entrain the deltaic sediment and deposit the sand in the leeside shoal located 30-130 km north and east of the main river discharge point (see Fig. 5 in Dupré, this volume). In the delta-front area, geostrophic water circulation is not vigorous and is reinforced by intermittent storm tides (Nelson and Creager, 1977; Nelson, this volume). Apparently, in this more complex delta setting, the leeside shoal develops a diffuse fan shape and contains a wider variety of internal sedimentary structures (Fig. 4-E and Fig. 2 in Howard, this volume).

ANCIENT SHORELINE SHOALS

Many areas of the Bering shelf are marked by well-developed fields of linear sand bodies formed by ancient shorelines (Fig. 1). The largest of these is a series of long, linear shoals that lie offshore from Port Clarence at water depths of 10-12, 20-24, 30, and 38 meters (Fig. 5). A well-defined linear field of ridges at similar water depths exists off Nome (Nelson and Hopkins, 1972; Hopkins, 1973; Tagg and Greene, 1973). West of St. Lawrence Island is a long, linear ridge at a depth of 30 m that also appears to be an

ancient shoreline (Fig. 1). All of the shoals described above occur in the Chirikov Basin, an area where detailed studies of ancient beaches have been made because strong currents have prevented burial by post-Holocene deposition (Nelson and Hopkins, 1972; McManus and others, 1974; see Nelson, this volume).

The sand bodies formed by ancient shoreline shoals are 15 to 30 km long, 3 to 7 km wide, and 10 to 15 m high. Seismic reflection and sampling reveals that the sand ridges off Port Clarence are at least 6 m thick and are composed of well-sorted fine to medium sand (Figs. 1 and 5). Troughs between the sand ridges contain very fine sand to silt (Fig. 5). Near Nome and northwest of St. Lawrence Island, the ancestral shoreline features have been incised into pebbly, sandy glacial till (Nelson and Hopkins, 1972; see Fig. 4 in Nelson, this volume) and consequently contain fine to coarse sand and gravel.

Near Port Clarence, bottom currents rework the crests of the ancient shoreline shoals into a series of mobile bedforms (Fig. 5). The largest features are sand waves with wavelengths up to 200 m and heights of 2 m (Nelson and others, 1978). Superimposed on them are smaller, slightly oblique sand waves that have wavelengths up to 10 m and heights of up to 0.5 m. Linguoid ripple fields with wavelengths of 10-30 cm and wave heights of a few centimeters occur on the stoss side of sand waves (Fig. 4-H). All of the bedforms have crests aligned transverse to the linear ridge crest and are asymmetric, steep side to the north, transverse to the flow direction of the strong geostrophic currents. Significant modification of ice gouges by these mobile bedforms shows that the bedform fields are presently active. Near Port Clarence, when strong north winds create large storm waves, the small-scale bedforms may be modified by ephemeral oscillation ripples until the normal northward current regime resumes. Near Nome, there is an even greater degree of mixing between asymmetric ripples developed by tidal current flow and

oscillation ripples developed inshore by storm waves (Hunter and Thor, this volume). The region of the large, linear ridge west of St. Lawrence Island also has mobile bedforms (Nelson and others, 1978).

In the largest area of ancient shoreline shoals near Port Clarence, reworking of the ancient shoreline shoals by modern currents results in well-developed sedimentary structures, especially on the shoals closer to shore. Ripple lamination is ubiquitous and bioturbation is dominant, particularly on offshore shoals and at several meters depth in all shoals. Ripple lamination commonly present near the surface, caps an underlying sequence of foreset beds. This cycle sometimes is repeated at about 50-cm intervals and may represent alternating episodes of linguoid ripple and small-scale (50 cm wave height) sand-wave migration along shoal crests (Fig. 5-C and 5-H). Thin mud-drapes and storm pebble lag horizons also are typical in the nearsurface sediment of ancient shoreline shoals (Fig. 5A).

The ancient shoreline shoals typically are flanked by older, limnic, peaty mud with radiocarbon dates ranging from 12,000 to more than 40,000 years B.P. (see Fig. 5 in Nelson, this volume). The presence of thin, modern mud (<50 cm) over peaty mud with radiocarbon dates exceeding 40,000 yrs B.P. indicates lack of modern deposition or scour between the shoals. Consequently, the intervening sand shoals on bedrock highs (Fig. 5) appear to represent ancient constructional ridges undergoing present-day modification on their crest by migration of surface bedforms; the main ridges, however, do not change significantly in size or shape.

The shape of the submerged shoals west of Port Clarence is similar to that of the modern, subaerial Port Clarence spit (Fig. 5F-F'); in addition their grain size is coarser (fine to medium sand) relative to that of enclosing inner shelf deposits (fine to very fine sand), or of leeside shoals

(very fine sand) in Chirikov Basin (Fig. 1)(see Figs. 3 and 6 of Nelson, this volume). Both characteristics suggest that the submerged shoals may be Pleistocene shoreline analogs to the Port Clarence Spit and that they formed by littoral drift processes, depositing fine to medium sand at lower stillstands of sea level (Figs. 1 and 5; Nelson, this volume). Submerged shoal crests off Port Clarence and St. Lawrence Island are similar in depth and grain size to ancient shoreline features at Nome and elsewhere in the northern Bering Sea (Figs. 1 and 5), again lending support to an origin during older sea-level stillstands at water depths of 10-12, 20-24, and 30 m (Nelson and Hopkins, 1972; Hopkins, 1973).

Many areas of the U.S. Atlantic shelf characterized by similar fields of linear sand ridges (Duane and others, 1972) have been interpreted as shoreface ridges stranded by a retreating shoreline (Field, 1980). Present-day reworking by shelf currents is modifying these features into active mobile bedform fields like those on Bering Shelf (Swift and Field, 1980).

GLACIAL MORAINES

A few large bodies of sand and gravel deposited by ancient glacial activity remain exposed and surrounded by Pleistocene transgressive sand on the seafloor in the Chirikov Basin region. A large outwash fan approximately 5 km in diameter is located offshore southeast of Nome (Fig. 1). Two very large coarse sand and gravel ridges about 75 km long and 25 km wide extend southward from Cape Prince of Wales toward the center of Chirikov Basin and northward from St. Lawrence Island to the same point. The two ridges are traceable as the ends of major moraines of continental glaciers that moved southward into Chirikov Basin from Siberia (see Fig. 4 in Nelson, this volume; Grim and McManus, 1970; Nelson and Hopkins, 1972).

The glacial features in general are coarser grained than the other shoals of the eastern Bering continental shelf (Fig. 1). Because gravel is difficult to sample, we have not been able to observe internal sedimentary structures.

SAND BODY GENESIS

Hydrographic and sedimentary processes vary from south to the north on the eastern Bering epicontinental shelf and consequently genesis and age of shelf sand bodies vary according to geographic location. Toward the southeast, tidal currents and wave energy dominate sedimentation as well as the local transport history, whereas in the northeastern shelf area, the effects of ice and geostrophic bottom currents flowing to the north are more important. The influx of fluvial sediment is particularly important in the southeastern and east-central region of the shelf, whereas glacial deposition and local transgressive history during the Pleistocene are more significant in the northeastern shelf area.

The extensive development of modern sand bodies in the southeastern and east-central Bering shelf relates to high influx of fluvial sediment in that area, which receives 90% of the Bering Sea's sediment load (Lisitsyn, 1966). The sand bodies in the southeastern shelf are modern features derived from sediment deposited by the Kuskokwim River and modified by tidal currents and waves in Kuskokwim Bay. The funnel-shaped estuary of the Kuskokwim River contains linear, coast-perpendicular sand ridges that are characteristic of a tide-dominated river mouth (Coleman and Wright, 1978). Shore-parallel sand bodies in west and northwest Kuskokwim Bay result from a mesotidal regime. In the microtidal (<2 m) environment off the Yukon River, channel sand bodies develop on the delta front platform mainly because of processes associated with shorefast ice and the high sediment discharge of the Yukon River (Dupré, this volume).

By contrast, sand and gravel bodies in the northeastern Bering shelf are the result either of relict or palimpsest deposition. The leeside sand bodies probably accumulated during the present Holocene high sea level and other Pleistocene highstands. Seismic-reflection profiles over the north end of the leeside shoal in east-central Shpanberg Strait and the shoal north of the Yukon delta show significant Holocene deposition (see Fig. 4 in Nelson, this volume). Profiles over leeside shoals indicate several episodes of deposition, most likely from sedimentation during several past high sea levels. The consistent lithology of very fine sand and horizontal flat laminations indicates that flow separation in the lee of obstructions results in deposition of the suspended sand load as bottom currents pass over the sand body. Ripple laminations and high-angle foreset beds in the Yukon shoal, show the influence of storm events on these typical flat-laminated deposits.

Unlike the leeside sand bodies, which exhibit significant Holocene deposition, the formation of the ancient shoreline sand bodies is related mainly to deposition of fine to medium sand by littoral drift currents on strandlines during lower stands of sea levels. The history of these ridges is complex, as deposits formerly at a lower sea level are now being modified into active ripple and sand wave fields by present-day bottom currents. Mobile bedforms are further disrupted by pebble lags and mud drapes formed during present-day storm events; thus, the resultant internal sedimentary structures do not represent the shoreline processes mainly responsible for formation of the main sand ridges. Internal structures, except for rare trough crossbedding, are mainly unknown in those relict sand and gravel bodies deposited by glacial events, but now are preserved by strong modern geostrophic currents.

GEOLOGIC SIGNIFICANCE OF SAND-BODY CHARACTERISTICS

The eastern Bering epicontinental shelf contains numerous offshore and nearshore large, linear sand bodies. Nearshore and offshore sand bodies resemble one another in that they are composed of well-sorted fine sand and are essentially linear, except for several of the leeside shoals and glacial features. They differ in that nearshore sand bodies orient with wave and tidal currents, but offshore shelf sand bodies mainly follow trends of geostrophic and storm-related currents.

Other distinctions may help to differentiate sand bodies because of differences in shape, grain size and internal sedimentary structures (Table 1). Shore-parallel shoals appear to be consistently shaped, smaller, and more coincident with shoreline trends than the other types of shoals. Linear tidal ridges and delta-front channels are generally perpendicular to shoreline trends and are quite consistent in gross size and shape, except for sinuosity of meanders in channel-fill bodies and sigmoidal shape in tidal ridges. Leeside shoals are oriented parallel to dominant shelf currents and are long and narrow where current speeds are consistently unidirectional and strong; elsewhere, they may be more fan-shaped. Overall size varies quite markedly depending on the size of the adjacent land barrier, the magnitude of flow, and sediment load. Ancient shoreline sand bodies also vary in size and have different shapes and orientations with respect to the shoreline (Fig. 1).

Grain size varies for different types of shelf sand bodies (Table 1). Deposits of subaerial glaciers dominated by coarse sand and fine gravel are distinctively coarser grained than all other types. In contrast, leeside shoals consisting of very fine sand because of deposition from the suspended sediment load, are typically the finest grained (Fig. 1). Ancient shoreline shoals are consistently coarser grained than deltaic or leeside deposits.

Internal sedimentary structures, although difficult to assess in cores from modern deposits, again help differentiate modern shelf shoals and perhaps provide one of the best criteria for ancient analogs. Leeside sand bodies, where uncomplicated by deltaic and storm sand sedimentation, are characterized by consistent, rhythmic flat lamination (Fig. 4-C). The very fine grain size of sand making up leeside sand bodies inhibits development of large-scale bedforms and thus such deposits generally should lack large- and medium-scale crossbedding, although ripple lamination of storms may interrupt flat lamination. Large-, medium-, and small-scale trough cross-laminations, on the other hand, are persistent in sand bodies and enclosing overbank deposits of delta-front channels. Because large-scale bedforms form in channel thalwegs, large-scale cross-bedding in clean sand should characterize the main-channel sand body, while smaller scale trough cross-lamination should characterize overbank mud that encloses the sand body. Rhythmic graded storm sand with vertical sequences of internal structure, organic debris, and mud caps also should be associated with younger channel-fill and laterally equivalent deposits. High-angle foreset beds in cyclic sequences with ripple and trough cross-lamination help identify shoreline sand bodies stranded by eustatic rises of sea level, but reworked by mobile bedforms while submerged. Modification of these ancient shoreline sand bodies by present-day mobile bedform fields and bioturbation suggests that internal structures of the original beach formation processes may rarely be present in such sand bodies.

In reconstructing ancient shelf environments, researchers must realize that 1) sand-body genesis is highly variable within the same shelf setting, 2) large sand bodies may be detached far from shore and not parallel later strandlines, and 3) features of different history and age may coexist (Table 1).

ACKNOWLEDGMENTS

Devin Thor, along with the scientific staff and crews of the R/V KARLUK and the R/V SEA SOUNDER, assisted in field data collection. Matthew and Bradley Larsen provided figure compilations, radiography, and grain size analyses. Louise M. Kiteley and Hugh McLean gave constructive review comments.

The cruises were supported jointly by the U.S. Geological Survey and by the Bureau of Land Management through interagency agreement with the National Oceanic and Atmospheric Administraton, under which a multi-year program responding to needs of petroleum development of the Alaska continental shelf is managed by the Outer Continental Shelf Environmental Assessment Program (OCSEAP) Office.

Table 1. Characteristics of Bering Shelf Sand Bodies

AGE	TYPE	ENVIRONMENT OF DEPOSITION	LENGTH (KM)	WIDTH (KM)	RELIEF (M)	LITHOLOGY	SEDIMENTARY STRUCTURES	DISTINGUISHING FEATURES
Holocene - Modern	Linear tidal sand ridges	Macrotidal funnel-shaped bay and estuary.	5-35	1-3	4-32	Fine sand	Parallel lamination, surface ripple fields, sand waves observed	Enclosed by tidal flat and shelf mud, shore-perpendicular, varying in size and shape--sometimes sigmoidal.
	Shore-parallel shoals (+ barrier islands)	Outer edge of subtidal flats in mesotidal regions.	5-10	0.5-1	15	do.	Same as above	Enclosed by tidal flat and shelf mud, shore parallel, consistent limited size and shape.
	Delta front (sub-ice) channels	Offshore extensions of major distributaries	20-30	2-4	5-15	Fine to very fine sand in thalweg, graded sand beds in overbank mud	Trough crossbedding graded sand beds with flat lamination, cross lamination in vertical sequence	Enclosed by graded overbank sand beds in mud, shore perpendicular, large-scale trough crossbeds in thalweg sand beds.
Pleistocene-Holocene Palimpsest	Leeside shoals	Lee of islands or peninsulas interrupting strong geostrophic bottom currents.	25-100	5-25	10-20	Very fine sand	Rhythmic flat laminations alternating with occasional thin ripple laminations	Enclosed by shelf sand and mud, orientation parallel to shelf currents not shoreline, widely varying shape and size, very fine sand size with rythmic flat lamination interrupted by ripples.
	Ancient shoreline shoals	Shoreline deposits formed during still-stands of sea level.	15-30	3-7	10-15	Fine to medium sand interinterrupted near surface by pebble lags and mud drapes	Alternating ripple and trough cross-lamination with high-angle foreset beds, bioturbation common	Enclosed by shelf sand and mud, parallel to ancient strandlines, high angle foresets interrupted by ripple and trough crosslamination, storm pebble and shell lags, bioturbation in lower and offshore sequences.
Pleistocene Relict	Morainal features	Glacial deposition during lowstands of sea level.	5-75	5-25	10-15	Medium-coarse sand and gravel	Rare trough cross-lamination and shell laminations	Enclosed by shelf sand and mud, size and shape variable, not shore parallel or perpendicular, coarse and variable grain size.

References

Arctic Environmental Information and Data Center, University of Alaska, National Climatic Center, Environmental Data Service, Asheville, N.C., and NOAA (1977) Climatic atlas of the outer continental shelf waters and coastal regions of Alaska. Bering Sea, 2, 443 p.

Cacchione, D.A., & Drake, D.E. (1979) Sediment transport in Norton Sound, Alaska: Regional patterns and GEOPROBE system measurements. U.S. Geological Survey Open-File Report 79-1555, 88 p.

Caston, V.N.D. (1972) Linear sandbanks in the southern North Sea. Sedimentology, 18, 63-78.

Coleman, J.M., & Wright, L.D. (1978) Sedimentation in an arid macrotidal alluvial river system: Ord River, Western Australia. Journal of Geology, 86, 621-642.

Drake, D.E., Cacchione, D.A., Nelson, C.H., & Muench, R.D. (1980) Sediment transport in Norton Sound, Alaska. Marine Geology, (in press).

Duane, D.B., Field, M.E., Meisburger, E.P., & others (1972) Linear shoals on the Atlantic inner continental shelf, Long Island to Florida. In: (Ed. by Swift, D.J.P., and others), Shelf sediment transport: Process and pattern. Dowden, Hutchison and Ross, Stroudsburg, PA., 447-498.

Field, M.E. (1980) Sand bodies on coastal plain shelves: Holocene record of the U.S. Atlantic inner shelf off Maryland. Journal of Sedimentary Petrology (in press).

Grim, M.S., & McManus, D.A. (1970) A Shallow-water seismic profiling survey of the northern Bering Sea. Marine Geology, 8, 293-320.

Hayes, M.O., (1975) Morphology of sand accumulation in estuaries. In: (Ed. by Cronin, L.E.), Estuarine Research, Geology and Engineering Academic Press, New York, 2, 3-22.

Hopkins, D.M. (1973) Sea level history in Beringia during the past 250,000 years. Quaternary Research 3, 520-540.

Kenyon, H., Belderson, R.H., Stride, A.H., & Johnson, M.A. (1979) Longitudinal tidal sand banks of north European Seas. In: Abstracts, International Meeting on Holocene marine sedimentation in the North Sea Basin, paper no. 49.

Lisitsyn, A.P (1966) Recent sedimentation in the Bering Sea. U.S.S.R. Academy of Science, Institute of Oceanology (English translation: Israel Program for Scientific Translations), (1969) 614 p.

McManus, D.A., Venkatarathnam, K., Hopkins, D.M., & Nelson, C.H. (1974) Yukon River sediment on the northernmost Bering Sea Shelf. Journal of Sedimentary Petrology, 44, 1052-1060.

Middleton, G.V., & Southard, J.B., (1977) Mechanics of sediment movement. Lecture notes for short course no. 3, Society of Economic Paleontologists and Mineralogists, Eastern Secton, Binghamton, N.Y.

Nelson, C.H., Cacchione, D.A., Drake, D.E., & Field, M.E. (1978) Areas of active large-scale sand wave and ripple fields with scour potential on the Norton Basin seafloor. In: Environmental assessment of the Alaskan Continental Shelf, Annual Reports of the Principal Investigators, U.S. Dept. of Commerce, NOAA, OCSEAP, Boulder, CO., 12, 291-307.

Nelson, C.H., & Creager, J.S. (1977) Displacement of Yukon-derived sediment from Bering Sea to Chukchi Sea during the Holocene. Geology, 5, 141-146.

Nelson, C.H., & Hopkins, D.M. (1972) Sedimentary processes and distribution of particulate gold in northern Bering Sea. U.S. Geological Survey Professional Paper 689, 27 p.

Nio, S.D., van den Berg, J.H., & Siegenthaler, C. (1979) Excursion guide to the Oosterschelde Basin, southwest Netherlands; an example of Holocene tidal sedimentation. International Association of Sedimentologists, International Meeting on Holocene marine sedimentation in the North Sea Basin, Guidebook for excursions, 9-35.

Nummendal, D. (1979) Tidal inlet sediment dispersal along the German North Sea coast. Abstracts volume, International Meeting on Holocene marine sedimentation in the North Sea Basin, paper no. 27.

Swift, D.J.P., & Field, M.E. (1980) Evolution of a classic sand ridge field: Maryland sector North American inner shelf. Sedimentology, in press, 37 p.

Tagg, A.R., & Greene, H.G. (1973) High-resolution seismic survey of a nearshore area, Nome, Alaska. U. S. Geological Survey Professional Paper 759-A, 23 p.

U.S. Dept. of Commerce, National Oceanic and Atmospheric Administration (1977) Tide Tables, 1977, west coast of North and South America. National Ocean Survey.

Figure Captions

Figure 1. Location of sand bodies on the eastern Bering epicontinental shelf.

Figure 2. Physiographic, hydrographic, and textural characteristics of Kuskokwim Bay sand bodies.

Figure 3. General geology of Kuskokwim Bay sand bodies.

Figure 4. Seafloor bedforms and internal sedimentary structures of sand body deposits on Bering Shelf. See Fig. 1 for photo locations.

A. Boxcore slab from crest of Ukivok ancient shoreline shoal west of Port Clarence showing storm shell lags and clay drapes (31 m water depth).

B. Boxcore slab containing thick well-sorted transgressive lag gravel from shoreline stillstand at depth of 30 m off NW Cape of St. Lawrence Island. Note faint crossbedding in center of cast.

C. Vibracore radiograph from crest of Tin City shoal west of Port Clarence showing ripple lamination, foreset bedding and trough cross-lamination in a typical sequence (18 m water depth).

D. Vibracore radiograph from leeside shoal north of Cape Prince of Wales (6 m water depth) showing rhythmic horizontal laminations and occasional ripple laminations.

E. Boxcore radiograph from Yukon leeside shoal northwest of Yukon Delta showing ripple lamination and foreset bedding (10 m water depth).

F. Vibracore radiograph from delta-front channel thalweg showing trough crossbedding off Yukon Delta (1 m water depth).

G. Photograph of vibracore epoxy peel from margin of delta front channel west of Yukon Delta showing a graded storm sand layer with a typical vertical sequence of flat, cross, and flat lamination from base to top of layer (1.5 m water depth).

H. 70-mm bottom photograph of a small sand wave (0.5 m wave height and 10 m wavelength) with superimposed linguoid ripples on the crest of York shoal west of Port Clarence (17 m water depth).

I. Oblique aerial photograph of a shore-parallel shoal in northeast Kuskokwim Bay. Note subdued cross sets of sand waves.

J. Ground-based photograph of ripples on a shore-parallel shoal in northwest Kuskokwim Bay.

Figure 5. Morphology, texture, and bedforms of sand ridges near Bering Strait.

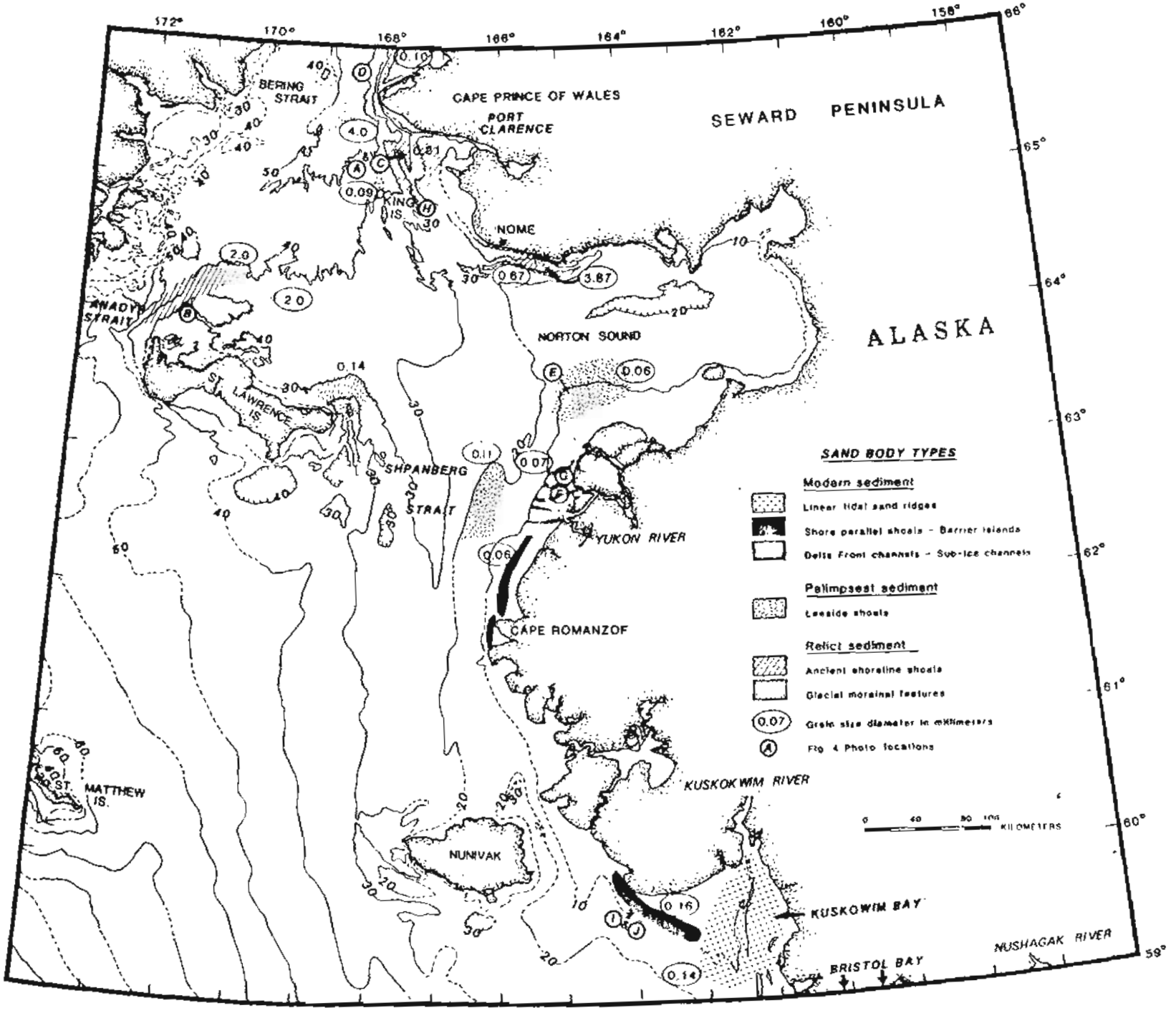
172°
170°
168°
166°
164°
162°
160°
158°
66°
65°
64°
63°
62°
61°
60°
59°
BERING STRAIT
CAPE PRINCE OF WALES
PORT CLARENCE
SEWARD PENINSULA
KING IS.
NOME
ANADYR STRAIT
NORTON SOUND
ALASKA
ST. LAWRENCE IS.
SHPANBERG STRAIT
YUKON RIVER
CAPE ROMANZOF
KUSKOKWIM RIVER
ST. MATTHEW IS.
NUNIVAK
KUSKOWIM BAY
BRISTOL BAY
NUSHAGAK RIVER
SAND BODY TYPES
Modern sediment
Linear tidal sand ridges
Shore parallel shoals - Barrier islands
Delta Front channels - Sub-ice channels
Palimpsest sediment
Leeside shoals
Relict sediment
Ancient shoreline shoals
Glacial morainal features
Grain size diameter in millimeters
Fig. 4 Photo locations
KILOMETERS

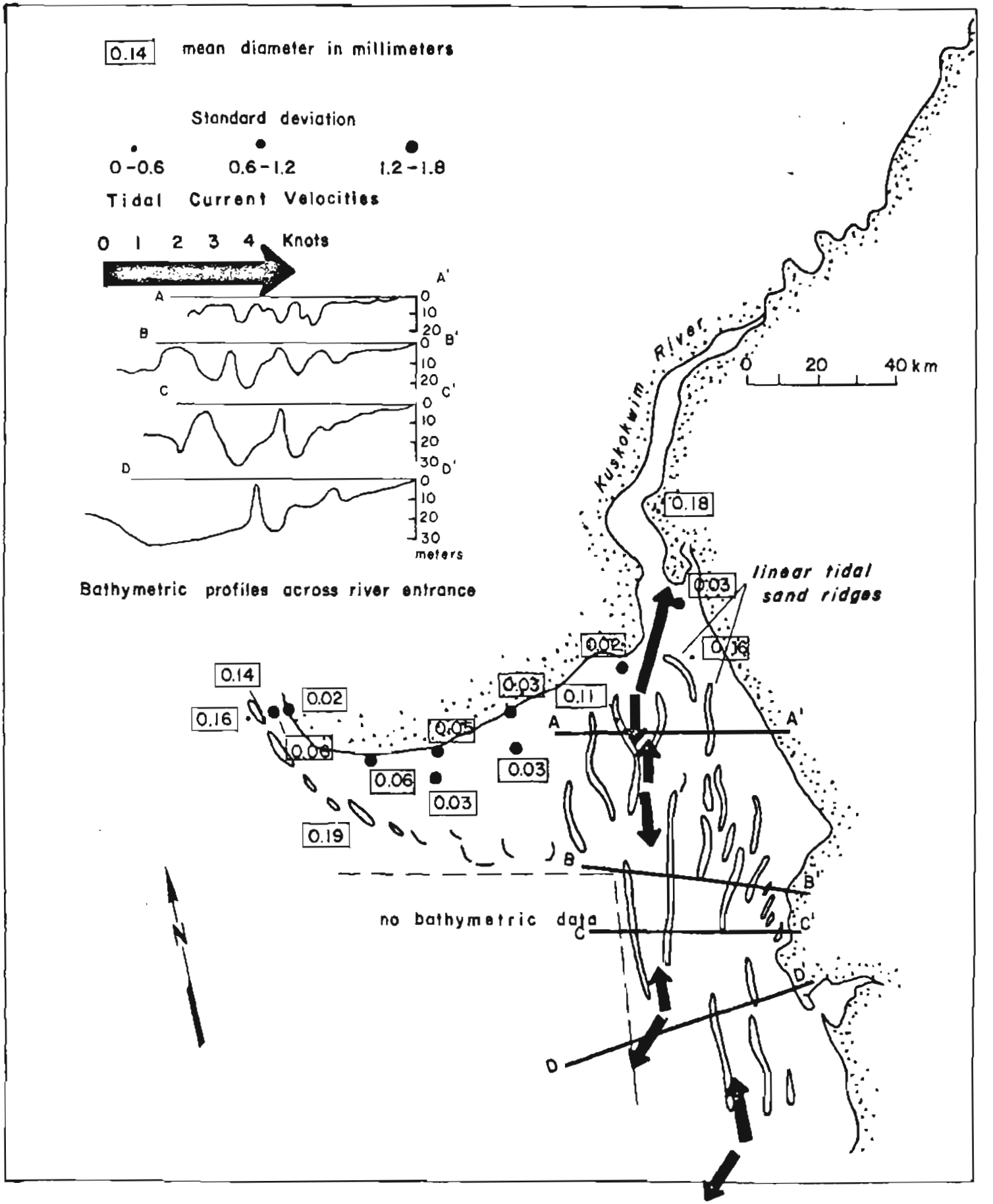
0.14 mean diameter in millimeters
Standard deviation
0-0.6
0.6-1.2
1.2-1.8
Tidal Current Velocities
0 1 2 3 4 Knots
A
A'
B
B'
C
C'
D
D'
meters
Bathymetric profiles across river entrance
Kuskokwim River
0 20 40 km
0.18
0.03
linear tidal sand ridges
0.02
0.16
0.14
0.02
0.03
0.11
0.16
0.05
0.06
0.03
0.03
0.19
no bathymetric data
N

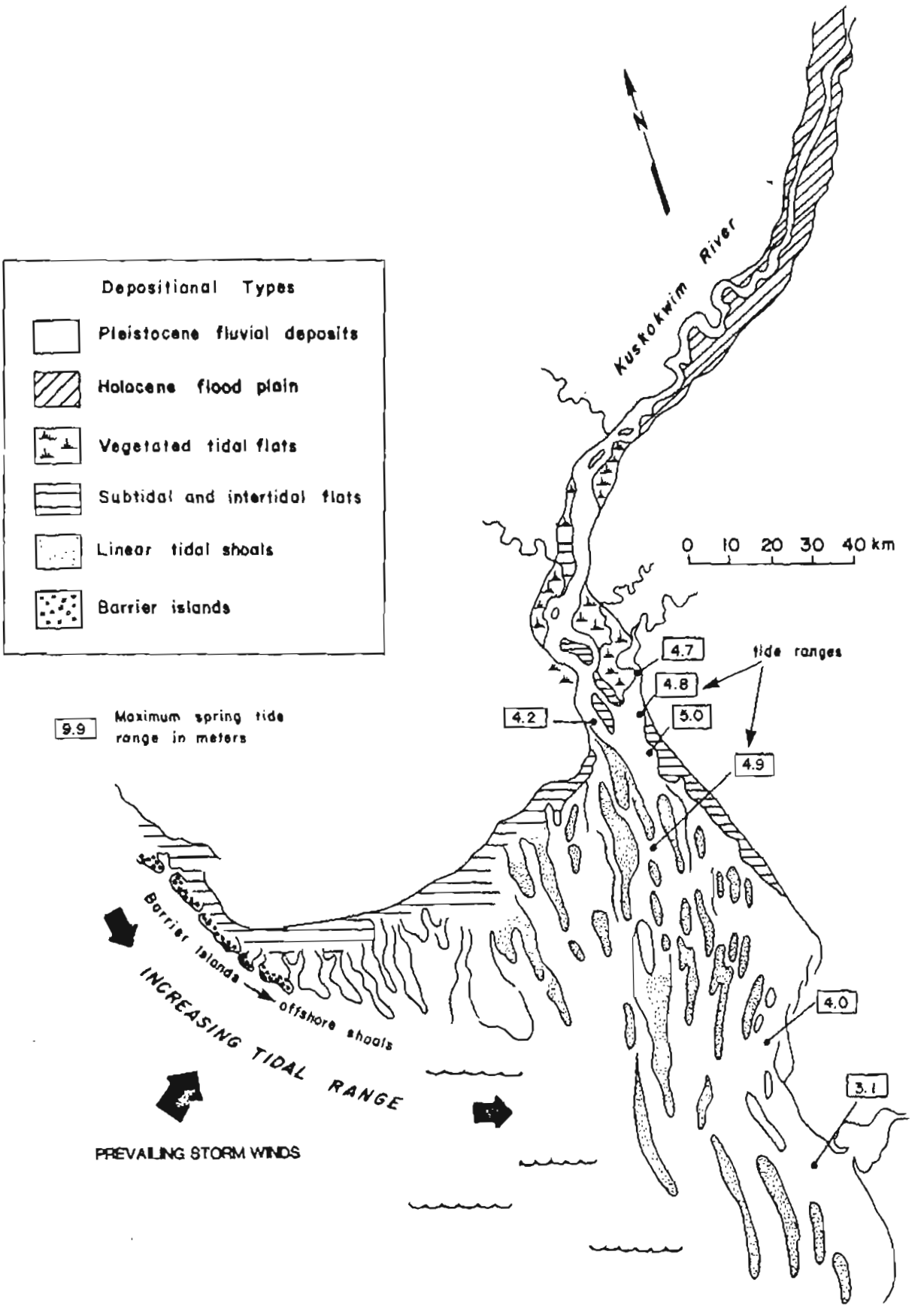
Depositional Types
Pleistocene fluvial deposits
Holocene flood plain
Vegetated tidal flats
Subtidal and intertidal flats
Linear tidal shoals
Barrier islands
N
Kuskokwim River
0 10 20 30 40 km
tide ranges
4.7
4.8
5.0
4.2
4.9
4.0
3.1
9.9
Maximum spring tide range in meters
Barrier islands
offshore shoals
INCREASING TIDAL RANGE
PREVAILING STORM WINDS

INTERNAL STRUCTURES

SURFACE BEDFORMS

Ancient Shoreline Shoal

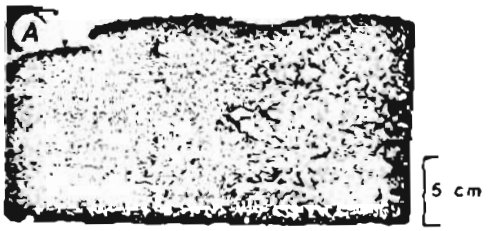

Ancient Shoreline Shoal–Glacial

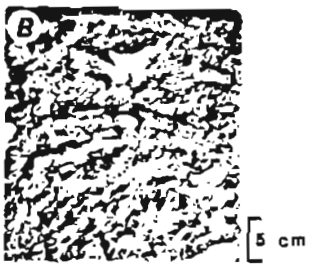

Ancient Shoreline Shoal

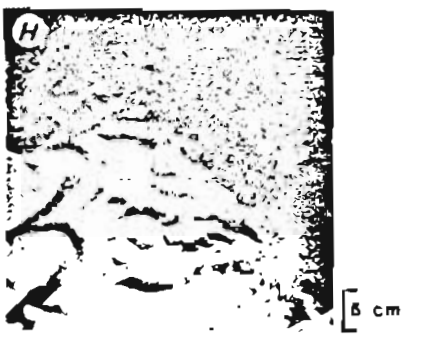

Leeside Shoal

Cape Prince of Wales

Yukon

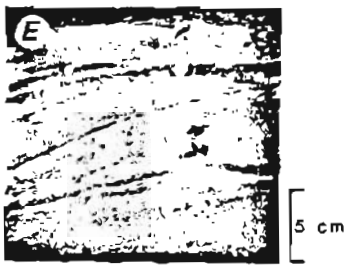

Shore Parallel Shoal

Ancient Shoreline Shoal

Yukon Delta Front Channel

Thalweg

Margin

Shore Parallel Shoal

BATHYMETRIC PROFILES

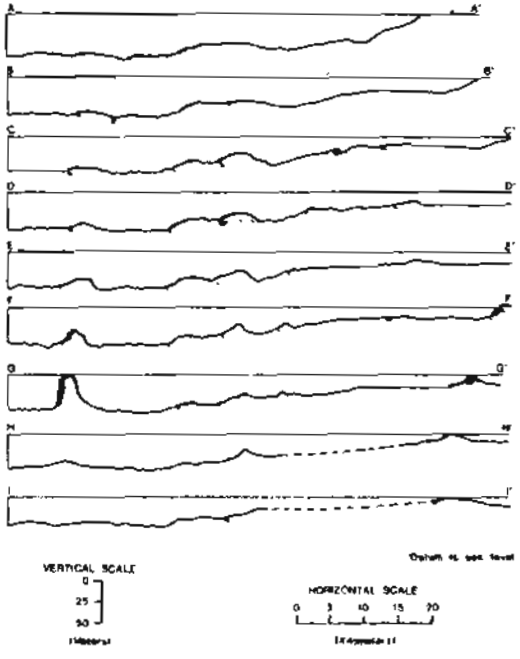

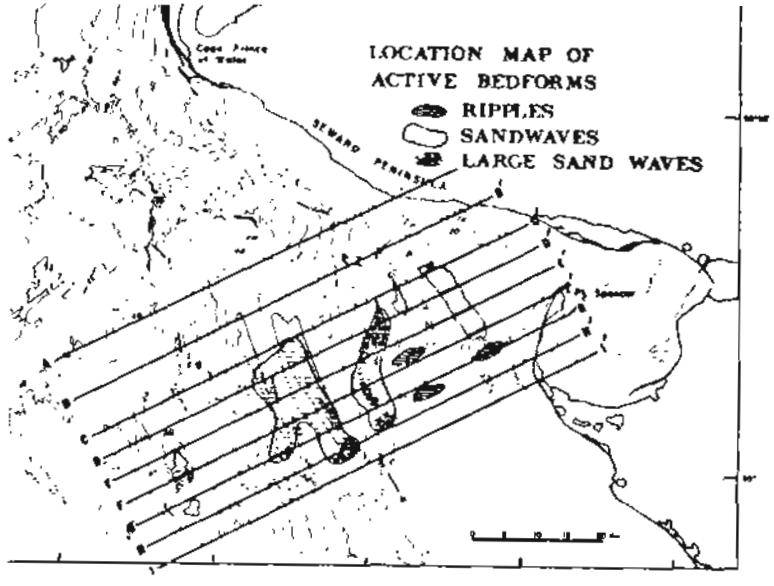

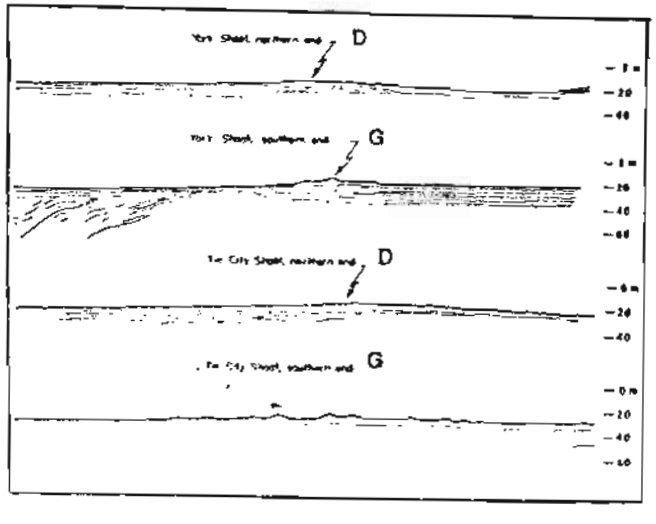

SEDIMENT DISTRIBUTION

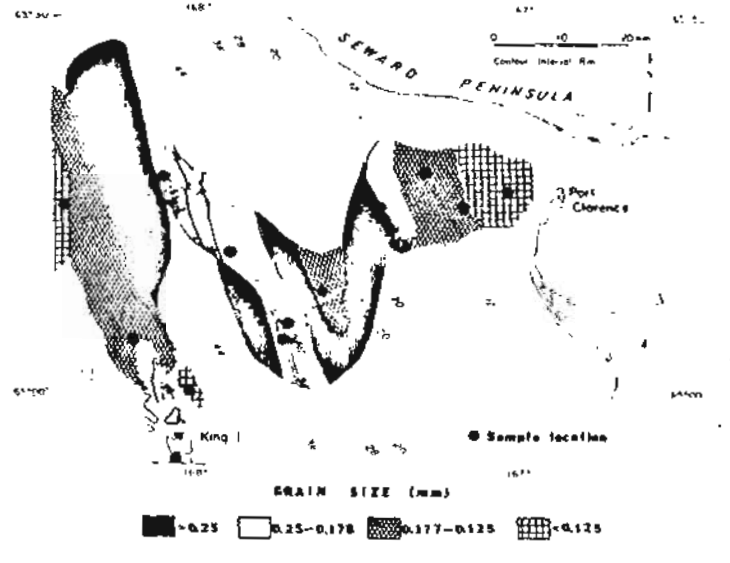

DEPOSITIONAL AND EROSIONAL FEATURES OF THE INNER SHELF, NORTHEASTERN BERING SEA

Ralph E. Hunter, Devin R. Thor, and Mary Lou Swisher

U. S. Geological Survey

Menlo Park, California 94025

ABSTRACT

Sonographs and bathymetric profiles from water depths less than 15 m in the Nome-Solomon, Port Clarence, and Yukon delta areas of the Alaskan Bering Sea coast show features generated by waves, currents, and drifting ice. The surficial sediments in the Nome-Solomon and Port Clarence areas range in grain size from sand to boulder gravel and have many surface features visible on sonographs, whereas the sediments of the Yukon delta are fine sands and silts that have few such features.

Materials in the Nome-Solomon and Port Clarence areas have been segregated by grain size into ribbons and irregular, elongate, and lobate patches. The sand patches commonly have convex-up profiles and probably rest on gravel lag deposits that are exposed in adjacent gravel patches. Coarse sand and fine gravel patches and ribbons are characterized by symmetrical ripples, spaced 0.5 to 2 m apart, that could only have been generated by storm waves. Gravelly sand waves in the Nome-Solomon area were formed by westward shore-parallel currents. Boulder gravel ridges in this area are of unknown origin.

Sand and gravel ribbons are common near the entrance to Port Clarence. Unlike ribbons elsewhere, which have been attributed to tidal or other currents, the ribbons in the Port Clarence area show features suggesting generation by storm waves. These ribbons are oriented approximately normal to the associated large wave ripples, and both the ripples and ribbons vary in orientation in ways that can be explained as effects of wave refraction over a shoaling bottom. Ribbonlike features of unknown origin occur locally on the Yukon delta front.

Ice-gouged furrows, though less common than in areas farther offshore, occur in all the nearshore areas studied. The gouges are 5 to 15 m wide, as much as hundreds of meters long, and usually less than 0.25 m deep. Some gouges off Nome and Safety Sound are caused by tugboat cables, barge cables, or anchors dragging on the bottom.

INTRODUCTION

Strong currents are known to occur in parts of the northern Bering Sea, particularly in the approaches to Bering Strait. These currents include a semipermanent northward drift toward Bering Strait and fluctuating tidal and wind-driven currents (Coachman et al., 1975). The geologic importance of these currents in areas more than a few kilometers from shore has been shown in studies by Nelson and Hopkins (1972), Moore and Welkie (1976), Field et al. (1977), Nelson et al (1977), Cacchione et al. (this volume), and Drake et al. (in press). Studies by Hunter et al. (1979), in contrast, have shown that waves and wave-induced currents are the dominant geologic agents on the beaches during the ice-free season. The shoreface, from the shoreline to a depth of 15 m, seemed likely to include the zone of transition from wave dominance to current dominance, and this previously little studied depth zone was the target of the present study.

We selected for detailed study three areas that offer a wide variety of sediment grain sizes and exposures to waves and currents: Port Clarence and vicinity, the stretch of coast from Nome to Solomon, and the Yukon delta (Fig. 1).

Data on these areas were gathered aboard the R/V KARLUK during June and July 1978. Data collected while underway include side-scan sonar, 7 kHz, and 200 kHz records; data collected at stations include underwater television

tapes, observations made while diving with scuba, and a few sediment samples to supplement those gathered during previous studies by Nelson and Hopkins (1972), Moore and Welkie (1976), and McManus et al. (1977).

SETTING

Port Clarence

Port Clarence is an embayment 25 to 30 km across (Fig. 2), protected from the Bering Sea by a Holocene gravel spit (Black, 1958). On the north, a Holocene gravel barrier separates Port Clarence from Brevig Lagoon. The inlet to Port Clarence is 7.3 km wide, has a maximum depth of 16 m, and is floored by mud (Moore and Welkie, 1976; McManus et al., 1977). The margins of the inlet, where most of the features visible on sonographs are located, are floored by sand and gravel. The surficial sediments are presumably Holocene, but the thickness of Holocene deposits is not known.

The mean tidal range in Port Clarence is 0.4 m. Currents through the inlet have not been studied, but the small tidal range and large cross-sectional area of the inlet ensure that the tidal currents are not extremely strong. Storm surges, known to be as high as 3.25 m (Sallenger et al., 1978), undoubtedly create stronger currents. The northward drift of the Alaskan Coastal Water toward Bering Strait (Coachman et al., 1975) may not affect the embayed coast near Port Clarence very strongly. The only long fetch for waves is to the southwest.

Nome-Solomon Area

The coast in the Nome area has developed by erosion of Pleistocene glacial and associated deposits (Hopkins et al., 1960; Nelson and Hopkins, 1972; Tagg and Greene, 1973). In the area from Safety Sound to Solomon,

Holocene barriers of sand and gravel have formed in front of the mainland (Fig. 3). The shoreface in the Nome-Solomon area slopes steeply to a depth of 12 m. Beyond the shoreface, the seafloor slopes more gently. The only Holocene deposits off Nome are gravel lag deposits and thin sand patches. Sand and gravel of presumed Holocene age occur off the Safety Sound-Solomon area, but the thickness of Holocene deposits is not known.

The mean tidal range at Nome is 0.3 m. Strong westward currents, tidal in part but reinforced by a net drift, are known to occur in northern Norton Sound (Nelson and Hopkins, 1972; Coachman et al., 1975). Currents associated with storm surges, which are as high as 4.75 m at the east end of Norton Sound (Sallenger et al., 1978), may be very strong. Fetches for waves are fairly long to the south and southeast and longest to the southwest.

Yukon Delta

The Yukon River debouches into the northern Bering Sea and forms a large arcuate delta complex in southwestern Norton Sound. The offshore part of this complex comprises three major components: (1) a sub-ice platform, (2) a delta front, and (3) a prodelta (Dupré, this volume) (Fig. 4). The sub-ice platform extends 10 to 30 km offshore as a bearkt featureless plain at water depths of 1 to 3 m. Dissecting the platform are several subaqueous distributary channels. The delta front, which is relatively steep and locally irregular, extends from the break in slope at the outer edge of the sub-ice platform to a water depth of 10 m. The prodelta slopes gently seaward from the toe of the delta front. Sediment of the delta complex is silt to fine sand.

Wave and current patterns in southwestern Norton Sound are poorly known. The major wave trains move northward from the southern Bering Sea and refract clockwise around the protruding Yukon shoals (Sallenger et al., 1978). Fetches are shorter to the north and northeast. The mean tidal range varies from 0.5 to 1.2 m around the delta margin.

Marine Climate

The coastal waters of the northeastern Bering Sea are usually free of ice from middle or late May to late October or early November. During the ice-free season the wind and wave regimens are variable; no distinctly dominant wind or wave direction is evident in data from the northeastern Bering Sea (Brower et al., 1977). The largest storms usually occur around the time of freeze-up in the fall, and the winds and waves during these storms are mostly from the east, northeast, or north. These storms may or may not affect the coastal waters, depending on the fetch in the direction of the storm winds and the timing of the storm with respect to freeze-up. In general, the direction of the dominant waves along a given stretch of shore is closely related to the direction of greatest fetch.

FEATURES PRODUCED BY WAVES AND CURRENTS

Areas off Southern Seward Peninsula

Features in the Port Clarence and Nome-Solomon inner shelf areas off the southern Seward Peninsula are similar, largely because of the similarly coarse sediment in the two areas. Wave- and current-produced features in these areas include sand and gravel patches and ribbons, wave ripples, and large current-produced transverse bedforms.

Patches

Irregular segregations of sand and gravel are ubiquitous in the Nome-Solomon area (Fig. 5). On sonographs, the sand patches are light toned and the gravel patches dark toned. The patches are extremely variable in width, ranging from 10 to 500 m. In the shallowest water depths studied, 4 to 8 m, the sand patches are sharply separated from gravel, which consists of cobbles and boulders. These shallow-water patches range in shape from very irregular (Fig. 5a) to roughly elongate at high angles to shore (Fig. 5b). Locally the sand patches are smoothly curved seaward-convex lobes spaced an average of 450 m apart (Fig. 6). On some of the bathymetric profiles, sand patches can be distinguished from gravel patches by differences in acoustic signature (Fig. 5c, d). The sand patches have smooth convex-up surfaces that typically rise above the intervening gravel, and with little doubt the sand forms lenses resting on a gravel substrate. Where the gravel surface is irregular, gravel ridges or mounds commonly rise above the sand lenses (Fig. 5).

In water deeper than 10 m, the patches become less distinct because patches of pebbly sand and pebble gravel commonly occur between the coarser gravel and the sand. Much of the pebbly sand and pebble gravel is visibly rippled on sonographs (Fig. 7). Many textural segregations are recognizable more by differences in ripple size and trend than by tonal differences on the sonographs (Fig. 7b).

The tendency for the patches to be elongate at high angles to shore and to have straighter boundaries at high angles to shore than at low angles represents a tendency toward ribbonlike forms. No well-developed ribbons are found in the Nome-Solomon area, however. The possible significance of the ribbonlike forms will be discussed in connection with the well-developed ribbons in the Port Clarence area. The lobate form and regular spacing of

some of the nearshore sand patches suggest an origin by stationary rip currents or edge waves.

Wave Ripples

Ripples with spacings of 0.5 to 2.0 m are commonly visible on sonographs in both the Nome-Solomon and Port Clarence areas (Fig. 7). These ripples were identified as wave generated by their symmetry as seen on the sonographs, by underwater television, and by diving. They occur wherever the sediment is moderately to well sorted and of a suitable grain size, in the very coarse sand to pebble gravel grades. Wave ripples of similar size in similarly coarse sediment are known from many areas (Trask, 1955; Vause, 1959; Newton and Werner, 1972; Channon and Hamilton, 1976). All of the large wave ripples were inactive when seen by television camera or by diving and must have formed during storms. In addition to the large inactive ripples, active ripples too small to be visible on sonographs were present in medium-grained sand.

All wave ripples in the Port Clarence inlet area trend northwest-southeast and can be explained as products of storm waves propagating northeastward out of the Bering Sea. In the Nome area, at least three sets of wave ripples can be seen at a depth of 12 m (Fig. 7d). The largest ripples (spacing 1.3 m) were formed by waves from the southwest, the middle-sized ripples (spacing 0.7 m) were formed by waves from the south, and the smallest ripples visible on the sonographs (spacing 0.4 m) were formed by waves from the south-southwest. Ripples of successively smaller size occur in successively finer sediment. Waves generated during a major storm must have formed the largest ripples in the coarsest rippled sediment. This large storm presumably formed ripples in finer sediment as well, but only the ripples in the coarsest sediment remained inactive and unmodified until the time of

observation. After the largest ripples were formed, successively smaller ripples were formed in successively finer material by what must have been successively smaller waves at successively later times.

In more detailed hydrodynamic terms, the wave ripples may be classified as vortex ripples because of their steepness (Dingler and Inman, 1977). At least the larger ripples are probably of orbital type, having a spacing similar to the orbital diameter of the waves (Clifton, 1976, Figs. 11-13). Calculations based on threshold velocities for grain movement (Rance and Warren, 1969; Komar, 1976; Dingler, 1979) and on the upper limit for the existence of orbital ripples (Mogridge and Kamphuis, 1972) suggest that the largest ripples (ripple spacing of 2.0 m in gravel having a median diameter of 2 to 8 mm at a water depth of 12 m) were formed by waves 2 to 5 m high having a period of 6 to 11 s.

Ribbons

Linear segregations or ribbons of sand and gravel are well developed at water depths of 4 to 8 m on the north side of Port Clarence, just outside and inside the inlet (Fig. 8). The ribbons are developed in three sizes of material with distinct side-scan sonar signatures similar to those in the Nome-Solomon area: unrippled cobble and coarse-pebble gravel, pebbly sand and fine-pebble gravel with wave ripples visible on sonographs, and sand with wave ripples too small to be visible on sonographs. Commonly the three materials lie next to one another in order of grain size (Fig. 8a, c). The ribbons show little regularity of spacing or width, but the average spacing is roughly estimated at 60 m. No relief is detectable on the bathymetric profiles, but underwater television suggests that the sand lies on the gravel.

Ribbons in other areas have been interpreted as longitudinal current-produced bedforms (Kenyon, 1970). The currents that produce most ribbons are tidal, though wind-driven currents have apparently produced some ribbons or similar textural bands (Stride and Chesterman, 1973; McKinney et al., 1974). For the Port Clarence area, however, a strong though not conclusive argument can be made that the ribbons are produced by wave action and are oriented parallel to the direction of wave propagation.

The evidence for a wave origin of the ribbons is in part negative. The ribbons are not parallel to the expected east-west direction of tidal or storm-surge currents through the inlet (Fig. 9). Nor are the ribbons approximately parallel to shore, as would be expected for Ekman currents driven by winds at almost any angle to shore in very shallow water (Neumann and Pierson, 1966, p. 202-203). The ribbons do not change in orientation significantly along irregularly curving isobaths on the north side of the inlet, as might be expected if the ribbons were parallel to currents that were deflected around seafloor irregularities.

Several positive kinds of evidence suggest an origin by wave action. The general northeast-southwest trend of the ribbons is parallel to the direction of greatest fetch and roughly normal to the trend of the accompanying wave ripples. Both the ribbons and the ripples curve in ways consistent with wave refraction; that is, the ribbons become more nearly perpendicular to shore as the bottom shoals and the ripples become more nearly parallel to shore.

Exactly how waves might produce ribbons is not known, though several mechanisms are conceivable. Originally irregular textural segregations produced by other causes might become streaked out by sediment transport caused either by wave-induced net water motion in the direction of wave propagation or, if net water motion is absent, by the time-velocity asymmetry

of wave orbital motion (short but strong pulses in the direction of wave propagation and longer but weaker pulses in the opposite direction). Langmuir circulation induced by waves or by wave-current interaction (Faller and Caponi, 1978) might be capable of forming linear textural segregations where no segregations had existed previously.

The hypothesis of ribbon generation by wave action is complicated by the fact that some of the ribbons in very shallow water are parallel to, and possibly bounded by, ice gouges (Fig. 8d). These ribbons may have somehow been produced by gouging. The occurrence of straight parallel ribbons through a depth range of 4 to 15 m, however, is difficult to reconcile with an origin by gouging, given the probability of ice grounding somewhere in that depth range.

An origin by wave action may explain the ribbonlike tendencies of the elongate textural segregations in the Nome-Solomon area. The poorer development of ribbonlike forms in that area than in the Port Clarence area could be explained by a greater variability of wave directions, as suggested by the greater variability in orientation of wave ripples.

Ribbons or elongate textural patches oriented at high angles to shore or normal to wave ripples have been observed elsewhere. McKinney and Pilkey (1969) observed textural bands oriented normal to large wave ripples on the Atlantic shelf of the southeastern United States. Newton et al. (1973) observed bands oriented at high angles to shore at relatively shallow depths (30-40 m) on the Atlantic shelf of northwest Africa. Swift et al. (1976) and Swift and Freeland (1978) observed textural bands oriented at high angles to shore off the northeastern United States but were not certain whether the bands were parallel to or transverse to the currents. Reimnitz et al. (1976) interpreted shore-normal rippled and unrippled bands off the west coast of

Mexico as products of rip currents. Such an interpretation is not feasible for the Port Clarence ribbons, which extend to water depths of 15 m, more than 3 km from shore. Textural bands tentatively interpreted as a product of Langmuir circulations generated by a combination of wind and waves have been observed on the San Pedro shelf off southern California (Karl, 1980).

Current-Produced Transverse Bedforms

Bedforms that can definitely be interpreted as produced by currents are not common in the Port Clarence and Nome-Solomon areas. Asymmetric sand waves having spacings of 2 to 4 m occur in the deeper parts of the inlet to Port Clarence (Fig. 9). Asymmetric transverse bedforms composed at least partly of pebble gravel occur in water depths of 12 to 15 m off Safety Sound (Fig. 10a). These bedforms are as much as 2.5 m in height, average 200 m in spacing, trend at a high angle to shore (N 12°E), and face westward.

Boulder ridges in water depths of 12 to 15 m off Nome trend at high angles to shore (trend N 33-60°E) and have relatively steep west-facing slopes (Fig. 10b). Underwater television showed that the west-facing slopes are composed of boulders and the more gentle east-facing slopes are composed of sand and relatively fine gravel.

The direction of asymmetry of the bedforms off Safety Sound is in accord with the dominance of westward currents in northern Norton Sound (Nelson and Hopkins, 1972; Coachman et al., 1975). These bedforms were probably produced by westward tidal currents reinforced by the semipermanent net westward drift, by storm-surge relaxation currents, or by a combination of these currents. The origin of the boulder ridges off Nome is not known. If they were produced by modern currents, only storm-surge relaxation currents could possibly be of adequate strength, and even these currents may not be capable of moving

boulders. An alternative explanation is that the boulder ridges were produced during the Holocene transgression at water depths shallower than present. If so, they may be similar in origin to the boulder ridges at water depths of 4 to 8 m off Nome (Fig. 5c) except that sand and finer gravel have been banked up against their east sides. Even assuming an origin in shallower water, it remains unknown whether the ridgelike form of the boulder masses was produced by wave and current action or resulted from the original distribution of boulders in the glacial or glaciofluvial material eroded during the Holocene transgression.

Areas Off Yukon Delta

Rolling and hummocky topography

Irregular rolling and hummocky topography characterizes the seaward edge of the sub-ice platform and the upper part of the delta front (Fig. 4b). North of the delta, the topography consists of east-west-trending sediment shoals that form a transition zone between the sub-ice platform and the delta front. Water depths over the shoal crests are 1 to 2 m and over the intervening troughs are 4 to 6 m. The shoal crests are 3 to 6 km apart. Seaward of the shoals, on the upper part of the delta front, the surface is undulatory or rolling. Relief is as much as 1 m, and the crests are 100 to 300 m apart. Below a water depth of about 5 m, the undulations disappear and the delta front slopes smoothly down to the nearly flat prodelta.

The morphologic character of the offshore part of the delta changes from the northern to the western side. The sub-ice platform on the western side is narrower than the platform on the northern side, and the slope of the delta front and prodelta on the western side is twice as steep as the slope on the northern side. The western delta front is irregular and hummocky but does not

have the shoals or rolling topography characteristic of the northern delta front. Locally, the western delta front has seaward-facing steps, which may be slump scarps, with as much as 0.5 m relief. Possible slump features are shown in Figure 11a. Current-scour depressions and erosion into underlying competent beds are also seen on the lower part of the western delta front or upper prodelta (Fig. 11b). Two major and numerous minor subaqueous distributary channels cut through the sub-ice platform and delta front. In contrast, the northern parts of the sub-ice platform and delta front have no channels. Scour in the channels (Fig. 11c) is proof that the channels are modern and active.

The differences in topographic features between the northern and western sides of the offshore delta complex suggest different processes or differences in degree and intensity of the processes at work. Unlike the northern side, which faces Norton Sound, the western side faces the open Bering Sea and is strongly affected by the north-flowing Alaskan Coastal Water Current. The northern delta front and sub-ice platform are in a destructive or erosive phase characterized by wave and current reworking of sediment into features such as shoals, ripples, and rolling topography. The western delta front and sub-ice platform are in a constructive phase characterized by rapid sedimentation and associated processes such as channeling, current scour, and slumping.

Sand waves and ripples

Sand waves and ripples are found on the upper parts of the delta front and on the flanks and bottoms of the major subaqueous distributary channels on the western side of the delta (Fig. 4b). Wavy bedforms on the upper part of the delta front have heights of 10 to 50 cm and wavelengths of 10 to 200 m.

These bedforms progressively increase in height toward the tops of the transition-zone shoals. The bedform crests trend generally east-west, subparalleling the trend of the shoals.

Asymmetric ripples on the flanks of subaqueous distributary channels have wavelengths of 3 to 5 m. Sand waves in the channels are strongly asymmetrical seaward-facing bedforms with wavelengths ranging from 25 to 200 m and heights of 0.5 to 1 m (Fig. 10c, d).

The sand waves and ripples are interpreted to be in equilibrium with the present wave and current regimes. Bedforms on the delta front are caused by waves and/or currents impacting the shoals of the delta front. Ripples on the flanks of subaqueous distributary channels are possibly caused by overbank flow during times of high river discharge. Sand waves on channel bottoms are caused by high flow velocities during times of high river discharge.

Ribbons

Features interpreted as sediment ribbons (Fig. 11d) are visible on sonographs from an area north of the Yukon delta, on the upper part of the delta front (Fig. 4b). The ribbons occur on the crests, flanks, and troughs of the broadly rolling ridges characteristic of the upper part of the delta front. The ribbons trend N 60-90°W, generally parallel to the trend of the rolling topography. Spacing between ribbons varies from 10 to 150 m. The wider spaced ribbons tend to occur more commonly in the trough areas. Associated with the ribbons are wavy bed-relief features, visible on depth profiles, that have wavelengths similar to ribbon spacing, but the lack of a one-to-one correspondence in location or spacing between these two features obscures their relations. As ribbon and interribbon areas were not sampled, the grain size of these features is not known. The character of the ribbons

on the sonographs, however, requires some acoustic difference (probably grain size) between ribbon and interribbon areas. The lack of correspondence between relief features and ribbons eliminates the possibility that the ribbon features are simply bedform shadows.

The ribbons occur in shallow water on the south side of the entrance to Norton Sound. This area is highly susceptible to southern Bering Sea storm waves, storm-surge run-off, the Alaskan Coastal Water Current, and tidal currents that would pass through the area either in a westward or an eastward direction. The ribbons here are subparallel to known or probable current directions and are possibly longitudinal features produced by one or more of these currents.

FEATURES PRODUCED BY ICE

Furrows produced by gouging of the seafloor are found in parts of the study area (Fig. 12). Three types of gouging occur: two are formed naturally by ice plowing the bottom sediment and one is formed artificially by anchors, anchor chains, or cables dragging the bottom. Single ice gouges are produced by a single ice keel plowing the bottom sediment. These gouges range in width from 5 to 20 m and are as much as one meter deep, although most are less than one-half meter deep (Fig. 12a, b). Multiple gouges are produced by multikeel ice plowing or "raking" the bottom sediment, creating numerous parallel furrows (Fig. 12c). Zones of raking are as much as 100 m wide. Artificial gouges are straighter and narrower (2 m or less) than most ice gouges (Fig. 12d).

Both single and multiple gouges are related to ice dynamics in Norton Sound. Landsat imagery has been used to study ice movement in northeastern Bering Sea (Dupré, 1978). Pack ice usually moves in a southwestward or

westward direction, pushed by the prevailing northeasterly winds. When this pack ice collides with other floes or with stationary shorefast ice, ice keels are forced deeper into the water. These keels keep moving with the ice pack but extend down far enough to plow the bottom. Gouges in Norton Sound generally trend subparallel to the shore (Fig. 4b), in agreement with ice movement directions as determined by satellite imagery. Ice-gouge trends in and around Port Clarence are more randomly oriented (Fig. 9), suggesting more complex ice movement in this embayed area.

Gouge furrows are not a common feature in the Nome/Safety Sound area because of ice movement patterns and because of current and wave action. Ice generally moves in a southwestward direction, making northern Norton Sound an area of ice divergence, not conducive to intense or dense gouging. Southwestern Norton Sound (Yukon prodelta area) is an area of ice convergence and consequently of high gouge density. Gouges are probably ephemeral features in this area because storm waves and tidal currents are capable of eroding the gouges or burying them by sediment.

Artificial gouges (Fig. 12d) have been found off Nome and off Safety Sound. They differ from ice gouges in that they are narrower, usually trend at a high angle to shore, and are found only in areas that have high barge traffic. Potential gouging tools are: (1) anchors and anchor chains that drag the bottom during deployment or recovery, (2) long tow cables between barges and tugboat, which tend to drag bottom even while underway, and (3) stabilization cables that trail from barge sterns.

CONCLUSIONS

A rich assemblage of wave- and current-produced features visible on sonographs is present in shallow water close to the southern shore of Seward Peninsula. The richness of the assemblage is dependent on the textural variability and general coarseness of the sediment. Few features were seen on sonographs from the fine sand and silt areas of the Yukon delta except in channels subject to river discharge.

In general, features known or thought to be produced by waves are more common than current-formed features. Where current-formed features do occur, they tend to be restricted to deeper parts of the shallow depth zone investigated here. Although the current-formed features are not common, some of them imply considerable sediment transport by strong currents. In the Nome-Solomon area, the current-formed features indicate westward sediment transport, opposite from the wave-induced net sediment transport along the beaches.

The more problematical features described here clearly need to be investigated further. Among such features are the lobate sand patches off Safety Sound, the ribbons interpreted to be produced by wave action in the Port Clarence area, the boulder ridges off Nome and Safety Sound, and the ribbons on the Yukon Delta.

ACKNOWLEDGMENTS

This study was supported jointly by the U.S. Geological Survey and the Bureau of Land Management through an interagency agreement with the National Oceanic and Atmospheric Administration, under which a multiyear program responding to needs of petroleum development of the Alaskan continental shelf is managed by the Outer Continental Shelf Environmental Assessment Program (OCSEAP) Office.

We wish to thank Tom Barnett, Captain of the R/V KARLUK, Bob Novak, Harry Hill, Jim Howard, Matt Larsen, Mark Holmes, and Dave McCulloch for their assistance during the cruises. We also thank Bill Dillon and Herman Karl for their reviews of the manuscript.

REFERENCES

Black, R. F. (1958) Permafrost, water-supply, and engineering geology of Point Spencer Spit, Seward Peninsula, Alaska. Arctic, 11, 102-116.

Brower, W. A., Jr., Diaz, H. F., Prechtel, A. S., Searby, H. W. & Wise, J. L. (1977) Climatic atlas of the outer continental shelf waters and coastal regions of Alaska. Vol. II, Bering Sea. Arctic Environ. Inf. and Data Center, Anchorage, Alaska, and Natl. Climatic Center, Asheville, N. C.

Cacchione, D. A., Drake, D. E. & Wiberg, Patricia (this volume) Bottom shear stress generated by waves and currents in the northern Bering Sea. Spec. Pub. Internat. Assoc. Sedimentologists.

Channon, R. D. & Hamilton, D. (1976) Wave and tidal current sorting of shelf sediments southwest of England. Sedimentology, 23, 17-42.

Clifton, H. E. (1976) Wave-formed sedimentary structures - a conceptual model. In (Ed. by R. A. Davis, Jr. & R. L. Ethington) Beach and nearshore sedimentation. Spec. Pap. Soc. econ. Paleont. Miner. 24, 126-148.

Coachman, L. K., Aagaard, Knut & Tripp, R. B. (1975) Bering Strait: the regional physical oceanography. Univ. Washington Press, Seattle.

Dingler, J. R. (1979) The threshold of grain motion under oscillatory flow in a laboratory wave channel. J. sedim. Petrol. 49, 287-294.

Dingler, J. R. & Inman, D. L. (1977) Wave-formed ripples in nearshore sands. Conf. Coastal Engring., 15th, Proc. 2109-2125.

Drake, D. E., Cacchione, D. A., Muench, R. D. & Nelson, C. H. (in press) Sediment transport in Norton Sound, Alaska. Mar. Geol.

Dupré, W. R. (1978) Yukon delta coastal processes study, in Environmental assessment of the Alaskan continental shelf, Annual reports of principal investigators for the year ending March 1978. Vol. XI, Hazards. Natl. Oceanic and Atmospheric Admin. and Bur. Land Management, 384-446.

Dupré, W. R. (this volume) Seasonal variations in deltaic sedimentation on a high-latitude epicontinental shelf. Spec. Pub. Internat. Assoc. Sedimentologists.

Faller, A. J. & Caponi, E. A. (1978) Laboratory studies of wind-driven Langmuir circulations. Jour. Geophys. Res. 83, 3617-3633.

Field, M. E., Nelson, Hans, Cacchione, D. A. & Drake, D. E. (1977) Dynamics of bedforms of an epicontinental shelf: northern Bering Sea (abs.). Am. geophys. Union Trans. (EOS), 58, 1162.

Hopkins, D. M., McNeil, F. S. & Leopold, E. B. (1960) The coastal plain of Nome, Alaska. Internat. geol. Cong., XXI Sess., 4, 46-57.

Hunter, R. E., Sallenger, A. H. & Dupré, W. R. (1979) Maps showing directions of longshore sediment transport along the Alaskan Bering Sea coast. Misc. Field Studies Map U. S. geol. Surv. MF-1049.

Karl, H. A. (1980) Speculations on processes responsible for mesoscale current lineations on the continental shelf, Southern California. Mar. Geol. 34, M9-M18.

Kenyon, N. H. (1970) Sand ribbons of European tidal seas. Mar. Geol. 9, 25-39.

Komar, P. D. (1976) Beach processes and sedimentation. Prentice-Hall, Englewood Cliffs, N. J.

Larsen, M. C., Nelson, Hans & Thor, D. R. (1980) Geologic implications and potential hazards of scour depressions on Bering shelf, Alaska. Environmental Geol. 3, 39-47.

MacIntyre, I. G. & Pilkey, O. H. (1969) Preliminary comments on linear sand-surface features, Onslow Bay, North Carolina continental shelf: problems in making detailed sea-floor observations. Maritime Sediments, 5, 26-29.

McKinney, T. F., Stubblefield, W. L. & Swift, D. J. P. (1974) Large-scale current lineations on the central New Jersey shelf: investigations by side-scan sonar. Mar. Geol. 17, 79-102.

McManus, D. A., Kolla, Venkatarathnam, Hopkins, D. M. & Nelson, C. H. (1977) Distribution of bottom sediments on the continental shelf, northern Bering Sea. Prof. Pap. U. S. geol. Surv. 759-C.

Mogridge, G. R. & Kamphuis, J. W. (1972) Experiments on bed form generation by wave action. Conf. Coastal Engring., 13th, Proc., 2, 1123-1142.

Moore, J. R. & Welkie, C. J. (1976) Metal-bearing sediments of economic interest, coastal Bering Sea. Alaska geol. Soc. Symposium on recent and ancient sedimentary environments of Alaska, Proc. K1-K17.

Nelson, C. H., Cacchione, D. A., Field, M. A., Drake, D. E. & Nilsen, T. H. (1977) Complex ridge and trough topography on a shallow current-dominated shelf, northwest Alaska (abs.). Bull. Am. Assoc. Petrol. Geol. 61, 817.

Nelson, C. H. & Hopkins, D. M. (1972) Sedimentary processes and distribution of particulate gold in the northern Bering Sea. Prof. Pap. U. S. geol. Surv. 689.

Neumann, Gerhard & Pierson, W. T., Jr. (1966) Principles of physical oceanography. Prentice-Hall, Englewood Cliffs, N. J.

Newton, R. S., Seibold, E. & Werner, F. (1973) Facies distribution patterns on the Spanish Sahara continental shelf mapped with side-scan sonar. "Meteor" Forsch-Ergebnisse, Reihe C., 15, 55-77.

Newton, R. S. & Werner, Friedrich (1972) Transitional-size ripple marks in Kiel Bay (Baltic Sea). Meyniana, 22, 89-94.

Rance, P. J. & Warren, N. F. (1969) The threshold of movement of coarse material in oscillatory flow. Conf. Coastal Engring., 11th, Proc. 1, 487-491.

Reimnitz, Erk, Toimil, L. J., Shepard, F. P. & Gutierrez-Estrada, Mario (1976) Possible rip-current origin for bottom ripple zones to 30 m depth. Geology, 4, 345-400.

Sallenger, A. H., Jr., Dingler, J. R. & Hunter, R. E. (1978) Coastal processes and morphology of the Bering Sea coast of Alaska, in Environmental assessment of the Alaskan continental shelf, Annual reports of principal investigators for the year ending March 1978. Vol. XII. Hazards. Natl. Oceanic and Atmospheric Admin. and Bur. Land Management, 451-502.

Stride, A. H. & Chesterman, W. D. (1973) Sedimentation by non-tidal currents around northern Denmark. Mar. Geol., 15, M53-M58.

Swift, D.J.P., Freeland, G. L., Gadd, P. E., Han, G., Lavelle, J. W. & Stubblefield, W. L. (1976) Morphologic evolution and coastal sand transport, New York-New Jersey shelf. In Middle Atlantic Continental Shelf and the New York Bight (Ed. by M. G. Gross). Am. Soc. Limnol. Oceanog. Special Symposia, 2, 69-89.

Swift, D. J. P. & Freeland, G. L. (1978) Current lineations and sand waves on the inner shelf, Middle Atlantic Bight of North America. J. sedim. Petrol. 48, 1257-1266.

Tagg, A. R. & Greene, H. G. (1973) High-resolution seismic survey of an offshore area near Nome, Alaska. Prof. Pap. U. S. Geol. Survey 759-A.

Trask, P. D. (1955) Movement of sand around southern California promontories. U. S. Corps Engrs. Beach Erosion Board Tech. Memo. 76.

Vause, J. E. (1959) Underwater geology and analysis of recent sediments off the northwest Florida coast. J. sedim. Petrol. 29, 555-563.

FIG. 1 -- Index map showing areas studied in the northeastern Bering Sea.

FIG. 2 -- Map showing tracklines and locations of illustrated features in the Port Clarence area.

FIG. 3 -- Map showing tracklines and locations of illustrated features in the Nome-Solomon area.

FIG. 4 -- a. Map of tracklines in Yukon delta area.

b. Map of morphologic features, and of features shown on sonographs in Yukon delta area.

FIG. 5 -- Irregular to elongate sand and gravel patches in the Nome-Solomon area. Distinctive points allowing comparison of a sonograph and its accompanying bathymetric profile are labelled x and y.

a. Sonograph of irregular patches.

b. Sonograph of elongate patches.

c. Bathymetric profile of area shown in a.

d. Bathymetric profile of area shown in b.

FIG. 6 -- Sonograph of cuspate sand and gravel patches off Safety Sound.

FIG. 7 -- Sonographs of wave ripples and associated features.

a. Sand (light-toned), gravel (dark-toned), and rippled fine gravel patches off Nome.

b. Patches off Nome distinguished by differences in ripple size and trend.

c. Sand, gravel, and rippled fine gravel patches in Port Clarence area.

d. Sand and rippled fine gravel patches off Nome. Note: the three areas distinguished by differences in ripple size and trend.

FIG. 8 -- Sonographs of ribbons in the Port Clarence area.

a. Sand (light-toned), gravel (dark-toned), and rippled fine gravel ribbons.

b. Sand and rippled fine gravel ribbons.

c. Elongate patches of sand surrounded by gravel, with narrow transitional zones of rippled fine gravel.

d. Sand and gravel ribbons oriented parallel to ice gauge (lower right); note gauge-like features at boundaries between sand and gravel.

FIG. 9 -- Map of features shown on sonographs in vicinity of Port Clarence entrance.

Fig. 10 -- Bathymetric profiles of sound waves and similar features.

a. Large transverse bedforms compared partly of gravel, off Safety Sound.

b. Somewhat asymmetric ridges whose steep west faces are of boulder gravel, off Nome.

c. Large sand waves in a channel that crosses the sub-ice platform, Yukon delta.

d. Small sand waves in a channel that crosses the sub-ice platform, Yukon delta.

FIG. 11 -- Features shown on sonographs in Yukon delta area.

a. Probable slump features.

b. Current-scour depressions and ice gouges.

c. Scour features in a channel that crosses the sub-ice platform.

d, Ribbon-like features.

FIG. 12 -- Sonographs of ice gouges and similar features.

a. Solitary gouge in the Port Clarence area.

b. Solitary gouges in the Port Clarence area.

c. Pressure-ridge raking off Safety Sound.

d. Artificial gouges off Nome; one is marked by arrows.

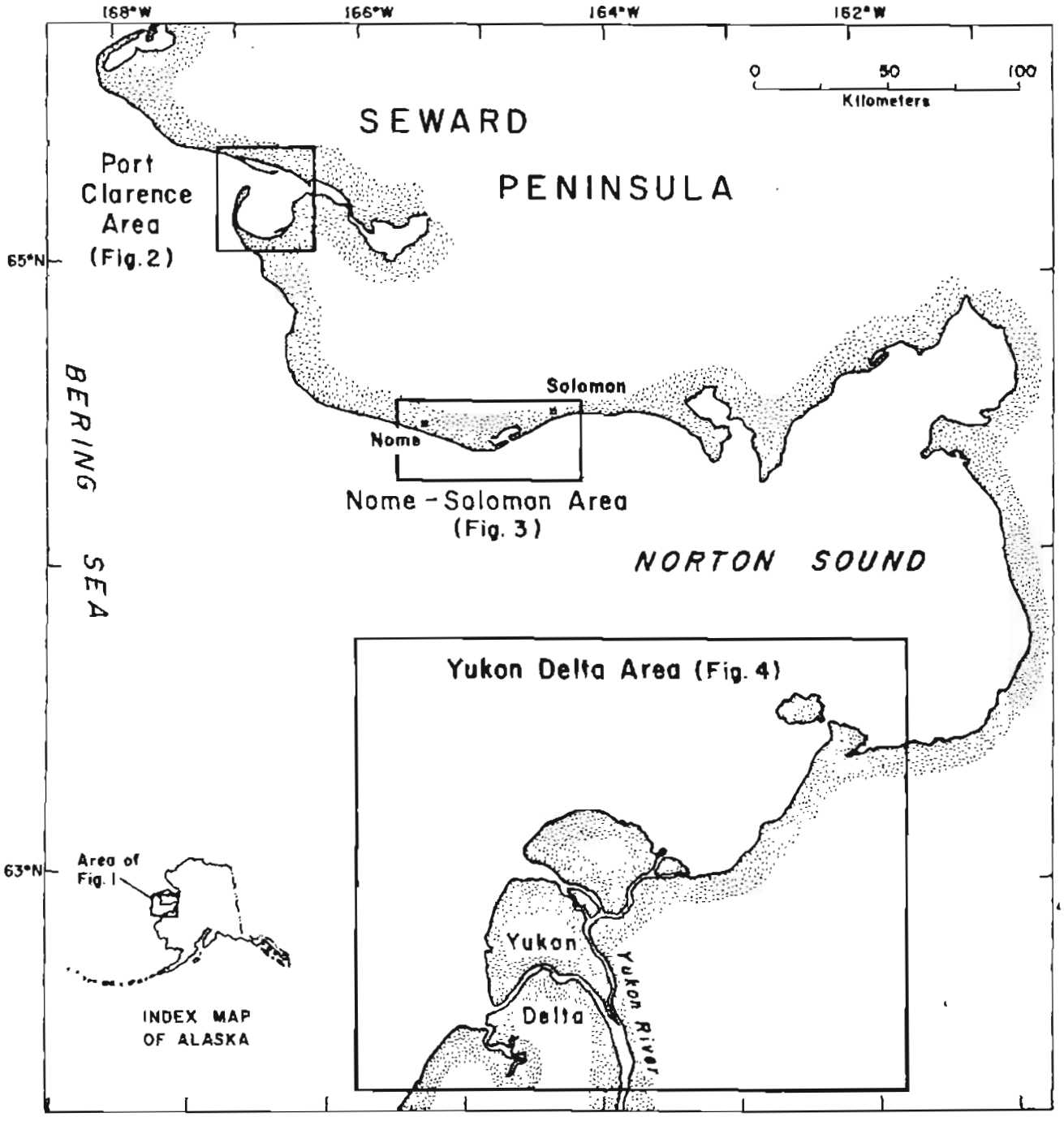
168°W
166°W
164°W
162°W
0
50
100
Kilometers
SEWARD
PENINSULA
Port
Clarence
Area
(Fig. 2)
65°N
BERING
SEA
Solomon
Nome
Nome - Soloman Area
(Fig. 3)
NORTON SOUND
Yukon Delta Area (Fig. 4)
63°N
Area of
Fig. 1
INDEX MAP
OF ALASKA
Yukon
Delta
Yukon River

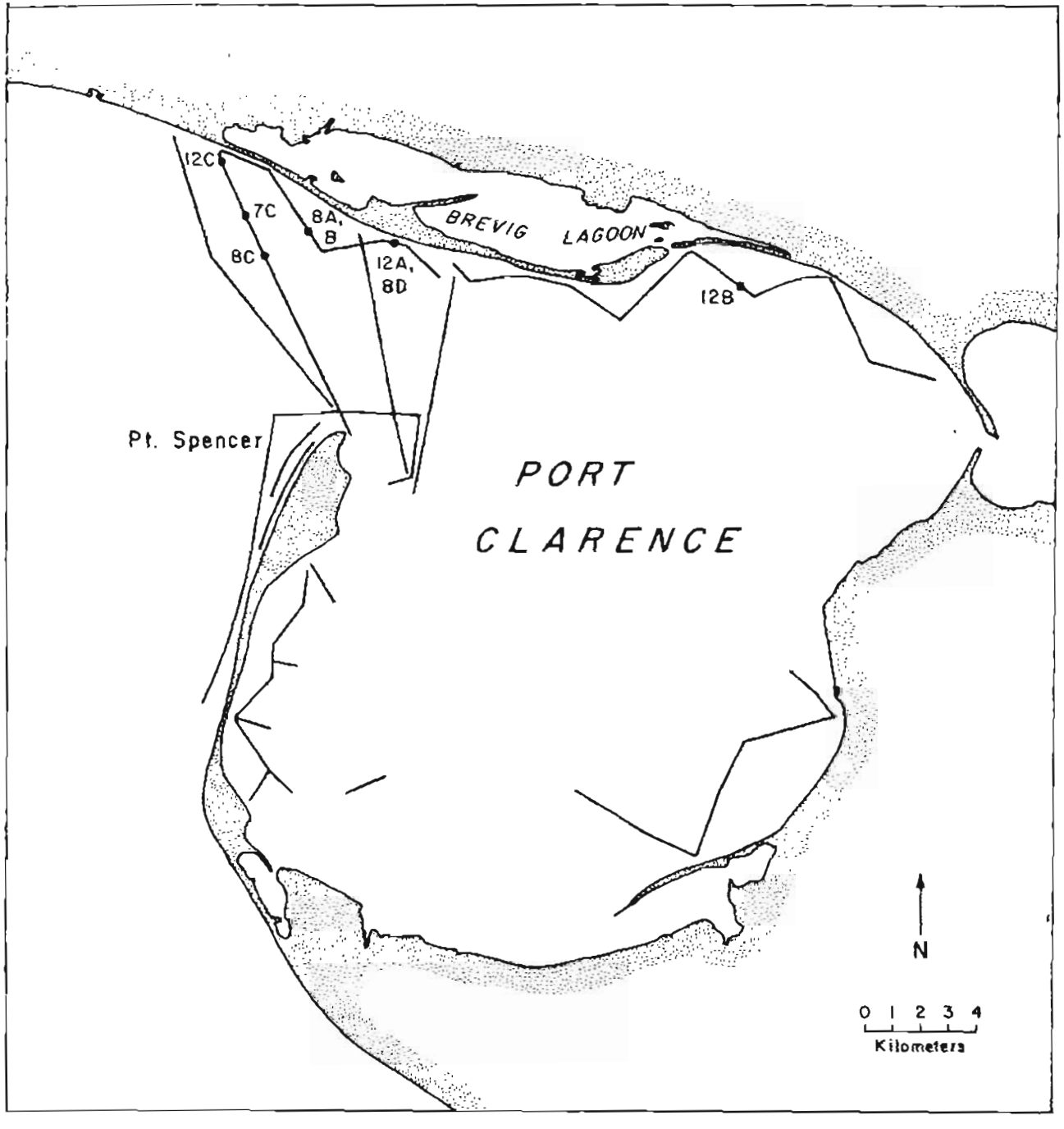
12C
7C
8A,
B
8C
12A,
8D
BREVIG LAGOON
12B
Pt. Spencer
PORT
CLARENCE
N
0 1 2 3 4
Kilometers

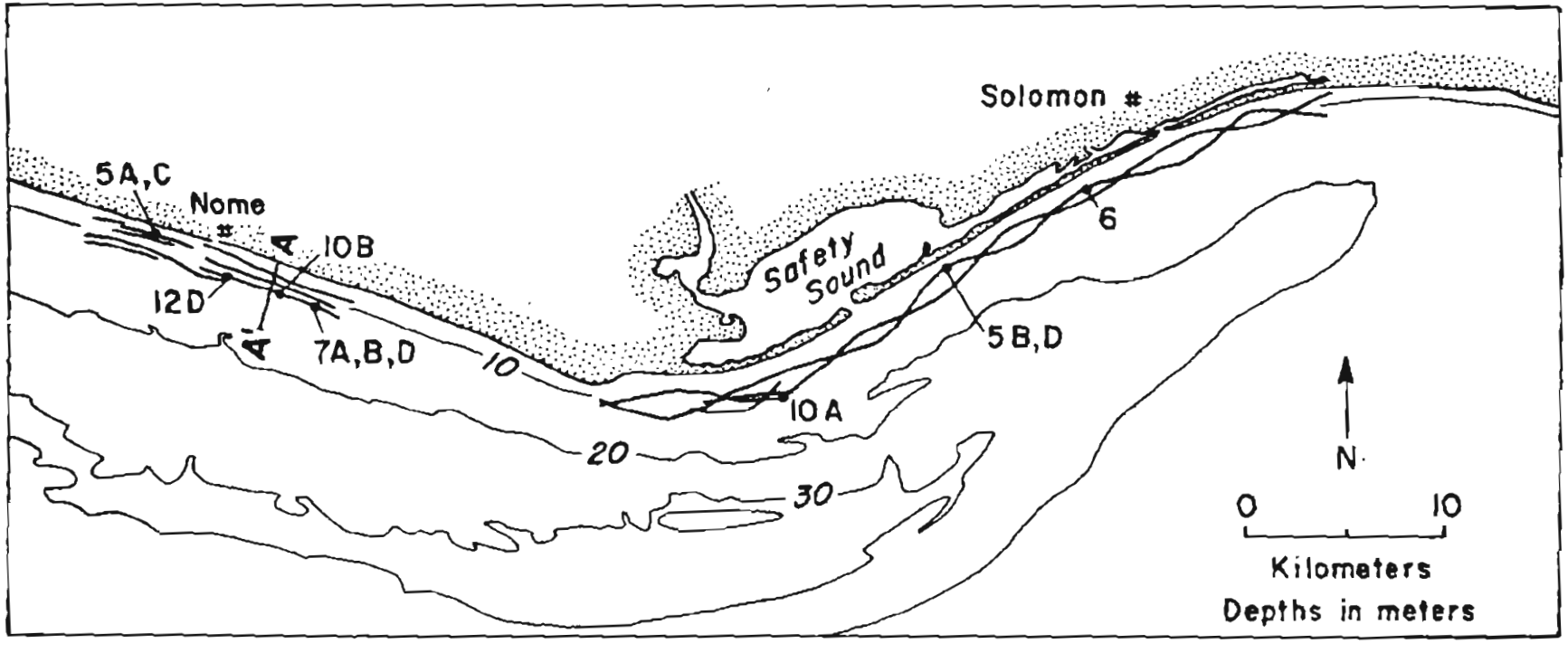
Solomon
5A,C
Nome
10B
12D
7A,B,D
10
20
30
Safety Sound
6
5B,D
10A
N
0
10
Kilometers
Depths in meters

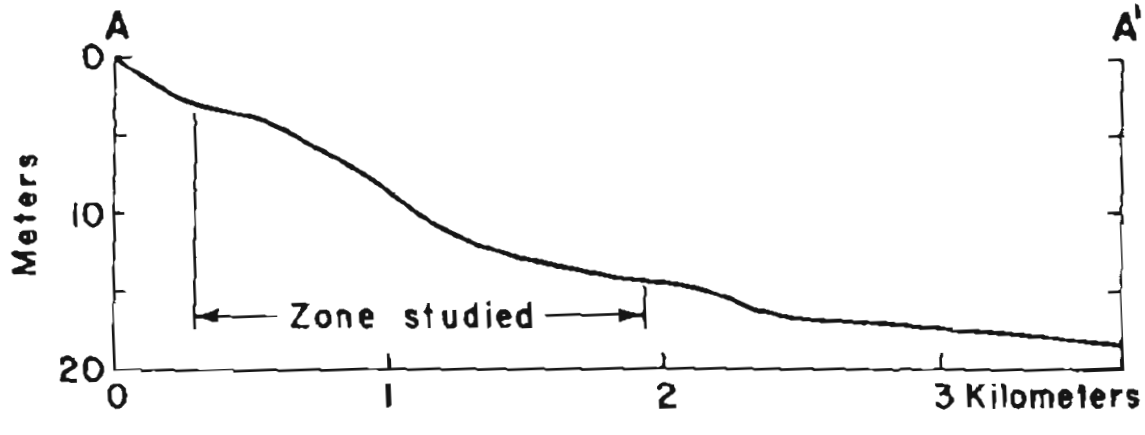
A
A'
0
10
20
Meters
Zone studied
0
1
2
3 Kilometers

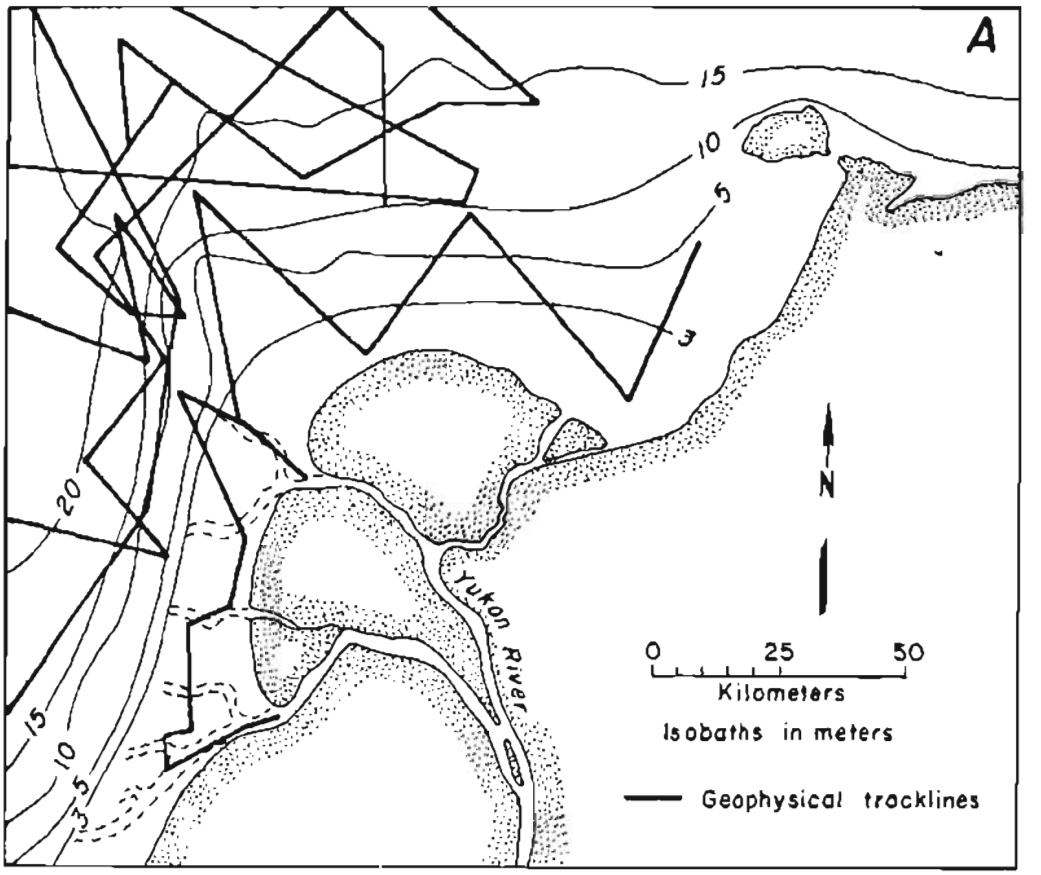
A
15
10
5
3
20
15
10
5
3
Yukon River
N
0
25
50
Kilometers
Isobaths in meters
Geophysical tracklines

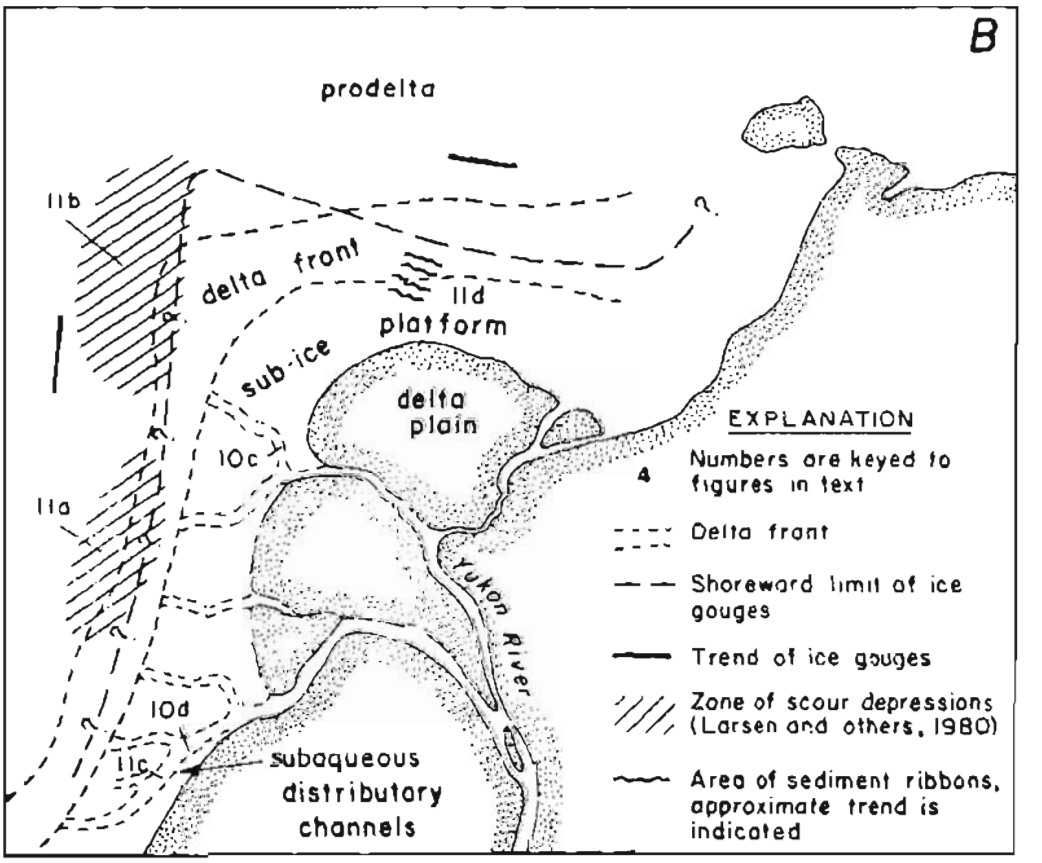
B
prodelta
11b
delta front
11d
platform
sub-ice
delta
plain
10c
11a
10d
11c
subaqueous
distributary
channels
Yukon River
EXPLANATION
4 Numbers are keyed to figures in text
Delta front
Shoreward limit of ice gouges
Trend of ice gouges
Zone of scour depressions (Larsen and others, 1980)
Area of sediment ribbons, approximate trend is indicated

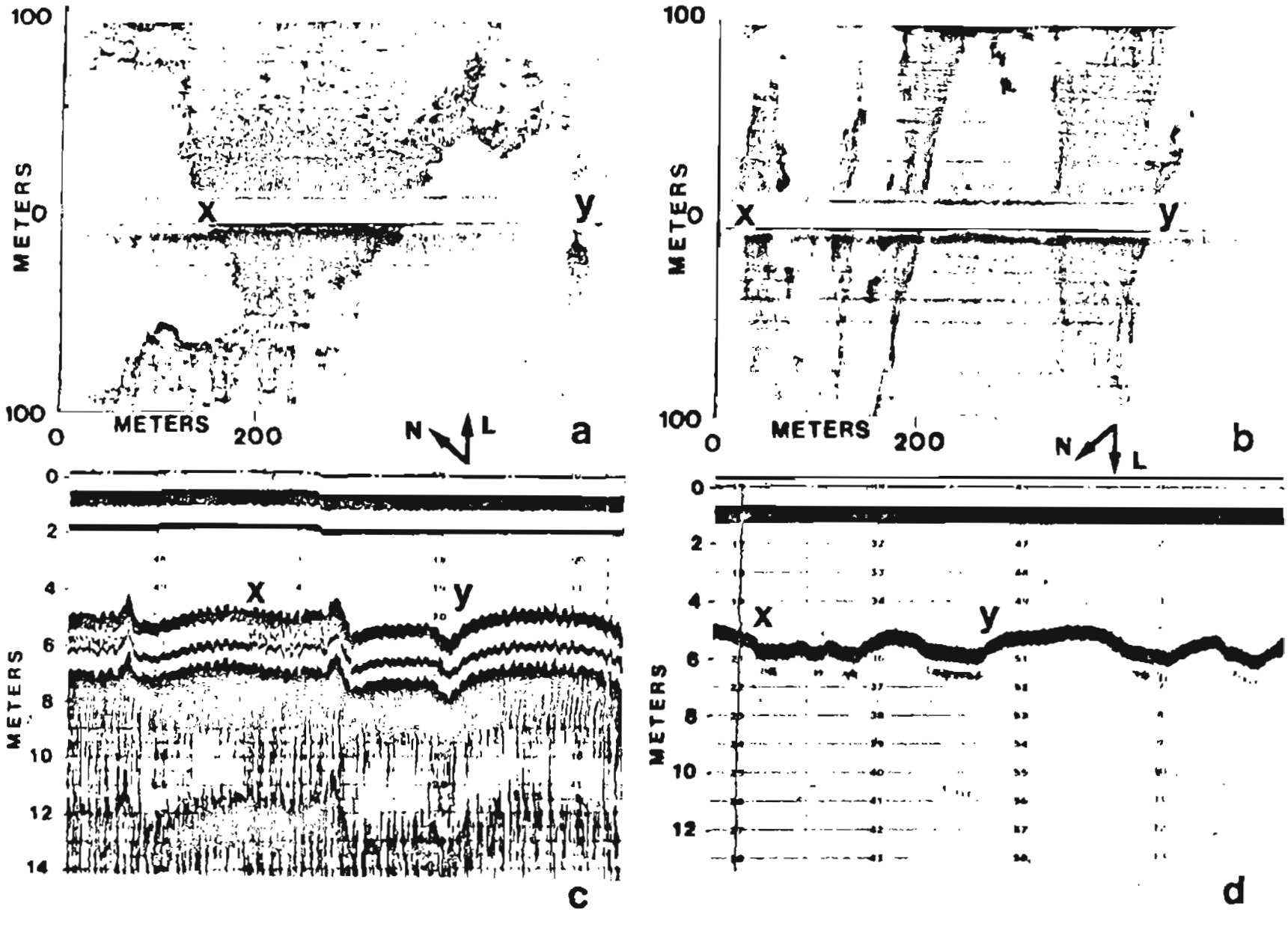
100
METERS
0
100
X
y
0
METERS
200
N
L
a
100
METERS
0
100
X
y
0
METERS
200
N
L
b
0
2
4
6
8
10
12
14
METERS
X
y
c
0
2
4
6
8
10
12
METERS
X
y
d

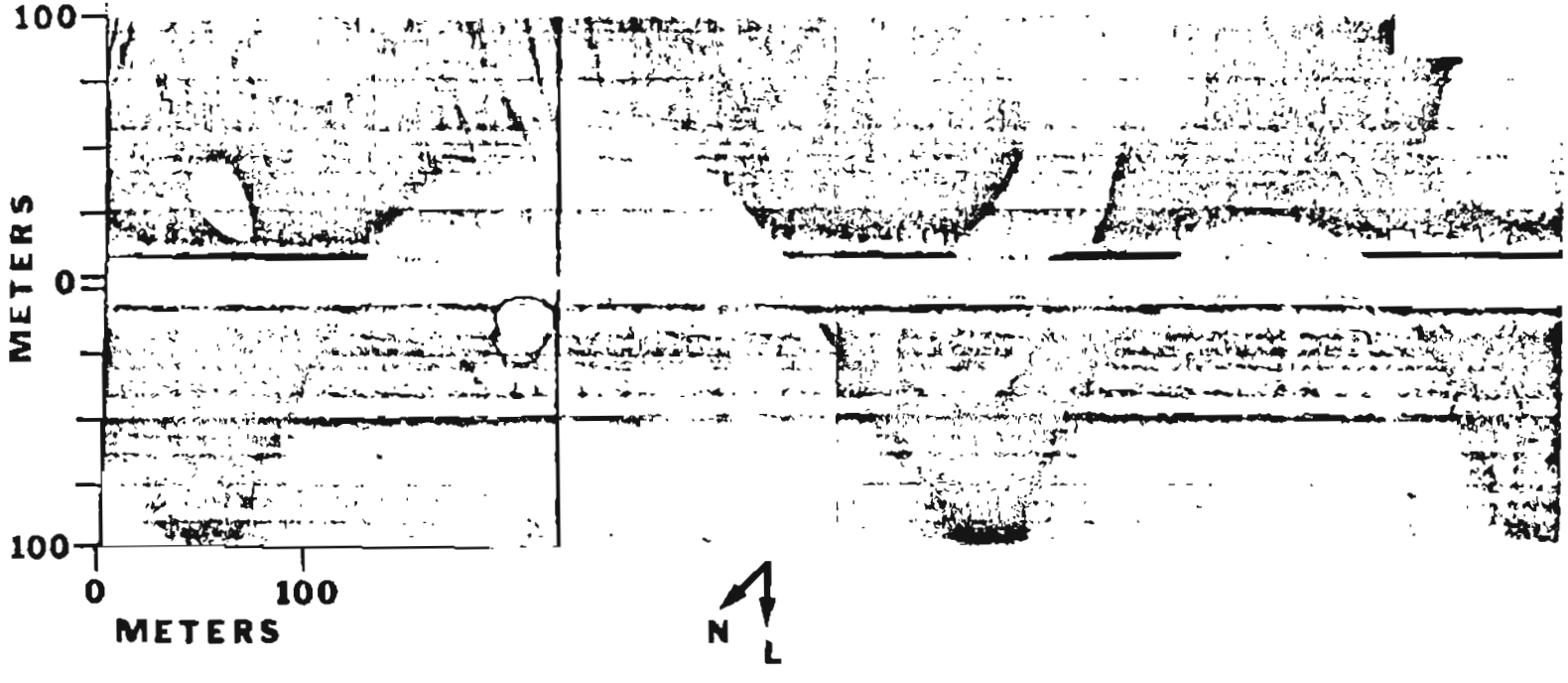
100
METERS
0
100
0
100
METERS
N
L

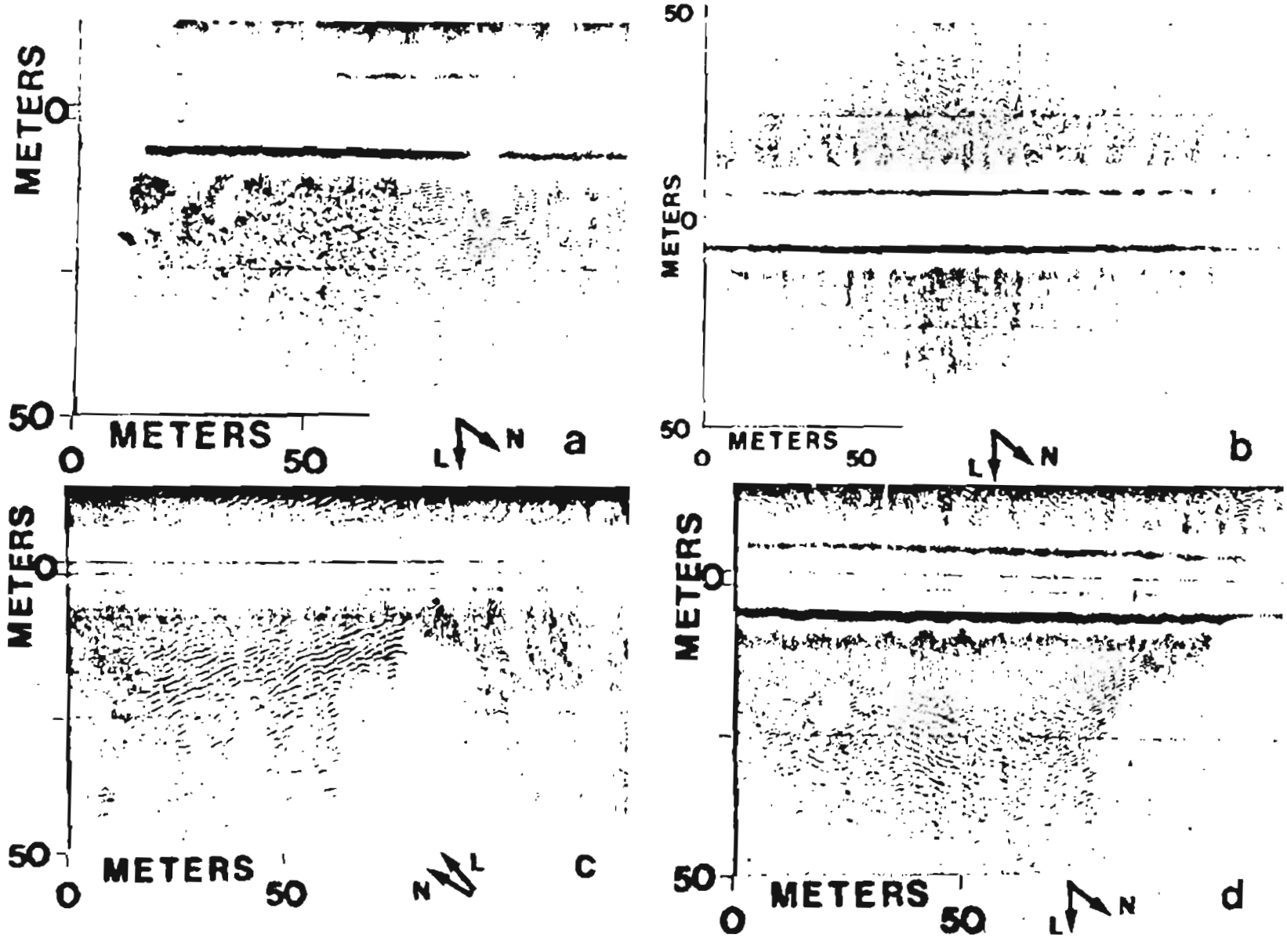
METERS
0
50
METERS
0
50
L
N
a
METERS
0
50
METERS
0
50
L
N
b
METERS
0
50
METERS
0
50
N
L
c
METERS
0
50
METERS
0
50
L
N
d

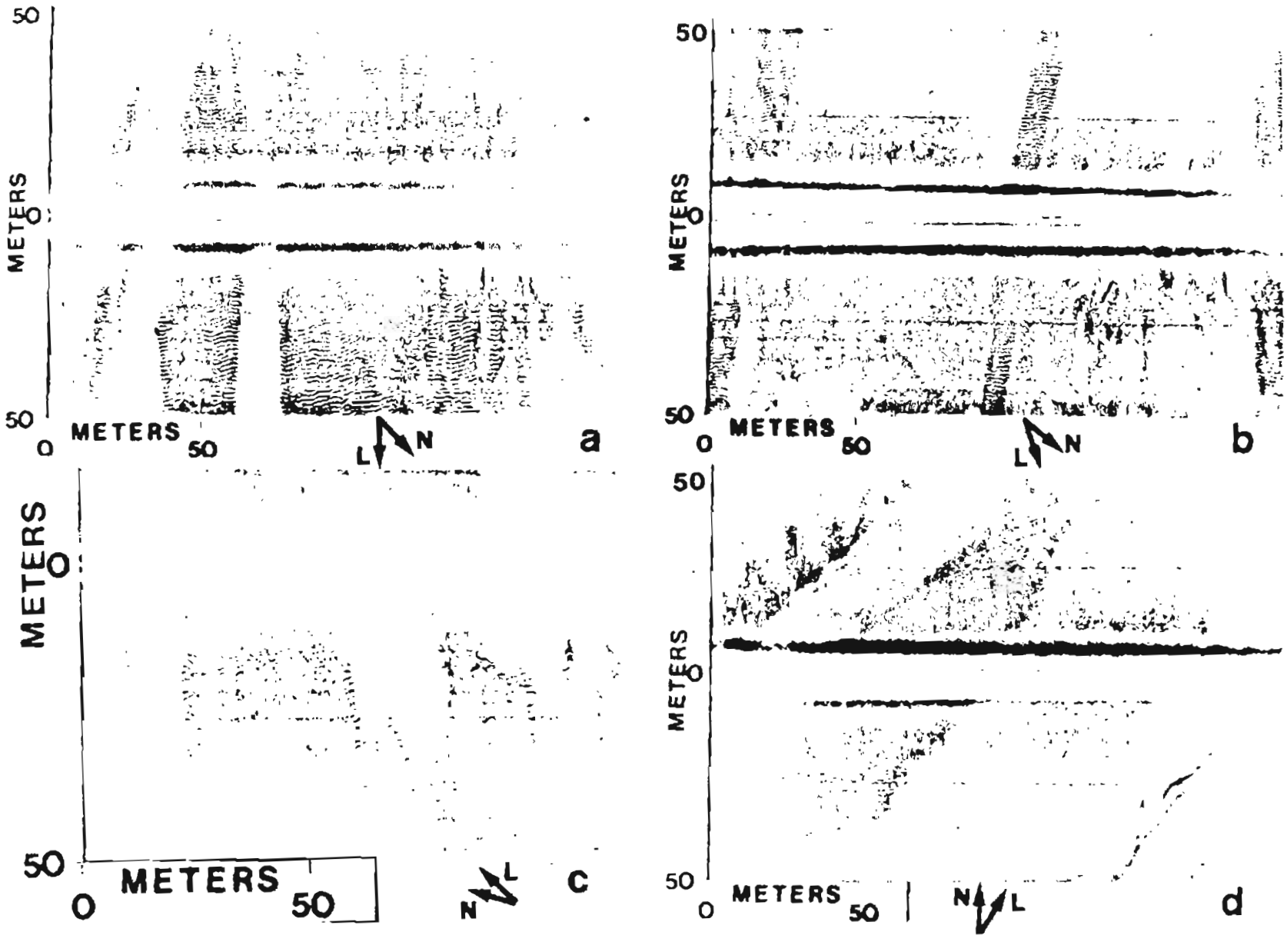
50
METERS
0
50
0
METERS
50
L
N
a
50
METERS
0
50
0
METERS
50
L
N
b
METERS
0
50
0
METERS
50
N
L
c
50
METERS
0
50
0
METERS
50
N
L
d

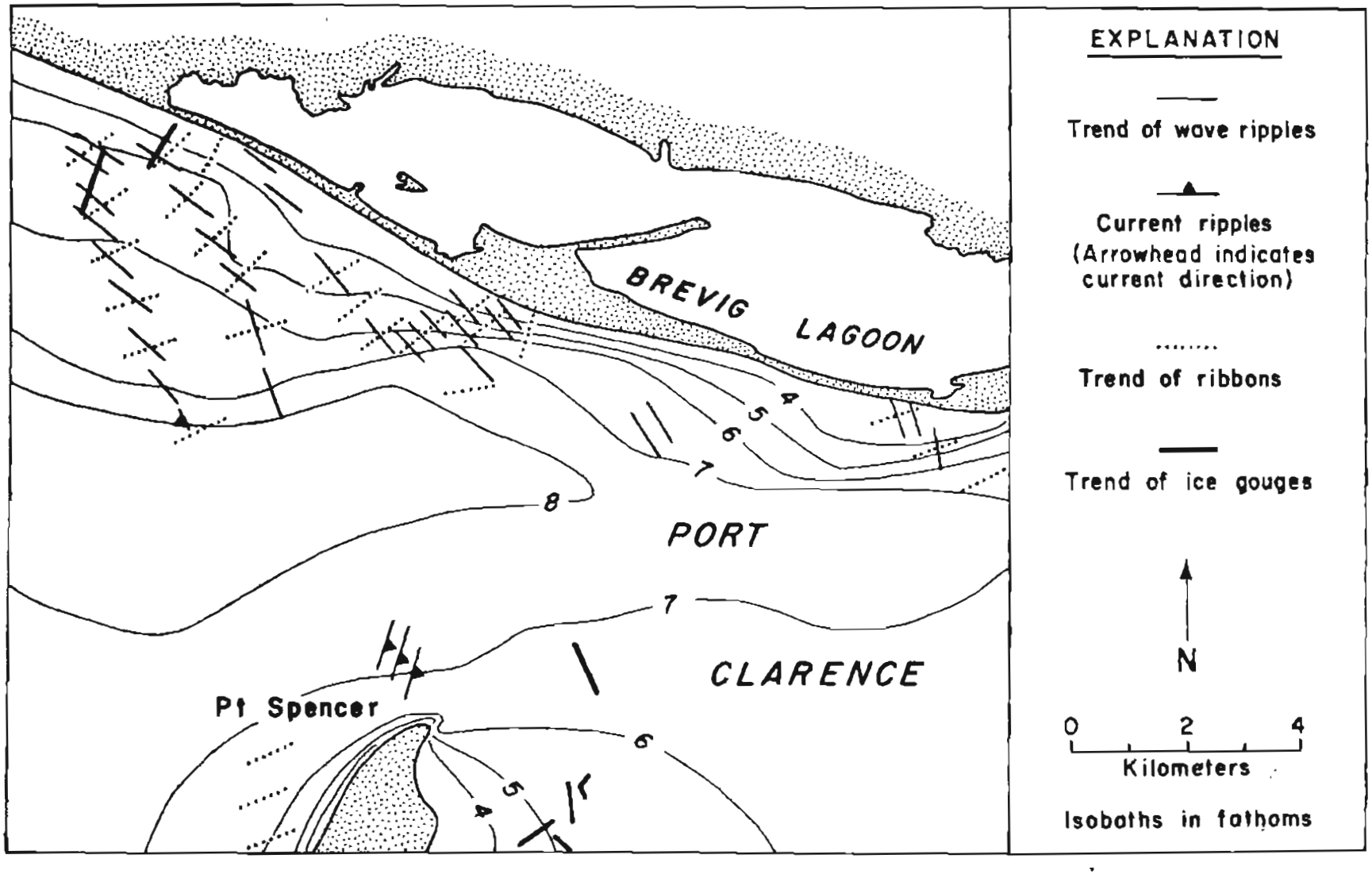
BREVIG LAGOON
PORT CLARENCE
Pt Spencer
4
5
6
7
8
7
6
5
4
EXPLANATION
Trend of wave ripples
Current ripples (Arrowhead indicates current direction)
Trend of ribbons
Trend of ice gouges
N
0 2 4
Kilometers
Isobaths in fathoms

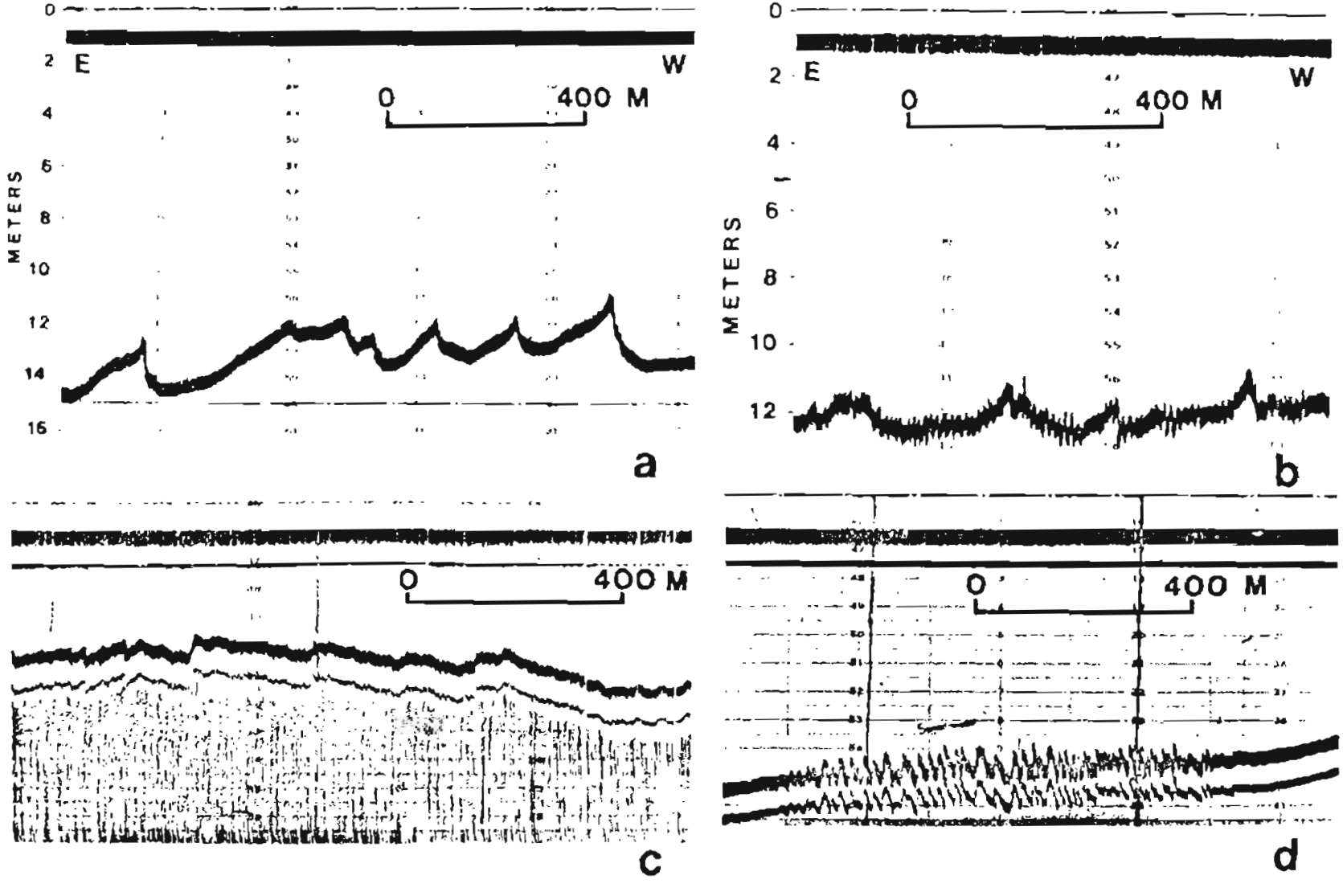
0
2
4
6
8
10
12
14
16
METERS
E
W
0
400 M
a
b
c
d

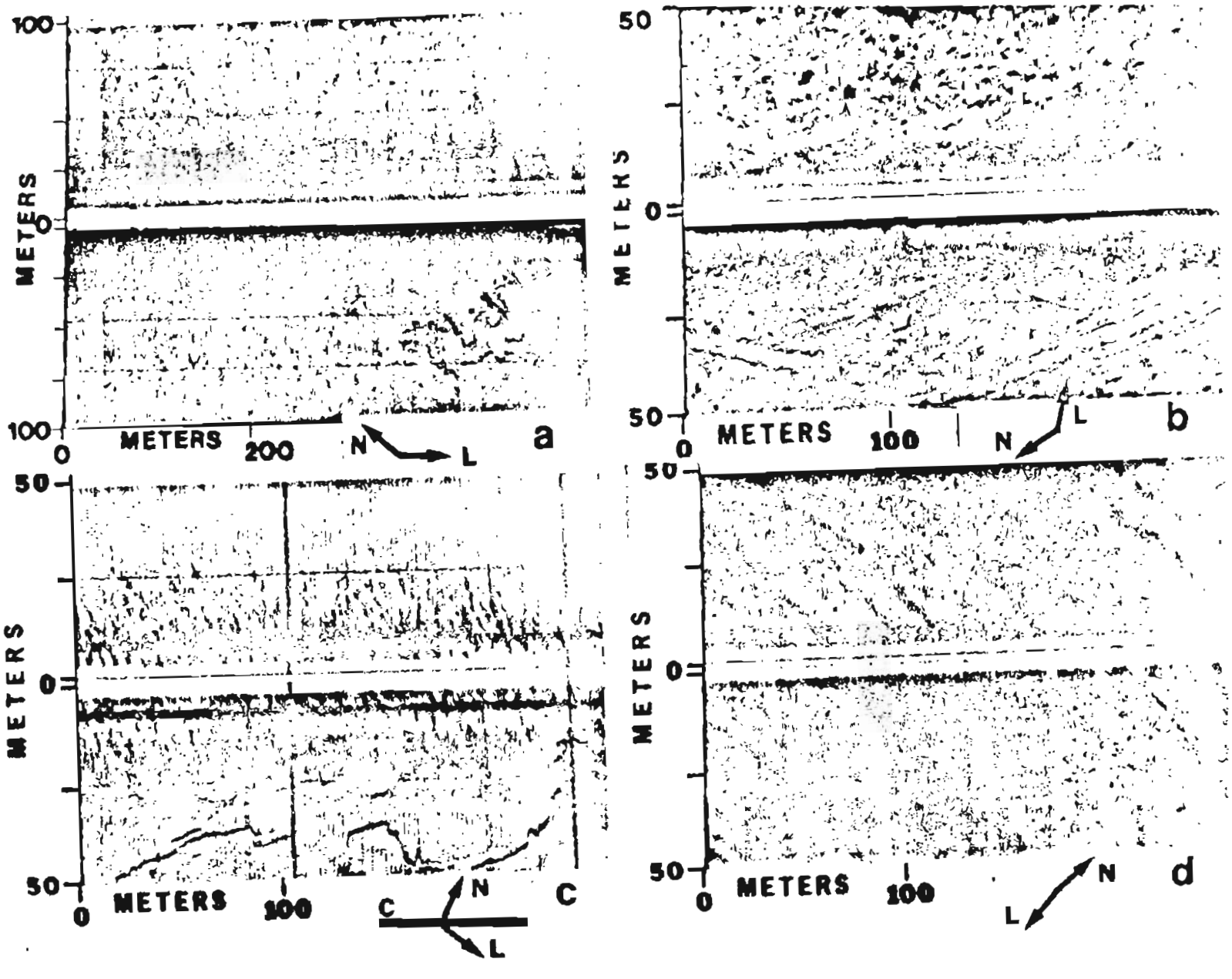
100
0
100
METERS
0
METERS
200
N
L
a
50
0
50
METERS
0
METERS
100
N
L
b
50
0
50
METERS
0
METERS
100
C
N
L
C
50
0
50
METERS
0
METERS
100
L
N
d

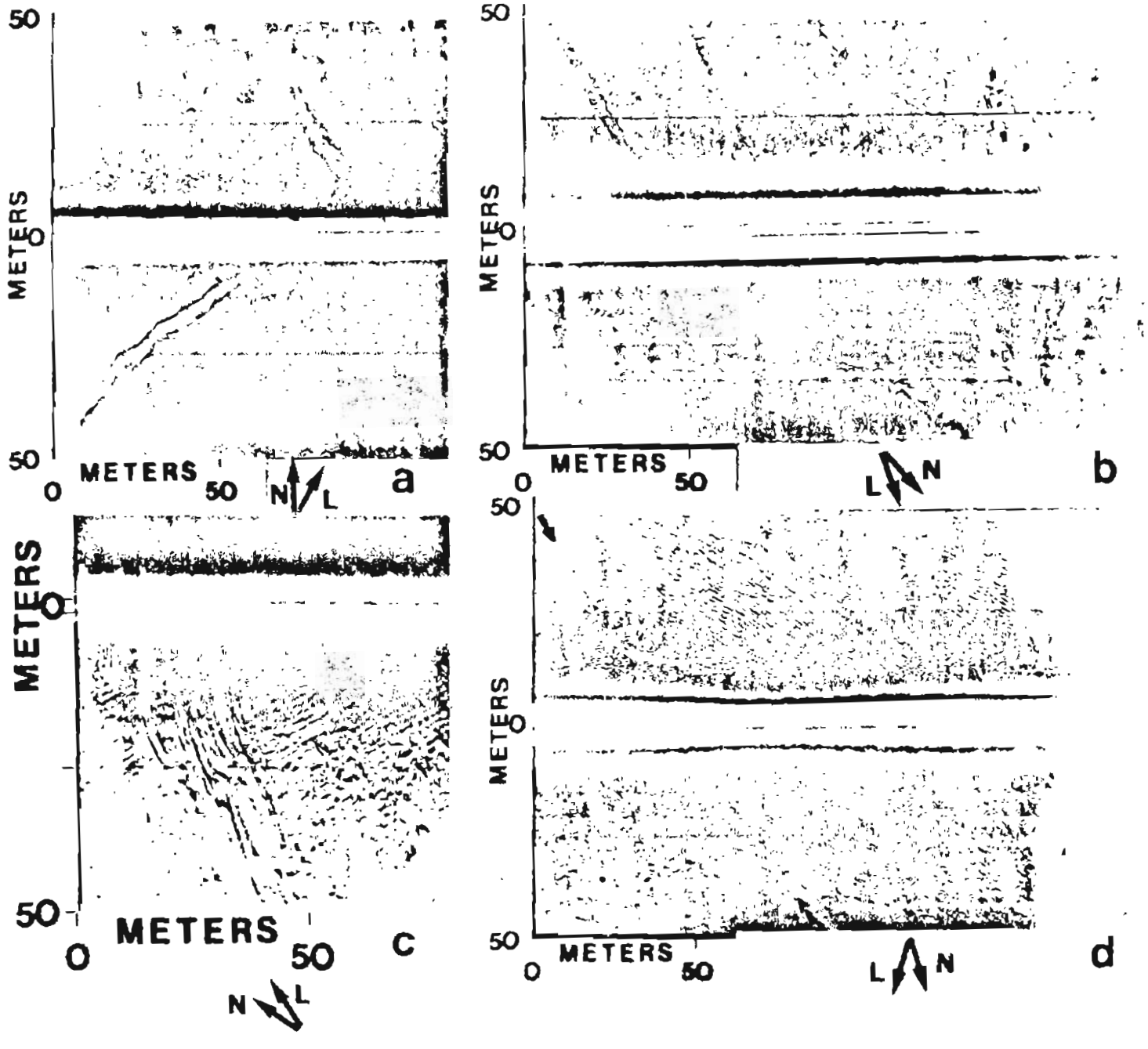
50
METERS
0
50
0
METERS
50
N
L
a
50
METERS
0
50
0
METERS
50
L
N
b
METERS
50
0
METERS
50
N
L
c
50
METERS
0
50
0
METERS
50
L
N
d

Velocity and Bottom-Stress Measurements in the Bottom Boundary Layer, Outer Norton Sound, Alaska

David A. Cacchione

David E. Drake

Patricia Wiberg

U.S. Geological Survey

Menlo Park, California 94025

Abstract

We have used long-term measurements of near-bottom velocities at four heights above the sea floor in Norton Sound, Alaska, to compute hourly values of shear velocity u_*, roughness z_o, and bottom-drag coefficient c_D. Maximum sediment resuspension and transport, predicted for periods when the computed value of u_* exceeds a critical level, occur during peak tidal currents associated with spring tides. The fortnightly variation in u_* is correlated with a distinct nepheloid layer that intensifies and thickens during spring tides and diminishes and thins during neap tides. The passage of a storm near the end of the experiment caused significantly higher u_* values than those found during fair weather. We attribute these increases in u_* to stronger bottom currents and larger surface waves.

INTRODUCTION

The most important dynamic parameter controlling the transport of sediment in the bottom boundary layer over continental shelves is the bottom shear stress τ_b. Historically, most estimates of τ_b in both natural and laboratory settings have been made by measuring the flow velocity at one or more heights above the bottom and applying an appropriate boundary-layer equation that relates the bottom shear stress to the velocity field. For example, in steady unidirectional turbulent flow over a flat bed whose only bottom irregularities are uniform sand grains, τ_b can be calculated from the relations (Schlichting, 1968):

$$\tau_b = \rho u_{*b}^2, \tag{1a}$$

and

$$\frac{u}{u_{*b}} = \frac{1}{k} \ln(z/z_o), \tag{1b}$$

where u is the current speed at a height z above the bottom, ρ is the fluid density, k is von Karman's constant (0.4), u_{*b} is the bottom shear velocity, and z_o is a roughness parameter. Equation (1b) applies within the turbulent lower part of the velocity profile, commonly referred to as the logarithmic zone; over continental shelves, this zone is within about 10 m of the sea floor (Wimbush, 1976). Sternberg (1968) found that approximately 85 percent of the vertical velocity distributions measured in six different tidal channels fit the logarithmic velocity profile given by equation (1b). Other velocity-profile measurements in dominantly shallow tidal flows also demonstrate the applicability of equation (1b) in estimating u_{*b}

(Bowden and others, 1959; McCave, 1973; Smith and McLean, 1977).

Two major difficulties that arise in applying equation (1b) to natural boundary-layer flows involve situations (1) where bottom irregularities or bed features exist whose vertical length scales exceed that of the sedimentary grains at the bed surface, and (2) when active sediment transport of bed load and near-bottom suspended load occurs. Smith and McLean (1977), who considered these problems, presented methods for dealing with the changes in shear velocity u_* that result. In particular, when more than one vertical scale of bed roughness is present, Smith and McLean argued that the velocity profile is separated into vertical zones that reflect the scales of these roughness elements. They suggested that equation (1b) applies within each vertical zone and that z_o for that zone is related to a particular physical roughness scale. For example, if the bottom consists of well-sorted sand grains and regularly spaced asymmetric sediment ripples, the slope of the velocity profile above these features changes at a height determined by the transition from a layer dominated by skin friction over the individual sand grains to an upper layer in which the form drag imposed by sediment ripples on the flow is dominant. This change in the velocity profile signifies a corresponding change in u_* and z_o, which in the lowest layer (where $u_* = u_{*b}$) are the appropriate parameters associated with skin friction acting on the surficial sedimentary grains.

When u_{*b} exceeds the value necessary to initiate bed-load transport, z_o is effectively proportional to the excess shear stress (Smith and McLean, 1977) and exceeds the values of z_o commonly given for turbulent boundary layers (Schlichting, 1968).

An additional problem in estimating u_* at the sea floor arises when surface waves generate bottom velocities (and stresses) that are of magnitudes comparable to those typical of the mean flow. Smith (1977) and Grant and Madsen (1979) showed that the wave and current stresses are nonlinearly coupled and that the net effect is to increase the mean stress above the value it would have if waves were absent. Both Smith (1977) and Grant and Madsen (1979) also showed that z_o values derived from velocity-profile measurements when waves and quasi-steady currents are both significant are increased by wave-current interaction. Grant and Madsen suggested that some of the anomalously high values of z_o reported by other researchers can be explained by this effect.

The estimates of u_* reported here were derived by the logarithmic-profile method, using measurements of near-bottom current velocities on an open continental shelf. The data were collected in outer Norton Sound, Alaska, during an 80-day period from July 8 to September 26, 1977, using an instrumented, in-situ bottom tripod (GEOPROBE; Fig. 1).

Cacchione and Drake (1980) and Drake and others (1980) have documented the importance of late-summer, early-fall storms in causing high rates of sediment transport throughout outer Norton Sound. They found that storm-driven bottom stresses are often large enough to resuspend surficial deposits at the GEOPROBE site and thereby enhance removal of these deposits by the regional northward flow. In addition, Drake and others (1980) also argue that during the more persistent fair-weather regime, tidal bottom stresses are significant in the near-bottom transport of sediment derived from the Yukon

River (Fig. 1), which occurs at relatively lower rates than during storms but over prolonged durations.

In this report we discuss the variation of u_* during fair-weather periods and emphasize the diunal and fortnightly tidal influence. We also include brief discussion of additional contributions to u_* during periods of high surface waves. Cacchione and Drake (1980) have already used these data to show the influence of stresses due to surface waves on mean or quasi-steady stress, as predicted by the theoretical formulations of Smith (1977) and Grant and Madsen (1979).

METHODS

The GEOPROBE system is an instrumented tripod designed to make onsite near-bottom measurements of currents, pressure, temperature, and light transmission and scattering, and to photograph the sea floor over durations of about 3 months (Cacchione and Drake, 1979). During 1977 the GEOPROBE was deployed in Norton Sound in 18-m mean water depth about 60 km south of Nome, Alaska (Fig. 1). Data were obtained at a basic interval of 1 h over a 3-mo period and recorded on a digital cassette tape. Two orthogonal components of horizontal current were measured with spherical electromagentic (e-m) current sensors at four heights-- 20, 50, 70, and 100 cm-- above the sea floor (Cacchione and Drake, 1979). At the hourly basic intervals, each component of current was sampled in a burst mode, once each second for a one-minute duration; bottom pressure was sampled at the same rate. Current speed and direction were measured with a Savonius rotor and vane, respectively, at hourly intervals. These latter measurements provided a consistency check on the e-m current-meter data.

The e-m current-meter data were treated as follows. First, individual pairs of velocity component measurements, u_i and v_i, at each vertical level were rotated to provide north-south (v) and east-west (u) components. The rotation angle was determined from photographs of an underwater compass mounted on the GEOPROBE and was corrected for magnetic declination; the accuracy of this procedure is about $\pm 5^{\circ}$.

Burst means $(\bar{u},\bar{v})$ for each component were then calculated over the one-minute sample durations:

$$\bar{u} = \sum_{i=1}^{60} u_i \; , \; \bar{v} = \sum_{i=1}^{60} v_i . \qquad (2)$$

Burst mean current speed s and burst mean current direction θ were also computed for each one-minute burst:

$$s = (\bar{u}^{-2} + \bar{v}^{-2})^{1/2} ; \quad \theta = \tan^{-1} \frac{\bar{v}}{\bar{u}} . \qquad (3)$$

A total of 1,920 values of s and θ were thus obtained over the 3-month experiment. The s values compared favorably with the hourly current speeds measured with the Savonius rotor, except during periods of relatively high surface waves (wave heights >1 m), when rotor values were spuriously large ("pumped up"; Karweit, 1974).

Because significant wave-induced stresses can interact nonlinearly with the quasi-steady stresses (Smith, 1977; Grant and Madsen, 1979) and thus modify equation (1b), it is important to identify periods of significant wave activity during the experiment. Variance estimates of the current speed were

computed to indicate these periods of increased wave activity.

Shear velocity u_* and bottom roughness z_o were determined for each hourly set of one-minute averages of current speeds s by fitting to a least-squares curve, using equation (1b) to the e-m the current-meter data obtained at the four heights. A regression coefficient r and standard error were also computed for each least-squares curve.

RESULTS

During fair-weather periods, bottom currents at the GEOPROBE site (Fig. 1) were characterized by mixed rotary tidal currents strongly polarized in a WNW-ESE orientation and by a weaker northerly mean flow. During stormy periods, moderate northerly wind-driven bottom currents and intense oscillatory wave currents were also observed (Cacchione and Drake, 1980). Figure 2 shows part of the current record taken with the e-m current meter at 100 cm above the sea floor. The mixed-tidal oscillations and fortnightly tidal cycle are readily apparent in the speed data. The east-west current speeds are larger than the north-south current speeds and contain a pronounced diurnal periodicity. Harmonic tidal analysis shows that the K_1 tidal constituent is the most energetic and that the K_1 tidal ellipse has pronounced WNW-ESE orientation; the ratio of major to minor axis length of this ellipse (K1) is about 10:1. The relatively low daily averages ("sticks") in curve cm 1 (Fig. 3) indicate a generally weak northerly flow (about 3 cm/s). Tidal and higher frequency motions in the current data have been removed from the daily mean currents (Q). The nontidal northerly current on July 25 and 26 was associated with an increase in wind speed. The effects of this event on the

computations of u_* are discussed later.

The variance of current speeds for each e-m current meter over the period July 8-September 8 are plotted in Figure 3. Significant increases in variance estimates above generally low values occur infrequently, most notably on July 25 and after September 1 (Fig. 3). The higher variance values on July 25 correspond to the higher nontidal daily-averaged currents shown in Figure 2. Late on July 24, weather records from the National Weather Service, Nome, indicate that hourly wind speeds increased to 15 to 20 knots; these higher winds persisted until early on July 26. Wind directions were persistently from the south-southeast throughout that time. The bottom pressure data taken on the GEOPROBE during this period indicate that wind waves increased on July 25 to about 1-m heights (data not shown), with corresponding wave-induced peak current speeds of about 15 cm/s (measured with the e-m current meter at 1 m above the sea floor). These wave currents were the highest recorded during the period July 8-September 1. After September 1, the energy levels in wave-induced bottom currents increased substantially in response to the more frequent passage of intense storms. The high variance values during the period September 3-8 were caused by high wave currents (Fig. 3).

Hourly values of u_* and current speed at 100 cm above the sea floor (u_{100}) are shown in Figure 4. Higher values of u_* and u_{100} regularly occur during spring tides at peak values of about 3.5 and 33 cm/s, respectively. The fortnightly rhythmic pattern in these parameters is also easily discernible in Figure 4. The bottom roughness z_o has a more irregular variation not readily correlated with the spring-neap cycle. The reason for this erratic variation in measured z_o is unknown; however, as discussed

earlier, sediment transport during periods when $u_* > u_{*c}$ could significantly alter the value of z_o (Smith, 1977). The estimated value of u_{*c} for surface deposits at the GEOPROBE site is about 1.3 cm/s (mean grain size is 70 μm); (Cacchione and Drake, 1979). This value of u_{*c} was derived from the modified Shield's curve shown by Smith (1977), applicable for uniform flow over a noncohesive sediment bed. The drag coefficient c_D, computed from $c_D = \left(\frac{u_*}{u_{100}}\right)^2$, is plotted for comparison with previous estimates (for example, Sternberg, 1968; McCave, 1973).

DISCUSSION

Although the computation of u_* and z_o was carried out for each of the hourly sets of e-m data points, as discussed above, it is useful to examine the accuracy of fitting a curve (in the least-squares sense) using equation (1b) to the burst-averaged speed data. A summary of correlation coefficients r, which are estimates of the goodness of fit of the least-squares curve to the data points (Davis, 1973), is shown in Table 1. The large number (approx. 80 percent of r values greater than 0.8) indicates the generally good fit of the least-squares curve given by equation (1b) to the entire data set. This result implies that hourly velocity profiles in this shelf region are dominantly logarithmic.

Figure 5 plots the relation of r^2 and u_{100}. In general (except for about 5 data points in the middle of the diagram), low values of r^2 occur at the low values of u_{100} (<10 cm/s); conversely, high values of r^2 predominantly are correlated with high values of u_{100} ($\geq$ 10 cm/s). This result suggests that the vast majority of poor logarithmic fits to the data occur at times of low

currents. This result is not surprising because low bottom currents, like periods of light surface winds, could be expected to vary considerably in both speed and direction in the bottom boundary layer and thus to deform the velocity profile.

We have already shown that the measured u_* values at times exceed u_{*c} (1.3 cm/s). Figure 4 indicates that significant bottom-sediment movement at the GEOPROBE site occurs on a fortnightly cycle, during periods of spring tides. Evidence for this rhythmic pattern of sediment movement associated with the tidal cycles during fair weather is also found in the bottom photographs and light-scattering measurements taken with the GEOPROBE. In particular, the turbidity in the water at about 2 m above the sea floor (as detected with the GEOPROBE nephelometer) increases and decreases with the spring and neap cycles, respectively. During peak spring tides, bottom photographs are totally obscured by the increased turbidity of the water. Since the critical bottom stress is exceeded during spring tides (Fig. 4), local resuspension of bottom material probably occurs, and the increased turbulence causes upward mixing of the suspended materials. This mixing could create a bottom turbid layer that diminishes and thins during times of low u_* (neap tides). Turbid bottom layers (nepheloid layers) have been reported in other continental-shelf areas (Drake, 1976; Pak and Zaneveld, 1977), although their precise mechanism is unresolved.

We note both the varying and periodically high values of measured z_o (Fig. 4). The average value of z_o for the period July 8-September 8 was about 2.2 cm; similar high values of z_o have been reported for tidally dominant flows using current-meter-profile data (Kagan, 1971). Measurements of z_o in a

shallow-marine environment also show considerable scatter (from 10^{-6} to 10^{1} cm) in any one locality over a range of hydraulic-flow conditions (Heathershaw, 1976).

The actual physical bottom roughness at the GEOPROBE site was difficult to determine from bottom photohgraphs because of the high turbidity. Shipboard underwater television and 70-mm bottom photographs taken two days after deployment of the GEOPROBE reveal a sedimentary surface characterized by low animal-generated mounds and burrows, with typical horizontal scales of 2 to 20 cm and vertical scales of 1 to 10 cm. The largest number of these features appear to protrude about 4 to 8 cm above the general bed level. A few isolated short-crested incipient sediment ripples also are scattered about the GEOPROBE site. The infrequent occurrence of ripples in this area is probably due to the relatively high silt content of the surface deposits and the active destruction of these features by the abundant organisms. If a physical roughness k_s of 6 cm is used to represent the bed, z_o, estimated from $z_o = k_s/30$ (hydraulically rough flow), would be about 0.2 cm (Schlichting, 1968), a value ten times smaller than the mean measured value of z_o determined from the velocity profiles. The reason for this discrepancy is unknown, but the estimate for k_s here is based on an extremely limited number of photographic observations of low accuracy. Other researchers have reported large values of measured z_o based on velocity-profile measurements on continental shelves (Scott and Csanady, 1976).

As pointed out earlier, Smith and McLean (1977) showed that z_o should be proportional to the excess shear stress when bed-load transport is occurring:

$$z_o = \frac{\alpha_o(\tau_b - \tau_c)}{(\rho_s - \rho)g} + z_N, \quad \tau_b \geq \tau_c, \tag{4}$$

where $\tau_c = \rho u_{*c}^2$, ρ_s is the density of the local sediment, g is the gravitational acceleration, z_N is the Nikuradse roughness (Schlichting, 1968), and α_o is an empirically determined constant (Smith and McLean, 1977). α_o was extimated to be 26.3 by Smith and McLean (1977) on the basis of their velocity-profile measurements in the Columbia River.

Equation (4) can be rewritten:

$$z_o = 1.63 \times 10^{-2}(u_{*b}^2 - 1.69) + z_N, \tag{5}$$

when $\rho_s = 2.65$ g/cm^3, $\alpha_o = 26.3$, and $u_b = 1.3$ cm/s. Apparently the values of z_o computed from equation (5) are considerably below the peak values shown in Figure 4. For example, using a value of $u_{*b} = 3.5$ cm/s, $(z_o - z_N)$ as determined from equation (5) is about 0.2. If z_N is about 0.2 cm (see above), z_o is about 0.4 cm.

Large variations in c_D have also been reported previously (Heathershaw, 1976). Sternberg (1968), using velocity data obtained in six tidal channels in Puget Sound, Washington, over a wide range of flow and bottom conditions, calculated a mean c_D value of 3.1×10^{-3}; the range in c_D values was from 0.87×10^{-3} to 11.1×10^{-3}. The mean value of c_D, using the data shown in figure 4, is 10×10^{-3}. We note that high values of c_D (and z_o) are correlated with low values of u_{100} (Fig. 4).

Finally, the relatively large values of u_* and u_{100} on July 25 are a result of the increased current speeds and bottom stresses caused by wind-

driven currents and surface waves. Measured oscillatory currents during the period July 25-26 had peak speeds of 15 cm/s at 100 cm above the sea floor; the average wave period determined from the burst pressure over 10 consecutive bursts was about 6.8 s. The hourly u_* values (reported in Fig. 4) during the period of increased wave stresses on July 25 (as well as after September) are probably underestimated. Smith (1977) and Grant and Madsen (1979) have shown that oscillatory wave stresses can interact nonlinearly with the quasi-steady stress components to increase the quasi-steady part. This wave-current interaction during the periods of increased wave activity, particularly September 7 to 17, 1977, in Norton Sound, is discussed elsewhere (Cacchione and Drake, 1980).

CONCLUSIONS

More than 80 percent of the measured velocity profiles taken with the GEOPROBE in Norton Sound vary logarithmically with distance above the bottom. Nonlogarithmic profiles generally occur during periods of low currents associated with turning of the tide. Logarithmicity of the profile persisted throughout periods of increased nontidal bottom currents, probably caused by higher local wind stress.

Diurnal and fortnightly variations in u_* and u_{100} appear throughout the measurements. Both c_D and z_o also show diurnal periodicities, although no fortnightly cycles are discernible. The values of c_D are higher than previous estimates for tidally dominant flows (Sternberg, 1968; McCave, 1973); however, unlike those of previous studies that were carried out in tidal channels, our measurements were obtained in the mouth of a wide embayment on an expansive

continental shelf. The mean values of C_D and z_o over the 65-day period were 10×10^{-3} and 2.2 cm, respectively. This mean value of z_o is considerably larger than that predicted for hydraulically rough flow over a bottom with irregular random roughness elements of 4- to 8- cm heights.

A distinct bottom nepheloid layer persisted throughout the experimental period; the turbidity and thickness of this layer increased in response to higher values of u_* during peak tidal flows. During maximum tidal currents, and particularly during spring tides, values of u_* exceeding u_{*c} indicate resuspension and transport of bottom materials. The increased turbulence associated with higher u_* values probably caused the near-bottom layer to thicken and to intensify in turbidity. Weaker mean regional flow probably advects the suspended materials northward away from the Yukon prodelta. Apparently, during fair weather this flow removes large amounts of the fine sediment supplied to the region by the Yukon River. Drake and others (1980) discuss the role of regional flow and storm-generated currents in transporting Yukon-derived materials into the Arctic basin.

The data reported here yield the longest continuous estimates of u_*, z_o, and C_D yet reported for a bottom boundary layer on an open continental shelf. Similar measurements in other continental-shelf areas, as well as other geologic and geophysical data collected with the GEOPROBE system, should increase our understanding of the response of surface deposits in particular regions to bottom stresses driven by different physical mechanisms.

ACKNOWLEDGMENTS

This work was carried out as part of the marine environmental studies program of the U.S. Geological Survey, Menlo Park, California, and was supported by the Bureau of Land Management through interagency agreement with the National Oceanic and Atmospheric Administration, under which a multiyear program responding to the needs of petroleum development of the Alaskan Continental Shelf is managed by the Outer Continental Shelf Environmental Assessment Program (OCSEAP0 office. We thank James Nicholson, George Tate, and Charles Totman for their assistance with the GEOPROBE tripod operation, and Paul Freitag for his technical aid.

REFERENCES

Bowden, K..F., Fairbairn, L.A., and Hughes, P. (1959) The distribution of shearing stresses in a tidal current. Geophys. Jour. Royal Astronom.Soc., 2, 288-305.

Cacchione, D.A. and Drake, D.E. (1979) A new instrument system to investigate sediment dynamics on continental shelves; Mar. Geol., 30, 299-312.

Cacchione, D.A. and Drake, D.E. (1980) Storm-generated sediment transport on a shallow continental shelf. J. Geophys. Res., in press.

Davis, J.C. (1973) Statistics and Data Analysis in Geology. John Wiley & Sons, New York, 550 pp.

Drake, D.E. (1976) Suspended sediment transport and mud deposition on continental shelves. In: Marine Sediment Transport and Environmental Management. (Ed. by D.J. Stanley and D.J.P. Swift), John Wiley and Sons, New York, 127-158.

Drake, D.E., Cacchione, D.A., Muench, R.D., and Nelson, C.H. (1980) Sediment transport in Norton Sound Alaska. Mar. Geol., in press.

Grant, W.D. and Madsen, O.S. (1979) Combined wave and current interaction with a rough bottom. J. Geophys. Res., 84 (C4), 1797-1808.

Heathershaw, A.D. (1976) Measurements of turbulence in the Irish Sea benthic boundary layer. In: The Benthic Boundary Layer (Ed. by I.N. McCave), Plenum Press, New York, 11-31.

Kagan, B.A. (1971) Sea bed friction in a one-dimensional tidal current. Izvestiya, Atmos. and Oceonic Phys., 8, 780-785.

Karweit, M. (1974) Response of a Savonius roter to unsteady flow. J. Mar. Res., 32, 359-364.

McCave, I.N. (1973) Some boundary-layer characteristics of tidal currents bearing sand in suspension. Memoires Societe Royale des Sciences de Liege, 6th series, VI, 187-206.

Pak, H. and Zameveld, J.R.V. (1977) Bottom nepheloid layers and bottom mixed layers observed on the continental shelf off Oregon. J. Geophys. Res., 82 (27), 3921-3931.

Schlichting, H. (1968) Boundary-Layer Theory. McGraw Hill, New York, 748 pp.

Scott, J.T. and Csanady, G.T. (1976) Nearshore currents off Long Island, J. Geophys. Res., 81 (30), 405-409.

Smith, J.D. (1977) Modeling of sediment transport on continental shelves. In: The sea: Marine Modeling (Ed. by Goldberg, E.D., McCave, I.N., O'Brien,J.J., and Steele, J.H.), Wiley-Interscience, New York, 539-577.

Smith, J.D., and McLean, S.R. (1977) Spatially averaged flow over a wavy surface. J. Geophys. Res., B2 (12), 1735-1746.

Sternberg, R.W. (1968) Friction factors in tidal channels with differing bed roughness. Mar. Geol., 6, 243-260.

Wimbush, M. (1976) The physics of the benthic boundary layer. In: The Benthic Boundary Layer (Ed by I.N. McCave), Plenum Press, New York, 3-10.

Table 1. Distribution of correlation coefficients (r) determined from a linear least-squares fit to the GEOPROBE hourly current speed profiles, Norton Sound, Alaska.

	1.00	0.90	0.80	0.70	0.60	0.50	0.40	0.3	0.2	0.1	0.0	<0*
Number of occurrences-----	1210	362	113	60	33	28	19	16	10	9	60	
Percentage of occurrences-----	63	19	6	3	2	1	1	<1	<1	<1	3	

* Values of r <0 indicate profiles whose slope was negative; i.e., velocity as taken from the fitted least-squares straight line decreased upward from the lowest level (z = 20 cm).

Figure Captions

Fig. 1. Bathymetric chart of Norton Sound, Alaska, showing location of GEOPROBE (A) during July-September 1977.

Fig. 2. Time series of currents measured at 100 cm above sea floor with GEOPROBE e-m current meter, showing variations in current speed u_{100} (a); current direction (b), east(+)-west(-) component u (c), north(+)-south(-) component v (d), and daily-averaged speed vectors ("sticks").

Fig. 3. Variance of burst-averaged current speeds for GEOPROBE e-m current meters at 20 (cm1), 50 (cm2), 70 (cm3) and 100 (cm4) cm above sea floor. Horizontal axis is marked at 4-day intervals.

Fig. 4. Time-series values of shear velocity (u_*), current speed at 100 cm above sea floor (u_{100}), drag coefficient (c_D), and roughness (z_o) during period July 8-September 10, 1977. Horizontal axis is marked at 6-day intervals.

Fig. 5. Square of correlation coefficient (r^2) obtained for least-squares-fitted curves to current-meter data and current speed at 100 cm above bottom (u_{100}).

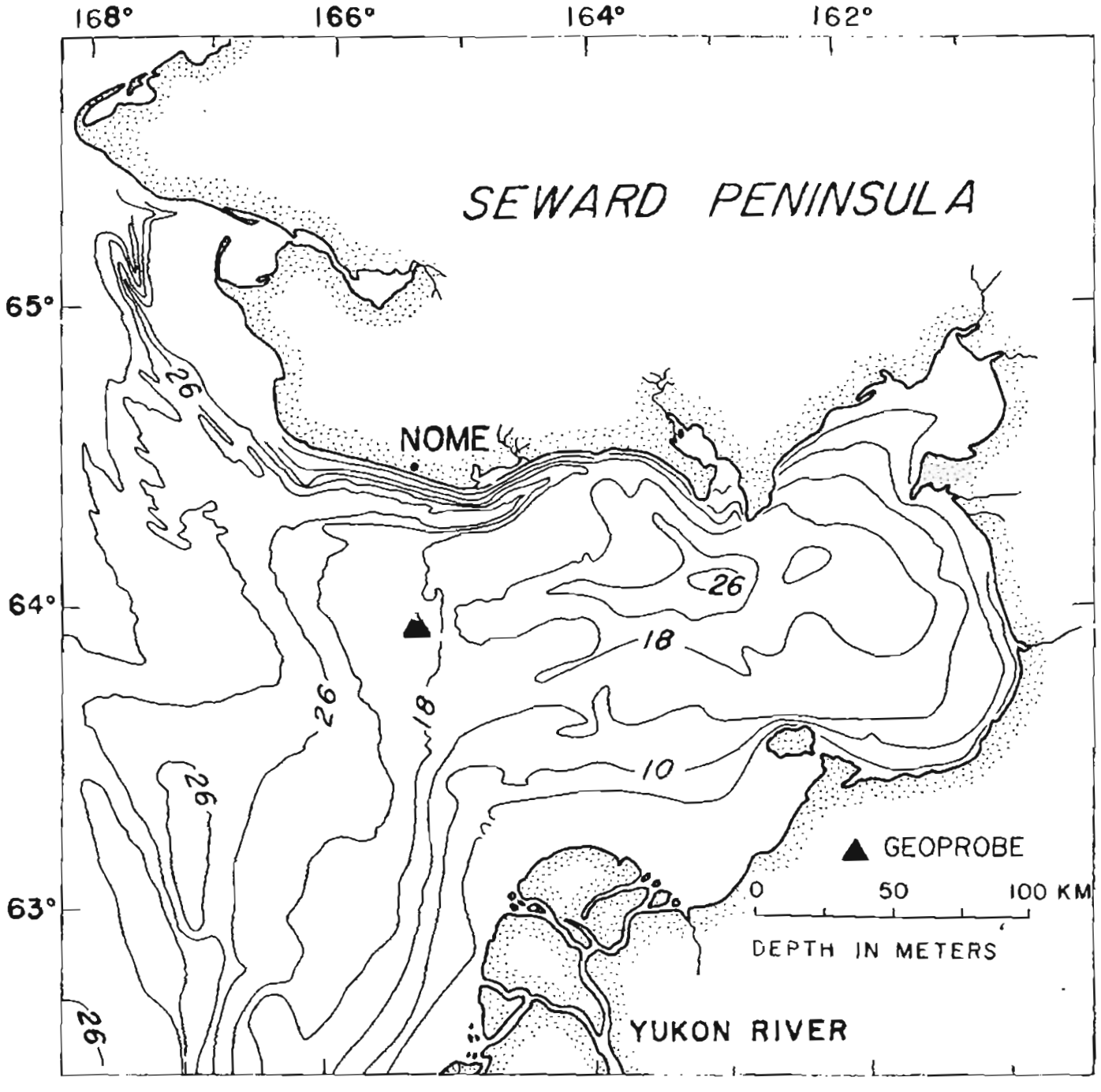
168°
166°
164°
162°
65°
64°
63°
SEWARD PENINSULA
NOME
26
18
10
GEOPROBE
0
50
100 KM
DEPTH IN METERS
YUKON RIVER

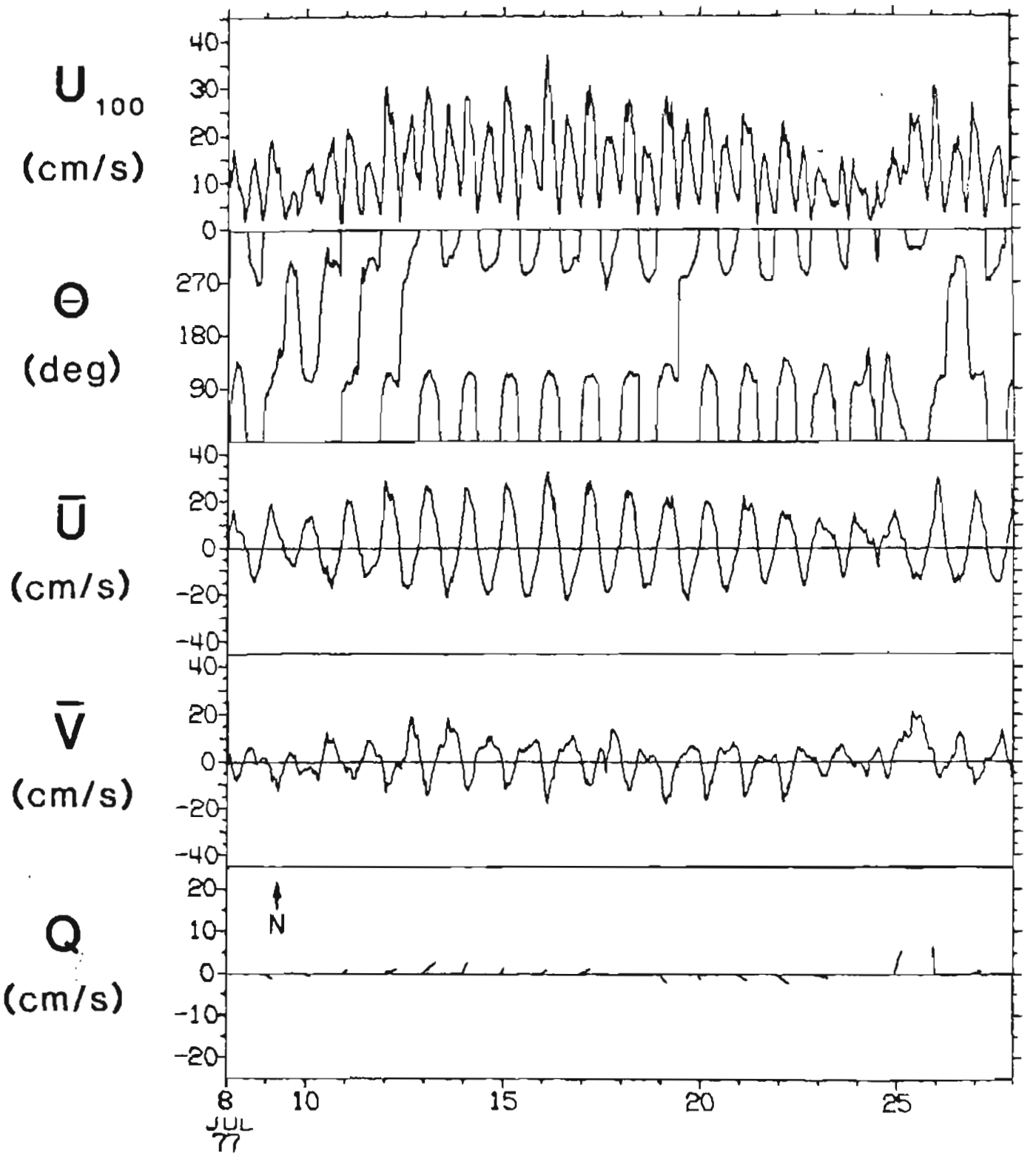
U_{100}
(cm/s)
40
30
20
10
0
Θ
(deg)
270
180
90
$\bar{U}$
(cm/s)
40
20
0
-20
-40
$\bar{V}$
(cm/s)
40
20
0
-20
-40
Q
(cm/s)
20
10
0
-10
-20
N
8
JUL
77
10
15
20
25

VARIANCE NORTON 1977

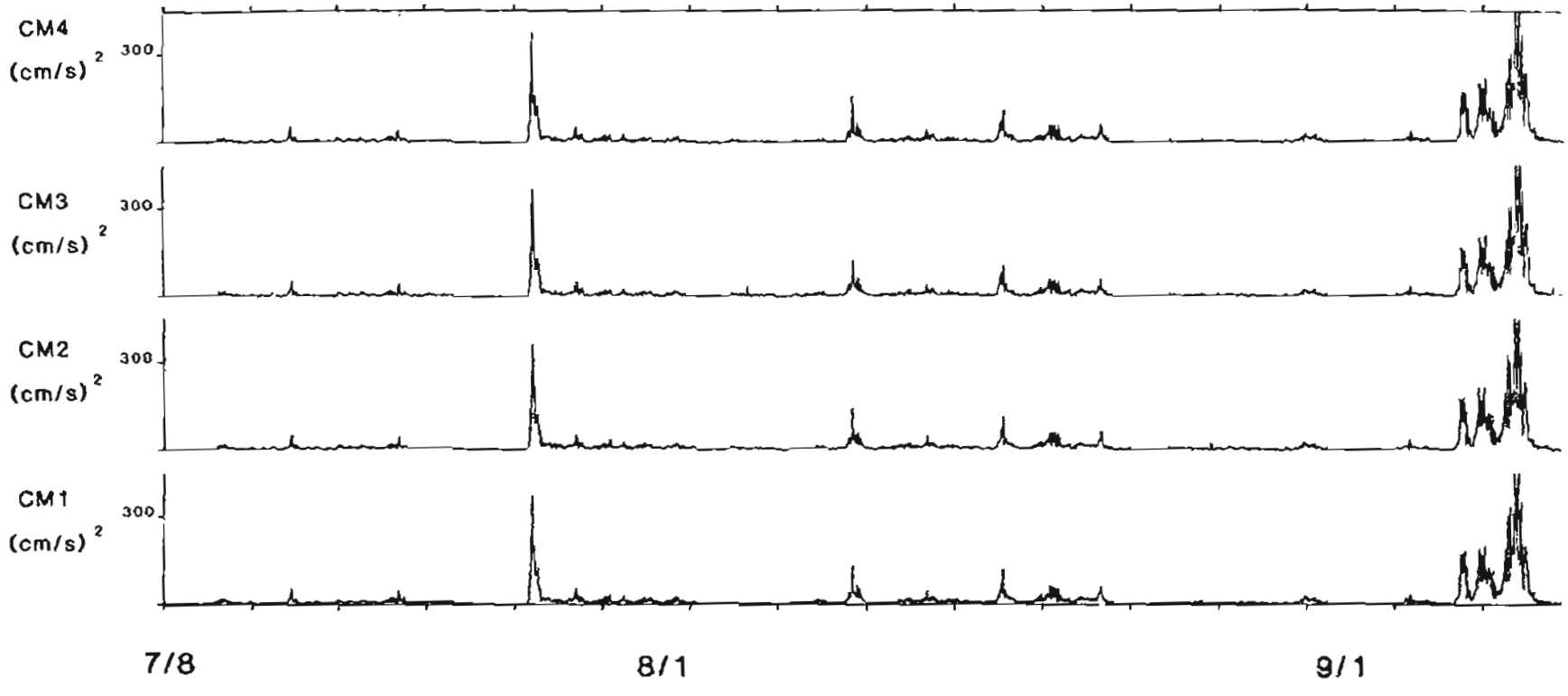

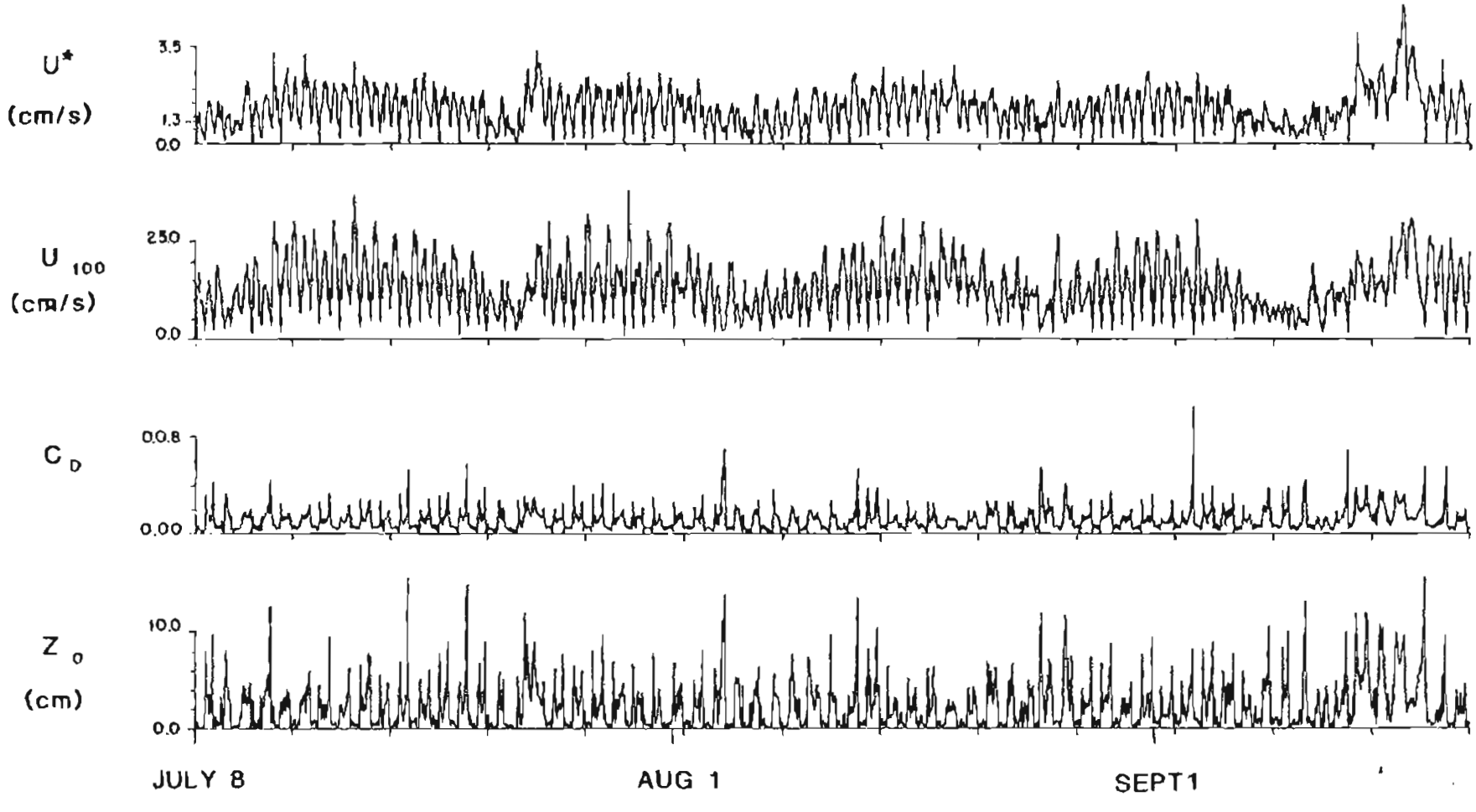
NORTON SOUND 1977
U*
(cm/s)
3.5
1.3
0.0
U 100
(cm/s)
250
0.0
C D
0.08
0.00
Z 0
(cm)
10.0
0.0
JULY 8
AUG 1
SEPT 1

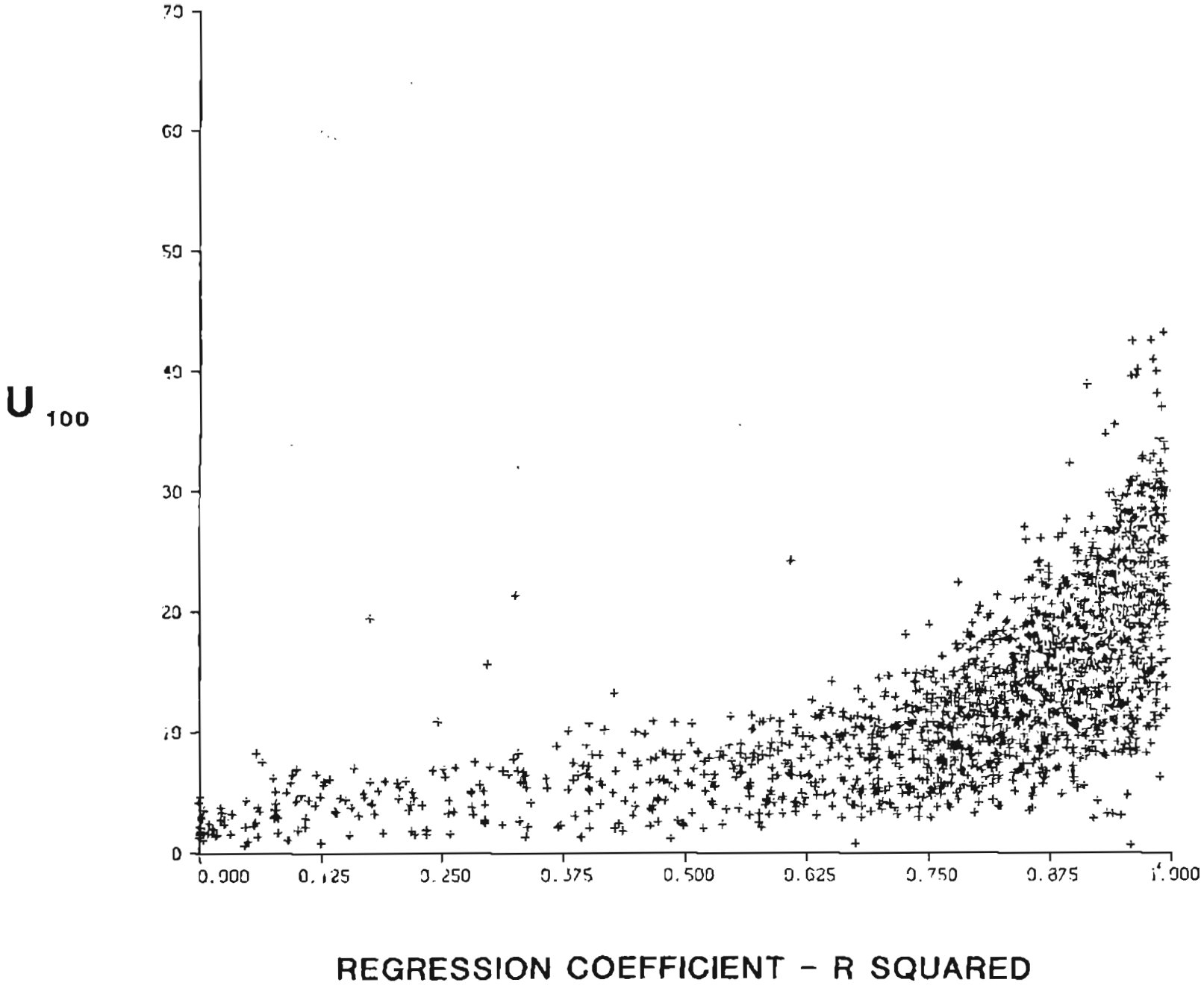
U 100
70
60
50
40
30
20
10
0
0.000
0.125
0.250
0.375
0.500
0.625
0.750
0.875
1.000
REGRESSION COEFFICIENT - R SQUARED

UNITED STATES DEPARTMENT OF THE INTERIOR

GEOLOGICAL SURVEY

Geotechnical Characteristics of Bottom Sediment in the Northern Bering Sea

By

Harold W. Olsen, Edward C. Clukey,

and C. Hans Nelson

Contents

	Page
Abstract	1
Introduction	2
Geologic and environmental framework	3
Geotechnical profiles	5
Consolidation and static triaxial data	10
Discussion of potential hazards	12
Acknowledgments	16
References	17

Table

Table 1.--Geologic and environmental framework for geotechnical studies in the northern Bering Sea..... 22

Geotechnical Characteristics of Bottom Sediment in the Northern Bering Sea

By

Harold W. Olsen[1], Edward C. Clukey[2], and

C. Hans Nelson[2]

Abstract

Yukon sediment of Holocene age, consisting dominantly of silty fine sand and sandy silt, covers the bottom of central and western Norton Sound, which is a high energy environment involving extensive ice loading, high waves, and strong bottom currents. The sediment contains significant amounts of sand in some areas and a generally minor amount of clay-size material ranging from 0 to 20 percent. Moreover, it is generally dense although loose and weak zones occur at the surface and also at depth between relatively dense layers. These characteristics, evidence of storm sand layers and scour depressions, and the results of preliminary analytical studies indicate this sediment is susceptible to liquefaction during major storms.

Substantially finer grained, weak, and highly compressible sediment of Holocene age, derived from the Yukon River and from local rivers and streams, covers eastern Norton Sound and the Port Clarence embayment, which are low

[1]U.S. Geological Survey, Box 25046, Mail Stop 903, Denver, Colorado 80225.

[2]U.S. Geological Survey, 345 Middlefield Road, Menlo Park, California 94025.

energy environments with negligible ice loading, low waves, and weak bottom currents.

Transgressive deposits of late Pleistocene age that cover the bottom of Chirikov Basin include an inner-shelf fine sand underlain by a basal transgressive medium sand that is exposed on the north and east flanks of the basin. Geotechnical data on the latter, obtained in the sand-wave fields near Port Clarence, show the material is loose near the surface but becomes firm rapidly with depth and could not be penetrated more than about 3 m with the Alpine vibratory sampler.

Pleistocene peaty deposits underlie the Holocene and late Pleistocene deposits in both Norton Sound and Chirikov Basin and are somewhat overconsolidated, probably because of subaerial desiccation during low sea level stands in the late Pleistocene. These materials have a higher clay content than the overlying deposits and they contain substantial amounts of organic carbon and gas. The presence of gas suggests that in situ pore pressures may be high. If so, the strength of the material could be low even though the material is generally overconsolidated.

Introduction

During the last few years the U.S. Geological Survey (USGS) has been acquiring geotechnical data on bottom sediment in the Northern Bering Sea. This effort has been part of a broad group of USGS studies in this region aimed at clarifying and evaluating those geologic conditions and processes that may be hazardous to offshore resource development activities (Thor and Nelson, 1979; Larsen, Nelson, and Thor, 1980).

Previous reports concerning this geotechnical effort include the papers by Clukey, Nelson, and Newby (1978); Nelson, Kvenvolden, and Clukey (1978); Nelson et al. (1979); and Sangrey et al. (1979). These reports describe near-

surface data on samples obtained during 1976 and 1977 with box corers, Soutar Van Veen samplers, and a Kiel vibracore sampler capable of penetrating 2 m beneath the ocean floor[3]. The data also include penetration rate measurements during vibracorer sampling operations. During 1978, additional samples and penetration records were obtained with an Alpine vibratory corer system equipped to obtain 8.89 cm diameter continuous samples to a maximum depth of 6 m. All of the data obtained to date have been compiled for the Bureau of Land Management in a USGS open-file report by Larsen, B. R., et al. (1980).

The purpose of this paper is to summarize the geotechnical information obtained in the above studies in relation to the geologic and environmental conditions in the northern Bering Sea and to assess the implications of these data with regard to potential hazards to offshore resource development activities in the region.

Geologic and environmental framework

The bottom of Norton Sound consists of silty fine sand and sandy silt of Holocene age discharged from the Yukon River, except for nearshore areas where Pleistocene (>10,000 years B.P.; Hopkins, 1975) transgressive deposits remain and tidally scoured troughs where transgressive and Holocene deposits are mixed (Fig. 1; Nelson, this volume, Fig. 6). In southern Norton Sound, the Holocene sediment is interbedded with fine sand layers as much as 20 cm thick near the Yukon Delta. Pleistocene freshwater silt interbedded with peaty muds and peat layers underlies the Holocene sediment.

---

[3]Use of brand names in this report is for descriptive purposes only and does not constitute endorsement by the U.S. Geological Survey.

Most of Chirikov Basin is covered by an inner shelf fine sand deposited by the late Pleistocene shoreline transgression across this region (Fig. 1; Nelson, this volume, Fig. 6). This deposit is underlain by a basal transgressive medium sand that is exposed on the north and east flanks of the basin. Lag gravels are exposed near the basin margins where the late Pleistocene shoreline transgression has reworked pre-Quaternary bedrock and glacial moraines and where strong modern currents have prevented subsequent deposition. Strong bottom currents and water circulation patterns have inhibited deposition of Holocene sediment from the Yukon River throughout Chirikov Basin, except for some accumulations with ice-rafted pebbles in local depressions in eastern and southern Chirikov Basin (McManus, Hopkins, and Nelson, 1977).

Prior to the deposition of the transgressive sand layers, tundra-derived peat deposits formed during several Pleistocene low sea-level stands that periodically exposed the entire northern Bering shelf until 12,000-13,000 years ago. These Pleistocene limnic peaty muds generally overlie Pleistocene glacial and alluvial deposits that are underlain by pre-Quaternary bedrock.

The Pleistocene peaty mud is a source of biogenic gas throughout the region. Seismic profiles showing acoustic anomalies associated with these materials indicate gas concentrations are of sufficient magnitude to affect sound transmission throughout Norton Sound (Holmes and Thor, this volume). The presence of shallow craters in the thin Holocene sediment in east-central Norton Sound suggests venting of biogenic gas accumulations from the underlying peaty muds. Generally low background levels of dissolved hydrocarbons in the waters of Norton Sound and high gas contents in the underlying peaty mud suggest venting is episodic, while the Holocene sediment generally acts as a seal preventing the biogenic gas from diffusing freely to

the sea floor as it appears to do through the transgressive sand in Chirikov Basin (Nelson et al., 1979).

A large submarine seepage of thermogenic gas in west-central Norton Sound was discovered in 1976 (Cline and Holmes, 1977; Kvenvolden et al., 1979b). Acoustic investigations indicate the presence of bubble-phase gas associated with the sediment in the seep in an area of 50 km^2 (Nelson et al., 1978). Detailed geophysical and geochemical studies indicate that hydrocarbons and CO_2 are migrating upward along a major growth fault in the sedimentary section (Kvenvolden et al., 1979a).

Bottom sediment in the northern Bering Sea is exposed to ice loading, cyclic stress from waves, and drag from bottom currents (Table 1). Ice loading is extensive in the vicinity of the Yukon Delta (Thor and Nelson, 1979). High waves and strong bottom currents occur in central and western Norton Sound and in Chirikov Basin. Storm waves and bottom currents cause significant reworking and erosion of the sediment in Norton Sound (Larsen, Nelson, and Thor, 1979) and also cause the transport of sediment from Norton Sound to the Chukchi Sea, almost 1000 km to the northwest (Cacchione, Drake, and Weiberg, this volume; Dupré and Thompson, 1979; Nelson and Creager, 1977; Drake et al., 1980). Two areas in this study, Port Clarence and eastern Norton Sound, are protected from large waves and strong bottom currents.

Geotechnical profiles

Methods

The geotechnical profiles (Figs. 2-6) present, for each of the regions outlined in Table 1, information concerning the composition and the relative density or consolidation state of the materials. Direct evidence concerning the composition of the materials includes the data on lithology, texture, Atterberg limits, and gas content. The other data on moisture content,

density, strength indices, and vibracore penetration resistance reflect the combined influences of the composition and the relative density or consolidation state. The latter can usually be inferred on a qualitative basis from the suites of information presented.

The data in Figs. 2-6 were obtained with shipboard and laboratory procedures as follows: penetration rates were derived from vibratory corer penetration rates during sampling; gas content data were obtained on shipboard from 10- to 15-cm sample tube sections using the procedures described by Kvenvolden et al. (1979a); bulk densities of tube sections were calculated from shipboard measurements of their volume and weight; visual descriptions, shear strength index measurements, and subsamples for moisture content, density, Atterberg limits, and texture analyses were obtained on shipboard from split tube sections of all cores except 78-1 through 78-5. The latter cores were preserved on shipboard and were subsequently extruded, logged, and tested in the USGS geotechnical laboratory in Denver. The Holocene-Pleistocene boundaries noted on Figs. 2-6 were derived from lithologic logging and radiocarbon dates (Nelson, this volume), and from microfaunal analyses (McDougall, this volume). Texture analyses were run with geologic (Larsen, B. R., et al., 1980), and engineering standard (American Society for Testing and Materials, 1977) sieving and sedimentation column techniques. Moisture content and density data were obtained on subsamples taken with the miniature coring device described by Clukey et al. (1978). Atterberg limits were run in accordance with ASTM Standards using the wet preparation method, D 2217 (American Society for Testing and Materials, 1977). Strength index data were obtained with laboratory vane, hand vane, pocket penetrometer, and unconfined compression test equipment. Circumstances did not generally allow these measurements to be made under controlled conditions with standardized

procedures that must be employed for the data to have quantitative significance regarding shear strengths. Nevertheless, these data show differences in strength that reflect variations in the composition and the relative density or consolidation states of the materials tested. The absence of strength index data in some of the profiles is also significant in that materials, such as clean sands that do not possess any apparent cohesion, cannot be tested with the strength index test methods used in this study.

Yukon Prodelta

The three profiles in the vicinity of the Yukon Delta (Fig. 2) show mostly Holocene materials that are dominantly silty fine sand, and sandy silt with occasional thin beds of organic clayey silt having clay contents generally less than 20 percent. Gas contents vary over a wide range at station 78-22 from about 0.2 to 70 ml/l of interstitial water; the range at stations 78-23 and 78-24 is considerably less, from about 0.8 to 4.0 ml/l. The relative density of the material varies over a wide range. Moderately dense to dense zones predominate. However, loose zones, indicated by a watery appearance and very low strengths, are particularly evident at a depth of 2-3 m at station 78-22, and from the surface to a depth of about 1.5 m at station 78-24. The watery appearance of the loose zones emerged fairly rapidly after the core was split, apparently because the material densified in response to vibrations generated by the ship engines. The variations of penetration resistance with depth generally correlate with the presence of loose or dense zones. The variations in gas content with depth do not show a close association either with relative density as inferred above or with the variations in texture, density, and strength with depth.

West-central Norton Sound

The five profiles in west-central Norton Sound (Fig. 3) are located in

the thermogenic (Kvenvolden et al., 1979a) gas seep acoustic anomaly (stations 78-1, 78-2, and 78-3), within a nearby biogenic (Kvenvolden et al., 1979a) gas acoustic anomaly (station 78-4), and adjacent to the biogenic gas acoustic anomaly (station 78-5). Very high gas contents occur at one location in the thermogenic anomaly (station 78-3) and in the biogenic anomaly (station 78-4). Much lower gas contents occur at stations 78-1 and 78-2 in the thermogenic anomaly and at station 78-5 adjacent to the biogenic anomaly. These profiles penetrate silty fine sand and sandy silt that are similar to the materials in the Yukon Delta region (Fig. 2) and that are probably Holocene deposits because of their lithology, texture, and consistently low moisture contents. The two profiles with very high gas contents also penetrate Pleistocene peaty muds at depths of about 3 m and 1 m at stations 78-3 and 78-4, respectively. Note that the high water contents and low densities are clearly associated with the peaty muds. The relative density of the materials varies over a wide range, which is similar to the range observed in the Yukon Delta region (Fig. 2) as indicated by watery-appearing zones and the wide variations in strength. The vibracore penetration resistance appears to correlate in general with the strength data, although not below 3 m depth at station 78-4. Low penetration resistance is associated with very high gas contents in the profile at station 78-3 and above 3 m in the profile at station 78-4. However, the increase in penetration resistance below 3 m at station 78-4, and the low penetration resistance at station 78-5 are not associated with changes in, or high values of, gas contents, respectively.

East-central Norton Sound

In east-central Norton Sound (Fig. 4) four of the five profiles (stations 78-6, 78-9, 76-121, 76-125) penetrate thin deposits of Holocene silty fine sand and sandy silt and extend into the underlying Pleistocene deposits which

include freshwater peaty mud. The profile at station 78-10 appears to penetrate only the Holocene material. Compared with the west-central Norton Sound and Yukon Delta regions (Figs. 2 and 3), these profiles show similar materials with relative densities that are low near the surface, but that increase much more rapidly with depth. In fact, the Alpine vibratory corer was unable to penetrate deeper than about 3 m in this region. The rapid increase in penetration resistance with depth occurs in both Holocene and Pleistocene materials, even though their gas contents are similar to those in weaker materials at other locations such as in the station 78-5 profile in west-central Norton Sound (Fig. 3).

Eastern Norton Sound and the Port Clarence embayment

The profiles from eastern Norton Sound, near Stuart Island, and from the Port Clarence embayment (Fig. 5) penetrate materials that are generally finer grained and have relatively high moisture contents, high plasticity, low density, low strength, and low penetration resistance compared with the materials in the regions previously discussed. The characteristics of these profiles (Fig. 5) appear to be associated with their low-energy environments. Station 78-21 is located in Port Clarence, the most protected environment in the region. The materials in this profile have substantially higher water contents (~90 percent) and lower strengths (~10 kPa) than other materials encountered in the northern Bering Sea. The very low strengths and their uniformity with depth suggest the Holocene materials in Port Clarence may be somewhat underconsolidated; i.e., not yet in equilibrium with the weight of the material.

Sand-wave fields near Port Clarence

Four profiles in the sand-wave fields near Port Clarence in the Chirikov Basin are shown in Fig. 6. Stations 78-14 and 78-16 are located on one sand-

wave crest, and the profiles penetrate medium sand that appears to be the basal transgressive deposit described by Nelson (this volume, Fig. 6). Station 78-15 is located in the adjacent sand-wave trough to the east, and penetrates the Pleistocene peaty mud that underlies the basal transgressive deposits in the region. The profile at station 78-17 is located on the adjacent sand-wave crest to the east. It penetrates the basal transgressive sand to a depth of about 1.5 m and the Pleistocene peaty mud from 1.5 to 2.2 m. The materials from 2.5 to 3.5 m are poorly to moderately sorted medium to fine sand with abundant pebbles and some silt- and clay-sized material. Below a sharp contact at 3.5 m the material appears to be glacial till consisting of a firm muddy sand with scattered pebbles.

The relative density of the basal transgressive sand is low near the surface but increases rapidly with depth, as indicated by the strength and penetration resistance data in the profiles for stations 78-14 and 78-16. The peaty mud at stations 78-15 and 78-17 is comparatively weak and has a very wide range of water contents due to the intermittent distribution and variable character of the peaty material. At station 78-17 the sand beneath the peaty mud appear to be firm and dense with a moderate to high resistance to vibracore penetration.

Consolidation and static triaxial data

Consolidation data (Fig. 7) on three box core samples of Holocene sediment show a wide range in the initial void ratio and compressibility of materials from the Yukon Delta and central regions of Norton Sound (Fig. 1; stations 76-154, 76-156). The wide range in these properties is consistent with the high variability in the strength and penetration resistance of these materials as shown in Figs. 2, 3, and 4. The compressibilities of the samples from station 76-156 may be high compared with other materials in these

regions, because this station is located near vibracore station 78-24, whose profile (Fig. 2) shows a very loose and weak zone at the surface.

Triaxial data on vibracore samples of Holocene Yukon sediment from stations 78-22 and 78-23 (Fig. 8) show moderate to high static strengths with friction angles in the range of 35° to 40°. The variation in friction angle is small for the samples from station 78-22, consistent with the small variations in texture and density among the samples. The wider variation in friction angle for the samples from station 78-23 appears to be associated with variations in both the texture and density of the samples tested.

Soils that tend to contract during shear (contractive) weaken and may liquefy during cyclic loading from earthquakes and ocean waves (Sangrey, et al., 1978). The stress paths in Fig. 8 show the materials tested are generally contractive at low deviator stress levels and become dilative (tend to dilate during shear) as they approach the yield surface. Moreover, with the exception of the sample from 2.34 m depth at station 78-22, the stress paths become less contractive and more dilative at decreasing initial volumetric stress levels. This behavior pattern is normal for homogeneous material. The in situ stresses at the depths from which the samples were obtained are on the order of 10 kPa to 30 kPa. These stresses are very low compared to the initial volumetric stresses used to obtain the data in Fig. 8. Therefore, the behavior of the materials in situ should be less contractive and more dilative than that shown by the stress paths in Fig. 8.

The stress path for the sample from 2.34 m depth at station 78-22 (Fig. 8) is of particular interest in that it shows this sample is more contractive at low stress levels than any of the samples tested. This behavior is consistent with the data in Fig. 2 which shows this sample represents the loosest zone in the profiles at stations 78-22 and 78-23. Thus

the data indicate that loose zones within the Holocene Yukon sediment are of the most concern with regard to strength loss and liquefaction during cyclic loading from earthquakes and ocean waves. Work in progress is aimed at defining the potential for strength loss in these materials on a more quantitative basis (Clukey, Cacchione, and Nelson, 1980).

Discussion of potential hazards

Potential hazards associated with the geotechnical characteristics of bottom sediment in the northern Bering Sea include the liquefaction of bottom sediments in response to ocean waves, earthquakes, and the upward migration of gas from thermogenic and biogenic sources; the scour and transport of bottom sediments and mobile bed forms in response to bottom currents; low strength and high compressibility of materials in low relative density and consolidation states; and gas-charged sediment.

Liquefaction is of particular concern in central and western Norton Sound because the area is exposed to strong cyclic loading from storm waves and is underlain by gas-charged material. Moreover, the susceptibility of the Holocene Yukon sediment in these regions to liquefaction is suggested by its dominantly silty fine sand and sandy silt texture and by the occurrence of relatively loose zones within it (Figs. 2, 3, 4). In addition, historic occurrences of wave-induced liquefaction are suggested by evidence of widespread storm-sand layers and scour depressions in the vicinity of the Yukon Delta (Nelson this volume; Larsen et al., 1979).

Work in progress is aimed at assessing on a quantitative basis the susceptibility of the Holocene Yukon sediment to liquefaction during storm waves. The approach involves the measurement of storm waves to define the cyclic bottom stresses induced during major storms; laboratory cyclic shear tests on Yukon Prodelta materials to determine the dynamic properties that

govern the rate of pore pressure increase and associated degradation of strength during cyclic loading; and analyses of these measurements with a finite-element model that takes into account both the buildup of pore pressure induced by cyclic loading and the concomitant dissipation of pore pressure that is governed by the permeability of the material.

Preliminary analyses have been completed (Clukey et al., 1980) for a semi-infinite half-space model of the Yukon prodelta using dynamic property and permeability data estimated from the geotechnical characteristics reported in this paper together with 3-m and 6-m sinusoidal surface waves. The 3-m wave represents worst-case conditions for a storm recorded in July 1977, and the 6-m wave corresponds to a 1-percent occurrence interval for storms in September and October (Arctic Environmental Information and Data Center, 1977). The results indicate the prodelta will not liquefy in response to the 3-m storm wave even for the extreme case when zero dissipation of pore pressure is assumed. However, the results for the 6-m storm wave, presented in Fig. 9, indicate the sediment will liquefy to a depth of approximately 3.5 m. The results in Fig. 9 further indicate that the depth of liquefaction varies with storm duration but does not increase significantly for durations greater than 1 hour. This relation is suggested by the 4-m pore pressure contour, which is increasing at a very slow rate at the end of the 1-hour storm assumed in the analysis.

Materials with low strength and high compressibility are present in eastern Norton Sound and the Port Clarence embayment. Comparison of Fig. 5 with Figs. 2, 3, and 4 shows that these materials are substantially finer grained and weaker than those in central and western Norton Sound. Because eastern Norton Sound and the Port Clarence embayment are protected from strong bottom currents and large waves, deposition has taken place in a low energy

environment. Also the materials have not been subjected to cyclic shear stresses associated with large waves, which have probably densified much of the sediment in other parts of the northern Bering Sea. The organic sandy clayey silt in the Port Clarence embayment is particularly weak and highly compressible because the very low strengths indicate the material may be somewhat underconsolidated.

Scour and transport of bottom sediment depend on the drag associated with bottom currents and the strength of the bottom sediment. Bottom currents are strong in central and western Norton Sound (Table 1). The bottom sediment is loose and weak at some locations in these regions (Figs. 2, 3, 4) and also in the sand waves near Port Clarence in Chirikov Basin (Fig. 6). In addition, the bottom sediment in central and western Norton Sound appear to be susceptible to liquefaction during major storms. These conditions are consistent with evidence of scour depressions in the vicinity of the Yukon Delta and also evidence for the large-scale transport and modification of sand waves near Port Clarence in the Chirikov Basin (Nelson, this volume; Larsen et al., 1979; Larsen et al., 1980).

The importance of gas in sediment depends on whether it is present in the bubble phase and whether the amount present is sufficient to cause significantly elevated pore fluid pressures. Elevated pore pressures can induce liquefaction in overlying materials, and they are associated with reductions in the strength of sediment in situ (Sangrey, 1977).

Seismic and core studies in Norton Sound suggest bubble phase gas is present in the anomaly associated with the thermogenic gas seep south of Nome and at several other locations where biogenic gas is being generated in the Pleistocene peaty mud beneath the Holocene silt (Kvenvolden et al., 1979a;

Holmes and Thor this volume; Kvenvolden et al., 1980; Nelson et al., 1978; Nelson et al., 1979).

Previous work that suggests bubble phase gas may be causing elevated pore pressures in situ includes: limited data showing an association of low vibracore sample penetration resistance with very high gas contents (Nelson et al., 1978); and studies of shallow craters on the bottom of east-central Norton Sound which attribute their origin to episodic venting of biogenic gas generated in the Pleistocene peaty mud and trapped by the overlying Holocene Yukon sediment (Nelson et al., 1979).

The geotechnical profiles in this paper (Figs. 2-6) show additional data concerning the association of vibracore penetration resistance and gas contents. Low penetration resistance is associated with very high gas contents in some of the profiles (see stations 78-3, 78-4, 78-8, and 78-15), but not in general as noted in the section on geotechnical profiles above. For example, the penetration resistance at station 78-5 is about the same as that at station 78-3 even though the gas contents in the two profiles differ substantially.

However, the lack of consistent correlations between gas content and penetration resistance in all the profiles does not eliminate the possibility that gas is causing elevated pore pressures in situ. The relative density or consolidation state of the materials also influences the penetration resistance and may be masking the effects of gas. In this regard the association of the shear strength and penetration resistance data in the profiles is of interest because both measurements are influenced by the relative density or consolidation state, but only the penetration resistance is influenced by in situ elevated pore pressures. The strength data were obtained from samples on shipboard and in the laboratory where elevated pore

pressures would have easily dissipated prior to the measurements.

The importance of the relative density or consolidation state of the material on penetration resistance is clearly evident in the geotechnical profiles from eastern Norton Sound and the Port Clarence embayment (Fig. 5). As noted in the discussion above very low strengths occur because these locations are not exposed to significant ice loading and waves that can densify and consolidate sediment. The penetration resistance is correspondingly low, it varies with the shear strength, and it does not appear to be influenced by variations in gas content. Similarly, in the profiles from the Yukon Delta region (Fig. 2), the penetration resistance is more closely associated with relative density, as indicated by the strength data, than with the gas content.

Hence the question remains whether significant elevated pore pressures associated with biogenic and thermogenic gas exist in the bottom sediment of the northern Bering Sea. Additional work is needed to determine the magnitudes of in situ pore pressures and their regional distribution.

Acknowledgments

The cruises for this study were supported jointly by the U.S. Geological Survey and the U.S. Bureau of Land Management through an interagency agreement with the U.S. National Oceanic and Atmospheric Administration, under which a multiyear program responding to the needs of petroleum development of the Alaska continental shelf is managed by the Outer Continental Shelf Environmental Assessment Program (OCSEAP) Office.

References

American Society for Testing and Materials (1977) Annual Book of ASTM Standards: Part 19, Philadelphia.

Arctic Environmental Information and Data Center, University of Alaska, Anchorage, and National Climatic Center, Environmental Data Service, NOAA, Asheville, North Carolina, (1977) Climatic Atlas of the Outer Continental Shelf waters and coastal regions of Alaska, vol. 2, Bering Sea.

Bishop, A. W., and Henkel, D. J. (1962) The measurement of soil properties in the triaxial test, 2d ed. Edward Arnold (Publishers) Ltd., London.

Cline, J. D., and Holmes, M. L. (1977) Submarine seepage of natural gas in Norton Sound, Alaska. Science, 198, 1149-1153.

Clukey, E. C., Cacchione, D. A., and Nelson, C. H. (1980) Liquefaction of Yukon Prodelta. Offshore Technology Conference Proceedings, Paper 3773.

Clukey, E. C., Nelson, H., and Newby, J. E. (1978) Geotechnical properties of Northern Bering Sea sediment. U.S. Geological Survey Open-File Report 78-408.

Drake, D. E., Cacchione, D. A., Meunch, R. D., and Nelson, C. H. (1980) Sediment transport in Norton Sound, Alaska. Marine Geology (in press).

Dupré, W. R., and Thompson, R. (1979) A model for deltaic sedimentation in an ice-dominated environment. Offshore Technology Conference Proceedings, Paper 3434, 2, 657-661.

Hopkins, D. M. (1975) Time-stratigraphic nomenclature for the Holocene Epoch. Geology, 3, 10.

Kvenvolden, K. A., Nelson, C. H., Thor, D. R., Larsen, M. C., Redden, G. D., Rapp, J. B., and DesMarais, D. J. (1979a) Biogenic and thermogenic gas in gas-charged sediment of Norton Sound, Alaska. Offshore Technology Conference Proceedings, Paper 3412, 1, 479-483.

Kvenvolden, K. A., Redden, G. D., Thor, D. R., and Nelson, C. H. (1980) Hydrocarbon gases in near-surface sediment of northern Bering Sea (Norton Sound and Chirikov Basin). In: Hood, D. W., editor, The Eastern Bering Sea Shelf, Chapter 19: Oceanography and Resources (in press).

Kvenvolden, K. A., Weliky, K., Nelson, C. H., and DesMarais, D. J. (1979b) Submarine seep of carbon dioxide in Norton Sound, Alaska. Science, 205, 1264-1266.

Larsen, B. R., Nelson, C. H., Larsen, M. C., Thor, D. R., Olsen, H. W., Clukey, E. C., and Esterlee, J. S. (1980) Physical properties of Norton Basin sediment. U.S. Geological Survey Open-File Report (in press).

Larsen, M. C., Nelson, H., and Thor, D. R. (1979) Geologic implications and potential hazards of scour depressions on Bering Shelf, Alaska. Environmental Geology, 3, 39-47.

Larsen, M. C., Nelson, C. H., and Thor, D. R. (1980) Sedimentary processes and potential geologic hazards of Norton Basin sea floor. In: Hood, D. W., ed., The Eastern Bering Sea Shelf, Chapter 19: Oceanography and Resources (in press).

McManus, D. A., Hopkins, D. M., and Nelson, C. H. (1977) Distribution of bottom sediments on the continental shelf, northern Bering Sea. U.S. Geological Survey Professional Paper 759-C.

Nelson, H., and Creager, J. S. (1977) Displacement of Yukon derived sediment from Bering Sea to Chukchi Sea during Holocene time. Geology, 5, 141-146.

Nelson, H., Kvenvolden, K. A., and Clukey, E. C. (1978) Thermogenic gases in near-surface sediments of Norton Sound, Alaska, 10th Offshore Technology Conference Proceedings, Paper 3354, 3, 2623-2633.

Nelson, C. H., Thor, D. R., Sandstrom, M. W., and Kvenvolden, K. A. (1979) Modern biogenic gas-generated craters (sea-floor "pockmarks") on the Bering Shelf, Alaska. Geological Society of America Bulletin, 90, 1144-1152.

Sangrey, D. A. (1977) Marine Geotechnology--State-of-the-Art. Marine Geotechnology, 2, 45-80.

Sangrey, D. A., Bouma, A. H., Hampton, M. A., Carlson, P. R., Molnia, B. F., Clukey, E. C., Nelson, C. H., and Olsen, H. W. (1979) Geotechnical engineering characteristics of the outer continental shelf lease areas in Alaska, Proceedings. 5th International Conference on Port and Ocean Engineering Under Arctic Conditions, August 13-18, 1979, 2, 963-976.

Sangrey, D. A., Castro, G., Poulos, S. J., and France, J. W. (1978) Cyclic loading of sands, silts, and clays. Proceedings of the ASCE Geotechnical Engineering Division Specialty Conference on Earthquake Engineering and Soil Dynamics, II, 836-851.

Thor, D. R., and Nelson, C. H. (1979) A summary of interacting surficial geologic processes and potential geologic hazards in the Norton Basin, northern Bering Sea. Offshore Technology Conference Proceedings, Paper 3400, 377-381.

Wissa, A. E. Z., Christian, J. T., Davis, E. H., and Heiberg, S. (1971) Consolidation at constant rate of strain. American Society of Civil Engineers, Journal of Soil Mechanics and Foundation Engineering, 97, SM 10, 1393-1412.

Figure Captions

1. Location map of northern Bering Sea showing regions and sampling stations cited in this paper.
2. Geotechnical profiles from the Yukon Prodelta.
3. Geotechnical profiles from west-central Norton Sound. Stations 78-1, 78-2, and 78-3 are in the thermogenic gas seep acoustic anomaly south of Nome. Station 78-4 is on a nearby biogenic gas acoustic anomaly. Station 78-5 is adjacent to the biogenic gas acoustic anomaly.
4. Geotechnical profiles from east-central Norton Sound where shallow gas craters are associated with thin deposits of Holocene Yukon silt overlying Pleistocene freshwater peaty mud.
5. Geotechnical profiles from eastern Norton Sound, including Stuart Island (78-8), and the Port Clarence embayment (78-21).
6. Geotechnical profiles from the sand-wave fields near Port Clarence in the Chirikov Basin. Stations 78-14 and 78-16 are located on one sand-wave crest. Station 78-17 is located on the adjacent sand-wave crest. Station 78-15 is in the trough between these sand-wave crests.
7. Consolidation data on samples of Holocene Yukon silt from box cores in the vicinity of the Yukon Delta and central Norton Sound. (See Fig. 1.) Box core station 78-156 is adjacent to vibracore station 78-24 whose geotechnical profile is shown in Fig. 2. ω = moisture content in percent dry soil weight; γ_t = bulk density in g/cm3; C_c = compression index. Tests run according to procedures described by the American Society for Testing and Materials (1977) and Wissa et al. (1971).

8. Consolidated-undrained triaxial data on samples of Holocene Yukon silt from Alpine vibracores at stations 78-22 and 78-23 near the Yukon prodelta (see Fig. 2). ϕ' = effective friction angle. σ_1 and σ_3 are the total vertical and horizontal stresses, respectively. σ_1' and σ_3' are the effective vertical and horizontal stresses, respectively. ω and γ_t are defined in the caption for Fig. 7. d_{50} and $<2\mu$ are the median grain size and minus 2 micron fraction, respectively. Tests run according to procedures described by Bishop and Henkel (1962).

9. Results of preliminary analyses of wave-induced liquefaction potential of Holocene Yukon silt near the Yukon prodelta, assuming a wave height of 6 m, a period of 10 seconds, a relative density of 54 percent, and a coefficient of permeability of $1.50X10^{-6}$ cm/s. U/σ = ratio of pore pressure to total overburden stress. The figure shows the variation of pore pressure ratio with time at depths below the sediment surface ranging from 0.25 m to 6 m.

Table 1.--Geologic and environmental framework for geotechnical studies in the northern Bering Sea

Region	Geologic units	Origin	Gas	Environmental Loading		
				Waves	Bottom currents	Ice
Yukon prodelta.	Holocene silty fine sand and sandy silt with interbedded storm sand layers less than 20 m thick.	Yukon River. High energy deposition and redeposition.	Biogenic	High	Strong	Extensive
West-central Norton Sound.	Holocene silty fine sand and sandy silt, bioturbated, 1-2 m thick, over	Yukon River. Medium energy deposition,	Thermogenic and biogenic	Medium to strong	Medium to strong	Low
	Pleistocene freshwater peaty mud.	Freshwater deposition; tundra-derived peat; subaerial desiccation.				
East-central Norton Sound.	Holocene silty fine sand and sandy silt, bioturbated, 1-2 m thick, over	Yukon River. Medium energy deposition,	Biogenic	Medium	Medium	Low
	Pleistocene freshwater peaty mud.	Freshwater deposition; tundra-derived peat; subaerial desiccation.				
Eastern Norton Sound and Port Clarence Embayment.	Holocene sandy clayey silt, over	Yukon River and streams discharging from nearby shorelines. Low energy. deposition.	Biogenic	Low	Low	Low
	Pleistocene freshwater peaty mud and (or) glacial till.	Origin of Pleistocene peaty mud, same as above.				
Sand-wave fields near Port Clarence in Chirikov Basin	Late Pleistocene transgressive sands, over	Sand derived from pre-Quaternary bedrock and glacial moraines.	Biogenic	High	Very strong	Low
	Pleistocene freshwater peaty mud and (or) glacial till.	Origin of Pleistocene peaty mud, same as above.				

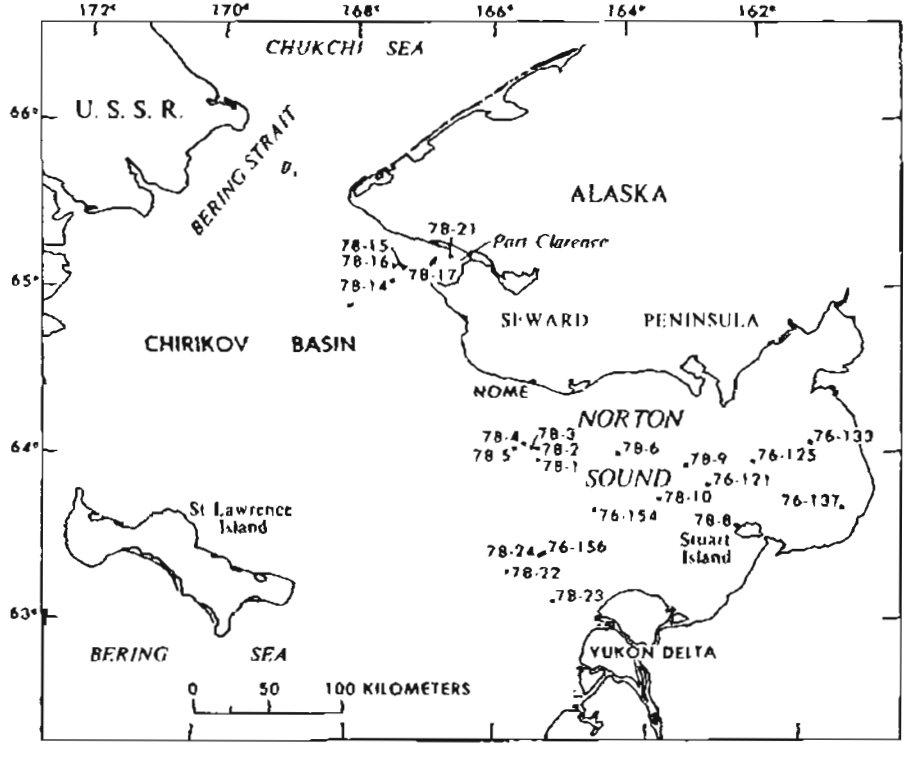
172°
170°
168°
166°
164°
162°
CHUKCHI SEA
66°
U. S. S. R.
BERING STRAIT
D.
ALASKA
78-21
Port Clarence
78-15
78-16
78-17
78-14
65°
SEWARD PENINSULA
CHIRIKOV BASIN
NOME
NORTON
SOUND
78-4
78-5
78-3
78-2
78-1
78-6
78-9
76-125
76-133
76-121
78-10
76-137
76-154
78-8
Stuart Island
78-24
76-156
78-22
78-23
64°
St Lawrence Island
63°
BERING SEA
YUKON DELTA
0 50 100 KILOMETERS

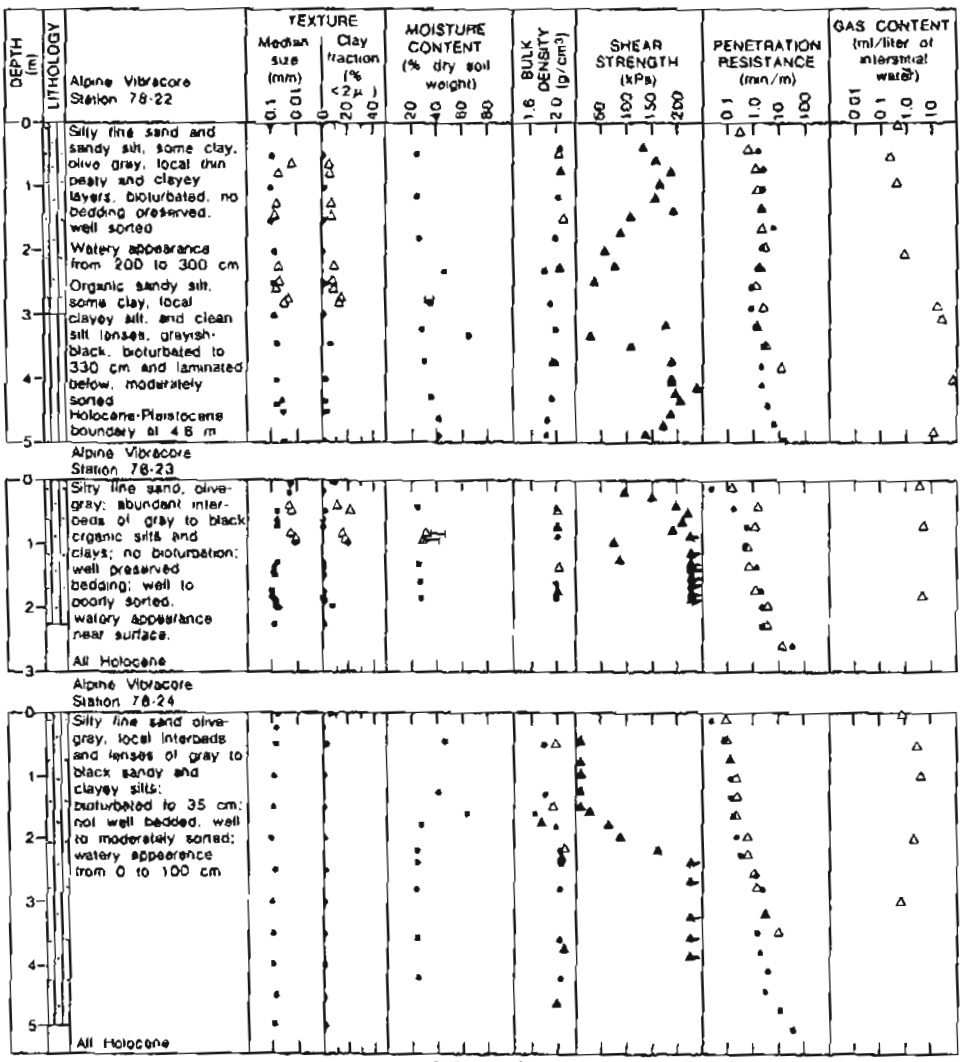

EXPLANATION

Solid symbol(●, ▲) shows data from core used primarily for geologic analysis

Open symbol(○, △) shows data from core used primarily for gas and engineering analysis

Symbols for shear strength data.
- △, ▲ pocket penetrometer
- ○, ● hand vane
- ▽, ▼ lab vane
- □, ■ unconfined compression

Symbols for density data.
- ●, ○ Based on subsamples
- △, ▲ Based on tube sections ~1 m long

Symbol for Atterberg Limits
Plastic limit ⟷ Liquid limit
These data are few because the materials are generally nonplastic

Symbols for lithology:
- Sand
- Silt
- Clay
- Organic silt or clay
- Peat and highly organic soils

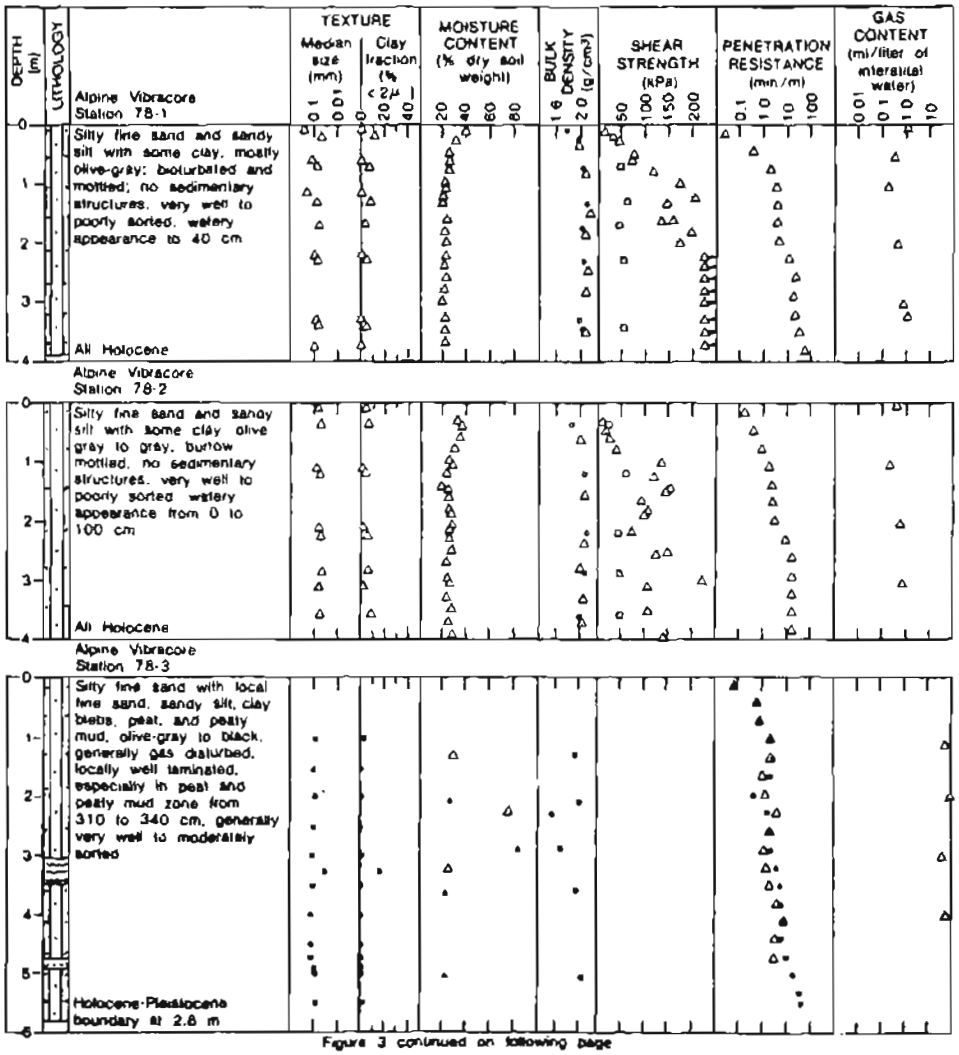

Figure 3 continued on following page

Figure 3 continued

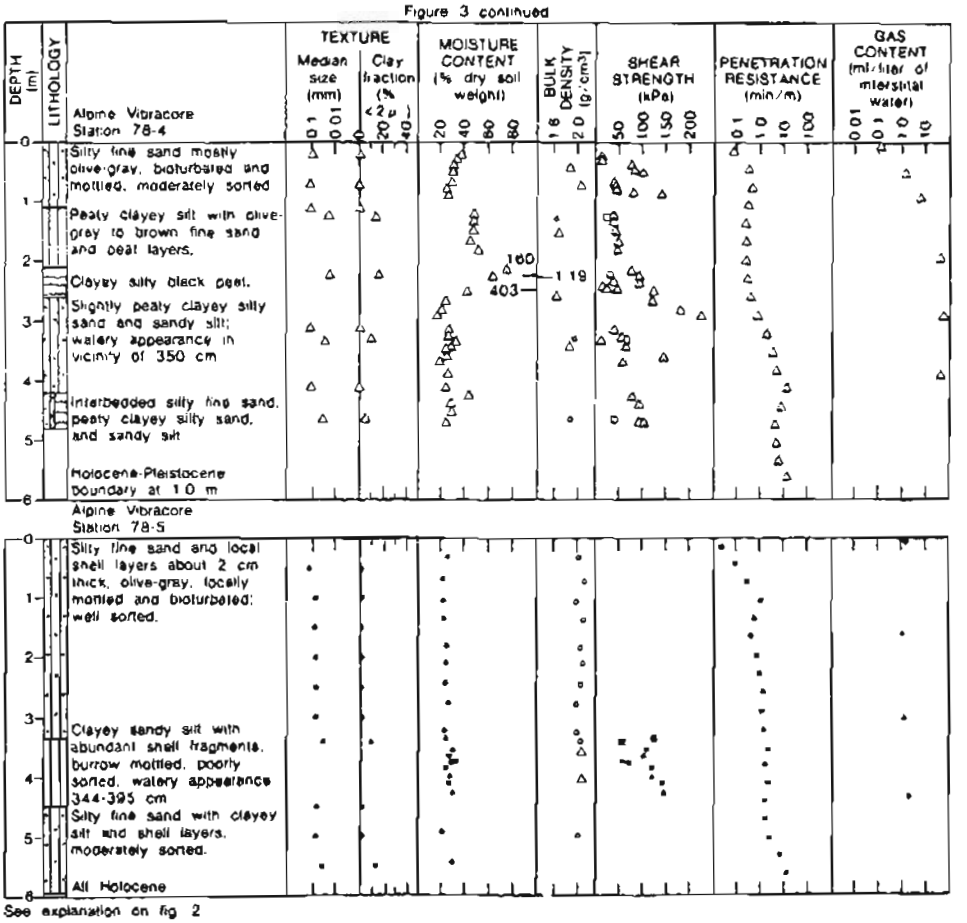

See explanation on fig. 2

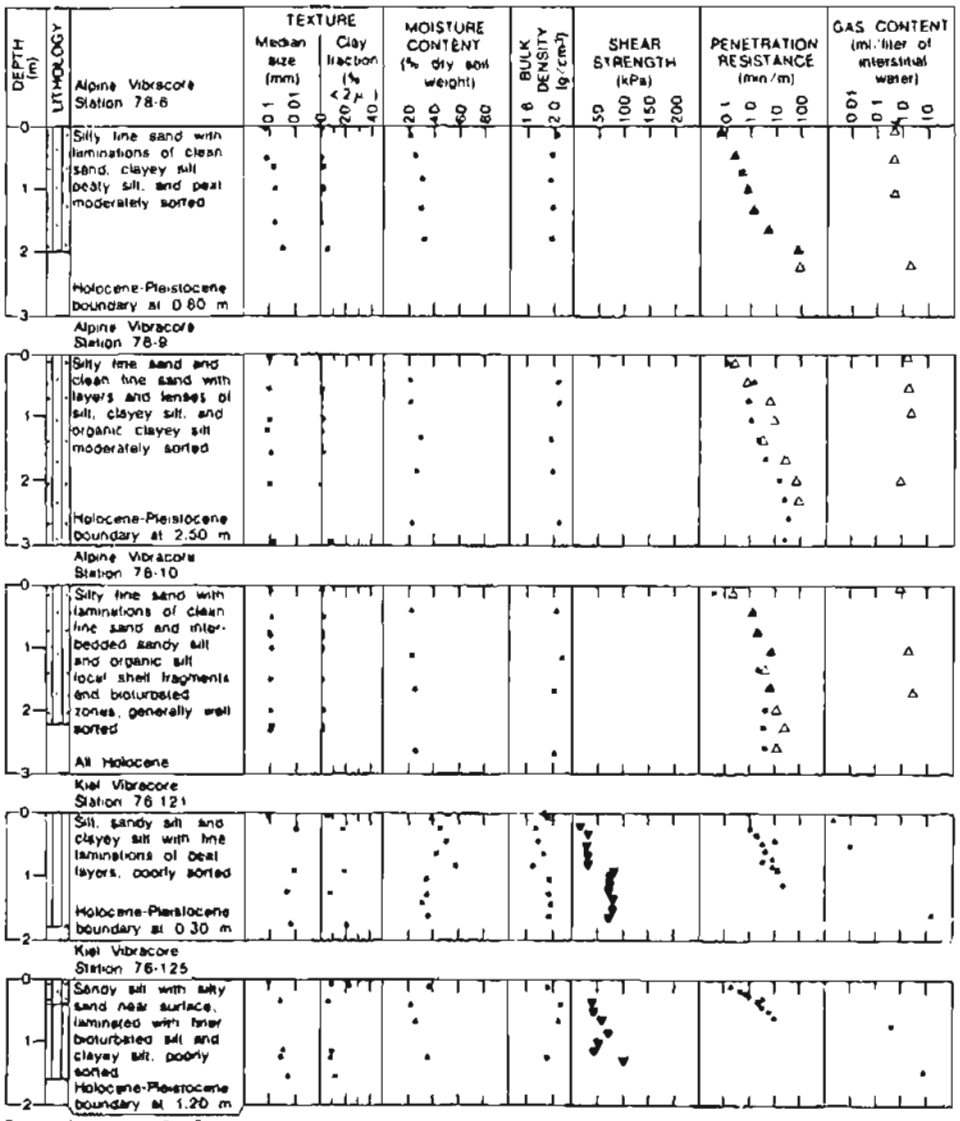

See explanation on fig. 2

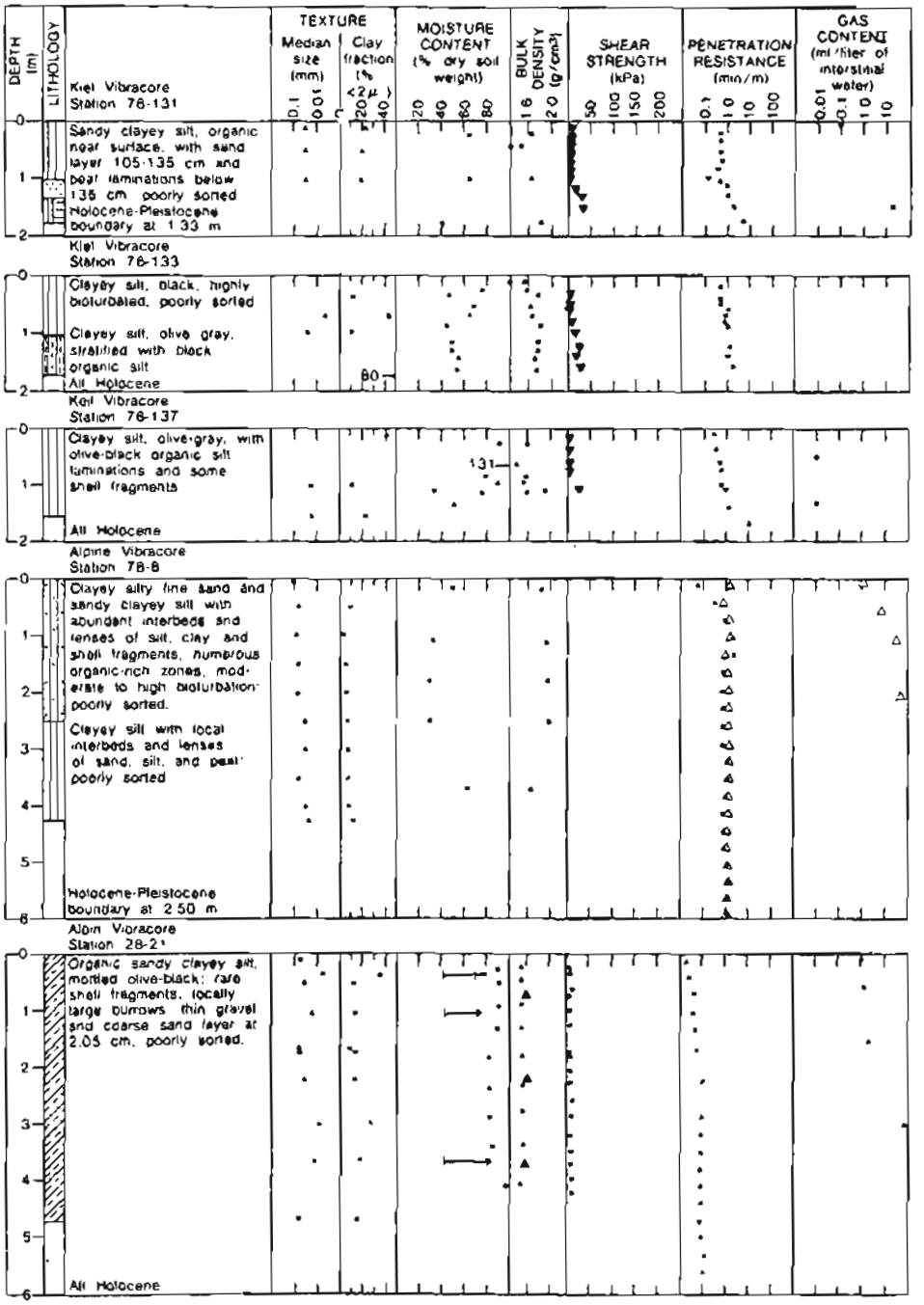

See explanation on fig. 2

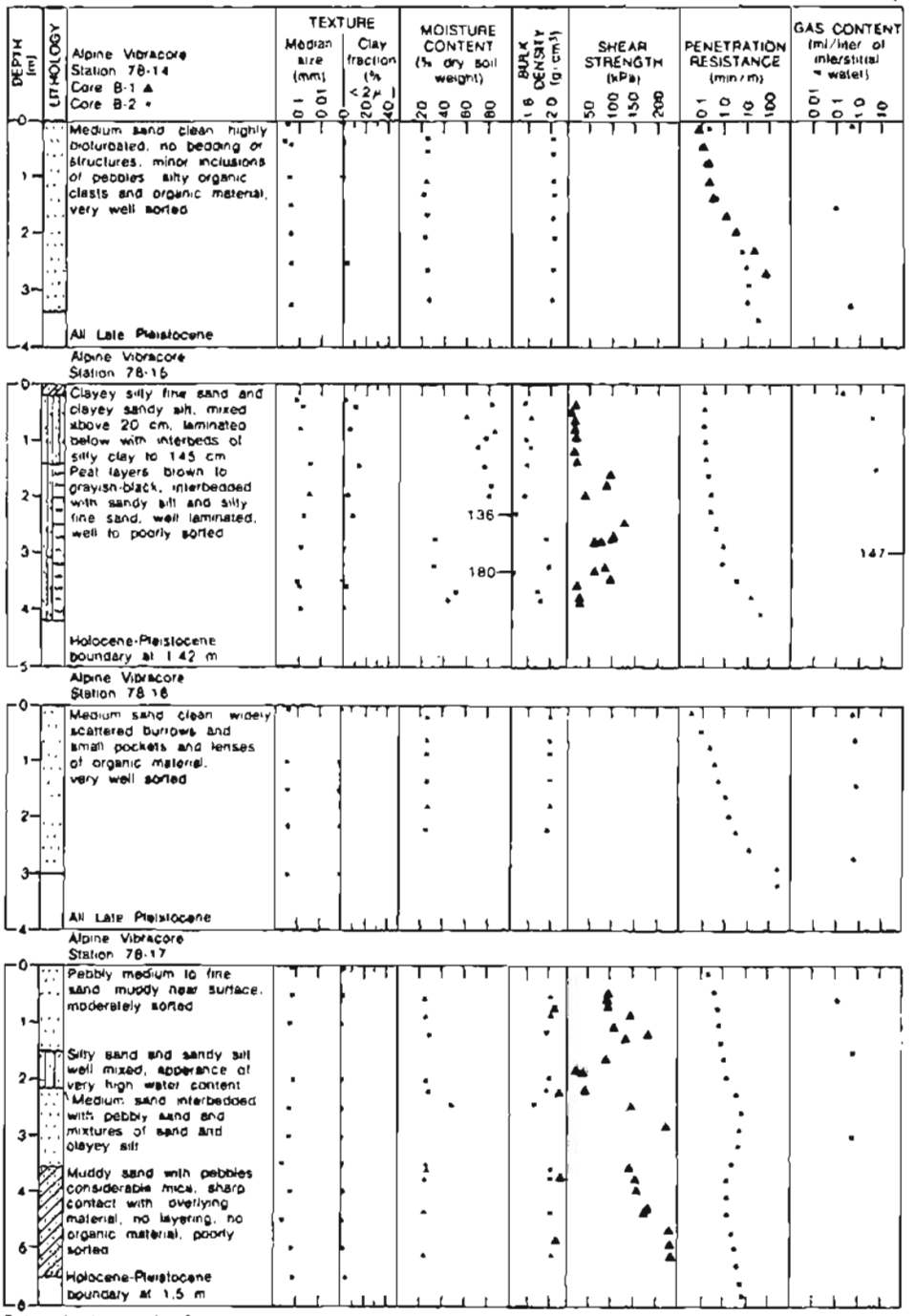

See explanation on pg 2

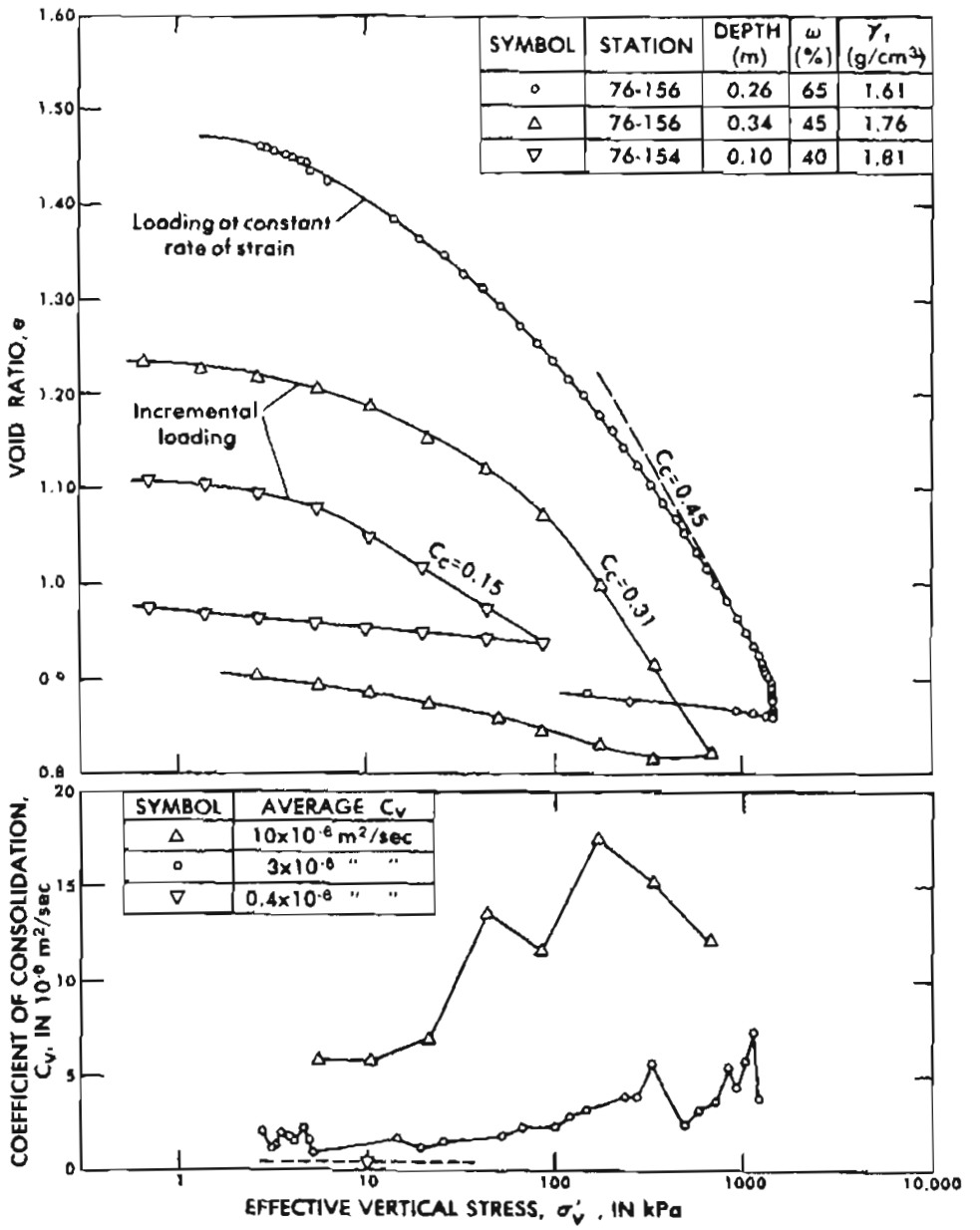
SYMBOL | STATION | DEPTH (m) | ω (%) | γt (g/cm³)
○ | 76-156 | 0.26 | 65 | 1.61
△ | 76-156 | 0.34 | 45 | 1.76
▽ | 76-154 | 0.10 | 40 | 1.81
Loading at constant rate of strain
Incremental loading
Cc=0.45
Cc=0.31
Cc=0.15
VOID RATIO, e
1.60
1.50
1.40
1.30
1.20
1.10
1.0
0.9
0.8
SYMBOL | AVERAGE Cv
△ | 10x10⁻⁶ m²/sec
○ | 3x10⁻⁶ " "
▽ | 0.4x10⁻⁶ " "
COEFFICIENT OF CONSOLIDATION, Cv, IN 10⁻⁶ m²/sec
20
15
10
5
0
1
10
100
1000
10,000
EFFECTIVE VERTICAL STRESS, σ'v , IN kPa

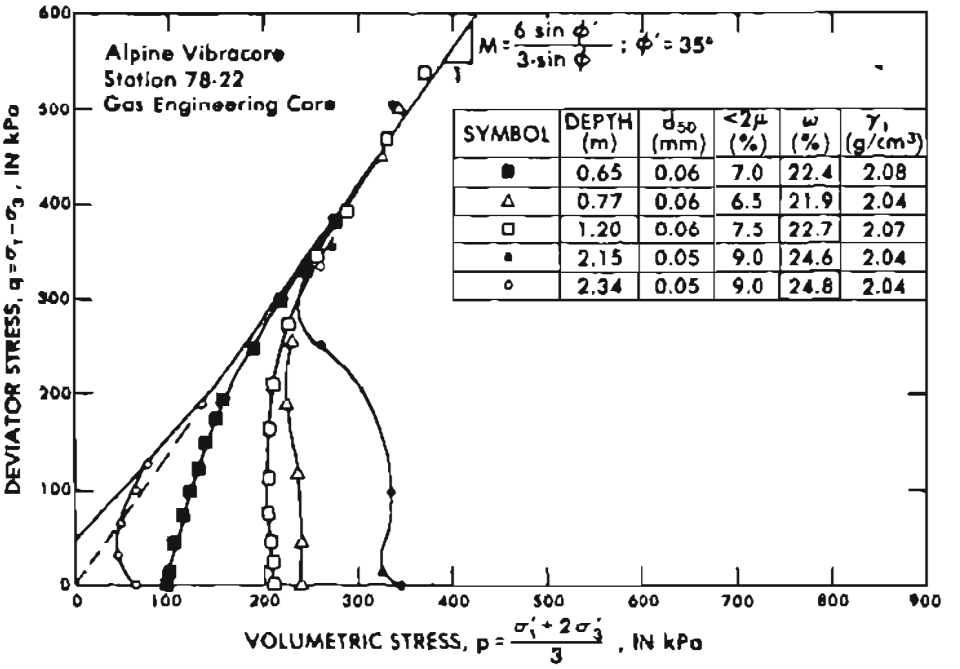

SYMBOL	DEPTH (m)	d_{50} (mm)	$<2\mu$ (%)	ω (%)	γ_t (g/cm³)
■	0.65	0.06	7.0	22.4	2.08
△	0.77	0.06	6.5	21.9	2.04
□	1.20	0.06	7.5	22.7	2.07
▪	2.15	0.05	9.0	24.6	2.04
○	2.34	0.05	9.0	24.8	2.04

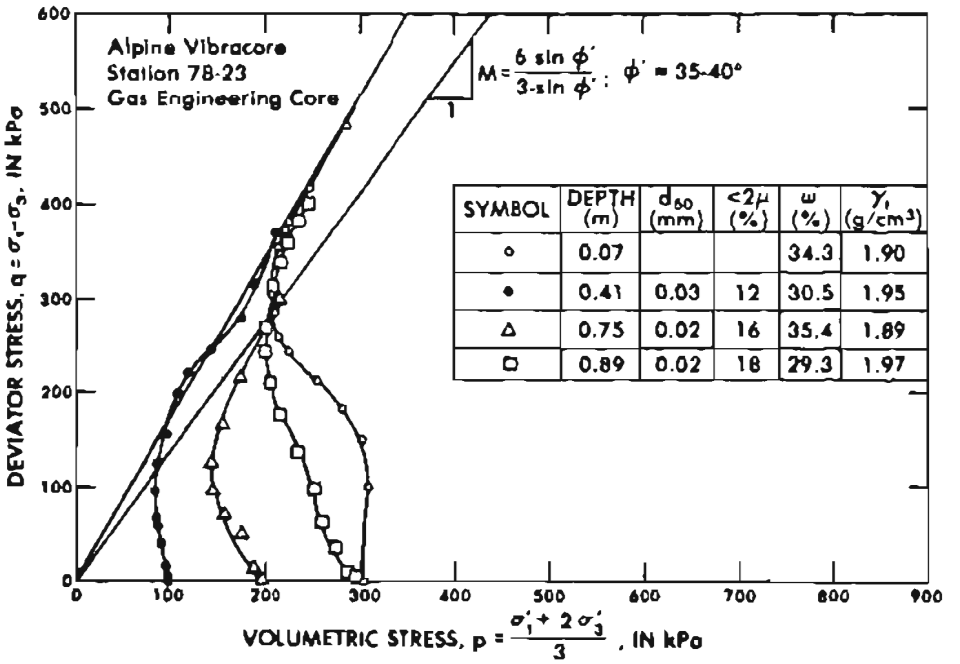

SYMBOL	DEPTH (m)	d_{50} (mm)	$<2\mu$ (%)	ω (%)	γ_t (g/cm³)
○	0.07			34.3	1.90
●	0.41	0.03	12	30.5	1.95
△	0.75	0.02	16	35.4	1.89
□	0.89	0.02	18	29.3	1.97

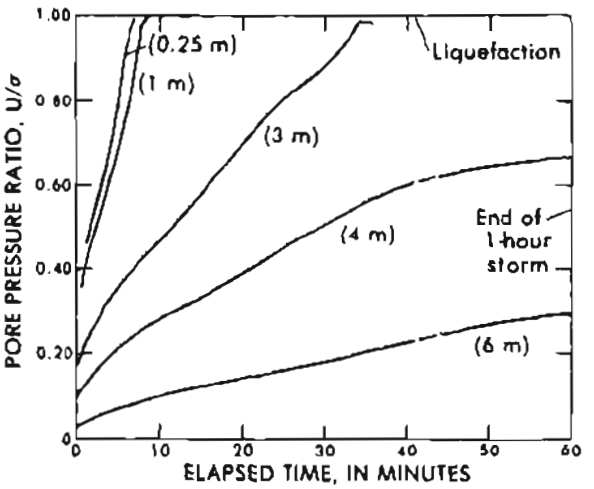
1.00
0.80
0.60
0.40
0.20
0
PORE PRESSURE RATIO, U/σ
(0.25 m)
(1 m)
(3 m)
(4 m)
(6 m)
Liquefaction
End of
1-hour
storm
0
10
20
30
40
50
60
ELAPSED TIME, IN MINUTES

United States
Department of the Interior
Geological Survey

DISTRIBUTION OF GAS-CHARGED SEDIMENTS IN NORTON BASIN, NORTHERN BERING SEA

by

Mark L. Holmes and Devin R. Thor

OPEN FILE REPORT 80-

This report is preliminary and has not been edited or reviewed for conformity with Geological Survey standards and nomenclature.

The use of trade names in this report is for descriptive purposes only and does not constitute an endorsement by the Geological Survey.

April 1980

DISTRIBUTION OF GAS-CHARGED SEDIMENTS IN NORTON BASIN, NORTHERN BERING SEA

M. L. Holmes and D. R. Thor

ABSTRACT

Seismic reflection records from Norton Sound and Chirikov basin contain numerous zones of anomalous acoustic responses caused by gas in the subsurface sediment layers. These acoustic anomalies have been detected using sound sources ranging in size and power from 3.5 kHz transducers to 1326 cubic inch air gun arrays. The frequency and distribution of these zones suggest that up to 7000 km^2 of the northern Bering Sea (Norton basin) may be underlain by gas-charged sediment. Much of the gas is of shallow biogenic origin, having been generated in buried peat deposits. Compressional velocity is about 1.5 km/sec in these layers, or 7 per cent below the velocity in gas free areas as determined from seismic refraction studies. Seismic velocity beneath a large gas seep south of Nome decreases to about 1.2 km/sec in the interval from 250-440 m below the sea floor. Here, thermogenic gases of deeper origin are migrating upwards along a system of basin margin faults.

INTRODUCTION

Discovery of the submarine seepage of natural gas south of Nome, Alaska, in 1976 (Cline and Holmes, 1977) prompted a comprehensive review of seismic reflection data from the Norton basin area (Fig. 1). The same types of anomalous acoustic responses associated with the seep zone (Cline and Holmes, 1977; Holmes and Cline, 1978; Nelson et al., 1978) were first encountered by Grim and McManus (1970) in the course of a high-resolution seismic study of the northern Bering Sea in 1967. They interpreted the zones of acoustically impenetrable sea floor on their sparker records as representing a Yukon River deposit very near the surface of the present-day sea floor. The highly reflective nature of this surficial deposit was thought to cause the sudden termination of deeper reflectors observed along portions of the seismic track (Grim and McManus, 1970). Air gun reflection records collected in Chirikov basin during a cruise by NOAA (then ESSA) in 1968 (Walton et al., 1969) also crossed a few of these reflector termination anomalies.

Cline and Holmes (1977) first suggested that these acoustic responses were caused by the presence of bubble phase gas in the near-surface sediment; Holmes and Cline (1978), Nelson et al. (1978), and Kvenvolden et al. (1979) presented detailed analyses of the deep penetration and high resolution seismic reflection records collected over the seep zone and the geochemistry of sediment samples from Norton Sound and Chirikov basin on USGS cruises in 1977 and 1978.

The main objective of this study was to determine the geographic extent and distribution of zones showing anomalous acoustic responses on seismic reflection records from Norton Sound and Chirikov basin. Certain

characteristics of these acoustic anomalies could then be analyzed to determine the most probable cause of the anomaly (gas, change in sediment type, etc.). Seismic records used for this study were collected aboard U.S. Geological Survey and University of Washington research vessels during the past 12 years along some 27,000 km of trackline (Fig. 2). Sound sources used in these geophysical studies included medium- and high-resolution sparker, 40 to 1300 cubic inch air gun, Uniboom, and subbottom profilers.

GEOLOGIC SETTING

The floor of the northern Bering Sea is a broad, shallow epicontinental shelf (Fig. 1). Water depths in Chirikov basin in the western part of the survey area range from 20-50 m. Norton Sound is bounded on the north by Seward Peninsula, on the east by the Alaska mainland, and on the south by the Yukon Delta. Water depths in Norton Sound range from 10-25 m. The surficial sediment of Norton Sound is primarily derived from the Yukon River and consists of coarse silt to very fine sand underlain by organic rich, nonmarine, peaty mud. Surficial sediment in Chirikov basin consists mostly of glacial gravel and transgressive fine sand (Nelson and Hopkins, 1974; McManus et al., 1974).

DESCRIPTION AND CAUSE OF ACOUSTIC ANOMALIES

Figures 3 and 4 show the locations of acoustically anomalous zones along more than 20,000 km of seismic reflection lines in Norton basin. The distribution of the many crossings of these zones suggests that they occur in large patches beneath much of the sea floor of Norton Sound; the total area may be as much as 7000 km^2. Two distinct types of acoustic anomalies were observed on the seismic reflection records: Reflector pull-downs and

reflector terminations (Holmes and Cline, 1978). Reflector pull-downs similar to those shown in Fig. 5 have been observed and described by several other investigators from both deep and shallow water areas where gas had accumulated in the subsurface strata (Lindsey and Craft, 1973; Cooper, 1978). The low compressional velocity in gas-charged horizons causes the recorded time section (seismic record) to be distorted relative to the true depth section. The greater travel time through the gassy sediment produces a zone of pulled down reflectors beneath it on the seismic record. The gas does not necessarily have to be in the free state (bubble phase) to produce this phenomenon; gas-water or oil-water solutions have compressional velocities less than water alone (Craft, 1973), although the decrease is much greater if gas is present in the sediment interstices. The strong horizontal reflector exhibiting a 180° phase shift which is associated with the observed pull-downs (Fig. 5) could be the result of reflections from interfaces between gas-charged zones and strata where water alone fills the pore spaces. The decrease in both compressional velocity and density due to the presence of gas in the sediment results in a large negative reflection coefficient at the top of the gas-charged layer (Craft, 1973; Savit, 1974). Such a condition would produce acoustic responses similar to the strong horizontal reflectors above the reflector pull-downs (Fig. 5).

Crossings of the acoustic anomaly associated with the gas seep south of Nome are shown in Figs. 5 and 6. The anomaly covers an area of about 50 km^2; it is characterized by a sudden termination of subbottom reflectors, and by a dramatic pull-down of the reflectors at its margins (Fig. 6). The depth to the top of the feature causing the anomalous acoustic signature appears to be quite shallow, on the order of 50-200 m. In places the surface of the acoustically opaque zone rises abruptly to within a few meters

of the sea floor (Nelson et al., 1978). These zones may indicate the locations of the active seeps (Kvenvolden et al., 1979).

Calculations by Cline and Holmes (1977, 1978) indicated that the concentrations of the low molecular weight hydrocarbons which had accumulated in the sediment beneath the seep zone were far below theoretical saturation values. This finding was in conflict with the seismic reflection data, which strongly suggested the presence of bubble phase gas in the sediment. The paradox was resolved by the recent discovery that the seep consists primarily of CO_2 rather than hydrocarbons, and that CO_2 is present in the free state in the sediment interstices (Kvenvolden et al., 1979).

Examples of other reflector termination anomalies observed on air gun records in Norton basin (Fig. 7) are quite different from the one associated with the gas seep. They exhibit only slight reflector pull-downs at their margins, and lack the dramatic "wipe-out" appearance of the seep anomaly. Low frequency reflections at 0.6, 0.9, and 1.2 seconds can be traced across the acoustic anomaly zone (Fig. 7); these reflectors show distinct pull-down relative to the corresponding reflectors in the normal section. The attenuation of all but the low frequency energy is a distinctive characteristic of the reflector termination zones (Figs. 3 and 4).

Other indirect evidence indicating abnormally low compressional velocities in these shallow zones is provided by the multichannel seismic reflection data collected by the USGS in August 1978. An oscillographic camera is used to monitor the signal from the hydrophone streamer every 50 shots. A "normal" shot record is shown in Figure 8. This is not a "gather" in the true sense of the word, but merely a recording of the output from each of the 24 streamer channels for one shot from the 1326 cubic inch (21.7ℓ) air gun array. Refracted arrivals (head waves), the water wave, and

reflected arrivals are clearly visible. In sharp contrast is a shot record over the gas seep reflector termination zone (Fig. 9). Little reflected energy is returned to the streamer over the gas-charged zone. Severe attenuation of the reflected arrivals is apparent, and the only arrival beyond trace 22 is the direct water wave (D). This phenomenon can easily be explained by invoking the model of near-surface gas-charged sediment; attenuation of the reflected arrivals, especially the high frequencies, will be pronounced (Mavko and Nur, 1979), as in the case of Figure 9.

Anomalous acoustic responses were also observed on mini-sparker and Uniboom reflection records (Grim and McManus, 1970; Nelson et al., 1978; Kvenvolden et al., 1979). Small reflector pull-downs observed on the air-gun records usually appear as abrupt reflector terminations on the high resolution profiles. Anomalies on Uniboom and mini-sparker records characteristically are near the surface (10 meters or less) and in some cases the top of anomalies are in the energy pulse of the record. Core-sample gas analysis substantiates that the top of gas-charged sediment zone is within a couple tens of centimeters of the surface (Kvenvolden et al., in press). The thickness of these near-surface gas zones is unknown, because only the top of the zone acts as a reflector, no energy is returned from lower reflectors. A minimum thickness of 5 m is set by the continuously high gas contents in a 5-m-long core.

Figure 10 shows a portion of a mini-sparker (800 joules) record over an anomaly approximately 20 km east of the Norton basin gas seep. The near surface zone of diffractions (point source reflectors) was at first thought to be related to the acoustic anomaly; this diffraction layer is commonly observed on high-resolution records over the reflector wipe-outs. However, careful examination of the seismic data (Fig. 10) shows that the diffractions are also present outside of the acoustic anomaly zones. The presence of

gas in the near-surface sediment apparently attenuates energy reflected from deeper horizons in the gas-charged zone, thereby making the zone of diffractions more apparent on records over the gas-charged zones. The patches of diffracted arrivals observed on the high resolution records in Norton Sound and Chirikov basin are probably caused by coarse sediment (cobbles and pebbles) buried in or a few meters beneath the Holocene section.

The extensive reflector termination anomalies observed throughout Norton basin (Figs. 3 and 4) are probably caused by a subsurface accumulation of gas in sufficient quantity that scattering and attenuation of the seismic signal, even from large sources, is almost complete. The drastic reduction in apparent amplitude of both the reflected and direct arrivals was observed over virtually all of the reflector termination anomalies crossed in the course of the geophysical surveys. It is indicative of an unusually low impedance mismatch at the sea floor; the most likely explanation is the presence of free (bubble-phase) gas in the sediment.

Geochemical analyses by Kvenvolden and others (1979) have shown that biogenic methane and thermogenic carbon dioxide are present at saturation volumes in near-surface sediment at many station sites in Norton basin. At many of the sampled sites, but not all, acoustic anomalies are associated with known saturated gas conditions.

Reflector Pull-Down Analysis

In an effort to gain more quantitative estimates of the velocity changes due to the presence of gas, a method was developed for computing the compressional velocity in gas-charged zones over which single channel seismic reflection records show a distinct pull-down of reflectors. Compressional velocity data obtained from sonobuoy refraction profiles (Holmes and Fisher, 1979) were first used to construct an average thickness versus reflection time curve for the "normal" gas-free section in Norton basin.

The next step was to carefully measure reflection times to several marker horizons which can be traced across a pull-down zone. The reflection times measured from the single channel seismic sections were first corrected for source to receiver offset using the formula

$$T_v^2 = T_r^2 - \frac{x^2}{V_o^2}$$

where T_r = apparent reflection time from the record, x = source to receiver offset, V_o = compressional velocity just beneath the sea floor (1.60 km/sec), and T_v = corrected (normal incidence) reflection time.

The depth to a given reflector could then be determined using the equation for the depth (thickness) versus reflection time curve derived from the sonobuoy measurements:

$$D = 0.80\ T_v + 0.167 T_v^2$$

It was then possible to construct average velocity curves for both the normal zones and the gas-charged zones:

$$\bar{V}^2 = \frac{4D^2 + x^2}{T_v^2}$$

where T_v = corrected vertical reflection time to a given reflector in the normal zone and to that same reflector in the pulled-down (gas-charged) section. These average velocity curves can then be used to compute interval velocities in each zone.

In actual practice, reflectors were picked at time increments of 0.1 sec, and these intervals were carried through the entire chain of calculations. Figure 11 is an example of such an analysis of the pull-down zone over the gas seep shown in Figure 6. The analysis extends only to

a subbottom depth of 640 m; the extent and character of the acoustically anomalous zone beneath the seep area prevents accurate picking of pulled-down reflectors below that depth. However, the general trend of the average and interval velocity curves for the gas-charged zone beneath the seep suggest that the entire section above basement (about 1.3 km) probably contains enough gas to significantly lower compressional velocity.

The interval velocity curve can also be used as a qualitative indicator of gas concentration in the sedimentary section. Figure 11 shows that compressional velocity reaches a minimum of 1.21-1.24 km/sec between 250-440 m subbottom depth. This represents a decrease of about 35 per cent from the velocity one would expect at that depth in a normal sedimentary section. If the interval velocity curve could be constructed for the entire section down to basement, it might exhibit several minima similar to the one shown in Figure 11. These minima are probably an expression of a change in sediment or rock type which allows gas to be concentrated in those horizons.

POSSIBLE SOURCES OF GAS

The distribution of acoustic anomalies (Figs. 3 and 4) suggests that near-surface accumulations of gas are most common in the central part of Norton basin northwest of the Yukon River delta. The apparent gas-free zones along the southern and eastern shores of Norton Sound (Fig. 3) are due to the absence of data from these very shallow water areas. Such is not the case for western Norton basin, however. Seismic reflection coverage is good (Fig. 2); there are simply few occurrences of acoustic anomalies.

The possible sources of the gas are still being investigated. The gas seep south of Nome is the only well-substantiated source of low

molecular weight hydrocarbon gases and carbon dioxide indicative of a deep thermogenic origin (Cline and Holmes, 1978; Nelson et al., 1978; Kvenvolden et al., 1979.

Carbon isotope measurements on the CO_2 and CH_4 components yielded $\delta^{13}C$ values (relative to PDB) of -.27‰ and -3.6‰, respectively (Kvenvolden et al., 1979). Holmes and Cline (1979) have used these data to estimate the source depth of these seep gases. A $\delta^{13}C$ value of -3.6‰ is characteristic of methane from a depth of about 2500 m (Galimov, 1969). This greatly exceeds basement depth (850-1450 m) beneath the seep, suggesting that the gas has migrated to the seep area from the deeper central portion of Norton basin. The southerly dip of beds and unconformities as well as numerous faults observed on the reflection records over the seep also support such an interpretation.

The location of many of the other reflector termination zones, especially in Norton Sound, coincides with known occurrences of buried tundra-derived peat deposits which were formed during low sea-level stands in the Quaternary (Nelson and Creager, 1977). Biogenic methane and carbon dioxide generated in these peat beds could cause the observed anomalous acoustic responses (Kvenvolden et al., in press); the peat layers themselves could also act to trap upward migrating petroleum-derived gases. A velocity analysis similar to the one previously discussed for the seep zone was performed for an acoustic anomaly associated with a suspected peat deposit. Although the reflector termination anomalies usually associated with this type of gas accumulation make it difficult to trace reflector pull-downs, preliminary results suggest that the gas has accumulated in near surface horizons up to a few tens of meters thick. Compressional velocity in these layers is approximately 1.5 km/sec, or about 7 percent less than in the surrounding gas-free sediment.

The absence of acoustic anomalies (gas-charged sediment) in western Chirikov basin is probably due to the different types of Quaternary deposits. Chirikov basin was extensively glaciated during the Pleistocene (Grim and McManus, 1970); the boundary between the glaciated and unglaciated terrain corresponds closely with the eastern limit of acoustic anomalies in Figs. 3 and 4. The Quaternary glacial and glacio-marine sediments deposited in Chirikov basin do not have a high potential for biogenic gas generation because advance and retreat of the ice sheets evidently destroyed or prevented the growth of tundra-derived peats common to Norton Sound. Also, the relatively thin Tertiary sedimentary section beneath Chirikov basin has not attained sufficient thickness to subject the basal sediments to the temperatures and pressures required for the generation of hydrocarbon gases.

SUMMARY

The distribution of acoustic anomalies indicates that almost 7000 km^2 of seafloor in Norton Sound and Chirikov basin is underlain by sediments containing sufficient gas to affect sound transmission through these zones. A method of indirectly determining compressional velocity in the gas-charged zones gave values from 7 to 35 per cent lower than would be expected in the case of gas-free sediment. The cause of one of the anomalies, that associated with the Norton basin gas seep, is well documented. Here thermogenic gases are seeping to the surface along a system of basic margin faults. Although other undiscovered seeps of the thermogenic gas may exist in Norton Sound or Chirikov basin, most of the acoustic anomalies in this area are probably caused by biogenic gases generated in buried peat layers. Further detailed processing and analysis of the seismic data will possibly permit quantitative estimates to be made of the amounts of gas present in these acoustically anomalous zones.

REFERENCES

Cline, J.D., and Holmes, M.L. (1977) Submarine seepage of natural gas in Norton Sound, Alaska. Science 198, 1149-1153.

_____ (1978) Anomalous gaseous hydrocarbons in Norton Sound: Biogenic or thermogenic? Proceedings, Offshore Technology Conference, Houston, p. 81-86.

Cooper, A.K. (1978) Hydrocarbon prospects for the frontier abyssal areas of the Bering Sea. The Oil and Gas Journal, Oct. 23, p. 196-201.

Craft, C.I. (1973) Detecting hydrocarbons--for years the goal of exploration geophysicists. The Oil and Gas Journal, Feb. 19, p. 122-125.

Galimov, E.M. (1969) Isotopic composition of carbon in gases of the crust. International Geology Review 11, 1092-1104.

Grim, M.S., and McManus, D.A. (1970) A shallow seismic-profiling survey of the northern Bering Sea. Marine Geology 8, 293-320.

Holmes, M.L., and Cline, J.D. (1978) Geological setting of the Norton basin gas seep. Proceedings, Offshore Technology Conference, Houston, p. 73-80.

_____ (1979) Source depth and geologic setting of the Norton basin gas seep. Journal of Petroleum Technology 31, 1241-1248.

Holmes, M.L., and Fisher, M.A. (1979) Sonobuoy refraction measurements from Norton basin, northern Bering Sea. Program, Amer. Assoc. Petroleum Geologists Annual Convention, Houston, p. 104 (abs).

Kvenvolden, K.A., Nelson, C.H., Thor, D.R., Larsen, M.C., Redden, G.D., and Rapp, J.B. (1979) Biogenic and thermogenic gas in gas-charged sediment of Norton Sound, Alaska. Proceedings, Offshore Technology Conference, Houston, p. 479-486.

Lindsey, J.F., and Craft, C.I. (1973) How hydrocarbon reserves are estimated from seismic data. World Oil, Aug. 1, p. 23-25.

Mavko, G.M., and Nur, A., (1979) Wave attenuation in partially saturated rocks. Geophysics 44:161-178.

McManus, D.A., Venkatarathnam, K., Hopkins, D.M., and Nelson, C.H. (1974) Yukon River sediment on the northernmost Bering Sea shelf. Journal of Sedimentary Petrology 44, 1052-1060.

Nelson, C.H., Hopkins, D.M., and Scholl, D.W. (1974) Cenozoic sedimentary and tectonic history of the Bering Sea. In D.W. Hood and E.J. Kelley (eds.) Oceanography of the Bering Sea, University of Alaska, Inst. Marine Sciences, p. 485-516.

Nelson, C.H., and Creager, J.S. (1977) Displacement of Yukon-derived sediment from Bering Sea to Chukchi Sea during Holocene time. Geology 5, 141-146.

Nelson, C.H., Kvenvolden, K., and Clukey, E.C. (1978) Thermogenic gases in near-surface sediments of Norton Sound, Alaska. Proceedings, Offshore Technology Conference, Houston, p. 2623-2633.

Savit, C.H. (1974) Bright spot in the energy picture. Ocean Industry, Feb., p. 60-65.

Walton, F.W., Perry, R.B., and Greene, H.G. (1969) Seismic reflection profiles, northern Bering Sea. Environmental Science Services Administration Operational Data Report C & GS DR-8, 26 p.

FIGURE CAPTIONS

FIGURE 1. Location map of study area showing Norton Sound, Chirikov basin, and the Norton basin gas seep (Cline and Holmes, 1977; Holmes and Cline, 1979).

FIGURE 2. Seismic reflection tracklines in the northern Bering Sea. Cruise dates and sound sources used are also shown.

FIGURE 3. Location of anomalous near-surface acoustic responses observed on single channel air-gun and minisparker seismic reflection records from Norton Sound and Chirikov basin. Also shown are the locations of the Norton basin gas seep (Cline and Holmes, 1977), and the seismic record sections shown in Figures 5,6,7,10.

FIGURE 4. Location of anomalous near-surface acoustic responses observed on Uniboom reflection records from Norton Sound and Chirikov basin.

FIGURE 5. Seismic reflection record across the Norton basin gas seep zone. Location of line shown in Figure 3. This record shows two types of acoustic anomalies indicative of gas in the sediment: Reflector terminations and reflector pull-downs.

FIGURE 6. Single channel reflection record across the Norton basin gas seep area. Location of line shown in Figure 3. Reflector termination zone and marginal pull-downs are clearly shown.

FIGURE 7. Single channel seismic reflection record from eastern Norton basin showing "normal" reflector zones and typical reflector termination anomalies. Location of line is shown in Figure 3.

FIGURE 8. Multichannel shot record over "normal" reflector sequence shown in Figure 7. Refracted head waves (H), and reflected arrivals (R) are clearly visible.

FIGURE 9. Multichannel shot record over the gas seep reflector termination anomaly shown in Figure 6. All arrivals are markedly attenuated due to gas in the near surface sediment. Amplifier settings slightly higher than in Figure 8.

FIGURE 10. Minisparker (800 joules) record from Norton basin showing reflector termination anomaly with near-surface diffractions. Location of line is shown in Figure 3.

FIGURE 11. Velocity analysis of reflector pull-down zone beneath the Norton basin gas seep (Fig. 6). The two right hand curves show average and interval velocity versus depth in the gas-free reflector sequence outside the seep zone. The two curves on the left are for the gas-charged section beneath the seep itself.

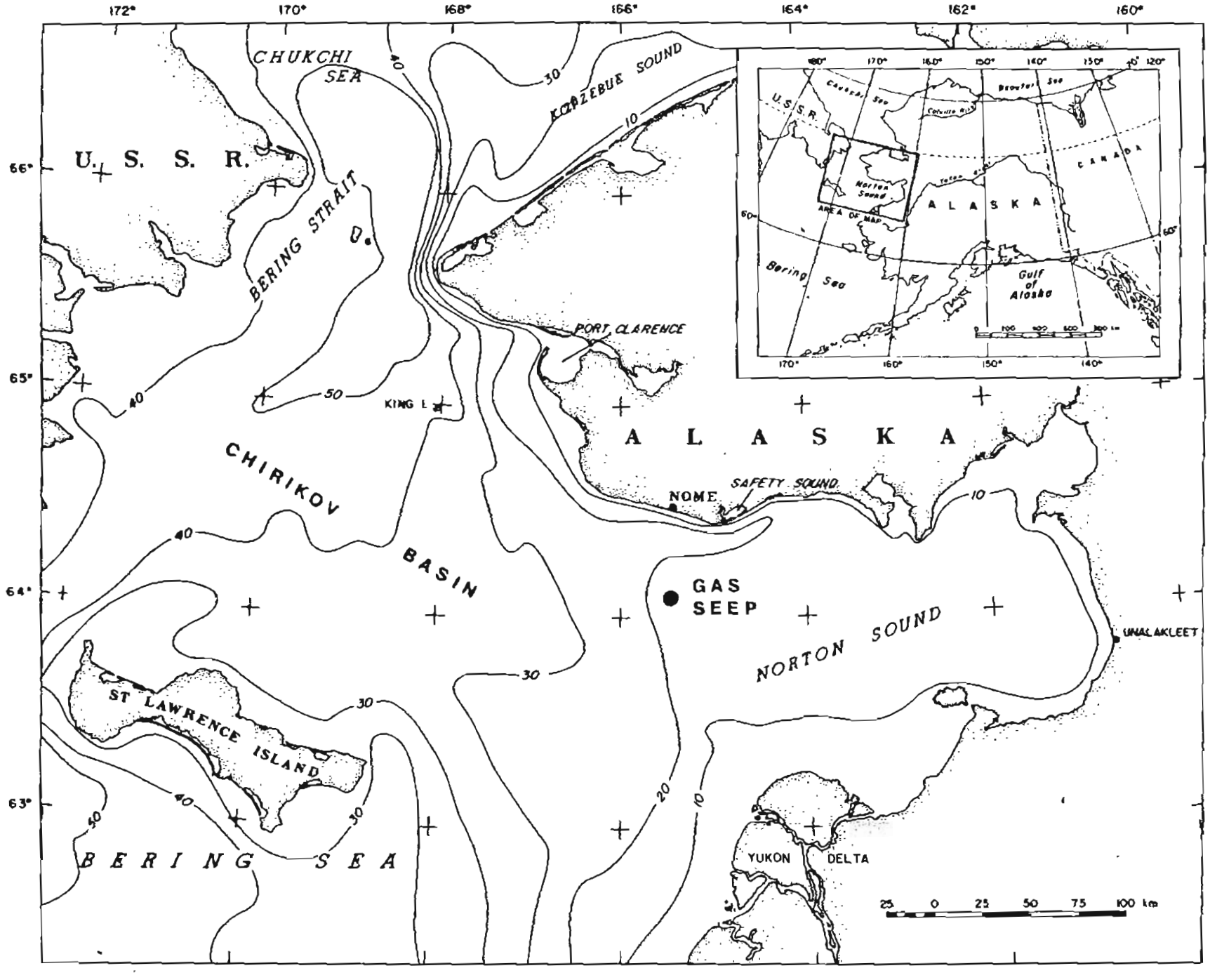
172°
170°
168°
166°
164°
162°
160°
66°
65°
64°
63°
CHUKCHI SEA
U. S. S. R.
BERING STRAIT
KOTZEBUE SOUND
PORT CLARENCE
KING I.
CHIRIKOV BASIN
A L A S K A
NOME
SAFETY SOUND
GAS SEEP
NORTON SOUND
UNALAKLEET
ST LAWRENCE ISLAND
BERING SEA
YUKON DELTA
40
30
10
50
20
0
25 0 25 50 75 100 km
U.S.S.R.
Chukchi Sea
Beaufort Sea
Colville R.
CANADA
Norton Sound
AREA OF MAP
ALASKA
Yukon R.
Bering Sea
Gulf of Alaska
180°
170°
160°
150°
140°
130°
120°
60°

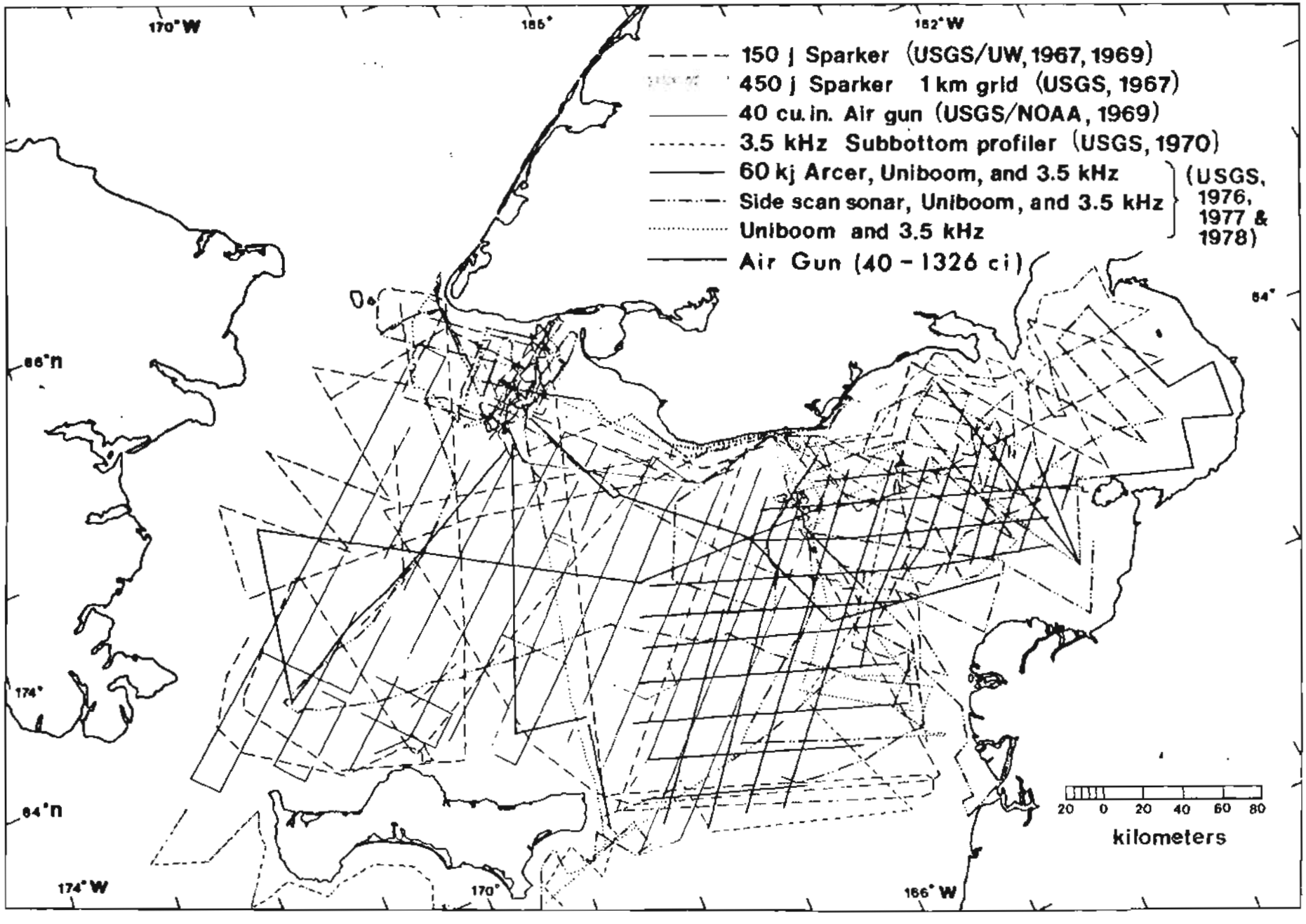
170°W
165°
162°W
150 j Sparker (USGS/UW, 1967, 1969)
450 j Sparker 1 km grid (USGS, 1967)
40 cu. in. Air gun (USGS/NOAA, 1969)
3.5 kHz Subbottom profiler (USGS, 1970)
60 kj Arcer, Uniboom, and 3.5 kHz
Side scan sonar, Uniboom, and 3.5 kHz
Uniboom and 3.5 kHz
(USGS, 1976, 1977 & 1978)
Air Gun (40 - 1326 ci)
66°n
64°
174°
64°n
174°W
170°
166°W
20 0 20 40 60 80
kilometers

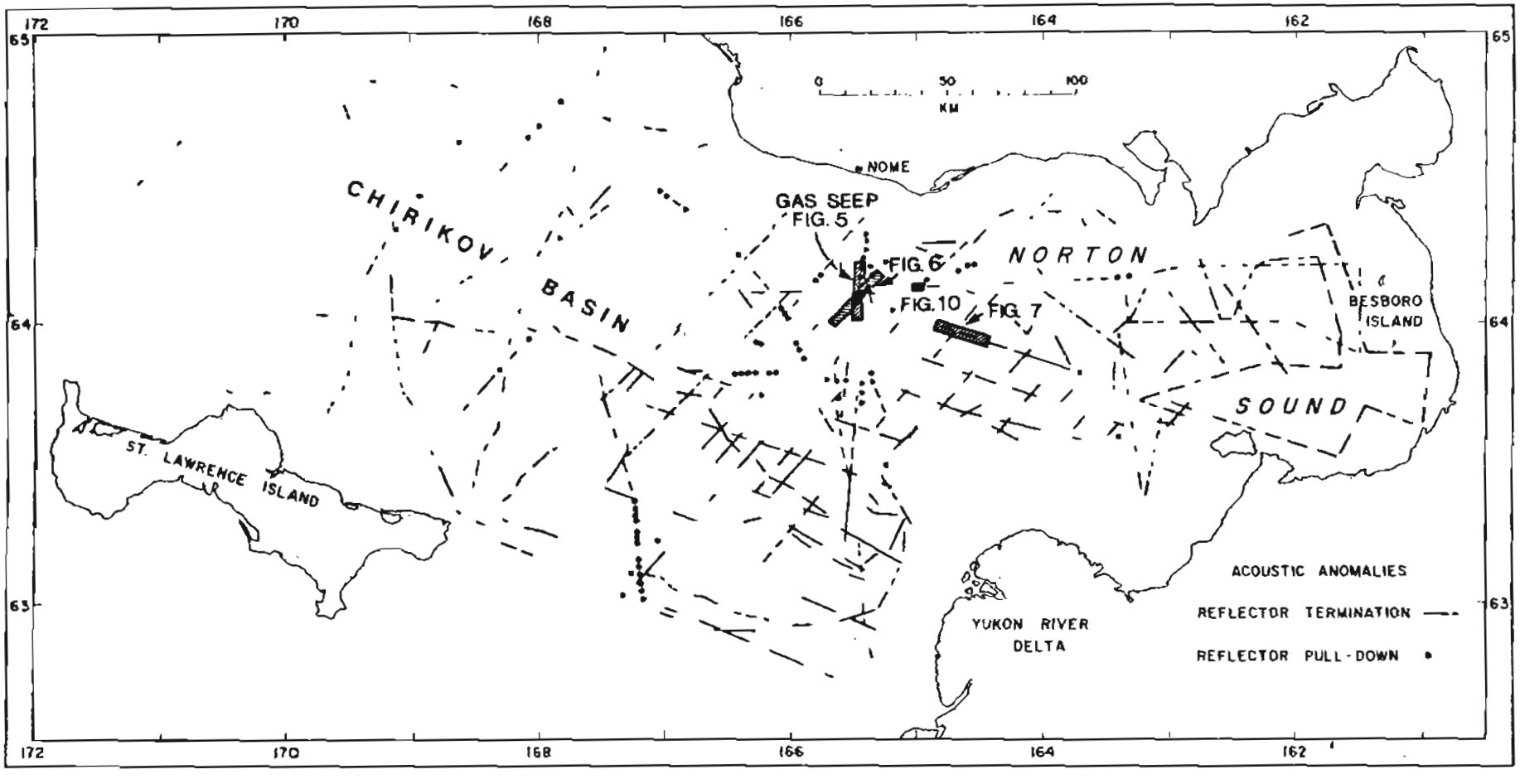
172
170
168
166
164
162
65
64
63
0
50
100
KM
NOME
GAS SEEP
FIG. 5
FIG. 6
FIG. 10
FIG. 7
CHIRIKOV
BASIN
NORTON
SOUND
BESBORO
ISLAND
ST. LAWRENCE ISLAND
YUKON RIVER
DELTA
ACOUSTIC ANOMALIES
REFLECTOR TERMINATION
REFLECTOR PULL-DOWN

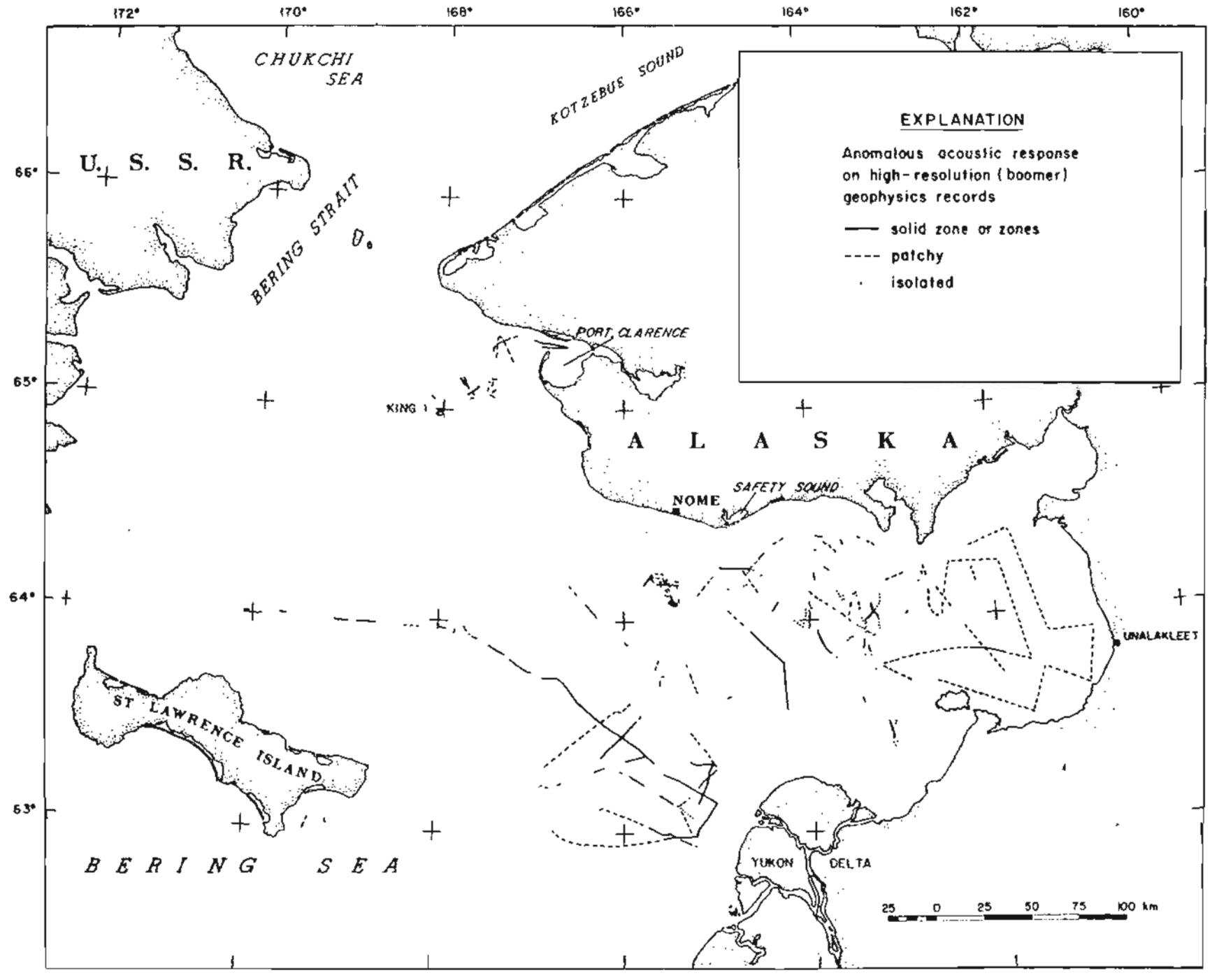
172°
170°
168°
166°
164°
162°
160°
66°
65°
64°
63°
CHUKCHI SEA
KOTZEBUE SOUND
U. S. S. R.
BERING STRAIT
PORT CLARENCE
KING I.
A L A S K A
NOME
SAFETY SOUND
UNALAKLEET
ST LAWRENCE ISLAND
BERING SEA
YUKON DELTA
EXPLANATION
Anomalous acoustic response on high-resolution (boomer) geophysics records
solid zone or zones
patchy
isolated
25 0 25 50 75 100 km

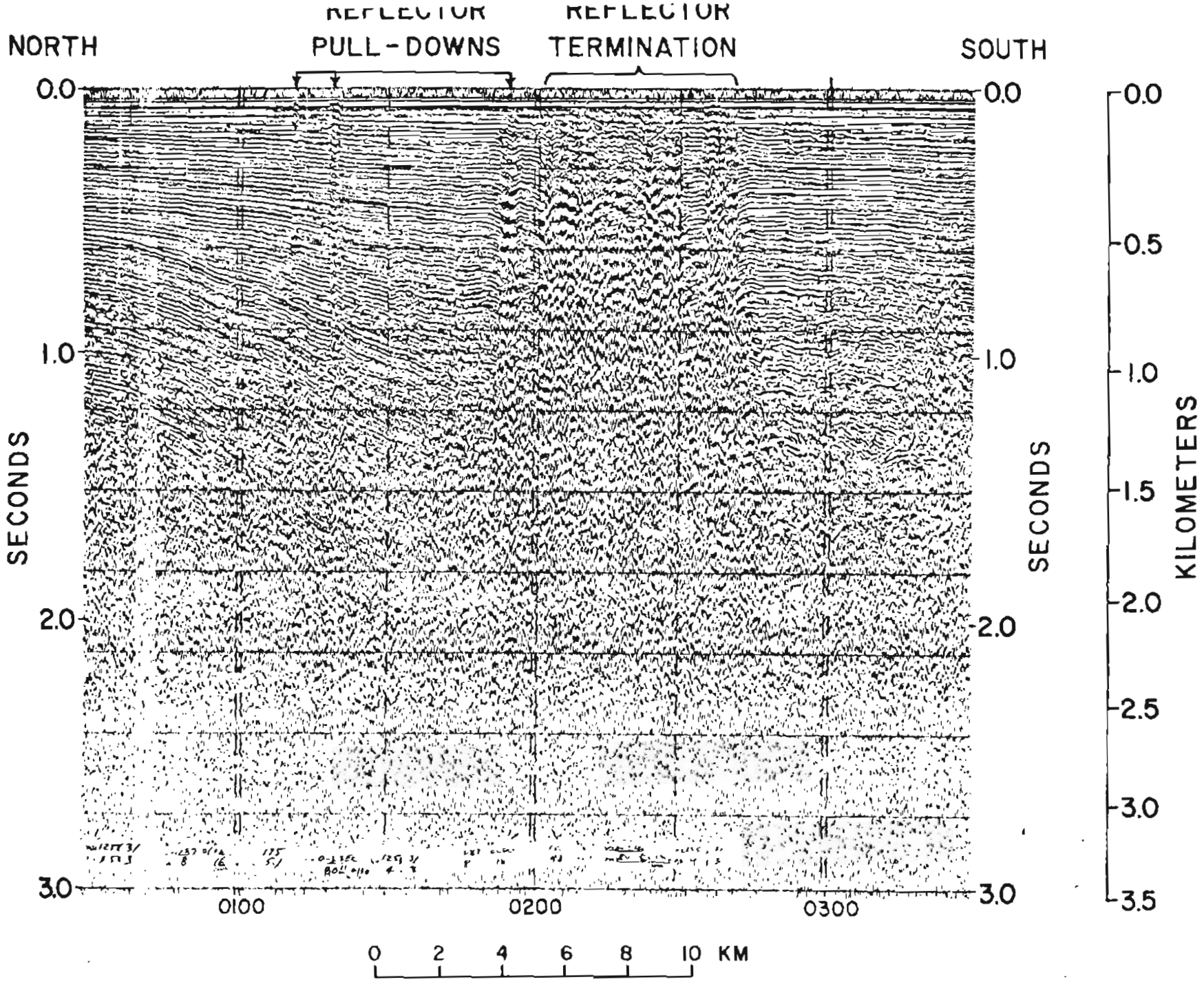
REFLECTOR PULL-DOWNS
REFLECTOR TERMINATION
NORTH
SOUTH
0.0
1.0
2.0
3.0
SECONDS
0100
0200
0300
0 2 4 6 8 10 KM
0.0
0.5
1.0
1.5
2.0
2.5
3.0
3.5
KILOMETERS

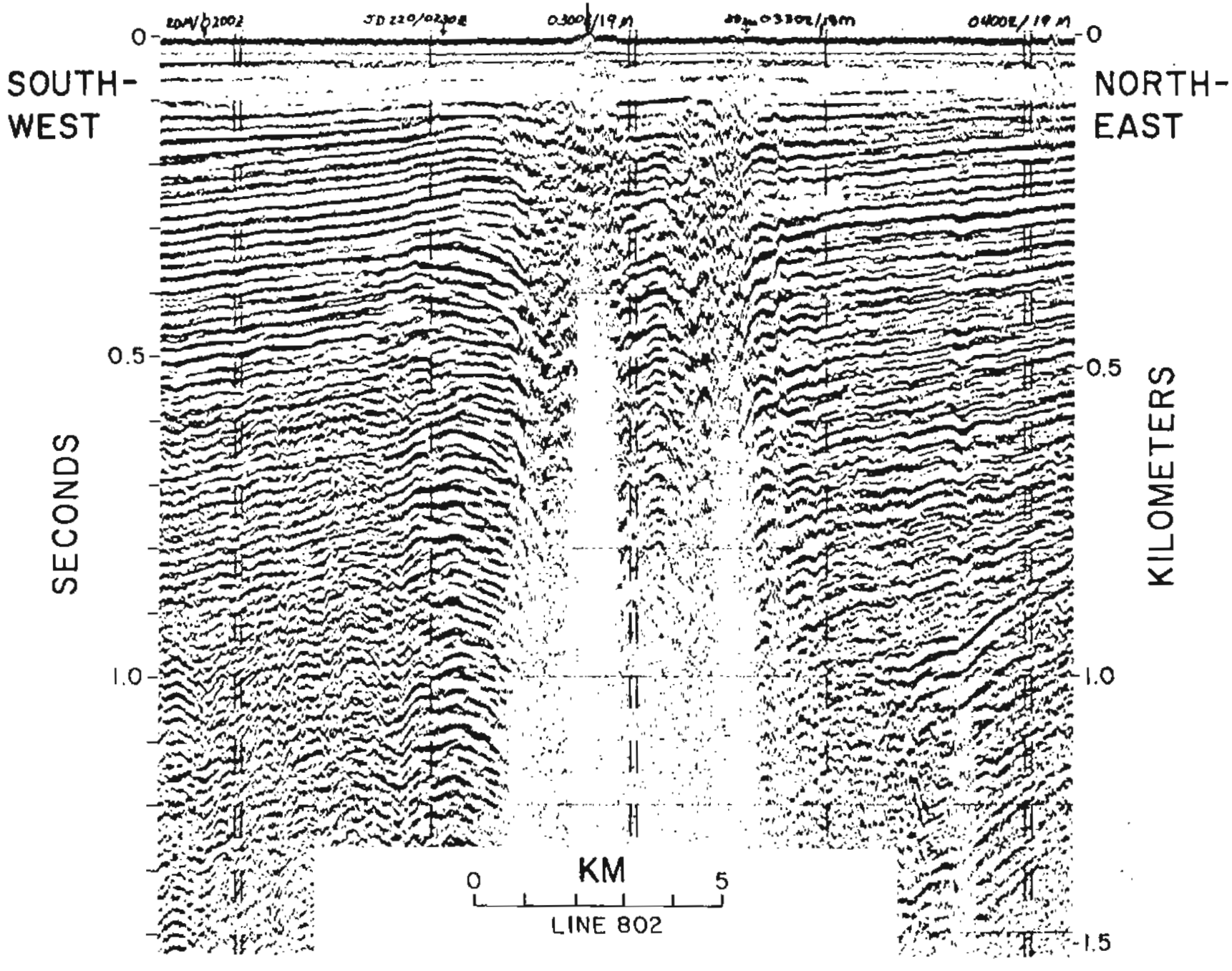
SOUTH-
WEST
NORTH-
EAST
SECONDS
KILOMETERS
0
0.5
1.0
1.5
0
KM
5
LINE 802

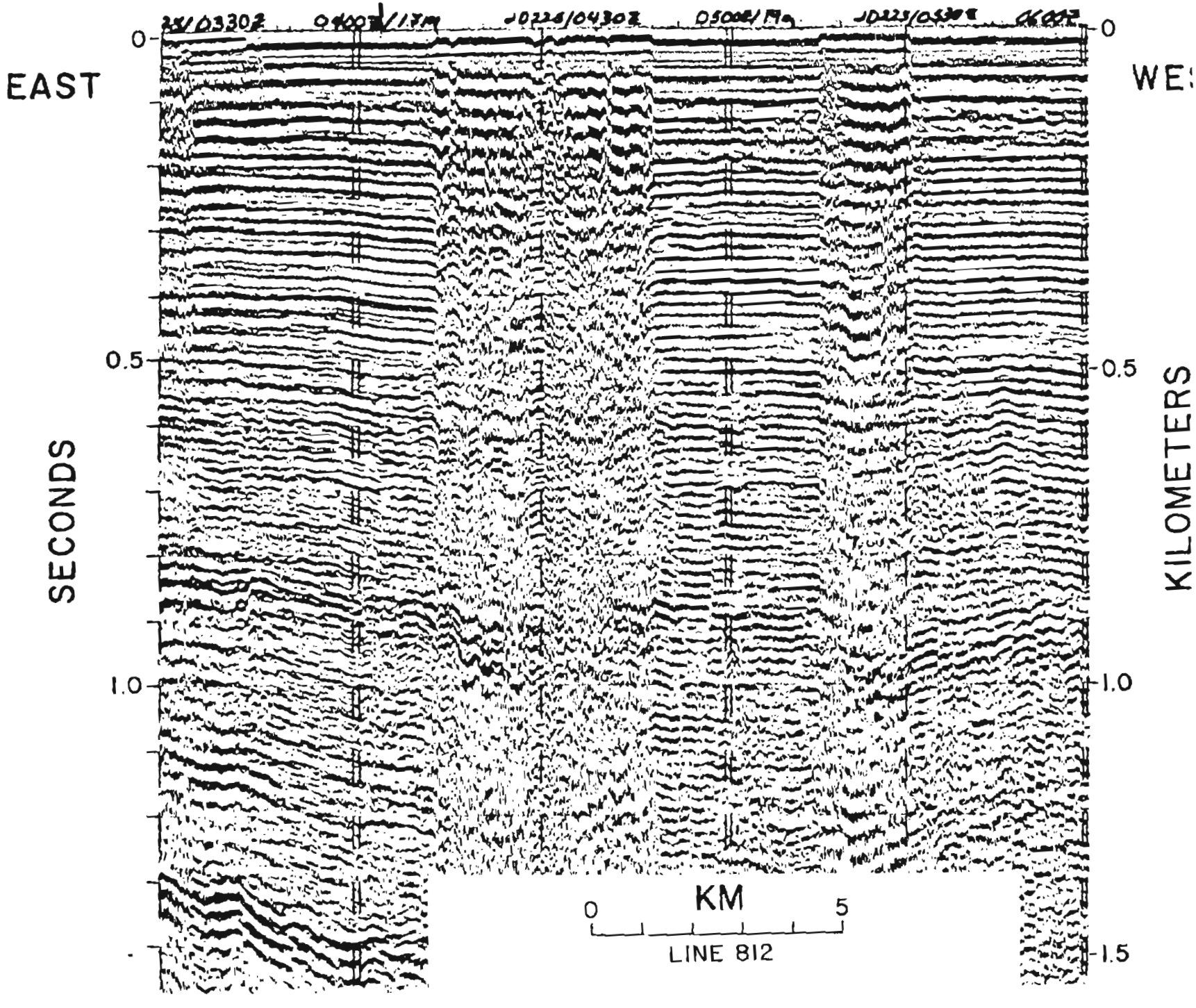
EAST
WE
SECONDS
KILOMETERS
0
0.5
1.0
1.5
0
KM
5
LINE 812

SHOT RECORD

CRUISE: L4-78-BS
DATE / TIME: 225 / 0404
LINE: 812

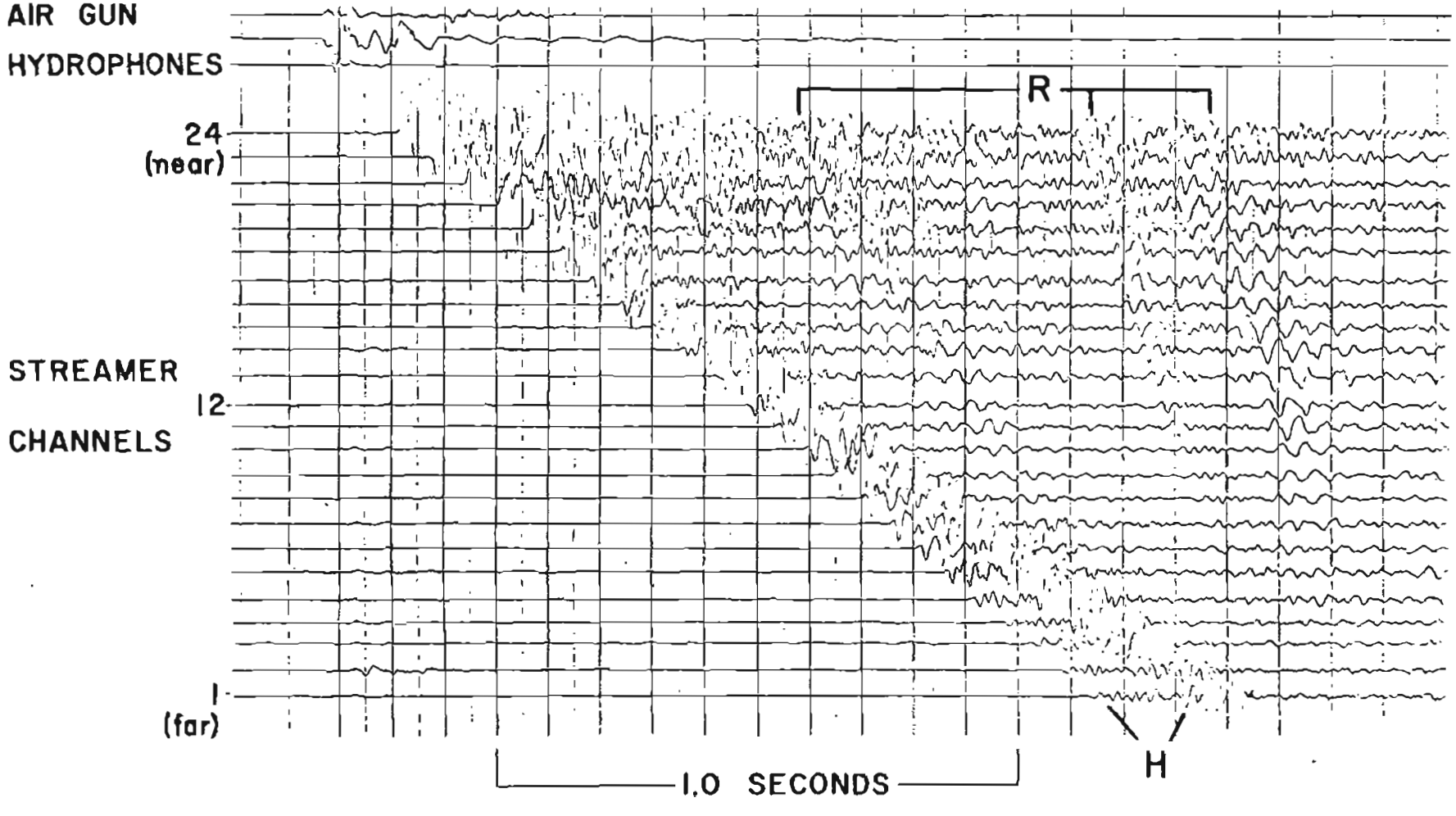

SHOT RECORD

CRUISE: L4-78-BS
DATE / TIME: 220 / 0254
LINE: 802

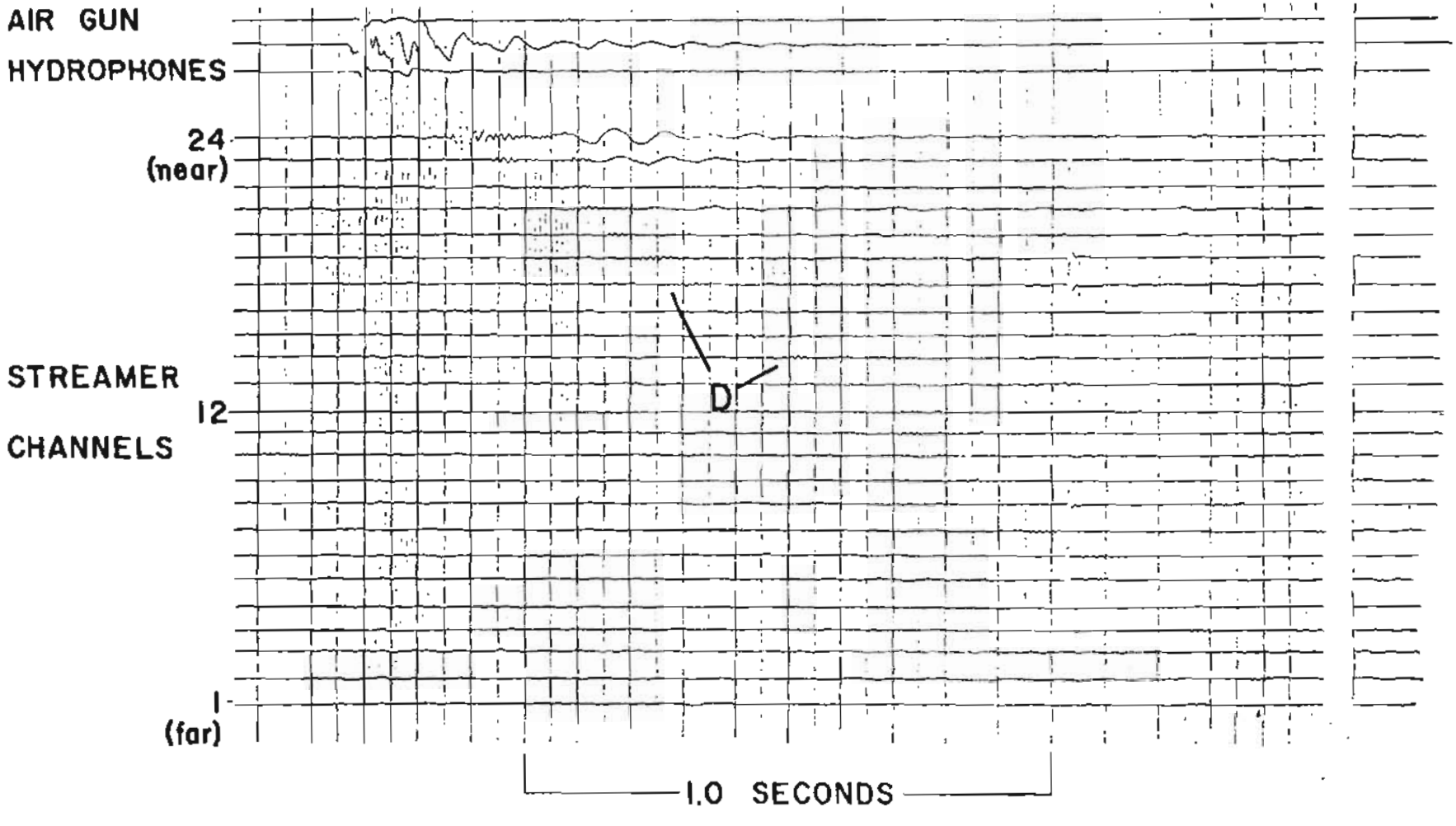

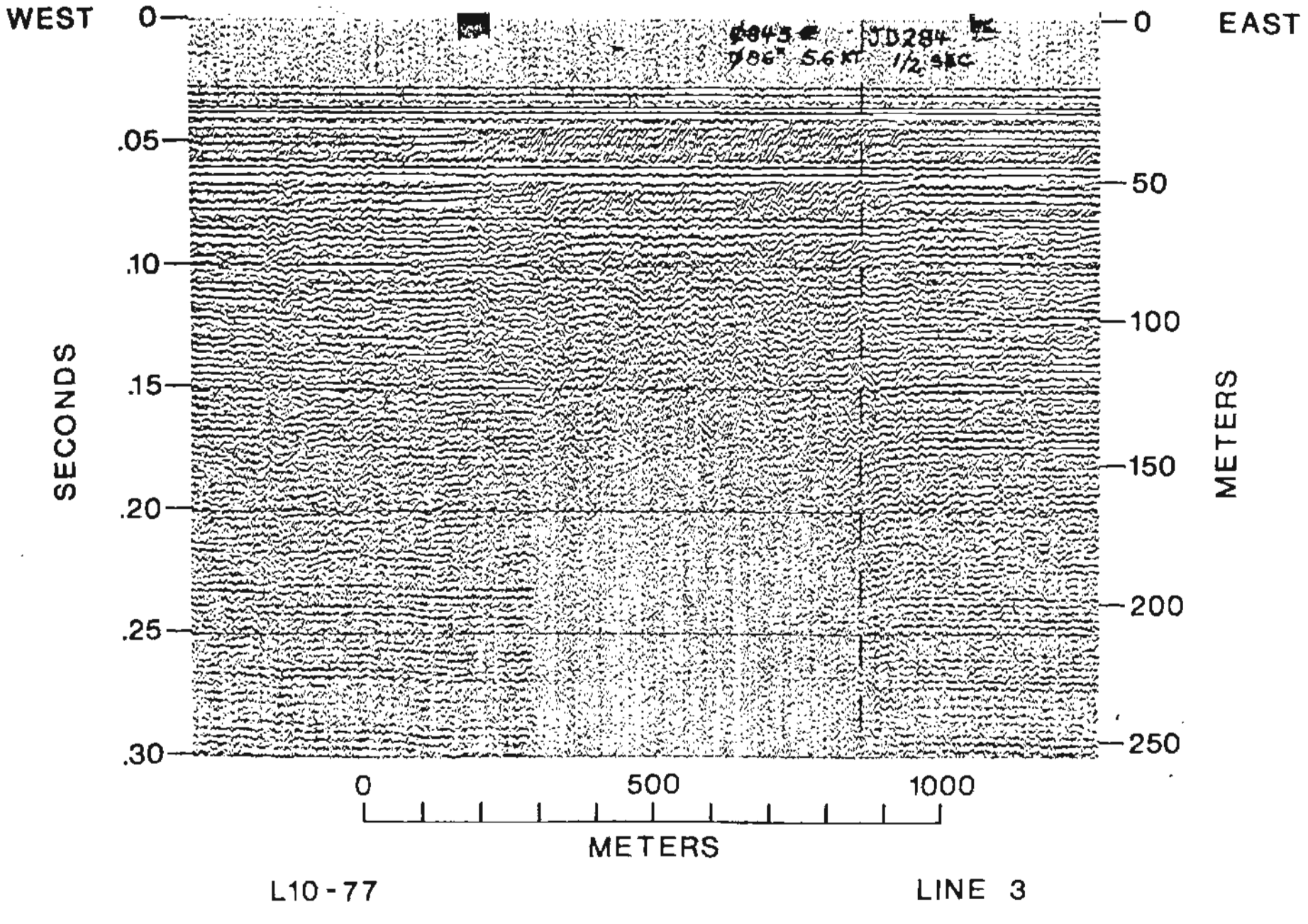
WEST
EAST
0
.05
.10
.15
.20
.25
.30
SECONDS
0
50
100
150
200
250
METERS
0
500
1000
METERS
L10-77
LINE 3

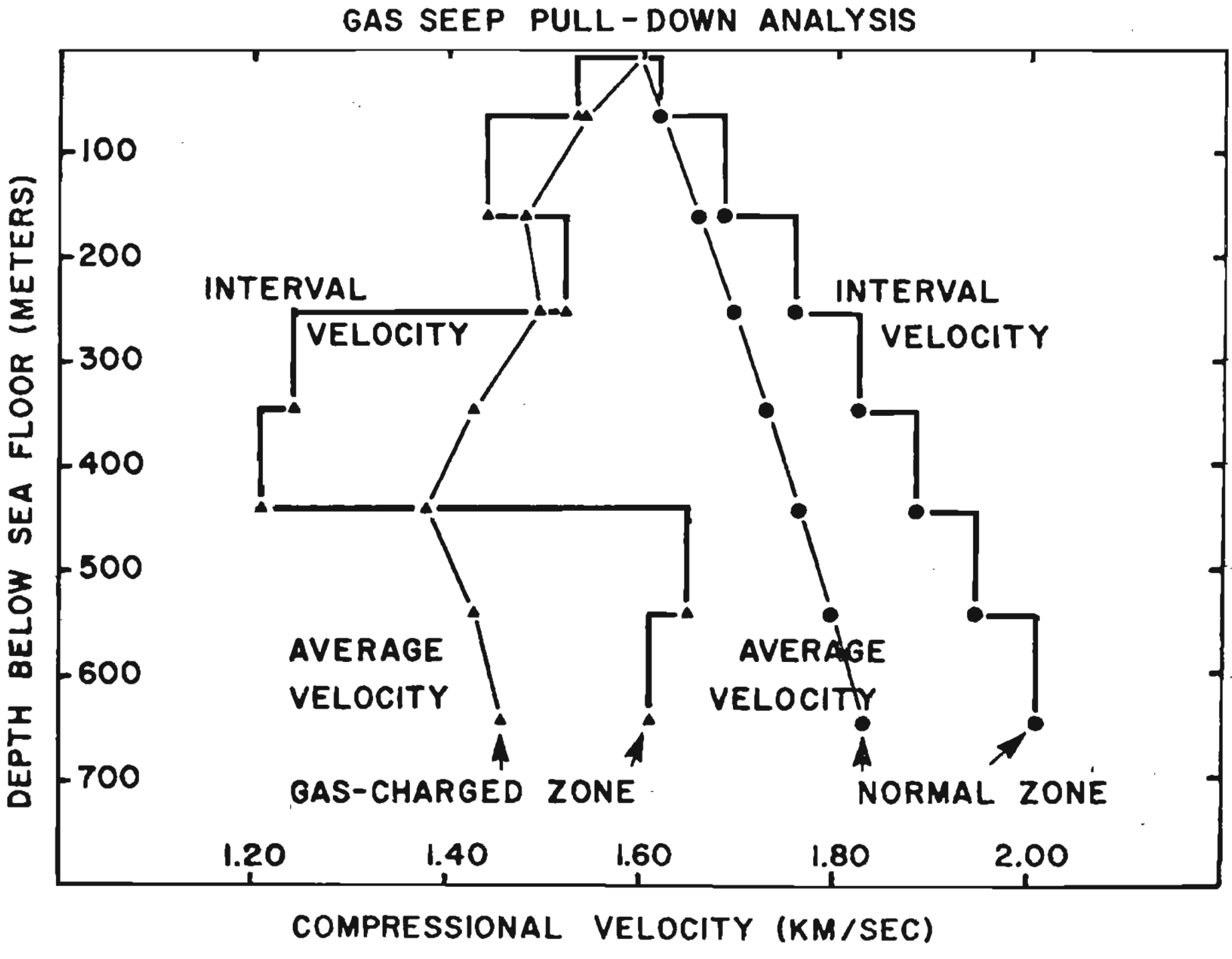
GAS SEEP PULL-DOWN ANALYSIS
DEPTH BELOW SEA FLOOR (METERS)
100
200
300
400
500
600
700
INTERVAL VELOCITY
INTERVAL VELOCITY
AVERAGE VELOCITY
AVERAGE VELOCITY
GAS-CHARGED ZONE
NORMAL ZONE
1.20
1.40
1.60
1.80
2.00
COMPRESSIONAL VELOCITY (KM/SEC)

Sources of papers included in this volume, indicated in right margin:

Sedimentary processes and potential hazards on the sea floor of Northern Bering Sea (EBS)
by: M.C. Larsen, C.H. Nelson, and D.R. Thor

Interplay of physical and biological sedimentary structures of the Bering epicontinental shelf (EBS
by: C. H. Nelson, R.W. Rowland, S.W. Stoker, B.R. Larsen

Ripples and sand waves in Norton Basin; bedform activity, and scour potential
by: C. H. Nelson, M.E. Field, D.A. Cacchione, D. E. Drake, and T. H. Nilsen

Graded storm sand layers offshore from the Yukon delta, Alaska
by: C. H. Nelson

Ice gouging on the subarctic Bering shelf (EBS)
by: D. R. Thor and C. H. Nelson

Liquefaction potential of the Yukon prodelta, Bering Sea (OTC)
by: E. C. Clukey, D.A. Cacchione, C.H. Nelson

Surface and subsurface faulting in Norton Sound and Chirikov Basin, Alaska
by: J. L. Johnson and M. L. Holmes

Hydrocarbon gases in near-surface sediment of northern Bering Sea (Norton Sound and Chirikov Basin) (EBS)
by: K. A. Kvenvolden, G. D. Redden, D. R. Thor, and C. H. Nelson

Introduction to papers from Holocene Marine Sedimentation in the North Sea Basin (HMS)
by: C. H. Nelson

Late Pleistocene-Holocene transgressive sedimentation in deltaic and non-deltaic areas of the Bering epicontinental shelf (HMS)
by: C. H. Nelson

Microfaunal analysis of late Quaternary deposits of the northern Bering Sea (HMS)
by: K. McDougall

Sedimentary structures on a delta-influenced shallow shelf, Norton Sound, Alaska (HMS)
by: J. D. Howard, C. H. Nelson

Linear sand bodies in the Bering Sea epicontinental shelf (HMS)
by: C.H. Nelson, W. R. Dupré, M.E. Field, and J. D. Howard

Depositional and erosional features of the inner shelf, northeastern Bering Sea (HMS)
by: R. Hunter, D. R. Thor, and M. L. Swisher

Velocity and bottom-stress measurements in the bottom boundary layer, outer Norton Sound, Alaska (HMS)
by: D. A. Cacchione, D. E. Drake, P. Wiberg.

Geotechnical characteristics of bottom sediments in the northern Bering Sea (HMS)
by: H. W. Olsen, E. C. Clukey, and C. H. Nelson

Distribution of gas-charged sediment in Norton Basin, northern Bering Sea (HMS)
by: M. L. Holmes and D. R. Thor

APPENDIX

Following is a list of papers included in this volume. Following the paper name, in parenthesis, is the name of the journal or book in which the paper can be found, when published, in the near future. If no journal or book name follows the paper title, this indicates that the paper appears only in this open file report.

Abbreviations used:

EBS- The Eastern Bering Shelf: Its Oceanography and Resources, Hood, D.W., editor. (in press).

OTC- Offshore Technology Conference, Proceedings, Houston, TX., paper 3773.

HMS- Holocene Marine Sedimentation in the North Sea Basin, Nio, S.C., Schattenhelm, R.T., and Van Weering, T.C.E., editors, International Association of Sedimentologists Special Publication, Blackwell Scientific Publications, London. (in press).